

THE JOURNAL
OF THE
INSTITUTE OF METALS

VOLUME LXXVI

1949-50

EDITOR

N. B. VAUGHAN, M.Sc.

The Right of Publication and of Translation is Reserved



*The Institute of Metals is not responsible either for the statements made or
for the opinions expressed in the following pages*

LONDON
PUBLISHED BY THE INSTITUTE OF METALS
4 GROSVENOR GARDENS, S.W.1
1950

Copyright]

[Entered at Stationers' Hall

PAST-PRESIDENTS.

Sir WILLIAM HENRY WHITE, K.C.B., LL.D., D.Eng., Sc.D., F.Inst.Met., F.R.S., 1908–1910 (*deceased*).

Sir GERARD ALBERT MUNTZ, Bart., 1910–1912 (*deceased*).

Professor WILLIAM GOWLAND, A.R.S.M., F.R.S., 1912–1913 (*deceased*).

Professor ALFRED KIRBY HUNTINGTON, A.R.S.M., 1913–1914 (*deceased*).

Engineer Vice-Admiral Sir HENRY JOHN ORAM, K.C.B., F.Inst.Met., F.R.S., 1914–1916 (*deceased*).

Sir GEORGE THOMAS BEILBY, LL.D., D.Sc., F.R.S., 1916–1918 (*deceased*).

Professor Sir HENRY CORT HAROLD CARPENTER, M.A., Ph.D., D.Sc., D.Met., A.R.S.M., F.Inst.Met., F.R.S., 1918–1920 (*deceased*).

Engineer Vice-Admiral Sir GEORGE GOODWIN GOODWIN, K.C.B., LL.D., F.Inst.Met., 1920–1922 (*deceased*).

LEONARD SUMNER, O.B.E., M.Sc., J.P., F.Inst.Met., 1922–1924 (*deceased*).

Professor-Emeritus THOMAS TURNER, M.Sc., A.R.S.M., F.Inst.Met., 1924–1926 (*deceased*).

Sir JOHN DEWRANCE, G.B.E., F.Inst.Met., 1926–1928 (*deceased*).

WALTER ROSENHAIN, D.Sc., B.C.E., F.Inst.Met., F.R.S., 1928–1930 (*deceased*).

RICHARD SELIGMAN, Ph.nat.D., F.Inst.Met., 1930–1932.

Sir HENRY FOWLER, K.B.E., LL.D., D.Sc., 1932–1934 (*deceased*).

HAROLD MOORE, C.B.E., D.Sc., Ph.D., F.Inst.Met., 1934–1936.

WILLIAM ROBB BARCLAY, O.B.E., F.Inst.Met., 1936–1938 (*deceased*).

CECIL HENRY DESCH, D.Sc., LL.D., Ph.D., F.Inst.Met., F.R.S., 1938–1940.

The Hon. RICHARD MARTIN PETER PRESTON, D.S.O., 1940–1942.

Lieut.-Colonel Sir JOHN HENRY MAITLAND GREENLY, K.C.M.G., C.B.E., M.A., F.Inst.Met., 1942–1944 (*deceased*).

Sir WILLIAM THOMAS GRIFFITHS, D.Sc., 1944–1946.

Colonel Sir PAUL GOTTLIEB JULIUS GUETERBOCK, K.C.B., D.S.O., M.C., T.D., D.L., J.P., M.A., A.D.C., F.Inst.Met., 1946–1948.

Sir ARTHUR JOHN GRIFFITHS SMOUT, J.P., 1948–1950.

OFFICERS AND COUNCIL

FOR THE YEAR 1950-1951

PRESIDENT:

H. S. TASKER, B.A.

PAST-PRESIDENTS:

SIR WILLIAM GRIFFITHS, D.Sc.

COLONEL SIR PAUL GUETERBOCK, K.C.B., D.S.O., M.C., T.D., D.L.,
J.P., M.A., A.D.C., F.Inst.Met.

SIR ARTHUR SMOOT, J.P.

VICE-PRESIDENTS:

MAJOR C. J. P. BALL, D.S.O., M.C.
S. F. DOREY, C.B.E., D.Sc., Wh.Ex.,
F.R.S.
PROFESSOR A. J. MURPHY, M.Sc.

PROFESSOR H. O'NEILL, D.Sc., M. Met.
C. J. SMITHHELLS, M.C., D.Sc.
PROFESSOR F. C. THOMPSON, D.Met.,
M.Sc.

HONORARY TREASURER:

W. A. C. NEWMAN, O.B.E., B.Sc., A.R.S.M., A.R.C.S.

ORDINARY MEMBERS OF COUNCIL:

JOHN ARNOTT.
G. L. BAILEY, M.Sc.
E. A. BOLTON, M.Sc.
D. F. CAMPBELL, M.A., A.R.S.M.
MAURICE COOK, D.Sc., Ph.D.
HARRY DAVIES.
C. H. DAVY.
T. M. HERBERT, M.A.
H. W. G. HIGNETT, B.Sc.

E. H. JONES.
D. P. C. NEAVE, M.A.
L. B. PFEIL, O.B.E., D.Sc., A.R.S.M.
A. R. POWELL.
PROFESSOR A. G. QUARRELL, D.Sc.,
Ph.D., A.R.C.S., D.I.C.
PROFESSOR G. V. RAYNOR, M.A.,
D.Sc., D.Phil.

EX-OFFICIO MEMBERS OF COUNCIL:

(Chairmen of Local Sections)

BIRMINGHAM : BERNARD THOMAS.
LONDON : E. A. G. LIDDIARD, M.A.
SCOTTISH : H. R. BEAUCHAMP.

SHEFFIELD : H. G. DALE.
SOUTH WALES : E. A. HONTOIR,
B.Sc.

REPRESENTATIVES OF OTHER BODIES.

The following, in accordance with Article 32, represent Government departments and allied societies at Council meetings for purposes of liaison :

ADMIRALTY :

CAPTAIN (E) L. A. B. PEILE, D.S.O.,
M.V.O., R.N.

IRON AND STEEL INSTITUTE :

J. R. MENZIES-WILSON, O.B.E.

INSTITUTION OF METALLURGISTS :
E. W. COLBECK, M.A.
L. ROTHERHAM, M.Sc.

WAR OFFICE :

MAJOR-GENERAL S. W. JOSLIN,
M.B.E., B.A.

SECRETARY:

LIEUT.-COLONEL S. C. GUILLAN, T.D.

ASSISTANT SECRETARY:

MAJOR R. E. MOORE.

EDITOR:

N. B. VAUGHAN, M.Sc.

**CHAIRMEN AND HONORARY SECRETARIES OF THE
LOCAL SECTIONS.**

at 30 June 1950.

Birmingham.

Chairman : BERNARD THOMAS, Leigh House, Bradmore Road,
Wolverhampton.

Hon. Secretary : E. H. BUCKNALL, M.Sc., "Ardarroch", 264 Harborne
Park Road, Harborne, Birmingham 17.

Hon. Treasurer : R. CHADWICK, M.A., 5 Fairmead Rise, King's Norton,
Birmingham, 30.

London.

Chairman : E. A. G. LIDDIARD, M.A., Fulmer Research Institute, Stoke
Poges, Bucks.

Hon. Secretary : E. C. RHODES, Ph.D., B.Sc., The Mond Nickel Company, Ltd.,
Development and Research Department, Bashley Road, London, N.W.10.

Hon. Treasurer : J. D. GROGAN, B.A., Metallurgy Division, National
Physical Laboratory, Teddington, Middlesex.

Scottish.

Chairman : H. R. BEAUCHAMP, Imperial Chemical Industries, Ltd., Metals
Division, 4 Blythswood Square, Glasgow, C.2.

Hon. Secretary : MATTHEW HAY, A. Cohen and Co., Ltd., Craigton Industrial
Estate, Barfillan Drive, Cardonald, Glasgow, S.W.2.

Hon. Treasurer : N. J. MACLEOD, Steven and Struthers, Ltd., 86 Eastvale Place,
Kelvinhaugh, Glasgow, C.3.

Sheffield.

Chairman : H. G. DALE, Sheffield Smelting Co., Ltd., Sheffield.

Joint Hon. Secretaries : A. J. MACDOUGALL, M.Met., and W. R. MADDOCKS,
Ph.D., B.Sc., Department of Applied Science, The University,
St. George's Square, Sheffield 1.

Hon. Treasurer : W. R. MADDOCKS, Ph.D., B.Sc., Department of Applied
Science, The University, St. George's Square, Sheffield 1.

South Wales.

Chairman : E. A. HONTOIR, B.Sc., Rio Tinto Co., Ltd., Port Talbot.

Hon. Secretary : K. M. SPRING, 36 Beechwood Road, Uplands, Swansea.

Hon. Treasurer : W. H. GRENFELL, "The Woods", Bryn Terrace, Mumbles,
Swansea.

CORRESPONDING MEMBERS TO THE COUNCIL.

at 30 June 1950.

Argentina.

H. N. BASSETT,

Shell Mex Argentina, Ltd., Casilla Correo 1759, Buenos Aires.

Australia.

Professor H. K. WORNER, D.Sc.,

Professor of Metallurgy, University of Melbourne, Carlton, N.3, Melbourne, Victoria.

Belgium.

H. P. A. FÉRON,

Administrateur-Directeur, Vissières et Tréfileries Réunies, 2 Avenue Général Leman, Haren, Bruxelles.

Canada.

Professor BRUCE CHALMERS, Ph.D., D.Sc.,

Department of Metallurgical Engineering, University of Toronto, Toronto 5, Ontario.

Professor G. LETENDRE, B.A., Ph.D., Professor of Metallurgy and Director, Department of Mining and Metallurgical Engineering, Faculty of Sciences, Laval University, Boulevard de l'Entente, Quebec City, P.Q.

France.

Professor P. A. J. CHEVENARD,

Directeur Scientifique, Société Anonyme de Commentry-Fourchambault et Decazeville, 84 rue de Lille, Paris 7e.

JEAN MATTER, Vice-Président et Directeur-Général, Société Centrale des Alliages Légers, Issoire, Puy-de-Dôme.

India.

N. P. GANDHI, M.A., B.Sc., A.R.S.M., D.I.C.,

Kennaway House, Proctor Road, Girgaon, Bombay 4.

Italy.

LENO MATTEOLI, Dott.chim.,

Vice-Director, Istituto Scientifico Tecnico Ernesto Breda, Sesto S. Giovanni, Milano.

Netherlands.

M. HAMBURGER, Director, N.V. Royal Nederlandsche Lood- en Zinkpletterijen voorheen A.D. Hamburger, Leidschekade 30, Utrecht.

South Africa.

G. H. STANLEY, D.Sc., A.R.S.M.,

24 Duncombe Road, Forest Town, Johannesburg, Transvaal.

Professor L. TAVERNER, A.R.S.M., D.I.C., Professor of Metallurgy and Assaying, University of the Witwatersrand, Johannesburg, Transvaal.

Spain.

Professor J. ORLAND, M.Sc., M.A., Ph.D., D.D., Head of the Department of Metallography and Strength of Materials, Instituto Católico de Artes e Industrias, Alberto Aguilera 23, Madrid.

Sweden.

Professor CARL BENEDICKS, Fil.Dr., Dr.-Ing.e.h., Dr.Techn.h.c.,
Drottninggatan 95 B., Stockholm.

Professor AXEL HULTGREN, Professor of Metallography, Kungl. Tekniska
Högskolan, Stockholm.

Switzerland.

Professor A. von ZEERLEDER, Dr.-Ing., Director, Research Laboratories,
Société Anonyme pour l'Industrie de l'Aluminium Chippis,
Rosenbergstrasse 25, Neuhausen a./Rheinfall.

United States of America.

Professor R. F. MEHL, Ph.D., Eng.D., Sc.D., Director, Metals Research
Laboratory, Carnegie Institute of Technology, Pittsburgh, Pa.

Professor C. S. SMITH, Sc.D., Professor of Metallurgy and Director of the
Institute for the Study of Metals, University of Chicago, Chicago 37, Ill.

Dr. R. A. WILKINS, Vice-President, Revere Copper and Brass Inc., Rome, N.Y.

CORRIGENDA

(1) In the paper by Mr. L. E. Samuels on "The Metallography of Copper
Containing Small Amounts of Bismuth," the following emendation should
be made :

The sentence in the third paragraph of p. 99 reading "Concentration of
solute atoms at the grain boundaries would increase with decreasing tem-
perature" should be replaced by : "Concentration of solute atoms at the
grain boundaries could occur only at temperatures below the solubility tem-
perature of the solute in the interior of the grain, the tendency to segregation
increasing as the temperature falls below the solubility temperature."

(2) In the paper by Mr. S. J. Carlile, Dr. J. W. Christian, and Dr. W.
Hume-Rothery on "The Equilibrium Diagram of the System Chromium-
Manganese," the following emendation should be made :

In Fig. 7 (p. 187) the $\alpha/(\alpha + \theta)$ boundary should be deleted between
1000° and 500° C., as it was not in fact determined below 1000° C.

CONTENTS

MINUTES OF PROCEEDINGS	PAGE
Extraordinary General Meeting, London, 29 March 1950	xiii
Annual General Meeting, London, 29, 30, and 31 March 1950 :	
Elections of Ordinary Members and Student Members	xiv
Walter Rosenhain Medal	xxii
Report of Council	xxii
Report of the Honorary Treasurer	xxii
Re-election of Auditors	xxii
Election of Officers for 1950-51	xxii
Senior Vice-President	xxiii
W. H. A. Robertson Medal for 1949	xxiii
Induction of the New President	xxiii
Vote of Thanks to the Retiring President	xxiii
Vote of Thanks to Other Retiring Officers	xxv
Presidential Address	xxv
The Institute of Metals (Platinum) Medal for 1950	xxv
Discussion of Papers	xxv
Conversazione and Exhibition	xxvi
Discussion of Papers	xxvi
PAPERS AND DISCUSSIONS	PAGE
	<i>Papers. Discn.</i>
1207. Recent French Investigations in the Field of Light Alloys. Twentieth Autumn Lecture. By Professor Georges Chaudron, Dr.ès.Sci.	1
1208. Some Aspects of the Production and Heat-Treatment of Electrolytic Copper Powder. By H. J. V. Tyrrell, M.A., B.Sc.	17
Discussion	659
1209. The Thermal Properties and Chilling Power of Some Non-Metallic Mould Materials. By R. W. Ruddle, M.A., A.I.M., and A. L. Mincher, B.Sc.	43
1210. The Metallography of Copper Containing Small Amounts of Bismuth. By L. E. Samuels, B.Met.E.	91
Discussion	660
1211. Modern Billet Casting, with Special Reference to the Solidification Process. By E. Scheuer, Dr.rer.nat.	103
Discussion	662

	PAGE <i>Papers. Discn.</i>
1212. Recrystallization of Single Crystals after Plastic Bending. By R. W. Cahn, B.A.	121
Discussion	672
1213. The Application of X-Ray Methods to the Determination of Phase Boundaries in Metallurgical Equilibrium Diagrams. By Professor E. A. Owen, M.A., Sc.D., and D. P. Morris, B.Sc.	145
Discussion	677
1214. The Equilibrium Diagram of the System Chromium-Manganese. By S. J. Carlile, B.A., J. W. Christian, B.A., D.Phil., and W. Hume-Rothery, M.A., D.Sc., F.R.S.	169
1215. A Note on the Effect of Nitrogen on the Structures of Certain Alloys of Chromium and Manganese, and on the Existence of an Intermediate Nitride Phase. By S. J. Carlile, B.A., and W. Hume-Rothery, M.A., D.Sc., F.R.S.	195
Discussion	718
1216. Overheating Phenomena in Aluminium-Copper-Magnesium-Silicon Alloys of the Duralumin Type. By J. Crowther, M.Sc., F.I.M.	201
Discussion	726
1217. The Mechanism of Deformation in Metals, with Special Reference to Creep. By W. A. Wood, D.Sc., and W. A. Rachinger, M.Sc.	237
Discussion	730
1218. On the Mechanism of Oxidation of Nickel-Platinum Alloys. By O. Kubaschewski, Dr.phil.nat.habil., and (Fr.) Ortrud von Goldbeck, Dr.rer.nat.	255
Discussion	738
1219. The Aluminium-Tin Phase Diagram and the Characteristics of Aluminium Alloys Containing Tin as an Alloying Element. By A. H. Sully, M.Sc., Ph.D., F.Inst.P., H. K. Hardy, M.Sc., Ph.D., A.R.S.M., A.I.M., and T. J. Heal, B.Sc., A.Inst.P.	269
Discussion	742
1220. Grain Refinement of Aluminium and Its Alloys by Small Additions of Other Elements. By Myriam D. Eborall, B.A.	295
Discussion	744
1221. The Mechanism of Grain Refinement of Sand Castings in Aluminium Alloys. By A. Cibula, M.A., A.I.M.	321
Discussion	744
1222. The Effect of Grain-Size on the Tensile Properties of High-Strength Cast Aluminium Alloys. By A. Cibula, M.A., A.I.M., and R. W. Ruddle, M.A., A.I.M.	361
Discussion	744
1223. A Method of Improving the Pressure-Tightness of Lead-Free Gun-Metal Sand Castings. By W. H. Glaisher, B.Sc.	377
1224. The Constitution of the Silver-Rich Silver-Magnesium-Zinc Alloys. By Professor G. V. Raynor, M.A., D.Sc., and R. A. Smith, B.Sc.	389

Contents

xi

SYMPOSIUM ON METALLURGICAL ASPECTS OF THE HOT WORKING OF NON-FERROUS METALS AND ALLOYS

	PAGE <i>Papers. Discn.</i>
1225. The Hot Rolling of Aluminium and Its Alloys. By F. Kasz, B.Sc., A.R.Ae.S., and P. C. Varley, M.B.E., M.A.	407
1226. The Extrusion of Aluminium Alloys. By Christopher Smith, F.I.M.	429
1227. The Hot Forging and Hot Stamping of Aluminium and Its Alloys. By F. E. Stokeld, F.I.M.	453
1228. The Hot Working of Magnesium and Its Alloys. By R. G. Wilkinson, B.Sc., and F. A. Fox, D.Sc., F.I.M.	473
1229. The Hot Working of Copper and Copper Alloys. By Maurice Cook, D.Sc., Ph.D., F.I.M., and Edwin Davis, M.Sc., F.I.M.	501
1230. The Hot Working of Tin Bronzes. By D. W. Dugard Showell, M.Sc.	527
1231. The Hot Working of Lead and Lead-Rich Alloys. By L. H. Back, B.Sc.	541
1232. The Rolling of Zinc and Zinc-Rich Alloys. By C. W. Roberts, B.Sc., A.I.M., and B. Walters, M.A.	557
Joint Discussion	752
<hr/>	
1233. The Behaviour of Nickel-Chromium-Iron Alloys in Carbon-Bearing Gases in the Range 900°-1000° C. By D. M. Dovey, M.A., A.R.I.C., A.I.M., and I. Jenkins, D.Sc., F.I.M.	581
1234. A Method for Assessing the Relative Corrosion Behaviour of Different Sea-Waters. By T. Howard Rogers, D.I.C., A.I.M.	597
1235. Static Models of Dislocations. By B. A. Bilby, B.A., Ph.D.	613
1236. Note on the Use of Electropolishing in the Metallographic Study of Plastic Deformation. By G. R. Wilms, B.Met.E., M.Eng.Sc.	629
1237. The Structure of Eutectics. By E. C. Ellwood, Ph.D., A.I.M., and K. Q. Bagley, B.Sc.	631
Discussion	780
Report of Council for the Year Ended 31 December 1949	643
Report of the Honorary Treasurer for the Financial Year Ended 30 June 1949	652
Further Discussion on Paper by Dr. H. K. Hardy : "Modern Descriptive Theories of Precipitation Processes" (<i>J. Inst. Metals</i> , 1948-49, 75 , 707, 1160)	784
Discussion on Paper by Professor A. Krupkowski and Mr. S. Kawinski : "The Phenomenon of Anisotropy in Annealed Polycrystalline Metals" (<i>J. Inst. Metals</i> , 1948-49, 75 , 869)	785
Obituary Notices	787
Name Index	789

LIST OF PLATES

- I-VI. Autumn Lecture by Professor G. Chaudron
between pp. 8 and 9
- VII-VIII. Paper by Mr. H. J. V. Tyrrell *between pp. 32 and 33*
- IX-XI. Paper by Mr. L. E. Samuels *between pp. 96 and 97*
- XII-XIII. Paper by Dr. E. Scheuer *between pp. 118 and 119*
- XIV-XIX. Paper by Mr. R. W. Cahn *between pp. 134 and 135*
- XX-XXI. Paper by Mr. S. J. Carlile, Mr. J. W.
 Christian, and Dr. W. Hume-Rothery
between pp. 182 and 183
- XXII-XXIII. Paper by Mr. S. J. Carlile and Dr. W. Hume-
 Rothery *between pp. 198 and 199*
- XXIV-XXV. Paper by Mr. J. Crowther . . . *between pp. 216 and 217*
- XXVI-XXXIII. Paper by Dr. W. A. Wood and Mr. W. A.
 Rachinger *between pp. 248 and 249*
- XXXIV-XXXVII. Paper by Dr. A. H. Sully, Dr. H. K. Hardy,
 and Mr. T. J. Heal *between pp. 280 and 281*
- XXXVIII-XLIII. Paper by Mrs. M. D. Eborall *between pp. 310 and 311*
- XLIV-XLIX. Paper by Mr. A. Cibula *between pp. 326 and 327*
- L-LIII. Paper by Mr. A. Cibula and Mr. R. W.
 Ruddle *between pp. 366 and 367*
- LIV. Paper by Professor G. V. Raynor and Mr.
 R. A. Smith *to face p. 390*
- LV-LVIII. Paper by Mr. F. Kasz and Mr. P. C. Varley
between pp. 422 and 423
- LIX-LXIV. Paper by Mr. C. Smith *between pp. 438 and 439*
- LXV-LXVI. Paper by Mr. F. E. Stokeld *between pp. 454 and 455*
- LXVII-LXX. Paper by Mr. R. G. Wilkinson and Dr. F. A.
 Fox *between pp. 486 and 487*
- LXXI-LXXIV. Paper by Dr. M. Cook and Mr. E. Davis
between pp. 518 and 519
- LXXV-LXXVI. Paper by Mr. L. H. Back *between pp. 550 and 551*
- LXXVII. Paper by Mr. C. W. Roberts and Mr. B.
 Walters *to face p. 566*
- LXXVIII-XCI. Paper by Mr. D. M. Dovey and Dr. I.
 Jenkins *between pp. 588 and 589*
- XCII-XCIX. Paper by Dr. B. A. Bilby *between pp. 620 and 621*
- C. Paper by Mr. G. R. Wilms *to face p. 629*
- CI. Paper by Dr. E. C. Ellwood and Mr. K. Q.
 Bagley *to face p. 636*
- CII-CV. Discussion on the paper by Dr. E. Scheuer
between pp. 666 and 667
- CVI-CVII. Discussion on the paper by Mr. R. W. Cahn
between pp. 674 and 675
- CVIII-CIX. Discussion on the paper by Mr. S. J. Carlile
 and Dr. W. Hume-Rothery *between pp. 722 and 723*
- CX-CXI. Discussion on the paper by Dr. W. A. Wood
 and Mr. W. A. Rachinger *between pp. 730 and 731*
- CXII. Discussion on the paper by Dr. O. Kubaschew-
 ski and Dr. O. von Goldbeck *to face p. 738*
- CXIII. Joint Discussion on Papers by Mrs. M. D.
 Eborall, Mr. A. Cibula, and Mr. R. W.
 Ruddle *to face p. 746*

THE INSTITUTE OF METALS

MINUTES OF PROCEEDINGS

EXTRAORDINARY GENERAL MEETING

AN EXTRAORDINARY GENERAL MEETING of the Institute of Metals was held at the Café Royal, Regent Street, London, W.1, at 10 a.m. on Wednesday, 29 March 1950. The President, Sir Arthur Smout, J.P., occupied the Chair.

The SECRETARY (Lieut.-Colonel S. C. Guillan, T.D.) read the notice convening the meeting.

The PRESIDENT then put to the meeting the following resolution, which was carried unanimously :

Resolution

" THAT the provisions of Clause 3 of the Memorandum of Association of the Institute of Metals with respect to the objects of the Association be altered as follows :

" (a) By the omission from sub-clause (b) thereof of the words 'and to assist the progress of inventions likely to be useful to the members of the Association and to the community at large'.

" (b) By the omission therefrom of sub-clauses (c) and (k).

" (c) By the omission from sub-clause (d) thereof of the words 'and between members of the Association' and the words 'wholly or in part'.

" (d) By the omission from sub-clause (g) thereof of the words 'and deal with'.

" (e) By the substitution in sub-clause (i) thereof of the words 'tending to promote the objects of the Association', for the words 'the undertaking whereof may seem desirable'.

" (f) By the substitution in sub-clause (m) thereof of the words 'services rendered to the science and practice of non-ferrous metallurgy', for the words 'research, for inventions of a specified character, or for improvements in the production or manufacture of non-ferrous metals and their alloys, and to expend money in researches and experiments, and in such other ways as may extend the knowledge of non-ferrous metals and their alloys'.

ANNUAL GENERAL MEETING

THE FORTY-SECOND ANNUAL GENERAL MEETING of the Institute of Metals was held in London on Wednesday, Thursday, and Friday, 29, 30, and 31 March 1950. The meeting was held at the Café Royal, Regent Street, W.1, on the morning of 29 March; at the Institution of Mechanical Engineers, Storey's Gate, S.W.1, on the afternoon of 29 March and all day on 30 March; and at 4 Grosvenor Gardens, S.W.1, all day on 31 March. The President, Sir Arthur Smout, J.P., occupied the Chair at the opening of the meeting.

Wednesday, 29 March

The CHAIRMAN extended a hearty welcome to members and visitors present from overseas.

The minutes of the previous General Meeting of the Institute, held in Paris from 3 to 8 October 1949, were taken as read and signed by the Chairman.

ELECTIONS OF ORDINARY MEMBERS, ASSOCIATE MEMBERS, AND STUDENT MEMBERS

The SECRETARY (Lieut.-Colonel S. C. Guillan, T.D.) announced that, since the last General Meeting, the following 216 Ordinary Members and Student Members had been elected on 21 October, 8 November, 9 December, and 31 December 1949 and 9 February and 14 March 1950.

ELECTED ON 21 OCTOBER 1949

As Ordinary Members

- AYALA, Urbano Lopez, Metallurgical Engineer, The Teziutlan Copper Company, Aire Libre Pue, Mexico.
- BAILEY, William, Chief Layout Draughtsman, Davy and United Engineering Company, Ltd., Park Iron Works, Sheffield.
- BUTLER, Edmund Marshall, Director and Assistant Manager, Kirkstall Forge, Ltd., Leeds 5.
- CLOGENSON, Georges Henry Jean, Dipl.-Ing., Joint General Manager, E. and E. Kaye, Ltd., Queensway, Ponders End, Enfield, Middlesex.
- DAVIES, George, Joint General Manager, E. and E. Kaye, Ltd., Queensway, Ponders End, Enfield, Middlesex.
- DAVIES, Roy Bartlett, B.Sc., Scientific Officer, Metallurgical Section, Research Department, British Insulated Callender's Cables, Ltd., 38 Wood Lane, London, W.12.
- FÉRON, André, Administrateur Directeur, S.A. Visseries et Tréfileries Réunies, Machelen, Belgium.
- FINCH, Donald Ira, B.S., Chief, Research Department, Metallurgical Division, Leeds and Northrup Company, 4901 Stenton Avenue, Philadelphia 44, Pa., U.S.A.
- FRANKLIN, William Walter, Chief Engineer, Davy and United Engineering Company, Ltd., Park Iron Works, Sheffield.
- GOODLAD, Wilfred Horace, Assistant Chief Engineer, Design and Development, Davy and United Engineering Company, Ltd., Park Iron Works, Sheffield.
- GRIMSTON, The Honourable John, Director and General Manager, Enfield Rolling Mills, Ltd., Millmarsh Lane, Brimsdown, Enfield, Middlesex.
- JOSEPHS, Ellis, Foundry Manager, Leopold Lazarus, Ltd., St. Stephen's Street, Birmingham 6.
- LEWIS, William Edmund Jenkin, B.Sc., Principal Surveyor for Metals, Lloyds Register of Shipping, 71 Fenchurch Street, London, E.C.3.
- MACDONALD, William Richardson Dickson, Director and Manager, The Yorkshire Copper Works, Ltd., Leeds.
- MILKO, John Anthony, B.S., Research Engineer, Battelle Memorial Institute, 505 King Avenue, Columbus, O., U.S.A.
- MORTON, James Storrs, D.F.C., M.A., Assistant Manager, Telcon Metals, Telegraph Construction and Maintenance Company, Ltd., Telcon Works, Greenwich, London, S.E.10.
- MUNNIK, Eric Howard, Engineer Technician, Rhodesian Iron and Steel Commission, P.O. Box 44, Que Que, Southern Rhodesia.

- NEEDLEMAN, Benjamin, B.Sc., Works Metallurgist, Union Steel Corporation of South Africa, Vereeniging, Transvaal, South Africa.
- PADLEY-SMITH, Arthur Edwin, General Manager, Aerlec (Aluminium), Ltd., Stoke Prior, Bromsgrove, Worcestershire.
- PLACE, Arthur, Rolling Mill Manager, Claywheel Rolling Mills, Claywheel Lane, Sheffield 6.
- ROGERS, Thomas Howard, D.I.C., Corrosion Investigator, Royal Naval Establishment, Halifax, Nova Scotia, Canada.
- SCHRAMM, Jacob, Dr.-Ing., Chief Metallurgist, Metall-Guss- und Presswerk Heinrich Diehl, Nuremberg, Germany.
- TIMMIS, Laurence Barnett, M.Sc., Librarian, Armament Research Establishment, Ministry of Supply, Fort Halstead, Sevenoaks, Kent.
- VAN LANCKER, Marc, Ing. Chim., Consultant Metallurgist, 40 Avenue des Colonies, Anvers, Belgium.
- WAKELING, Albert Lorraine, Metallurgist, J. Stone and Company, Ltd., Charlton, London, S.E.7.

As Student Members

- BHAT, Uppinangady Gopalkrishna, B.Sc., Apprentice Metallurgist, Indian Smelting and Refining Company, Ltd., Bhandup, Bombay, India.
- BRADLEY, Donald, Scientific Assistant, Royal Aircraft Establishment, Farnborough, Hampshire.
- ELLIOTT, Sam John Lloyd, B.Met.E., Metallurgical Engineer, c/o Commonwealth Bank of Australia, Australia House, Strand, London, W.C.2.
- FRANCES, Claude, Engineer, Société Schneider, 15 rue Pasquier, Paris, France.
- WATERS, Brian Harry Coles, B.A., Research Metallurgist, Metallurgy Department, The University, Pembroke Street, Cambridge.

ELECTED ON 8 NOVEMBER 1949

As Ordinary Members

- ASTON, Charles Frederick, General Manager, Heaton and Dugard, Ltd., Shadwell Street Mills, Birmingham 4.
- BAILEY, Harold John, Sales Manager, Evered and Company, Ltd., Surrey Works, Smethwick, Staffs.
- BANNISTER, William Joseph, B.Sc., Divisional Manager, Wire Mills Production Division, British Insulated Callender's Cables, Ltd., Prescot, Lancashire.
- BOTHAM, George Henry, B.Sc., Laboratory Manager, A.P.V. Company, Ltd., Wandsworth Park, London, S.W.18.
- HÄGG, Gunnar, Ph.D., Professor of General and Inorganic Chemistry, University of Uppsala, Uppsala, Sweden.
- MARÉCHAL, Jean, Ing. civil des Mines, Chef du Service des Recherches et des Laboratoires de l'Usine de Dives, Compagnie du Duralumin et du Cuivre, Dives-sur-Mer, Calvados, France.
- MEREDITH, George, General Sales Manager, James Booth and Company, Ltd., Argyle Street Works, Nechells, Birmingham 7.
- ROCA SOLER, José, General Manager, Cia. Roca-Radiadores, S.A., Gavá, Spain.
- SMITH, James Arthur, B.Met., Metallurgist, Research Department (Metallurgy Section), The English Electric Company, Ltd., Stafford.
- TAYLOR, Henry George, D.Sc., Director of Research, British Welding Research Association, 29 Park Crescent, London, W.1.
- TAYLOR, Robert Clive, Chief Chemist and Metallurgist, T. J. Priestman, Ltd., Cupro Foundry, Leopold Street, Birmingham 12.

*Annual General Meeting**As Student Members*

- CUPP, Calvin Robert, Student of Metallurgy, The University, Toronto, Ont., Canada.
- EL-MEHAIRY, Ahmed Ezzat, B.Sc., Metallurgical Research Student, Sir John Cass Technical Institute, Jewry Street, Aldgate, London, E.C.3.
- GREENFIELD, Peter, B.Sc., Student of Metallurgy, The University, Edgbaston, Birmingham.
- JORDAN, Michael Frederic, Student of Metallurgy, The University, Edgbaston, Birmingham.
- MOFFATT, Robert Sydney Martin, B.Sc., Metallurgist, Appleby-Frodingham Steel Company, Ltd., Scunthorpe, Lincolnshire.
- RYDER, Colin David, Student of Metallurgy, The University, Liverpool.
- SHARP, Peter Edward, Technical Assistant, Tungsten Wire Department, British Thomson-Houston Company, Ltd., Rugby, Warwickshire.

ELECTED ON 9 DECEMBER 1949

As Ordinary Members

- BELL, Raymond Charles, B.A., B.A.Sc., Research Engineer, Consolidated Mining and Smelting Company of Canada, Ltd., Trail, B.C., Canada.
- CATLING, Jack Harold, Joint Managing Director, Reynolds Light Alloys, Ltd., Redfern Road, Tyseley, Birmingham 11.
- CUTLER, Percy, Assistant Works Manager, Government of India (Ministry of Defence) Ordnance Factory, Ambarnath, near Bombay, India.
- DICKENS, Arthur, Engineering Trades Sales Manager, Imperial Chemical Industries, Ltd., National Provincial Bank Buildings, Bute Street, Cardiff.
- DUTTA, Sudhendu Kumar, M.Sc., Assistant Foreman, Metallurgical Laboratory, Inspectorate of Metal and Steel, Ishapore, West Bengal, India.
- ELLIOTT, Eric, A.Met., Liaison Officer, Aluminium Development Association, 33 Grosvenor Street, London, W.1.
- JACKSON, Horace Ernest, Delegate Director, Imperial Chemical Industries, Ltd., Metals Division, Witton, Birmingham 6.
- MORRISON, John Lamb Murray, D.Sc., Professor of Mechanical Engineering, Engineering Laboratories, University of Bristol, Unity Street, Bristol 1.
- NEWTON, James Welsby, B.Sc. (Eng.), Engineering Manager, Staffordshire Factories of Thomas Bolton and Sons, Ltd., Froghall, Stoke-on-Trent, Staffordshire.
- PAISH, Ralph, Assistant Metallurgist, Rotol, Ltd., Gloucester.
- PRIMUS, Francis Charles, Professor of Mechanical Technology, České Vysoké Učení Technické, Karlovo nam 13, Prague, Czechoslovakia.
- RICKSECKER, Ralph E., M.S., Chief Metallurgist, Cleveland Division, Chase Brass and Copper Company, Inc., 1121 East 260th Street, Cleveland, O., U.S.A.
- RYBCZYNSKI, Ludwik, Student of Engineering, Metallographic Laboratory, Zakłady Przemysłowe H. Cegielski, Poznan, Poland.
- SERGEANT, William John Clive, Production Control Chemist, Copper and Alloys, Ltd., Greets Green Road, West Bromwich, Staffordshire.
- SHARP, Herbert John, B.Sc., Metallurgist, Hoover, Ltd., Perivale, Greenford, Middlesex.
- SHELVINGTON, William Edwin, Metallurgical Chemist, Copper and Alloys, Ltd., Greets Green Road, West Bromwich, Staffordshire.
- SMITH, Eugene Monroe, M.S., Development Engineer, Youngstown Sheet and Tube Company, Youngstown, O., U.S.A.
- THOMPSON, Lawrence S., Ph.D., A.M., A.B.L.S., Librarian, University of Kentucky Libraries, Lexington 29, Ky., U.S.A.

- TUCHSCHMID, Eugen Heinrich, Assistant to the Professor of Physical Metallurgy, Eidgenössische Technische Hochschule, Zürich, Switzerland.
WILLIAMS, Sidney Jonas, Assistant Metallurgist, International Alloys, Ltd., Aylesbury, Buckinghamshire.
WILSON, Clifford, Ph.D., B.Sc., A.R.S.M., D.I.C., Chief Production Metallurgist, High Duty Alloys, Ltd., Trading Estate, Slough, Bucks.

As Student Members

- ARNOLD, Brian, Student of Metallurgy, Coventry Technical College, Coventry.
BARTNIK, George, Student of Metallurgy, Battersea Polytechnic, London, S.W.11.
BELL, Henry B., Student of Metallurgy, Royal Technical College, Glasgow.
BERRY, Brian Shepherd, B.Sc., Research Student, Department of Metallurgy, University of Manchester.
BETON, Robin Hartley, Student of Metallurgy, Manchester University.
CHATTERJEE, Ajit Kumar, B.Sc., Research Student, Manchester University.
CONGREVE, Walter Kendall, B.A.Sc., Student of Metallurgy, Manchester University.
GREEN, Terence Edwin, Student of Metallurgy, Manchester University.
HARRIS, Louis Reuben, B.A., Assistant Research Metallurgist, National Smelting Company, Ltd., Avonmouth, Bristol.
HAWKINS, Neville, Student of Metallurgy, Manchester University.
HOUSEMAN, David Henry, B.A., Student of Metallurgy, Cambridge University.
HUGO, Jacques Pierre, B.Sc., Student of Metallurgy, Sheffield University.
JAMIESON, Archibald, Foundry Metallurgist, Argus Foundry, Ltd., Thornliebank, near Glasgow.
KAY, Gerald Harry, Student of Metallurgy, Birmingham University.
KEEN, (Miss) Maureen Sheila Marie, Student of Metallurgy, Manchester University.
KOENIG, Hans M., Student of Engineering, Imperial Chemical Industries, Ltd., Metals Division, Gowerton, Glamorgan.
LAURIENTE, Mike, B.S., M.S., Student of Engineering, Johns Hopkins University, Mechanical Engineering Department, 34th and Charles Avenue, Baltimore 18, Md., U.S.A.
LEA, Albert Dennis, Student of Metallurgy, University of Manchester.
MITCHELL, Gordon H., Student of Metallurgy, Royal Technical College, Glasgow.
NISBETT, Edward George, Student of Metallurgy, Royal Technical College, Glasgow.
POMEROY, Patrick Reginald Dan, Bursar, British Non-Ferrous Metals Research Association, Euston Street, London, N.W.1.
POOLE, David Michael, Student of Metallurgy, Manchester University.
RYDER, Dennis Arthur, Student of Metallurgy, Birmingham Central Technical College.
SCUTTS, William, Foundry Metallurgist, G. and J. Weir, Ltd., Cathcart, Scotland.
SPEIRS, Archibald, Student of Metallurgy, Royal Technical College, Glasgow.
TERRY, Robert Brian, Student of Metallurgy, University of Birmingham.

ELECTED ON 31 DECEMBER 1949

As Ordinary Members

- BANKS, Clarence Kenneth, A.B., M.Sc., Ph.D., Director of Research and Development, Metal and Thermit Corporation, Box 255, Rahway, N.J., U.S.A.
b (76)

- BARNES, Sidney Mellish, Director and Technical Representative, Barronia Metals (Great Britain), Ltd., Hereford.
- DOWDING, Michael Frederick, M.A., Research Engineer, Davy and United Engineering Company, Ltd., Park Iron Works, Sheffield 4.
- FODOR, Gabriel, Technical Director, Société Anonyme Gilby-Wire, 29 Quai de la Marne, Rueil-Malmaison (S. et O.), France.
- HERNE, Howard James Louis, M.A., Mathematician, Physics Laboratories, The British Iron and Steel Research Association, 104 Battersea Park Road, London, S.W.11.
- HOLTH, Tore, M.Sc., Scientific Officer, Norwegian Defence Research Establishment, Lillestrøm, Norway.
- MERCER, Randolph, B.Sc., Technical Manager, Enfield Rolling Mills (Aluminium), Ltd., Bradford Works, Bowling Back Lane, Bowling, Bradford, Yorkshire.
- MILLWARD, Humphrey John, Chief Metallurgist, Light Alloys, Sterling Metals, Ltd., Northey Road, Coventry, Warwickshire.
- RATHENAU, Gerhart W., Dr. Phys., Research Physicist, Research Laboratory, N.V. Philips' Gloeilampenfabrieken, Eindhoven, Holland.
- REITSEMA, Roelof, Director of the Department for Metals, Centraal Instituut voor Materiaalonderzoek, Delft, Holland.
- RUSSELL, John, Representative, Engineering Trades' Department, Imperial Chemical Industries, Ltd.; (mail) 32 Dorian Drive, Clarkston, Renfrewshire.
- WAINE, Fred, J.P., Executive Director, British Insulated Callender's Cables, Ltd., Surrey House, Temple Place, London, W.C.2.
- WILLIAMS, Cyril Hector, Development Engineer and Metallurgist, Barronia Metals (Great Britain), Ltd., Hereford.

As Student Members

- ASBURY, Frederick Ernest, Student of Metallurgy, Sheffield University.
- BIGGS, William Derrick, B.Sc., Metallurgist, Research Department, Murex Welding Processes, Ltd., Waltham Cross, Hertfordshire.
- BOURNE, Alan Arthur, Johnson, Matthey and Company, Ltd., Exhibition Grounds, Wembley, Middlesex.
- CHATTERJEE, Asit Kumar, B.Sc., B.Met., Lecturer in Metallurgy, B.E. College, P.O. Botanic Gardens, Howrah, Calcutta, India.
- CILTON, John Pollock, Student of Metallurgy, Cambridge University.
- DAVIES, Colin James, Technical Assistant, Imperial Chemical Industries, Ltd., Metals Division, Waunarlwydd, near Swansea.
- DAVIS, Richard John, B.A., Research Student, Oxford University.
- ELLIOTT, Ronald, Student of Metallurgy, Leeds University.
- EVANS, Brian, M.A., Metallurgist, Enfield Rolling Mills, Ltd., Brimsdown, Enfield, Middlesex.
- GREGG, John Fleming, Student of Metallurgy, University College, Swansea.
- HAMPTON, Donald, Assistant Experimental Officer, Royal Arsenal, Woolwich, London, S.E.18.
- HESLOP, John, Student of Metallurgy, Leeds University.
- HUDSON, Robert Frederick, B.Met.E., Metallurgist, Commonwealth Aircraft Corporation Pty., Ltd., Box 7794, G.P.O., Melbourne, Vic., Australia.
- JESSOP, Alan Fields, Student of Metallurgy, Birmingham University.
- JOHANSSON, Thor, Student of Metallurgy, Constantine Technical College, Middlesbrough, Yorkshire.
- NODEN, Joseph Desmond, B.Sc., Research Student, Birmingham University.
- OLDS, Geoffrey Charles Edward, B.Sc., Physicist, Research Laboratory, The British Thomson-Houston Company, Ltd., Rugby, Warwickshire.

SAMUEL, Philip, B.Met., Research Student, Sheffield University.
WAINHOUSE, Donovan Michael, Student of Metallurgy, Leeds University.

ELECTED ON 9 FEBRUARY 1950

As Ordinary Members

- CARLSSON, Carl Georg, Metallurgical Engineer, Metallografiska Institutet, Drottning Kristinas väg 48, Stockholm, Sweden.
- CHANDARIA, Devchand P., Director and Manager, Kenya Aluminium and Industrial Works, Ltd., Rodgers Road, P.O. Box 341, Mombasa, Kenya.
- GARDNER, Robert Nathan Henry, B.Sc., Metallurgist, C. H. Parsons, Ltd., Britannia Works, Wharfdale Road, Tysley, Birmingham.
- GOODWIN, Harold, Joint Managing Director, Birmetals, Ltd., Woodgate, Works, Quinton, Birmingham 32.
- HENTZ, Åke G., Chief of the Metallurgical Laboratory, AB Lumalampen, Lumavägen 6, Stockholm 20, Sweden.
- HUGHES, Charles Robert William, Senior Metallurgical Engineer, The Anglo-Argentine Iron Company, Ltd., Casilla de Correo 1627, Buenos Aires, Argentine.
- KALLING, Bo Michael Sture, Director of Research, Stora Kopparbergs Bergslags AB, Domnarvet, Sweden.
- KING, Ronald, B.Sc., Reader in Physics, University College, Gower Street, London, W.C.1.
- LAMOURDEDIEU, Marcel, Director, Société Centrale des Alliages Légers, 66 Rue de la Chaussée d'Antin, Paris, France.
- LIANDER, Nils Halvard, ASEA, Västerås, Sweden.
- LISSELL, Erik Olof, M.Sc., Gjuteriavdelningen, Sveriges Mekanförbund, Floragatan 5, Stockholm, Sweden.
- LORD, James Osborn, B.Chem.Eng., Associate Professor of Metallurgy, Ohio State University, Columbus 10, O., U.S.A.
- MANTLE, Edward Charles, M.Sc., British Non-Ferrous Metals Research Association, Euston Street, London, N.W.1.
- MOCARSKI, Stanislaw, Dr.Ing., Metallurgist, David Brown Foundries Company, Ltd., Penistone, near Sheffield.
- MODIN, Sten Olof, Metallurgical Engineer, Metallografiska Institutet, Drottning Kristinas väg 48, Stockholm, Sweden.
- MOLINDER, Anders Göran, S.M., Chief Metallurgist, Uddeholms AB, Munkfors, Sweden.
- de NARDO, Juan Bautista, Professor of Physical Metallurgy, University of La Plata, La Plata, Argentina.
- OLT, Theodore F., Director, Research Division, Armco Steel Corporation, Middletown, O., U.S.A.
- RAVEN, Richard Tebbitt, B.Sc., General Works Manager, Birmetals, Ltd., Woodgate Works, Quinton, Birmingham 32.
- SCHAUB, Cyril, Director of Research, Fagersta Bruks AB, Fagersta, Sweden.
- SPIEGELBERG, Arne Per Wilhelm, Metallografiska Institutet, Drottning Kristinas väg 48, Stockholm, Sweden.
- STEVENS, John Rupert, Head of Research Department, E. Silver and Company, 80 New Bond Street, London, W.1.
- STEWART, Maxwell Hector, Chemist and Metallurgist, The Steel Improvement Company Pty., Ltd., 102 Bay Road, North Sydney, Australia.
- WALLACE, Eben Richard, B.Sc., Chief Chemist, British Insulated Callender's Cables, Ltd., Prescot, Lancashire.
- WATKINS, Harry Clifford, Research Metallurgist, H. J. Enthoven and Sons, Ltd., 89 Upper Thames Street, London, E.C.4.

Annual General Meeting

- WHITFIELD, John France, B.Sc., Chief Engineer, Birmetals, Ltd., Woodgate Works, Quinton, Birmingham 32.
 WHYMPER, Harry William, Foundry Manager, Birmetals, Ltd., Woodgate Works, Quinton, Birmingham 32.

As Student Members

- BECKER, Jean, 20 rue de Passy, Paris XVIIe, France.
 CHAUDHURI, Arup Ratan, B.Sc., Research Student, University of Manchester.
 COOPER, Norman, Student of Metallurgy, Royal Aircraft Establishment, Farnborough, Hampshire.
 DAVIES, Brian Gowan, Post-graduate Student of Metallurgy, University College, Cardiff.
 DENNIS, Thomas John, Student of Metallurgy, University of Birmingham.
 FAULKNER, Charles Raymond, B.Sc., Research Student, University of Birmingham.
 HARRIS, Solomon Wilfred, Student of Metallurgy, Royal Technical College, Glasgow.
 JACKSON, William James, Student of Metallurgy, University of Birmingham.
 KULA, Eric Bertil, S.B., Research Assistant, Institut fur Metallografi, Royal Institute of Technology, Stockholm 26, Sweden.
 KUO, Ke-hsin, B.Sc., Research Assistant, Royal Institute of Technology, Stockholm 26, Sweden.
 LLOYD, Raymond Charles, Assistant Metallurgist, James Booth and Company, Ltd., Argyle Street, Nечells, Birmingham 7.
 MARSHALL, J. B., Assistant Metallurgist, English Electric Company, Ltd., Preston, Lancashire.
 NYGREN, Erik, Box 68, Munkfors, Sweden.
 SHAKESPEARE, William George, Student of Metallurgy, University of Birmingham.
 SMALLMAN, Raymond Edward, Student of Metallurgy, University of Birmingham.
 SWANSON, Colin John, B.Sc., Research Bursar, British Non-Ferrous Metals Research Association, Euston Street, London, N.W.1.
 TAYLOR, Alan Frederick, Student of Metallurgy, University of Birmingham.
 VAUGHAN, Charles Stanley, Assistant Metallurgist, Cannon Iron Foundries, Ltd., Deepfields, near Bilston, Staffordshire.
 WHITWHAM, Donald, M.A., Research Student, Laboratoire du Centre Nationale de la Recherche Scientifique, Paris, France.

ELECTED ON 14 MARCH 1950

As Ordinary Members

- APPLETON, Ronald John Walter, Chairman and Managing Director, Esavian, Ltd., 181 High Holborn, London, W.C.1.
 BINNEY, Humphrey Lockhart, M.A., Engineer, Capper Pass and Son, Ltd., Bedminster Smelting Works, Bristol.
 CARMINA, Rosario, Technical Manager, Industria Nazionale Alluminio, via F. Turati n. 18, Milano, Italy.
 EWEN, Ian Elrick, Chief Engineer and Deputy Director, The United Wire Works, Ltd., Granton, Edinburgh.
 LÁSZLÓ, Franz Michael, Dr.Ing., Lecturer in Engineering, Engineering School, University of Melbourne, Melbourne, Vic., Australia.
 LINDH, Erik Gunnar, Metallurgist, A.B. Bofors, Bofors, Sweden.

- McCONNELL, Alexander McDonald, Metallurgical Chemist, Vulcan Boiler and General Insurance Company, Ltd., 67 King Street, Manchester 2.
- NICHOLLS, Christopher, Chief Assistant Metallurgist, The North-Eastern Marine Engineering Company (1938), Ltd., Wallsend-on-Tyne, Northumberland.
- NORÉN, Tore M. I., Chief of the Metallurgical Laboratory, ESAB, Gothenburg, Sweden.
- PANDURANGIAH, Vummidi, Partner, Vummidi Ramiah Chetty Guruswamy Chetty and Company, 23-25 N.S.C. Bose Road, Madras, India.
- PONTREMOLI, Pio, Joint Technical Manager, Industria Nazionale Alluminio, via F. Turati n. 18, Milano, Italy.
- SCHRERO, Morris, B.S., Technology Librarian, Carnegie Library of Pittsburgh, 4400 Forbes Street, Pittsburgh 13, Pa., U.S.A.
- SIDDIQI, Rafir Ahmad, B.Sc., c/o Royal Arsenal Laboratory, Metallurgy Branch, A46, Woolwich, London, S.E.18.
- TUCKER, Herbert Toyne, B.Sc., Chief Chemist, Metal Sales Company (Pty.), Ltd., P.O. Box 44, Benoni, South Africa.

As Student Members

- AUSTIN, Peter, Student of Metallurgy, Sheffield University.
- AZIZ, Mostafa Kamal Abdel, B.Sc., Post-Graduate Student of Metallurgy, Eidgenössische Technische Hochschule, Zürich, Switzerland.
- BIGGS, Derek Leonard, Student of Metallurgy, Battersea Polytechnic, London, S.W.11.
- CARTMELL, Leo John, Student of Metallurgy, Royal School of Mines, London, S.W.7.
- CONDEN, Peter, Student of Metallurgy, Royal School of Mines, London, S.W.7.
- CROWTHER, John Raymond, B.Sc., Metallurgist, Northern Aluminium Co., Ltd., Handsworth, Birmingham 21.
- DONALDSON, John William, Student of Metallurgy, Royal School of Mines, London, S.W.7.
- ELKINGTON, Ronald William, Student of Metallurgy, Royal School of Mines, London, S.W.7.
- FLEMING, Graham, Student of Metallurgy, Royal School of Mines, London, S.W.7.
- HALL, John Richard, Student of Metallurgy, Royal School of Mines, London, S.W.7.
- HARBORD, Reginald John, Student of Metallurgy, Royal School of Mines, London, S.W.7.
- HARRIS, Derek William, Student of Metallurgy, Rotherham Technical College, Rotherham, Yorkshire.
- HAWLEY, William H., Jr., B.S., Post-Graduate Student of Metallurgy, Hammond Metallurgical Laboratory, Yale University, New Haven, Conn., U.S.A.
- HOLT, Martin Oswald, Student of Metallurgy, Royal School of Mines, London, S.W.7.
- LAKER, William Eric, B.Sc., Physicist, West Works Laboratory, Bristol Aeroplane Co., Ltd., Filton, Bristol.
- MACKAY, James Matthew, Student of Metallurgy, Royal School of Mines, London, S.W.7.
- MEHTA, Surendra Raj, Student of Metallurgy, University College, Cardiff, South Wales.
- MICHAEL, Anthony Dennis, B.Sc., Research Metallurgist, J. Stone and Co., Ltd., Deptford, London, S.E.14.

- MOIR, Douglas Newlands, Student of Metallurgy, Royal School of Mines, London, S.W.7.
- PALMER, Arthur Robert, Student of Metallurgy, Royal School of Mines, London, S.W.7.
- PELL, Frederick Roy, Metallurgist, Hayward-Tyler and Co., Ltd., Luton, Bedfordshire.
- PILE, Bryan Harold, Student of Metallurgy, Royal School of Mines, London, S.W.7.
- PORTER, John Moser, Student of Metallurgy, Leeds University.
- POTTER, Pat, Student of Metallurgy, Royal School of Mines, London, S.W.7.
- SPRAY, Charles Alan Francis Thomas, Student of Metallurgy, Royal School of Mines, London, S.W.7.
- STRONG, Geoffrey Victor, Student of Metallurgy, Royal School of Mines, London, S.W.7.
- TREHEARNE, Edward Brian Geoffrey, Student of Metallurgy, University of Birmingham.
- WILLIAMS, Clifford Douglas, Student of Metallurgy, Royal School of Mines, London, S.W.7.
- WINGROVE, David John, Chemist, Associated Lead Manufacturers, Ltd., 308 West Ferry Road, London, E.14.

WALTER ROSENHAIN MEDAL

The CHAIRMAN announced that, thanks to the generosity of a donor firm (Imperial Chemical Industries, Ltd.), the Council had received a sum of money sufficient to enable it to found a Medal, in memory of the brilliant British metallurgist, Walter Rosenhain, that would be awarded annually in recognition of exceptional merit in the field of physical metallurgy.

REPORT OF COUNCIL

The CHAIRMAN (Sir Arthur Smout, J.P.) formally moved the adoption of the Report of Council for the Year Ended 31 December 1949, which is printed on pp. 643-651 of this volume.

Dr. F. A. Fox (Ordinary Member) seconded the motion, which was carried unanimously.

REPORT OF THE HONORARY TREASURER

The HONORARY TREASURER (Mr. W. A. C. Newman, O.B.E.) presented the Report of the Honorary Treasurer and the Accounts for the Financial Year Ended 30 June 1949, which are printed on pp. 652-658 of this volume, and moved their adoption.

Mr. H. H. SYMONDS (Ordinary Member) seconded the motion, which was carried unanimously.

RE-ELECTION OF AUDITORS

It was proposed, seconded, and carried that Messrs. Poppleton and Appleby be re-elected Auditors to the Institute for the ensuing year.

ELECTION OF OFFICERS FOR 1950-51

The SECRETARY read the names of officers elected to fill vacancies on the Council for 1950-51, as follows :

President :

H. S. TASKER, B.A.

Vice-Presidents :

Professor H. O'NEILL, D.Sc., M.Met.

Professor F. C. THOMPSON, D.Met., M.Sc.

Ordinary Members of Council :

G. L. BAILEY, M.Sc.

HARRY DAVIES

E. H. JONES

L. B. PFEIL, O.B.E., D.Sc., A.R.S.M.

Professor G. V. RAYNOR, D.Sc., D.Phil., M.A.

SENIOR VICE-PRESIDENT

The CHAIRMAN announced that the Council had elected Professor A. J. MURPHY, M.Sc., to be Senior Vice-President for 1950-51, and that he would be its next nomination for the Presidency.

W. H. A. ROBERTSON MEDAL

The PRESIDENT announced that the first award of the W. H. A. Robertson Medal had been made to Mr. W. J. Thomas and Mr. W. A. Fowler for their paper on "Some Technical Problems Influencing Production Economy in the Rolling of Aluminium" (*Journal*, 1948-49, vol. 75, pp. 921-948). He then presented the medal to Mr. W. J. Thomas, who made a brief acknowledgement on behalf of his co-author and himself.

INDUCTION OF THE NEW PRESIDENT

The PRESIDENT (Sir Arthur Smout, J.P.), in inducting into the Chair the new President of the Institute, Mr. H. S. TASKER, B.A., said that the Presidency of the Institute was an honour which carried with it certain responsibilities, some anxieties on occasion, but many joys and many opportunities for service both to the industry and to the members. The unique qualifications which Mr. Tasker had for this office were well known, and he had already served the Institute well in several capacities. He had been a member for 17 years, he had served on many of its Committees, he had been a most competent Honorary Treasurer through a very difficult period in the Institute's history, and had also done a great deal on the educational side.

Mr. Tasker, he said, was Chairman of Goodlass Wall and Lead Industries, Ltd. His work on the administrative side of the industry was well known not only in Great Britain but also overseas. He (Sir Arthur) said that he inducted Mr. Tasker into the Presidential Chair with every confidence, knowing that, under his leadership, the Institute would go from strength to strength.

Mr. H. S. Tasker then took the Chair.

The PRESIDENT (Mr. H. S. TASKER, B.A.) briefly thanked the members for the honour of election to the Presidency.

VOTE OF THANKS TO THE RETIRING PRESIDENT

Mr. G. L. BAILEY, M.Sc. (Ordinary Member of Council), in proposing a very hearty vote of thanks to Sir Arthur Smout for his services to the Institute, as President, said that the demands which today were made by various Institutes on the voluntary services of technicians and scientists from industry were very heavy. The Institute of Metals was no exception. It was

very important that the members of the Institute should not only know that that was so, but should also make very clear to their President how much they appreciated the time that he had given to the Institute's affairs out of such little spare time as he had had. Not only was he called on to preside at Council meetings and to attend very many Committee meetings, but he also had to do a very great deal of other work behind the scenes.

Sir Arthur Smout, he continued, had done all those things with conspicuous ability and with his usual energy and enthusiasm. He had conducted the Council very efficiently through its business. Outside the Council room, and in various ways in Committees, he had made a special point of interesting in the work of the Institute the men engaged in the practical sides of the industry. He had encouraged wholeheartedly the Metallurgical Engineering Committee, which had been formed during his Presidency. He had been very assiduous in performing the duty of visiting the Local Sections and Associated Societies.

He (Mr. Bailey) therefore had very much pleasure in proposing that a very hearty vote of thanks be accorded to Sir Arthur Smout for his services as President of the Institute.

Professor A. J. MURPHY, M.Sc. (Senior Vice-President), in seconding the motion, said that anyone who had been a member of this Institute for as long as he had could not fail to have been impressed by the good fortune that the members had enjoyed in the quality of the men whom they had selected to lead them as Presidents. It was fortunate that that had been so, since the responsibilities were heavy and the duties arduous and time-consuming.

Sir Arthur Smout had brought to this high office the special benefits of his authoritative position as a leader of the British metallurgical industry, and of his long membership of the Institute, during which he had given much thought to its problems and opportunities. He brought also a clear idea of the ways in which the difficulties could be surmounted, and a capacity to persuade and enlist the enthusiastic support of all concerned for the action which he judged necessary for the progress of the Institute.

Though in wider circles there appeared to be divided views on the wisdom of referring to election addresses, he had looked at the Presidential Address which Sir Arthur had read two years ago, and could say at once that Sir Arthur had come out of it very well indeed.

Two years ago Sir Arthur had sounded what he (Professor Murphy) thought he would agree was the keynote of his Presidential policy, when he referred to the success already achieved by the Institute in bringing into close contact scientists and practical men engaged in works operations. Sir Arthur strongly urged that still further efforts should be put into this service, commanding papers dealing with works technique and practices and the adaptation of scientific principles to the metallurgical industry. He thought that it was well known to members that Sir Arthur was the inspirer of a symposium on "Metallurgical Aspects of Non-Ferrous Metal Melting and Casting of Ingots for Working", which had provided one of the most successful meetings that the Institute had held. They looked forward to a repetition of this experience in the symposium on the "Metallurgical Aspects of the Hot Working of Non-Ferrous Metals and Alloys", which was also conceived by Sir Arthur as the second of what he proposed should be a series of symposia on related subjects.

In his Address, Sir Arthur had spoken of the need for eliminating idle time in the metal industry. No one would dispute that he had very thoroughly eliminated idle time so far as the Presidency was concerned. If it were true that, as he had said, the more we contributed to the Institute the more we

should get out of it, Sir Arthur was due for a handsome yield, and he thought that the reward which he would prize most would be the sincerity of the appreciation which those present would now express, on behalf of all the members of the Institute, for the enthusiasm, the friendliness, and the wisdom with which he had guided the members during the past two years.

The motion was then put to the meeting and carried with acclamation.

Sir ARTHUR SMOUT, in acknowledging the Vote of Thanks, said that he had enjoyed the opportunities given to him to serve still further the profession and the industry to which he owed so much.

No President could have been better served both by the officers of the Institute and by the staff, and he wished to pay a very sincere tribute to the work of Colonel Guillan and his staff.

VOTE OF THANKS TO OTHER RETIRING OFFICERS

The Hon. R. M. PRESTON, D.S.O. (Past-President) proposed a vote of thanks to the retiring officers, Lieut.-Col. Sir John Greenly (Past-President), Mr. John Cartland (Vice-President), and Dr. N. P. Allen and Dr. J. W. Jenkin, (Ordinary Members of Council).

Mr. H. W. G. HIGNETT, B.Sc. (Ordinary Member of Council) seconded the motion, which was put to the meeting and carried with acclamation.

PRESIDENTIAL ADDRESS

The PRESIDENT, Mr. H. S. Tasker, B.A., then delivered his Presidential Address, which is printed on pp. 99-109 of Vol. 77 of the *Journal*.

A vote of thanks to the President for his Address was proposed by Professor H. O'NEILL, D.Sc., M.Met. (Vice-President), seconded by Mr. CHRISTOPHER SMITH (Member), and carried with acclamation.

The meeting then adjourned.

LUNCHEON

A luncheon was held at the Café Royal, Regent Street, London, W.1, at which Mr. H. S. TASKER, B.A., President, presided. Among the guests was the French Ambassador, M. Massigli.

AWARD OF THE INSTITUTE OF METALS (PLATINUM) MEDAL FOR 1950

At the conclusion of the Luncheon, the President presented to Professor ALBERT PORTEVIN (Honorary Member) the Institute of Metals (Platinum) Metal for 1950, in recognition of his outstanding services to the non-ferrous metal industries, and Professor Portevin addressed the members.

DISCUSSION OF PAPERS

The meeting was resumed, in the afternoon, at the Institution of Mechanical Engineers, Storey's Gate, London, S.W.1, when the President, Mr. H. S. Tasker, B.A., occupied the Chair.

The following papers were presented and discussed. In each case a hearty vote of thanks to the authors was proposed by the Chairman and carried with acclamation.

"Modern Billet Casting, with Special Reference to the Solidification Process", by E. Scheuer, Dr.rer.nat.

"Grain Refinement of Aluminium and its Alloys by Small Additions of Other Elements", by Myriam D. Eborall, B.A.

"The Mechanism of Grain Refinement of Sand Castings in Aluminium Alloys", by A. Cibula, M.A., A.I.M.

"The Effect of Grain-Size on the Tensile Properties of High-Strength Cast Aluminium Alloys", by A. Cibula, M.A., A.I.M., and R. W. Ruddle, M.A., A.I.M.

Thursday, 30 March

At the resumed meeting, held at the Institution of Mechanical Engineers, Storey's Gate, London, S.W.1, the President, Mr. H. S. Tasker, B.A., occupied the Chair.

SYMPOSIUM ON "METALLURGICAL ASPECTS OF THE HOT WORKING OF NON-FERROUS METALS AND ALLOYS"

A general discussion, reported in this volume of the *Journal*, took place on the following papers. Dr. C. J. Smithells, M.C. (Vice-President) and Mr. G. L. Bailey, M.Sc. (Member of Council) acted as rapporteurs. A vote of thanks to the authors of the papers was proposed by the Chairman and carried with acclamation.

"The Hot Rolling of Aluminium and its Alloys", by F. Kasz, B.Sc., A.R.Ae.S., and P. C. Varley, M.B.E., M.A.

"The Extrusion of Aluminium Alloys", by Christopher Smith, F.I.M.

"The Hot Forging and Hot Stamping of Aluminium and its Alloys", by F. E. Stokeld, F.I.M.

"The Hot Working of Magnesium and its Alloys", by R. G. Wilkinson, B.Sc., and F. A. Fox, D.Sc., F.I.M.

"The Hot Working of Copper and Copper Alloys", by Maurice Cook, D.Sc., Ph.D., F.I.M., and Edwin Davis, M.Sc., F.I.M.

"The Hot Working of Tin Bronzes", by D. W. Dugard Showell, M.Sc.

"The Hot Working of Lead and Lead-Rich Alloys", by L. H. Back, B.Sc.

"The Rolling of Zinc and Zinc-Rich Alloys", by C. W. Roberts, B.Sc., A.I.M., and B. Walters, M.A.

CONVERSAZIONE AND EXHIBITION

In the evening an informal conversazione was held at 4 Grosvenor Gardens, London, S.W.1, at which there was an exhibition of specimens, equipment, instruments, &c., of non-ferrous metallurgical interest.

Friday, 31 March

The meeting was resumed at 4 Grosvenor Gardens, London, S.W.1, the President, Mr. H. S. Tasker, B.A., occupying the Chair.

DISCUSSION OF PAPERS

In the morning, a discussion took place on the following paper:

"The Application of X-Ray Methods to the Determination of Phase Boundaries in Metallurgical Equilibrium Diagrams", by Professor E. A. Owen, M.A., Sc.D., and D. P. Morris, B.Sc.

The meeting was resumed in the afternoon, when discussions took place on the following papers:

"The Mechanism of Deformation in Metals, with Special Reference to Creep", by W. A. Wood, D.Sc., and W. A. Rachinger, M.Sc.

"Recrystallization of Single Crystals After Plastic Bending", by R. W. Cahn, B.A.

In each case a hearty vote of thanks to the authors was proposed by the Chairman and carried with acclamation.

The meeting then concluded.

AUTUMN LECTURE, 1949.

1207

RECENT FRENCH INVESTIGATIONS IN THE FIELD OF LIGHT ALLOYS.

By PROFESSOR GEORGES CHAUDRON,* Dr.ès.Sci., MEMBER.

TWENTIETH AUTUMN LECTURE TO THE INSTITUTE OF METALS, DELIVERED IN PARIS, 3 OCTOBER 1949.

SYNOPSIS.

A review is given of the researches on light alloys carried out in France since the liberation, in particular of the work of the Vitry laboratory of the Centre National de la Recherche Scientifique. The subjects briefly discussed include : the macro-mosaic structure of very pure aluminium; the properties of grain boundaries and intragranular boundaries; the recrystallization and mechanical properties of very pure aluminium; the preparation of large metallic crystals and the occurrence of isolated crystals; the production of oxide-free surfaces on aluminium; structures obtained in semi-continuously cast ingots; preferred orientation; anodic oxidation; and special-purpose alloys.

I.—INTRODUCTION.

IT is well known that the only important ore of aluminium is bauxite, which is an impure aluminium hydrate. It was discovered by a French engineer named Berthier, who described the mineral in *Annales des Mines* in 1821. His account begins as follows : " There exists near Arles, in the department of Bouches du Rhône, on a hill which bears the name of the nearby village of Les Baux, a considerable deposit of iron ore resembling in its appearance and its mode of occurrence the iron ore called alluvion. I have examined it and I have found that in fact it is composed of aluminium hydrate mixed with red oxide of iron. Aluminium hydrate not having been found previously in Europe, so far as I know, I feel I should report the evidence which has led me to recognize its existence in the ores of Les Baux."

Berthier had just discovered one of the richest deposits of bauxite in the world.

The use of bauxite for the production of aluminium was first thought of by Henri Sainte Claire Deville in 1859, when he was a professor at the Sorbonne. Indeed, if the discovery of aluminium was due to the

* Professeur à la Sorbonne; Directeur du Laboratoire de Vitry-sur-Seine du Centre National de la Recherche Scientifique.

German Wöhler, it is to Sainte Claire Deville that we owe the production of the metal in the molten state and the first fabrication on an industrial scale. And it was a French engineer, Héroult, who conceived and perfected the present electrochemical method of extraction.¹

It cannot be denied, however, that at the beginning of the century French industry perhaps did not appreciate the potentialities of the new metal. Researches on aluminium and its alloys were also neglected in French laboratories.

It was not until about 1925 that a revival of research into light metals took place. It is a pleasure to me to recall the beautiful dilatometric experiments of Chevenard and Portevin on the age-hardening of light alloys² and the work on the castability of aluminium and its alloys carried out at the Ecole Centrale under the direction of Albert Portevin. It was at this time that the great engineer Caquot, then director of technical research at the Ministère de l'Aéronautique, had the idea of fostering numerous researches in the laboratories of the Universities and technical schools. Specialists were trained in these laboratories who subsequently had brilliant careers in industry.

Since the liberation of France in 1944 it appears that research in this field has attracted an increasing number of outstanding physicists, chemists, and crystallographers. In spite of our modest resources, as compared with those of American industry and laboratories, French work in recent years has certainly won the regard of our foreign colleagues, and it may be said that our industry has begun to reap the benefit of this new scientific effort. In Table I I have attempted to show the various centres of activity of the French aluminium industry. Numerous research centres have been fully occupied for several years. You will certainly know very well the names of the heads of laboratories indicated in Table I, for most of them have published some of their results in the *Journal* of this Institute. It would be difficult therefore in a review which must necessarily be very brief to give you a picture of all the work carried out in France since the end of the war. For this reason I shall limit myself to some work recently carried out in the laboratory at Vitry or originating there. These researches relate to the following three main problems :

(a) Impurities in a metal have been found to play a part which depends on their location in the structure, and this has given rise to researches on the structure of metals.

(b) The surface conditions of aluminium produced by electrolytic polishing, and the new techniques of micrographic attack of aluminium and its alloys.

(c) New researches on aluminium alloys prepared from high-purity materials.

TABLE I.—*The French Aluminium Industry : The Principal Companies, Works, and Research Centres.*

ALUMINA WORKS.			
Cie. Alais, Froges et Camargue et Société d'Electrochimie :			
Usines de Gardanne et de La Barasse (Bouches du Rhône), de Salindres (Gard), de Saint Auban (Basses Alpes).			
ALUMINIUM REDUCTION PLANTS.			
Cie. Alais, Froges et Camargue		Société d'Electrochimie	
Saint Jean de Maurienne (Savoie) L'Argentière (Hautes Alpes)		Rioupéroux (Savoie) Les Clavaux (Isère)	
SEMI-FABRICATORS OF ALUMINIUM AND ITS ALLOYS.			
Société CEGEDUR		Tréfileries et Laminoirs du Havre (T.L.H.)	Compagnie Française des Métaux
Couzon (Haute Loire) Farmoutiers (S. et M.) Vitry sur Seine (Seine) Reyquillères (S. et O.) Le Bourget (S. et O.)		Le Havre (Seine inf.) Montreuil-Belfroy (M. et L.) Dijon (Côte d'Or) Rugles (Eure)	Givet (Ardennes) Castelsarrazin (T. et G.) Beville les Rouen (S. inf.) Saint Denis (Seine)
INDUSTRIAL LABORATORIES.			
Aluminium Français		T.L.H. et Soc. Fran- çaise des Métaux	Soc. d'Electrochimie
Chambéry (Savoie) Dir. : M. Chevigny	Le Bourget (S. et O.) Dir. : M. Tournaire	Antony (Seine) Dir. : M. Hérenguel	Ugine (Hte. Savoie) Dir. : M. Jolivet
TECHNICAL TRAINING CENTRE.			
Centre de l'Aluminium Français, Bd. de Grenelle, Paris. Directeur : M. Gadeau.			
SCIENTIFIC LABORATORIES ENGAGED IN RESEARCH ON ALUMINIUM AND ITS ALLOYS.			
Laboratoire Ecole Centrale : Prof. A. Portevin; Prof. P. Bastien. Laboratoire de Vitry du C.N.R.S. : Prof. G. Chaudron; Prof. P. Lacombe. Laboratoire Conservatoire des Arts et Métiers : Prof. A. Guinier. Laboratoire Ecole des Mines. Directeur : Ch. Crussard. Laboratoires Techniques des Services de l'Aéronautique. M. l'Ingénieur principal Faguet. Laboratoires de la Marine Nationale-Physique des Métaux. Chef de Service : M. P. Jacquet.			

II.—THE MACRO-MOSAIC STRUCTURE OR POLYGONIZED STATE OF CERTAIN CRYSTALS.

Lacombe and Beaujard showed in the *Journal* of this Institute in 1947³ the great importance of etch figures in the study of the structure of aluminium, and the quality of the photomicrographs presented in that paper has attracted your attention. The authors had for the first time used a combination of very pure aluminium (99.99%), electrolytic polishing, and etching reagents particularly suitable for the purpose,⁴ and as a result have brought to light a new phenomenon having numerous consequences, namely, the macro-mosaic structure of certain crystals.

At first sight the etch figures on the surface of a single crystal produced by a critical amount of cold work appear to lie entirely at random. But it is possible to observe the formation of lines that reveal a network, the size of which varies in different parts of a single crystal (see Fig. 20 of reference 3). It might at first be thought that these lines were due to surface faults, but Lacombe and Beaujard have shown that the opposite face of the metal sheet presents exactly the same appearance, though slightly displaced. They have therefore concluded that these lines represent the traces on the surface of the single crystal of discontinuities which extend through the whole thickness of the metal sheet, the displacement observed between the outlines obtained on the two opposite faces being due solely to the inclination of the boundaries of the various blocks relative to the surface (see Fig. 21 (a) and (b) of reference 3).

It might be objected that the more or less polyhedral outline observed is due simply to the persistence of imperfections or to intercrystalline deposits of impurities in a previous fine-grained structure. The authors have, however, advanced numerous arguments against this explanation; in particular, the outlines of this sub-structure are confined entirely within those of the initial grain (see Fig. 22 of reference 3).

This arrangement of intracrystalline blocks, which Lacombe and Beaujard have called a "macro-mosaic structure" to distinguish it from the very fine structure postulated by Darwin,⁵ does not appear on all recrystallized crystals, but it is visible on metals other than aluminium and also on solid solutions. Lacombe and Berghézan have revealed the phenomenon in the course of their study of the ageing of solid solutions of aluminium with 8, 10, and 12% zinc.⁶ Large grains are produced in these alloys by prolonged heating at 550° C., after a critical reduction of 2%. After cooling the specimens in air, electrolytic polishing shows up only the boundaries of the crystals, but after ageing for a certain time, e.g. 1 hr. at 20° C., fresh electrolytic polishing reveals within the grains a network of very fine lines which appear in depression. It is important to point out that the true crystal boundaries do not present the same appearance as the intracrystalline lines which indicate the discontinuities (Fig. 1, Plate I). Electrolytic polishing can also reveal the intracrystalline discontinuities in pure aluminium (Fig. 3, Plate II). X-ray examination by the Laue method shows in every case of macro-mosaic structure a very diffuse Laue spot, which indicates that the crystal consists of a collection of small disorientated blocks.⁷ This result is confirmed by the technique of high-resolution Laue diagrams recently described by Guinier and Tennevin.⁸

Guinier and Lacombe⁹ have found by this method that after de-

formation of the crystal the diffraction spots are elongated and show continuous blackening—the phenomenon well known as asterism. But after annealing, these spots, while retaining the same shape, are resolved into small, fine striæ. This evidence the authors interpret as showing that the distorted crystal is broken up into a great number of blocks slightly disorientated with respect to one another.

As already stated, the macro-mosaic structure does not appear on all crystals, but depends in particular on the amount of cold work before annealing, being observed only in the case of a small amount of work. Orowan has described a mechanism of recrystallization of crystals of zinc and cadmium deformed by bending, and he has shown that after annealing the crystals consist of little blocks very slightly disorientated, a phenomenon for which he suggests the name "polygonization".¹⁰

It is possible that the phenomena discovered by Lacombe and by Orowan¹⁰ and Cahn¹¹ may be identical. It is clear that research must be actively pursued in this field, for it would be very important to be able to explain the mechanism of formation of the intracrystalline blocks and to determine the relations between the recovery of the crystal and polygonization. This is a subject that will be discussed further by Lacombe at a meeting of the Société Française de Métallurgie.

III.—PROPERTIES OF GRAIN BOUNDARIES.

Ever since the earliest days of metallography, the problem of the grain boundary has attracted the attention of research workers. In corrosion, the grain boundary is often the weak point of a metal, even of a high-purity metal. Certain authors have postulated a narrow transition zone in which the arrangement of the atoms represents a compromise between the arrangements of atoms in the two adjacent grains. But on the other hand we believe that the surface region of a crystal can be enriched in impurities even in the case of a metal of over-all high purity.

In work published in 1944, Lacombe and Beaujard¹² studied the relative orientation of crystals of very pure aluminium by means of etch figures, using a reagent containing hydrochloric, nitric, and hydrofluoric acids. In the course of this work they were able to observe the very great differences in the rate of attack at the grain boundaries, depending on the relative orientation of the two adjacent crystals. These observations led Lacombe and Yannaquis¹³ to carry out a systematic study of the phenomenon, using 10% hydrochloric acid as the etching reagent. The specimens were of high-purity aluminium,

rolled and recrystallized to give very large grains and then electrolytically polished in the Jacquet bath before the acid attack in order to avoid any interference due to a thin film of oxide. Very deep and narrow attack was observed at the grain boundaries except where the neighbouring crystals bore the relation of twins; in that case there was no attack. Chalmers and his co-workers¹⁴ had already shown that in homogeneous copper-beryllium and aluminium-magnesium alloys precipitation occurred in a very unequal way on the different faces of the crystals but did not take place on the contact face between twins. It must be remembered, however, that this work was concerned with supersaturated solid solutions.

We have also observed that the grain boundaries between crystals of different orientation in aluminium of 99.99 and 99.998% purity have a melting point below that of the main body of the crystals and can be molten while the boundaries of the twins remain solid.¹⁵ Fig. 2 (Plate I) shows the melting of the grain boundaries except that between the two crystals *A* and *B* which form twins. This preliminary fusion at the boundaries would support the theory of the concentration of impurities, in accordance with Benedicks' well known views.

IV.—PROPERTIES OF INTRAGRANULAR BOUNDARIES.

The intragranular boundaries are those between the blocks which form the macro-mosaic structure. Lacombe and Berghézan have shown repeatedly that the intragranular boundaries have properties entirely different from those of true grain boundaries. The blocks forming the macro-mosaic structure are slightly disorientated with respect to one another, and their boundaries undergo attack by 10% hydrochloric acid in the same way as adjacent grains of sharply different orientation. The intragranular boundaries can be distinguished from the grain boundaries by other methods of attack.

Burgers,¹⁶ and subsequently Shockley and Read,¹⁷ have interpreted these intragranular boundaries as a consequence of dislocations, the average size of which can be calculated as a function of the disorientation of neighbouring blocks.

Lacombe and Berghézan have shown that in the decomposition of an aluminium-zinc solid solution there was a concentration of precipitated atoms in the intragranular boundaries. They have observed similar phenomena in the aluminium-4% copper solid solution, in which, after quenching and then ageing at 180°-220° C. the intermediate θ' phase is precipitated. A photomicrograph taken by these authors (Fig. 4, Plate III) shows selective precipitation along the intra-

granular boundaries in the form of a border, and it may be seen that in parts of this border there is a concentration of precipitate in the form of fine needles. On the other hand at the true grain boundaries there is a deficiency of precipitate. Precipitation of θ' can also occur, as in the case of aluminium-zinc solid solutions, after plastic deformation of the crystal, the precipitation taking place along the slip planes where the imperfections are concentrated¹⁸ (Fig. 5, Plate III).

V.—THE ROLE OF STRUCTURAL IMPERFECTIONS IN THE KINETICS OF AGE-HARDENING.

It is interesting to observe that structural defects, of whatever kind, appear to play an essential part in the age-hardening of solid solutions. Hérenguel and I have shown that aluminium-zinc solid solutions cooled in air can undergo very appreciable age-hardening.¹⁹ By the micro-hardness method it is possible to demonstrate that in a polycrystalline specimen hardening does not take place in the same way in all the crystals. It is likely that the polygonized crystals of the aluminium-zinc solid solution harden slightly. If it is assumed that the structural defects are concentrated in the intracrystalline boundaries, it follows that there will be a concentration of precipitate in certain zones of the crystal, while other parts will undergo no structural change. On the other hand, a metal recrystallized after very heavy reduction does not give rise to a polygonized structure, and its hardening is a maximum. In this case the faults are distributed at random throughout the structure and are close to one another.

VI.—THE RECRYSTALLIZATION OF VERY PURE ALUMINIUM.

It is well known that the recrystallization temperature of a metal depends on the impurity content. But there is another factor, namely, the degree of cold work to which the metal has been subjected before heat-treatment. For the smallest amounts of cold work a progressive change in hardness takes place from the lowest annealing temperature. It may perhaps be concluded from this that the process of recrystallization can vary widely, according as the metal has been lightly or heavily cold worked. In the researches carried out at Vitry, recrystallization phenomena have been studied by micro-mechanical tests using Chevenard machines, which enable measurements to be carried out on very small specimens, and also by micro-examination.²⁰ Recrystallization is said to take place in a cold-worked metal when it is possible to observe the formation of nuclei and the development from them of new crystals having an orientation different from that of the original metal.

The isothermal study of the return of the initial mechanical properties in cold-worked aluminium has revealed the existence of a phase of recovery of the lattice which precedes primary recrystallization. These experiments provide evidence in support of the existence of this intermediate stage, which is still the subject of controversy.²¹

The question arises whether this stage of recovery is not identical with the polygonized state. However, up to the present the polygonized state has been observed only after annealing even very pure aluminium at an elevated temperature, whereas the recovery and even the recrystallization can be effected very little above room temperature.

VII.—THE PRODUCTION OF LARGE METALLIC CRYSTALS; ISOLATED CRYSTALS.

The production of large metallic crystals is of great importance in present-day metallurgical research. In the method of production by recrystallization after a critical amount of cold work, one very often comes across small isolated crystals that resist absorption by the large crystal surrounding them, even after very prolonged heating. These crystals are sometimes described as "inclusions",²² but as this name is liable to cause confusion it has been thought better in France to call them "isolated crystals".

Lacombe and Berghézan have demonstrated the existence of several kinds of isolated crystals :

- (a) those that bear strictly the relation of a twin to the surrounding large crystal;
- (b) those having an orientation close to that of the surrounding crystal and having generally a circular form which it is difficult to reveal;
- (c) those which, having any orientation, exhibit a very marked macro-mosaic or polygonized structure.

The last-mentioned are the remains of a former crystallization which the large crystals have not been able to absorb during growth. In Fig. 6 (Plate IV) an isolated polygonized crystal and one bearing the relation of a twin can be seen in the same photograph.

VIII.—THE MECHANICAL PROPERTIES OF PURE ALUMINIUM.

It is well known that the mechanical properties of a metal depend on the size of the crystals in the test-piece. A test-piece composed of very large crystals may often easily be deformed by hand. Up to the present there have been no precise data for the fundamental mechanical

PLATE I.

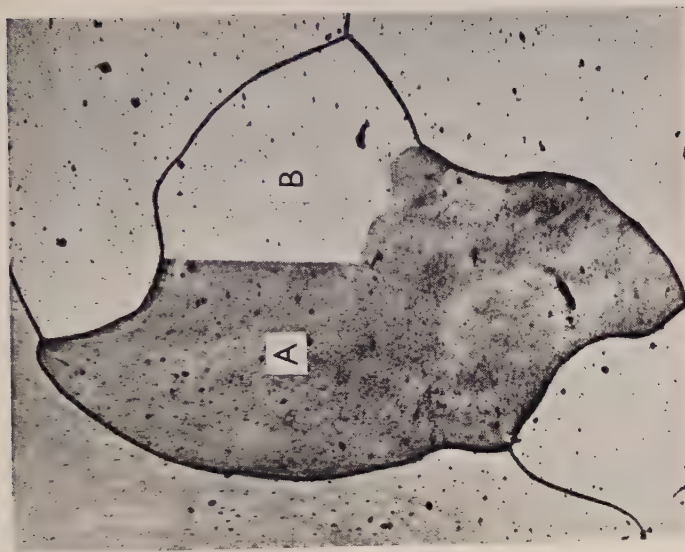


FIG. 2.—Electrolytically Polished Specimen Showing the Absence of Fusion in the Boundary Separating the Two Crystals *A* and *B* which Bear the Relation of Twins. $\times 10$.

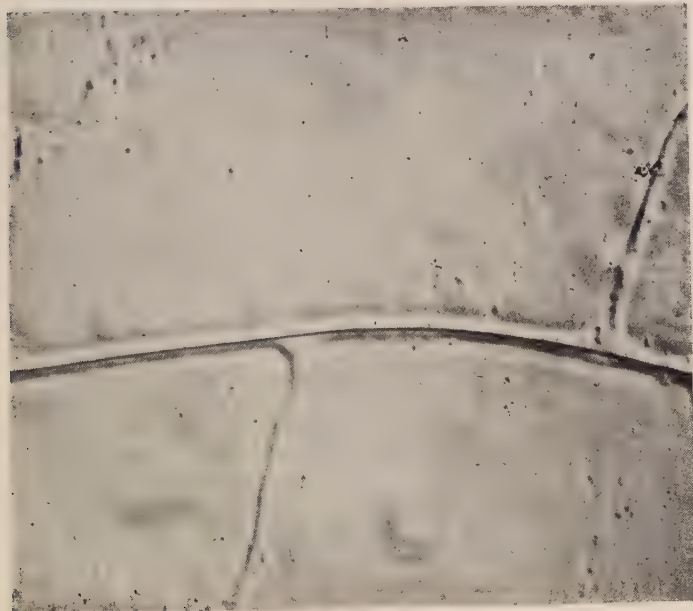


FIG. 1.—Comparison of a Grain Boundary and Intracrystalline Boundaries Obtained by Preferential Attack by Electrolytic Polishing (Aluminium-Zinc Solid Solution). $\times 250$.

[To face p. 8.

PLATE II.

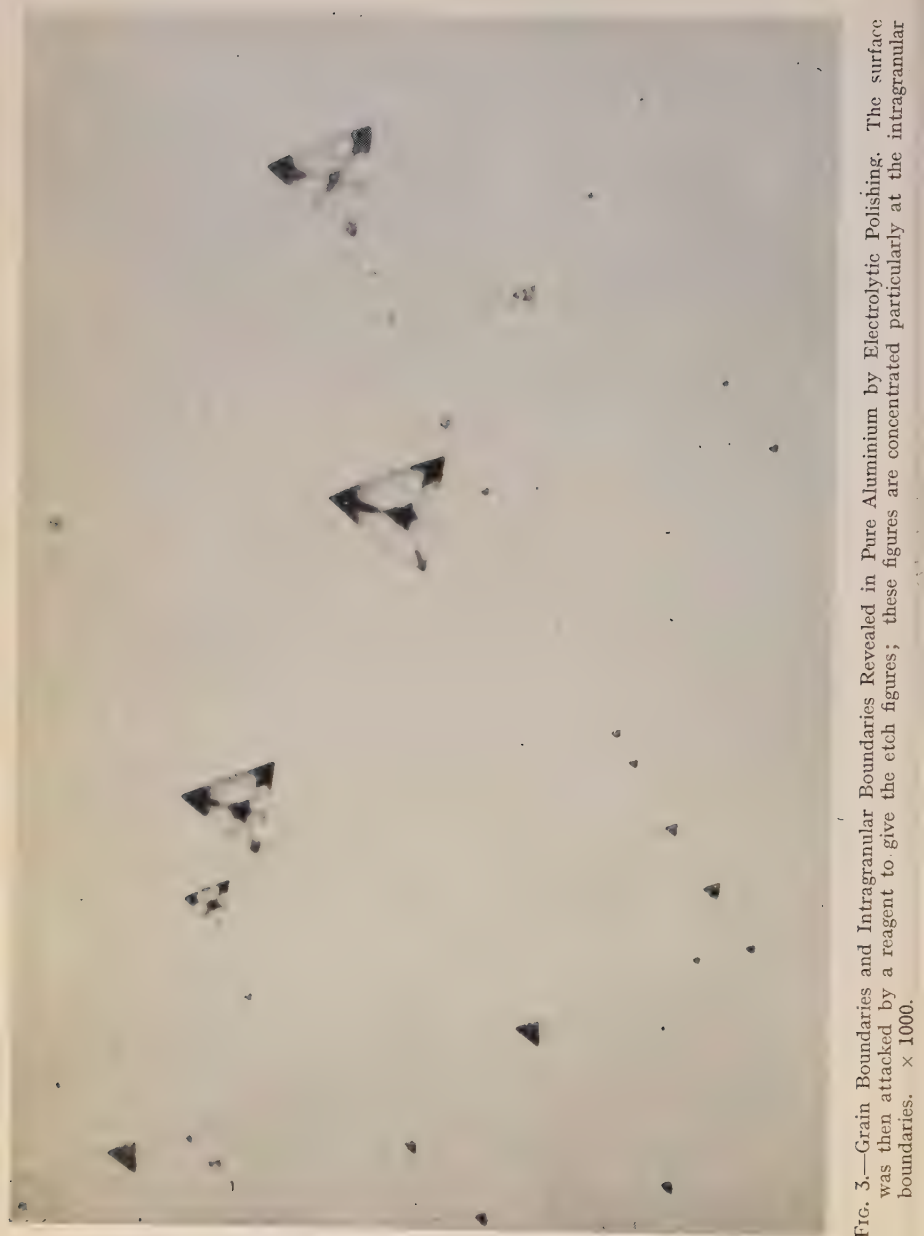


FIG. 3.—Grain Boundaries and Intragranular Boundaries Revealed in Pure Aluminium by Electrolytic Polishing. The surface was then attacked by a reagent to give the etch figures; these figures are concentrated particularly at the intragranular boundaries. $\times 1000$.

PLATE III.

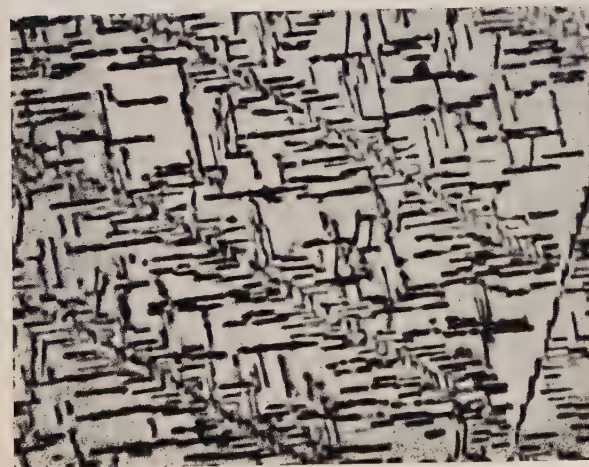
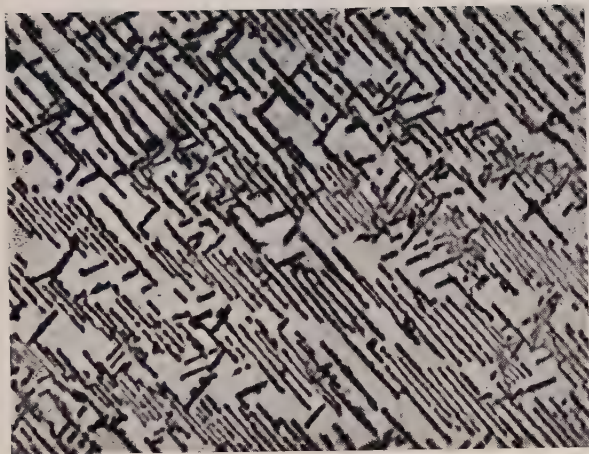


Fig. 4.—Preferential Precipitation of θ' Phase in the Intragranular Boundaries I of Crystals of Aluminium-Copper Solid Solution. (I is a true grain boundary.) $\times 1000.$

Fig. 5.—Preferential Precipitation of θ' Phase Along the Lines of Deformation L Caused by Water Quenching. $\times 1000.$

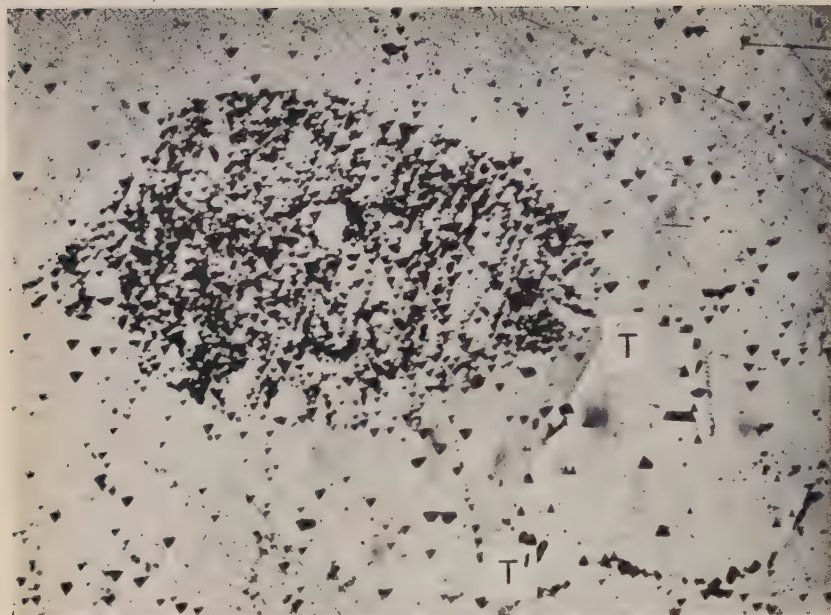


FIG. 6.—Two Isolated Crystals Observed After Attack to Reveal Etch Figures. Considerable concentration of etch figures occurs in one crystal, which is polygonized; the other bears the relationship of a twin to the large crystal surrounding it. (TT' is the twinning plane). $\times 250$.



FIG. 7.—Surface Electrolytically Polished in Accordance with the Conditions Laid Down by Morize, Showing Points of Anodic Attack Concentrated at the Boundaries of Mosaic Blocks. $\times 500$.

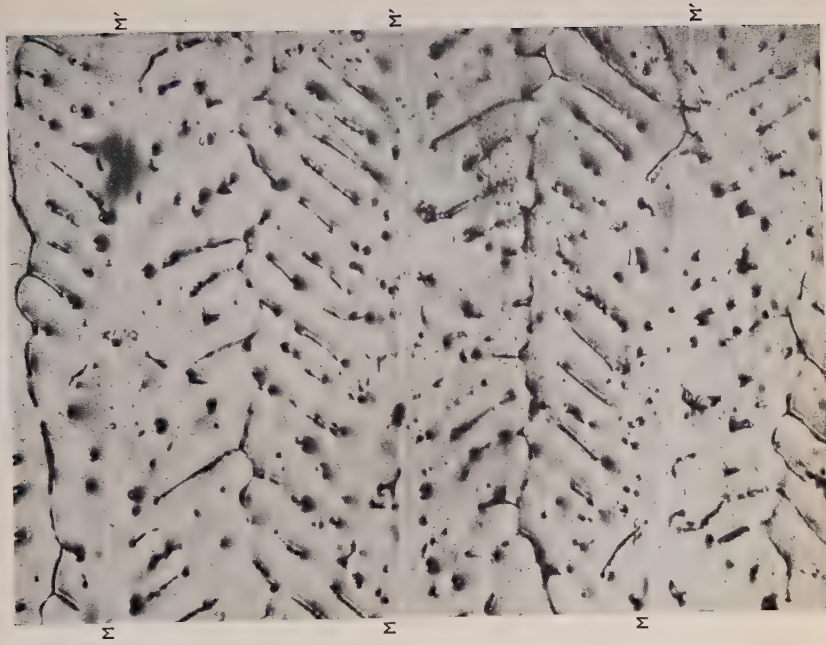


FIG. 9.—Distribution of Impurities Within the Structure of the Semi-Continuously Cast Ingot.

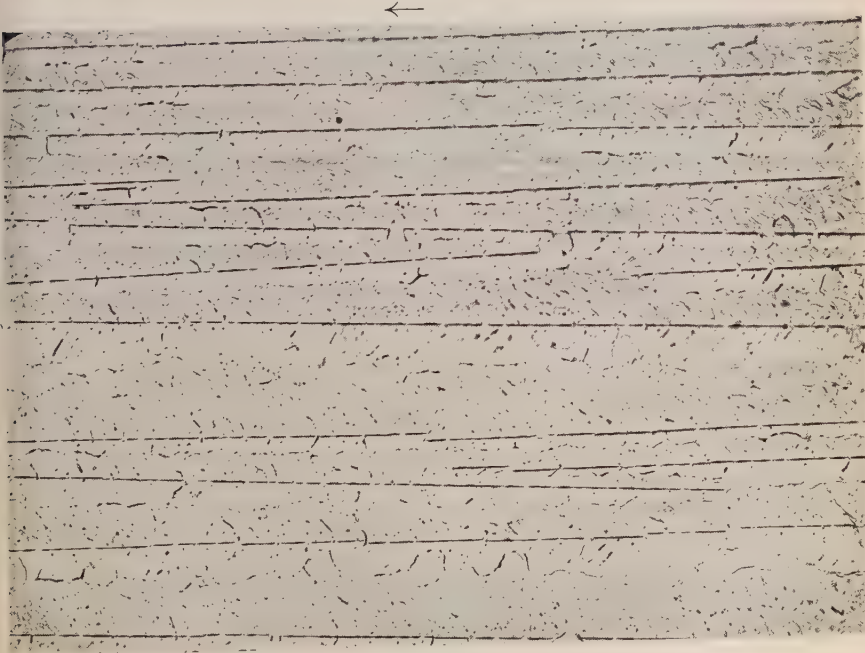


FIG. 8.—Structure of a Semi-Continuously Cast Ingot. The direction of casting is indicated by the arrow.

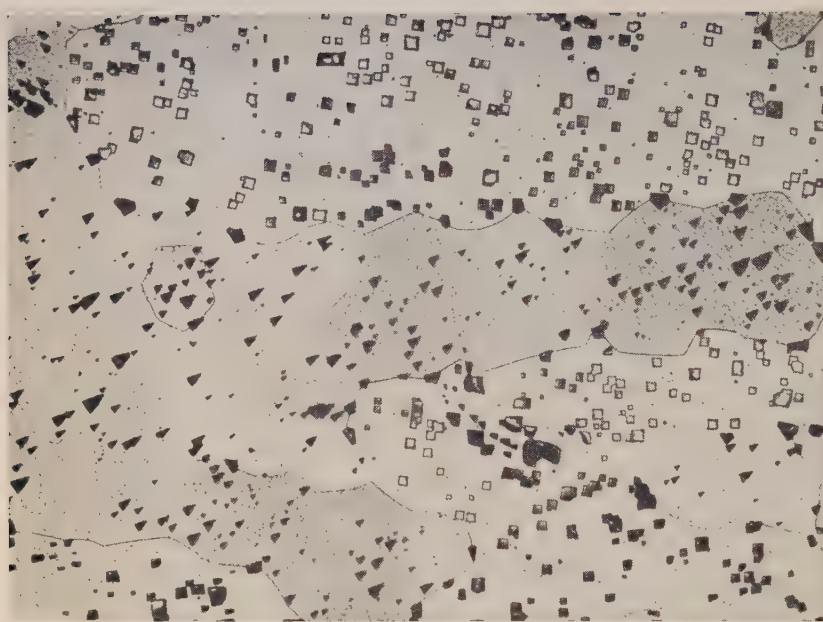


FIG. 10.—The Oriented Structure Exhibits Several Large-Scale Cells, the Relative Orientations Being Revealed by the Etch Figures. $\times 200$.

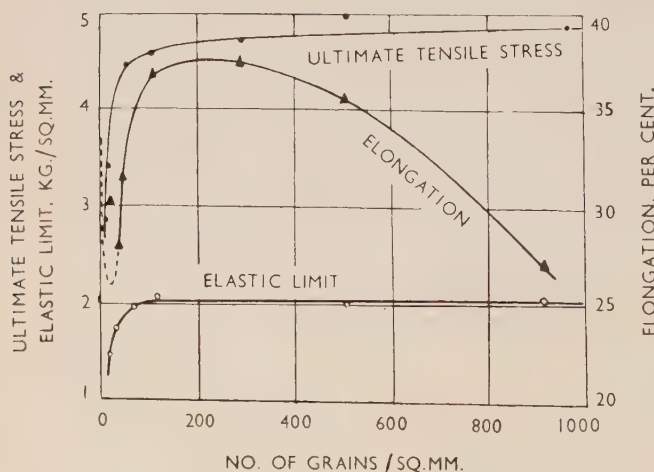


FIG. 11.—Variation of the Mechanical Properties of 99.99% Aluminium with Grain-Size.

properties (ultimate tensile stress, elastic limit, and elongation) of high-purity aluminium (99.99%). Chossat²³ has made a study of these properties in relation to grain-size, using a Chevenard micro-machine. He has also studied at the same time the conditions of recrystallization of this pure aluminium in relation to temperature and to certain additions.

In the case of 99.99% aluminium reduced 95%, the recrystallized grain-size varies from 900 grains/mm.² for a 30-min. anneal at 320° C. to 17 grains/mm.² for an anneal at 500° C. In this temperature interval the mean grain-size is related to the temperature by an exponential law. Above 500° C. this law is not valid, probably as a result of the phenomenon of secondary recrystallization. The exponential law has also been found to apply to impure metals, though within somewhat narrower temperature limits, e.g. 320°–410° C. for aluminium containing 0.1% zinc and 320°–500° C. for aluminium with 0.12% magnesium.

The mechanical properties of pure aluminium as a function of grain-size are summarized in Fig. 11 (Plate VI). It will be noted that the elongation passes through a maximum at 300 grains/mm.² The elastic limit and tensile stress are substantially constant above 100 grains/mm.²

A noteworthy fact has emerged in the course of these tests. In certain cases stress-strain curves of a quite characteristic form have been obtained : beyond the elastic limit the curve falls off in a series of steps. Similar observations have previously been made by Portevin and Le Chatelier²⁴ on Duralumin, by Körber and Pomp²⁵ on steel, and by McReynolds²⁶ on aluminium-copper alloys. Most of these authors relate the stepwise deformations to the existence of a particular structure in the test-piece or to physical heterogeneity. Chossat advances an explanation based on Cottrell's recent theory²⁷ of the existence of clusters of solute atoms round faults in the crystal. According to Cottrell, for slip to occur it must be possible for the dislocations to be displaced within the crystal; but the dislocations would be obstructed by the clusters of solute atoms. Depending on the temperature, annealing would cause either centripetal migration towards the fault in the crystal or, at higher temperatures, a centrifugal migration which would homogenize the crystal and lead to the disappearance of the phenomenon observed.

In the case of isothermal tests on 99.99% aluminium, we have found these series of steps on the stress-strain curves after periods of annealing which vary inversely with the temperature; for example, at 225° C. they appear at the end of 50 hr., at 245° C. after 3 hr., and at 280° C. after 1 hr. Above 300° C. they are not observed.²⁸

These last results show once again the importance of the part played by impurities and above all of their distribution within the crystal.

IX.—PRODUCTION OF NEW SURFACE STATES ON ALUMINIUM.

Metallic surfaces are now prepared in the laboratory either by mechanical polishing or by electrolytic polishing by the method devised by Jacquet.²⁹ Ever since the work of Osmond and of Beilby it has been known that metals polished mechanically by means of abrasives suffer marked surface distortion which forms a sort of skin on the metal. The skin consists of very heavily cold-worked metal, that is, metal which has been broken down into very small crystallites. We have had occasion to study this phenomenon by the X-ray back-reflection method.³⁰ Using this technique it is possible to explore the metal at various depths by carrying out a succession of anodic attacks and making an X-ray examination of the new surface exposed each time. Mechanical polishing produces in addition to a very heavily cold-worked surface layer a more or less deep distortion of the crystal structure. Moreover, mechanically polished metal is covered with an oxide film. In short, it may be said that two skins are formed: the one structural, which is more or less deep, and the other chemical, consisting of an oxide film. These two skins often mask the real surface properties and even the properties of the metal in massive form.

On the other hand electrolytic polishing, carried out in a bath of acetic anhydride and perchloric acid, consists of a simple anodic solution of the surface of the metal. There is therefore no formation of a structural skin, though the chemical skin persists to a greater or lesser extent, that is, the aluminium is covered with an oxide film.

The formation of this chemical skin depends on the nature of the bath, the method of washing the surface to rid it of electrolyte, and on the time it is exposed to the air. We have found that the thickness of the film is very closely related to the electrode potential of the metal surface in a 3% sodium chloride solution. Under these conditions the sheet of aluminium studied behaved, from the point of view of reproducibility of the measurements, like a reversible electrode. In addition, this method has proved much more sensitive than electron diffraction in revealing the presence of very thin oxide films.³¹

The potential of aluminium polished electrolytically is -1.20 V., while that of the metal mechanically polished is -0.74 V.³² Morize obtained the value -1.20 V. by taking special precautions. The viscous layer due to polishing was eliminated by the use of a strictly anhydrous solvent. On exposure to the air such a surface becomes

covered with an increasingly thick film of oxide and its potential tends towards the value — 0·74 V.

The surface corresponding to a potential of — 1·20 V. exhibits new properties of the metal, in particular the formation, in contact with the sodium chloride solution, of a brown oxide film quite different from the oxide film of stoichiometric composition. The sodium chloride attack reveals weak spots which occur particularly at the boundaries of the mosaic blocks (Fig. 7, Plate IV).

However, the value — 1·20 V. was still far from reaching the theoretical value of — 1·95 V. calculated from thermodynamic data.³³ It was reasonable to suppose, therefore, that this surface state represented a very slightly oxidized condition, and that it would be interesting to carry out all the polishing operations and the measurement of potential in a tube swept by a current of nitrogen. Under these conditions a much more negative potential was determined, — 1·60 V., a value which is also obtained when the potential is measured with a trace of mercuric chloride present in the electrolyte. In the presence of a mercury salt, the aluminium oxide film is destroyed, and it is natural to assume therefore that under these conditions the potential measured is that of the bare metal.

Clearly, it would be interesting to pursue the researches on the new surface state obtained in an inert atmosphere.

X.—SEMI-CONTINUOUS CASTING AND THE DISTRIBUTION OF IMPURITIES IN THE INGOT.

The semi-continuous casting process is widely used in France. In this technique, as you know, the ingot mould is reduced to a kind of water-cooled ring, from which the ingot emerges progressively to enter a pit full of water, a procedure which enables very long ingots to be cast. The drastic quenching of the metal permits certain classical defects in cast ingots to be avoided, though new ones make their appearance.

The process has been systematically studied by Hérenguel and his co-workers;³⁴ in particular they have observed a new type of structure. If the vertical section of an ingot is examined after an attack by the reagent used to produce etch figures, two structures are observed :³⁵ an outer zone consisting of the classical columnar crystals and an inner zone characterized by a new structure which takes the form of fibres substantially parallel to the axis of the ingot, the direction *MM'* in Fig. 8 (Plate V). These fibres are in reality sections through very thin laminæ. Photomicrographs, by means of etch figures, and Laue

reflection diagrams have shown that these laminæ, which have an average thickness of 0·1–0·2 mm., are formed by the contact of two flat crystals bearing the relation of twins to one another. The principal impurities in the metal (iron and silicon) separate on solidification in a well defined way: in part they are concentrated at the boundary of two adjacent laminæ and in part they are deposited within the laminæ in the form of flat scales or flakes parallel to the 100 planes of the crystal. Finally, the traces of the twinning planes (MM' in Fig. 9, Plate V) are entirely free from precipitate. It is interesting in this connection to recall Northcott's work on columnar structures.³⁶

XI.—PREFERRED ORIENTATION AFTER ROLLING.

As you know, to obtain good results in pressing, the sheet used must consist of fine equi-axed crystals orientated at random. On the other hand, it is possible after rolling and annealing to obtain a more or less preferred orientation in the sheet which gives rise to well-known troubles. X-rays can be used for the analysis of these preferred structures, but it appears that in practice micrographic methods can give much more complete information. Hérenguel uses etch figures. Fig. 10 (Plate VI) shows a structure having large-scale cells, some being formed by a structure made up of cubes having (100) faces parallel to one another. Hérenguel thus reveals very easily the existence of macrographic features and then analyses grain by grain the orientation of an aggregate.³⁷

XII.—THE ANODIC OXIDATION OF ALUMINIUM AND ITS ALLOYS.

The well known Bengough process has been much studied in France in recent years.* After anodic oxidation there appear on aluminium and aluminium alloy articles certain defects which have been classified by Hérenguel according to the nature of their origin.³⁸ Systematic researches have been carried out on the factors that govern the appearance of oxide films produced on aluminium. They can be divided into three groups:³⁹

- (a) The surface condition before oxidation.
- (b) The composition of the metal or alloy.
- (c) Previous thermal and mechanical treatment.

A fundamental fact has emerged, namely that the whole of the previous metallurgical history of the metal or alloy may be clearly revealed in the appearance and structure of the oxide film. Anodic

* The researches were co-ordinated and encouraged by the Commission des Etats de Surface des Métaux.

oxidation is a very sensitive means of detecting the precipitation of a new phase in an aluminium alloy.

On the basis of these researches it may be said that the production of a perfect anodic film appears to demand a series of very careful metallurgical operations, using high-purity material. The French aluminium industry now makes a special high-purity aluminium-magnesium alloy to ensure perfect anodic oxidation. This has resulted in the use of the metal not only for decorative purposes, but also for particular applications, such as electrical insulation, where a perfectly continuous anodic film is necessary.

XIII.—SPECIAL-PURPOSE ALLOYS.

Until recent years the aluminium industry in the various countries has been solely engaged in producing the five or six principal alloys required to meet the most important conditions of service. In regard to the so-called secondary applications, the user has often been in difficulties. For a long time attention has been concentrated on the production of Duralumin-type alloys of as high a strength as possible. Nowadays account is taken of other interesting properties of aluminium and its alloys, e.g. electrical conductivity, quality of oxide film, high cold workability, corrosion-resistance, &c. These special alloys must often be made using very pure metals and taking particular precautions. These exacting metallurgical requirements appear to have been successfully met by the French light-alloy industry. The following special alloys may be noted.

1. Aluminium-Magnesium Alloys for Anodic Oxidation.

Aluminium-magnesium alloys made from high-purity materials are very resistant to corrosion and give an anodic film as clear as that on super-pure aluminium.⁴⁰ These alloys contain 3 and 5% magnesium and must fulfil the following conditions : the α phase of which they are composed must be perfectly homogeneous; the structure must be isotropic and fine-grained, as anodic oxidation reveals anisotropy; and electrolytic polishing must precede anodic oxidation.

2. Alloys for Severe Plastic Deformation.

The aluminium-magnesium alloys have strength properties that increase rapidly with magnesium content and certain alloys have been developed with a view to drawing and pressing. They must be fine-grained and exhibit no preferred orientation.

3. Alloys for Fusion Welding.

These are medium-strength aluminium-magnesium and aluminium-magnesium-zinc alloys of moderate alloy content. They must contain few insoluble elements and must have been degassed and then rapidly solidified to avoid the large concentration of insoluble constituents that give rise to defects in gas welding.

4. Alloys to Resist Sea Water.

These are aluminium-magnesium alloys, as pure as possible, or at any rate free from heavy metals.

5. New Alloys of the Al-Mg-Zn Type.

The very high mechanical properties of aluminium-magnesium-zinc alloys are well known. Researches are being carried out with the object of realizing the highest possible strength, perhaps in excess of 60 kg./mm.² (42 tons/in.²), while maintaining complete stability of properties. This has led in particular to researches on aluminium-zinc alloys.⁴¹ Héren-guel has shown that alloys can be produced which are very ductile, and hence easy to work, and which after quenching from about 400° C. age-harden to give relatively high mechanical properties. Thus an alloy containing 3·5% zinc and 1·75% magnesium has the following advantages :

- (a) its hot workability is extremely good,
- (b) it is quenched from between 350° and 450° C.,
- (c) age-hardening is not rapid, which enables it to be worked.

Immediately after quenching the ultimate tensile stress is 20 kg./mm.² (14 tons/in.²); on age-hardening it increases to 35 kg./mm.² (24·5 tons/in.²), the corresponding elastic limit being 25 kg./mm.² (17·5 tons/in.²).

This alloy appears to fill a gap in the medium-strength light alloys.

XIV.—CONCLUSION.

We are celebrating this week the centenary of the birth of the famous metallographer, Floris Osmond. In his day he developed very greatly the possibilities of the metallographic technique, and showed by his own researches the powerful nature of this experimental method. It is noteworthy that at the present time a revival of classical metallography is taking place, as is exemplified by the discovery of the sub-structure of aluminium and its consequences.

The scientific work carried out in France in recent years on the properties of very pure aluminium, its surface condition, cold working, alloys, &c., has led the light-alloy industry in the direction of real precision metallurgy in which metals and alloys are produced that are specially suited to their particular applications. This industrial advance shows once again that there should be no essential difference between the methods of scientific research and those of industrial research.

REFERENCES.

1. P. Héroult, French Patent No. 175,711 (23 April 1886).
C. M. Hall, U.S. Patent No. 400,766 (9 July 1886).
2. P. Chevenard and A. Portevin, *Compt. rend.*, 1923, **176**, 296; 1925, **180**, 1927; 1928, **186**, 144.
3. P. Lacombe and L. Beaujard, *J. Inst. Metals*, 1947/8, **74**, 1.
4. P. Lacombe and L. Beaujard, *ibid.*, p. 4.
5. C. G. Darwin, *Phil. Mag.*, 1914, [vi], **27**, 315.
6. P. Lacombe and A. Berghézan, *Compt. rend.*, 1948, **226**, 2152.
7. P. Lacombe and A. Berghézan, *Physica*, 1949, **15**, 161.
8. A. Guinier and J. Tennevin, *Compt. rend.*, 1948, **226**, 1530.
9. A. Guinier and P. Lacombe, *Métaux et Corrosion*, 1948, **23**, 212.
10. E. Orowan, Congrès de la Société Française de Métallurgie, Paris, 1947.
11. R. W. Cahn, *Phys. Soc. : Rep. Conf. on Strength of Solids*, **1948**, 136.
12. P. Lacombe and L. Beaujard, *Compt. rend.*, 1944, **219**, 66.
13. P. Lacombe and N. Yannaquis, *Compt. rend.*, 1947, **224**, 921.
14. P. J. E. Forsyth, R. King, G. J. Metcalfe, and B. Chalmers, *Nature*, 1946, **158**, 875.
15. G. Chaudron, P. Lacombe, and N. Yannaquis, *Compt. rend.*, 1948, **226**, 1372.
16. W. G. Burgers, *Proc. K. Ned. Akad. Wetensch.*, 1947, **50**, 452; also *Phys. Soc. : Rep. Conf. on Strength of Solids*, **1948**, 134.
17. W. Shockley and W. T. Read, *Phys. Rev.*, 1949, [ii], **75**, 692.
18. P. Lacombe and A. Berghézan, *Compt. rend.*, 1949, **229**, 365.
19. J. Hérenguel and G. Chaudron, *Compt. rend.*, 1943, **216**, 687
20. H. Chossat, M. Moufard, P. Lacombe, and G. Chaudron, *Compt. rend.*, 1948, **227**, 432.
21. H. Chossat, P. Lacombe, and G. Chaudron, *Compt. rend.*, 1948, **227**, 593.
M. Cook and T. Ll. Richards, *J. Inst. Metals*, 1947, **73**, 1.
A. Krupkowski and M. Balicki, *Ann. Acad. Sci. Tech. Varsovie*, 1937, **4**, 270.
22. W. May, T. J. Tiedema, and W. G. Burgers, *Nature*, 1948, **162**, 740.
23. H. Chossat, *Compt. rend.*, 1949, **228**, 1344.
24. A. Portevin and F. Le Chatelier, *Rev. Mét.*, 1924, **21**, 233.
25. F. Körber and A. Pomp, *Mitt. K.-W. Inst. Eisenforsch.*, 1927, **9**, 346.
26. A. W. McReynolds, *J. Metals*, 1949, **1**, (III), 32.
27. A. H. Cottrell, *Phys. Soc. : Rep. Conf. on Strength of Solids*, **1948**, 30.
28. H. Chossat, Thesis, Paris : 1949; and *Rev. Mét.*, 1949 (in the press).
29. P. A. Jacquet, "Le Polissage Electrolytique des Surfaces Métalliques et ses Applications". Tome I.—"Aluminium, Magnésium, Alliages légers". Saint-Germain-en-Laye (S. et O.) : 1948. (Editions Métaux.)
30. J. Benard, P. Lacombe, and G. Chaudron, *Journées des Etats de Surface*, 1945, 73.
31. H. Raether, *Compt. rend.*, 1948, **227**, 1247.
32. P. Morize, Thesis, Paris : 1947.
33. U. R. Evans, "Metallic Corrosion, Passivity and Protection". Second edition. London : 1946, p. xxiv.
34. J. Hérenguel, *Rev. Mét.*, 1948, **45**, 139.
35. J. Hérenguel and P. Lacombe, *Compt. rend.*, 1949, **228**, 846.
36. L. Northcott, *J. Inst. Metals*, 1946, **72**, 283.

16 Recent French Investigations of Light Alloys

37. J. Hérenguel, *Rev. Mét.*, 1948, **45**, 505.
38. J. Hérenguel, *Etudes sur les Aspects des Pellicules d'Oxydation Anodique formées sur l'Aluminium et ses Alliages*, 1944, 19.
39. G. Chaudron, *ibid.*, p. 95.
40. J. Hérenguel and M. Scheidecker, *Métaux et Corrosion*, 1948, **23**, 167.
J. Hérenguel and R. Segond, *Rev. Mét.*, 1949, **46**, 377.
41. G. Chaudron, J. Hérenguel, and P. Lacombe, *Compt. rend.*, 1944, **218**, 404.

SOME ASPECTS OF THE PRODUCTION AND 1208 HEAT-TREATMENT OF ELECTROLYTIC COPPER POWDER.*

By H. J. V. TYRRELL,† M.A., B.Sc.

SYNOPSIS.

The preparation of electrolytic copper powder from acid copper sulphate and acid sodium cupro-chloride electrolytes has been studied on the laboratory scale, and the effect of the cell conditions on the nature of the product elucidated. The powders prepared from the two electrolytes were quite different both in appearance and properties, that from the chloride bath giving higher-strength compacts than that obtained from the sulphate bath using the conditions described in this work. Sulphate powder particles consisted of a number of radially oriented micro-crystals; chloride particles were frequently true dendrites, and consisted of two or three crystals only. Power efficiencies for chloride powders have been found to be considerably higher than those obtained for sulphate powders, both in this work and in German production plants. The effects of heat-treatment on properties were studied in most detail for the sulphate powders. The annealing atmosphere was of great importance in determining the stability of the annealed powder, traces of ammonia, such as may have been present in the cracked-ammonia atmosphere used in some experiments, giving samples which tended to discolour rapidly on storage. It was found possible to stabilize such powders by coating the particles with a mono-layer of stearate ions. The relationships between the tensile strength of the sintered compacts and the temperature at which the powders were annealed, the pressure at which they were formed, their density, and their change in density on sintering, were investigated, and the results are expressed in statistical form.

I.—INTRODUCTION.

THE technique of making metal articles by pressing metal powder in a suitable die and then sintering, has grown steadily in importance during the last few decades, and there has been an increasing demand for metal powders of various kinds. Copper powder, particularly that prepared by electrolysis, is probably the most widely used, most of it being obtained before the war from Germany or the U.S.A. The manufacturing processes have not been described in detail. The present paper describes some aspects of an attempt to develop a domestic source of supply which reached the stage of pilot-plant production. It is concerned particularly with laboratory investigations of the production of electrolytic powders, and with the effect of heat-

* Manuscript received 20 January 1949.

† Department of Chemistry, Sheffield University; formerly Research Department, Imperial Chemical Industries Ltd., Widnes, Lancashire.

treatment on the stability and moulding properties of powders produced both on the plant and in the laboratory. No description is given of the design, lay-out, or operation of the pilot plant.

Two electrolytes were selected for detailed study, namely, acidified copper sulphate solutions, and solutions of cuprous chloride in acidified brine. The first is a common type of electroplating bath, the second has been suggested for electro-refining¹ and for the preparation of copper powder from scrap brass.² A few experiments were carried out on cupro-cyanide electrolytes using a modified du Pont "High Speed Copper" formula,³ but these were unpromising and the work was not continued.

The heat-treatment investigation developed from a study of the storage stability of powders from the plant. Since these were exclusively produced from sulphate electrolytes, the laboratory heat-treatment work was principally concerned with two bulk samples of sulphate powder prepared under slightly different conditions on the plant, although a few experiments were also carried out with a large sample of chloride powder prepared experimentally in a 500-amp. cell.

II.—EXPERIMENTAL.

1. Preparation.

Laboratory-scale experiments were usually carried out in a 2-l. beaker, heated in a large water bath to facilitate temperature control. The electrodes consisted of a thick copper anode and a stainless steel cathode, which were suspended in the electrolyte. This was usually stirred vigorously. It was not possible, in a cell of this type, to control the degree of turbulence in the neighbourhood of the cathode very precisely, and in order to examine this factor a more elaborate cell was used. This consisted of a cylindrical cathode, which could be rotated about a vertical axis at a known speed, surrounded by a co-axial perforated copper anode. A few larger-scale experiments were carried out using a scaled-up version of the simple laboratory cell described above. This operated with a load of about 500 amp. In all cases, the product was removed by manual scraping of the cathodes at intervals, washed with water on a Buchner filter until it was free from electrolyte, and then dried in a low vacuum. In the case of powders prepared from a cupro-chloride electrolyte, it was necessary to give an initial wash with 5% sodium chloride solution to remove any cuprous chloride before washing with water.

2. Heat-Treatment.

The heat-treatment furnace consisted of a 2-in. internal dia. tube-furnace, 16 in. long, heated electrically. A loose tubular liner of heat-resisting steel was placed inside the furnace, projecting far enough for the ends to be closed with rubber bungs. The powder was contained in a stainless steel boat, 6 in. long, of semi-circular section, which fitted closely into the liner and could be slipped from the water-cooled zone at the inlet end of the furnace into the hot zone by means of a copper rod attached to it. A Chromel-Alumel thermocouple measured the temperature of the hot zone. Cylinder hydrogen purified by passing over red-hot copper, and dried by bubbling through concentrated sulphuric acid, was led into the heat-treatment furnace after removing acid spray. Oxygen-free nitrogen was used to purge the apparatus before and after passing the hydrogen. A capillary flow meter and a mercury lute were included in the common gas supply line to the furnace.

Samples were annealed for either 1 or 2 hr., and were then quenched by withdrawing the boat into the water-cooled zone, or allowed to cool slowly in the furnace over a period of several hours. Each batch of powder was submitted to these four treatments at each annealing temperature.

3. Materials Used in Heat-Treatment Experiments.

Two batches of powder produced on the pilot plant were used for the majority of the experiments. One of these had been made from a plain acid sulphate bath containing about 10 g./l. of copper and 100 g./l. of sulphuric acid, using a bath temperature of about 60° C., and a cathode current density of the order of 20 amp./dm.². This is referred to as powder *A*. The other batch, referred to as powder *B*, was prepared from a similar electrolyte to which sufficient common glue had been added during the operation of the cell to maintain a concentration of approximately 0·1% (weight/volume) in the bath. These two powders were supplied from the pilot plant as representative samples of the material in production at the time. Their properties are given in Table I.

A small number of experiments were carried out with a batch of chloride powder, prepared on the 500-amp. cell, the properties of which are given later.

4. Testing.

The size-distribution of the powders was determined by hand-sieving, using B.S. sieves down to 200 mesh. Some of the results are quoted in terms of a 250-mesh "Finex" sieve; this was a sub-standard 200-mesh B.S. sieve which at the time was the only one available.

TABLE I.—Properties of Experimental Copper Powders.

Properties	Powder A	Powder B
Sieve Analysis :		
% + 100 mesh B.S.S.	27	22
% - 100 + 150	24	29
% - 150 + 200	9	14
% - 200	40	35
Apparent Density of Powder, g./ml.	2.0	2.3
Tapped Density of Powder, g./ml.	2.8	3.0
Green Density of Compact, g./ml. :		
(a) 50 tons/in. ² pressure	8.45	...
(b) 24 tons/in. ² pressure	7.53	...
Tensile Strength of Sintered Compact, tons/in. ² :		
(a) 50 tons/in. ² pressure	5.6	...
(b) 24 tons/in. ² pressure	7.8	...
Glue Content, wt.-%	None	0.014

The apparent density was measured by pouring the powder into an open flat-topped vessel of known volume, removing the excess powder from the top, and determining the weight of the contents. If, before weighing, the vessel was tapped gently until no further decrease in volume was observed, the "tapped density" could be determined. The flow properties of the powder were measured by determining the time required for a given weight of the powder to flow out of a funnel of arbitrary dimensions. This is not described, since no figures are quoted for flow times.

The powders were pressed, without the addition of lubricant, in a ring die,⁴ giving compacts approximately 1 in. in dia. with a wall thickness of about $\frac{1}{16}$ in. The "green" compacts were strong enough to handle and their density (green density) could be determined directly. They were then sintered at 1000° C. for 30 min. in an atmosphere of cracked ammonia. Tensile-strength measurements were carried out using a Hounsfield tensometer, the ring being held by two semi-cylindrical jaws fitting loosely inside. One jaw was fixed and the other moved in order to apply a measured load to the periphery of the ring. This extended and finally broke, the extension being measured by the movement of the jaw applying the load. A stress-elongation curve could thereby be plotted. The tensile strength of the ring was given by the following expression :

$$\text{tensile strength, tons/in.}^2 = \frac{\text{breaking load, tons}}{2 \times \text{cross-sectional area of ring}}$$

The cross-sectional area of the ring was taken as the original area of the annulus before any load was applied. Under the conditions of the test, the breaking load as measured was equal to the maximum stress transmitted through the ring. Tensile-strength measurements of this type give results which are linearly related, to a first approximation, to those obtained when normal test-pieces are used.^{4, 5}

The stability of a powder was assessed in terms of the colour change from pink to brown, purple, and black which accompanies the progressive oxidation of such powders. Samples were exposed in specimen tubes ($6 \times \frac{3}{4}$ in.), about two-thirds full, over calcium chloride, and over 30% sulphuric acid, this corresponding at room temperatures to an atmosphere with a relative humidity of 75%. Colour changes were followed with a Lovibond Tintometer, but the numerical results obtained were of little use quantitatively because of the complex changes in hue and intensity which occurred on storage. Ultimately, the figures obtained were used solely to classify the powders as stable or unstable, any appreciable change with time in the Lovibond figures being sufficient for that sample to be classified as unstable.

The samples of powder which had been heat-treated at any but the lowest temperatures were found to be sintered into a friable cake. The degree of sintering was estimated by measuring the depth to which a loaded needle of known dimensions would penetrate. A Hutchinson Penetrometer,⁶ a standard instrument used in testing tar products, was available and was used for this purpose. Before applying the other tests described above, it was necessary to break down the sintered cake; this was done as gently as possible, but those samples treated at 650° C. or above required a light grinding in an impact mill (Christie and Norris "Junior") before they could be examined.

III.—RESULTS.

1. *Electrode Reactions in Metal-Powder Cells.*

It is well known that, for sulphate electrolytes, the principal anode reaction under normal conditions is the solution of copper to form cupric ions. There was no evidence in this work of side reactions or of polarization phenomena of any important kind, at the anode current densities used (about 15 amp./dm.²), the anode solution efficiency based on solution as cupric ions being always close to 100%. There appeared to be four possible anode reactions in cupro-chloride solutions :

- (a) The formation of cuprous ions and their subsequent precipitation as solid cuprous chloride in the neighbourhood of the anode, or

their transformation into soluble anionic complexes if the total chloride concentration in the solution was sufficiently high.

(b) The oxidation of the cuprous complexes to the cupric state.

(c) The discharge of the complex copper anion and the deposition of metallic copper. Feodotieff⁷ found that this only occurred at very high current densities (80 amp./dm.²).

(d) The liberation of chlorine.

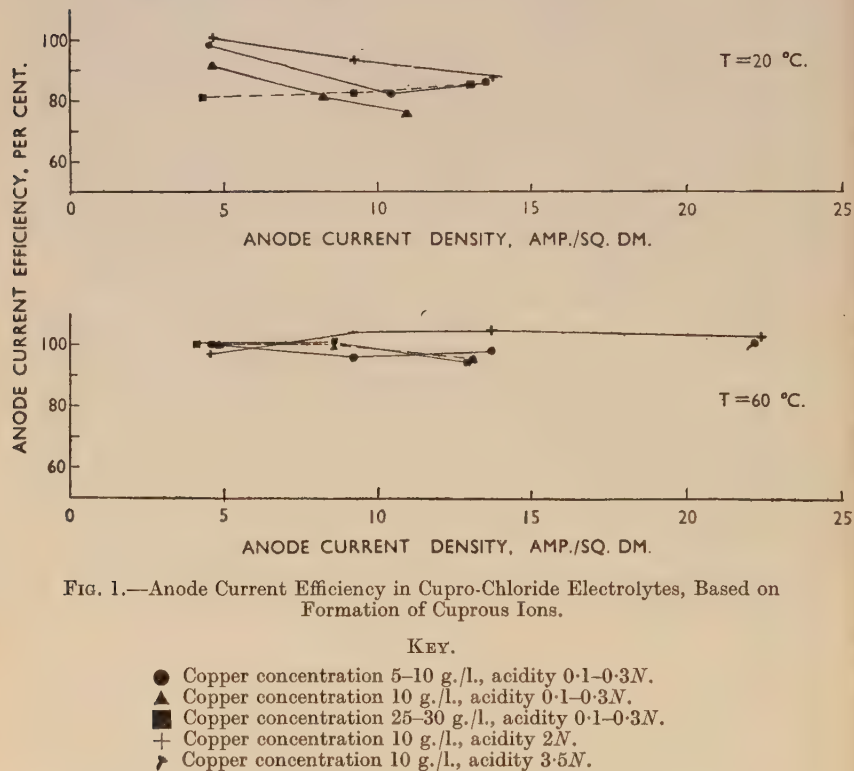


FIG. 1.—Anode Current Efficiency in Cupro-Chloride Electrolytes, Based on Formation of Cuprous Ions.

KEY.

- Copper concentration 5–10 g/l., acidity 0.1–0.3N.
- ▲ Copper concentration 10 g/l., acidity 0.1–0.3N.
- Copper concentration 25–30 g/l., acidity 0.1–0.3N.
- + Copper concentration 10 g/l., acidity 2N.
- ↗ Copper concentration 10 g/l., acidity 3.5N.

The effect on the anode solution efficiency of variations in the cell conditions is illustrated in Fig. 1, where the mean measured efficiency is plotted against the anode current density used. Each curve corresponds to a group of experiments for which the other cell conditions remained constant. Clearly the solution efficiency was generally greater at 60° than at 20° C., remaining close to 100% up to the highest current densities studied, particularly in acid solutions. Since, in the majority of experiments, the concentration of cupri-

chloride did not rise, or the total concentration of chloride fall, the formation of cuprous ions was undoubtedly the principal anode reaction.

The appearance of the anode at the end of an experiment with a chloride electrolyte varied according to the operating conditions. Normally it was etched, and covered with a thin black slime, apparently cupric oxide. Occasionally, however, it was highly polished. This

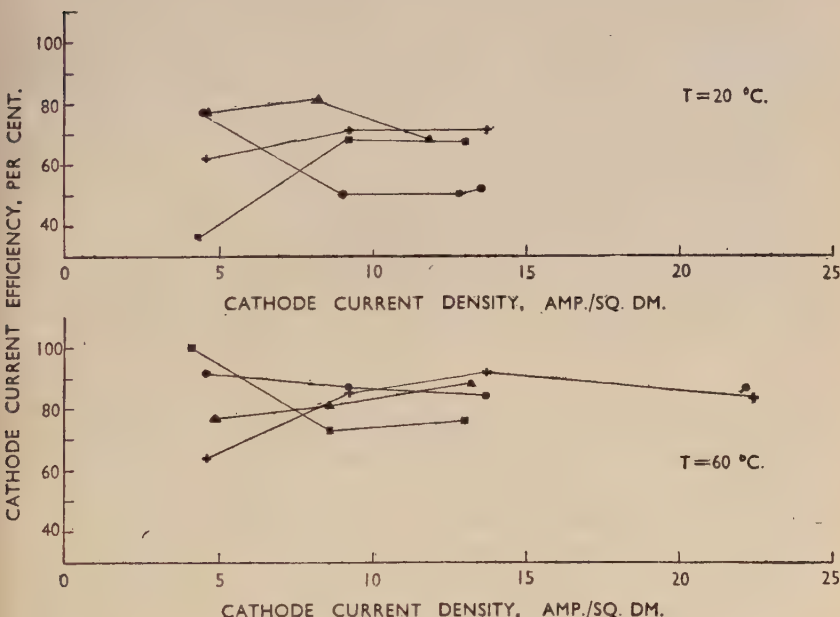


FIG. 2.—Cathode Current Efficiency in Cupro-Chloride Electrolytes, Based on Deposition of Cuprous Ions.

Key as in Fig. 1.

polishing was observed when low temperatures and high anode current densities, a low copper concentration in the electrolyte (5 g./l. of copper), and a pH between 0.5 and 1.0 were used. It was associated with the occurrence of strong anodic polarization in the cell, and has been reported previously^{8, 9} for both chloride and cyanide baths. The phenomenon was not important in the preparation of the powders, since the conditions producing it were not those most favourable for powder production.

The principal cathode reaction in the sulphate electrolyte was the discharge of cupric ions as metallic copper, but at the current densities

used in powder cells (about 15 amp./dm.²) a small amount of hydrogen was formed, especially in unstirred electrolytes. In consequence, powders formed under these conditions were contaminated with basic material. Cathode current efficiencies obtained from small laboratory cells were low (50–60%) even when the electrolyte was stirred, owing to difficulties of collection. However, values of about 95% were regularly reported from the pilot plant, and the side reactions could not have been serious.

In chloride electrolytes the discharge of cuprous ions and of hydrogen ions were also in competition as cathode reactions, though there was, in addition, a third possibility, the reduction of any cupric complexes present to cuprous. Fig. 2 shows that cathode efficiencies based on deposition of cuprous ions as metal, depended mainly on the temperature of operation of the cell. A temperature of 60° C. gave efficiencies which were considerably higher than those obtained in experiments carried out at 20° C. The other factors were apparently less important. The figures quoted were obtained from small-scale experiments and would be expected to be rather lower than those obtained from continuous operation of larger cells.

2. *Properties of Powders.*

Specifications for metal powders normally include the particle-size distribution expressed in terms of standard sieves, and the apparent density. This is partly a function of the particle size, and partly of the shape and surface characteristics. Consequently, changes in the cell conditions produced changes in the particle size and the apparent density which were, to some extent, independent. The results of a number of experiments are summarized below:

(a) The size distribution of the particles was principally determined by the frequency with which the powder was removed from the cathode, the apparent density remaining almost unaffected (Table II). Data in this Table were obtained from experiments on an acid sulphate electrolyte (copper 10, sulphuric acid 100 g./l., temperature 60° C.), using a cell with a vertical cylindrical cathode, the peripheral speed being 35.65 cm./sec., and the cathode current density 18.9 amp./dm.².

(b) Increasing the acidity and the total copper concentration of the electrolyte, raising the operating temperature, or decreasing the cathode current density, increased the average particle size and the apparent density. Any major change in these variables led, in the case of the sulphate solutions, to the formation of adherent deposits.

the best conditions for powder formation being those quoted above for Table II. Powder was formed from chloride baths over almost the whole range of conditions tested (see key to Fig. 1).

TABLE II.—*Frequency of Removal from the Cathode and Physical Properties of the Powder.*

Frequency of Removal, per hr.	% + 100 mesh B.S.S.	% - 100 mesh B.S.S.	Physical Properties of — 100 Mesh Fraction	
			% - 250 Finex	Apparent Density (g./ml.)
2	75	25	21	3.8
4	33	67	35	3.5
12	9	91	47	3.2

(c) The nature of the cathode deposit was changed by the addition of small amounts of foreign substances to the bath, e.g. colloids, wetting agents. In general, these tended to increase the apparent density of the dried powder, and it was the accepted practice to add common glue to the pilot-plant cells at one time. It is shown later that this gave rise to an inferior product.

(d) The results obtained on the laboratory cells were greatly affected by the turbulence of the electrolyte. When the bath was unstirred the copper was deposited at the cathode as a fluffy powder contaminated with basic material (sulphate electrolyte). Similar powders were formed in stirred solutions of low copper concentration, i.e. the type of product formed in unstirred solutions arose because of the rapid impoverishment of the solution in the neighbourhood of the cathode. Evidently, the normal diffusion processes were too slow to keep up the copper concentration in this region unaided. Similar results were obtained for chloride solutions. In larger cells sufficient stirring seemed to arise from gas evolution at the cathode, convection currents in the cell, &c., to make mechanical agitation unnecessary. The effect was studied quantitatively using the vertical cathode cell and the conditions described in (a) above. The results are shown in Fig. 3. The copper concentration in the cathode layer evidently reached its maximum when the peripheral velocity of the cathode reached 35 cm./sec., further increments of velocity having only a small effect.

Powders of a very wide range of size distribution were prepared in the above experiments (cf. Table II). The apparent densities of these varied between 0.7 and 3.7 g./ml., the value increasing as the cell conditions approached those normally used in electroplating, i.e. high

electrolyte concentrations, high temperatures, and low cathode current densities. As has been stated, conditions for powder formation were comparatively critical in sulphate baths; in chloride baths they were much less so. An electrolyte containing 150 g./l. of sodium chloride,

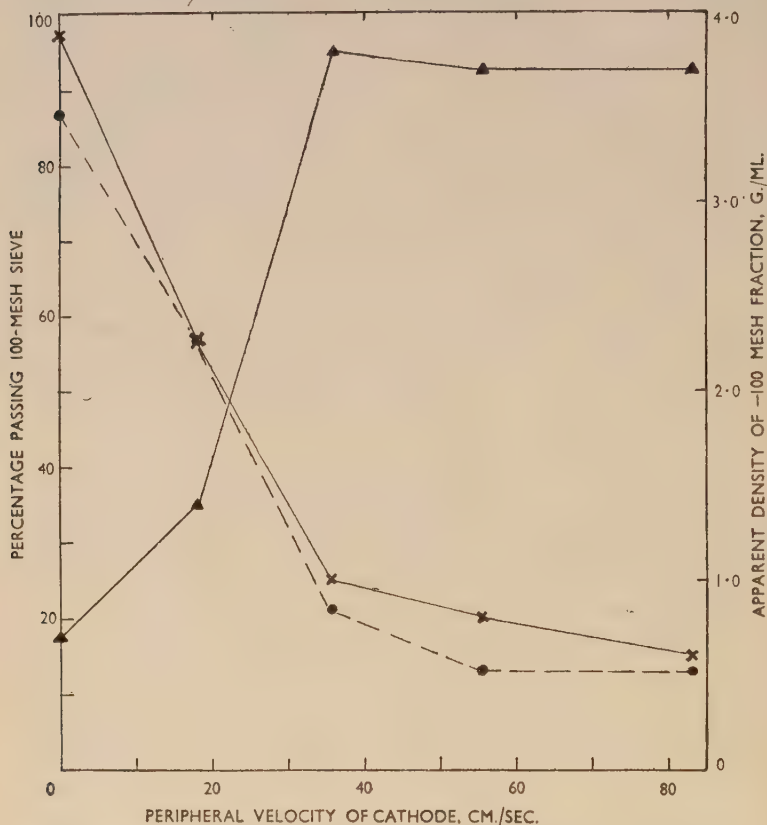


FIG. 3.—Effect of Rotation of the Cathode. (Product removed from cathode every 3 min.)

KEY.

- × Proportion of product passing 100-mesh B.S. sieve.
- Proportion of -100 mesh fraction passing 250-mesh (Finex) sieve.
- ▲ Apparent density of -100 mesh fraction.

20 g./l. of copper as cuprous chloride, and sufficient hydrochloric acid to make the solution about 0.5*N* in acidity gave satisfactory results in some large-scale experiments, the temperature used being about 60° C., and the cathode current density about 8 amp./dm.²

3. Structure of Powders.

The powders obtained from the chloride and sulphate baths were quite different in appearance and in structure. Chloride powders had a bright metallic look and, on microscopic examination, the individual particles were found to show well defined crystal faces and to be dendritic in form (Fig. 4, Plate VII). Sulphate powders, on the other hand, were not noticeably metallic in appearance, the particles having an irregular surface with no apparent structure, and being rather nodular in form (Fig. 5, Plate VII). Examination of polished, etched sections showed that, while the sulphate particles consisted of clumps of small radiating crystallites, the chloride particles were made up of two or three relatively large crystals (Figs. 6 and 7, Plate VIII). Clearly the rate of formation of new nuclei on the cathode compared with the rate of growth of already existing crystals was greater in the sulphate than in the chloride bath. It was not possible to investigate this interesting phenomenon any further, but it may have been connected with the fact that the copper-ion concentration in the cupro-chloride solution was low but relatively constant, being controlled by the dissociation of the complex anion. The structure of the electrolytic chloride powder was similar to that reported for powders precipitated chemically from chloride solutions.⁴

4. Comparative Power Efficiencies.

The pilot plant, operating with an acid sulphate electrolyte under the optimum conditions specified above, gave an average power efficiency over long periods of 3.53 kWh./kg. of dry powder produced.¹⁰ The cells were water-cooled to keep them at the operating temperature. Two small batches of powder were made on a 500-amp. cell, using a chloride electrolyte under the conditions specified above. The energy dissipated as heat in the solution was insufficient to maintain the bath temperature at 60° C. without using some form of auxiliary heating. The power consumption, ignoring that required for maintaining the temperature of the solution, was 1.14 kWh./kg. in one experiment and 0.77 in the other. The experimental cell was not identical in form with those used on the plant, but there was no doubt that higher power efficiencies could be obtained with the chloride bath. This was partly due to the lower voltage drop across the chloride cell and partly to the much higher cathode current yields, which approached the theoretical value expected for the deposition of cuprous ions.

5. Stability of Powders.

A large number of copper powder samples were examined during the course of this work, and all of them were found to be unaffected by prolonged storage in a dry atmosphere. The change in colour observed for certain powders stored in the laboratory atmosphere was due to surface oxidation, a type of reaction which only occurs at room temperature in the presence of water vapour.

The earliest stability tests were carried out on samples supplied from the pilot plant. It was found that most batches which had been heat-treated in a reducing atmosphere below 550° C. were unstable, while very few of those heat-treated above 650° C. failed to satisfy the stability test. These heat-treatments had been carried out in a continuous furnace using an atmosphere of cracked ammonia. Different results were, however, obtained when samples of sulphate powder were heat-treated in a laboratory furnace using a purified hydrogen atmosphere (Table III). In these experiments the propor-

TABLE III.—*Effect of Heat-Treatment Temperature on Stability.*
(Laboratory furnace, purified cylinder hydrogen atmosphere.)

Powder A—42 samples.

Temperature Range, °C.	Stable, %	Unstable, %	Ratio Stable : Unstable
200°–400°	21·4	11·8	1·81
400°–600°	33·4	2·4	13·80
600°–800°	26·2	4·8	5·45
Total	81·0	19·0	4·26

Powder B—65 samples.

Temperature Range, °C.	Stable, %	Unstable, %	Ratio Stable : Unstable
200°–400°	17·8	3·6	5·00
400°–600°	38·4	1·8	21·50
600°–800°	31·2	7·2	4·38
Total	87·4	12·6	6·91

tion of stable samples was high at all annealing temperatures. There was a barely significant increase in the proportion of unstable specimens when powder A was treated at temperatures in the 200°–400° C. range, but otherwise the observed differences were not statistically significant on an 0·05 level. There was no marked difference between the two untreated powders as far as stability was concerned.

In order to investigate this discrepancy, experiments were carried out using the same annealing atmosphere in the laboratory furnace as had been used in the plant furnaces. This was prepared by passing cylinder ammonia over a heated catalyst in an I.C.I. cracking unit, and contained nitrogen and hydrogen with possibly a trace of free ammonia. It was completely free from oxygen and water vapour, unlike the purified cylinder hydrogen which may have contained small traces of these substances. Table IV shows that samples treated under these conditions were less stable than samples treated under similar conditions in hydrogen. The stability was improved by saturating the cracked gas with water and drying over calcium chloride, this procedure introducing a pressure of water vapour equal to that over anhydrous calcium chloride and removing any ammonia present.

TABLE IV.—*Composition of Annealing Atmosphere and Effect on Stability.*

Annealing Atmosphere (see key below)	Temperature Range, °C.	Stable, %	Unstable, %	Ratio Stable : Unstable	Number of Specimens
I	200°-400°	18.2	6.1	3.0	
	400°-600°	37.8	0.0	∞	
	600°-800°	28.8	9.1	3.2	
	Total	84.8	15.2	5.1	33
II	200°-400°	0.0	22.2	0.0	
	400°-600°	11.1	27.8	0.4	
	600°-800°	11.1	27.8	0.4	
	Total	22.2	77.8	0.29	18
III	200°-400°	15.0	10.0	1.5	
	400°-600°	40.0	5.0	8.0	
	600°-800°	20.0	10.0	2.0	
	Total	75.0	25.0	3.0	20
IV	200°-400°	0.0	28.6	0.0	
	400°-600°	0.0	28.6	0.0	
	600°-800°	42.8	0.0	∞	
	Total	42.8	57.2	0.75	14

KEY TO ANNEALING ATMOSPHERES.

- I. Purified cylinder hydrogen.
- II. Cracked ammonia.
- III. Cracked ammonia saturated with water vapour and dried over calcium chloride.
- IV. Purified cylinder hydrogen containing 0.1 vol.-% of added ammonia. Tested for 2 weeks only.

This increase in stability was not due to any scrubbing action by passage through a long purifying train, since passage of the gas through an empty train before it entered the furnace produced no improvement. These observations can be explained in two ways:

- (i) The traces of water vapour and oxygen possibly present in the purified cylinder hydrogen may have caused the formation of a thin protective film of oxide on the surface of each particle, cf. the bright annealing process for copper. No such film could have been formed by the dry oxygen-free cracked ammonia, though it could conceivably have formed after the gas had been saturated with water vapour and dried.
- (ii) When gaseous ammonia is passed over heated copper the surface becomes pink and spongy owing to the formation of copper nitride and its subsequent reduction by hydrogen derived from partial cracking of the ammonia at the metal surface. If ammonia had been present in the cracked gas used, the resulting increase in surface area of the powder might account for the decrease of stability.

A choice between these two hypotheses could have been made, but for the use of calcium chloride as a drying agent. No cracking unit was available at the time to permit the repetition of these experiments using a drying agent which would not react with ammonia, but two sets of experiments were carried out with powder *B* which suggested strongly that the second hypothesis was the correct one. Cylinder hydrogen was purified as described, and dried as thoroughly as possible, phosphorus pentoxide being used in the final drying stage. No change in the stability of the copper samples annealed in these experiments was observed. Further experiments were then carried out using a stream of hydrogen, purified and dried as in the majority of experiments, to which 0·1 vol.-% of dry gaseous ammonia had been added. The proportion of stable samples fell sharply, as can be seen from Table IV. These results suggest that the high proportion of unstable samples obtained from material annealed at low temperatures on the pilot plant was due to the presence of ammonia in the reducing atmosphere, the ammonia producing a reactive surface on the powder particles by alternate formation and decomposition of copper nitride.

6. *Chemical Stabilization.*

In addition to studying the possibility of stabilization by controlling the conditions of heat-treatment, a number of substances were tested as antioxidants. Samples of a sulphate powder known to be unstable were stirred with a dilute solution of the substance in a

suitable solvent, filtered, and washed with the solvent until all the excess addition agent was removed. The moist powders were then dried in vacuum. Results are shown in Table V, the term "good"

TABLE V.—*Organic Stabilizers.*

Antioxidant Substance	Concentration, wt.-% in Applied Solution	Solvent	Result
Nonoxol DCP	0·25	Alcohol	Good
Nonoxol D	0·25	Alcohol, benzene	Good
Disalicyl ethylene diamine	0·125	Alcohol	Good
Diphenyl <i>p</i> -phenylene diamine	0·25	Benzene	Poor
β -Naphthol	0·25	Hot water	Good
Hydroquinone	0·25	Water	Moderate
Bedafln HN	0·25	Aqueous ammonia	Good
Stearic, oleic, linoleic, ricin- oleic acids	0·25	Alcohol, aqueous ammonia	Good
Sodium soap	0·25	Water	Good

signifying that no appreciable deterioration occurred on storage in a 75% humid atmosphere for 1 month, "moderate" that some discolouration occurred, and "poor" that little improvement was observed.

The stabilized powders (apart from that treated with hydroquinone) differed from the unstabilized powders in that they were not wetted by water. Evidently the stabilizer had formed a water-repellent film on the surface of each particle. This was shown to be a monolayer in the case of stearic acid, by determining the minimum amount of the acid which was required to render unwettable a sample of powder whose surface area had been determined independently by a permeability method. It was found that the powder would disperse in water if less than 0·05 g. of stearic acid/100 g. of dry powder were used in the ammoniacal solution applied to it. Using this figure, and the cross-sectional area of the stearic acid molecule quoted by Adam,¹¹ the surface area of the powder was calculated to be 0·4 m.²/c.c., which compared favourably with the independent value of 0·275 m.²/c.c. The stabilized particles were therefore shown to be covered with a single layer of stearate ions, the carboxyl groups being next to the metal and the hydrocarbon chains lying perpendicular to the surface.¹² The other effective stabilizers (except hydroquinone) presumably acted in a similar manner.

The most promising material for large-scale use was stearic acid dissolved in ammonia (i.e. ammonium stearate in excess ammonia), since it was cheap and did not require the use of organic solvents. A few 20-kg. batches were made by adding the stearate solution to

powder from pilot-plant cells which had been washed free from electrolyte. After washing free from excess stearate, the powder was dried in steam-heated vacuum ovens. It oxidized slightly during drying, but was water-repellent. The colour was considerably improved, and the water-repellent properties retained, by a low-temperature anneal (below 300° C.) in hydrogen, the resulting powder being stable. This process of stabilizing, drying, and heat-treating at a low temperature in hydrogen appeared to be a practical method of producing a stable, oxide-free material, but it was never worked on a large scale.

It was also found possible to stabilize a powder by mixing it with dry stearic acid or zinc stearate in small amounts, the mixing being most conveniently carried out in an empty ball mill. The chief objection to the process was that the flowing properties of the treated powder were poor, the deterioration being more marked than would have been expected from the slight increase in the proportion of "fines" during the milling. However, this was probably not as important as it appeared, since stearates are frequently used as die lubricants, being mixed with the powder before pressing. Powders stabilized by the wet processes described above have flow properties similar to the original material.

7. Physical Properties.

Some degree of sintering occurred at the higher temperatures (up to 750° C.) at which the heat-treatment experiments were carried out. Measurements of the depth of penetration of a loaded needle into the heat-treated powder showed that slight sintering occurred at 300° C. Thereafter the penetration of the needle decreased steadily up to 650° C., the rate of increase then tending to fall off to some extent; there was no indication of any sudden change.

No marked changes occurred during heat-treatment in the apparent density, the flow time, or the size-distribution of the powders, except for those powders which had sintered sufficiently to require breaking down in an impact mill. The final product was then finer and denser than the original with a similar flow time. The results were similar for powders *A* and *B*.

8. Moulding Properties.

Samples annealed at temperatures between 200° and 750° C., using the four standard conditions of heat-treatment, were prepared from both the experimental powders. The physical properties and the stability were examined as indicated above, and sintered compacts made from each. The densities of these were measured before and



FIG. 4.—Appearance of Powder Particles.
Chloride powder. $\times 20$.

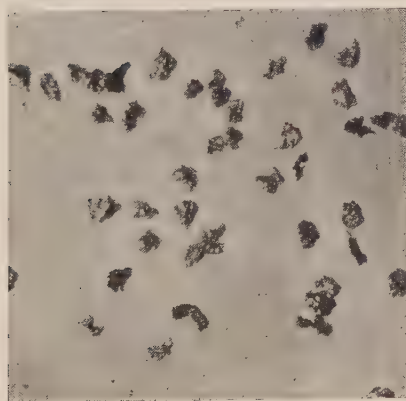


FIG. 5.—Appearance of Powder Particles.
Sulphate powder. $\times 20$.

[To face p. 32.



FIG. 6.—Structure of Powder Particles. Etched section of sulphate powder.
Etched in H_2O_2 + ammonia. $\times 200$.



FIG. 7.—Structure of Powder Particles. Etched section of chloride powder.
Etched in H_2O_2 + ammonia. $\times 200$.

after sintering, together with the tensile strength of the sintered compacts. The relationships between annealing conditions and properties of the compacts were not simple; samples of the same powder annealed under apparently identical conditions often gave compacts of different densities and strengths. These variations, which were in general more marked for powder *B* than powder *A*, did not obscure the general statistical relationships between annealing conditions and properties. Accordingly, the results have been expressed by calculating certain statistics from each set of data, namely the linear regression equation of the measured property on the temperature of annealing, and the correlation coefficient between these quantities. The first gives what may be regarded as the average value of the property for a given value of the temperature, and the second a numerical estimate of the closeness of the relationship.¹³ The correlation coefficient may vary between 0 and 1, a zero value indicating that the two variables are independent, and a high value that they are closely related.

The densities of the unsintered compacts pressed at 24 tons/in.² were positively correlated to some extent with the annealing temperature (correlation coefficients about 0.5 for both powders). Compacts from powder *A* were denser than those from *B*, the average increase in density with annealing temperature being about the same for both (0.05 g./ml. for an increase of 100° C.). The results on 50-ton compacts were similar, the average density being about 0.8 g./ml. higher than for the 24-ton compacts.

The tensile-strength results for the above compacts sintered at 1000° C. are shown in Figs. 8 and 9. Considering all the results for each powder it may be seen that the annealing temperature was more closely correlated with the strength of the sintered compact for powder *A* than for *B*, i.e. effects other than that of the annealing temperature were apparently more important for *B* than for *A*. The variables were most closely correlated for the slowly cooled samples of *A*, indicating that the full effect of the heat-treatment was not produced after only 2 hr. in the heated zone. In addition to this closer correlation for *A*, the average strength of the compacts from this material was greater than for those from *B*; in particular, there was no sample which gave a very low or zero-strength compact on sintering as did certain samples of *B*.

Compacts were also pressed from annealed samples of *A* at 50 tons/in.², sintered under the standard conditions, and the tensile strength measured. The results differed from those obtained for the 24-ton compacts, as can be seen from Fig. 10. When the annealing temperature was below 500° C., the effect on the tensile strength of the

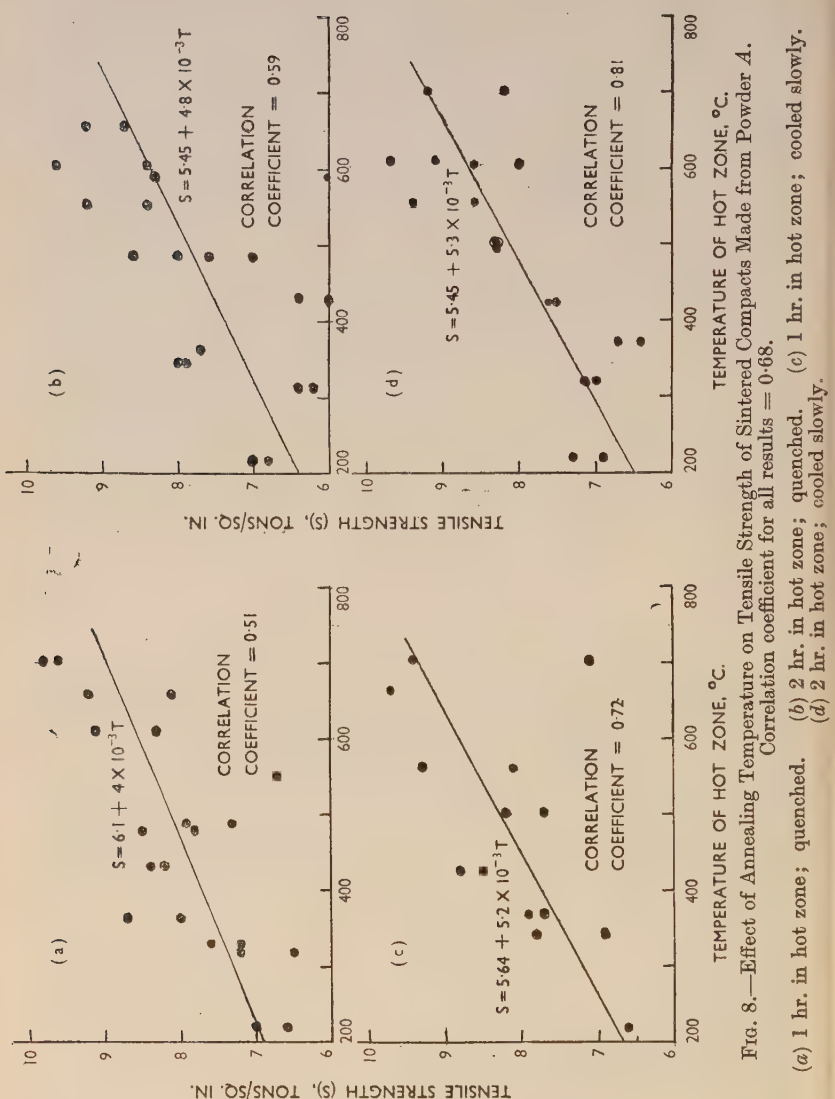


Fig. 8.—Effect of Annealing Temperature on Tensile Strength of Sintered Compacts Made from Powder A.
Correlation coefficient for all results = 0.68.

- (a) 1 hr. in hot zone; quenched.
- (b) 2 hr. in hot zone; quenched.
- (c) 1 hr. in hot zone; cooled slowly.
- (d) 2 hr. in hot zone; cooled slowly.

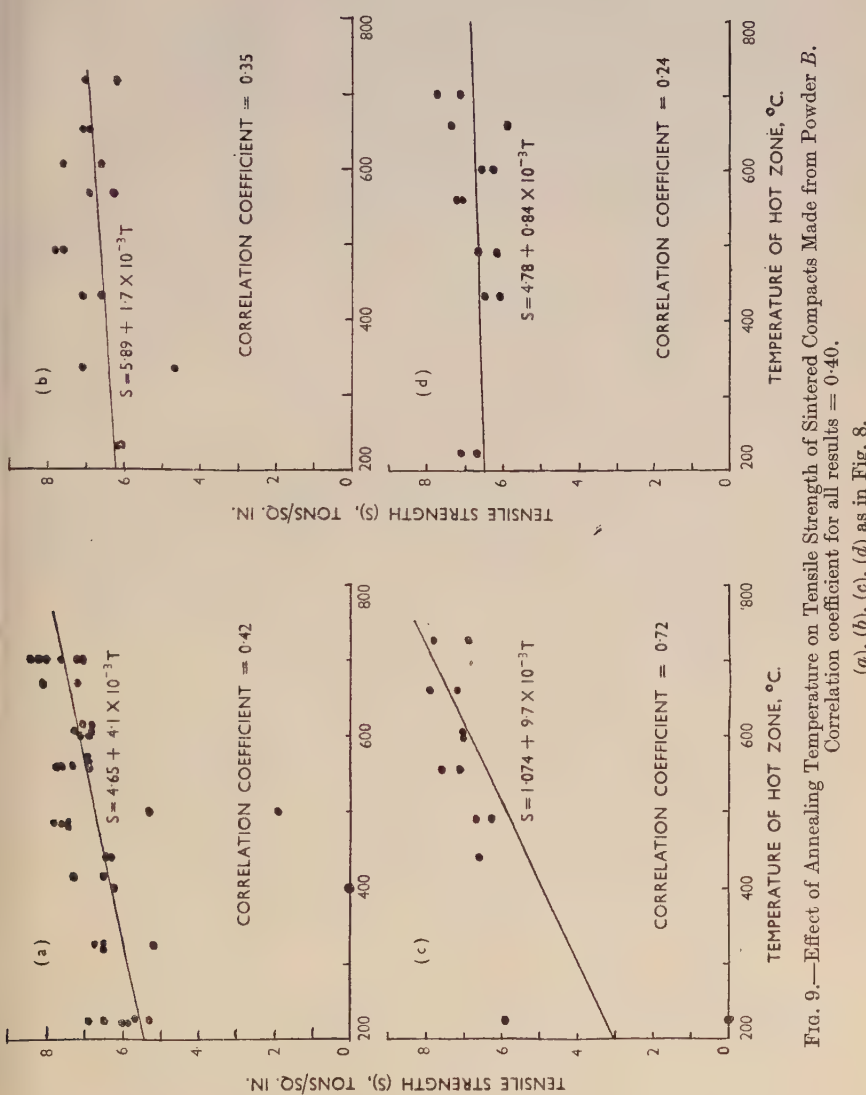


Fig. 9.—Effect of Annealing Temperature on Tensile Strength of Sintered Compacts Made from Powder B.
 Correlation coefficient for all results = 0.40.
 (a), (b), (c), (d) as in Fig. 8.

final compact was small; in general, these compacts were weaker than the corresponding 24-ton compacts. Above 500° C. the effect of the annealing temperature was very marked, and the strengths of the 50-ton compacts from samples annealed at 700° C. were comparable with those of the corresponding 24-ton compacts.

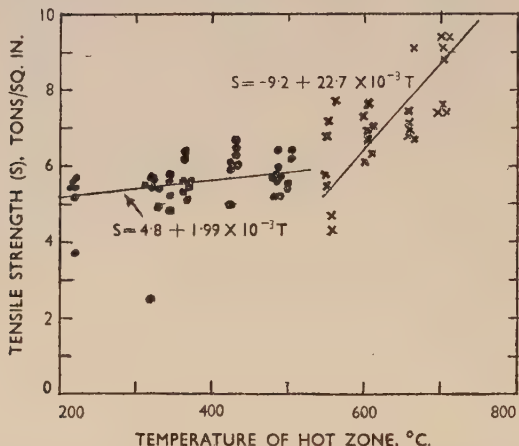


FIG. 10.—Effect of Annealing Temperature on Tensile Strength of Sintered Compacts of Powder A, Pressed at 50 tons/in.² (All results, irrespective of annealing time and method of cooling.)

Samples annealed at and below 500° C. Correlation coefficient = 0.28.
Samples annealed above 500° C. Correlation coefficient = 0.76.

The effect of varying size-distribution on the tensile strength of 24-ton compacts from powder B was tested by hand sieving and blending the resulting sieve cuts to give three powders of different size gradings. Table VI shows that the strongest compacts were on the

TABLE VI.—Effect of Particle-Size Distribution on Tensile Strength.
(Compacts prepared at 24 tons/in.² pressure.)

Heat-Treatment Temperature, °C.	320°			485°			585°		
	1	2	3	1	2	3	1	2	3
Blend									
Mean Tensile Strength, tons/in. ²	...	5.2	6.7	5.7	7.2	6.3	7.0	8.0	9.1

Note : The blends were made from powder B as follows :

		Blend 1	Blend 2	Blend 3
Wt.-% + 100 mesh B.S. sieve	.	40	20	5
Wt.-% — 100 + 150 "	.	30	30	30
Wt.-% — 150 + 200 "	.	15	20	25
Wt.-% — 200 "	.	15	30	40

whole given by the finest powders. The tests were not, of course, very extensive.

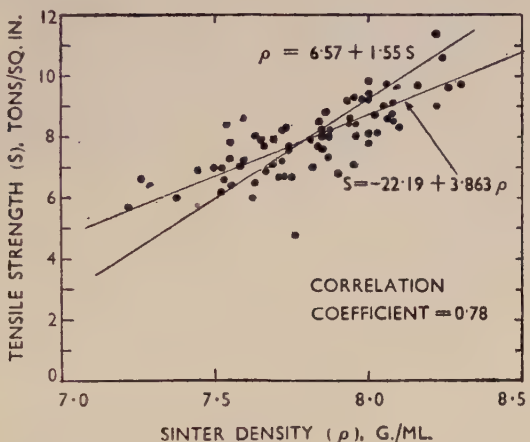


FIG. 11.—Tensile Strength and Density of Sintered Compacts of Powder A, Prepared at 24 tons/in.² Pressure.

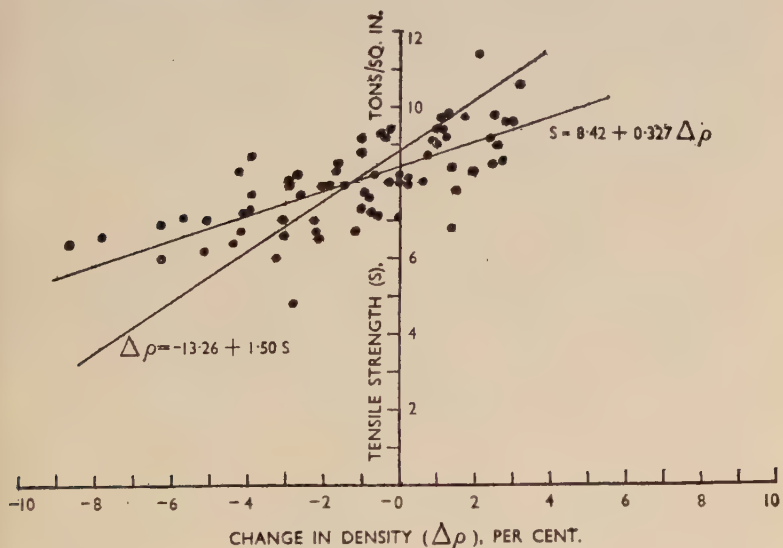


FIG. 12.—Tensile Strength and Change in Density on Sintering Compacts of Powder A, Prepared at 24 tons/in.² Pressure.

During the process of sintering the dimensions of the compact usually changed. Since the change in weight during sintering was

negligible, the dimensional changes were followed by measuring the change in density. The most detailed results were obtained for 24-ton compacts prepared from powder *A*, the relationships between tensile strength and sintered density, and tensile strength and percentage change in density being shown in Figs. 11 and 12. It can be seen that both these pairs of variables were closely correlated, the highest-strength compacts being those with the highest sinter densities, the density having increased on sintering. The results on 50-ton compacts were similar.

9. Heat-Treatment of Chloride Powders.

All the above-mentioned data on heat-treatment apply to sulphate powders. A small batch of chloride powder prepared as described (p. 18) was also examined. After removing the portion retained on a 100-mesh sieve, 63% of the powder passed a 250-mesh sieve, the apparent density of the -100 fraction being 1.5 g./ml. Heat-treatment in hydrogen for 1 hr. at temperatures up to 615° C. increased the density up to a maximum of 1.8 g./ml., and reduced the proportion of the -250 fraction to 29%. The density of the green compacts pressed at 24 tons/in.² varied from 7.9 g./ml. (225° C. anneal) to 8.1 g./ml. (615° C.), the density increasing on sintering at 1030° C. for 30 min. by about 0.5 g./ml. The lowest tensile strength recorded was 11.2 tons/in.², and the highest 13.9 tons/in.². This particular chloride powder, therefore, was capable of giving sintered compacts, under the conditions stated, with strengths up to 91% of that of massive copper, a figure higher than that attained with either of the sulphate powders examined.

IV.—DISCUSSION.

The preparation of copper powder of uniform quality by electrolysis required a close control of cell operation. In addition to the usual variables of cathode current density, bath composition and temperature, and degree of agitation, small changes in the rate at which the powder was removed from the cathode had an appreciable effect on the particle-size distribution. This, and the apparent density of the powder, could be varied independently to some extent, though it was generally true to say that as the bath conditions approached those normally used in electroplating, the powder became coarser and denser, provided that it was removed at a constant rate from the cathode. More frequent removal gave a finer powder, the density not being much affected. The reason for the partial independence of the size distribution and the apparent density was due to the fact that the latter depended on the shape and porosity of the powder

particles as well as on their size. In the case of the sulphate electrolyte the cell conditions for the production of a usable powder were more critical than for the chloride solutions. In the former, decrease in temperature or in copper concentration, increase in acidity or cathode current density gave a light, fluffy powder, while too great a change in the opposite direction gave rough adherent deposits of copper plate. On the other hand, it was found to be virtually impossible to obtain coherent plate from chloride electrolytes, though naturally the nature of the powder formed varied with the cell conditions. According to Leadbeater,¹⁴ an acid sulphate electrolyte, 3*N* in sulphuric acid, and containing 8–23 g./l. of copper was used in Germany for the production of copper powder, the cathode current density being 32 amp./dm.² The power consumption under these conditions was 2.96 kWh./kg., which is similar to the figure of 3.53 kWh./kg. obtained on the pilot plant which was quoted earlier. Both these figures are higher than those obtained in the preparation of two large batches from a chloride electrolyte, namely 1.14 and 0.77 kWh./kg.

The moulding properties of the sulphate and chloride powders referred to in the present work varied considerably. Material prepared from a glue-free sulphate electrolyte was better than that prepared from one containing glue, while that made from a chloride electrolyte was appreciably better than either. The difference between the two sulphate powders was apparently due to the presence of co-deposited glue in the second; this may have segregated at the grain boundaries, preventing or hindering recrystallization during heat-treatment. There was a striking difference in the structure of the sulphate and chloride powders, the particles of the latter being formed of a few large crystals instead of a multitude of small ones, and this probably accounted for the differences in pressing properties.

On the whole, therefore, it seems probable that the cupro-chloride would be more satisfactory for the large-scale production of copper powder, since the power costs were lower, the cell conditions less critical, and the product of better quality. It has not, however, been possible to test this conclusion by operating a suitable plant unit over a long period.

The difficulties encountered in the storage of certain samples of sulphate copper powder could be avoided by enclosing a desiccant in the powder container, since no deterioration occurred in a dry atmosphere. Chemical stabilization by application of a mono-layer of a suitable organic compound such as stearic acid, or simply by mixing with stearic acid or zinc stearate was also successful. The essence of this process appeared to be the "waterproofing" of the surface and

the consequent prevention of the formation there of an adsorbed water layer, this probably being an essential preliminary to the oxidation which was responsible for the discoloration of the powder. Experiments on the heat-treatment of sulphate powders showed that the stability of the annealed sample was affected to some extent by the temperature of annealing, a low-temperature anneal in a reducing atmosphere being likely to give an unstable material. The most important factor was, however, the nature of the annealing atmosphere. Unstable samples were rarely obtained when purified cylinder hydrogen was used, the proportion increasing markedly especially at the lower annealing temperatures, when cracked ammonia was substituted. Addition of a trace of dry ammonia to hydrogen had the same effect, and it was concluded that the presence of this compound was responsible for the instability of samples annealed in cracked ammonia, possibly because of the increased surface area resulting from reaction between the copper and ammonia.

The powders sintered to some extent during the heat-treatment process. The degree to which this occurred increased with the temperature of annealing, slight cohesion being found in samples annealed at 300° C. There was no evidence that any sudden change occurred as the temperature increased, the sintered cake of powder becoming steadily more difficult to break down until, at temperatures of 650° C. or over, it was necessary to give it a light grinding in an impact mill. This tendency to sinter slightly on annealing made it impossible to ensure that the annealed samples from the same batch of powder possessed an identical size distribution; in addition, the particles of the samples which had been milled had probably been distorted slightly. This may have accounted for the fact that the relationships between the properties of the compacts and the annealing temperature were of a statistical nature, the spread of the results being rather large. On the average the green density and the tensile strength increased with the annealing temperature. Compacts prepared from the powder containing glue were weaker and lighter than corresponding compacts from a glue-free powder, the temperature of annealing being less important in determining the final properties. In addition, several compacts of zero strength were obtained from the former (powder *B*), and it may be concluded that the practice of adding glue to the electrolyte produced an inferior powder.

A number of compacts were prepared from powder *A* by pressing at 50 tons/in.² These were denser than the corresponding 24-ton compacts, but the tensile strengths after sintering were usually less. The annealing temperature, if 500° C. or below, scarcely affected the

strength of the sintered compact; this was always considerably less than that of the corresponding 24-ton compacts. Above 500° C. the strength increased with annealing temperature, until at 700° C. there was no difference between the two series. Since the powders annealed at the higher temperatures gave compacts of similar strength, the discrepancy at the lower temperatures could not have been due to differences in the pressing operations. The density of the low-strength compacts decreased considerably on sintering, and it seemed that the effect was due to the presence of adsorbed gas on the annealed powders; the amount adsorbed must be assumed to have decreased as the annealing temperature increased above 500° C. The 24-ton compacts were initially less dense, and therefore more porous, than the 50-ton compacts, and most of the gases evolved during sintering could escape without expanding the compact unduly, if at all. This was not possible in the case of the 50-ton compacts which were swollen by the expansion of the trapped gases during sintering, losing strength because of their higher porosity. Cook and Pugh⁴ found a similar phenomenon occurring in certain instances when using an electrolytic powder annealed at 300° C. in hydrogen, the strength of sintered compacts prepared at high pressures being less than that of those made at low pressures. They explained their results in a similar way. It is important that they found the sintering temperature to affect the results, and the above analysis of the effect of annealing temperature on the properties of the sintered compacts is therefore incomplete, since all compacts prepared from sulphate powders were sintered at one temperature.

ACKNOWLEDGEMENTS.

The author's thanks are due to his colleagues for their help and advice, to the Alkali Division of Imperial Chemical Industries Ltd. for carrying out a determination of the surface area of a copper powder sample, and to the Dyestuffs Division for suggesting and supplying many of the substances used in the stabilization experiments. He is particularly indebted to Mrs. Dickenson and to Mr. J. Keogh for pressing, sintering, and carrying out tensile-strength measurements on the compacts.

REFERENCES.

1. British Patent No. 264,116, 1926.
2. British Patent No. 558,722, 1942.
3. "Modern Electroplating". New York : 1942 (Electrochemical Society).
4. M. Cook and C. F. Pugh, *Iron Steel Inst. Special Rep.* No. 38, 1947, 162.
5. P. Bradley and J. Mitchell, unpublished work.
6. "Standard Methods of Testing Petroleum and its Products". 8th edition. London : 1947 (Institute of Petroleum).

42 Heat-Treatment of Electrolytic Copper Powder

7. P. P. Feodotieff, *Z. anorg. Chem.*, 1928, **173**, 81.
8. C. A. Littler with H. V. Tartar, *Trans. Electrochem. Soc.*, 1938, **74**, 533.
9. J. V. Petrocelli, *Trans. Electrochem. Soc.*, 1939, **77**, 133.
10. P. Harrower, unpublished report, I.C.I. General Chemicals Division.
11. N. K. Adam, "The Physics and Chemistry of Surfaces". 3rd edition, p. 50. London : 1941 (Oxford University Press).
12. L. H. Germer and K. H. Storks, *J. Chem. Physics*, 1938, **6**, 280.
13. G. U. Yule and M. G. Kendall, "Introduction to the Theory of Statistics". 13th edition, p. 209; London : 1945 (Charles Griffin & Co. Ltd.).
14. C. J. Leadbeater, *Iron Steel Inst. Special Rep.* No. 38, 1947, 191.

THE THERMAL PROPERTIES AND CHILLING 1209 POWER OF SOME NON-METALLIC MOULD MATERIALS.*

By R. W. RUDDLE,† M.A., A.I.M., MEMBER, and A. L. MINCHER,‡ B.Sc., STUDENT MEMBER.

(Communication from the British Non-Ferrous Metals Research Association.)

SYNOPSIS.

The earlier sections of the paper are devoted to a brief mathematical treatment of the flow of heat in moulds of low thermal conductivity and to a review of existing information relevant to the subject.

The experimental work, described in the main part of the paper, was carried out with the dual objects of (*a*) testing the validity of the mathematical treatment, and (*b*) determining the chilling powers of the materials examined. Cylinders, 5 in. in dia. \times 10 in. long, were cast in moulds made in each of the following materials: synthetic sand (green and dry), naturally bonded sand (green and dry), bonded magnesite, bonded silicon carbide, and plaster. The casting was made in different alloys to examine the influence of freezing temperature on the heat flow in the different moulds. During the solidification of the castings heating curves were taken at various points in the moulds and the temperature distributions thus obtained experimentally were compared graphically with those predicted by mathematical analysis. Good agreement was found with most of the dry moulds. The mathematical treatment could not be applied to the green moulds, but the rate of heat extraction by these moulds was found directly from the experimental temperature-distribution curves. The rate at which all the moulds removed heat from the casting was found to be greatest when metals of high freezing temperature were cast; this is due primarily to the steeper temperature gradient in the mould, but is also in part caused by intergranular radiation which increases the apparent thermal conductivity of the mould at high temperatures.

Approximate figures have been derived for the following thermal constants of the dry moulds: temperature diffusivity, apparent thermal conductivity, heat diffusivity, and "mould constant". Figures are also given for the "mould constants" of the green moulds. It is shown that these constants may be used to calculate the freezing times of simple castings with fair accuracy.

I.—INTRODUCTION.

THIS research, which forms part of a long-term study of the solidification of castings, was undertaken in order to obtain fundamental information on the rate at which a mould will remove heat from the metal cast

* Manuscript received 12 March 1949.

† Head of Melting and Casting Section, British Non-Ferrous Metals Research Association, London.

‡ Formerly Research Bursar, British Non-Ferrous Metals Research Association, London.

Note.—The results of this work were made available to members of the British Non-Ferrous Metals Research Association in a confidential report issued in July 1948.

therein. The importance of this knowledge to any study of the solidification of castings does not require stressing, for it is clear that the phenomena which occur during the solidification of a mass of pure metal or alloy are closely dependent upon the rate at which the latent heat of fusion is extracted from the metal. A knowledge of the heat-extractive properties of mould materials may also be of more immediate practical importance, by providing data on the relative chilling capacities of the materials, which data may be used in a more or less qualitative manner in industrial foundry practice. Furthermore, if it were possible to calculate the progress of solidification in a casting, the design and proper disposition of gates and feeders would be facilitated; this is the ultimate object of the research.

In Section II of the paper is described a mathematical treatment of the problem of the extraction of heat from a casting by a plane mould wall, supposed semi-infinite. The results of other investigations of the thermal properties of non-metallic mould materials and the rate of heat extraction by such moulds are critically reviewed in Section III.

The technique and results of experiments in which heating curves were taken in moulds made in several different materials of low and moderate chilling power are described in Sections IV and V. Bearing in mind the ultimate aim of the research, the immediate object of this experimental work was two-fold. First, it was desired to determine how far the mathematical treatment given in Section II could be applied to a real mould of finite size consisting of an agglomeration of discrete particles, as opposed to an idealized isotropic and homogeneous material semi-infinite in extent; and, if applicable, to put this theoretical treatment on as firm a basis as possible. The second object of the research was to obtain some idea of the chilling powers and thermal constants of the materials examined and of their dependence upon temperature. It was hoped that the constants thus approximately determined, together with data provided from other sources, would enable calculations of the heat-extraction rates by moulds and of the freezing times of castings to be made with a reasonable degree of accuracy.

II.—BASIC THEORY OF HEAT FLOW IN MOULDS.

The amount of heat extracted by a mould from unit surface area of a casting at a given time after pouring is equal to the product of the specific heat, density, and temperature* of the mould integrated over that volume of the mould which has risen appreciably in temperature;

* Expressed as temperature above the initial temperature of the mould.

correspondingly, the rate of heat extraction of the mould is the differential, with respect to time, of this product. In a given instance the rate of heat extraction may be found by multiplication of the areas under a series of experimentally determined temperature-distribution graphs by the specific heat and density. Results obtained in this way, however, are only valid for the particular conditions existing when the measurements are made, and are not of general applicability; if, for example, another casting were made using a metal of different freezing point it would be necessary to repeat the temperature measurements under the new set of conditions.

Fortunately the problem is to some extent amenable to mathematical treatment which, in part at least, overcomes the difficulty described above. It may be shown¹ that the change in temperature of an element of dimensions $2dx$, $2dy$, and $2dz$, of a homogeneous, isotropic solid through which heat is flowing is given by :

$$\frac{\partial \theta}{\partial t} = \frac{K}{\rho c} \left(\frac{\partial^2 \theta}{\partial x^2} + \frac{\partial^2 \theta}{\partial y^2} + \frac{\partial^2 \theta}{\partial z^2} \right) = \frac{K}{\rho c} \cdot \nabla^2 \theta \quad \dots \quad (1)$$

where θ = temperature of element,

t = time,

K = thermal conductivity of the solid,

ρ = density of the solid,

and c = specific heat of the solid.

The quantity $K/\rho c$ is designated the temperature diffusivity of the solid and is frequently represented by α .* For heat conduction in one direction the equation reduces to :

$$\frac{\partial \theta}{\partial t} = \alpha \cdot \frac{\partial^2 \theta}{\partial x^2} \quad \dots \quad (2)$$

It may also be shown¹ that, if the plane boundary of a semi-infinite solid body initially at a temperature θ_0 is instantaneously raised to a temperature θ_1 at time $t = 0$, then after time t the temperature θ of any point whose perpendicular distance from the boundary is x , is given by :

$$\theta = \theta_0 + (\theta_1 - \theta_0) erfc \left(\frac{x}{2\sqrt{\alpha t}} \right) \quad \dots \quad (3)$$

where :

$$erfc(x/2\sqrt{\alpha t}) = 1 - erf(x/2\sqrt{\alpha t}) = 1 - \frac{2}{\sqrt{\pi}} \int_0^{x/2\sqrt{\alpha t}} e^{-\beta^2} d\beta$$

* In this country $\alpha = K/\rho c$ is usually termed the "thermal diffusivity"; in this paper α is called the "temperature diffusivity" in accordance with German practice, to distinguish it from the related quantity $b = \sqrt{K\rho}$, which is named the "heat diffusivity".

and α is the quantity defined in equation (2). The integral $erf x$ is known as the error function and its properties are briefly described in the Appendix (p. 89).

Equation (3) may be applied to the problems of a mould absorbing heat from a solidifying casting provided the following assumptions are made :

- (a) That the temperature of the interface between the metal and the mould remains sensibly constant throughout the solidification period.
- (b) That the temperature diffusivity α of the mould material is sensibly independent of temperature.
- (c) That errors introduced by non-homogeneity of the mould are not large.
- (d) That the error introduced by the finite size of the mould wall is not large (equation (3) is theoretically only valid for a mould wall of infinite thickness and area).

The validity of these assumptions and the errors introduced by them are considered later in the discussion of the experimental results obtained.

Assuming that the distribution of temperature in the mould is given by equation (3) for any time t after the casting has been poured, up to the end of solidification, the rate, $\partial Q/\partial t$, at which heat is removed from the casting by unit area of the mould surface is given by the following expression¹ :

$$\frac{\partial Q}{\partial t} = -K \left[\frac{\partial \theta}{\partial x} \right]_{x=0}$$

and by differentiation of equation (3) :

$$\frac{\partial Q}{\partial t} = \frac{K(\theta_1 - \theta_0)}{\sqrt{\pi \alpha t}} = 0.564 \frac{K(\theta_1 - \theta_0)}{\sqrt{\alpha t}} \quad . \quad . \quad . \quad (4)$$

This expression may more conveniently be written :

$$\frac{\partial Q}{\partial t} = \frac{0.564(\theta_1 - \theta_0)b}{\sqrt{t}} \quad . \quad . \quad . \quad . \quad (5)$$

where $b = \sqrt{K\alpha}$ is termed the "heat diffusivity" of the material.

The total heat absorbed in time t by unit area of the mould surface is readily obtained by integrating equation (5) :

$$Q = b(\theta_1 - \theta_0) \int_0^t \frac{0.564}{\sqrt{t}} \cdot dt = 1.128b\sqrt{t}(\theta_1 - \theta_0) \quad . \quad . \quad . \quad (6)$$

Equation (6) is sometimes written for simplicity as :

$$Q = q\sqrt{t} \quad . \quad . \quad . \quad . \quad . \quad . \quad (7)$$

where $q = 1.128b(\theta_1 - \theta_0)$, is called the "mould constant", and is a measure of the chilling power of the mould.

Assuming the validity of the assumptions detailed above, equations (3), (5), and (6) enable the temperature distribution in, and heat extraction by, a plane mould wall to be calculated from knowledge of the three constants, thermal conductivity, specific heat, and density. Alternatively the value of the temperature diffusivity may be determined by fitting an equation of the form of equation (3) to the temperature distribution found experimentally by measurements made in the mould. Using this figure for the temperature diffusivity, the value of any one of the three basic constants may then be derived if values for the other two are known, and Q and $\partial Q/\partial t$ may be calculated by use of equations (5) and (6). This latter approach to the problem was adopted in the present work to verify the theory and to determine directly the mean values of the temperature diffusivity. The available data for the thermal properties of moulding materials are rather scanty and in many instances are of doubtful accuracy, especially at high temperatures. It was hoped that the experimentally determined diffusivities would provide a useful check on these data, and would enable estimates to be made of the thermal conductivity, which of the three basic constants is the one most likely to be affected by variations in the grain-size of the material and other factors.

III.—PREVIOUS WORK.

The earliest important investigation of the thermal properties of moulds is that carried out by Briggs and Gezelius.^{2,3} These workers cast 6-in.-dia. steel spheres in moulds made from a number of different materials and measured the rise in temperature of the mould at various distances from the metal/mould interface, expressing their results as time-temperature curves. Briggs and Gezelius grade the materials investigated in the following decreasing order of "heat transference": (1) Chamotte, (2) Downer sand (dry), (3) German Industrial Extra sand (dry), (4) green synthetic sand, and (5) cement-bonded sand. These authors base their estimate of the "heat transference" property of the moulds upon the rate of rise of temperature at locations remote from the interface; the "heat transference" is therefore related to the temperature diffusivity, but it does not follow that materials of high "heat transference" extract heat from the casting more rapidly than materials of low "heat transference". As explained above, the rate of heat extraction is dependent upon the heat diffusivity, and materials possessing high thermal conductivity combined with low specific heat

and density will have high temperature diffusivity combined with low heat diffusivity.

Briggs and Gezelius^{2,3} also present curves for the rise in temperature of a dry-sand mould during the casting of a 9-in.-dia. steel sphere, which show that the temperature at the metal/mould interface was sensibly constant for about 20 min. after casting. They state that the rates of solidification of 6-in.-dia. spheres cast in green- and dry-sand moulds were almost identical, and conclude that the heat extraction properties of green and dry sand are practically the same. This statement must be regarded with reserve since their measurements of solidification rates were taken only 2 min. after casting, when the rate of heat extraction is very high; it is not to be expected that minor variations in the rates of heat extraction would be very apparent until some while after casting. Briggs and Gezelius made no attempt to analyse their results mathematically, although many of their curves seem quite suited to such analysis.

Curves showing the temperature changes in moulds made in Ottawa sand bonded with fireclay have been published by Diercker,⁴ and Scott⁵ has presented results obtained with a steel moulding sand; again, no attempt at mathematical analysis has been made by either of these authors.

The investigation carried out by Chvorinov⁶ is apparently the only quantitative study hitherto made. This author measured temperatures at various locations in sand moulds used for steel casting, and interpreted his results by a method similar to that described above in Section II. Series of mould-heating curves are given in Chvorinov's paper, for several different shapes and sizes of sand-castings. Some curves are also presented for the heating of a mould made in magnesite brick. The author shows that the temperature-distribution graphs derived from the heating curves agree closely with the theoretical distributions obtained by plotting equation (3), provided a suitable value for the temperature diffusivity α be assumed. Chvorinov gives in this and another paper⁷ a table of the thermal properties of a few moulding materials, which is reproduced below as Table I; some of the figures for moulding sand in this table were derived from Chvorinov's temperature measurements, the remainder apparently being taken from the literature.

Chvorinov⁶ states that, while some fall in the temperature of the metal/mould interface takes place during the solidification of steel castings, the mean temperature may be used in making calculations with sufficient accuracy for all practical purposes. He further states that his experimental figures for interface temperatures agree almost exactly with those calculated on theoretical grounds; the way in which his calculations have been made is, however, not very clear.

TABLE I.—*Thermal Properties of Some Moulding Materials : Figures Quoted by Chvorinov.^{6, 7}*

Mould Material	Density, g./c.c.	Thermal Conductiv- ity, C.G.S. units	Specific Heat, cal./g./° C.	Temper- ature Diffusivity, C.G.S. units	Heat Diffusivity, C.G.S. units
Steel moulding sand	1.73	0.0018 (0.65)	0.26	0.00402 (0.00145)	0.0286 (17.1)
Chamotte brick	1.80	0.00305 (1.10)	0.26	0.00652 (0.00235)	0.0378 (22.7)
Magnesite brick	2.70	0.0083 (3.0)	0.25	0.0124 (0.00445)	0.0750 (45.0)
Silicon carbide (solid)	2.20	0.0333 (12.0)	0.22	0.058 (0.021)	0.138 (82.8)
Silicon carbide (clay- bonded)	2.00	0.0083 (3.0)	0.26	0.016 (0.0058)	0.0650 (39.0)

Figures in brackets are corresponding values expressed in metre-kilogramme-hour units, which are frequently more convenient.

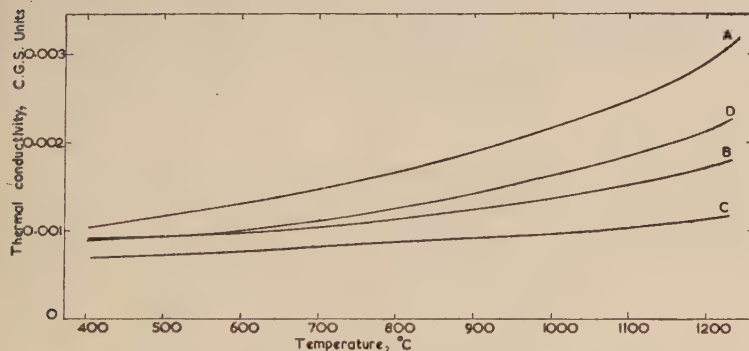


FIG. 1.—Curves Obtained by Lucks, Linebrink, and Johnson,⁸ for the Variation with Temperature of the Thermal Conductivities of Four Silica Sands : (a) Coarse Sand; (b) Medium Sand; (c) Fine Sand; (d) Mixed Sand.

The thermal conductivities of three closely graded unbonded silica sands have recently been determined over the temperature range 400°–1230° C. by Lucks, Linebrink, and Johnson.⁸ These workers obtained their figures by measuring the temperature gradient in and heat flow through a large mass of the sand, heat being continuously supplied to one face of the sand mass, and being continuously removed from the opposite face. Gradings of the three sands investigated are given in

Table II and the curves showing the variation with temperature of the thermal conductivities of the sand are reproduced in Fig. 1. This Figure shows :

(a) The marked effect of sand grain-size on conductivity, that of the coarse sand being 50% greater than the conductivity of the finest sand at 400° C. and about 160% greater at 1200° C.

(b) The way in which conductivity increases with temperature; this increase is least for the fine sand and greatest for the coarse sand, figures of about 60% and about 180%, respectively, being found over the range studied.

TABLE II.—*Gradings of Sands Studied by Lucks, Linebrink, and Johnson.⁸*

Sand A (density = 1.73 g./c.c.)		Sand B (density = 1.63 g./c.c.)		Sand C (density = 1.46 g./c.c.)	
Grading		Grading		Grading	
U.S. Standard Sieve No.	Percentage	U.S. Standard Sieve No.	Percentage	U.S. Standard Sieve No.	Percentage
—16 + 20	...	—40 + 50	...	—70 + 80	5
—20 + 25	78	—50 + 60	72	—80 + 100	76
—25 + 30	22	—60 + 70	27	—100 + 120	17
—30	...	—70 + 80	1	—120 + 140	2
...	...	—80	...	—140	...

In a later paper,²⁰ the same authors report the results of similar conductivity measurements made on a sand mixture consisting of 60% of sand A and 40% of sand C; the density of the mixture was 1.78 g./c.c. The conductivity-temperature curve for the mixture (curve D in Fig. 1) showed the same general features as the curves obtained earlier with the closely graded sands and was found to lie approximately midway between the curves for sands A and C.

Measurements of the thermal conductivity of bonded Ottawa sand have been reported by Dietert, Hasty, and Doelman.⁹ These workers measured the conductivities in the temperature range 90°–1250° C., of rammed and dried specimens of a coarse sand (—30 + 40 U.S. sieve nos.) and a fine sand (—100 + 140 U.S. sieve nos.), both bonded with 4% bentonite. The curves obtained, which are reproduced in Fig. 2, are very similar to and reveal the same general features as those obtained by Lucks, Linebrink, and Johnson,⁸ but they are all displaced in the direction of higher conductivities by a factor of about 30%. The reason for this is not clear, but the higher conductivities found by Dietert,

Hasty, and Doelman cannot be ascribed to the effect of ramming, since the densities of the bonded sands were rather lower than those of the unbonded material investigated by Lucks, Linebrink, and Johnson.⁸ Fig. 2 also shows that when the two sands had the same density the conductivity curves practically coincided, despite the disparity in grain-size. This, however, is in apparent disagreement with the results of Lucks, Linebrink, and Johnson,^{8, 20} who found the highest conductivity in their sand *A*, the mixture of sands *A* and *C* having a lower conductivity although possessing a higher density.

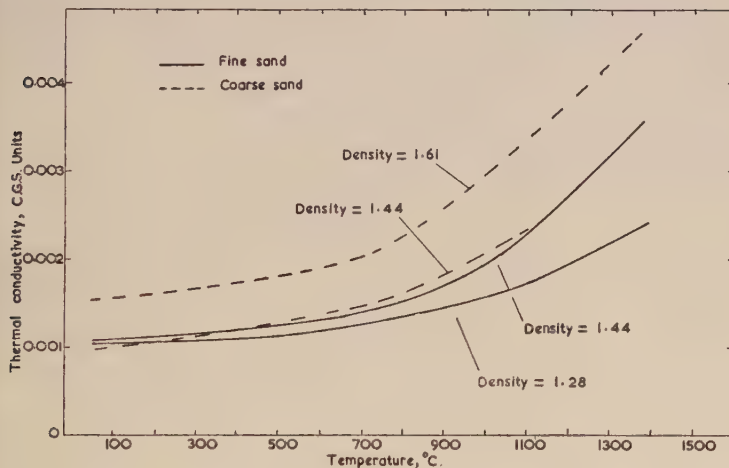


FIG. 2.—Curves Obtained by Dietert, Hasty, and Doelman,⁹ Showing the Variation with Temperature of Thermal Conductivities of Two Bonded and Rammed Sands. Figures refer to the density ρ in g./c.c.

The transmission of heat through porous solids has been treated theoretically by Russell²¹ and Eucken.²² Russell divides these materials into two classes—those consisting, to a first approximation, of discrete pores embedded in solid (continuous-solid type of material), and those consisting of an agglomeration of solid particles surrounded by air (continuous-air type of material). Neither of these two idealized types of structure has any counterpart in reality, the majority of porous substances having structures which are somewhere between the two ideal types postulated. However, a sand mass approaches the continuous-air type of structure quite closely and a theory of heat conduction based on the assumption of a continuous-air structure should be applicable without serious error.

Russell assumes that his idealized substance consists of uniformly

spaced cubic particles separated by a uniform layer of air and derives the following equation for the continuous-air structure:

$$\frac{K_b}{K_s} = \frac{K_a}{K_s} \cdot \frac{K_s/K_a(1-P)^{2/3} + 1 - (1-P)^{2/3}}{K_s/K_a[(1-P)^{2/3} - 1 + P] + [2 - (1-P)^{2/3} - P]} \quad (8)$$

where :

K_b = apparent conductivity of the aggregate,

K_s = true conductivity of the pure solid,

K_a = apparent conductivity of the air spaces,

and P = the porosity (fraction of total volume).

If K_s/K_a is greater than 20, equation (8) may be simplified, without much loss of accuracy to :

$$K_b = K_a \frac{(1-P)^{2/3}}{(1-P)^{2/3} - 1 + P} \quad \dots \dots \quad (9)$$

By use of the binomial expansion of $(1-P)^{2/3}$ equation (9) may be further approximated to :

$$K_b = K_a \left(\frac{3}{P} - 2 \right) \quad \dots \dots \quad (10)$$

It follows from equations (9) and (10) that, if in a continuous-air type of material $K_s/K_a > 20$, then the apparent thermal conductivity of the material is to a first approximation independent of the conductivity of the solid and depends only on the conductivity of the air and on the porosity.

The treatment given by Eucken²² is similar to that of Russell but postulates spherical particles instead of cubes. Use of Eucken's equation leads to results almost identical to those obtained from Russell's equation.

Since porosity is related to density, it follows from equations (9) and (10) that the conductivity increases with increasing density of the sand. This provides an explanation of the observation made by Dietert, Hasty, and Doelman,⁹ that two sands of differing grain-size had the same apparent conductivity when rammed to the same density.

At elevated temperatures, however, the simple relation between apparent conductivity and porosity, or density, is modified by the increasing part played by intergranular radiation in the transfer of heat. Assuming black-body conditions, Russell²¹ gives the following equation for the equivalent conductivity K_r of a pore due to radiation :

$$K_r = 1.36 \left(\frac{T}{100} \right)^3 x \quad \dots \dots \quad (11)$$

where T = temperature in °K.

and x = width of the pore in cm.

The value of K_r must be added to the true conductivity of the air to obtain K_a , the apparent conductivity of the pore spaces. Since K_r is proportional to T^3 it increases very rapidly with temperature, and there can be little doubt that intergranular radiation is the cause of the marked increase in the apparent conductivity of sands, above about 400° C., as shown by Figs. 1 and 2. According to equation (11) the radiation component of conductivity is proportional to the pore size; hence at elevated temperatures the apparent conductivity of a sand depends not only on density but also on grain-size. This may be the reason why, despite its greater density, the mixed sand *D* investigated by Lucks, Linebrink, and Johnson²⁰ had a lower apparent conductivity than the coarse sand *A*.

A method for the calculation of pore size has been proposed by Bell in an appendix to one of the papers²⁰ by Lucks, Linebrink, and Johnson. It is assumed that the sand consists of spheres of two sizes having radii R and r ; f is the fraction of the total weight of sand which consists of spheres of radius R . The pore size is then given by :

$$x = \frac{\frac{4rP}{3}}{(1-P)\left[1-f\left(\frac{R-r}{R}\right)\right]} \quad \dots \quad (12)$$

Using this equation and Russell's equation (8), Bell has calculated the apparent conductivities of all the sands investigated by Lucks, Linebrink, and Johnson. These calculations were carried out for three different temperatures, and agreement with the observed values was good; most of the figures agreed to within 2 or 3%, and the biggest discrepancy found was about 12%.

The part played by radiation in effecting heat transfer in moulding sands has also been discussed by Schwartz,¹⁰ who gives the following equation for the apparent conductivity at a temperature T° K. :

$$K_a = K_0 + 324rT^3 \times 10^{-13} \quad \dots \quad (13)$$

in which K_0 is the apparent conductivity at 0° C. and r is the mean radius of the sand grains. Schwartz's treatment yields results which are too high. This is probably due to his taking the width of the air spaces to be equal to the distance between the centres of the grains in adjacent rows of a close-packed arrangement; the mean pore width is in fact much smaller than this distance.

Values of the thermal conductivities of a number of insulating-sand mixes are given in the Second Report¹¹ of the Moulding Materials Sub-Committee of the Steel Castings Research Committee of the Iron

and Steel Institute and the British Iron and Steel Federation, but the method by which these values were determined is not revealed.

A few papers have been published describing the results of *ad hoc* experiments in the foundry to determine the effect of different moulding materials on the solidification of castings. Dietert, Fairfield, and Hasty¹² have compared the effect of four sands (both green and dry) on the rate of "skin formation" in steel castings and have shown that this increases with increasing density of the sand. This fact is predicted by equation (5), since an increase in density increases the value of the heat diffusivity b , and thus increases $\partial Q/\partial t$ and hence the rate of "skin formation". The above authors¹² present curves showing the effect on density of a number of variables including moisture, clay content, and grain spread, and have determined the relationship between sand density and mould hardness.

The effect of a variety of different mould materials on the temperature gradients present during the solidification of magnesium alloy plates has been studied by Chamberlin and Mezoff.¹³ These workers use various means to assess the "chilling capacities" of the different mould materials; the best assessment appears to be based on the reciprocal of the time taken by the plate to cool to 399° C. The chilling capacities thus assigned are roughly in order of the heat diffusivities of the materials concerned.

One of the present authors has compiled, after a critical study of the literature, lists of selected values for the thermal properties of mould materials.¹⁴

IV.—EXPERIMENTAL TECHNIQUE.

The work described in the succeeding paragraphs was carried out to check the validity of the theoretical approach defined in Section I and to assess the chilling powers of some moulding materials of low and medium conductivity. To this end, measurements were made of the temperature distribution in a number of these moulds, by taking heating curves at points in the mould at various perpendicular distances from the interface between the mould and a plane wall of a large casting. The casting used was a 5-in.-dia. \times 10 in. cylinder, the plane wall against which the measurements were made being the end of the cylinder opposite the runner. Since it was desired to study a range of interface temperatures which would cover the majority of non-ferrous-metal casting conditions, each mould was cast in an aluminium-base and a copper-base alloy. A few experiments were made with a third alloy of intermediate freezing temperature.

A point of importance which had to be considered when planning the experimental work was the necessity for keeping the interface temperature as nearly as possible constant for a reasonable period, since the theoretical relations are only strictly applicable to the case of a constant interface temperature. It had been found in other work¹⁵ that the interface temperature of 5-in.-dia. \times 10 in. cylinders sand cast in aluminium-30% copper alloy (eutectic temperature 548° C.) remained constant for about 30 min.; this alloy was therefore used for all the castings made in the aluminium-base range. It had also been shown¹⁵ that the interface temperature remains constant for a fair time in alloys of short freezing range which solidify to give an equi-axial structure. According to Northcott,¹⁶ the presence of lead in copper has a marked grain-refining effect; copper containing 0.5% lead, melted under a charcoal cover, was therefore used for experiments in the copper-base range. The interface temperature was substantially constant with this alloy for about 10 min., but fell appreciably after this time. The intermediate interface temperature was obtained by making the casting in a bronze containing 23% tin. This alloy freezes at 798° C., and the interface temperature of sand-cast cylinders remains reasonably constant for about 15 min. The following materials were used in making up these alloys; cathode copper, super-purity aluminium (both of 99.99% purity), and Mellanear tin (99.8% purity).

A further point of importance is the temperature drop across the sand/metal interface. Preliminary experiments in which thermocouples were placed on either side of the interface showed that the temperature of the metal side of the interface during the constant-temperature period was that of the freezing point of the metal, while the temperature on the mould side of the interface was generally a few degrees below this temperature, for sand moulds. The difference between the two temperatures was, however, somewhat variable, and it is thought that the reading of the thermocouples placed on the sand side of the interface may have been low owing to the finite size of the thermocouple junction. The difference was considerably greater in the case of moulds of chilling capacity higher than sand. In carrying out calculations based upon the results of the temperature measurements, the temperature of the interface has been taken to be near that indicated by the thermocouple placed on the mould side of the interface. The temperatures assumed and the reasons for doing so are given later.

Normal melting procedures were used with all the alloys and each was degassed by an appropriate treatment before being cast. The casting temperatures employed corresponded to about 100° C. superheat. The moulds were poured as rapidly as possible through a 1½-in.-

dia. downgate and the recorder was started when the mould was half full.

The temperatures in the mould were measured with seven 28-gauge B. & S. Chromel-Alumel thermocouples which were moulded into the drag so that their junctions lay along the central axis (produced) of the cylinder. One of these couples was invariably placed as near as possible to the metal/mould interface; the remainder were at various distances behind the interface. These distances varied somewhat in the different moulds, the locations selected depending upon the rate of heat penetration into the moulds. The actual distance of each couple junction from the interface was determined after casting by carefully scraping away the mould until the junction was exposed and measuring with a pair of dividers. The thermocouple wires were bare in the dry moulds, but fireclay insulators were employed for the green moulds, only the hot junctions being exposed. The parting line was curved and above the mid-section of the cylinder, so that the couple junctions were all well removed from the parted surfaces. Two thermocouples were also placed in the casting, one at the interface opposite to the corresponding couple in the sand, and the other in the estimated heat centre of the casting.

The apparatus used to record the temperature measurements consisted of a Tinsley D.C. amplifier with a straight line characteristic, and a high-speed milliammeter pen recorder. The magnification provided by the amplifier was such that the output of 20 m.amp., giving full scale (4 in.) deflection of the recorder, corresponded to an input of 12 mV., equivalent to about 300° C. The major part of the e.m.f. generated by the thermocouples was opposed by a back e.m.f. supplied by a calibrated potentiometer suppressor unit. The speed of response of the equipment was about 1 sec. so that it was possible to make up to 60 readings per minute. Each of the thermocouples was in turn connected to the instrument by a magnetically operated selector switch controlled by a push button. Readings were commenced immediately the casting had been poured and were continued until the interface temperature had fallen well below the freezing point of the alloy.

Heating curves were obtained in moulds made from the following materials: (1) a typical synthetic sand of medium grading, (2) a common naturally bonded sand (Mansfield Red), (3) dead-burnt magnesite powder bonded with linseed oil, (4) clay-bonded silicon carbide grit, (5) a proprietary plaster specially made for metal casting. Both green and dry moulds were made from the two sands; the moulds made from the other materials were used dry only. To minimize re-absorption of

moisture, the dry moulds were cast as soon as practicable after removal from the core oven, and for this reason the initial temperatures of these moulds were frequently above atmospheric temperature. Considerable difficulty was experienced in completely freeing the plaster moulds from combined moisture. In addition, these moulds were found to re-

TABLE III.—*Details of Moulds Studied.*

Mould Material	Grading		Bond	Moisture Content, %	Baking Treatment	Density, g./c.c.
	B.S. Sieve No.	Percentage				
Dry synthetic sand (Parish's No. 1)	— 30 + 44 — 44 + 60 — 60 + 85 — 85 + 120 — 120 + 150 — 150	2·7 27·9 53·6 12·6 1·8 1·4	5% bentonite	2·5-3	12 hr. at 220° C.	1·49 *
Green synthetic sand (Parish's No. 1)	As above	...	5% bentonite	2·5-3	None	1·54 *
Dry naturally bonded sand (Mansfield Red)	— 30 + 44 — 44 + 60 — 60 + 85 — 85 + 120 — 120 + 150 — 150 + 200 — 200	2·4 2·8 5·8 20·1 31·3 27·5 10·0	Natural	5	12 hr. at 220° C.	1·56 *
Green naturally bonded sand (Mansfield Red)	As above	...	Natural	5	None	1·64 *
Bonded magnesite (dead-burnt powder)	+ 30 — 30 + 60 — 60 + 100 — 100	22 25 6 47	2% heavy boiled linseed oil	...	3 hr. at 100° C. followed by 12 hr. at 220° C.	1·95 †
Bonded silicon carbide (RA60 grit)	— 30 + 44 — 44 + 60 — 60 + 85 — 85	0·6 59·2 39·5 0·6	4% bentonite, 1·3% dextrine	3	12 hr. at 220° C.	1·63 †
Plaster (Hydrocal metal casting plaster)	3 hr. at 100° C. followed by 16 hr. at 220° C.	0·745 †

* Determined by comparison of hardness measurements made on the mould, with those made on standard A.F.S. compression-test specimens of known density, made from the same material. For dry moulds, hardness measurements were made on the mould before baking and the density quoted is that of the corresponding A.F.S. specimen after baking.

† Determined on separate specimen.

absorb moisture from the atmosphere very readily, and for these reasons it was not found possible to cast into completely dehydrated plaster moulds. Details of the moulds and materials from which they were made are given in Table III. Each mould was made from new materials with the exception of those made in bonded silicon carbide, some of the moulds in which were made from material which had been used a few times.

V.—DISCUSSION OF RESULTS.

The simplest way of interpreting the heating curves obtained from the moulds is to plot, for a particular time or times after casting, the temperature at various points in the mould against the distance of the points from the casting/mould interface, and to fit to the plotted points a theoretical temperature distribution curve derived by inserting the appropriate numerical values in equation (3). In this way the validity of the mathematical treatment can be tested and, if a good fit can be obtained by adjusting the value of α in equation (3), the value of α giving the best fit is an approximate figure for the temperature diffusivity of the material. It is tacitly assumed that α is independent of temperature.

However, a better method, originally used by Chvorinov,⁶ permits far more experimentally determined temperatures to be incorporated in a single plot. Equation (3) shows that the temperature of any point in the mould depends solely upon the value of $(x/2\sqrt{\alpha t})$. Clearly then, if α is assumed independent of temperature, all points for which the ratio x/\sqrt{t} is the same, must be at the same temperature (e.g. a point distant 2 cm. from the interface will, at 4 min. after casting, be at the temperature which the point 1 cm. from the interface reached 1 min. after casting, since the ratio x/\sqrt{t} is the same in both instances). If, therefore, the temperature is plotted against x/\sqrt{t} , a smooth curve is obtained from measurements made at different distances from the interface and different times after casting, so that by increasing the number of arbitrarily selected times a large number of points may be incorporated in a single plot. The curve thus obtained will correspond numerically to the temperature distribution in the mould 1 unit of time after casting; if the temperature distribution after n units of time is required, the quantity $x\sqrt{n}/\sqrt{t}$ must be plotted. This method of interpreting the heating curves has been applied whenever possible in the present work (it cannot be applied to green-sand moulds), and, for convenience, metre-kilogramme-hour units have been employed; with these units plotting x/\sqrt{t} gives the temperature distribution 1 hr. after casting, $x/\sqrt{2t}$ the distribution after $\frac{1}{2}$ hr., &c.

For easy comparison of the temperature-distribution curves obtained from the different moulds, θ has in all instances been plotted against $x/\sqrt{2t}$ and the distribution $\frac{1}{2}$ hr. after casting has thus been obtained, although in some cases the taking of readings had been discontinued long before this period had elapsed.

The procedure adopted in fitting to the experimental points an equation of the form :

$$\theta = \theta_0 + (\theta_1 - \theta_0) erfc \left(\frac{x}{\sqrt{2\alpha t}} \right) (14)$$

obtained by inserting $t = \frac{1}{2}$ in equation (3), is briefly as follows. The value of θ_0 , the initial mould temperature, was taken as the mean of the values recorded by all the thermocouples immediately prior to casting (this temperature was frequently above atmospheric for the reasons given in the preceding Section). The interface temperature θ_1 was then assumed; this temperature was normally taken to be close to that indicated by the thermocouple placed at the interface, but when the interface temperature did not remain constant for long, a rather lower temperature was assumed. Different values of the temperature diffusivity α were then tried in the equation until the best possible fit was obtained. In many instances a theoretical curve could be found which fitted the experimental points well, and in such instances the value assumed for α is probably correct to $\pm 10\%$. In other cases, however, where the experimental points were more scattered, fairly good fits could be obtained from more than one theoretical curve; in these cases the figures quoted may be in error by as much as $\pm 20\%$. The accuracy of the figures given in the ensuing discussion for the temperature diffusivity and the other thermal constants is therefore somewhat variable and more weight should be given to figures derived in instances where the theoretical equations fitted the experimental points well.

The heating curves have been further interpreted by the construction of curves showing the variation with time after casting of $\partial Q/\partial t$, the rate of heat extraction per unit area of mould surface, and of Q , the total heat removed per unit area. These curves were constructed by calculating b from the experimentally determined values for α and ρ and from values for c taken from the literature; the figures for b were then inserted in equations (5) and (6).

The heating curves obtained from the various moulds, and their interpretation, are discussed individually in the succeeding paragraphs.

1. Dry Synthetic Sand.

Heating curves were obtained from these moulds for the three different casting temperatures and the sets of curves for the nominal interface temperatures of 548° C. and 1083° C. are reproduced in Figs. 3 and 4. The corresponding temperature-distribution curves for $\frac{1}{2}\text{ hr.}$ after casting, obtained in the manner described above, are plotted in Fig. 5; the horizontal scale in this Figure is in units of $x/\sqrt{2t}$, but, as explained in the preceding paragraphs, the units are numerically equal to the distance in metres from the interface for a time after casting of $\frac{1}{2}\text{ hr.}$

An interesting feature of the distribution curves is the slowness with

which heat penetrates sand moulds; even $\frac{1}{2}$ hr. after casting, points more than a few centimetres from the interface had scarcely begun to rise in temperature.

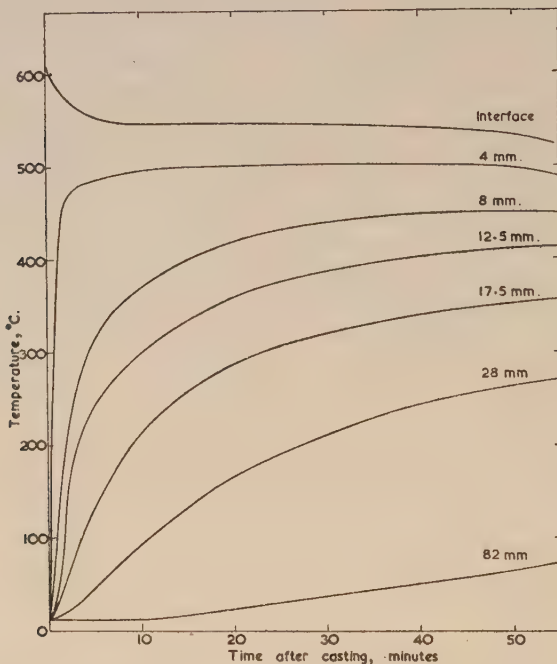


FIG. 3.—Dry Synthetic Sand Mould. Heating curves obtained with interface temperature of $548^{\circ}\text{ C}.$

It will be observed that the theoretical curves corresponding to the equations:

$$\theta = 25 + 523 \operatorname{erfc} \left(\frac{x}{\sqrt{2} \times 0.0010} \right) \quad (15)*$$

(nominal interface temperature = $548^{\circ}\text{ C}.$)

$$\theta = 15 + 1065 \operatorname{erfc} \left(\frac{x}{\sqrt{2} \times 0.0015} \right) \quad (16)$$

(nominal interface temperature = $1083^{\circ}\text{ C}.$)

fit the experimental points closely, showing that the flow of heat into dry-sand moulds may be represented mathematically with a good degree of accuracy. A similar distribution was found for the interface

* Numerical values are in metre-kilogramme-hour units.

temperature of 798° C., and the following equation gave a reasonably good fit :

$$\theta = 13 + 780 \operatorname{erfc} \left(\frac{x}{\sqrt{2 \times 0.0012}} \right) (17)$$

(nominal interface temperature = 798° C.)

The three equations above lead to values for the mean temperature diffusivity α of 0.0010, 0.0012, and 0.0015 m.²/hr. for the respective

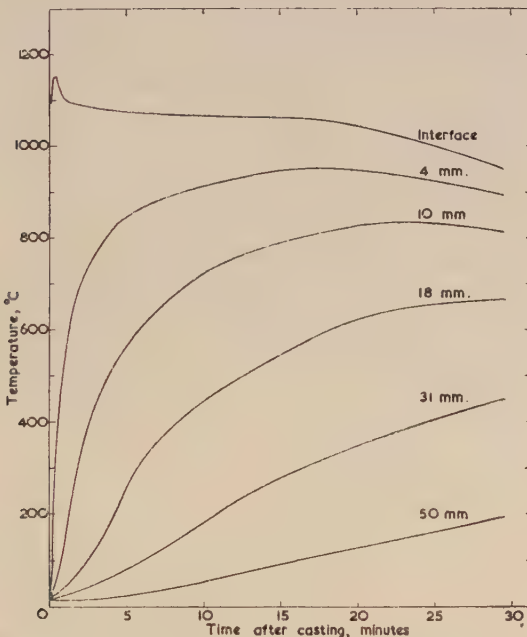


FIG. 4.—Dry Synthetic Sand Mould. Heating curves obtained with interface temperature of 1083° C.

interface temperatures of 548° , 798° , and 1083° C., from which it appears that the mean value of α increases approximately linearly with temperature; despite this variation equation (3) can evidently be used with reasonable accuracy. It is impossible to obtain figures for the apparent thermal conductivity of the sand from the literature, since, as is shown in Section III, this quantity is very variable and depends upon several factors which have not been adequately studied. However, the specific heat of a moulding sand should be close to that of pure silica sand, for which figures are available, since the few per cent. of bonding material

in the sand should not greatly affect the specific heat; in addition, this quantity is obviously not affected by grain-size and other similar considerations. Hence, using published figures for the specific heat and assuming that the density of the sand is not much affected by temperature, the mean apparent thermal conductivity may be calculated from the temperature diffusivity figures. This has been done for the diffusivity figures above, employing figures for the mean specific heat obtained by Cohn and MacGee,¹⁷ and the conductivities thus calculated

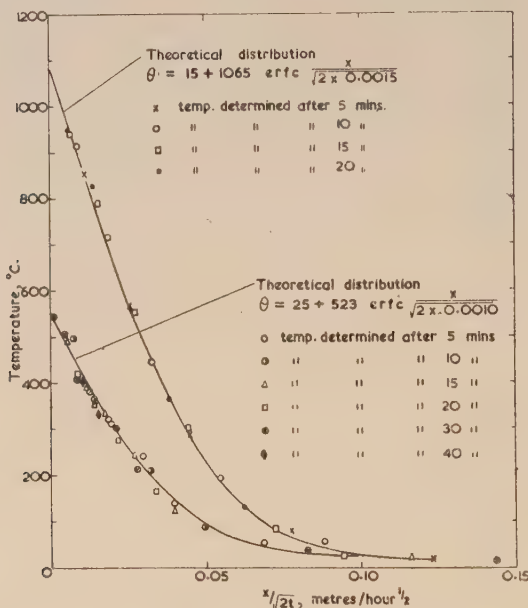


FIG. 5.—Dry Synthetic Sand Moulds. Temperature distributions after $\frac{1}{2}$ hr. for interface temperatures of 548° and 1083° C.

are given in Table IV, together with values for the other thermal constants. Table IV and Figs. 1 and 2 show that the mean conductivity figures calculated in this way are quite consistent with the conductivities quoted by Lucks, Linebrink, and Johnson,⁸ and by Dietert, Fairfield, and Hasty.¹² It must be borne in mind, when comparing the present results with those of the other workers, that the figures given here are mean values over the range room temperature to the interface temperature of the experiment, while the values in Figs. 1 and 2 refer to the apparent conductivity at the temperature indicated. The results show an increase in the mean conductivity of about 70% on increasing the

TABLE IV.—Thermal Properties of Moulds.

Mould Material	Temperature Range, ° C., room temp. to	Assumed Mean Specific Heat, cal./g.	Observed Mean Temperature Diffusivity	Calculated Mean Thermal Conductivity	Calculated Mean Heat Diffusivity	Calculated Mould Constant, cal./cm. ² . min. ^{1/2}
Synthetic sand (dry) (density = 1.49 g./c.c.)	548°	0.246 ¹⁷ *	0.0010 * 0.0028 †	0.36 ₄ * 0.0010 ₃ , †	11.6 * 0.019 ₃ , †	89.4
	798°	0.257 ¹⁷	0.0012 * 0.0033 †	0.46 ₀ * 0.0012 ₃ , †	13.3 * 0.022 ₃ , †	151
	1083°	0.272 ¹⁷	0.0015 * 0.0042 †	0.60 ₈ * 0.0017 ₀ , †	15.7 * 0.026 ₃ , †	244
Mansfield sand (dry) (density = 1.56 g./c.c.)	548°	0.246 ¹⁷	0.0010 * 0.0028 †	0.38 ₄ * 0.0010 ₇ , †	12.1 * 0.020 ₃ , †	93.6
	1083°	0.272 ¹⁷	0.0012 * 0.0033 †	0.50 ₈ * 0.0014 ₀ , †	14.7 * 0.024 ₅ , †	228
Bonded silicon carbide (density = 1.63 g./c.c.)	548°	0.245 ¹⁹	0.0015 * 0.0042 †	0.59 ₈ * 0.0016 ₆ , †	15.5 * 0.025 ₈ , †	119
	798°	0.255 ¹⁹	0.0024 * 0.0066 †	0.99 ₈ * 0.0027 ₈ , †	20.4 * 0.034 ₀ , †	232
	1083°	0.265 ¹⁹	0.0024 * 0.0066 †	1.04 * 0.0028 ₈ , †	21.2 * 0.035 ₃ , †	330
Bonded magnesite (density = 1.95 g./c.c.)	548°	0.259 ¹⁸	0.0035 * 0.0097 †	1.7 ₂ * 0.0049 ₁ , †	29.9 * 0.049 ₈ , †	230
	1083°	0.277 ¹⁸	0.0018 * 0.0050 †	0.97 ₂ * 0.0027 ₀ , †	22.9 * 0.038 ₂ , †	354
Plaster (density = 0.745 g./c.c.)	548°	?0.4	0.0011 * 0.0031 †	0.3 ₅ * 0.0009 ₇ , †	10 * 0.017 †	80
	798°	?0.4	0.0007 * 0.0019 †	0.2 ₂ * 0.0006 ₁ , †	8.3 * 0.014 †	95
	1083°	?0.4	0.0008 * 0.002 ₁ , †	0.2 ₈ * 0.0007 ₈ , †	7.4 * 0.012 †	125
Green synthetic sand (density = 1.54 g./c.c.)	548° 1083°	7108 258
Green Mansfield sand (density = 1.64 g./c.c.)	548° 1083°	105 237

* Metre-kilogramme-hour units.

† C.G.S. units.

‡ For initial temperature of mould = 20° C.

upper limit of the range from 548° to 1083° C.; this implies a much greater increase in the instantaneous value of the apparent conductivity.

Using the thermal constants of Table IV and equations (5) and (6), the curves in Fig. 6 showing the variation with time of $\partial Q/\partial t$, the rate of heat extraction per square centimetre of mould surface, and Q , the total heat extracted, were constructed. The curves, especially that for Q , are useful in calculating approximate solidification times of castings; this may be readily done by calculating the heat content of the casting above the solidus temperature (latent heat and super-heat), dividing this figure by the surface area of the casting, and determining, from the Q -

curve appropriate to the freezing temperature of the casting, the time taken for this amount of heat to be absorbed by the mould. For an alloy of long freezing range a reasonably accurate result may be obtained by assuming a mean value for the interface temperature; in doing this due weight should be given to the rate of deposition of solid at different points in the freezing range. For example, in aluminium-copper alloys containing a few per cent. of copper the freezing range is of the order of 100° C., but, since the greater part of the alloy solidifies in the first few

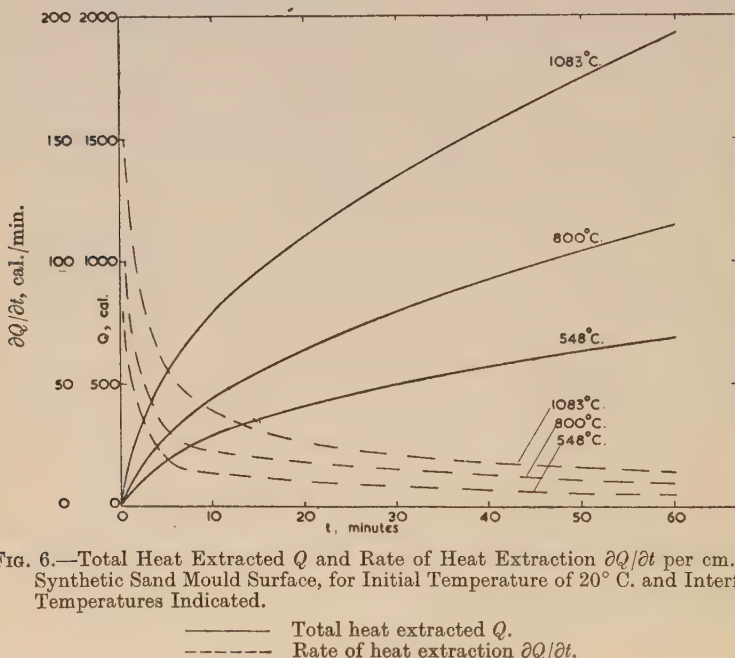


FIG. 6.—Total Heat Extracted Q and Rate of Heat Extraction $\partial Q/\partial t$ per cm^2 of Synthetic Sand Mould Surface, for Initial Temperature of 20° C. and Interface Temperatures Indicated.

— Total heat extracted Q .
- - - Rate of heat extraction $\partial Q/\partial t$.

degrees of this range, it is clearly right to take the mean interface temperature near the top of the freezing range.

The figures calculated for the mould constant q (equation (7)), and used in deriving the curves for Q and $\partial Q/\partial t$, have also been included in Table IV. For convenience, these figures are expressed in $\text{cal}/\text{cm}^2/\text{min.}^\frac{1}{2}$.

The figures for the mould constants and heat diffusivities in the last two columns of Table IV are of particular importance in metal casting, for these quantities are essentially measures of the chilling power of the material of the mould.

The value found for the heat diffusivity at an interface temperature of 1083° C. (15.7 M.K.H. units) is in substantial agreement with the

figure obtained by Chvorinov⁶ (17.1 M.K.H. units), since Chvorinov's work was carried out at steelmaking temperatures, and it is to be expected that the mean diffusivity would be higher at these temperatures.

2. Dry Mansfield Sand.

Only two interface temperatures (548° and 1083° C.) were used to obtain heating curves for moulds in this material. These curves are

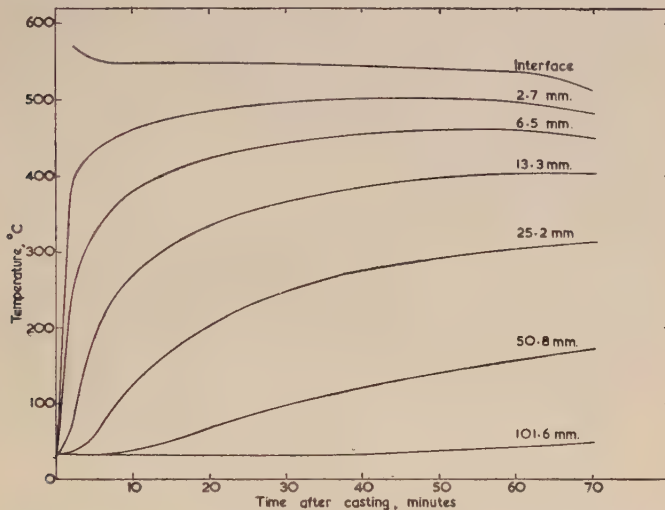


FIG. 7.—Mansfield Sand Mould. Heating curves obtained with interface temperature of 548° C.

reproduced in Figs. 7 and 8 and the corresponding temperature-distribution curves are given in Fig. 9. The equations which best fitted the experimental distributions were :

$$\theta = 32 + 508 \operatorname{erfc} \left(\frac{x}{\sqrt{2} \times 0.0010} \right) \dots \quad (18)$$

(nominal interface temperature = 548° C.)

$$\theta = 18 + 1040 \operatorname{erfc} \left(\frac{x}{\sqrt{2} \times 0.0012} \right) \dots \quad (19)$$

(nominal interface temperature = 1083° C.)

It will be noticed that the interface temperature recorded by the interface couple (see Fig. 8), and assumed in equation (13) is about 25° C. below the nominal figure. While it is impossible to say whether or not

the actual interface temperature was that indicated by the interface couple, the possibility of a sharp temperature drop occurring across the interface, due to air-gap formation or other cause, cannot be neglected, although no such effect could be positively detected in the present work. The low interface temperature recorded could also be accounted for by small errors in the measured positions of the thermocouples situated

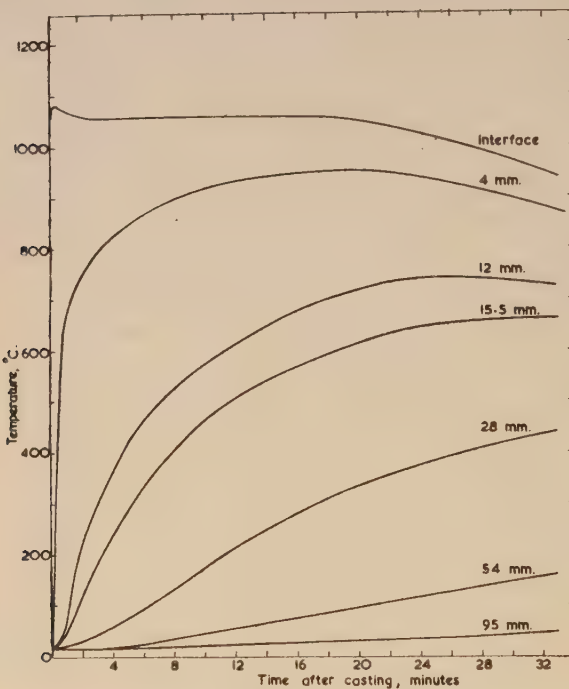


FIG. 8.—Mansfield Sand Mould. Heating curves obtained with interface temperature of 1083° C.

near the interface. Similar reasoning also applies to the copper castings made in other moulds (described below).

Equations (18) and (19) lead to values of the temperature diffusivity of 0.0010 and 0.0012 m.²/hr., respectively, and these in turn yield the figures given in Table IV for the apparent conductivity and other constants. It will be seen that both conductivity and temperature diffusivity, and especially the latter, increase with temperature less rapidly than is the case with synthetic sand. This effect is no doubt due to the finer grain-size of the Mansfield sand which, according to Russell's

equation (equation 11), should result in a smaller radiation component at high temperatures. Naturally bonded sands frequently contain considerable quantities of clay, and for this reason the use, in calculating the conductivity, of the specific heat of pure silica sand may be open to criticism, since the specific heat of most clays is considerably greater than that of sand (about 0.5 as compared with about 0.25). The effect is, however, not large, the presence of, for example, 10% of clay resulting

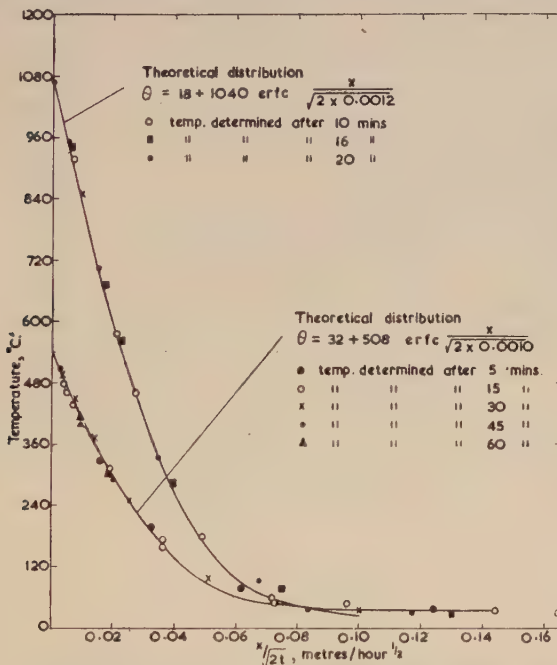


FIG. 9.—Mansfield Sand Moulds. Temperature distributions after $\frac{1}{2}$ hr. for interface temperatures of 548° C. and 1083° C.

in an increase in the specific heat of about 10%. The heat diffusivities given in Table IV show that for an interface temperature of 548° C., Mansfield sand extracts heat at about the same rate as the synthetic sand. At an interface temperature of 1083° C., the rate of heat extraction is rather less than for the synthetic sand, but the difference is small, because the rate of heat extraction is proportional to the square root of the conductivity.

Curves in which the rate of heat extraction and total heat extracted are plotted against time for the two different temperatures, are given in

Fig. 10. Values for the "mould constant" employed in calculating these curves are quoted in Table IV.

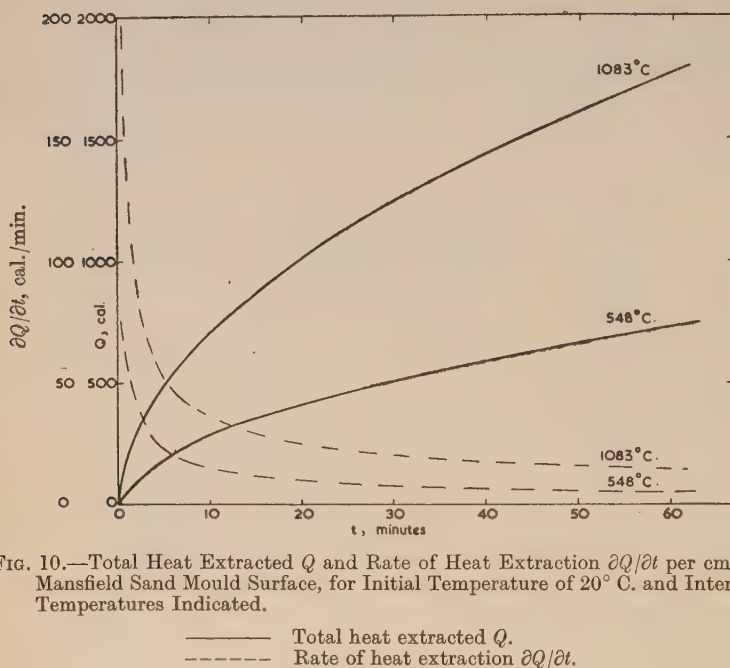


FIG. 10.—Total Heat Extracted Q and Rate of Heat Extraction $\partial Q/\partial t$ per cm^2 of Mansfield Sand Mould Surface, for Initial Temperature of 20°C . and Interface Temperatures Indicated.

— Total heat extracted Q .
- - - Rate of heat extraction $\partial Q/\partial t$.

3. Silicon Carbide.

The heating curves obtained from the moulds in bonded silicon carbide are shown in Figs. 11 and 12 for interface temperatures of 548° C . and 1083° C . respectively; a third set of curves obtained with an interface temperature of 798° C . is not reproduced.

The recorded interface temperatures were found to be considerably lower than the nominal interface temperature, especially at the higher temperatures, and, in addition, the interface temperatures began to fall fairly soon after the castings had started to freeze, instead of remaining sensibly constant for a relatively long time, as was the case with the sand moulds. For these reasons, in fitting theoretical temperature-distribution curves to the experimental points shown plotted in Fig. 13, interface temperatures considerably below the nominal were assumed. Thus, taking the interface temperatures to be 535° , 780° , and 1053° C .

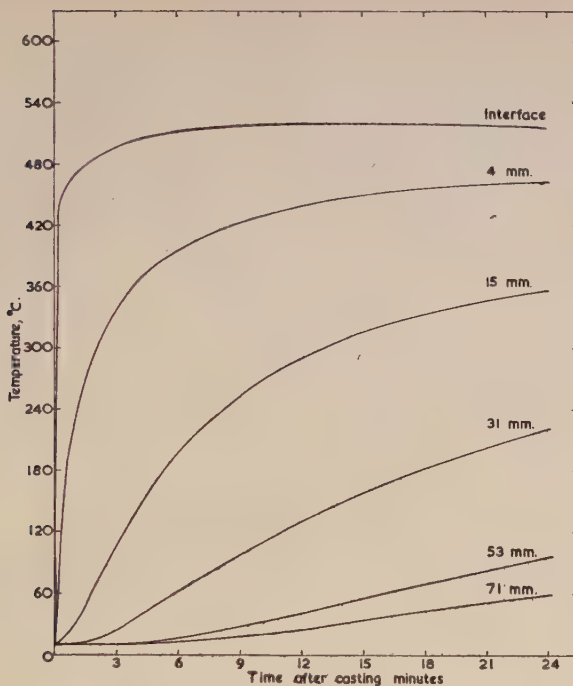


FIG. 11.—Silicon Carbide Mould. Heating curves obtained with interface temperature of 548° C.

the experimental points were best fitted by the following $\frac{1}{2}$ -hr. distributions:

$$\theta = 12 + 523 \operatorname{erfc} \left(\frac{x}{\sqrt{2} \times 0.0015} \right) \dots \quad (20)$$

(nominal interface temperature = 548° C.)

$$\theta = 66 + 714 \operatorname{erfc} \left(\frac{x}{\sqrt{2} \times 0.0024} \right) \dots \quad (21)$$

(nominal interface temperature = 798° C.)

$$\theta = 18 + 1035 \operatorname{erfc} \left(\frac{x}{\sqrt{2} \times 0.0024} \right) \dots \quad (22)$$

(nominal interface temperature = 1083° C.)

The theoretical distribution given by equation (22) was found to give a very good fit with the experimental points, but the agreement was not so good at the two lower interface temperatures; a possible reason

for the less good agreement at lower temperatures is variation of the temperature diffusivity with temperature.

The values for the temperature diffusivity of 0.0015, 0.0024, and 0.0024 m.²/hr. given by equations (20)–(22), for the respective interface temperatures of 548°, 798°, and 1083° C., yield the figures presented in Table IV for the other thermal constants. In calculating these figures some doubt arose as to the values to be taken for the specific heat of the

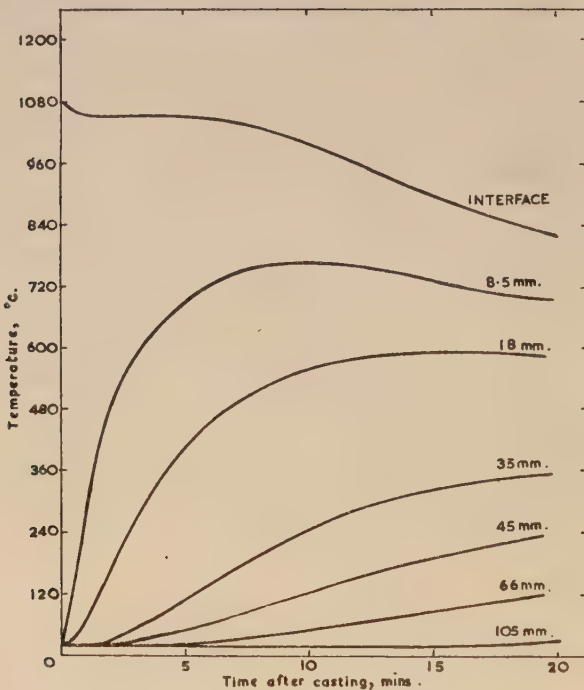


FIG. 12.—Silicon Carbide Mould. Heating curves obtained with interface temperature of 1083° C.

material. The equation suggested by Kelley¹⁸ for the specific heat of silicon carbide yielded mean values, the use of which led to rates of heat extraction which were clearly too low, since they corresponded to times of total solidification of the castings which were only slightly less than those obtaining with sand moulds and very much greater than those actually observed. Kelley's values for the specific heat were therefore rejected in making the calculations, and figures published by Miehr, Immke, and Kratzert¹⁹ for carborundum containing 10% bond, were used instead.

Assuming their correctness, the figures thus obtained for the apparent thermal conductivity (Table IV) show the mean value of this constant to increase by nearly 100% between 548° and 1083° C., and, even if the figure obtained at the lowest temperature is somewhat in error, it is clear that a substantial increase in apparent conductivity occurs. It seems likely that this is due to marked intergranular radiation, since most of the published figures for the conductivity of bonded silicon

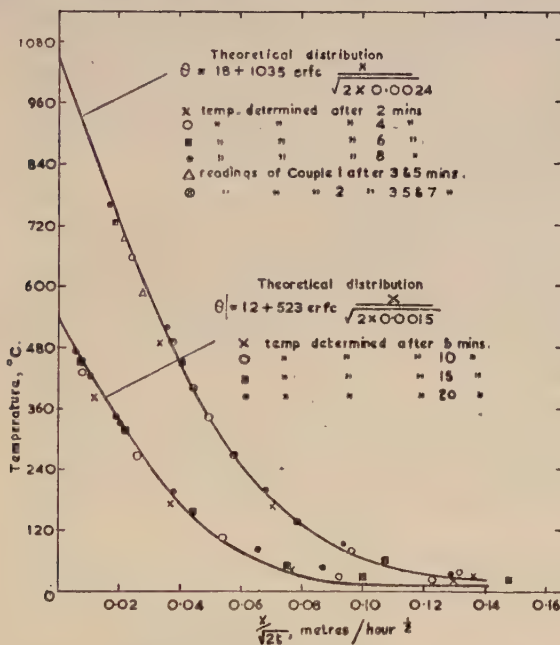


FIG. 13.—Silicon Carbide Moulds. Temperature distributions after $\frac{1}{2}$ hr. for interface temperatures of 548° and 1083° C.

carbide, carborundum brick, &c., show a decrease in conductivity of about 50% on going from 500° to 1000° C.

The substantial decline in true conductivity with increasing temperature, combined with the marked increase in apparent conductivity which occurs at high temperatures due to radiation, suggests that the apparent conductivity has a minimum value at some intermediate temperature. This might account for the small discrepancy noted above between the experimental points and the theoretical distribution curves for the interface temperatures of 548° and 798° C. The temperature diffusivity would be greater at low than at intermediate

temperatures, so that the experimental points in the distributions for the interface temperatures of 548° and 798° C. might be expected to fall to the right of the theoretical curves at low temperatures. As Fig. 13 shows, this does in fact happen with an interface temperature of 548° C. On the other hand, at high temperatures the diffusivity should increase again, and it might well be that the experimental points in the distribution for the interface temperature of 1083° C. would be fitted by a

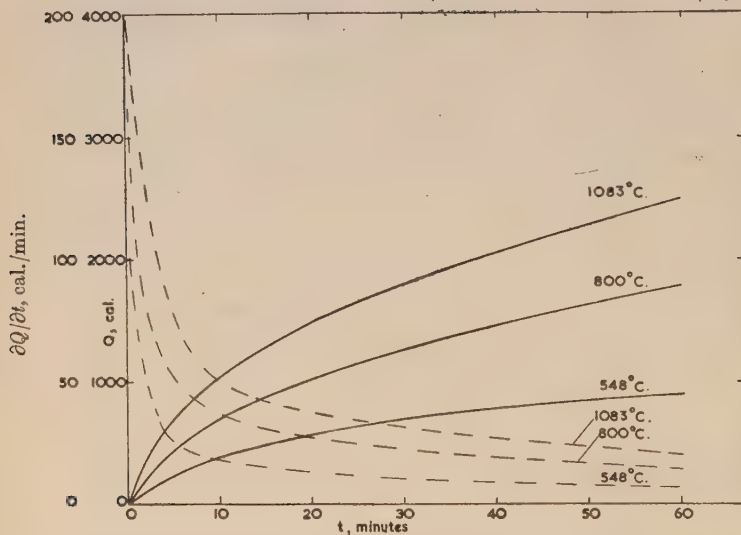


FIG. 14.—Total Heat Extracted Q and Rate of Heat Extraction $\partial Q/\partial t$ per cm^2 of Silicon Carbide Mould Surface, for Initial Temperature of 20° C. and Interface Temperatures Indicated.

— Total heat extracted Q .
- - - Rate of heat extraction $\partial Q/\partial t$.

theoretical curve at the upper and lower ends of the range, there being only a very small discrepancy at the intermediate temperatures.

As before, the heat diffusivities and mould constants have been calculated for the three temperatures (Table IV) and curves for the rate of heat extraction and total heat extracted are shown in Fig. 14. These curves and figures show that the chilling power of bonded silicon carbide is greater than that of the synthetic sand by roughly one-third for all the interface temperatures studied.

4. Bonded Magnesite.

The heating curves obtained at interface temperatures of 548° and 1083° C. are shown in Figs. 15 and 16. The temperature-distribution

curves reproduced in Fig. 17 show that at the higher interface temperature the experimental points are well fitted by the following equation, which assumes an interface temperature of 1025° C. and a temperature diffusivity of 0.0018 m.²/hr.:

$$\theta = 20 + 1005 \operatorname{erfc} \left(\frac{x}{\sqrt{2} \times 0.0018} \right) \quad \dots \quad (23)$$

(nominal interface temperature = 1083° C.)

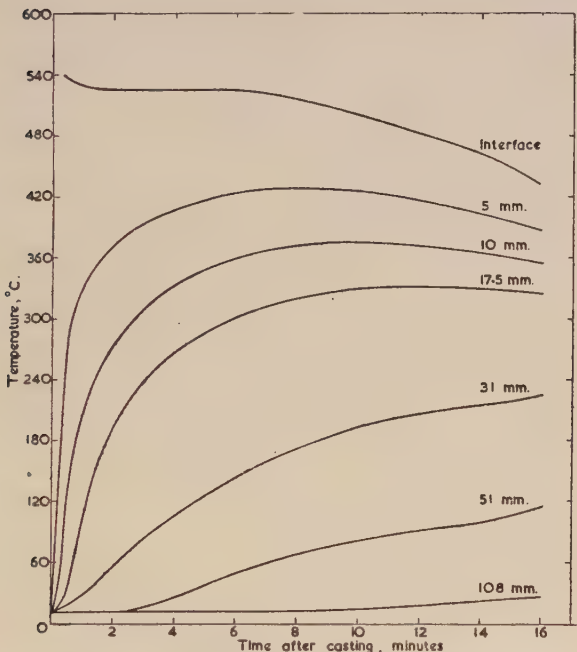


FIG. 15.—Magnesite Mould. Heating curves obtained with interface temperature of 548° C.

At the lower interface temperature, on the other hand, no very good fit could be found, the upper portion of the experimental curve apparently corresponding to a temperature diffusivity of about 0.0025 m.²/hr., while the lower half was fitted by a curve for which the diffusivity was 0.0040 m.²/hr. The best over-all fit was obtained from the curve :

$$\theta = 10 + 510 \operatorname{erfc} \left(\frac{x}{\sqrt{2} \times 0.0035} \right) \quad \dots \quad (24)$$

(nominal interface temperature = 548° C.)

which postulates a diffusivity of $0.0035 \text{ m}^2/\text{hr.}$ and an interface temperature of 520° C.

The difficulty of fitting the experimental data obtained at the interface temperature of 548° C. is probably due to variation of the temperature diffusivity, for values taken from the literature of the thermal conductivity of magnesite brick and similar substances show a decrease in conductivity and hence in temperature diffusivity between 0° and

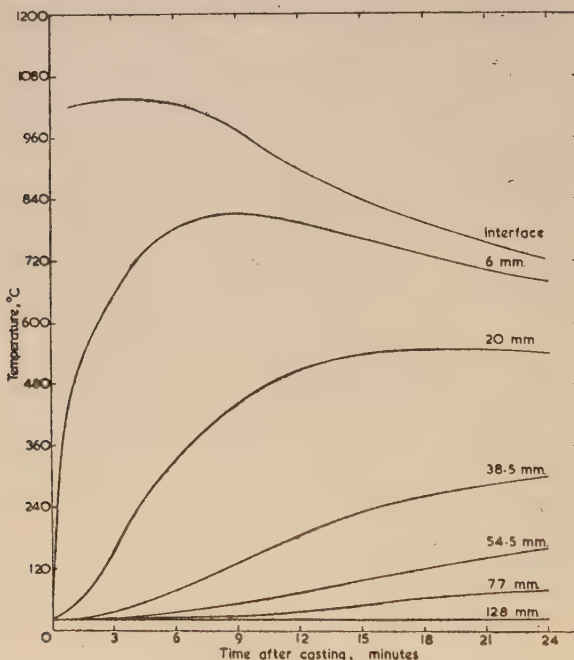


FIG. 16.—Magnesite Mould. Heating curves obtained with interface temperature of 1083° C.

600° C. of the order of 100%. It may be noted that, at very low temperatures, the experimental points fall well above and to the right of the theoretical curve, as would be expected if the diffusivity were markedly greater at low temperatures. The same is true of the curve for an interface temperature of 1083° C. , but the over-all fit is better since the points fit the curve well at temperatures above about 250° C. ; it may be that at higher temperatures the conductivity and diffusivity decrease less rapidly with temperature.

The values of the other thermal constants, calculated from the above

temperature diffusivities, are given in Table IV; in making these calculations it was assumed that the specific heat of the dead-burnt magnesite used could be taken as that of pure magnesia, and mean specific heats derived from Kelley's equation for magnesia¹⁸ were employed.

It will be seen from Table IV that the apparent conductivity decreases by about 40% between 548° C. and 1083° C., and since, as the literature

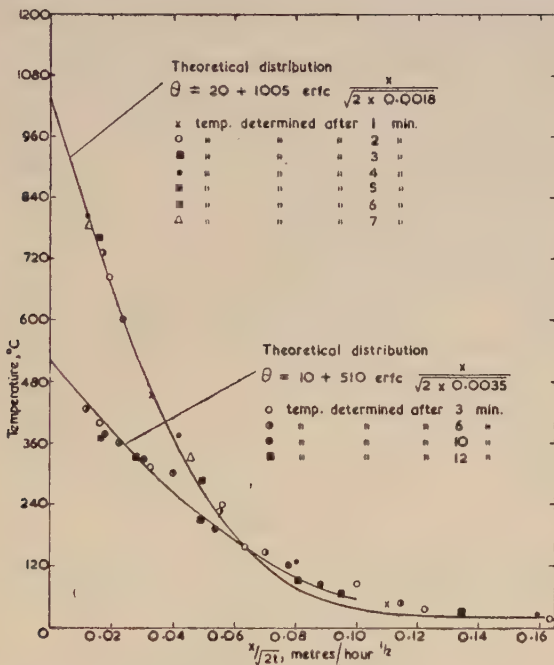


FIG. 17.—Magnesite Moulds. Temperature distributions after $\frac{1}{2}$ hr. for interface temperatures of 548° and 1083° C.

shows, this is paralleled by a similar decrease in the true conductivity, it is unlikely that in the material examined radiation at high temperatures greatly affects the conductivity. The magnesite used contained a large proportion of fines, and as Lucks, Linebrink, and Johnson⁸ show, this minimizes the effect of radiation in increasing the apparent conductivity; this effect is also predicted by the theoretical approaches of Russell²¹ and Eucken.²²

The heat diffusivities and mould constants for the two temperatures are also given in Table IV and derived curves for the rate of heat

extraction and total heat extraction are given in Fig. 18. At the lower temperature the rate of heat extraction of magnesite is about two and a half times that of synthetic sand and twice that of silicon carbide. However, since magnesite is unusual in that its temperature diffusivity decreases with temperature, the rate of heat extraction at copper-casting temperatures is only one and a half times that of the synthetic sand and little greater than that of silicon carbide.

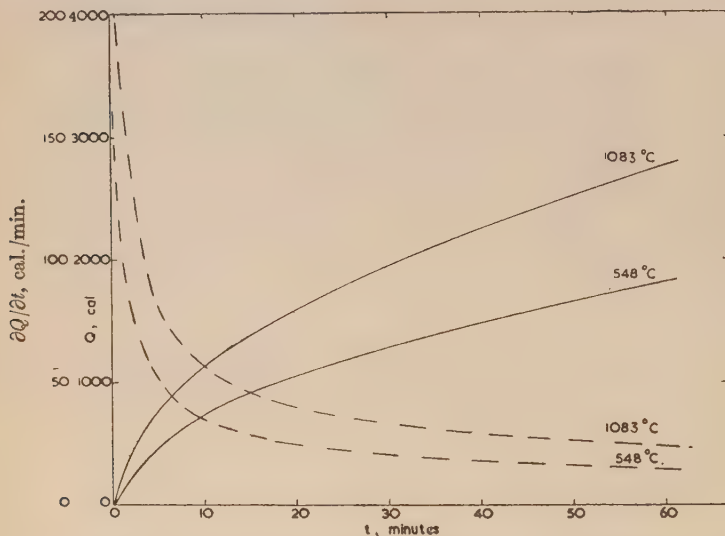


FIG. 18.—Total Heat Extracted Q and Rate of Heat Extraction $\partial Q / \partial t$ per cm^2 of Magnesite Mould Surface, for Initial Temperature of 20° C . and Interface Temperatures Indicated.

— Total heat extracted Q .
- - - Rate of heat extraction $\partial Q / \partial t$.

The remarks above with regard to the chilling power of magnesite moulds, and the figures given in Table IV, apply only to moulds made from a particular consignment of magnesite powder. Later experiments with a different consignment have shown that the thermal properties of this material vary quite markedly. For example, using a new consignment, a repeat of the experiment carried out with the aluminium-30% copper alloy (interface temperature = 548° C), led to a mean value of the temperature diffusivity α of about 0.0015 M.K.H. units, compared with the value of 0.0035 M.K.H. units found in the first experiment. In this second experiment, as in the first, the temperature diffusivity appeared to alter considerably over the temperature range

of the experiment, varying between about 0.0020 and 0.0012 M.K.H. units. The solidification time for the 5-in.-dia. cylinder casting was very much greater in the second experiment than in the first (22 min. against 8 min.), and calculation shows that the change in temperature diffusivity almost exactly accounts for the longer solidification time observed. Furthermore, since in this calculation the same values of specific heat and density were assigned to the two moulds, it is clear

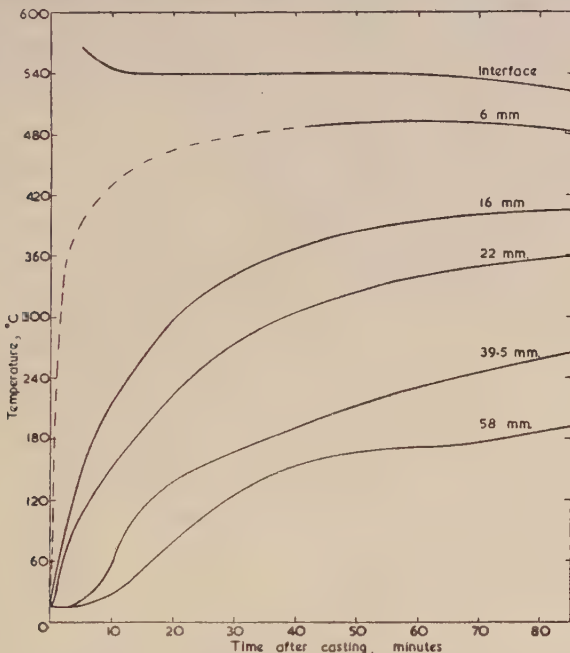


FIG. 19.—Plaster Mould. Heating curves obtained with interface temperature of 548° C.

that the two consignments of magnesite differed principally in apparent thermal conductivity. The value for this quantity deduced from the results of the second experiment is 0.76 compared with 1.77 M.K.H. units from the first experiment. No explanation can be offered for this marked variation in conductivity, but it was noted that the second consignment of magnesite was rather coarser than the first.

5. Plaster.

Despite very thorough baking it was found almost impossible entirely to eliminate combined moisture from the moulds in this material, and

for this reason the majority of the heating curves obtained show kinks due to the occurrence of the dehydration reaction. This effect is most marked in the curves obtained at interface temperature of 548° C. (Fig. 19) and 798° C. (not reproduced). The curves obtained at 1083° C. (Fig. 20) were practically free from kinks.

However, since the irregularities in the curves were quite small, it was not thought that they would greatly affect the temperature distribution in the mould, and the usual method of plotting θ against $x/\sqrt{2t}$ was employed to obtain the temperature distributions shown in Fig. 21. The experimental points were found to be best fitted by the following curves :

$$\theta = 15 + 533 \operatorname{erfc} \left(\frac{x}{\sqrt{2} \times 0.0011} \right) \dots \quad (25)$$

(nominal interface temperature = 548° C.)

$$\theta = 40 + 755 \operatorname{erfc} \left(\frac{x}{\sqrt{2} \times 0.0007} \right) \dots \quad (26)$$

(nominal interface temperature = 798° C.)

$$\theta = 18 + 1062 \operatorname{erfc} \left(\frac{x}{\sqrt{2} \times 0.0008} \right) \dots \quad (27)$$

(nominal interface temperature = 1083° C.)

The fit of the curve corresponding to equation (27) was very good down to 100° C. The other curves fitted rather less well, and in all instances the experimental points diverged somewhat from the theoretical curves at low temperatures; this is no doubt due to the irregularities caused in the heating curves by the presence of moisture and the occurrence of allotropic transformations in the plaster.

In interpreting the values of 0.0011, 0.0007, and 0.0008 m.²/hr. obtained for the temperature diffusivities for the respective interface temperatures of 548°, 798°, and 1083° C., a difficulty again arose with regard to the specific heats to be adopted. Figures obtained by the use of Kelley's specific-heat equation for gypsum¹⁸ were clearly not applicable, since the mould constants calculated using these values predicted times of total solidification far in excess of those observed. Furthermore, it was known that the proprietary plaster used contained considerable quantities of other substances which might add markedly to the specific heat of the mixture.

By comparing the freezing times of identical castings made in sand and in plaster and using the relation :

$$q_1 \sqrt{t_1} = q_2 \sqrt{t_2} \dots \quad (28)$$

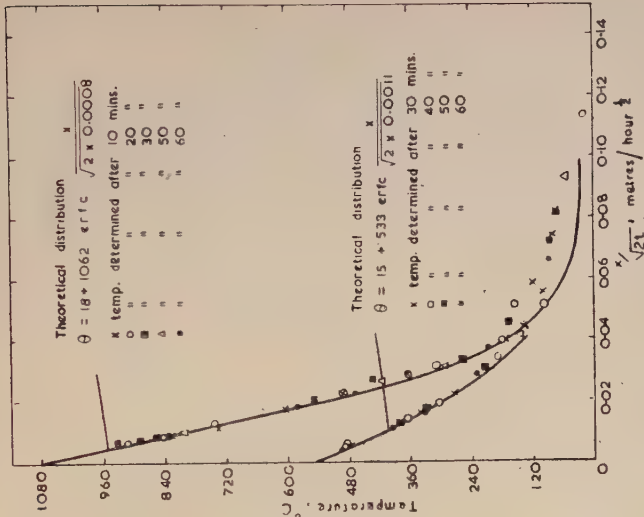


FIG. 21.—Plaster Moulds. Temperature distributions after $\frac{1}{2}$ hr. for interface temperatures of 548° and 1083° C.

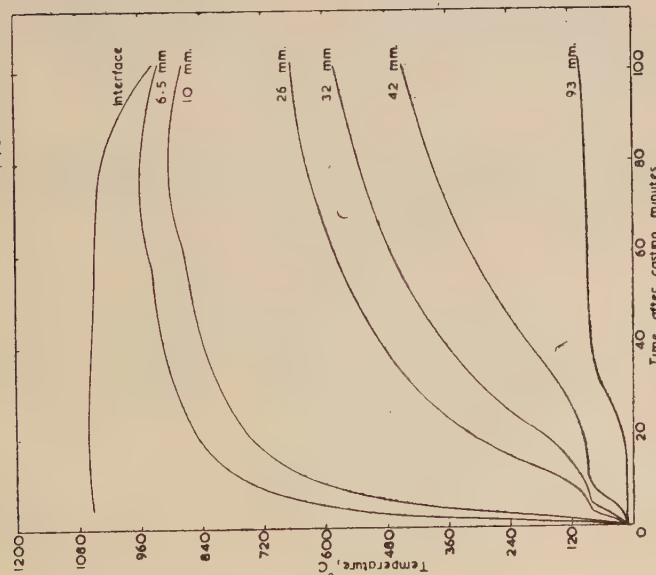


FIG. 20.—Plaster Mould. Heating curves obtained with interface temperature of 1083° C.

where q_1 and t_1 , and q_2 and t_2 are the mould constants and freezing times for sand and plaster respectively, an approximate value of 125 cal./cm.²/min.¹ for the mould constant of plaster at 1083° C. interface temperature was obtained. Using this value of the mould constant, and the temperature diffusivity of 0.0008 m.²/hr. found experimentally, a value of about 0.4 cal./g. was derived for the mean specific heat, and employed in all subsequent calculations. The figures thus obtained for the other thermal properties are given in Table IV.

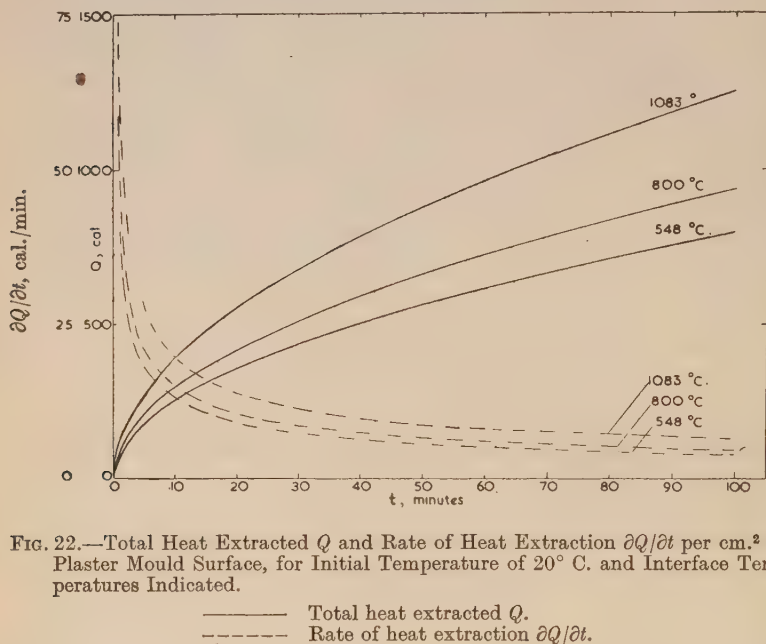


FIG. 22.—Total Heat Extracted Q and Rate of Heat Extraction $\partial Q / \partial t$ per cm.² of Plaster Mould Surface, for Initial Temperature of 20° C. and Interface Temperatures Indicated.

— Total heat extracted Q .
- - - Rate of heat extraction $\partial Q / \partial t$.

The heat diffusivities and mould constants in Table IV and the heat-extraction curves in Fig. 22 show that the chilling power of plaster is only a little less than that of synthetic sand for an interface temperature of 548° C. The temperature diffusivity of plaster, like that of magnesite, falls irregularly with increasing temperatures, so that at an interface temperature of 1083° C. the chilling power of plaster is only about one-half that of synthetic sand.

It appears that the thermal properties of plaster moulds are also very variable and are greatly influenced by factors at present unknown and uncontrolled in the making of the mould. Evidence for this is provided by the results of replicate experiments using the same plaster

and carried out with cylinders cast in copper (interface temperature = 1083° C.). In one repeat experiment the value of the temperature diffusivity α found was 0.0006 M.K.H. units (corresponding to $q = 120$ cal./min. $^{\frac{1}{2}}$), and in a second repeat, carried out on a mould which was baked at a higher temperature (about 600° C.), α was found to be equal to 0.0011 M.K.H. units (corresponding to $q = 140$ cal./min. $^{\frac{1}{2}}$). In all instances the solidification times of the casting varied correspondingly, and calculations based on the value of α and the time of solidification

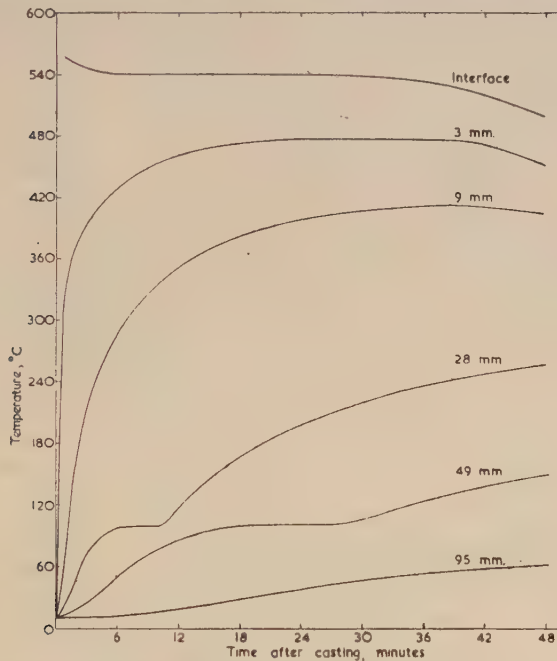


FIG. 23.—Green Synthetic Sand Mould. Heating curves obtained with interface temperature of 548° C.

lead to approximately the same figure for the specific heat (0.4 cal./g./° C.). It is clear therefore that, as with magnesite, the variability in plaster moulds is caused by differences in apparent thermal conductivity. The figures calculated for this quantity are 0.1₉, 0.2₈, and 0.3₇, M.K.H. units, corresponding respectively to the three experimentally determined diffusivities of 0.0006, 0.0008, and 0.0011 m.²/hr.

6. Green Sands.

All the heating curves obtained from green-sand moulds showed pronounced inflections at 100° C., and it was evident that these curves

could not be interpreted by the method used with the dry moulds. Heating curves obtained from green synthetic sand, with interface temperatures of 548° C. and 1083° C., are reproduced in Figs. 23 and 24, respectively; the curves obtained from green Mansfield sand moulds (not reproduced) were closely similar to those from the synthetic sands.

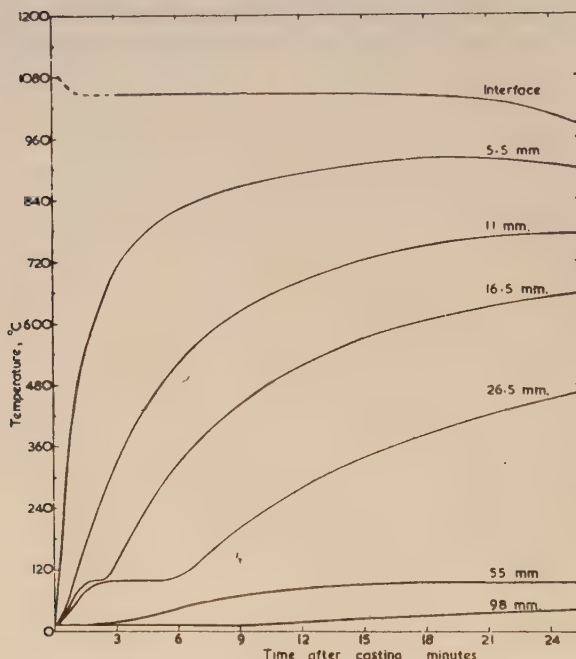


FIG. 24.—Green Synthetic Sand Mould. Heating curves obtained with interface temperature of 1083° C.

As plotting the temperature against $x/\sqrt{2t}$ was found to be useless, the temperature-distribution curves were obtained by plotting the temperature directly against the distance from the interface. This was done with each mould for several different times after casting, and families of curves were thus obtained of which those shown in Figs. 25 and 26 for synthetic sand, for interface temperatures of 548° and 1083° C., are typical.

Although the mathematical treatment cannot be applied to green moulds, the heat absorbed by these moulds in a given time can nevertheless be estimated by measuring the area under the temperature-distribution curve, multiplying by the mean specific heat and density,

and adding to the figure thus obtained a further figure to account for the heat content (above the initial heat content) of the moisture in the mould. This latter figure is derived by assuming that all the moisture initially present in that part of the mould which is at or above 100° C. will have been heated to this temperature; the heat absorbed by this moisture will then be the product of its mass, specific heat, and the temperature difference between 100° C. and the initial temperature of the

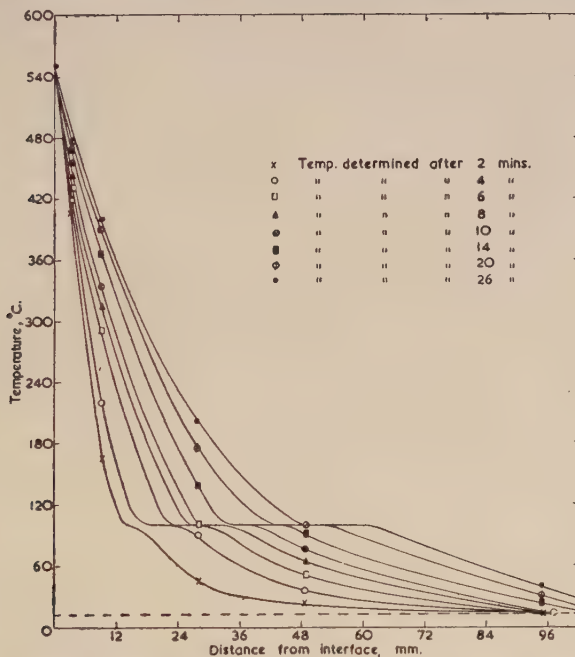


FIG. 25.—Curves Showing Temperature Distribution in Green Synthetic Sand Mould at Various Times after Casting. Interface temperature 548° C.

mould; the moisture in that part of the mould, the temperature of which is between the initial temperature and 100° C., is assumed to have been raised to a mean temperature of about 60° C. and its heat content calculated accordingly.

The heat contents of each of the moulds were thus calculated for a number of different times after casting; the figures so obtained for the total heat extracted by unit surface area of the moulds were plotted against the time (Fig. 27). Comparison of the curves in Fig. 27 with the corresponding curves for dry-sand moulds (Figs. 6 and 10) shows that, at an interface temperature of 548° C., heat is extracted more rapidly

by green-sand than by dry-sand moulds. The same is true at 1083° C., but here the relative difference is much smaller, because the heat absorbed by the moisture in the moulds is a much smaller part of the total. The above-stated finding that green sand has a higher rate of heat extraction than dry sand is in contradiction to the work of Briggs and Gezelius^{2,3} and others who have investigated both materials, but at steel-casting temperatures the differences would probably be very small.

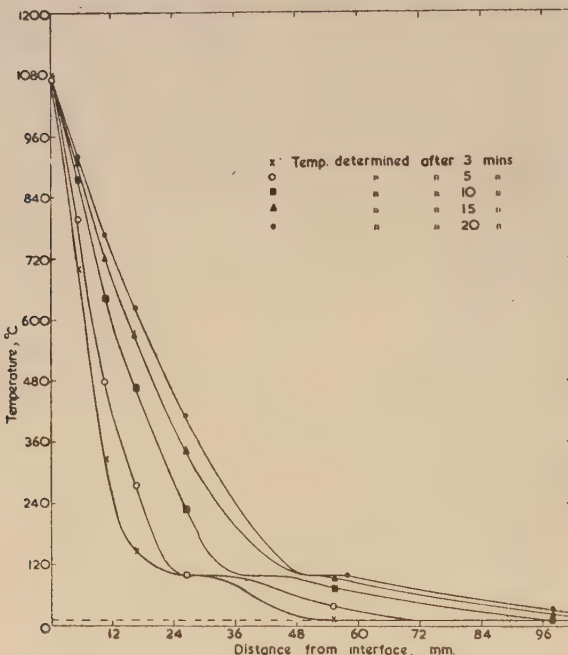


FIG. 26.—Curves Showing Temperature Distribution in Green Synthetic Sand Mould at Various Times after Casting. Interface temperature 1083° C.

and might not be revealed by the relatively cruder methods employed by these workers.

An attempt was made to derive an approximate mould constant for the green-sand moulds by plotting Q against \sqrt{t} and measuring the slope of the best straight line through the experimental points and the origin. Reasonably good straight lines, passing through the origin, were obtained for both sands at higher temperature and for Mansfield sand at the lower temperature. The values of the mould constant thus found are given in Table IV and, as is shown below, were consistent with the freezing times of the castings. With the synthetic sand, at 548° C. interface

temperature, no good line passing through the origin could be fitted to the experimental points, which, however, all fell close to a straight line which intersected the Q axis at about 60 cal. The value for the mould constant given by the slope of this was 108, but it is evident that this figure is very approximate.

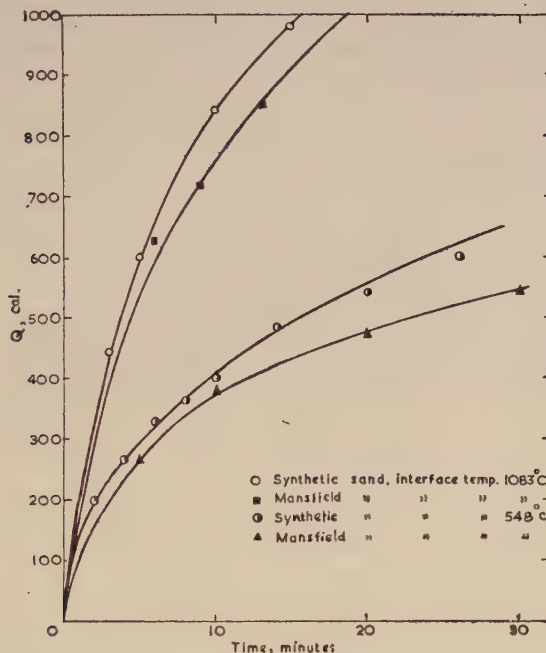


FIG. 27.—Approximate Curves Showing Heat Extraction by Green-Sand Moulds per cm^2 Surface Area.

7. General Discussion.

The accuracy of the results described above and the applicability of the mathematical treatment may be gauged to some extent by considering the solidification times of the castings made in the various moulds, for it follows from equation (7) that the solidification times of identical castings made in different moulds are inversely proportional to the square of the mould constant, since the total heat extracted from the castings must be the same in each instance. The observed solidification times t and calculated mould constants q have been tabulated in Table V for the aluminium-30% copper alloy castings (interface temperature 548° C.) and the copper castings (interface temperature 1083° C.)

together with values of the product $q\sqrt{t}$ which is equal to Q , the heat removed from the casting by each square centimetre of mould surface. It can be seen that the values of the product $q\sqrt{t}$ agree reasonably well for the individual castings in the two series. The freezing times of castings of the type used are subject to variations of 10–15% due to various accidental influences, as has been shown in other work¹⁴; this factor together with possible errors in the values assumed for the temperature diffusivity, more than accounts for such discrepancies as are apparent in Table V.

TABLE V.—Freezing Times of Castings : Heat Extracted per cm.² of Mould Surface.

Mould Material	Interface Temperature : 548° O.			Interface Temperature : 1083° O.		
	Freezing Time, t , min.	Mould Constant, q	$Q = q\sqrt{t}$, cal.	Freezing Time, t , min.	Mould Constant, q	$Q = q\sqrt{t}$, cal.
Magnesite . . .	8	230	650	8	354	1000
Silicon carbide . . .	>26	119	>608	10	330	1010
Green synthetic sand . . .	41	108	692	20	258	1150
Green Mansfield . . .	42	105	680	21	237	1090
Synthetic sand . . .	50	89·4	635	20	244	1090
Mansfield sand . . .	60	93·6	720	22	228	1070
Plaster . . .	73	80	710	75	125	1080

The experimental results described and discussed in the preceding paragraphs suffice to show that the heating of a mould in contact with a casting and the heat extraction from the casting by the mould are amenable to mathematical calculation on the lines laid down in Section II. These calculations should prove of great benefit in future studies of the progress of solidification in castings. The most serious cause of such discrepancies as may exist between the results of theoretical calculations and the observed results appears to lie in the variations with temperature of the temperature diffusivity, and errors due to this factor are more likely to occur with some materials than with others.

Non-constancy of the interface temperature is probably not an important source of error. Where alloys of short freezing range are cast in sand the effect is not large, and the interface temperature may be taken equal to the freezing point of the casting; with long-freezing-range alloys a mean interface temperature can safely be used in making the calculations. With moulds in materials such as magnesite, which have a fairly high chilling capacity (relative to sand), the interface temperature is a few degrees below the freezing temperature of the casting, but a correction can readily be made for this.

The conclusions above only apply to materials of low or moderate chilling power; with materials of high chilling capacity the errors would probably be very much larger, especially those due to non-constancy of the interface temperature. It will probably be necessary to extend the mathematical analysis of the problem before these cases can be considered. The possibility of air-gap formation between a mould of high chilling power and the casting will also have to be borne in mind.

The possibility of any extensive application of calculations of the heat extraction by moulds, which is likely to prove of great value in research and industry, must necessarily be based upon accurate thermal data, and further work will be largely dependent upon a more accurate knowledge of the relevant constants than is at present available.

As a matter of interest the apparent thermal conductivities of some of the mould materials studied in this work have been calculated using Russell's equations (equations (8) and (11)). These calculations have been made for two temperatures— 500° and 1000° C.—and the results are given in Table VI, together with the figures obtained from the experimental data by calculation using equation (3). The constants used in making the calculations are listed in Table VII. In studying

TABLE VI.

Mould Material	Thermal Conductivity Calculated from Russell's Equations, C.G.S. units		Mean Conductivity Found Experimentally, C.G.S. units	
	500° C.	1000° C.	Room Temper- ature to 548° C.	Room Temper- ature to 1083° C.
Synthetic sand . . .	0.0009	0.0016	0.0010	0.0017
Mansfield sand . . .	0.0008	0.0010	0.0010	0.0014
Bonded magnesite . . .	0.0008	0.0012	0.0049	0.0027
Bonded silicon carbide	0.0009	0.0020	0.0016	0.0028

TABLE VII.

Mould Material	Mean Grain Dia., mm.	Thermal Conductivity of Pure Substance, C.G.S. units		Density of Pure Sub- stance, g./c.c.
		500° C.	1000° C.	
Synthetic sand . . .	0.25	0.013 ²²	0.0098 ²²	2.65 ²⁵
Mansfield sand . . .	0.11	0.013 ²²	0.0098 ²²	2.65 ²⁵
Bonded magnesite . . .	{ 48% of 0.46 52% of 0.09	0.032 ²⁴	0.010 ²⁴	3.62 ²⁶
Bonded silicon carbide	0.27	0.78 ²²	0.48 ²²	3.21 ²⁷

The thermal conductivity of air was taken to be 0.000129 C.G.S. units at 500° C. and 0.000182 C.G.S. units at 1000° C.²³

the figures in Table VI it must be remembered that those calculated from Russell's equations are values of the apparent conductivity at a particular temperature; the experimental figures, on the other hand, are mean figures.

Comparison of the calculated and observed results shows fair agreement of the figures for the synthetic sand, although the calculated figures are perhaps rather low since it is to be expected that the instantaneous values at 500° or 1000° C. would be larger than the mean figures. The calculated figures for the other materials are all distinctly too low; this is especially true of the figures for magnesite, where the calculated figures are not even of the same order as the observed values.

It is difficult to suggest any adequate reason for these discrepancies, but it may be that Russell's theory is inapplicable to mixtures of relatively coarse particles with large quantities of fines. The discrepancy between the observed and calculated figures for silicon carbide may be due to the particle shape which departs widely from the idealized shape assumed by Russell.

The comparison made in Table VI of the observed and calculated figures for the sands, coupled with the similar comparison made by Lucks, Linebrink, and Johnson,²⁰ suggest that use of Russell's equations leads to moderately accurate values of the apparent conductivity of moulding sand; further work will, however, be necessary before this theory can be accepted without reserve. It is evident that great caution is necessary when applying Russell's theory to materials other than sand.

VI.—CONCLUSIONS.

The principal conclusions emerging from the work described above are summarized briefly as follows:

(1) The heating of a plane mould wall, of low or moderate chilling power, in contact with a casting, and the rate of heat extraction by the mould wall are amenable to mathematical treatment with a good degree of accuracy, provided that the interface temperature is fairly constant, the temperature diffusivity of the material is not greatly affected by temperature, and the mould is free from moisture.

(2) The values for the temperature diffusivities of the various materials obtained during the course of the work are reasonably consistent with the figures obtained by other workers.

(3) The grain-size distribution of the material of a non-metallic mould is an important factor which, by influencing the porosity and the extent of intergranular radiation, greatly affects the apparent thermal conductivity and chilling power, especially at high temperatures.

(4) The chilling capacity of green sand is greater than that of dry sand at aluminium-casting temperatures, but the relative difference decreases with increasing temperature reaching a low value at copper-casting temperatures.

(5) Taking the chilling power (the value of the mould constant in Tables IV and V) of the dry synthetic sand investigated as unity at aluminium-casting temperatures, the approximate relative chilling powers given in Table VIII may be assigned to the materials examined. These ratings are different at aluminium- and copper-casting temperatures.

TABLE VIII.

Mould Material	Relative Chilling Power	
	Aluminium-Casting Temperatures	Copper-Casting Temperatures
Bonded magnesite	2½	4
Bonded silicon carbide	1½	3½
Green synthetic sand	1¼	2¾
Green Mansfield sand	1¾	2½
Dry synthetic sand	1	2¾
Dry Mansfield sand	1	2½
Plaster	7/8	1½

(6) It is possible to calculate approximately the freezing times of castings of simple shape, from knowledge of the thermal properties of the mould material.

ACKNOWLEDGEMENTS.

The authors are indebted to the Director and Council of the British Non-Ferrous Metals Research Association for permission to publish this paper. Their thanks are also due to their colleagues, and in particular to Dr. A. G. Quarrell and Mr. W. A. Baker, for helpful advice and assistance.

APPENDIX.

THE ERROR FUNCTION.

The solution of many of the differential equations arising in problems of heat conduction involves a definite integral of the form :

$$\frac{2}{\sqrt{\pi}} \int_0^x e^{-\beta^2} \cdot d\beta$$

which is known as the error function and is commonly written "erf x ". This integral cannot be evaluated directly, but approximate solutions may be obtained, when x is small, by expressing $e^{-\beta^2}$ as a uniformly

convergent series and integrating term by term, or when x is large, by repeated integration by parts.

The values of the error function when x is equal to 0 and ∞ are given by :

$$\operatorname{erf}(0) = 0$$

$$\operatorname{erf}\infty = 1$$

while for all values of x between 0 and ∞ , the error function assumes values between 0 and 1. A further important property of the error function is that :

$$\operatorname{erf}(-x) = -\operatorname{erf}x.$$

The error function frequently appears in heat-flow problems as $1-\operatorname{erf}x$, and this expression is usually written $\operatorname{erfc}x$.

The values of $\operatorname{erf}x$, $\operatorname{erfc}x$, and other related functions have been tabulated and are given in the literature.^{28, 29}

REFERENCES.

1. H. S. Carslaw and J. C. Jaeger, "Conduction of Heat in Solids". London : 1947 (Oxford University Press).
2. C. W. Briggs and R. A. Gezelius, *J. Amer. Soc. Naval Eng.*, 1933, **45**, 462.
3. C. W. Briggs and R. A. Gezelius, *Trans. Amer. Found. Assoc.*, 1935, **43**, 274.
4. A. H. Diercker, *Trans. Amer. Inst. Min. Eng.*, 1930, **90**, 83.
5. M. A. Scott, *Trans. Amer. Found. Assoc.*, 1939, **47**, 513.
6. N. Chvorinov, *Giesserei*, 1940, **27**, 177, 201, 222.
7. N. Chvorinov, *Proc. Inst. Brit. Found.*, 1938-39, **32**, 229.
8. C. G. Lucks, O. L. Linebrink, and K. L. Johnson, *Trans. Amer. Found. Assoc.*, 1947, **55**, 62.
9. H. W. Dietert, E. J. Hasty, and R. L. Doelman, *Foundry*, 1947, **75**, (9), 84.
10. H. A. Schwartz, *Trans. Amer. Found. Assoc.*, 1945, **53**, 159.
11. *J. Iron Steel Inst.*, 1942, **146**, 393 p.
12. H. W. Dietert, H. H. Fairfield, and E. J. Hasty, *Trans. Amer. Found. Assoc.*, 1947, **55**, 175.
13. M. V. Chamberlin and J. G. Mezoff, *Trans. Amer. Found. Assoc.*, 1946, **54**, 648.
14. R. W. Ruddle, *Inst. Metals Monograph and Rep. Ser. No. 6*, 1949 (in the press).
15. R. W. Ruddle, *J. Inst. Metals* (in the press).
16. L. Northcott, *J. Inst. Metals*, 1938, **62**, 101.
17. W. Cohn and A. E. MacGee, *Ber. deut. keram. Ges.*, 1926, **7**, 149.
18. K. K. Kelley, *U.S. Bur. Mines Bull.* No. **371**, 1934.
19. W. Miehr, H. Immke, and I. Kratzert, *Tonind.-Zeit.*, 1925, **50**, 1671.
20. C. F. Lucks, O. L. Linebrink, and K. L. Johnson, *Trans. Amer. Found. Soc.*, 1948, **56**, 363.
21. H. W. Russell, *J. Amer. Ceram. Soc.*, 1935, **18**, 1.
22. A. Eucken, *V.D.I. Forschungsheft*, 1932, [B], **3**, 353.
23. M. ten Bosch, "Die Wärmeübertragung", p. 257. Berlin : 1936 (J. Springer).
24. J. B. Austin, [A.S.T.M.] *Symposium on Thermal Insulating Materials*, 1939.
25. Y. Tu, *Phys. Rev.*, 1932, [ii], **40**, 662.
26. M. Ponte, *Compt. rend.*, 1929, **188**, 909.
27. G. Borrmann and H. Seyfarth, *Z. Krist.*, 1933, **86**, 472.
28. W. F. Sheppard, "The Probability Integral". (*Brit. Assoc. Advancement Sci. Math. Tables*, 1939, 7.)
29. E. Jahnke and F. Emde, "Tables of Functions". Leipzig : 1933 (Teubner).

THE METALLOGRAPHY OF COPPER CONTAINING SMALL AMOUNTS OF BISMUTH.*

By L. E. SAMUELS,† B.Met.E., STUDENT MEMBER.

SYNOPSIS.

The dark lines noted at the grain boundaries of electrolytically polished specimens of brittle bismuth-containing copper are not films, as previously supposed, but are step-like grooves. Deep etched grooves are also developed at the grain boundaries of both mechanically polished and electrolytically polished specimens of this material by a number of etching reagents. It is suggested that brittleness of such material is attributable to a brittle zone resulting from the concentration, without precipitation, of bismuth at the grain boundaries; a mechanism of embrittlement based on one previously advanced for the temper-brittleness of steels is suggested.

I.—INTRODUCTION.

In a recent paper, Voce and Hallowes¹ reported the results of an extensive investigation into the mechanism of embrittlement of deoxidized copper by bismuth, and concluded that the embrittlement was primarily attributable to the presence of thin films of elementary bismuth at the grain boundaries of the copper. This conclusion was largely dependent upon the co-operative metallographic work carried out by Schofield and Cuckow,² who detected "dark lines" in electrolytically polished samples of brittle materials. Electron micrographs of plastic replicas of the polished surface of these samples showed broad bright lines each flanked on one side by a thin dark line, which was interpreted by Schofield and Cuckow to indicate that the broad bright lines corresponded to parts which stood proud above the general surface of the specimens. It was concluded, therefore, that the bright lines were the exposed edges of intercrystalline films of a discrete second phase in the material.

Cuckow³ later reported the further examination of an electrolytically polished specimen of the brittle copper by means of a phase-contrast microscope. The micrographs obtained by this method were very similar in appearance to the original electron micrographs of surface replicas, and were also interpreted by Cuckow to indicate the presence of exposed edges of intercrystalline films.

Schofield and Cuckow's² paper gave rise to discussion by Limb and the

* Manuscript received 14 April 1949.

† Metallurgist, Defence Research Laboratories, New South Wales Division, Lidcombe, Australia.

present author⁴ and, as a result of this and of correspondence between the latter and Mr. Schofield, duplicate specimens of the material examined by Schofield and Cuckow were made available to the author by the British Non-Ferrous Metals Research Association, primarily with the object of attempting to detect the apparent intercrystalline films by mechanical polishing. This paper covers the results of the metallographic examination of these copper samples.

II.—MATERIAL.

The material examined consisted of four samples of cold-rolled and annealed non-arsenical phosphorus-deoxidized copper strip designated KAV 71, KAV 91, KAV 105, and JXH 4, containing 0·00005 ("bismuth-free"), 0·005, 0·0075, and 0·015% bismuth, respectively. Each sample was received in two conditions, namely : (a) bright annealed at 550° C. for 1 hr. and quenched in water (brittle condition, except the "bismuth-free" sample), designated by the suffix "A" to the identification numbers; (b) bright annealed at 750° C. for $\frac{1}{2}$ hr. and quenched in water (ductile condition), designated by the suffix "B" to the identification number.

III.—PREPARATION OF THE SPECIMENS FOR METALLOGRAPHIC EXAMINATION.

1. *Mechanical-Polishing Technique.*

After rough preparation on files, the specimens were rubbed successively by hand on grades "280" and "400" waterproof Alundum abrasive papers, using flowing water as a lubricant. Subsequent polishing was carried out in four stages :

Stage (a). Hand rubbing on a dry wax-impregnated linen lap charged with "20 sec."-grade elutriated-alumina abrasive (prepared by the methods developed by Rodda⁵).

Stage (b). Hand polishing on a linen pad charged with a water paste of "3 min."-grade elutriated-alumina abrasive.

Stage (c). Hand polishing on a "Selvyt"-cloth pad charged with a water paste of "30 min."-grade elutriated-alumina abrasive, using a small amount of high-grade soap as lubricant.

Stage (d). Final hand polishing on a "Selvyt"-cloth pad charged with a water paste of calcined magnesium oxide.

The multi-stage nature of this process and the use of carefully graded abrasives facilitates rapid polishing, a short time only being required at each stage to remove the scratches of the previous stage. The rapid

rate of polishing, particularly in the intermediate stages, also increases the likelihood of the removal at each stage of the disturbed layer beneath the previous scratches.

2. Electrolytic-Polishing Technique.

Specimens for electrolytic polishing were first prepared by mechanical polishing up to stage (b) above. The electrolyte used consisted of an aqueous solution of orthophosphoric acid (1000 g. (density 1.75 g./ml.)/l.) saturated with copper before use. The specimen, mounted in bakelite, was arranged with the polishing face horizontally upwards, at a distance of approximately 2.5 cm. below a 5-cm.-dia. sheet-copper cathode; the electrolyte was at room temperature and was not stirred. A bleeder resistance of 0.8 ohm was used in parallel with the polishing cell, as recommended by Horowitz and Maltz.⁸

The nominal polishing range in this cell was 1.05–1.35 V.; at 1.3 V. the preliminary polishing scratches were removed in less than 5 min.

IV.—DESCRIPTION OF MICROSTRUCTURES.

1. Specimens Prepared by Mechanical Polishing.

Although intercrystalline films were not detected in any as-polished specimens after correct mechanical polishing by the methods outlined above, a number of interesting features, which are described in some detail below, were noted after etching. The features discussed were confined to the brittle samples and were in no case observed in specimens of ductile material.

Polished specimens of brittle material etched in standard alkaline reagents, such as ammonium persulphate, cupric ammonium chloride, and ammonium hydroxide–hydrogen peroxide, characteristically showed small, dark, somewhat triangular features at the junctions of grain boundaries (Fig. 1, Plate IX); apparent intercrystalline films, however, could not be developed even by deep etching in these reagents.

Apparent intercrystalline films could, however, be developed in all brittle specimens by etching in standard acid etching reagents such as 50% aqueous nitric acid (Fig. 2, Plate IX), acid ferric chloride, chromic oxide–hydrochloric acid reagents (Fig. 3, Plate IX), and also by etching in the electrolytic-polishing cell at approximately 0.8 V. (Fig. 4, Plate IX).

The extent and width of the apparent films was dependent upon both the etching time and the nature of the reagent. Light etching, particularly with nitric acid, developed only dark triangular features at the grain-boundary junctions similar to those developed by the alkaline reagents. (This type of feature is indicated by the arrows in

Fig. 9, Plate XI ; as explained below, this specimen had been very lightly etched in dilute nitric acid). Normal etching developed the apparent intercrystalline films referred to above, whereas further over-etching increased the width of the apparent films without increasing their number and extent. After normal etching, the films were most prominent in electrolytically etched specimens, were slightly less marked in specimens etched in nitric acid, and considerably less marked in specimens etched in the remaining reagents (compare Figs. 2, 3, and 4, Plate IX). Careful comparative examination showed, however, that the apparent films were developed in the same number and to the same extent in a particular specimen by the various acid reagents. The maximum width of apparent film developed by any of the reagents was of the order of 1μ .

If specimens which had been etched electrolytically or in nitric acid were repolished on the magnesia pad (polishing stage (d)), the apparent films remained prominent after the general etch had been removed; the microstructure of the specimens was then somewhat similar to that of electrolytically polished specimens (see Section IV. 2). The apparent films slowly disappeared, however, during further repolishing. Apparent films developed by the less active reagents were removed with the general etch during repolishing.

Since the width of the apparent films depended upon the severity of the etch, and since they could be gradually removed by subsequent polishing, it was apparent that a standardized preparation technique was essential for comparative examination of the samples. The technique chosen was light etching in nitric acid followed by sufficient polishing on the magnesia pad to remove only the general etch, the process being repeated several times in order to develop fully the apparent films. This technique, which is subsequently referred to as the "nitric-acid-etch method", gave reproducible results.

The results of examination of the specimens prepared by this method were in conformity with the observations reported by Schofield and Cuckow² for electrolytically polished specimens, i.e. apparent intercrystalline films were detected only in specimens KAV 91A, KAV 105A, and JXH 4A, the number of apparent films increasing with the bismuth content. A typical micrograph of a specimen of JXH 4A prepared by this method is shown in Fig. 7 (Plate X).

2. Specimens Prepared by Electrolytic Polishing.

The examination of specimens in the as-electrolytically-polished condition confirmed the observations previously described by Schofield and Cuckow.² A micrograph of a specimen of JXH 4A after electrolytic

polishing at 1.3 V. for 15 min. is shown in Fig. 8 (Plate X). It will be noted from a comparison of Figs. 7 and 8 that, although the apparent films are developed to approximately the same extent by the two methods of polishing, the apparent films developed by electrolytic polishing were considerably thinner and less marked than those developed by mechanical polishing and etching (nitric-acid-etch method).

The apparent films developed by electrolytic polishing completely disappeared after a very short period of polishing on the magnesia pad (polishing stage (*d*)).

Electrolytic polishing at voltages over the entire nominal polishing range of the cell (1.05–1.35 V.) and for widely different periods of time did not alter the appearance of the apparent films. The films became much more marked, however, when specimens polished at the normal voltage were subsequently etched by reducing the cell voltage to approximately 0.8 V., the width of the apparent films increasing with longer etching times in the cell (compare Figs. 5 and 6, Plate X). Etching by this means, however, did not increase the number and extent of the apparent films. The microstructure of specimens etched in this manner was similar to that of mechanically polished and electrolytically etched specimens (compare Fig. 5, Plate X, and Fig. 4, Plate IX); the triangular features at the grain-boundary junctions were not as marked, however, in the electrolytically polished specimens as in the similarly etched mechanically polished specimens.

The apparent films in specimens which had been electrolytically polished and electrolytically etched as above remained prominent after the general etch had been removed by hand polishing on the magnesia pad (polishing stage (*d*))); the microstructure of the specimens was then identical with that of specimens prepared by the mechanical nitric-acid-etch method. In this case also, the apparent films were gradually removed by further mechanical polishing.

Etching electrolytically polished brittle specimens in the standard acid reagents also widened the apparent films. The apparent films in electrolytically polished specimens were less pronounced, however, after light etching in the alkaline etching reagents, and after further etching it was not possible to distinguish between apparent films and normal grain boundaries; triangular features were again developed at the grain-boundary junctions by heavier etching in these reagents.

V.—NATURE OF APPARENT INTERCRYSTALLINE FILMS.

It was thought that the features described above indicated that the "dark lines" (referred to as "apparent films") developed in brittle

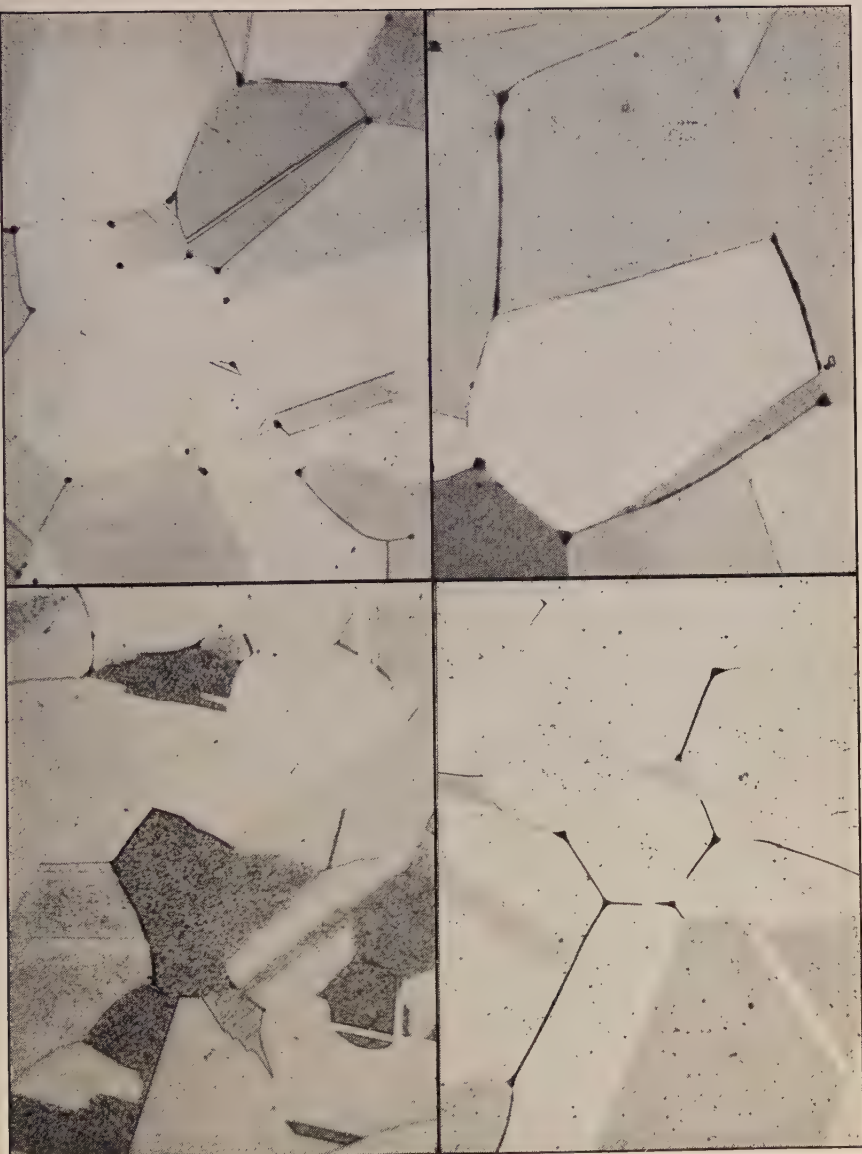
material both after mechanical and electrolytic polishing were etched grooves rather than the exposed edges of intercrystalline films. In particular, it was considered that the manner in which the dark lines gradually disappeared during repolishing on the magnesia pad is consistent with the lines being discrete films only if it is assumed that the surface was severely "flowed" during repolishing. It is believed that the polishing methods used do not flow the polished surface, and some evidence to support this belief is given below. Further, if the dark lines are discrete films, it is difficult to understand why the width of the lines should be dependent upon etching conditions, or why the lines developed by electrolytic polishing should have become considerably more marked when the specimens were etched by reducing the cell voltage.

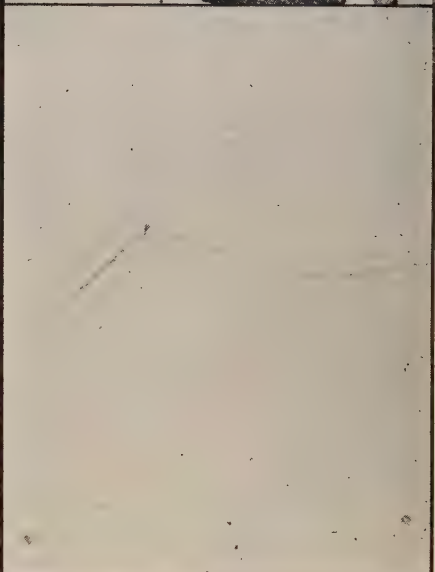
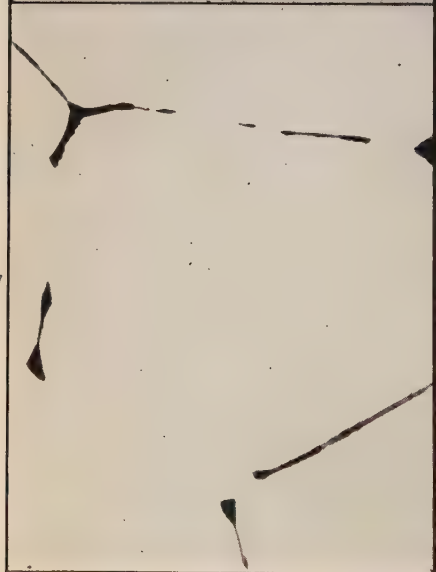
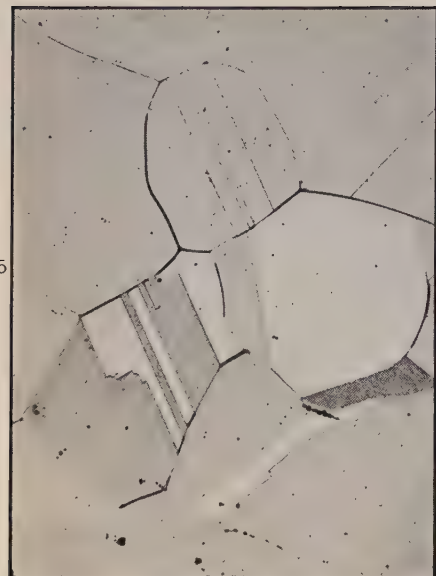
With a view to obtaining definite evidence as to the nature of the apparent films, a number of polished specimens of JXH 4A were heavily electroplated with copper, sectioned perpendicular to the original polished surface, and the sectioned surface mechanically polished by the standard technique. In order to avoid relief between the electroplating and the original specimen, the sections could only be etched lightly, 30% aqueous nitric acid being used in all cases. The triangular features at the grain-boundary junctions only were developed in these sections. Electrolytic polishing of these specimens resulted in too much relief for satisfactory examination.

The original polishing treatments of specimens examined in this way were as follows :

- (i) Mechanical polish, nitric-acid-etch method (as in Fig. 7, Plate X).
- (ii) Mechanical polish, etched in chromic oxide-hydrochloric acid reagent (as in Fig. 3, Plate IX).
- (iii) Electrolytic polish, as-polished (as in Fig. 8, Plate X).
- (iv) Electrolytic polish, electrolytic etch (as in Fig. 6, Plate X); general etch just removed by hand polishing on the magnesia pad.

Examination of these sections clearly showed that the dark lines or apparent films developed at the grain boundaries in specimens prepared by method (i) (see Figs. 9 and 10, Plate XI), method (ii), and method (iv) (see Fig. 11, Plate XI) are, in fact, etched grooves or channels. In this respect, it is noted that Voce and Hallowes¹ observed that massive globules of bismuth in coppers containing high concentrations of bismuth were less rapidly dissolved than the copper during normal electrolytic polishing. It is to be anticipated that this differ-

FIG. 1.—JXH 4A. Mechanical polish, etched in ammonium persulphate solution. $\times 500$.FIG. 2.—JXH 4A. Mechanical polish, etched in nitric acid solution. $\times 500$.FIG. 3.—JXH 4A. Mechanical polish, etched in chromic oxide-hydrochloric acid reagent. $\times 500$.FIG. 4.—JXH 4A. Mechanical polish, electrolytic etch, 0.8 V., 3 sec. $\times 500$.

FIG. 5.—JXH 4A. Electrolytic polish, electrolytic etch, 0.8 V., 3 sec. $\times 500$.FIG. 6.—JXH 4A. Electrolytic polish, electrolytic etch, 0.8 V., 10 sec. $\times 500$.FIG. 7.—JHX 4A. Mechanical polish, nitric-acid-etch method. $\times 1500$.FIG. 8.—JHX 4A. Electrolytic polish. $\times 1500$.

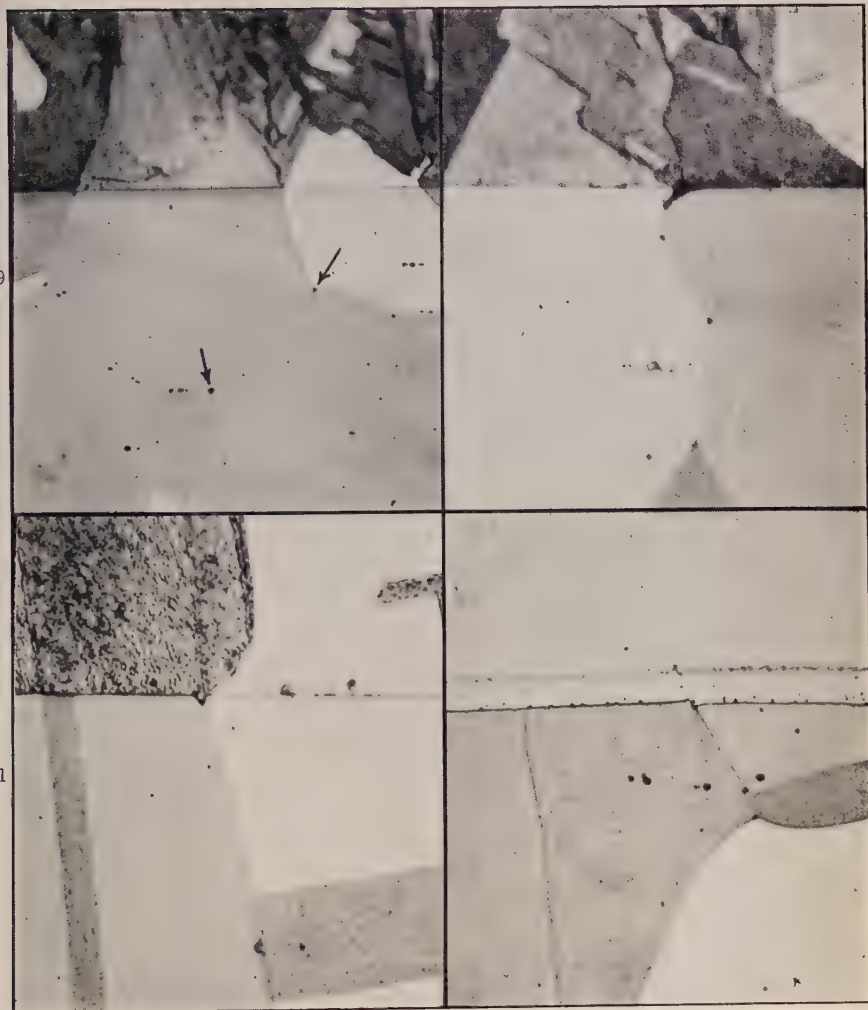


FIG. 9.—Perpendicular Section, JXH 4A. Original surface prepared by mechanical polish, nitric-acid-etch method. $\times 500$.

FIG. 10.—As Fig. 9. $\times 1500$.

FIG. 11.—Perpendicular Section, JXH 4A. Original surface electrolytically polished and electrolytically etched. $\times 1500$.

FIG. 12.—Taper Section, JXH 4A. Original surface electrolytically polished. $\times 15,000$. (Effective magnification perpendicular to original surface.)

ence in solution rate would be exaggerated at the lower cell voltages which result in etching. On this basis, it would be expected that even the finest bismuth film would afford some evidence of a ridge at the root of the groove shown in Fig. 11 (Plate XI). It is evident, therefore, that the entirely groove-like nature of the apparent films in the electrolytically polished, electrolytically etched specimen is not consistent with the conclusion that dark lines in as-electrolytically-polished specimens are bismuth films of even sub-microscopic dimensions.

The evidence obtained by examination of the perpendicular section of the as-electrolytically-polished surface (method (iii)) was not conclusive. A further electrolytically polished specimen of JXH 4A was therefore prepared as above, except that the specimen was flash nickel-plated before copper plating (in order to delineate sharply the original polished surface) and the plated specimen was taper-sectioned at an angle of approximately $5^{\circ} 43'$ to the original polished surface. By this means, the depth of irregularities in the original polished surface, such as ridges or grooves, are mechanically magnified by approximately 10 dia. in the surface of the taper section.

The taper section of a typical portion of the electrolytically polished surface is shown in Fig. 12 (Plate XI), the portion shown including both a normal grain boundary and a grain boundary at which a dark line or apparent film had been located. It is clear that the apparent film is actually a step at the grain boundary, flanked by a slight ridge in one of the adjoining grains and a shallow groove in the other adjoining grain. This contour, which is characteristic of the apparent films, is not that to be expected of a discrete film of a second phase but must have resulted from uneven solution during electrolytic polishing of the copper at and adjacent to the grain boundary. It should be noted that the contour shown in Fig. 12 provides a ready explanation of the electron micrographs of surface replicas obtained by Schofield and Cuckow,² the step and ridge corresponding with the broad bright line of the electron micrographs and the adjoining shallow groove corresponding with the thin dark line.

No attempt was made to determine the nature of the dark triangular features developed at grain-boundary junctions, particularly by alkaline etching reagents; it would seem reasonable to assume, however, that these features are also etched grooves or pits. The action of alkaline etching reagents on electrolytically polished specimens of brittle copper would therefore be to reduce the prominence of, or even to eliminate, the dark lines by removing uniformly the surface layer of the specimen and to develop triangular-shaped pits at the grain-boundary junctions. This behaviour may explain the "dark tail-like features" at the grain-

boundary junctions, noted by Schofield and Cuckow² in electron micrographs of replicas of surfaces which had been etched in ammonium persulphate.

Attention is drawn to Fig. 9 (Plate XI), which is a micrograph of the section shown in Fig. 10 (Plate XI) at a lower magnification; the original surface of this specimen had been prepared entirely by mechanical polishing and was in the unetched condition before plating. It will be noted that the grains of the electrodeposited copper are completely conformable with the grains at the original polished surface. It has been suggested by Jacquet^{7, 8} that conformability of the electrodeposit can only be obtained when the polished surface is completely free from "flow" and/or distortion. It would appear possible, therefore, that the methods of mechanical polishing used in this investigation finally produce "flow"-free, undistorted surfaces; it is intended to investigate this matter further.

One other point of interest was noted during the course of the examination. Electrolytic etching and etching in nitric acid developed the grooves or apparent films to a much more marked extent than electrolytic polishing alone, and also developed clearly the normal grain boundaries; it was possible to establish definitely, therefore, that the apparent films were developed entirely at the grain boundaries of these samples.

VI.—DISCUSSION.

On the basis of the above-quoted metallographic evidence, it is concluded that any discrete grain-boundary films present in the brittle copper must be of sub-microscopic dimensions; in this event, the films cannot be bismuth films, but would have to be films of a constituent whose solution rate during electrolytic polishing and etching is greater than that of the surrounding copper. Even if it is assumed that films which comply with these requirements are present in the brittle material, it is still necessary to explain the heavy selective etching of a relatively wide zone adjacent to the more brittle grain boundaries by a number of specific etching reagents. It would seem more reasonable, therefore, to ascribe the brittleness to the presence of brittle zones at the grain boundaries rather than to the presence of films of a brittle constituent.

Recent work carried out on copper-antimony alloys and on temper-brittle steels has shown analogies with the copper-bismuth alloys, in that the grain boundaries of the alloys are embrittled by heating at temperatures within a certain range, and that some of the embrittled grain boundaries are preferentially etched by specific metallographic methods.

The work on copper-antimony alloys was carried out by McLean and Northcott,⁹ who observed discontinuous intercrystalline features or apparent films in electrolytically polished and etched specimens of brittle material. McLean¹⁰ subsequently concluded from observations of the electrolytically polished specimens with an interference microscope that these features were etched grooves rather than discrete films. It is of particular interest to note that the contour deduced by McLean for these grooves is very similar to that shown in Fig. 12 (Plate XI).

Cohen, Hurlich, and Jacobson¹¹ have developed a special reagent which attacks heavily and preferentially the grain boundaries of steels in the temper-brittle condition, but which attacks the grain boundaries lightly or not at all when the material is in a ductile condition. McLean and Northcott¹² have confirmed this work and have concluded that the features etched at the grain boundaries are grooves or channels and are not associated with precipitated constituents. These authors also showed that the fracture surface of impact test-pieces of brittle material follows the path of the network etched by the reagents.

McLean and Northcott¹² have suggested that temper-brittleness is due to the segregation, without precipitation, of carbon atoms at the grain boundaries, i.e. the carbon atoms diffuse to the grain boundary and build up a local concentration, which may be considerably in excess of the normal solubility limit, without precipitation of carbon occurring. The segregation would result in severe local lattice distortion and consequently in grain-boundary brittleness. Concentration of solute atoms at the grain boundaries would increase with decreasing temperature. Below a certain temperature, however, the tendency to concentration would decrease as a result of the increasing importance of decrease in diffusion rate. These authors base this mechanism on the conclusion that, when the solute and solvent atoms are of different sizes, the distribution of solute atoms having minimum energy is one in which the solute atoms are concentrated at distorted regions such as grain boundaries and possibly also internal surfaces of misfit.

McLean¹⁰ has also briefly suggested that the mechanism of embrittlement of copper-bismuth alloys may be similar to that described for temper-brittleness of steels. Embrittlement of the alloys would then be attributable to the concentration by diffusion of bismuth at the grain boundaries, the bismuth concentration being a maximum at the grain boundary and decreasing for some distance from it. In view of the relatively large atomic diameter of bismuth, a concentration of this type is particularly likely to occur, and it is of interest to see how the theory can explain the experimental observations of Voce and Hallowes.¹ It

should be noted that this theory differs fundamentally from that originally proposed by Voce and Hallowes¹ only in that it supposes that relatively high concentrations of bismuth may develop at the grain boundaries without actual precipitation of elementary bismuth occurring.

The concept of severely distorted bismuth-rich zones adjacent to the grain boundaries adequately explains the action of metallographic etching reagents on the material, since it is reasonable to suppose that such a zone would be preferentially attacked by specific reagents. The manner in which the width of the etched groove varies with etching conditions is also in conformity with the concept of a concentration gradient in the bismuth-rich zone. It might also be deduced, from the manner in which the etched grooves end abruptly along a grain boundary, that the width of the concentration zones may change abruptly. Further, since the length of grain boundary attacked does not increase even after severe over-etching, it must be concluded that the width of the zone at the unattacked portions is sub-microscopic and probably of the same order of magnitude as a normal grain boundary.

The type of embrittlement curve produced by Voce and Hallowes¹ can also be immediately explained. As indicated above, the brittleness would be expected to disappear at temperatures above the solid solubility limit of bismuth within the grains (see Fig. 15 of paper by Voce and Hallowes¹) and to become progressively more marked at temperatures below the solubility temperature; at a certain temperature, however, the tendency to segregation would be balanced by a low diffusion rate and the brittleness would become less marked with further fall in temperature (see Fig. 1 of their paper).

By analogy with similar systems, it is reasonable to expect that the tendency to grain-boundary diffusion would be markedly increased by previous cold work. Voce and Hallowes¹ showed that embrittlement can occur in both annealed and cold-worked material, but that the embrittlement is considerably more marked in cold-worked than in annealed material. The theory is also in accord with Schofield and Cuckow's² observation that spheroidization of the "dark lines" in electrolytically polished specimens of brittle material does not occur even after extended periods of heating in the critical range, and with Voce and Hallowes's¹ experiments indicating that no sudden change in brittleness occurs at the melting point of bismuth. Neither of these features could be satisfactorily explained on the theory based on the presence of elementary bismuth films.

It is clear that the degree of embrittlement resulting from grain-boundary concentration of solute atoms would be dependent upon both the total content of solute atoms and the total grain-boundary area,

i.e. the grain-size. Voce and Hallowes¹ have also shown, however, that maximum embrittlement is attained when approximately sufficient bismuth is present to permit the formation of a monatomic layer of bismuth at the grain boundaries. In order to explain this feature satisfactorily by the modified theory, it must be assumed that almost the entire bismuth content of the alloy may segregate at or adjacent to the grain boundary, and that the presence of such a concentration of bismuth atoms is sufficient to cause brittleness. Further increase in bismuth content would increase the width of the segregated zone but would not markedly increase brittleness. These assumptions are in conformity with the deductions made above from the etching characteristics of the material.

VII.—SUMMARY.

It has been shown that the dark lines detected in electrolytically polished specimens of brittle copper by previous investigators are not films, as previously supposed, but are step-like grooves at the grain boundaries. It has also been shown that deep grooves are etched at the grain boundaries of both mechanically polished and electrolytically polished specimens by a number of acid reagents, the width of the grooves being dependent upon both the nature of the reagent and the severity of the etch; pits at the grain-boundary junctions but not grooves at the grain boundaries are developed by standard alkaline etching reagents.

A mechanism of embrittlement, based on one previously advanced to explain the temper-brittleness of steels, has been discussed; this mechanism attributes the brittleness to the concentration, without precipitation, of bismuth at and immediately adjacent to the grain boundary. The suggested mechanism offers a reasonable explanation of a number of major features of the embrittlement phenomena.

ACKNOWLEDGEMENTS.

The author wishes to acknowledge his indebtedness to Mr. Schofield and Mr. Hallowes for their encouragement and for providing the specimens examined. Acknowledgements are also due to the General Superintendent, Defence Research Laboratories, Australia, for permission to publish this paper.

REFERENCES.

1. E. Voce and A. P. C. Hallowes, *J. Inst. Metals*, 1947, **73**, 323.
2. T. H. Schofield and F. W. Cuckow, *J. Inst. Metals*, 1947, **73**, 377.
3. F. W. Cuckow, *J. Iron Steel Inst.*, 1949, **161**, 1.
4. L. E. Samuels and H. R. Limb, *J. Inst. Metals*, 1947, **73**, 805 (discussion).
5. J. L. Rodda, *Trans. Amer. Inst. Min. Met. Eng.*, 1932, **99**, (Inst. Metals Div.), 145.
6. J. Horowitz and J. Maltz, *Metal Progress*, 1947, **51**, 263.
7. P. A. Jacquet, *J. Chim. Phys.*, 1936, **33**, 226.
8. P. A. Jacquet, *Rev. Mét.*, 1938, **35**, 41.
9. D. McLean and L. Northcott, *J. Inst. Metals*, 1946, **72**, 583.
10. D. McLean, *J. Inst. Metals*, 1947, **73**, 791 (discussion).
11. J. B. Cohen, A. Hurlich, and M. Jacobson, *Trans. Amer. Soc. Metals*, 1947, **39**, 109.
12. D. McLean and L. Northcott, *J. Iron Steel Inst.*, 1948, **158**, 169.

MODERN BILLET CASTING, WITH SPECIAL **1211** REFERENCE TO THE SOLIDIFICATION PROCESS.*

By E. SCHEUER,† Dr.rer.nat., MEMBER.

SYNOPSIS.

The characteristic feature of the continuous-casting process, as opposed to the conventional billet-casting processes, is the stationary condition of the liquid part of the billet and of the solidification zone during the casting operation. The method is the outcome of a long and varied development, the main goals of which have been to secure improvement in production economy and in quality of the billet. The present paper is mainly concerned with the question of quality.

The requirements of an ideal billet-casting process are outlined on the basis of the structure of an ideal billet. Conventional billet-casting methods fail to meet these requirements in many respects, and developments aiming at overcoming these deficiencies are reviewed. The latest of them is the continuous-casting process, which comes much nearer to satisfying the requirements of the ideal casting process than the methods previously in use. In the aluminium industry it has, since the war, become by far the most popular casting process.

Improvements are still needed in :

- (a) Elimination of radial internal stresses which can produce hot tears and cracking of finished billets.
- (b) Application of the method to high-melting-point alloys (copper alloys, steels, &c.).
- (c) Development of the continuous strip-casting process to a point where it can become a popular production method.

I.—INTRODUCTION.

BILLET casting lends itself more readily to detailed theoretical and mechanical study than does the production of other castings, because simple geometrical shapes have to be produced in very large quantities. On the other hand, alloys used for billets are mostly difficult to cast as they are generally alloys with a long melting range, which, as far as possible, are avoided in foundries because of defects caused by their behaviour during freezing. In spite of this, billets must be of a uniformly high and consistent quality, so that considerable expenditure on research and equipment to produce them is justified.

II.—WHAT IS THE CONTINUOUS-CASTING PROCESS?

The conventional processes of billet casting are represented diagrammatically in the three sections of Fig. 1. The essential feature is the

* Manuscript received 17 February 1949. Read before the London Local Section on 9 December 1948.

† Chief Metallurgist and Head of Laboratories, International Alloys Ltd., Aylesbury, Bucks.

mould cavity of the required shape which is filled with liquid metal from the top or from the bottom, after which the metal is left to solidify. During the course of pouring and freezing, a number of changes take place in the mould and in the billet. The metal level rises from the bottom to the top of the mould, the temperature of the mould walls increases in a very complicated pattern in space and time, and the temperature in the billet falls in an equally or even more complicated

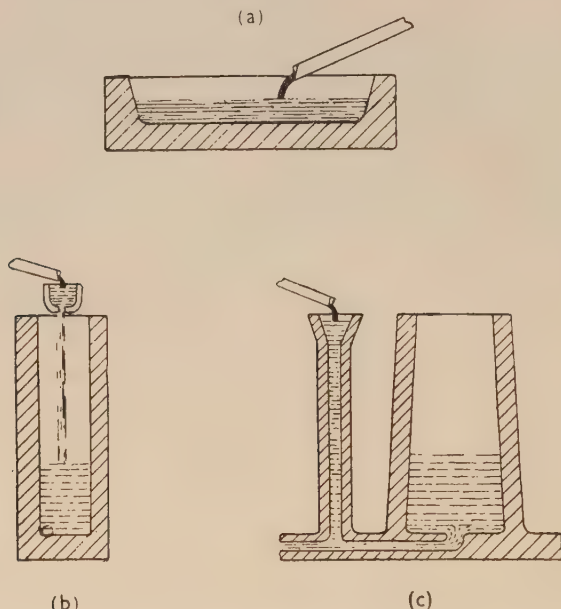


FIG. 1.—Conventional Billet-Casting Processes. (a) Flat cake; (b) Upright top-cast; (c) Upright bottom-cast.

way. At no time during the whole casting process is there a stationary condition, and, of course, each new billet starts the same cycle of changes.

Compare with this the diagram (Fig. 2) which represents the continuous-casting process. Here only a small part of the side walls of the billet is contained by the mould. The billet protrudes downwards and moves in this direction at a constant speed, while liquid metal is poured on to the top at a corresponding rate, so keeping the level of liquid metal in the mould practically stationary. By controlling the cooling process, the liquid-metal feed, and the speed and travel of the solid billet, the level of the liquid metal is kept steady and, most important of all, the boundary between the liquid and solid metal is fixed in

space. The result is that at any moment the physical and thermal conditions are the same, and if a sufficient supply of liquid metal and means of disposal of the billet are available, casting may be carried on continuously.

The characteristic feature of the continuous-casting process (termed for convenience C.C.P.) is the stationary condition during the casting process of the liquid part of the billet and the solidification zone, with

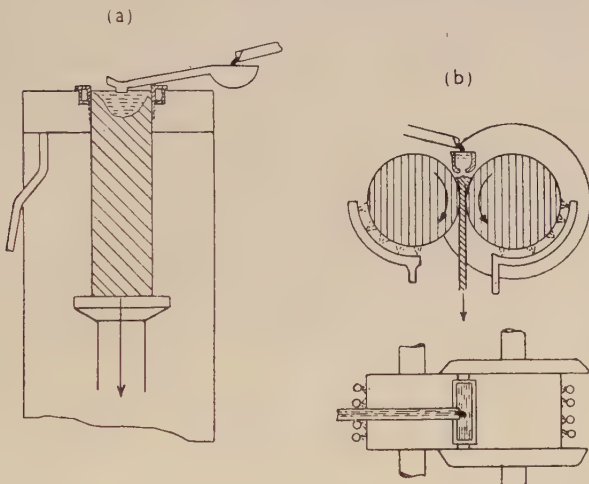


FIG. 2.—Continuous-Casting Processes. (a) Sleeve mould; (b) Roller mould.

respect to position in the mould and the temperature distribution in the freezing metal.

There is, in fact, hardly anything less exciting visually than the operation of a perfectly functioning casting machine¹ (Fig. 3, Plate XII).

It is obvious that, although the requirements of the C.C.P. are simple enough, the equipment necessary to secure a steady and uniform supply of liquid metal and an infinitely variable and reliable method of billet removal must be complicated and expensive and, consequently, the capital expenditure will be much greater than that required for equipment for conventional methods of casting.

The reasons justifying the expense and elaboration are :

- (i) Considerable economy in manpower.
- (ii) The production of billets of a metallurgical quality superior to those produced by any other process.

Of course, these two factors are not strictly separated in the long and varied development from the first conception to the practical production plant, but they can still be distinguished in the two machines typical of recent development, the continuous or semi-continuous billet-casting machine and the roller-type strip-casting machine. Both of these combine advantages of quantity and quality, but the accent is more on quality in the case of the sleeve-type billet-casting plant (Fig. 2 (a)), and more on quantity production in the roller-type strip-casting machine (Fig. 2 (b)).

III.—REQUIREMENTS OF AN IDEAL BILLET-CASTING PROCESS.

In this Section a short survey is made of the main metallurgical requirements for a billet, and of the principal features of an ideal casting process which can be deduced from these requirements. The properties of an ideal billet can be summed up as :

- (a) Absence of inclusions and flaws, i.e. slag, oxide, shrinkage and gas cavities, and cracks.
- (b) Uniform composition, i.e. absence of segregation of all kinds.
- (c) Fine and regular distribution of constituents in the micro-structure, i.e. small or finely branched primary crystals and eutectic grain to make homogenization easy.
- (d) Small grain-size of the matrix (small enough to make the billet mechanically homogeneous under the stresses of the first stages of deformation).
- (e) A clean and smooth surface.

In order to achieve such properties (apart from an ideal condition of the metal), an ideal casting process is needed. It will have to fulfil the following conditions :

- (1) Filling the mould without turbulence and oxidation to avoid trapped oxide, slag, and gases.
- (2) Lowest pouring temperature possible to avoid danger of gassing the metal and to facilitate rapid solidification.
- (3) Rapid heat extraction, producing fine grain and preventing release of gas dissolved in the melt, gravity segregation, and inter-crystalline shrinkage.
- (4) Directional solidification progressing from the "freezing end" of the billet (generally the bottom end) towards the "feeding end" (generally the top end). This eliminates piping.
- (5) Plane solidification front, i.e. during solidification the surface separating the liquid from the solid portion should not be curved. This prevents piping, eliminates internal stresses which may lead to cracking during and after solidification, and helps in overcoming inverse

segregation. The solidification front should also be normal to the longitudinal axis of the billet in order to eliminate inverse segregation completely.

IV.—THE IDEAL CASTING PROCESS AND THE CONVENTIONAL BILLET-CASTING PROCESS.

Let us now review the three standard billet-casting processes in their simplest form and consider how far they meet these requirements. Later some refinements applied to them will be described, and eventually the developments leading to the C.C.P.

1. *Filling the Mould without Turbulence and Oxidation.*

Obviously the top-pouring of an upright mould is most unfavourable in this respect. The metal has to travel the longest possible path before it reaches its final position, and it arrives in the liquid pool with some velocity, causing a more or less turbulent stirring effect. During this time there is considerable possibility of oxidation. Dross or slag carried into the mould is difficult to remove, as access to and observation of the metal sump in the mould is difficult, particularly during the earlier stages of filling (see Fig. 1).

The bottom-pouring method effects a real improvement on the top-pouring method in the matter of turbulence. As the metal stream is confined in a closed channel, its velocity can be controlled so as to ensure a comparatively quiet and smooth movement without any splashing. Even so, there will be a flow of the metal throughout the length of the billet from the bottom to the top during the filling period, which will mean a considerable amount of stirring. In the closed channel the question of oxidation does not arise.

The open, flat mould can be filled with comparatively little turbulence, and the metal surface is easily accessible for skimming. However, it is difficult to avoid some turbulence before the large bottom area of the mould is covered with liquid metal when starting the pour. The large open surface is also likely to oxidize to a considerable extent during pouring and freezing. All open-mould billets are, therefore, likely to have two sides with different properties. It is known that the top surface layer of copper billets cast in open moulds often contains considerable amounts of cuprous oxide, apart from gases which have accumulated in it during solidification. Fig. 4 (Plate XII) shows the unsymmetrical structure in a copper wire-bar.²

2. Low Casting Temperature.

The casting temperature must be high enough to allow for the heat loss in transferring the liquid metal from the furnace or casting ladle to its final position in the mould.

In this respect the flat, open mould is obviously very favourable. The path from the lip of the ladle to the centre of the mould is short, and that from the centre of the mould to the periphery is also as short as possible. The solidification, mainly from the bottom to the top, has only to progress through the smallest dimension of the billet. Feeding will require less superheat, as the feeding channels to be kept open are only half the length of those of an upright mould.

In the bottom-poured upright billet the path of the liquid metal is longest, and owing to the fact that the pouring stream goes right through the length of the billet, a considerable superheat will be required if the mould is to be completely filled.

The top-poured upright mould holds an intermediate position between these two extremes.

3. Intensive Heat Extraction.

The possible rate of heat extraction is controlled by the temperature gradient and the heat conductivity of the mould walls, the heat transfer between casting and mould walls, and the heat conductivity of the solid shell of metal formed along the mould wall.

By the use of thin-walled water-cooled moulds the temperature gradient in the mould wall can be increased to such a degree that it is no longer the limiting factor. The thermal conductivity of the solidified shell depends on the composition of the metal being cast, and cannot be altered. It is not a limiting factor as regards the possible heat-extraction rate, but plays an important role in limiting its practicable range in certain cases, as will be seen later. The real limiting factor of heat extraction proper is the heat transfer between billet and mould wall. This remains quite high while the metal is liquid and has proper contact with the wall, but as soon as a solid shell has formed around the billet, further cooling of the shell produces a contraction which results in the appearance of an air-gap between billet and mould, thus introducing considerable resistance to heat extraction just when the increasing thickness of solid metal between the freezing zone and the surface of the billet would call for more intensive cooling of the wall. The calculated temperature distribution³ in mould wall and billet during solidification of a steel ingot is shown in Fig. 9.

In all upright billet moulds, freezing proceeds more or less from the

sides towards the axis and, therefore, they are all subject to the insulating effect of the air-gap. Even in the case of the flat, open mould, where cooling is effected mainly through the bottom surface, and it might be

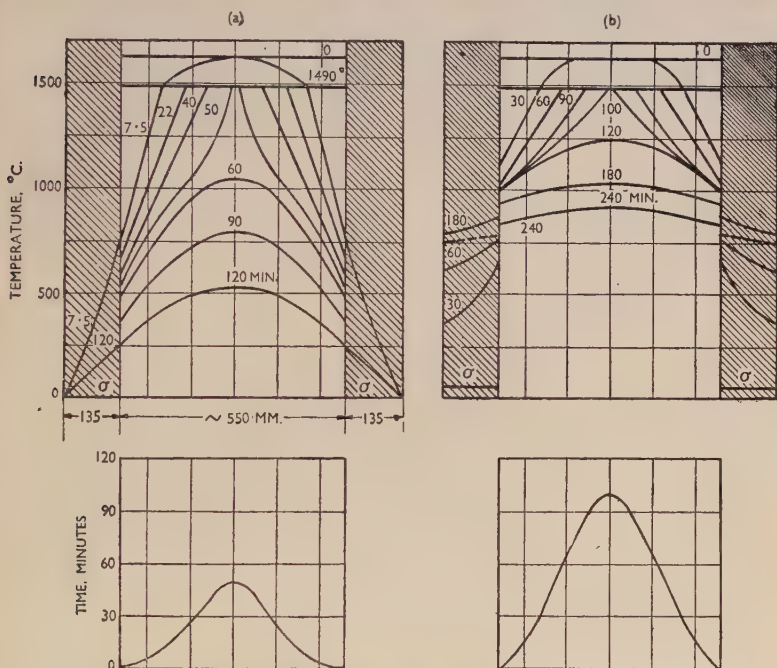


FIG. 9.—Calculated Temperature Distribution in Mould Wall and Billet during Solidification of a Steel Ingot Cast at 1620°C . (a) Continuous contact with mould wall; (b) 2-mm. air-gap between billet and mould wall. Curves showing progress of solidification given below. (Adapted from Schwarz.³)

expected that the weight of the billet would maintain proper surface contact, warping of the billet as the result of uneven cooling soon reduces the effectiveness of this contact.

4. Directional Solidification.

Directional solidification is a fundamental necessity if shrinkage cavities are to be avoided. In order to achieve it there must be established in the zone of solidification a temperature gradient great enough to prevent the trapping of liquid pockets by solid metal. For obvious reasons it is difficult to keep the top part of a liquid mass cold while the bottom is hot, therefore the general direction of the heat flow is mostly downwards. If the three standard moulds are considered from the point

of view of temperature distribution it will be seen that none of them comes very near to the ideal requirements (Fig. 10). The flat, open mould goes at least some way to meet the case. The side walls have only a limited effect, and the main cooling action comes from the bottom surface. Furthermore, liquid metal is added from the top with relatively low turbulence, and thus helps to increase the gradient, producing isotherms resembling in shape a shallow dish with rather steep sides.

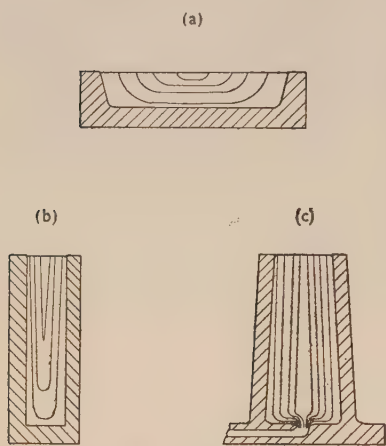


FIG. 10.—Shape of Isotherms in Three Conventional Billet-Casting Processes. (a) Flat cake; (b) Upright top-cast; (c) Upright bottom-cast.

The top-poured upright mould is intermediate between the two former cases. The predominant horizontal heat flow along the side walls is there, but the liquid metal flowing in from the top has at least some effect in the direction of tilting the gradient in the desired direction.

One incidental feature of this casting process can be and is being used to improve considerably the rather unfavourable temperature distribution in an upright mould. To avoid turbulence the mould is always filled rather slowly and the pouring time is generally long enough to allow the freezing to proceed in some measure along with the pouring. Thus, instead of the solidification of the whole billet starting at the same time along the vertical walls, it follows the rising level of liquid at some distance, forming the well-known funnel-shaped isothermal surfaces.

5. Plane Solidification Front.

Macro-shrinkage will be avoided if there is communication between all liquid parts during all stages of solidification, and it is true that a

rather deep and narrow cup can fulfil this requirement. But there are two defects connected with radial heat flow which can only be avoided by a much more pronounced approximation to the ideal plane solidification front. They are inverse segregation and shrinkage stresses.

Inverse segregation is now generally ascribed to displacement in the casting of the residual low-melting part of an alloy after most of the metal has solidified.^{4,5} This occurs in alloys with a considerable melting range, the low-melting-point liquid, rich in certain alloying additions, moving under the influence of shrinkage in the direction of the heat flow. The result is a concentration gradient of some alloying constituents in the direction of the heat flow. In the normal upright-die billet mould (6–9 in. dia.) the effect is such that in an aluminium–4% copper alloy (Duralumin) the copper content in the outer zone may be 0.7% higher than in the central zone (Fig. 11 (a))—enough to cause appreciable differences in the properties of the two zones.⁵ This effect is concentrated in the zone in which freezing starts.

It is easy to see that if the solidification front moves on until nearly the end of solidification, a stationary condition will develop, each freezing layer losing as much to the preceding layer as it gains from the following layer⁶ (Fig. 11 (b)). This fact provides a possible means of eliminating the segregation defect from the bulk of the billet. If it can be contrived that the solidification front is normal to the axis and is made to travel along that axis from one end to the other of the billet, then there will only be a shallow zone of a few inches at the bottom and still less at the top which shows any segregation in the axial direction, while over the whole remainder of the length the composition is uniform owing to the establishment of the stationary condition. There will be no segregation between centre and surface if the solidification front is really flat.

Obviously there are intermediate effects in the event of the solidification front not being flat, but more or less cupped.

The same geometrical considerations apply to the question of internal stresses. These are mostly radial-tension stresses caused by the hot interior of the billet cooling faster at a certain stage than the already comparatively cool outside layers. If this happens while the interior is still liquid, no stresses are set up, but piping will occur. If the metal in the centre of the billet is in the pasty condition between the liquidus and solidus temperature, an internal hot tear is formed. In the case of large-diameter billets rapidly cooled in the mould, shrinkage differences are built up also after the whole cross-section is solid. They set up severe internal elastic-tension stresses sufficient to lead a billet to crack after complete cooling, either spontaneously or on the slightest additional stress during handling.

If severe exterior cooling is applied during freezing, the surface can temporarily come under peripheral and longitudinal tension, which is sometimes released by gradual splitting of the billet lengthwise during freezing, similarly to the way in which billets occasionally split during rolling. Diagrammatic and photographic⁶ records of this effect are given in Fig. 5 (Plate XII).

As in the case of segregation, the ideal method of eliminating these

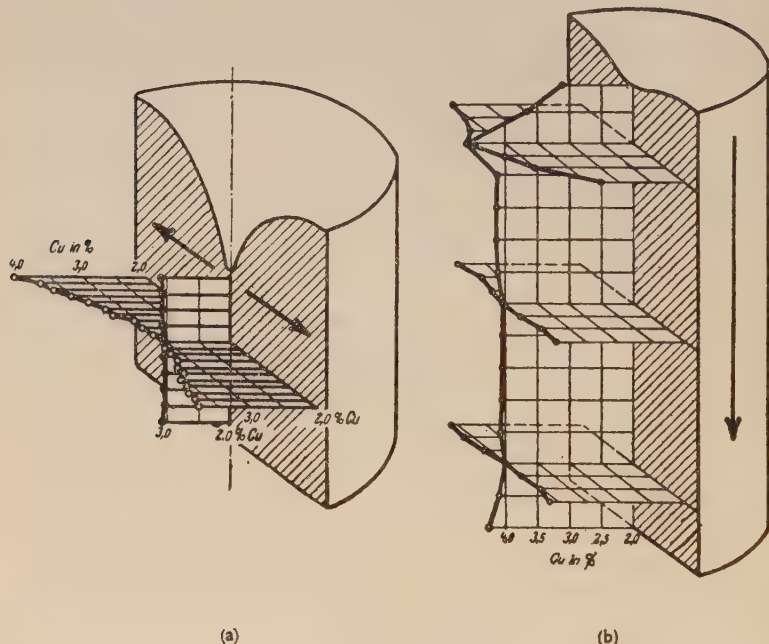


FIG. 11.—Distribution of Copper Content in Billets with Different Directions of Heat Flow. (a) Radial heat flow; (b) Axial heat flow. (Brenner and Roth.⁵)

stresses is to avoid any radial temperature gradient, i.e. to have a flat solidification front travelling along the axis of the billet.

The flat, open mould can produce some approximation to a flat solidification front even where intensive cooling occurs. In the case of the top-poured upright billet a certain approximation can be achieved by the expedient of slow pouring, as already described, but this can only be used to a limited extent because at the same time rapid solidification is desirable. Below a certain pouring rate, severe cold shuts or folds on the billet surface (Fig. 7, Plate XIII), will force the caster either to

increase the pouring rate or to decrease the cooling rate. It is quite impossible with a bottom-poured upright mould to achieve a flat solidification front.

V.—DEVELOPMENT OF THE CONTINUOUS-CASTING PROCESS.

In describing the development of the C.C.P. it is proposed to mention only a selection of the more valuable solutions offered to the casting

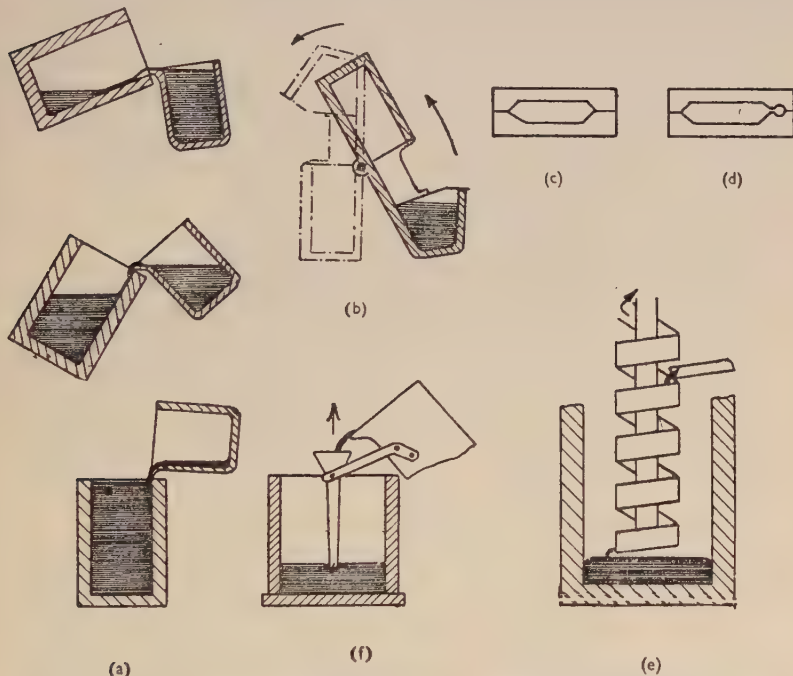


FIG. 12.—Devices for Reducing Turbulence in Pouring. (a) Tilting of mould; (b) Durville process; (c) Metal stream along mould wall; (d) Metal stream entering through slot; (e) Spiral channel; (f) Funnel.

problems outlined above, and to leave out the very large number of less important remedies described in the patent literature, some of which are very elaborate and even fantastic.

The developments eventually leading from the simple top-poured or bottom-poured vertical mould to the continuous-casting process, can be dealt with under the same headings as were used in the previous Section.

1. Non-Turbulent Flow.

Improvement has been attempted by tilting the mould when starting the pour and reverting to the upright position only after the metal level comes near to the top (Fig. 12 (a)). Durville⁷ went so far as to build the casting ladle and mould into one rigid unit which was slowly turned upside down (Fig. 12 (b)).

In some cases a separate pouring channel was introduced along the side of the billet, from which the metal entered the mould proper through a slot (Fig. 12 (c) and (d)).

Fairly modern processes provide a spiral channel wound round a heated column,⁸ or a funnel with a long and narrow vertical tube attached.⁹ These are lowered into the mould from the top and discharge the metal immediately on to the liquid level (Fig. 12 (e) and (f)).

2. Low Casting Temperature.

In a more elegant, but more elaborate way, the same object is achieved by combining it with the next desirable feature, a short pouring channel, in order to reduce the casting temperature.

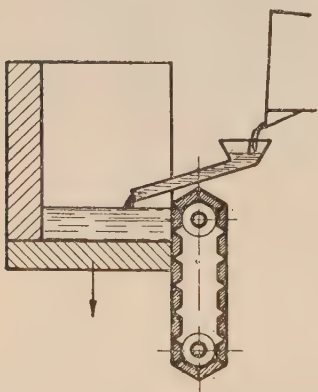


FIG. 13.—Züblin Casting Process.

This group of processes provides for a slot in the side of the mould through which a short pouring channel is introduced at a level always just above the metal in the mould. As the mould is lowered, this slot is closed by building up blocks of cast iron or, in a later version, by a caterpillar chain^{10, 11} (Fig. 13). A mould of this description was used in the large-scale production of high-strength aluminium alloys in Germany before the war. This method obviously came very near to providing a stationary condition of the solidification zone, but did not produce a flat solidification front.

The next step achieves the stationary condition completely. It is the introduction of a mould entirely formed by endless belts which link together at the top of the mould and part at the bottom, releasing the billet formed during the interval (Fig. 14). These machines have been the subject of a large number of patents, and one of them is reported to have had a considerable experimental production run in America on

brass.^{12, 13, 14} The idea seems, however, to have been abandoned, probably owing to the failure of the mould segments by distortion and other mechanical difficulties.

3 and 4. Rapid Heat Extraction and Directional Solidification.

Regarding the problem of securing a real directional solidification, the methods so far described were not much better than the ordinary top-poured vertical mould, providing it was filled slowly. The efforts

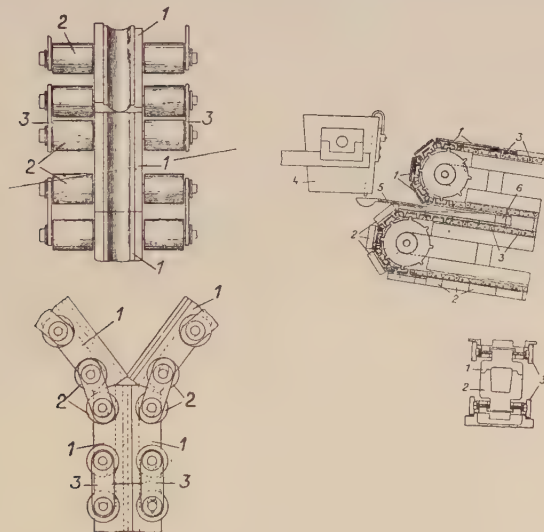


FIG. 14.—Two Typical Designs of the Caterpillar-Chain Casting Machine.
(Herrmann,¹²)

aimed at improvement in this respect at first took a different direction.

Slow pouring was abandoned. Instead of this, the metal was poured with the greatest practicable speed into a very thin-walled steel mould which did not cool the metal below the freezing point. Only after the mould had been completely filled and dross and slag had risen to the top—in some cases even after a prolonged holding period at constant temperature—was the mould cooled either by water rising in a tank around it or by the mould being lowered into a tank filled with water (Fig. 15).

Hundreds of thousands of tons of heavy high-class extrusion and forging billets in strong aluminium alloys were produced in this country during the war by this method. The process is expensive, as much metal

is lost in machining the tapered billet to cylindrical shape and in removing the top and bottom ends. In Germany a prominent producer of magnesium alloys considers this method still to be the best for very large-diameter billets.¹⁵

The cooling is severe while the outside zone of the billet is still liquid or very soft, but the appearance of the well-known air-gap as soon as the "crust" has hardened limits the intensity of cooling. To avoid the introduction of an air-gap in the heat-transfer system the cooling agent must impinge directly on the billet. This was achieved by a return to

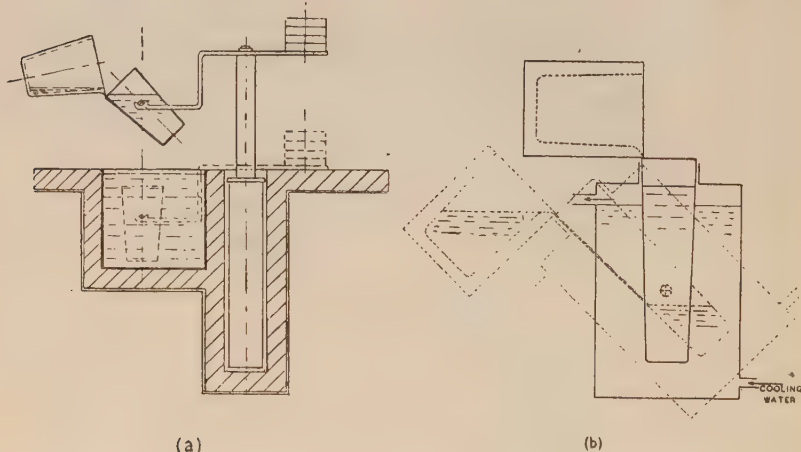


FIG. 15.—Axial Cooling in Thin-Walled Water-Cooled Steel Moulds.
(a) German method; (b) British method.

the use of the open-bottom mould (see Fig. 2), but this time the mould was made much shorter and, instead of elaborate measures being taken to remove the mould and billet simultaneously, a method was applied which had been known for a long time in connection with casting of lead pipe and first mentioned as a recognized procedure in a patent by Laing in 1843. The billet slides in the mould and is extracted at the same rate as it is cast. As soon as the billet emerges from the short mould it is exposed to direct cooling, e.g. by a water bath or water spray.*

5. Plane Solidification Front.

The method just described also very nearly solved the problem of obtaining a flat solidification front in the right position. As the cooling

* Junghans process; Zunkel and V.L.W. process; Alcoa D.C. process.

in the mould proper is adjusted to a degree just sufficient to form a thin vertical solid crust on the mould walls, and the lower part is cooled as severely as the metal can stand, the depth of the liquid metal cup is rarely

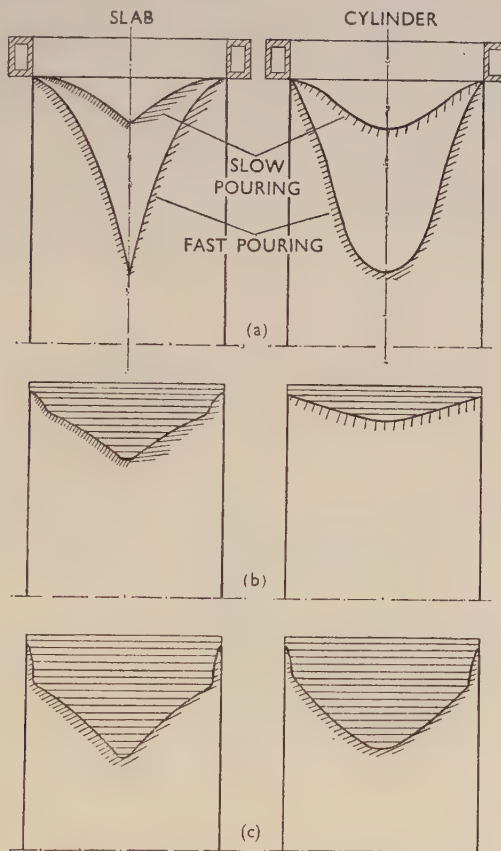


FIG. 16.—Shape of Liquid Cup in Top of Billets Cast by the Continuous Process.
(a) Calculated; (b) Experimental, slow pouring; (c) Experimental, fast pouring.
(Roth.¹⁶)

much more than the diameter or the thickness of the billet, and the shape is as shown in Fig. 16. The limitation "as the metal can stand" refers to the internal stresses set up by severe temperature gradients in the solidification zone, which in certain alloys tend to produce longitudinal cracks (hot tears).

6. Advantages of the Continuous-Casting Process.

The direct-cooling continuous-casting process combines in a very simple and efficient way, and to a high degree, the features required for the casting of a good billet, which in the older casting processes could be achieved only in part and often at the sacrifice of one requirement to another.

It is easy to see that the same applies also to the roller-type of continuous-casting process originated by Bessemer in 1865 and brought to the production stage mainly as a result of the work of Hazelett¹⁷ (see Fig. 2).

There is the same advantage in feeding right to the top of the metal sump, making possible low pouring turbulence and low pouring temperature. The intense cooling is in this case maintained in the lower parts of the solidification zone by the plastic compression of the billets between the rollers, which eliminate the air-gap. Further, the V-shaped arrangement of the cooling surfaces helps considerably in flattening the solidification cup.

Apart from the advantages of improved quality, the continuous-casting process is also a convenient and economical process. The pouring speed and the pouring temperature which control the process can be easily measured and need not be changed during the operation. This makes a rigid control of casting conditions possible and enables a higher degree of uniformity to be attained than is possible with older processes. The equipment required is more complicated and expensive than with conventional billet-casting methods, but the output is considerable, as small billets can be cast simultaneously in a series of moulds¹⁸ (Fig. 6, Plate XII). The moulds are small, easy to handle, and inexpensive compared with the cast-iron moulds with their great weight and large space requirements for storage, or the thin-walled steel mould which can stand only a small number of casts.

VI.—FIELDS OF APPLICATION.

The field in which the continuous-casting process has developed most rapidly and successfully is the aluminium industry. During the war a large part of the aluminium-billet production in all the main industrial countries was changed over to the continuous-casting method, and after the war it became by far the most widely used for this purpose. The reasons for this include the high-quality demands of the aircraft industry, and the fact that aluminium has the lowest melting point of any metal used on a large scale for highly stressed structures. The high standard achieved in the casting of aluminium alloy billets is illustrated

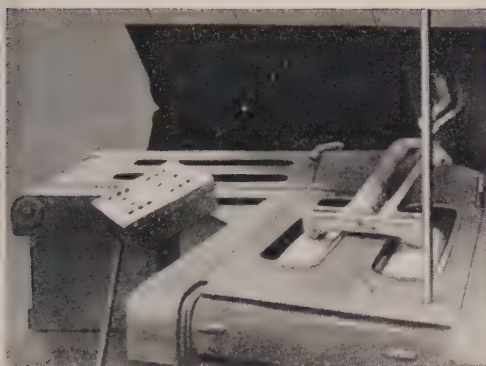


FIG. 3.—Top of Continuous-Casting Machine in Action.
(Péloutier.¹)

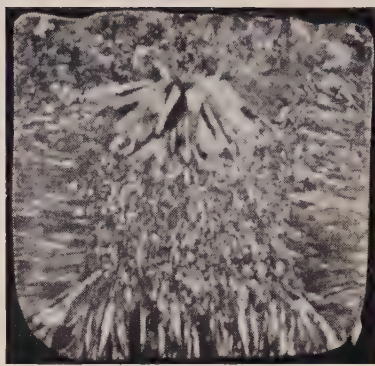


FIG. 4.—Macrostructure of Section of Copper Wire-Bar. (Sachs.²)

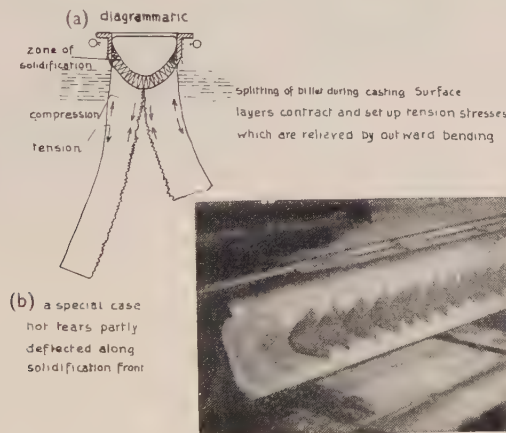


FIG. 5.—Splitting of Billets under the Influence of Axial Tension in the Surface Layers. (Case (b) Patterson.⁶)

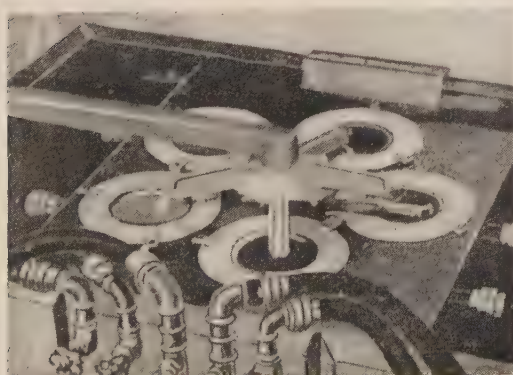


FIG. 6.—Multiple Billet Arrangement for Continuous Casting. (Küstner.¹⁸)



[Courtesy of International Alloys, Ltd.]

FIG. 7.—Cold Shuts in Surface of Cylindrical Billet.



[Courtesy of International Alloys, Ltd.]

(a)

(b)

FIG. 8.—Microstructure of Extrusion Billets in Aluminium Alloy.
(a) Cast in cast-iron mould; (b) Cast by continuous-casting process.

in Fig. 8 (Plate XIII). The microstructure of the continuously-cast billet (Fig. 8 (b)) shows a fine distribution of constituents, while the billet cast in an upright mould (Fig. 8 (a)) shows microporosity and relatively coarse distribution of micro-constituents.

For zinc, lead, and tin the process offers no difficulties. It appears that considerable efforts are being made to bring to the production stage the applications of the same principle to copper, brass, bronze^{19, 20} (Fig. 17) and steel,²¹ all of which have already been more or less successfully cast without so far bringing about as widespread a switch-over to the new method as has occurred with aluminium.

VII.—FUTURE DEVELOPMENTS.

What can be expected of future developments?

There is still a great deal to be done in connection with the adaptation of the processes for higher-melting-point metals. To overcome the difficulties of maintaining the mould surface in a proper condition under the attack by liquid metal at high temperature and under the constant thermal strain, will require much patience and hard work.

There are also still some limitations in the field where the process is already in full production. The flatness of the solidification front is good enough to reduce the difficulties with segregation, but not quite sufficient to eliminate difficulties with internal stresses. This limits the amount of chilling which can be applied to billets of large diameter and to certain alloys which have a large freezing interval.

The strip-casting machine will have to undergo some further development, especially in the stability of the mould surface, before it can hope for a popularity similar to that of the sleeve machine.

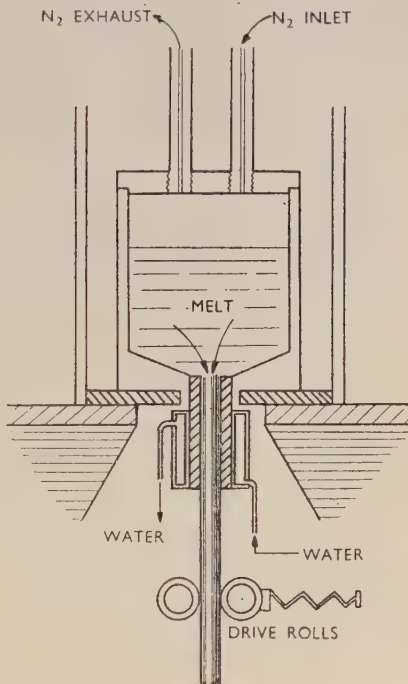


FIG. 17.—Sectional View of Asarco Continuous-Casting Machine for Copper and Copper Alloys. (Smart and Smith.¹⁹)

These difficulties should, however, not diminish the value of a development which is equally impressive and satisfactory from the theoretical, the mechanical, and the production point of view.

ACKNOWLEDGEMENTS.

The author wishes to thank Mr. J. Wood for helpful criticism, Mrs. E. Scheuer-Zindel for the preparation of the diagrams, and Mr. H. Harris for preparation of the photographs.

Thanks are due to the Directors of International Alloys Ltd., Aylesbury, for permission to publish the paper.

REFERENCES.

1. J. M. Péloutier, *Rev. Aluminium*, 1947, **24**, 87.
2. G. Sachs, "Praktische Metallkunde". Berlin : 1933 (J. Springer).
3. C. Schwarz, *Arch. Eisenhüttenwesen*, 1931, **5**, 139, 177.
4. G. Masing and E. Scheuer, *Z. Metallkunde*, 1933, **25**, 173.
5. P. Brenner and W. Roth, *Z. Metallkunde*, 1940, **32**, 10, 90.
6. W. Patterson, *Aluminium*, 1943, **25**, 77.
7. P. H. G. Durville, Brit. Patent No. **23,719**, 1913.
8. *Brit. Intelligence Objectives Sub-Cttee. Misc. Rep.* No. **79**.
9. A. v. Zeerleder, "Technologie der Leichtmetalle". Zürich : 1947 (Rascher Verlag).
10. J. Züblin, German Patent No. 489,385.
11. E. Kotteritzsch, German Patent No. 468,829.
12. E. Herrmann, *Aluminium-Archiv*, 1940, (16).
13. T. W. Lippert, *Trans. Amer. Inst. Min. Met. Eng.*, 1945, **161**, 479.
14. L. H. Day, *Metal Treatment*, 1943, **10**, 173.
15. P. Menzen and W. Patterson, *Aluminium*, 1943, **25**, 375, 413.
16. W. Roth, *Aluminium*, 1943, **25**, 283.
17. C. W. Hazelett, *Trans. Amer. Inst. Min. Met. Eng.*, 1945, **161**, 512.
18. H. Kästner, *Stahl u. Eisen*, 1947, **67**, 15.
19. J. S. Smart, Jr., and A. A. Smith, Jr., *Iron Age*, 1948, **162**, (9), 72; and *Metal Ind.*, 1948, **73**, 347, 372.
20. Anon., *Steel*, 1946, **118**, 140.
21. T. W. Lippert, *Iron Age*, 1948, **162**, (8), 72.

RECRYSTALLIZATION OF SINGLE CRYSTALS 1212 AFTER PLASTIC BENDING.*

By R. W. CAHN, B.A.,† STUDENT MEMBER.

SYNOPSIS.

Experiments have been carried out to determine under what conditions it is possible to procure in deformed crystals a special type of recrystallization which leads to discontinuous asterisms in the Laue patterns. It has been found that bent single crystals are particularly liable to this type of recrystallization, which has been observed with zinc, magnesium, aluminium, and rock-salt. Systematic experiments with zinc crystals have established an optimum bending radius, annealing time, and annealing temperature. The microstructures of the bent and of the annealed specimens have also been examined; the annealed specimens consisted of many crystallites separated by straight boundaries perpendicular to the slip planes.

The theory of the phenomenon is discussed, and it is concluded that it is the result of the motion of dislocations during annealing. The bearing of the results on the general theory of recrystallization is briefly considered.

I.—INTRODUCTION.

WHEN the process of plastic deformation in crystals of metals or other substances is followed by means of X-ray diffraction (using the Laue technique), it is almost invariably found that the originally sharp reflections, corresponding to various lattice planes, become drawn out into streaks. This phenomenon, known as *asterism*, corresponds to a departure from perfect parallelism in the crystal, affecting either large parts or only isolated regions. In the former case there is elastic bending of the lattice without the creation of sharp discontinuities, while in the latter, minute fragments or *crystallites* are torn from their positions in the lattice and rotated bodily. There has been much argument about which interpretation is correct in particular instances; in most of the present work, the former certainly applies.

It had been observed by a few workers that asterism in some of their Laue photographs did not take the usual form of long, continuous streaks, but appeared as groups of separate spots. This must mean that the original crystal has become subdivided into a number of grains of slightly differing orientation. Thus Konobeevsky and Mirer¹ show a particularly clear pattern of this type from a bent and annealed rock-salt crystal, while Andrade and Tsien² found that

* Manuscript received 15 March 1949.

† Formerly at Cavendish Laboratory, Cambridge. Now with Ministry of Supply, Atomic Energy Research Establishment, Harwell, Berks.

crystals of sodium and potassium when extended at room temperature gave rise to such split asterisms, as did also iron crystals on subsequent annealing. Hirst³ had clear evidence of splitting during the deformation by creep of single crystals of lead. Bungardt and Osswald⁴ found that the sharp spots in the Debye-Scherrer rings in diffraction photographs from coarse-grained aluminium became diffuse and split up after light rolling; Chitruk⁵ detected a similar effect in pulled tensile test-pieces of mild steel. Again, Boas and Honeycombe,⁶ in their experiments on the thermal fatigue of crystallographically anisotropic metals, found that splitting took place in the asterisms from cadmium specimens subjected to many repeated cycles of heating and cooling which led to deformation. Kabata⁷ obtained double asterisms in single crystals of aluminium prepared by recrystallization; while particularly good results, showing a multiple and sharp fine structure in X-ray photographs of slightly extended aluminium crystals, subsequently annealed, were obtained by Crussard⁸; Collins and Mathewson⁹ had made some similar observations earlier. In the course of experiments on the recrystallization of silicon ferrite aggregates, Dunn¹⁰ sometimes detected splitting of asterisms in diffraction patterns from parts of crystals near boundaries or deformation bands.

Some very recent work by Guinier and Tennevin¹¹ shows up the effect particularly well. By applying a refined focusing technique to very weakly bent aluminium crystals, they observed a minute subdivision of the diffraction spots on annealing. This subdivision becomes progressively coarser with continued annealing.

It is clear that a form of recrystallization is involved in all the cases cited above, since both the size and the orientation of the crystals giving rise to X-ray patterns has changed and evidence of strain has disappeared. Such a change in the structure of the specimens is of the kind defined as recrystallization; it differs, however, from the usual type in the essential point that the new crystals are very close in orientation to the original ones. Since recrystallization always requires previous plastic deformation, and usually annealing at a raised temperature for an appreciable time, further study involved finding the mode of deformation and the time and temperature of annealing which will lead to the phenomenon in question. Because of the somewhat haphazard fashion in which most of the results quoted above were observed, the present author's search for the conditions began in rather a random way. For this reason the early stages of the work will be only briefly mentioned, and chief attention will be given to the detailed results obtained when it had become possible to produce this kind of recrystallization readily.

II.—PRELIMINARY EXPERIMENTAL WORK.

1. *Experiments with Copper.*

The first plan of attack rested upon the argument that if a polycrystalline aggregate is very heavily deformed and then annealed at such a low temperature that any changes take place only very sluggishly, the effect may be observed; for the appearance of the X-ray pattern suggests that what is involved is not growth from new nuclei formed at random, but rather a gradual relieving of the strains in the lattice as a whole, the old orientation being more or less preserved. This may well occur under conditions which cannot furnish the considerable activation energy necessary for nucleus formation. Heavy deformation followed by low-temperature annealing provides such conditions; the complementary method is to give light deformation and a high-temperature anneal. Copper has suitable recrystallization temperatures and was used for these experiments.

For the first method, copper strip was rolled by various amounts, with up to 98% reduction, and annealed at low temperatures in a thermostatically controlled oil bath. When recrystallization took place at all, it was always by the nucleation of new grains, as was shown by the fact that the deformation and recrystallization textures were different.

For the complementary method, fine-grained copper foil was given a small extension and annealed to give coarse grains. It was found that these grains were by no means perfect, though stable to high temperatures. The diffraction spots exhibited much fine structure; Fig. 1 (Plate XIV) shows an example. Thus it appears that ordinary primary recrystallization can in certain circumstances lead to the formation of grains divided into blocks of slightly differing orientation. This agrees with the metallographic findings of Lacombe and Beaujard¹² who observed that aluminium crystals produced by the method of critical straining and annealing consisted of many blocks of slightly differing orientation, the boundaries of which could be revealed by etching.

2. *Experiments with Zinc.*

It was decided to try again the method of a high-temperature anneal following weak deformation, this time using zinc. The large grains obtained were again not strain-free, but the degree of diffuseness in the spots was slight and there was little clear evidence of splitting of the asterisms.

At this stage it was decided to use single crystals and thus to

simplify the conditions. The crystals were made from lengths of spectroscopically pure zinc wire, 1 mm. in dia., using a travelling furnace apparatus similar to that described by Andrade and Roscoe.¹³

Some crystals were extended slightly and annealed, but did not recrystallize; nor did a crystal which was annealed after strong torsion. Finally, bending was tried. After some unsuccessful experiments the photograph shown in Fig. 2 (Plate XIV) was obtained from a crystal bent sharply (0·5 cm. radius) and annealed for 30 min. at 370° C. This photograph was taken with the X-ray beam parallel to the plane of bending and perpendicular to the crystal at the point of incidence. Another crystal, bent to a radius of 0·8 cm., recrystallized in a similar manner, but in this case annealing at a temperature of 395° C. was necessary before any change took place.

It seems, then, that the necessary conditions with zinc crystals, for discontinuous asterisms to be obtained, are (*a*) deformation by sharp bending, and (*b*) annealing at a temperature not far below the melting point.

3. Experiments with Magnesium.

The promising results with zinc gave encouragement to continue work with another metal. Another hexagonal metal—magnesium—was chosen, as it seemed possible that the fact that zinc has a hexagonal structure had something to do with the nature of the recrystallization, more especially since the structure has a profound effect on the plastic properties of zinc. This time single crystals were used from the start. No magnesium wire was at first available for use with the Andrade furnace, so an attempt was made to produce large grains by recrystallization of weakly strained strip. By using a very small extension (about 0·3%) and very gradual heating, grains of 1–2 cm.² in area and about 1 mm. thick were produced. Most of these contained a few fine twins. Some of the grains were cut out and etched deeply (down to about $\frac{1}{2}$ mm.) to remove the worked layers due to sawing. As in the case of copper, the X-ray patterns of the crystals showed signs of deformation, and the diffuse spots were split very clearly in one specimen. The diffuseness was due neither to surface deformation nor to geometrical factors, as the etching down and the use of a fine collimator showed. The crystals were heated to 250° C. in a salt bath and quickly bent over a pre-heated former. This was done to avoid as far as possible deformation twinning. Some of the specimens recrystallized in the ordinary way on annealing, giving new sharp spots. In several others, the asterisms became subdivided into extraordinarily fine and sharp reflections. Fig. 3 (Plate XIV) shows

an enlargement of one such set of reflections from another X-ray photograph. No others are included because it is difficult to show up the detail in a reproduction. These subdivided spots cannot be images of the crystal with the blank spaces corresponding to the twin bands in the specimen, because to produce such an image would require much more perfect collimation than it was possible to use. The very fine spots in the recrystallized specimens must therefore be due to a large number of tiny crystallites of similar orientation.

Later, some work was carried out with crystals made in the Andrade furnace, when magnesium wire was available. At this stage of the work it became necessary to determine the orientation of the crystals to permit of their being set up and photographed in a standard way. The method adopted was as follows: (a) the crystal was bent in a plane containing the wire axis and the normal to the glide plane, thus ensuring that the individual lamellæ were bent about a single axis only, to a first approximation; and (b) the X-ray photograph was taken with the beam approximately normal to the glide plane; this showed up the discontinuous asterisms particularly well. The orientation of the magnesium crystals was found by a two-film X-ray method originally introduced by Davey.¹⁴ By deforming crystals in accordance with the above scheme and annealing, photographs showing extensive fine structure in the asterisms were obtained. Fig. 7 (Plate XV) is a good example. It was made from a crystal wire, 0·1 cm. in dia., bent in an oil bath at 200° C. to 1·1 cm. radius, and annealed for 18 hr. at 560° C. The long annealing time was intended to make sure that the subdivision of the asterisms went as far as it would go.

4. Experiments with Rock Salt.

Since, as mentioned earlier, Konobeevsky and Mirer¹ obtained particularly clear discontinuities in a Laue photograph from a bent and annealed rock-salt crystal, it was thought worth while to repeat the experiment.

Specimens of suitable size were obtained by cleavage from a larger piece of natural rock salt (cleavage takes place parallel to the (100) plane); an X-ray photograph of one such crystal showed it to be undistorted. The crystals were bent under the surface of warm water, thus rendering them plastic as a result of the dissolution of surface imperfections (Joffé *et al.*¹⁵). After this they were sealed up in a silica tube and annealed. Fig. 8 (Plate XV) shows the Laue pattern from one such crystal, 0·1 cm. thick, bent to a radius of 0·5 cm. and annealed for 16 hr. at 740° C.* The pattern shows completely sub-

* The streaks in the principal asterism are parallel to the axis of bending.

divided asterisms, but the scale of the effect is finer than that found by Konobeevsky and Mirer. Fig. 4 (Plate XIV) is an enlargement from another photograph.*

One of the recrystallized specimens was examined under the microscope, and revealed line-markings on the surface, many of them delimiting lamellæ parallel to the axis of bending. This observation is of interest in connection with the mechanism of recrystallization, if it can be assumed that the markings represent a "thermal etching" of the boundaries of the new grains.

5. Experiments with Aluminium.

Single crystals were made in the Andrade furnace, and their orientation determined by an optical method, as described in Section III, 1. Fig. 9 (Plate XV) is a photograph from a crystal bent to a radius of 1·1 cm. and annealed for 2 hr. at 580° C. in an evacuated glass tube. Generally, the spots were much closer together than in this photograph and were barely resolved. The metallographic observations are described separately below.

III.—DETAILED INVESTIGATIONS WITH ZINC.

It had now been established that discontinuities in the Laue pattern occur in a variety of metals (*a*) to a slight degree and not very clearly in the primary recrystallization of weakly deformed polycrystalline aggregates after annealing, and (*b*) sharply if single crystals are annealed after plastic bending. However, the results were somewhat erratic. A bent and annealed crystal of zinc, for instance, might not recrystallize at all, or it might recrystallize in the ordinary way by nucleation and growth to give a few crystals of unrelated orientation, or it might recrystallize to give discontinuities in the Laue asterism. If it recrystallized in the second way, it might do so after a short anneal, or it might require a long period at high temperature. Thus it was desirable to find out the conditions of bending and annealing which most favoured this type of recrystallization. Since one obvious possible source of the erratic results was the unknown orientation of the crystals used, a series of experiments was carried out with crystals of known orientations, under various conditions of bending and annealing. Zinc was chosen for this work, partly because this metal has only one glide plane and the effect of orientation would therefore be simpler than for a cubic metal, and partly because it was available in greater purity than any other metal (see Appendix I, p. 141).

* The streaks in the principal asterism are parallel to the axis of bending.

1. Preparation of Specimens.

The crystals were grown from cold-drawn zinc wire of 0·1 cm. dia. cut into 10-cm. lengths, using the travelling furnace referred to earlier. The crystals were very carefully handled throughout to avoid any unintended deformations.

Pieces of crystal about 2 cm. long were welded by means of a tiny flame to special flat brass holders, the tips of which were coated with

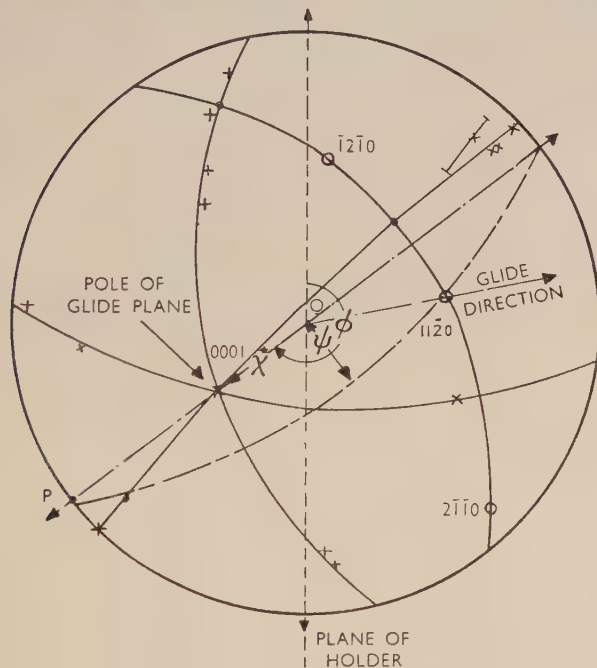


FIG. 22.—Stereographic Plot of Crystal No. 7. The crystal axis is at the centre.
 $x^* = \chi - 90^\circ$.

zinc. The holder served to fix the crystal in the bending jig and in the annealing bath, and provided a reference plane for defining the positions of the crystal axes.

When it was found in the course of the work that the best orientations for bending were those in which the glide plane was inclined at or near 45° to the crystal axis (i.e. those giving the best ductility), a small piece of each crystal was first cut off and pulled between pliers. If it would pull into a ribbon before breaking, the rest of the crystal was considered suitable. The orientation of the crystal pieces was

determined optically, with the aid of a two-circle goniometer, using a rapid method described by Barrett and Levenson.¹⁶

The angular readings were plotted on a stereogram. Fig. 22 shows a typical plot. It will be seen that the etch brings out sets of facets lying on six pyramidal zones at 60° intervals. Barrett and Levenson¹⁶ say that these are $(10\bar{1}l)$ zones, and the glide directions, which are parallel to $[\bar{1}\bar{1}20]$, are therefore placed on the stereogram at positions

shown by the small circles. Knowledge of the angle χ^* between the normal to the glide plane and the crystal axis determines the suitability of the crystal for the experiment and allows it to be set up in the standard position for X-ray diffraction. The angle ϕ must also be known for this, and to allow the crystal to be rotated into the correct position for bending, in which the crystal axis and the normal to the glide plane are both in the plane of bending (i.e. normal to the axis of bending). ψ is a measure of the amount by which the nearest glide direction is

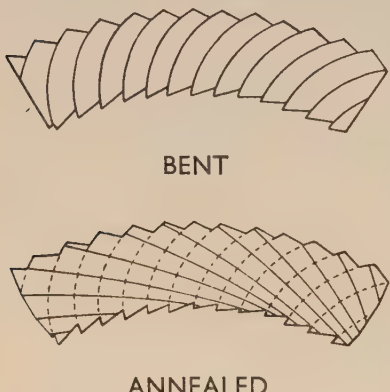


FIG. 23.—Section of a Bent Crystal Parallel to Plane of Bending (schematic).

out of the plane of bending. The idealized process of plastic bending as sketched in the top half of Fig. 23 can only be realized if $\psi = 0$.

The value of ψ does not seem to make any difference to recrystallization in the case of the zinc crystals, even though, if ψ is more than a few degrees, torsion is added to bending, and the state of elastic strain must be complicated in comparison with that obtaining in the ideal state illustrated in Fig. 23. A few of the crystals were checked by X-rays, and in this way it was possible to confirm the orientations and to show the crystal to be strain-free.

2. Bending and Annealing.

When the orientation of the specimen had been determined, it was set up in the bending jig shown in Fig. 24. The spindle *A* was rotated until the plane *OP* (see Fig. 22) was vertical; then the specimen was screwed down by turning spindle *B* until it was in contact with the appropriate former, over which it was then bent. For experiments on bending at raised temperatures, hot medicinal paraffin was poured into

the vessel *C* before the bending operation; for low temperatures, liquid air from a Dewar wash-bottle was squirted over the crystal for some time before bending.

No X-ray photograph was generally taken at this stage, since the first few experiments all showed a similar set of continuous asterisms. Fig. 10 (Plate XVI) is an example. The same specimen set up in the same way after recrystallization gave the pattern shown in Fig. 11 (Plate XVI). This has asterisms of much the same lengths. (It must be remembered that there was inevitably a slight margin of error

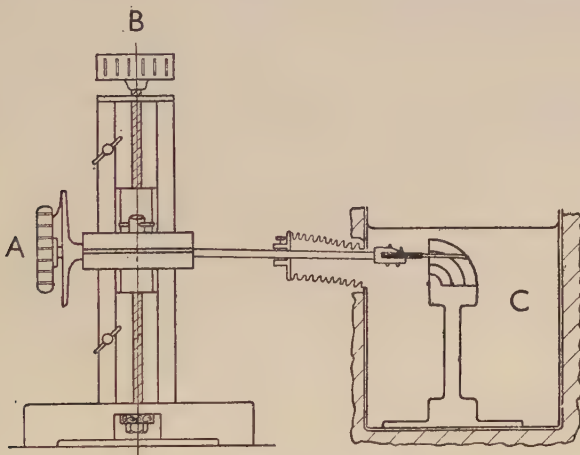


FIG. 24.—Bending Jig.

in setting up the crystal in the camera.) The pattern after recrystallization thus gave all the information required. The specimen was next annealed. After some experiments to establish the minimum temperature at which recrystallization would consistently take place, a standard annealing treatment of 2 hr. in a salt bath at 400° C. was usually given. This form of annealing had the advantages that the specimen was not oxidized after withdrawal because a protective salt film was formed, and that the sublimation usual when zinc is heated *in vacuo* was avoided.

3. X-Ray Examination.

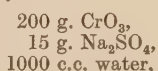
After annealing, the specimen was set up for a transmission flat-film Laue photograph, in such a way that the X-ray beam was approximately normal to the basal plane at the point of incidence, while the plane of bending was vertical. All the Laue photographs of zinc here reproduced, and also Figs. 4, 7, 8, 9 (Plates XIV and XV) were taken

in this way.* The use of this standard orientation allowed the photographs of different crystals to be directly compared. The beam was collimated by two fine horizontal slits about $\frac{1}{3}$ mm. wide and 5 cm. apart, the back slit being about 1 cm. from the specimen. The beam was only allowed to impinge upon one half of the width of the crystal. This was because the absorption was so high that the central part of the crystal hardly contributed at all to the Laue photograph, and if the beam had been allowed to straddle the crystal doublet spots would have resulted. Unfiltered molybdenum radiation at 70 kV. was used; the specimen-to-film distance was 5 cm.

4. Metallographic Examination.

Several of the crystals were examined microscopically, some before and some after annealing. The former were examined without being specially mounted. The free surface was given a high polish by an electrolytic method before bending. After bending, the polished crystals were set up on a microscope so that the apex of the convex side was in the plane of vision. Fig. 12 (Plate XVI), is a photograph showing the slip lines. It will be seen that there are lines of all degrees of blackness, betokening various amounts of slip of the individual glide packets; but those of medium blackness are spaced roughly uniformly. In counting the lines to obtain the mean thickness of the glide lamellæ, all those lines which could be clearly distinguished at a magnification of 800 were counted, but even so the values can be significant only to within a factor of two or three.

The specimens that were prepared for examination after they had been annealed were mounted with the plane of bending in the surface of the mount. The mounted crystals were ground down until the central section was exposed and then polished electrolytically. It proved extremely difficult to get a good polish, probably because of the shape and small size of the surface exposed. The few specimens which received a satisfactory polish were etched to bring out the boundaries of the new grains revealed in the X-ray photograph. This again was very difficult, because the degree to which a boundary will etch decreases as the difference of orientation between the adjacent grains decreases, and is usually vanishingly small if this difference is only a matter of a degree or less (see Lacombe and Beaujard¹²). The etching reagent which gave the best results was the standard chromate etch for zinc, of composition :



* Figs. 4, 9, 10, 11, 19, 20, and 21 have been turned on their sides in reproduction.

followed by a plain chromic acid solution as a rinse. It was necessary to give a gross over-etch, leading to waviness of the polished surface. There was general pitting, with a concentration of pits at the boundaries. In some cases dark-ground illumination was necessary to bring out the structure. Figs. 13–16 (Plates XVI and XVII) are examples of the photographs obtained. The crystal of Fig. 13 had been bent to a radius of 2·2 cm. and annealed; Fig. 14 is a portion of the same crystal at higher magnification, showing the concentration and discontinuity of etch-pits at the boundary, and the remarkable straightness of the latter. Figs. 15 and 16 were made from the more sharply and less sharply bent portions, respectively, of a crystal bent to a nominal radius of 1·1 cm., but in fact unevenly along its length. It is important to note that the directions of the boundaries always coincided, to within a few degrees, with the hexagonal axis (which lies in the plane of the photographs).

5. Results.

Table I gives a résumé of the results obtained in this series of experiments.

TABLE I.—*Results Obtained with Spectrographically Pure Zinc Crystals.*

Specimen Nos.	χ	ψ	Radius, cm.	Temperature	Annealing Treatment	Discontinuous Asterisms	Figure References
7d	42°	26°	3·2	Room	14 hr. at 400° C.	Doubtful traces only	
5a	43°	17°	2·2	Room	$\frac{1}{2}$ hr. at 350° C. + 14 hr. at 390° C.	Incipient Good	
7c	42°	26°	2·2	Room	6 hr. at 405° C.	Partial	
7b	42°	26°	2·2	Room	40 hr. at 350°–400° C.*	Almost complete	Figs. 13 and 14 (Plates XVI & XVII)
12b	44°	0°	2·2	Room	2 hr. at 400° C.	Partial	
11b	52°	10°	2·2	Room	$2\frac{1}{2}$ hr. at 400° C. + 8 hr. at 400° C.	Partial Almost complete	Fig. 5 (Plate XIV)
5b	43°	17°	1·5	Room	19 hr. at 345° C.	Good	Figs. 10 and 11 (Plate XVI)
13c	43°	9°	1·5	Room	2 hr. at 400° C.	Partial but sharp	Fig. 6 (Plate XIV)
11c	52°	8°	1·5	110° C.	2 hr. at 400° C.	Good	
14b	52°	2°	1·5	Liquid air	2 hr. at 400° C.	None	
15b	44°	23°	1·5	Liquid air	2 hr. at 400° C.	None	
11a	52°	10°	1·1	110° C.	2 hr. at 400° C.	Good	Figs. 15 and 16 (Plate XVII)
15c	44°	28°	1·1	Liquid air	2 hr. at 400° C.	None	
—	?	?	0·8	Room	$2\frac{1}{2}$ hr. at 395° C.	Good	Fig. 2 (Plate XIV)
13a	43°	9°	0·8	Room	2 hr. at 400° C.	Good	Fig. 19 (Plate XIX)
—	?	?	0·5	Room	$\frac{1}{2}$ hr. at 370° C.	Good	
13d	43°	9°	0·35	Room	2 hr. at 400° C.	Good	
14d	52°	2°	0·35	110° C.	2 hr. at 400° C.	Good	Fig. 20 (Plate XIX)

* The temperature sank to this value accidentally.

Some examples of the Laue photographs obtained are reproduced in Figs. 5, 6, and 19–21 (Plates XIV and XIX). A selection of photographs were measured to check the mean angles between the spots (α) and the approximate total angles involved (β). This was done in each case for several asterisms, in or near the plane of bending, and the results are given in Table II.

TABLE II.—*Mean Angles Between Spots (α) and Total Angle Involved (β) in Laue Photographs of Zinc Crystals.*

Specimen No.	Conditions of Bending	Conditions of Annealing	Mean α	Mean β
11b	2.2 cm. rad. at 110° C.	10½ hr. at 400° C.	0.3°	2°
13c	1.5 cm. rad. at R.T.	2 hr. at 400° C.	0.25°	2.5°
5b	1.5 cm. rad. at R.T.	19 hr. at 345° C.	0.4°	3.5°
11c	1.5 cm. rad. at R.T.	2 hr. at 400° C.	0.25°	4°
11a	1.1 cm. rad. at 110° C.	2 hr. at 400° C.	0.35°	6.5°
13a	0.8 cm. rad. at R.T.	2 hr. at 400° C.	0.25°	6°
14a	0.35 cm. rad. at 110° C.	2 hr. at 400° C.	0.3°	7°
13d	0.35 cm. rad. at R.T.	2 hr. at 400° C.	0.25°	5.5°

It must be pointed out that the total length of asterism as measured is not highly significant because of the sharp change in intensity of the incident "white" X-rays with change in wave-length, and because of geometrical effects due to the shape of the specimen. The mean angle between the spots is fairly accurate. With these provisos, it can be said that the mean angle between the spots is approximately independent of the sharpness of bending, but that the total angular range of spots (and therefore the number of spots) on the whole increases with sharpness of bending, as it should do.

From the photomicrographs, Figs. 13–16 (Plates XVI and XVII), it will be seen that the average width of the grains decreases as the bending becomes sharper. This is in agreement with the X-ray results; for the number of grains through which the X-ray beam passes is inversely proportional to their mean width, and if the angle between successive grains is roughly independent of the degree of bending, the total angular range and the number of spots will increase with the sharpness of bending.

It remains to give the mean thickness of the glide lamellæ as obtained from several crystals polished before bending. In arriving at these values, which are shown in Table III, the inclination of the glide lamellæ to the surface was allowed for.

As mentioned before, these values are only reliable to within a factor of two or three because of the difficulty of distinguishing fine lines. The error will be towards too large mean spacings; 2μ may be

taken as being a rough mean value. There is no evidence that the spacing depends significantly on the temperature of bending.

TABLE III.—*Mean Spacing of Glide Lamellæ in Zinc Crystals.*

Specimen No.	χ	Conditions of Bending	Mean Spacing, cm.
16b	47°	1.5 cm. at R.T.	0.0004
16a	47°	1.5 cm. in liquid air	0.0001(3)
16c	47°	1.5 cm. at 120° C.	0.0003(3)
17c	33°	1.5 cm. at 120° C.	0.0001(5)
17a	33°	1.5 cm. at R.T.	0.0001(2)
			Over-all mean value 0.0002(3) cm.

IV.—METALLOGRAPHIC EXPERIMENTS WITH ALUMINIUM.

Quite recently, the author has succeeded in etching the boundaries in bent and annealed aluminium crystals. Here again, they are straight and perpendicular to the glide planes, as may be seen from Figs. 17 and 18 (Plate XVIII). These are photomicrographs from two such crystals ($\chi = 49^\circ$, $\psi \sim 2^\circ$) bent in the standard position, to 6.0 and 3.0 cm. radius respectively, and annealed for several hours at 625° C. Sections were prepared parallel to the plane of bending and electrolytically polished and etched in Lacombe and Beaujard's reagent.¹² The crystal of Fig. 18 was then bent a little further; the fresh slip lines, taken in conjunction with the orientation of the section, confirm directly that the boundaries are perpendicular to the glide planes.

Full details of these experiments, which form part of a study of the deformation of aluminium crystals, will be published separately.

V.—DISCUSSION OF RESULTS.

It will be helpful to collect together the conclusions which can be drawn from the results, before trying to interpret them. It will then be easy to see what facts a theory of the effect must explain :

(1) The effect can be produced in a number of materials.

(2) It can be produced in an imperfect form by primary recrystallization of lightly-worked fine-grained metals, especially copper and magnesium. It was not obtained in any of the experiments involving more or less homogeneous deformation of zinc single crystals, but was frequently obtained after bending. The one experiment on torsion gave a negative result.

(3) To produce the effect by bending (to which attention will be confined for the moment), it was necessary to give considerable deformation, i.e. bend to a small radius of curvature. For 1-mm. dia. crystals, the maximum radius to give the effect fairly consistently was 2.2 cm.; 3.2 cm. was insufficient, 1.5 cm. was always small enough.

(This applied to bending at room temperature or above.) At the smallest radius used, 0.35 cm. (which corresponds to a maximum strain of 0.14) the type of recrystallization was still the same, and there was no sign of its taking place in the ordinary way.

(4) The experiments were not critical in fixing the minimum times and temperatures of annealing to produce recrystallization in zinc; at 350° C. a considerable time of annealing was usually necessary, while at 400° C., 2 hr. sufficed for all except the smallest amounts of bending. The fact that even this treatment sometimes resulted in partial recrystallization only, suggests that the process always requires at any rate more than a few minutes to reach completion. The experiments on zinc, as well as other substances, show that the temperature of annealing must not be far removed from the melting point to produce recrystallization in a few hours.

(5) If zinc is bent at the temperature of boiling liquid air (about -180° C.), it does not recrystallize even after a long period of subsequent annealing. Crystals bent at 110° C. show no appreciable difference in the ease or nature of recrystallization from those bent at room temperature.

(6) Recrystallization seems to take place more easily if the metal is very pure. The time necessary to produce resolvable discontinuous asterisms in magnesium was considerably greater than it was for pure zinc, and they were always very fine in the former case; the magnesium was only 99.95% pure, the zinc 99.999%.

(7) The microstructure after recrystallization consists of long, narrow grains with their length perpendicular to the glide plane, i.e. parallel to the hexad axis (within 2°-3°); the boundary often curves round slightly to keep itself parallel to the changing direction of the hexad axis. The boundary etches as a series of pits with about the same mean spacing as the glide planes. The "thermally" etched surface of a recrystallized rock-salt crystal showed a lamellar structure which may have represented the new grain boundaries. Fig. 23 shows diagrammatically the situation as found for zinc.

From the microscopic evidence, then, it can be said that the new grains have a certain shape definitely related to the glide system of the original crystal; and from the X-ray results it is clear that the orientations of these grains, which are free from elastic strain, never depart much from that of the original crystal. The crystal axes are curved in the deformed crystal; the boundaries of the new grains are curved correspondingly, so that they are everywhere normal to the glide plane. The fact that the angle between successive spots in the



- FIG. 1.—Single Grain in Coarse-Grained Copper Foil. Enlarged Laue spot.
- FIG. 2.—Zinc Crystal, bent to 0.5 cm. radius and annealed for $\frac{1}{2}$ hr. at 370° C. Laue pattern.
- FIG. 3.—Magnesium Crystal, bent to approx. 0.5 cm. radius and annealed for $\frac{3}{4}$ hr. at 500° C. Greatly enlarged Laue spot.
- FIG. 4.—Rock Salt Crystal, bent to approx. 0.5 cm. radius and annealed for 16 hr. at 760° C. Enlarged Laue spot.
- FIG. 5.—Zinc Crystal No. 11b, bent to 2.2 cm. radius and annealed for $10\frac{1}{2}$ hr. at 400° C. Enlarged Laue spots.
- FIG. 6.—Zinc Crystal No. 13c, bent to 1.5 cm. radius and annealed for 2 hr. at 400° C. Enlarged Laue spots.



FIG. 7.—Magnesium Crystal, bent to 1·1 cm. radius at 200° C. and annealed for 18 hr. at 560° C. Laue pattern.



FIG. 8.—Rock-Salt Crystal, bent to 0·5 cm. radius and annealed for 16 hr. at 740° C. Laue pattern.



FIG. 9.—Aluminium Crystal, bent to 1·1 cm. radius and annealed for 2 hr. at 580° C. Laue pattern.

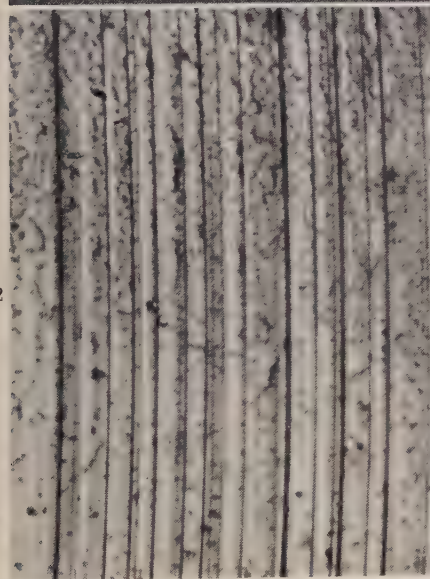
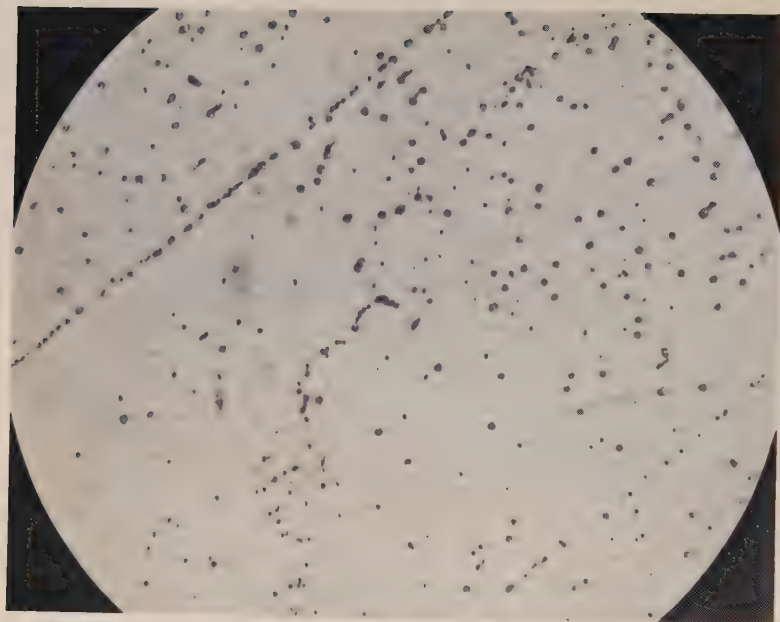


FIG. 10.—Zinc Crystal No. 5b, bent to 1.5 cm. radius, unannealed.

FIG. 11.—As Fig. 10, after annealing for 19 hr. at 345° C.

FIG. 12.—Zinc Crystal No. 17c, bent to 1.5 cm. radius at 120° C. Slip lines and unetched surface. $\times 800$.

FIG. 13.—Zinc Crystal No. 7b, bent to 2.2 cm. radius and annealed for 40 hr. at 350°–400° C. Etched section. $\times 65$.

FIG. 14.—As Fig. 13. $\times 800$.

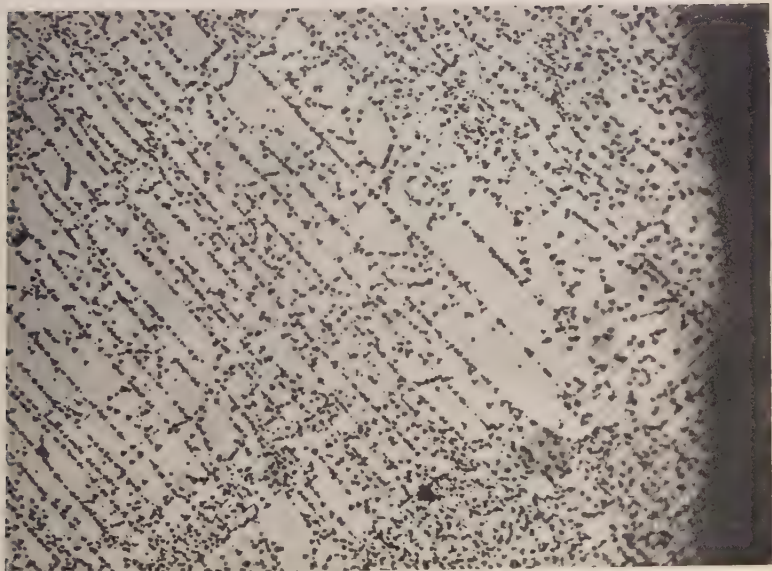
15

FIG. 15.—Zinc Crystal No. 11a, bent to approx. 1.1 cm. radius at 110°C. and annealed for 2 hr. at 400°C. Dark-ground illumination. $\times 130$.FIG. 16. As Fig. 15. Portion of specimen bent less sharply. Dark-ground illumination. $\times 130$.

PLATE XVIII.



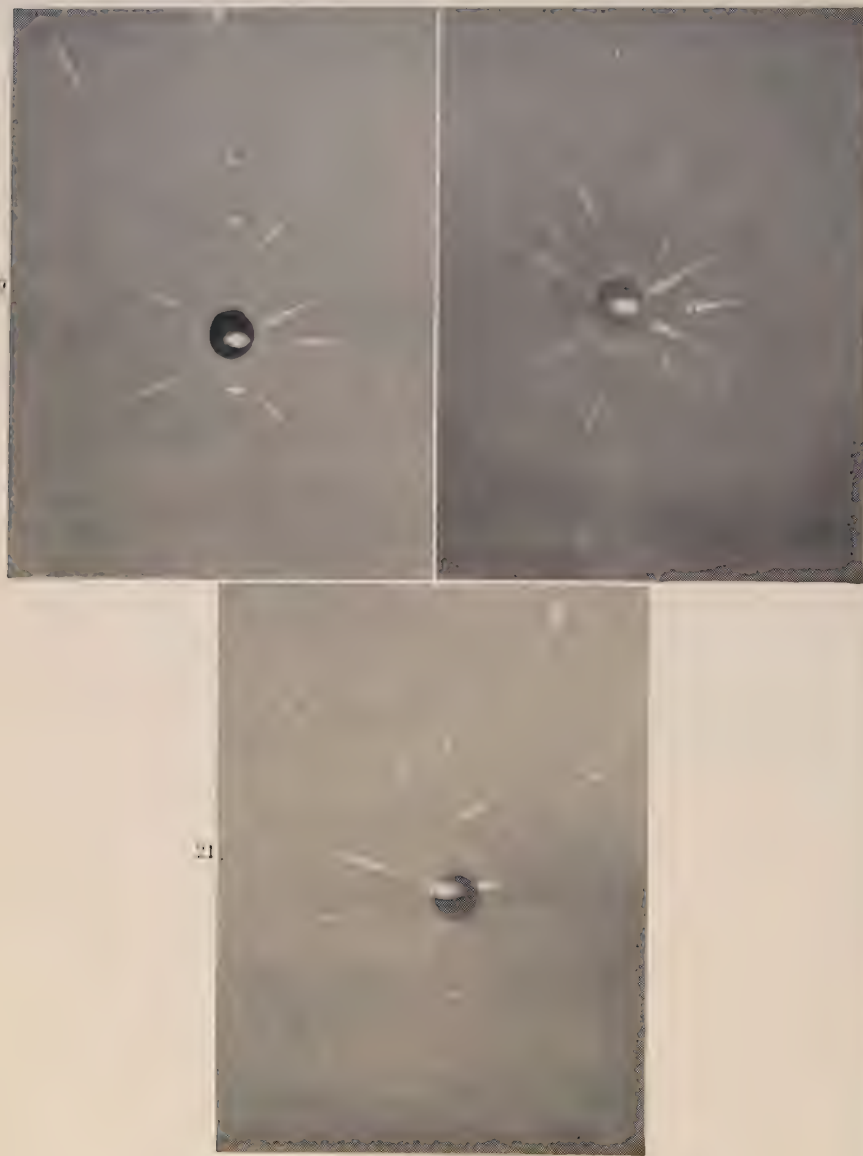
17



18

FIG. 17.—Aluminium Crystal, bent to 6.0 cm. radius and annealed for 18 hr. at 625° C. Etched section. $\times 70$.

FIG. 18.—Aluminium Crystal, bent to 3.0 cm. radius and annealed for 18 hr. at 625° C. Crystal bent further after sectioning and etching. $\times 90$.



LAUE PHOTOGRAPHS.

- FIG. 19.—Zinc Crystal No. 13*a*, bent to 0.8 cm. radius and annealed for 2 hr. at 400° C.
FIG. 20.—Zinc Crystal No. 14*d*, bent to 0.35 cm. radius and annealed for 2 hr. at 400° C.
FIG. 21.—Zinc Crystal No. 15*b*, bent to 1.5 cm. radius under liquid air and annealed for 2 hr. at 400° C.

X-ray pattern is usually fairly constant implies that the grains make constant angles with each other. This angle is a maximum for lattice directions in the plane of the sketch (Fig. 23), which coincides with the vertical plane through the central spot in the X-ray photographs. (It should be remembered that several of these have been turned on their sides in reproduction.) It will be seen that the spots in a horizontal line through the central spot are hardly distorted at all and have no fine structure. In all the grains the directions perpendicular to the plane of Fig. 23 are therefore crystallographically identical.

It seems perfectly clear that these grains cannot have grown from recrystallization nuclei forming at random in the old grain, as is usually the case; for grains growing in this way have either random orientations, or a mean orientation with considerable spread of the individual grains about this mean value (Burgers and Louwerse¹⁷). Moreover, such elongated grains are rarely observed in recrystallization from nuclei, because the latter form in random positions (there being no question of concentration at grain boundaries here) and then grow uniformly in all directions, with perhaps slight local variations. To explain the present results, nuclei of particular orientation would have to form at about equal distances apart at the same time and grow at the same rate. No reasons appear to exist for such a sequence of events.

The alternative explanation is that the grains do not form by growth from nuclei, as usually understood, but by a kind of "recovery" of the original lattice. This would involve an elimination of the elastic stresses in successive narrow regions of the lattice, each region taking up the mean of the range of orientation originally present in it. Many of the results observed could be accounted for in this way. It must be noted that the recovery could not occur by a sudden "clapping over" of the lattice in such regions, as is the case in twinning. The reason for this is well put by Dehlinger¹⁸: "It is in fact not possible to remove a bend [in a lattice] by lifting a single atom over a potential barrier, in such a way that it is followed by the remaining atoms without their having to surmount any barriers. [This is just what happens in twinning.] The special feature of bending is the difference of density in the upper and lower sides of a bent lamella; and only after this has been eliminated does the bend become unstable." To overcome this difficulty he proposes a mechanism involving the movement of atoms from the compressed to the extended side of a lamella; to achieve this three separate "avalanches" of atomic movements, separately activated but suitably timed by chance, are postulated. This leads, as he shows, to a very marked dependence on temperature, which has not been observed in the present work.

A simpler way to achieve the recovery of narrow lattice regions becomes apparent when we remember that the surfaces of bent lamellæ contain many dislocations of the "edge" type (Orowan,¹⁹ Taylor,²⁰ Burgers²¹). When flexural slip takes place, a large excess of dislocations of one sign must remain at the surfaces of each glide lamella, for there must be crystallographic continuity between adjacent lamellæ. Since the lattices on either side of the glide zone are respectively compressed and extended, this can only be achieved by the presence of dislocations (all of the same sign), which by definition involves a difference of density on opposite sides of the plane in which they lie. If these dislocations should move along the glide plane, either discontinuities must arise between the lamellæ, or the radius of curvature of the lamellæ increases locally, thereby reducing the elastic strain.* The former process is impossible because the attraction between atoms is too great, but the latter could occur; further, since it would be attended by a decrease in strain energy, there would be a definite tendency for it to occur. The motion of dislocations will require some activation; this can be furnished by the thermal oscillation of the atoms in the lattice, and therefore the process should become easier as the temperature is raised. The direction of movement of dislocations would vary at different points; once movement had begun at one point, the mutual repulsion of the dislocations would lead to others being pushed in the same direction, and then the direction would remain the same, since reversal would lead to a renewed building up of strain. Dislocations would build up along surfaces separating the regions in which the direction of movement was opposite. Now Bragg²³ has shown that the boundary between two crystals inclined slightly to each other about an axis coincident with the present bending axis, is in effect built up of a succession of edge dislocations of the same sign. The process described above can thus lead to the formation of a number of grains of orientation always near to that of the parent crystal, and of roughly uniform width (with statistical variation of the latter).

It is suggested that the process might be named *polygonization*, to distinguish it from other forms of recrystallization. The name derives from the fact that the crystallographic direction which coincides with the wire axis, while bent along an arc before annealing, becomes part of a polygon afterwards. The term *primary recrystallization* will be used for ordinary recrystallization by nucleation and growth.

* The author is indebted to Dr. A. H. Cottrell for the suggestion that motion of dislocations might be involved. A recent paper by W. G. Burgers²² predicts such motion of dislocations on theoretical grounds.

An attempt has been made to work out quantitatively the mechanism for polygonization just advanced. The elastic theory of beams was applied to the lamellæ to derive the dependence of the stored elastic energy on the radius of curvature. An essential factor, not exactly known however, in such a treatment is the variation of the lamellar thickness with curvature, and two different but equally plausible treatments of this problem are possible, leading to quite different final results. The difficulty can be by-passed by examining the process of plastic bending more closely. The individual lamellæ (Fig. 23, upper half) behave quite differently from freely bent elastic beams, because the radii of curvature of both surfaces must be equal; if this were not so, voids would appear between each pair of lamellæ. This difference of lamellæ from ordinary beams is caused precisely by the concentration of dislocations along their bounding surfaces, and the elastic stress system is the resultant of the stress system of the lamellæ considered as simple beams and the many small local systems associated with the dislocations. Now it is easily shown* that the number of dislocations per unit cross-sectional area necessary to maintain lattice continuity depends only on the curvature applied to the crystal, and is inversely proportional to the radius. The energy associated with the dislocations is therefore independent of the lamellar thickness, and if the latter is very small, this energy will be large compared with the "beam energy" of the lamellæ. It is suggested that this is in fact the case when the lamellæ, as in the present experiments, are only about 2μ in thickness. Then we can say that the elastic energy in the bent crystals is approximately inversely proportional to the radius of curvature.

When polygonization is complete, the lattice has been relieved (a) of all the "beam energy" of the lamellæ, and (b) of most of the strain energy associated with the dislocations. At first sight it would seem that when the dislocations have gathered along the bounding surfaces, this strain energy would actually increase because of their mutual repulsion. However, this is not true when the dislocations lie in a plane perpendicular to the glide plane, because in this position they mutually relieve their stress-fields to a considerable extent, and their mutual repulsion is therefore a minimum.²¹ Briefly, this is due to the fact that when edge dislocations are arranged in this way, the extra half-plane of atoms of one dislocation comes directly above the missing half-plane of the next. Cottrell²⁴ has recently explained very clearly why the observed orientation of the boundaries is a necessary consequence of dislocation theory. This consideration explains both the

* See Appendix II, p. 141.

observed directions and the remarkable straightness, at high magnifications, of the boundaries, and the stability of the new-grown structure, once it is formed, to further heating. A further objection which may be made is that the proposed mechanism would require several dislocations to bunch close together on each active glide plane. This is not a real obstacle, however, since Heidenreich and Shockley²⁵ have shown that apparently single active glide planes consist of a family of planes so close together that only an electron microscope can resolve them. Each dislocation will therefore diffuse along a different plane, and the boundary will consist of small bunches of dislocations, the dislocations in each bunch being spaced out along the length of the boundary. This is supported by the curious nature of the etching (Fig. 17, Plate XVIII). The mean distance apart of the separate pits is found to be equal to the mean lamellar thickness.

The conclusion that high purity of the metal favours polygonization is not surprising when it is remembered how sensitive is the yield-point of a single crystal, which is also connected with the motion of dislocation, to the presence of impurities. The latter form around themselves regions of elastic stress, and this stress will in general oppose the passage of dislocations (see, for instance, Mott and Nabarro²⁶).

It remains to account for the observed fact that coarse grains of copper and magnesium, produced by primary recrystallization, generally showed signs of distortion and polygonization. This was almost certainly due to the progressive redistribution of the intercrystalline stresses present in a cold-worked polycrystalline specimen,²⁸ by the growth of the new grains. This redistribution caused the new grains themselves to become slightly distorted, and during the remaining period of annealing they underwent polygonization. This explanation is supported by the observation that when deformed *single crystals* of magnesium underwent primary recrystallization, the resulting grains were strain-free. Here, of course, there were no intercrystalline stresses to redistribute.

There has also to be explained the curious fact that zinc crystals bent at -180° C. would not polygonize on subsequent annealing. No explanation in terms of an exceptionally small thickness of the lamellæ was possible, in view of the data given in Table III. A possible explanation is that the captive dislocations which have been discussed above are all of one sign. It is not, of course, to be expected that only dislocations of one sign are present. According to the dislocation theory of plastic deformation,²⁹ it is the interaction of positive and

* In this connection Cottrell's²⁷ concept of "atmospheres" of impurities around dislocations, restraining their motion, should also be relevant.

negative dislocations, arranged on a "superlattice", which causes work-hardening of a deformed specimen. In the case of plastic bending, there will be a "background" of positive and negative dislocations, plus an extra number of one kind. The hardening depends largely on the background concentration of dislocations. It is well known that crystals deformed at very low temperatures work-harden much more than when the deformation takes place at room temperature. Therefore the background concentration of dislocations in the crystals bent in liquid air must be high. Now polygonization can only relieve the strain due to the excess of one kind of dislocation; that due to the background can only be removed by primary recrystallization. If, then, the background concentration is high, there will be little tendency for polygonization to take place, for only a small proportion of the strain present could be relieved by it. Moreover, the higher the background concentration, the more is the diffusion of the excess dislocation inhibited; anything which inhibits slip must also inhibit polygonization.

Since the present work was done, a paper has appeared by Guinier and Tennevin,¹¹ which shows that the limiting radius of curvature and annealing temperature found necessary to produce polygonization in zinc are merely due to the small resolving power of the Laue method. By means of a refined focusing X-ray technique they have detected polygonization in aluminium crystals bent to radii as large as 30 cm., and annealed at temperatures as low as 350° C. These experiments have recently been extended to zinc,³⁰ and polygonization has been detected in a crystal bent to 10 cm. radius and annealed for 15 hr. at 300° C. Annealing at 400° C. led to a great reduction in the number of polygonization blocks. Apparently, a very small distortion of the lattice and a relatively low temperature suffice to bring about the first stages of polygonization, but the later stages, during which a few of the blocks absorb all the others, require a high temperature and occur most readily in severely bent crystals. The present author's observation that the mean angle between the blocks was almost independent of the radius of curvature implies that there is a limit to this process of absorption.

VI.—POLYGONIZATION AND RECRYSTALLIZATION THEORY.

Experiments have previously been carried out on annealing single crystals after plastic bending (Beck and Polanyi,³¹ Beck³²). Here aluminium was used, and the immediate purpose was to observe how recrystallization by nucleation and growth was affected by reversed bending. It was found that the specimen recrystallized in the outermost deformed layers, to a depth depending on the orientation and

the degree of deformation. No X-ray study was made of the unrecrystallized remainder. The present author's specimens were much thinner than Beck's, and this is probably why even sharply bent zinc crystals generally polygonized instead of recrystallizing.

In deformed polycrystalline aggregates, of course, there will always be elastic distortion, because of the great difference in degree and direction of distortion of adjacent grains (see, for example, Boas and Hargreaves,³³ Greenough²⁸). When deformation is slight, considerable local distortion is still possible and some polygonization may occur. Some of the papers mentioned in the introduction^{4, 5, 6, 10} have described observations on polycrystalline materials which point to this. Dunn¹⁰ found multiple X-ray reflections, particularly near "deformation bands" in annealed silicon ferrite; he also showed that there is intense elastic strain in the vicinity of these bands. He called the process leading to multiple X-ray reflections "recovery of the third type".

It is necessary to point out that even single crystals deformed in an externally homogeneous way are by no means free from elastic distortion. This is particularly well shown by the fact that in general it is possible to avoid asterism in the Laue pattern altogether only if crystals are deformed by pure shear,³⁴ although with aluminium even this does not entirely get rid of it.³⁵ Experiments by Komar and Mochalov³⁶ on magnesium point to the same conclusion. Crussard⁸ obtained very clear evidence of polygonization (which he calls "recrystallization *in situ*") in X-ray patterns of aluminium crystals pulled in tension to a few per cent. elongation; a Laue photograph showing this was also published by Collins and Mathewson.⁹ Again, Andrade and Tsien² found pronounced spottiness in the Laue pattern of single crystals of sodium and potassium pulled in tension at room temperature (i.e. quite near the melting point).

Recent, as yet unpublished, experiments by the present author have clarified these findings considerably. It was found that extended aluminium crystals contained narrow "deformation bands" which were apparently the places where *Biegegleitung* or flexural glide occurred during the extension, which was not quite even along the length of the crystals. The lattice was very sharply bent in these bands, and on annealing local polygonization took place there, as was demonstrated by means of X-rays and the microscope.

The experiments briefly touched upon in the previous paragraph suggest that polygonization may be expected wherever the lattice is bent, even locally. This has led the author to the hypothesis that in primary recrystallization nuclei form by the polygonization of minute

"local curvatures" in the slip bands. This hypothesis makes it possible to explain a number of previously puzzling observations, and a paper on this subject is in course of publication.

ACKNOWLEDGEMENTS.

The author's thanks are due to Dr. E. Orowan for suggesting the problem, and for his interest and advice in the course of the work; to the British Iron and Steel Research Association, under whose auspices this work was done, for financial assistance; and to Mr. H. Haines, for his assistance with the photographic side of the work.

APPENDIX I.

PURITY OF MATERIALS USED.

The purities of the metals used, from Hilger "H.S." reports on "Speepur" materials, are as follows :

(1) *Zinc*.—No chemical analysis was possible by reason of the exceptional purity. Spectrographic analysis revealed only minute traces of iron, magnesium, and (doubtful) copper. Purity certainly $>99.99\%$, perhaps $>99.999\%$.

(2) *Magnesium*.—Chemical analysis : 0.03% manganese, 0.0075% iron, 0.004% aluminium. Silicon, copper, and zinc were not detected chemically, though spectrograms showed these and various other metals. Estimated purity = 99.95%.

(3) *Aluminium*. Chemical analysis : 0.002% magnesium, 0.0015% silicon, 0.0005% copper, 0.005% iron. Spectrographic lines detected due to magnesium, copper, calcium, silicon, barium. Estimated purity of metal $>99.995\%$.

APPENDIX II.

THE DENSITY OF EXCESS DISLOCATIONS OF ONE SIGN IN A BENT CRYSTAL.

Fig. 25 represents a small section of a bent crystal, taken perpendicular to the direction of the dislocation lines (i.e. the glide direction lies in the plane of the figure). The radius of curvature is R .

The elastic strain at the surface of each lamella = $s = \pm \frac{d}{2R}$.

The total amount of misfit there would be between a pair of adjacent lamellæ if no dislocations were present = $D \cdot 2s = \frac{Dd}{R}$.

Each dislocation relieves the misfit by one atomic parameter a .

\therefore There must be $N = \frac{Dd}{Ra}$ excess dislocations between each pair of lamellæ.

The total number of excess dislocations crossing the section shown
 $= N \cdot \frac{D}{d} = \frac{D^2}{Ra}$.

\therefore The total number of dislocations per unit cross-section $= \frac{1}{Ra}$.
This is independent of d , and inversely proportional to the radius of curvature.

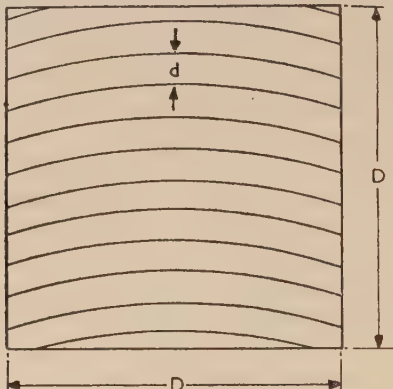


FIG. 25.—Polygonization of a Bent Crystal (schematic).

REFERENCES.

1. S. Konobeevsky and I. Mirer, *Z. Krist.*, 1932, **81**, 69.
2. E. N. da C. Andrade and L. C. Tsien, *Proc. Roy. Soc.*, 1937, [A], **163**, 1.
E. N. da C. Andrade and Y. S. Chow, *Proc. Roy. Soc.*, 1940, [A], **175**, 290.
3. H. Hirst, *Proc. Austral. Inst. Min. Met.*, 1941, (121), 11, 29.
4. W. Bungardt and E. Osswald, *Z. Metallkunde*, 1939, **31**, 45.
5. V. Chitruk, private communication.
6. W. Boas and R. W. K. Honeycombe, *Proc. Roy. Soc.*, 1946, [A], **186**, 57.
7. M. Kabata, *Mem. Coll. Sci. Kyoto Imp. Univ.*, 1936, **19**, 223.
8. Ch. Crussard, *Rev. Mét.*, 1944, **41**, 111.
9. J. A. Collins and C. H. Mathewson, *Trans. Amer. Inst. Min. Met. Eng.*, 1940, **137**, 150.
10. C. G. Dunn, *Trans. Amer. Inst. Min. Met. Eng.*, 1946, **167**, 373.
11. A. Guinier and J. Tennevin, *Compt. rend.*, 1948, **226**, 1530.
12. P. Lacombe and L. Beaujard, *J. Inst. Metals*, 1948, **74**, 1; and *Phys. Soc. : Rep. Conf. on Strength of Solids*, 1948, 91.
13. E. N. da C. Andrade and R. Roscoe, *Proc. Phys. Soc.*, 1937, **49**, 152.
14. W. P. Davey, *Phys. Rev.*, 1924, [ii], **23**, 764.
15. A. Joffé, M. V. Kirpicheva, and M. A. Levitsky, *Z. Physik*, 1924, **22**, 286.
16. C. S. Barrett and C. H. Levenson, *Trans. Amer. Inst. Min. Met. Eng.*, 1940, **137**, 76.
17. W. G. Burgers and P. C. Louwerse, *Z. Physik*, 1931, **67**, 605.

18. U. Dehlinger, *Z. Metallkunde*, 1941, **33**, 16.
19. E. Orowan, *Z. Physik*, 1934, **89**, 634.
20. G. I. Taylor, *Proc. Roy. Soc.*, 1934, [A], **145**, 362.
21. J. M. Burgers, *Proc. K. Ned. Akad. Wetensch.*, 1939, **42**, 293, 378; and *Proc. Phys. Soc.*, 1940, **52**, 23.
22. W. G. Burgers, *Proc. K. Ned. Akad. Wetensch.*, 1947, **50**, 425, 595, 719, 858.
23. W. L. Bragg, *Proc. Phys. Soc.*, 1940, **52**, 54.
24. A. H. Cottrell, "Progress in Metal Physics", Vol. I, p. 93. London : **1949**.
25. R. D. Heidenreich and W. Shockley, *Phys. Soc. : Rep. Conf. on Strength of Solids*, **1948**, 57.
26. N. F. Mott and F. R. N. Nabarro, *Proc. Phys. Soc.*, 1940, **52**, 86.
27. A. H. Cottrell, *Phys. Soc. : Rep. Conf. on Strength of Solids*, **1948**, 30.
28. G. B. Greenough, *Proc. Roy. Soc.*, 1949, [A], **197**, 556.
29. G. I. Taylor, *Proc. Roy. Soc.*, 1934, [A], **145**, 362, 388, 405.
30. A. Guinier, private communication.
31. P. Beck and M. Polanyi, *Z. Elektrochem.*, 1931, **37**, 521.
32. P. A. Beck, *Trans. Amer. Inst. Min. Met. Eng.*, 1937, **124**, 351.
33. W. Boas and M. E. Hargreaves, *Proc. Roy. Soc.*, 1948, [A], **193**, 89.
34. A. Kochendörfer, "Plastische Eigenschaften von Kristallen und metallischen Werkstoffen", p. 12. Berlin : **1941**.
35. W. G. Burgers and F. J. Lebbink, *Nature*, 1946, **157**, 47.
36. A. Komar and M. Mochalov, *Physikal. Z. Sowjetunion*, 1936, **9**, 613.

THE APPLICATION OF X-RAY METHODS 1213 TO THE DETERMINATION OF PHASE BOUNDARIES IN METALLURGICAL EQUILIBRIUM DIAGRAMS.*

By PROFESSOR E. A. OWEN,† M.A., Sc.D., MEMBER, and
D. P. MORRIS,† B.Sc.

SYNOPSIS.

Recent criticisms of the X-ray powder method of determining phase boundaries in metallurgical equilibrium diagrams (notably by Hume-Rothery and Raynor, *J. Sci. Instruments*, 1941, **18**, 74) are considered in detail and are shown to be unfounded. Certain objections to the microscopical method are pointed out, and in the light of X-ray investigations carried out on solid specimens, it is concluded that in general the study of equilibrium conditions is best conducted with material in powder form.

I.—INTRODUCTION.

THE relative advantages of the X-ray and classical metallurgical methods for the determination of phase boundaries in equilibrium diagrams have been considered, among others, by Hume-Rothery and Raynor,¹ who arrived at the conclusion that for ordinary equilibrium-diagram work at the higher temperatures the classical methods appear to be the more satisfactory and reliable, but that the X-ray methods become increasingly valuable at the lower temperatures, provided that the specimens are annealed for sufficiently long periods. Hume-Rothery and Raynor criticized the X-ray method on several grounds. The purpose of the present paper is to give further consideration to the matter in the light of more recent researches, especially on the behaviour of solid specimens as compared with powder specimens under various conditions of treatment. It is hoped that this communication will be helpful in dispelling some of the fears expressed concerning the X-ray powder method, and in showing the great value of this method in determining phase boundaries in equilibrium diagrams not only at low but also at high temperatures. Some objections have been raised

* Manuscript received 15 March 1949.

† Physics Department, University College of North Wales, Bangor.

to the X-ray method which apply not to this method alone, as would be gathered from the paper cited, but to some of the classical methods also. It would be well to submit some of the statements made to critical examination before finally accepting them, and to modify the emphasis placed on certain aspects of the work. A wrong impression will be gained of the value of the X-ray powder method of determining phase boundaries in equilibrium diagrams if the matter is left as stated by Hume-Rothery and Raynor, so it will be the aim of the present authors to consider in some detail each objection raised by them in their paper.

The usefulness of X-ray methods in the study of such phenomena as atomic migration and superlattice changes is not in question; the objections raised refer to the determination of phase boundaries in equilibrium diagrams, and it is this aspect of the work only that will be considered here.

II.—HEAT-TREATMENT OF FILINGS.

The method of producing filings for X-ray examination has been described previously,^{2, 3} and differs in some important respects from that described by Hume-Rothery and Raynor. They omit to mention, for instance, the precautions taken to ensure that the ingot is in an initially homogeneous state. Elaborate tests are made to ensure that there is absence of segregation both longitudinally and transversely in the ingot before the final samples of filings are taken from it. Usually the ingot, which is prepared in cylindrical form, is cold worked alternately with annealing over considerable periods, depending upon the alloy, until it shows no segregation. This may be very difficult with some alloys, and several methods of cooling from the molten state have usually to be tried before a satisfactory result is obtained. A homogeneous ingot having been produced, which is possible in the small ingots prepared for the work since they weigh usually only a gramme or two, filings are taken and annealed at the required temperatures.

In the work hitherto done in this laboratory on lump and powder material, it has been found that filings reach equilibrium sooner than the lump. It may be true, as stated by Hume-Rothery and Raynor, that "in many cases" the times of annealing to produce equilibrium are of the same order for the two forms, but the present authors have found no cases so far in which this occurs, even at the higher temperatures.

When testing for the equilibrium of the filings it is usual to take, in the first instance, two samples, one of which is annealed for about twice as long as the other.⁴ If the two do not yield identical crystal parameters within the error of measurement, further samples are taken and annealed for longer periods until the lattice parameter is found to be constant. It depends upon the nature of the alloy and upon the temperature, whether the period of annealing to produce equilibrium at that temperature is of the order of hours, weeks, months, or even years. But the same test applies. If plates of material were used they would often require months of annealing, whereas powder would require only weeks. In fact, in plate form some alloys require alternate annealing and cold working over very long periods to bring them to a state *approaching* equilibrium. Hume-Rothery and Raynor refer to the distrust of X-ray work by some metallurgists on account of the shorter periods of annealing used with filings as compared with lump material in some instances, but these times of annealing are determined by definite tests as indicated above. It is doubtful whether the metallurgist has as definite a test to apply to his lump specimens, and as we shall see later the physicist has even more ground for distrusting the results of metallurgists when these results are deduced from the microscopical examination of prepared surfaces.

To summarize, the X-ray powder method consists in first obtaining a homogeneous ingot, and then in preparing from this ingot filings which are annealed for long enough to produce equilibrium at the required temperature, definite tests based on lattice-parameter measurements being applied at each stage.

III.—COMPOSITION OF INGOT AND FILINGS.

In addition to the state of homogeneity of the ingot being known before filings are taken from it, the composition of the ingot is accurately known. Several ingots prepared as described in previous papers^{2, 3} were submitted to accurate chemical analysis, and as a rule the results of analysis agreed, within 0·1 wt.-%, with the composition as calculated from the weights of the constituents used in their production, even when the ingots contained volatile constituents. For example, a copper-zinc alloy prepared to contain 8·01% zinc and 91·99% copper proved on analysis to contain 7·98% zinc and 91·98% copper; a silver-zinc alloy prepared to contain 36·00% zinc and 64·00% silver on analysis was found to contain 36·05% zinc and 63·98% silver; a silver-tin alloy prepared to contain 5·97% tin and 94·03% silver contained

5.95% tin and 93.94% silver by analysis. The volatile constituent agrees within 0.05% with the estimated value in each case, showing there is no appreciable loss by volatilization in preparing the ingot. On the average the actual composition agrees within 0.05 wt.-% of the estimated value for both volatile and non-volatile constituents. The weight of each ingot is compared with the weight of the ingredients used to make it, and the weights agree usually to a few parts in 10,000.³

The purity of the filings has been questioned, but it is possible to test for soluble impurities by X-ray examination probably as accurately as can be done by any method of analysis of very small quantities. Hume-Rothery and Raynor are much exercised concerning the purity of the filings, but experiment shows that their fears are unfounded. Suppose samples of filings of pure metal, for instance silver which is cited in their paper, are prepared and sieved, and that each contains a particular but different range of particle size, it is unlikely that all the samples will be contaminated to the same extent, and yet on annealing there is no difference in lattice parameter within the error of experiment.⁵ Below are the figures for silver of 99.999% purity, each specimen having been annealed at 450° C. for 12 hr.

<i>Grade of Particle</i>	<i>Lattice Parameter of Silver at 18° C., kX.</i>		
Passed through 300 mesh . . .	4.0776 ₆		
" 250-300 mesh . . .	4.0775 ₈		
" 140-250 " . . .	4.0775 ₉		
Retained by 140 " . . .	4.0776 ₀		

Similar tests were carried out with copper, gold, iron, and lead; the copper (99.999% purity) and the gold (spectroscopically pure) samples were annealed at 500° C. for 12 hr.; iron (99.98% purity) was annealed at 500° C. for 115 hr., and lead (99.999% purity) annealed at 100° C. for 1 hr. The results were the same as with silver, no change in parameter being observed. There would certainly be a greater divergence between the parameter values if there had been contamination of the filings such as might be inferred would be the case from the statement of Hume-Rothery and Raynor.

With aluminium of high purity (99.998%) a slight change in parameter amounting to ± 0.0002 kX. from the mean was observed over the range of particle size examined. More extensive tests indicated that there may be a real change in parameter with particle size in the case of pure aluminium; low-purity aluminium (99.39%) does not show the effect. But even with pure aluminium the whole change is only just outside the experimental error of measurement.

All the filings used in the above measurements were prepared by hand and were enclosed in evacuated tubes for annealing as soon as possible after sieving.

If these pure metals do not show contamination, it is reasonable to infer that this is also the case with alloys prepared by the same technique.

There is yet another test which may be carried out in this connection. Suppose samples of filings, sieved or unsieved, from a solid solution are prepared, and that these are annealed for various times at various temperatures. When these are quenched in cold water, it is found that the lattice parameter of an alloy of a given composition in the range of solid solution is the same whatever the temperature and the period of annealing. This test has frequently been carried out and reported on various occasions in papers published from this laboratory.⁶ If the filings were appreciably contaminated, the lattice parameters after annealing at different temperatures, especially if a long range of temperature is covered as in the paper above referred to, should show more variation than was actually observed.

In the latter case it should be mentioned that the actual filings of many samples were analysed. From the criticism of Hume-Rothery and Raynor it might be inferred that the X-ray physicist deliberately avoided submitting the actual filings to the test of chemical analysis. This in general is certainly not the case.

The main point to be emphasized in connection with the question of contamination is that in the X-ray method tests such as have been mentioned can be applied which supply information on the point at issue, whereas no such tests are available in the microscopical method.

The next consideration is the exact composition of the filings. It has already been mentioned that in the technique adopted the ingot is first examined for segregation. Small ingots are deliberately used, and even these are not accepted unless the test to which they are subjected, namely that the unsieved filings prepared from different parts of the ingot yield the same parameter within experimental error, is satisfied. The question of segregation is therefore settled in the initial stages of the investigation.

Hume-Rothery and Raynor suggest the possibility of volatilization of one constituent during the annealing of the filings. To reduce the loss by volatilization to a minimum the filings are annealed in small bulbs drawn out to a narrow neck which allows the filings to pass through and which can be readily sealed off in a small flame without heating the filings.³ In this way the dead space can be made very

small indeed. The total volume of the container is generally about 200 mm.³ The usual expedient adopted to test loss by volatilization is to divide an annealed sample into two portions: one half is again annealed at the same temperature for a longer period, or if it is an unsaturated solution, at a higher temperature; the other half is maintained at room temperature. There was no perceptible loss of the volatile constituent after this treatment, as judged from the parameter values.^{2, 4} This test was carried out frequently at the beginning of our investigations on equilibrium diagrams, but not so often at the later stages because we were satisfied that the loss from this source was imperceptible with the technique adopted.

When dealing with polyphase alloys Hume-Rothery and Raynor state that "it is quite common for the filing process to produce particles of very different sizes from the different phases, and in such cases the composition of the filings varies with the fineness of the sieve through which they are passed". It may also be added that since only the finer grades are used in our technique, this, according to the above statement, may magnify the effect. When this statement is examined in detail (see Section IV), it will be found that no error can arise from this source.

IV.—TECHNIQUE OF PHASE-BOUNDARY DETERMINATION.

It would be well here to consider briefly the technique adopted to arrive by X-ray methods at the position of a phase boundary in an equilibrium diagram. Two methods are possible: (1) the disappearing-phase method, and (2) the lattice-spacing method, and their sensitivities may be very different.

The sensitivity of the disappearing-phase method depends upon several factors. If a strong line exists in the structure spectrum of the second constituent which is watched as it appears or disappears when the composition of the alloy is altered, the amount of the second phase necessary to give a trace of its presence in the structure spectrum may be as low as 0·2 at.-% if radiation can be chosen which does not produce too much general scattering and so provides a fairly clear background in the photograph. If, however, the background is heavy, even though strong lines in the spectrum of the second phase are available, the sensitivity may decrease to 0·5 or even 1 at.-%. In the iron-nickel system, for instance, where the background is rather pronounced, the accuracy of phase-boundary determination by this method is of the order of 0·5%. Furthermore, of course, preferential

sieving out of one constituent may seriously affect the accuracy, and for this reason the method is usually carried out with unsieved filings. In practice, however, this method is employed for a preliminary survey of the system only or when the lattice parameter is difficult to measure with accuracy owing to bad definition or unfavourable position of spectral lines. A Debye-Scherrer camera is usually employed, so that the whole of the spectrum may be recorded. A preliminary survey having been made by this method, the position of the boundary is fixed with precision by the lattice-spacing method.

For this method the camera employed in the authors' laboratory is of the focusing type,⁷ and is chosen for a special reason, namely that the lattice spacings can be obtained from the dimensions of the instrument without having to resort to extrapolation. This is useful because the spacing can be deduced with a high degree of accuracy from individual sets of planes in the crystal. In order to increase the accuracy of measurement, continuous lines must be produced in the X-ray photograph, and this can be achieved only by employing a fine grade of powder.

The first step in the process of finding the position of a phase boundary by this method is to determine with the greatest accuracy possible the relation between the lattice parameter and the composition of alloys across the pure-phase region. The alloys are annealed at various temperatures within the phase and quenched; as already stated, an alloy in an unsaturated phase gives the same parameter value whatever the temperature within the phase from which it is quenched. It is important that the composition of the alloy remains constant. This is found to be the case in alloys that are free from segregation as determined in the manner already described. There is no difficulty usually in determining the parameter-composition curve with accuracy.

The next step is to move into the adjacent duplex region. In this region of two saturated phases, the parameter of each constituent at any temperature remains constant across the region. A number of alloys are prepared within the range of the two-phase region, filings taken from them as before and annealed at given temperatures for sufficiently long periods to produce the equilibrium condition at those temperatures, and then efficiently quenched to retain their condition at the temperatures of annealing. In the case of alloys in duplex regions it is usual to anneal all the powder and sieve it after the annealing treatment to obtain the finest grains for the X-ray camera. Both the constituents, quenched from any temperature, show constant parameters across the region. The boundary of the pure phase at any

temperature is the point where the horizontal at that temperature determined from alloys in the duplex region meets the parameter-composition curve of that phase.

Returning now to the criticism of Hume-Rothery and Raynor (mentioned at the end of Section III) that in sieving filings of alloys in the duplex region the composition of the specimen examined may be very different from that of the parent sample owing to differential selection in the sieving process, it is quite immaterial whether this is so or not, since the method depends not on the estimation of the relative proportions of the two phases present in the specimen but in the determination of the composition of *one* of the phases as measured by its lattice parameter. Actually the second constituent could be entirely removed by sieving without affecting the method in the slightest. The exact composition of the powder as a *whole* in the duplex region is not essential to the accuracy of this method of determining the position of phase boundaries. In all our researches on phase boundaries in this laboratory we have encountered no difficulty on the score of the separation of the constituents of a duplex alloy. We therefore disagree entirely with the conclusion of Hume-Rothery and Raynor that "for accurate work nothing except the analysis of the filings in their final stage is satisfactory", when stated in this connection.

The sensitivity of the lattice-spacing method is generally higher than that of the disappearing-phase method because the limit of solubility is obtained by the measurement of definite quantities which can be determined with precision. The final accuracy depends upon the accuracy of the determination of the lattice spacing of one constituent in the mixed-phase region, and the lattice-spacing-composition curve in the single-phase region and its inclination to the axis of composition, and these determinations are not affected by the sieving process.

It has been pointed out by Hume-Rothery and Raynor¹ that many investigators have assumed that the lattice-spacing-composition curve is linear, and that in some cases rather lengthy extrapolations have been employed. This procedure is obviously unjustifiable, but this is not a true criticism of the X-ray powder method itself, but merely an example of its misuse. The exact shape of the curve is immaterial, since it can be determined right across the single-phase region by suitable choice of alloys.

To conclude this Section, it will be well to consider briefly the sensitivity of the microscopical method of determining phase boundaries and the identification of constituents. It is clear that with regard to sensitivity no hard and fast rule may be given, since with a disappearing-

phase method of this sort the conditions will vary with the particular system examined. In general, however, it is considered by metallurgists to be more sensitive than the X-ray disappearing-phase method, although to take one specific example in which no etching difficulties were apparently encountered, a redetermination of the $\alpha/(\alpha + \zeta)$ boundary in the copper-germanium system placed the boundary about 0·5 at.-% lower in germanium at 300° C. than that determined in earlier work from the same laboratory.⁸ This difference was attributed to the failure to detect precipitated ζ in the earlier work owing to the use of small specimens, although it is not clear how this could affect the method.

With regard to the identification of constituents, the relative advantages of the microscopical and X-ray methods have been discussed by Hume-Rothery and Raynor.¹ For ternary and more complicated systems the advantage lies with the X-ray method, while in all systems it is supreme for the study of superlattices and atomic migration. For the simple binary alloys it is claimed that the microscopical method is usually shorter and more simple. Whilst this may be true, it is worth while emphasizing that the information supplied by this method is always purely qualitative, and it is not possible to establish from the appearance of the phases whether they are saturated, that is, whether the alloy is actually in equilibrium. The structure spectra of the constituents obtained by the X-ray method, however, not only supply information about the identity of the constituents but also indicate whether they have reached thermodynamic equilibrium, and it is here that the essential difference between the two methods lies. The position may be summarized by saying that the most important feature of the precision X-ray method of locating a phase boundary is that it depends on quantitative measurements made on single-phase alloys and on the major constituent of duplex alloys, whereas the microscopical method depends on visual and qualitative observations made on the minor constituent of duplex alloys, in which it must be present in regions at least one thousand times greater than the atomic dimensions.

V.—ALLOY SYSTEMS WITH PHASES UNSTABLE AT ROOM TEMPERATURE.

The procedure described above refers to work on quenched filings, the assumption being that the condition of the alloy at a given temperature of annealing is retained by quenching. Sometimes this is

not the case, the alloy whose high-temperature condition it is desired to retain at room temperature transforming on quenching into another phase or phases. The cases cited by Hume-Rothery and Raynor are those of the β phases of the copper-zinc and silver-zinc systems. These alloy systems were examined in this laboratory by the X-ray method using quenched specimens,^{6, 9} and in both cases the boundaries of the β -region appear not to be correctly located¹⁰ because on quenching, especially in the case of specimens of composition near to the boundary of the phase, the conditions of the alloys were not retained. These results are compared by Hume-Rothery and Raynor with the results of the classical metallurgical methods, and it is concluded that "these alloys are unsuitable for examination by X-ray methods with quenched filings". Although apparently the positions of the phase boundaries in these two systems may be satisfactorily determined by microscopical examination, it was necessary to check the conclusions by high-temperature X-ray investigations. We would therefore extend the above statement and say that in general such systems are unsuitable for examination by *any* method employing quenched specimens, whether filings or lump material. It should be emphasized that it is not the X-ray method as such that is at fault; rather is it the technique whereby an endeavour is made to retain the condition of an alloy at high temperature by quenching, and this criticism can be levelled equally well against the classical metallurgical methods which employ this technique of quenching.

Alongside the two alloy systems above mentioned should be considered two other alloy systems which were examined by the X-ray method before the silver-zinc system was investigated. These are the aluminium-zinc¹¹ and the iron-nickel¹² systems. They well illustrate the real usefulness of the X-ray method when the alloy system contains a phase which cannot be retained by quenching, and they are different in type in that one contains a volatile constituent, while in the other the two constituents are non-volatile, though in both cases it is necessary to investigate the alloys in some region of the equilibrium diagrams at high temperatures. In these two alloy systems the X-ray method is seen to good advantage, the alloys being examined at the temperatures at which they are annealed. This would also have been the technique employed with the silver-zinc and copper-zinc systems had it been suspected that the β phase could not be retained by quenching. The work done by the X-ray method on these two systems points, therefore, to the desirability of examining certain alloys in all systems at high temperatures to check the results obtained with quenched specimens.

The Aluminium-Zinc System.

In the case of the aluminium-zinc system¹¹ it was known from work by ordinary metallurgical methods that the β phase transformed readily on quenching. The X-ray investigation was therefore carried out at high temperature, with results that elucidated the form of the equilibrium diagram at elevated temperatures more accurately than had hitherto been possible. The equilibrium diagram presented by Tanabe,¹³ which was about the twenty-fifth contribution on the system by classical metallurgical methods, is reproduced in Fig. 1 (dotted lines), with some phase boundaries (full lines) as determined by X-rays. Owen

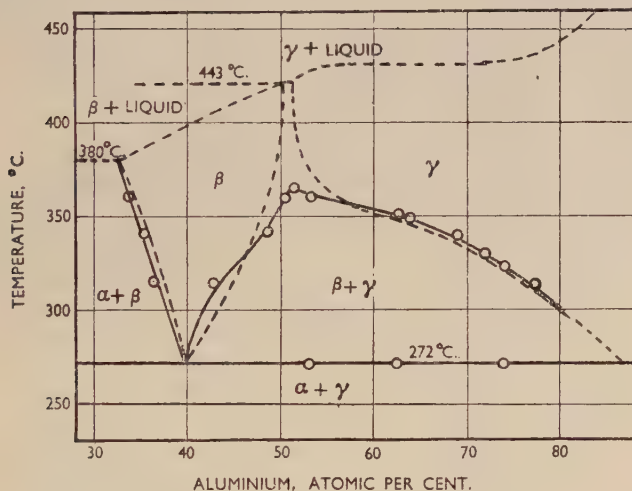


FIG. 1.—Equilibrium Diagram of Aluminium-Zinc Alloys.

KEY.
 - - - Tanabe,¹³
 —— Owen and Pickup.¹¹

and Pickup¹¹ found that the structure of the β and γ phases of Tanabe's diagram were both face-centred cubic, and they stated that their X-ray data did not confirm the existence of the $(\beta + \gamma)$ region above about 360° C . If this is so, then the α and γ regions join above this temperature to form one field, and this was later corroborated by classical metallurgical methods.¹⁴ There is no doubt that the X-ray method was the means of clearing up a difficulty in connection with this diagram which had baffled metallurgists before the system was investigated by X-rays at elevated temperatures.

The Iron-Nickel System.

As regards the iron-nickel system, about 65 contributions had been made concerning the equilibrium diagram of the system before Owen and Sully¹² undertook an extensive investigation of the system by the X-ray method, which included the examination of quenched specimens as well as specimens maintained at elevated temperatures.

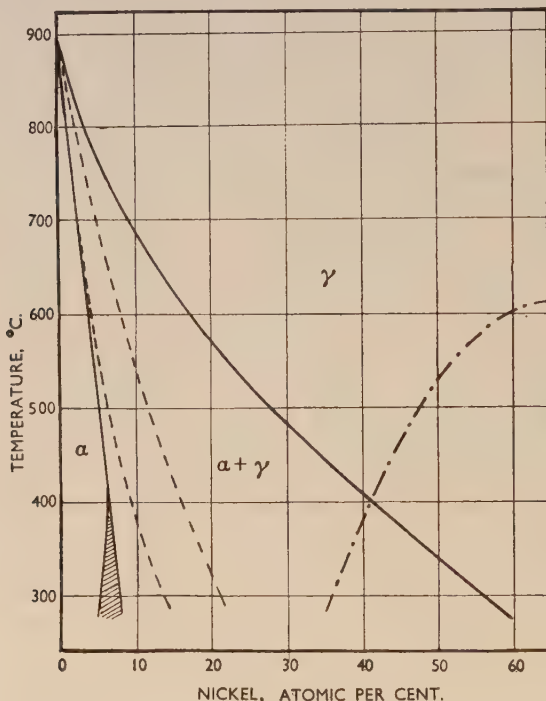


FIG. 2.—Equilibrium Diagram of Iron-Nickel Alloys.

KEY.

- Selected iron-nickel diagram (Marsh¹³).
- Owen and Sully¹² and Owen and Liu.
- Magnetic transformation.

The suggested equilibrium diagram of the system, after many changes, before the X-ray investigation was undertaken is shown dotted in Fig. 2,¹⁵ the full lines in this figure being the boundaries in the equilibrium diagram found by X-rays. Here there is a marked difference between the results by the two methods of investigation. It is significant that the X-ray method supplied information concerning these alloys which had not up to that time been obtained by classical

metallurgical methods, particularly in regard to alloys containing up to about 25 at.-% nickel quenched from temperatures above about 580° C.

These two diagrams are cited as instances of work carried out by the X-ray method which show that observations made on quenched alloys supplemented by observation made on alloys maintained at elevated temperatures, the specimens being in powder form, provide a satisfactory means of arriving at phase boundaries in equilibrium diagrams.

VI.—DETERMINATION OF LIMIT OF SOLUBILITY.

Solubility of Aluminium in Silver.

Hume-Rothery and Raynor refer to the determination of the solubility of aluminium in silver, comparing their results by microscopical methods with those of Foote and Jette¹⁶ by the X-ray method. We had determined the α -boundary in this laboratory¹⁷ before these results were published, and since there are one or two points in doubt according to the above authors we now include our results in Fig. 3, together with theirs and the boundary given by Hume-Rothery, Mabbott, and Channel-Evans¹⁸ when they considered the solubility limits of a number of alloys of silver and copper with the elements of the *B* sub-groups. This composite diagram will serve to illustrate two points: firstly, the X-ray results agree all along the portion of the boundary which has been investigated in common by the two groups of observers. The divergence at any temperature does not exceed 0·4 at.-%, and along

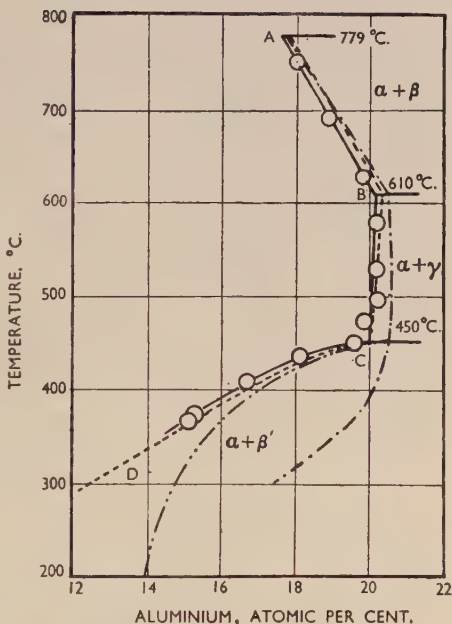


FIG. 3.—Solubility of Aluminium in Silver.

KEY.

- Hume-Rothery, Mabbott, and Channel-Evans.¹⁸
- Hume-Rothery and Raynor.¹
- Foote and Jette.¹⁶
- Owen and Roberts.¹⁷

the portion *BC* is much less than this. The point *C*, which appears to be in doubt according to Hume-Rothery and Raynor,¹ is found at 19.92 at.-% aluminium by Foote and Jette, at 20.0 by Owen and Roberts, and at 20.5 by Hume-Rothery and Raynor and by Hume-Rothery, Mabbott, and Channel-Evans. The X-ray results place the portion *BC* of the

boundary at a lower aluminium content than the metallurgical results. The second point is the variation observed below about 450° C. Whereas the X-ray results agree, the two investigations by microscopical methods disagree widely amongst themselves; at 400° C. they disagree by about 3.2 at.-% aluminium, and at 300° C. by about 2.7 at.-%, and these values disagree with the X-ray results. That is, the position of the boundary below about 450° C. is quite indefinite according to the two metallurgical results, but quite definite according to the X-ray results. In the former, lump specimens were used, but in the latter the material was in the form of filings. These results would indicate that at the lower temperatures equilibrium, and therefore reproducible results, are more readily obtained with powder than with lump material. The work on this system does not

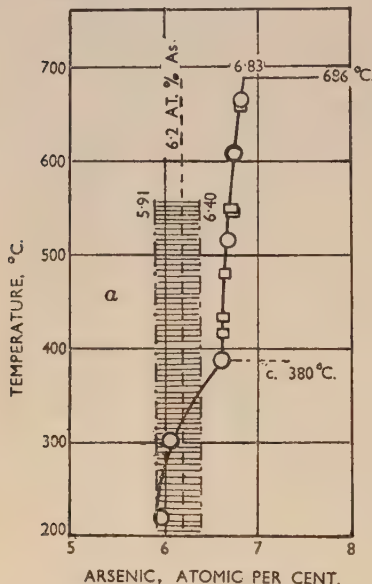


FIG. 4.—Solubility of Arsenic in Copper.

KEY.

- — — Hanson and Marryat.¹⁹
- · · Hume-Rothery, Mabbott, and Channel-Evans.¹⁸
- Owen and Rowlands⁴ and Owen and Roberts.¹⁷

justify, in our opinion, the conclusion arrived at by Hume-Rothery and Raynor that "as the temperature is raised the older methods become relatively more suitable, and the X-ray methods may well be confined to cases where the solubility range is very small or the boundaries nearly vertical". To investigate this point further a number of solubilities were examined.

Solubility of Arsenic in Copper.

The solubility of arsenic in copper had been investigated by the classical methods and found by Hanson and Marryat¹⁹ to be 6.21

at.-% arsenic and independent of temperature. Hume-Rothery, Mabbott, and Channel-Evans¹⁸ carried out a further investigation and found the solubility at 550° C. to lie between 5·91 and 6·40 at.-% arsenic and that no change occurred on re-annealing at lower temperatures, in agreement with Hanson and Marryat. These results and those obtained in two separate investigations^{4, 17} by the X-ray method conducted in this laboratory by different experimenters with different material prepared specially for the investigations, are included in Fig. 4. It will be observed that the two X-ray investigations agree exactly over the range of composition and temperature common to both, but they disagree with the results obtained by the classical methods. Above about 400° C. the limit of solubility of arsenic in copper found by the X-ray method at all temperatures up to 688° C. is outside the limits of solubility given by the classical metallurgical investigations above mentioned, and, contrary to the results of these investigations, X-rays reveal a gradual increase in the solubility of arsenic in copper with temperature, namely 6·64 at.-% arsenic at 400° C., and 6·83 at.-% at 686° C. Below 400° C. the solubility decreases from 6·63 at.-% at 384° C. to 5·90 at.-% at 200° C. In this case the position of the boundary at temperatures below about 360° C., as determined by X-rays, falls within the limits of the range given by Hume-Rothery, Mabbott, and Channel-Evans, but at higher temperatures the boundary lies outside this range.

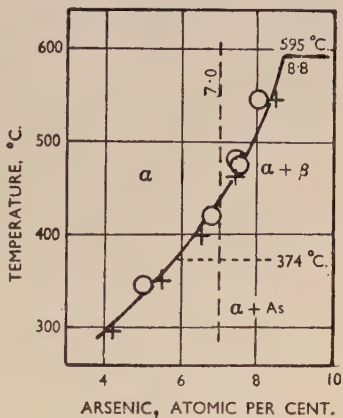


FIG. 5.—Solubility of Arsenic in Silver.

KEY.

— Heike and Leroux,²⁰
 — Owen and Rowlands⁴ and Owen and Roberts.¹⁷

Solubility of Arsenic in Silver.

With silver-arsenic alloys (Fig. 5) the difference between the results of the two methods is more pronounced; whereas Heike and Leroux²⁰ by classical methods found the solubility at all temperatures up to the peritectic temperature of 595° C. to be constant at 7 at.-% arsenic, the X-ray method¹⁷ shows a definite change of solubility with temperature, increasing from 5·2 at.-% at 350° C. to 8·8 at.-% at 595° C., these figures having a probable error of $\pm 0\cdot15$ at.-%. Arsenic is a

material which readily tarnishes and is also volatile. The range of the probable error is therefore greater than usual for these reasons.

These two systems—copper–arsenic and silver–arsenic—taken at random from several systems examined by X-rays in this laboratory, serve to contradict the general conclusion arrived at by Hume-Rothery and Raynor, and incidentally they illustrate how detailed and definite is the information obtained by the X-ray method as compared with that supplied by the classical metallurgical methods in these two instances.

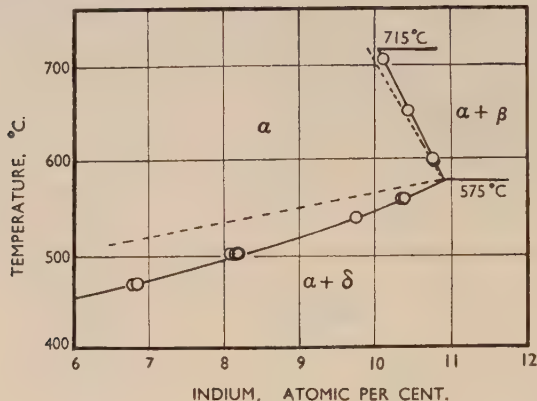


FIG. 6.—Solubility of Indium in Copper.

KEY.

— — — Hume-Rothery, Raynor, Reynolds, and Packer.⁸
— — — Owen and Roberts.¹⁷

Solubility of Indium in Copper.

Another instance to disprove the last-mentioned conclusion of Hume-Rothery and Raynor may be cited. This is the system copper–indium, the α -boundary of which has been determined by Hume-Rothery and his collaborators⁸ and also by Owen and Roberts¹⁷ in this laboratory. Here we have good agreement between the results of the two groups of workers at high temperatures (from 576° C. up to the peritectic temperature, 710° C.), but no agreement at low temperatures, and, contrary to the usual findings at low temperatures by the two methods, the X-ray method now shows more solution of indium in copper than that found by the microscopical method. The results are shown in Fig. 6.

Solubility of Gallium in Silver.

One other system, namely silver–gallium, should be considered because Hume-Rothery has commented on our determination of this

boundary by the X-ray method.⁴ He has stated that our determination of the maximum limit of solubility is incorrect²¹ because the lattice-parameter-composition curve should be drawn with a slight curvature

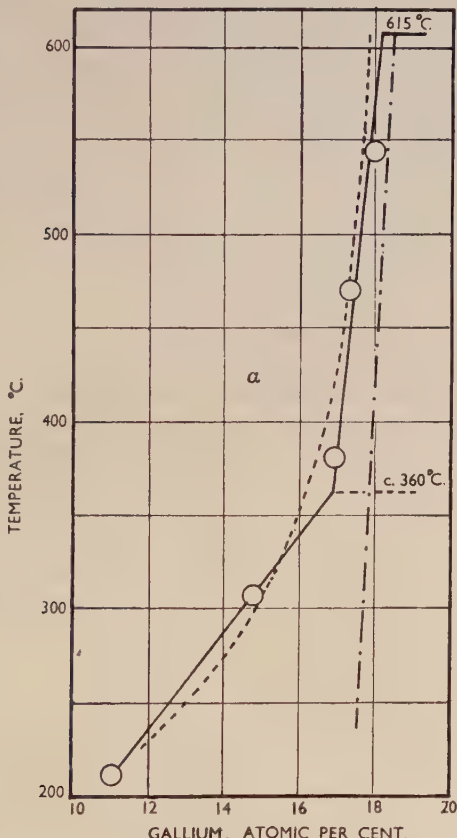


FIG. 7.—Solubility of Gallium in Silver.

KEY.

- Hume-Rothery, Mabbott, and Channel-Evans.¹⁸
- - - Owen and Rowlands (original boundary).⁴
- Owen and Rowlands (adjusted boundary).

instead of a straight line as we had drawn it to the accuracy of the measurements. There may be some justification for this criticism. Allowing then for this slight curvature, the values of the boundary have only small differences from our former values as shown in Fig. 7. The maximum solubility at the peritectic temperature of 615° C. becomes 18.2 instead of the previous value of 17.8 at.-% gallium,

still differing slightly from the value of 18.6 at.-% given by Hume-Rothery, Mabbott, and Channel-Evans.¹⁸ The boundary found by these authors by the classical methods is included in Fig. 7. In order to fix the position of the boundary above 550° C. more securely by the X-ray method, it would be desirable to make further observations at temperatures nearer to that of the peritectic, thereby obviating the somewhat extended extrapolation which has previously been necessary. The difference at the peritectic temperature between the positions of the boundary by the two methods is small, however, compared with the serious discrepancies observed at lower temperatures; about 1.0 at.-% at 400° C., 3.3 at.-% at 300° C., and about 5.0 at.-% at 250° C. The point shown at 211° C. in Fig. 7 has been deduced from our parameter-composition curve, using the lattice-parameter value in the duplex region at 211° C. determined by Hume-Rothery. The point falls closely on the continuation of the boundary as previously drawn by us.

This system serves as an instance of the great discrepancies between the two methods observed at the lower temperatures. There is no doubt that the X-ray method leads to a more accurate location of the phase boundary, taken as a whole, over the range of temperature investigated.

The above examples from alloy systems already examined suffice to show that the X-ray powder method gives satisfactory and reliable results at both high and low temperatures if the precaution is taken of examining those alloys that are unstable at room temperature, at the actual temperature at which the boundary point is to be determined.

VII.—BEHAVIOUR OF STRESSED MATERIAL.

It would be well at this stage to consider the problem of phase-boundary determination in the light of recent work which has been done on stressed materials.²² Briefly stated, a filed or a finely polished surface of aluminium is found to be in a state of stress after these operations, the lattice parameter being different from that corresponding to the equilibrium state of the metal. Moreover, after a metal has been compressed the initial parameter is higher than the equilibrium value, and in course of time changes to a value which remains constant but is different from the equilibrium value. The material appears to reach a metastable condition at room temperature after this treatment, and can be changed to its equilibrium state only by further annealing at an elevated temperature. These results, together with others which arise from cold working a material, will be considered in relation to

the technique adopted in investigations on lump material by classical metallurgical methods in which the microscope plays an important part.

VIII.—SURFACE CONDITION OF POLISHED SPECIMENS.

The main objection to the microscopical method is the fact that metallurgical specimens require preparation after the final heat-treatment. Although particular kinds of treatment may have to be adopted in certain cases, especially for the investigation of equilibrium conditions, the procedure is not essentially different from the general technique described in text-books²³ and specialized papers dealing with particular alloys.²⁴ This consists in the cutting and filing (and sometimes grinding) of the specimen to obtain a flat surface and to examine different sections, followed by the polishing of the surface with polishing papers and pads, the latter requiring the use of polishing powders and a lubricating medium. The specimen is then rinsed and dried, generally in a current of warm air, and examined under the microscope either before or after etching or both. In addition, in certain cases, depending mainly on the size and shape of the specimen, it has to be mounted in a suitable medium before polishing begins, although presumably this technique would not be adopted in the study of equilibrium conditions.

Now clearly these various processes are undesirable, particularly for the investigation of equilibrium conditions, since they involve the risk of upsetting the initial condition of the specimen, set up possibly after weeks or even months of annealing, through cold work and the effects of polishing and through exposure to many different environments.

The preliminary cutting and filing and the necessity of holding the specimen in some form of vice, produce cold-worked layers whose thickness and extent will depend upon the severity of the treatment, and although this is reduced to a minimum it is certain that the specimen, and particularly the surface layers, are no longer in the initial condition at the end of this treatment. This conclusion becomes even more important when it is remembered that the majority of specimens are examined in the quenched condition and, being in an unstable state, may be more susceptible than usual to the effects of cold work. It has been suggested²⁵ that straining increases the instability of the supersaturated state, and this increases the tendency for the solute atoms to be deposited from solution, though this change may need time or a rise in temperature. It is not known to what extent the incipient precipitation visualized above proceeds, since the specimen still requires polishing before microscopical examination; but it seems reasonable to regard the specimen at this stage in its preparation as

being more susceptible than usual to the effects of further deformation and rise of temperature.

There has been some difference of opinion in the past about the actual mechanism of the polishing process, but it is now generally agreed that "the existence of a flowed layer on polished surfaces is an experimental fact which cannot be denied".²⁶ Bowden and Ridler²⁷ have shown that the surface temperature during polishing becomes high enough to cause local melting, and that the molten or softened solid flows or is smeared over the surface and very quickly solidifies to form the polished Beilby layer. The latter is not homogeneous, but consists of rapidly cooled solid containing very small aggregates or micro-crystals of varying size, in which particles of oxide and polishing powder are embedded. Moreover, polishing in air has been shown by Preston and Bircumshaw²⁸ and by Dobinski²⁹ to cause rapid surface oxidation, while, as already mentioned, Owen, Liu, and Morris²² found the polished surface of aluminium in a state of stress and yielding a lattice parameter different from the equilibrium value, and because of penetration of the X-ray beam into the specimen this represents the state of affairs considerably below the surface of the specimen. It is therefore quite certain that the condition of the surface of the specimen and of a layer of appreciable thickness has been profoundly modified by the polishing process. Any attempt to infer the constitution and condition of the specimen by the microscopical examination of unetched polished surfaces is therefore likely to be misleading, although this seems to be fairly common practice for certain purposes.^{30, 31, 32}

This may be illustrated by the investigations of Wulff and his collaborators by electron diffraction on the phase transformations induced in stainless steel (18% nickel, 8% chromium) by polishing and grinding.³³ The surface layers resulting from wet or dry grinding were found to be austenitic, indicating that they had been heated above 200° C., whilst about 6×10^{-4} cm. below the surface was a layer which had been reduced to ferrite by cold work. Samples which had received any type of polishing had a ferritic layer 1.5×10^{-5} cm. or less in thickness.

IX.—ETCHED SURFACES.

Generally speaking, the polished surface, as would be expected from the nature of the Beilby layer, has to be etched in order to develop the structure, the etching reagent acting by preferential attack on the grain boundaries and at regions of strain, and on the various phases of which the specimen is composed. The etching reagents and the

conditions employed differ widely from alloy to alloy and on the particular aspect of the structure which is being investigated, but for phase identification the practice appears to be to try various reagents and conditions until those which give a reasonably satisfactory contrast between the various phases have been found.³¹ In many cases, the action of the etching reagent is very uncertain and the various tints and colours are not reproducible.^{8, 30} It is suggested that this may be due to variations in the deformation and strain produced in the polished surface. There are undoubtedly, therefore, difficulties associated with the identification of phases on etched specimens even in binary systems. Moreover, McLean³⁴ has shown that the deformation of a specimen during preparation for microscopical examination may penetrate to a depth of nearly 0.25 mm. in α -brass, for example, so that unless the etching process removes at least this thickness of material, the surface examined cannot be regarded as being in true equilibrium, and owing to the tendency for incipient precipitation mentioned earlier, there may be a danger of obtaining values for solid-solubility limits which are too low.

X.—X-RAY INVESTIGATION OF SOLID SPECIMENS.

An investigation of solid specimens by X-ray methods would appear to provide the possibility of overcoming the difficulty attaching to the preparation of the specimen *after* heat-treatment, since it does not depend upon having polished or etched surfaces. The required shape of surface can be obtained by filing or grinding the specimen *before* subjecting it to heat-treatment. Such an investigation was carried out in an attempt to compare by one method and with the same camera the behaviour of powder and lump specimens, and in the hope that some of the more controversial regions of one or two published equilibrium diagrams could be re-examined with the new technique.

A special camera was designed to execute the work; this will be described elsewhere. The results obtained place in doubt the feasibility of the application of X-ray diffraction techniques directly to solid specimens, as opposed to the normal powder technique, for the measurement of equilibrium lattice spacings, not from any difficulty of X-ray technique but rather from the point of view of establishing equilibrium conditions in polycrystalline specimens.

The powder method has the advantage that consistent and reproducible values of lattice spacings can be obtained after comparatively short heat-treatments, and the agreement in the values obtained by different workers in this field places beyond doubt the fact that their

values may be properly regarded as physical constants of the materials and as being representative of the equilibrium state.

The failure to obtain consistent results with solid specimens can only be interpreted as being due to the difficulty of establishing equilibrium conditions. One possible cause of this is the mutual interference of neighbouring crystals during grain growth and in recovering from the effects of deformation; other contributing factors may be thermal stresses set up on cooling and, in anisotropic materials, stresses due to different expansion coefficients.

XI.—GENERAL CONCLUSIONS.

The results of the investigation just mentioned provide indirect evidence in favour of the X-ray powder method of investigating equilibrium conditions in alloy systems, and as such they have an important bearing on the criticism of the method by Hume-Rothery and Raynor dealt with earlier in this paper. Undoubtedly the filing and sieving processes can lead to the introduction of impurities, but this can be remedied by careful technique. Decomposition by quenching, as already noted, is just as likely with solid as it is with powder specimens, and the effects of this can hardly be described as a failing of the powder method. On the other hand, the quantitative measurements of the X-ray powder method are an invaluable criterion of equilibrium, a criterion which appears to be lacking in the usual microscopical method of determining solid-solubility limits and equilibrium diagrams. The work carried out in this laboratory shows quite definitely that different crystals in the same large-grained solid specimen can have different lattice spacings even in specimens which one would normally assume to have been annealed to equilibrium. This shows that polycrystalline specimens are really aggregates of individual crystals of different shapes and lattice spacings. Measurements on individual crystals have been made and they show these variations; it is therefore not surprising that the results obtained with comparatively coarse-grained specimens are not always consistent.

It is possible that these local variations will occur from crystal to crystal in a fine-grained solid specimen also, although the effect is smoothed out, since the measured lattice spacing is the mean of those of a large number of crystals. Further, if the specimen is simultaneously rotated and oscillated during exposure, the measured lattice spacing could reasonably be expected to be free from complications due to the selective action of the incident X-rays which, in a stationary specimen, results in grains of one particular orientation only contributing to the

diffraction lines and thereby, as shown by Smith and Wood,³⁵ giving an expansion or contraction effect in stressed specimens. Work which has been carried out in this Department and which will shortly be published, has shown, however, that even for fine-grained solid specimens anomalous lattice spacings are obtained even after long annealing treatments, and this is attributed to the difficulty of removing the strains set up during cold working. This difficulty is overcome in the case of powders, since each particle consists of only a few crystals and they are relatively much more free to assume the equilibrium configuration than is the case in solids.

Solid specimens even after prolonged annealing cannot properly be regarded as being in a true equilibrium state, and the preparation of metallurgical specimens for microscopical examination is likely to lead to further deviation from equilibrium.

The final conclusion arrived at is that when the study of equilibrium conditions is the ultimate goal, the X-ray powder method has decided advantages over any other method provided that due care is taken to avoid contamination and that observations are made at high temperature as well as on quenched specimens at room temperature. In the first paper⁶ published from this laboratory on the X-ray study of phase boundaries in equilibrium diagrams of alloy systems it was concluded that a phase boundary can be determined by the X-ray method from parameter measurements alone, and that an accurate determination can be made irrespective of the amount of the second phase present. Subsequent work has confirmed these findings, and in addition justifies the view that the X-ray investigator who tries to determine an equilibrium diagram by the X-ray powder method alone is more likely in general to arrive at a diagram representing the true equilibrium state of an alloy system than the metallurgist who employs only classical metallurgical methods for which solid specimens are necessary.

Previous to our more recent researches on lump specimens, we were inclined to the view that equilibrium conditions such as are necessary to construct an equilibrium diagram of an alloy system, would be better studied with material in lump form by classical metallurgical methods in conjunction with powder material by the X-ray method, but now we are forced to the opposite view that in general the main emphasis should be on the X-ray powder method with the microscopical and other methods requiring lump specimens as subsidiary to it.

REFERENCES.

1. W. Hume-Rothery and G. V. Raynor, *J. Sci. Instruments*, 1941, **18**, 74.
2. E. A. Owen and E. W. Roberts, *Phil. Mag.*, 1939, [vii], **27**, 294.
3. E. A. Owen and E. A. O'D. Roberts, *J. Inst. Metals*, 1945, **71**, 213.
4. E. A. Owen and V. W. Rowlands, *J. Inst. Metals*, 1940, **66**, 361.
5. Y. H. Liu, Ph.D. Thesis, Univ. Wales, **1947**.
6. E. A. Owen and L. Pickup, *Proc. Roy. Soc.*, 1932, [A], **137**, 397.
7. E. A. Owen and E. L. Yates, *Phil. Mag.*, 1933, [vii], **16**, 606.
8. W. Hume-Rothery, G. V. Raynor, P. W. Reynolds, and H. K. Packer, *J. Inst. Metals*, 1940, **66**, 209.
9. E. A. Owen and I. G. Edmunds, *J. Inst. Metals*, 1938, **63**, 291.
10. K. W. Andrews, H. E. Davies, W. Hume-Rothery, and C. R. Oswin, *Proc. Roy. Soc.*, 1941, [A], **177**, 149.
11. E. A. Owen and L. Pickup, *Phil. Mag.*, 1935, [vii], **20**, 761.
12. E. A. Owen and A. H. Sully, *Phil. Mag.*, 1938 [vii], **27**, 614.
13. T. Tanabe, *J. Inst. Metals*, 1924, **32**, 415.
14. M. L. V. Gayler and E. G. Sutherland, *J. Inst. Metals*, 1938, **63**, 123.
15. J. S. Marsh, "The Alloys of Iron and Nickel". Vol I, p. 53. New York : **1938**. (McGraw-Hill Book Co., Inc.)
16. F. Foote and E. R. Jette, *Trans. Amer. Inst. Min. Metal Eng.*, 1941, **143**, 151.
17. E. A. Owen and E. A. O'D. Roberts, unpublished data.
18. W. Hume-Rothery, G. W. Mabbott, and K. M. Channel-Evans, *Phil. Trans. Roy. Soc.*, 1934, [A], **233**, 1.
19. D. Hanson and C. B. Marryat, *J. Inst. Metals*, 1927, **37**, 121.
20. W. Heike and A. Leroux, *Z. anorg. Chem.*, 1915, **92**, 119.
21. W. Hume-Rothery and K. W. Andrews, *J. Inst. Metals*, 1942, **68**, 133.
22. E. A. Owen, Y. H. Liu, and D. P. Morris, *Phil. Mag.*, 1948, [vii], **39**, 831.
23. C. H. Desch, "Metallography". London : **1942**. (Longmans, Green and Co., Ltd.)
R. H. Greaves and H. Wrighton, "Practical Microscopical Metallography". London : **1939**. (Chapman and Hall, Ltd.)
24. N. H. Mason, G. J. Metcalfe, and B. W. Mott, *J. Inst. Metals*, 1944, **70**, 197.
25. C. A. Edwards, D. L. Phillips, and Y. H. Liu, *J. Iron Steel Inst.*, 1943, **147**, 145 p.
26. C. H. Desch, "Metallography". London : **1942**, p. 276.
27. F. P. Bowden and K. E. W. Ridler, *Proc. Roy. Soc.*, 1936, [A], **154**, 640.
F. P. Bowden and T. P. Hughes, *Proc. Roy. Soc.*, 1937, [A], **160**, 575.
28. G. D. Preston and L. L. Bircumshaw, *Phil. Mag.*, 1936, [vii], **22**, 654.
29. S. Dobinski, *Phil. Mag.*, 1937, [vii], **23**, 397.
30. D. J. Strawbridge, W. Hume-Rothery, and A. T. Little, *J. Inst. Metals*, 1947-48, **74**, 191.
31. D. W. Wakeman and G. V. Raynor, *J. Inst. Metals*, 1948-49, **75**, 131.
32. G. V. Raynor and D. W. Wakeman, *Phil. Mag.*, 1949, [vii], **40**, 404.
33. J. Wulff, *Trans. Amer. Inst. Min. Eng.*, 1941, **145**, 295.
34. D. McLean, *J. Inst. Metals*, 1947-48, **74**, 95.
35. S. L. Smith and W. A. Wood, *Proc. Roy. Soc.*, 1944, [A], **182**, 404.

THE EQUILIBRIUM DIAGRAM OF THE SYSTEM CHROMIUM-MANGANESE.*

By S. J. CARLILE,† B.A., J. W. CHRISTIAN,‡ B.A., D.Phil., STUDENT MEMBER, and W. HUME-ROTHERY,§ M.A., D.Sc., F.R.S., MEMBER.

SYNOPSIS.

The equilibrium diagram of the system chromium-manganese has been determined for the whole range of compositions above 1000° C., and for the range 60–100 at.-% manganese at lower temperatures. There is a wide solid solution of manganese in chromium extending up to approximately 70 at.-% manganese, and the corresponding liquidus and solidus curves fall smoothly from the melting point of chromium to 1310° C., at which temperature the solid solution reacts with the liquid to form an intermediate phase of variable composition denoted θ , having a complex crystal structure probably based on the composition CrMn₃. The liquidus and solidus continue to fall to 1276° C., where the θ phase and liquid react peritectically to form a solid solution of chromium in γ -manganese, whilst at 1246° C., δ -manganese is formed peritectically from the liquid and the γ -manganese phase. At low temperatures the chromium-base solid solution undergoes transformations which have not yet been studied; the solid solution readily absorbs nitrogen at high temperatures, and in the region of 40 at.-% manganese the whole alloy can be transformed into a brittle white solid. The α , β , and γ modifications of manganese all take up about 10 at.-% chromium into solid solution, but the solubility of chromium in δ -manganese is very small.

I.—INTRODUCTION AND PREVIOUS WORK.

THE system chromium-manganese is of interest because the constituent elements lie in Groups VI and VII of the Periodic Table, where the interatomic distances and melting points suggest that the atomic cohesion is at a maximum.|| If the views of Pauling¹ are accepted, Groups VI and VII are those in which electrons begin to enter the atomic *d* orbitals, but this interpretation seems to be increasingly doubtful. No previous determination of the equilibrium diagram appears to have been made, and the system is one whose study involves many experimental difficulties owing to the reactivity of chromium and the volatility of manganese at high temperatures.

* Manuscript received 8 April 1949.

† Lecturer in Physics, Huddersfield Technical College.

‡ Inorganic Chemistry Laboratory, Oxford.

§ Royal Society Warren Research Fellow, Oxford.

|| The melting point of manganese is lower than that of chromium or iron, possibly because of the abnormal crystal structure, but the general tendency for the melting points to reach maxima in Groups VI to VII is clear.

II.—EXPERIMENTAL METHODS.

A. *Materials Used.*

The chromium used in the present work was electrolytic metal, one batch of which had been prepared at the National Physical Laboratory and the remainder by Messrs. Johnson, Matthey and Company, Ltd. In agreement with previous workers (cf. Adcock²), it was found that the electrolytically deposited metal contained about 1% of oxygen in a form which could not be detected in the original deposit, but which on annealing in a vacuum at 800° C., produced oxide particles readily visible under the microscope. Attempts made to prepare alloys from the electrolytic metal by melting in hydrogen gave alloys containing appreciable quantities of oxide, and all the chromium used for the equilibrium-diagram work was therefore treated in hydrogen for 6 hr. at 1400°–1500° C., and by this means the oxygen content was reduced to about 0·1%, which is equivalent to 0·3% of chromic oxide, Cr₂O₃. Figs. 8 and 9 (Plate XX) indicate the improvement caused by the hydrogen treatment. The chromium which had been treated in hydrogen contained less than 0·02% of nitrogen, and was free from metallic impurities except that the first batch of N.P.L. metal contained from 0·04 to 0·07% iron.

The manganese used was electrolytic metal of 99·98% purity, and was treated in hydrogen at 800° C. in order to remove superficial oxidation.

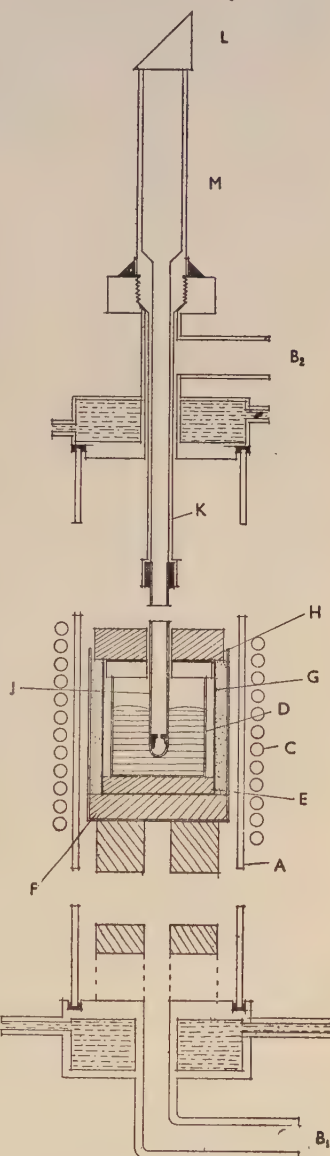
B. *The Preparation of the Alloys.*

The first batch of alloys was prepared in a spark-gap induction furnace at the National Physical Laboratory, and the authors must express their thanks to Dr. N. P. Allen and the staff of the Metallurgy Division for their help. The alloys prepared at Oxford were melted in a valve-operated induction furnace in an atmosphere of hydrogen at about 500 mm. (of mercury) pressure. Some experimental details of this work are given in Appendix I (p. 192).

All the alloys used were melted in crucibles of A.R.R. recrystallized alumina made by the Morgan Crucible Company, Ltd., and for the alloys of high chromium content the crucibles were lined on the inside with thoria. The furnace arrangements were such that the melt could be viewed through a glass window, and after the alloy was completely molten the furnace was switched off, and the hydrogen was pumped away; the alloy was then allowed to cool in a vacuum.

C. The Liquidus above 1500° C.

The liquidus curve above 1500° C. was determined by thermal analysis in the induction furnace, using ingots of approximately 100 g. which had been previously melted under the conditions described in Section IIB. The temperatures were measured by an optical pyrometer of the disappearing-filament type, and the general arrangements are shown in Fig. 1. In this figure *A* is a thick-walled silica tube of length 24 in. and internal diameter 2½ in., whose ends are closed by brass end-pieces with water-cooled wax vacuum seals. The tubes *BB* enable the large tube to be evacuated and filled with hydrogen. The middle part of the tube is surrounded by the work coil *C* of the H.-F. generator. The thoria-lined alumina crucible *D* containing the alloy stands on an alumina block *E* inside the outer alumina crucible *F*. The crucible is surrounded by a molybdenum heater sleeve *G* and is provided with alumina lids *H* bored centrally to admit the alumina sighting tube *J*, which is clamped into the brass tube *K* passing out of the furnace unit through a vacuum seal as shown in Fig. 1. A totally reflecting glass prism *L* is waxed to the top of the



KEY.

- A* Silica furnace tube.
- B₁* To vacuum system.
- B₂* To hydrogen supply.
- C* Work coil of H.F. generator.
- D* Thoria-lined alumina crucible.
- E* Alumina block.
- F* Outer alumina crucible
- G* Molybdenum heater sleeve.
- H* Alumina lids.
- J* Alumina sighting tube.
- K* Brass tube.
- L* Glass prism.
- M* Brass tube.

FIG. 1.—Apparatus for Cooling Curves above 1500° C.

brass tube M , and the resulting horizontal beam of light is viewed through the telescope of the optical pyrometer, which is always placed at the same distance from the prism.

The previously melted ingot was drilled centrally to allow insertion of the sighting tube J (Fig. 1), and was then placed in the crucible, care being taken to allow sufficient space between the ingot and crucible to prevent the latter from being broken by the thermal expansion of the metal.

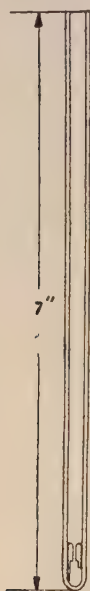


FIG. 2.—Sighting Tube of Optical Pyrometer, showing alumina baffle plug.

The H.F. generator used was made by Messrs. Philips, Ltd., and was such that the extent of the coupling between the oscillatory circuit and the anode circuit of the valve, and hence the rate of heating or cooling, was controlled by rotation of a handwheel. In order to obtain a regular rate of heating this control wheel was fitted with a worm gear wheel by means of which the control wheel could be rotated very slowly; in practice it was found convenient for the observer to give the small handwheel of the worm a definite number of rotations every one or two minutes. The most satisfactory rate of heating or cooling was found to be of the order of 6° – 8° /min., because slower rates made it impossible to distinguish the beginning of arrests owing to the spread of the optical-pyrometer readings.

In order to obtain black-body conditions the sighting tube was fitted with a baffle plug pierced with a small hole, as shown in Fig. 2. The telescope of the optical pyrometer was then adjusted so that the hot filament was viewed across the image of the hole in the baffle plug.

The optical pyrometer was calibrated at the National Physical Laboratory, but in the present work a correction had to be made for absorption in the glass prism, and for possible errors arising from the experimental conditions which made the entrance aperture of the instrument smaller than was desirable. If T_1 and T_2 are the true and apparent temperatures respectively on the absolute scale, it can be shown that for both kinds of error

$$T_1 - T_2 = KT_2^2,$$

provided that KT_2 is very much smaller than 1. In this way a determination of $(T_1 - T_2)$ at a single temperature enables the corrections to be calculated for the whole range. For this purpose use was made

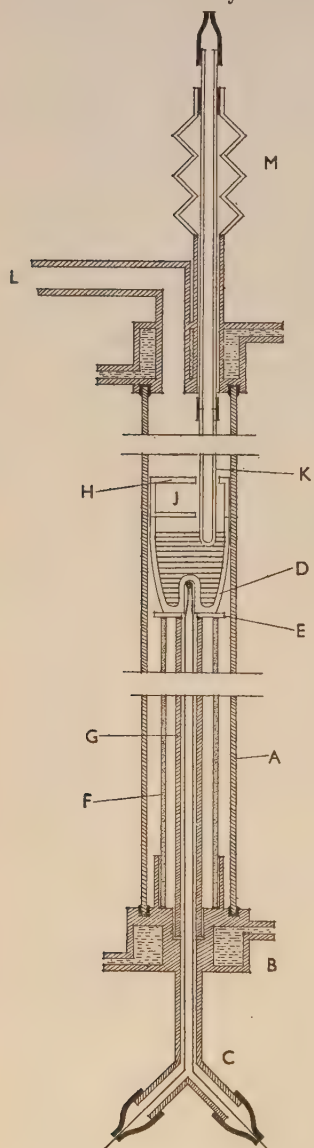
of the Mond nickel shot of 99.94% purity, the freezing point of which is 1455° C. (1728° K.) and is easily reproducible.* We have to thank Mr. H. W. G. Hignett of The Mond Nickel Company, Ltd., for supplying us with this material. The correction at 1455° C. was found to be 15° C., in good agreement with the value 14.5° C. at 1400° C., given by the National Physical Laboratory as the probable correction for a glass prism of the size used. In this way the constant K was determined, and theoretically this alone should be sufficient. As an additional precaution, the value of $(T_1 - T_2)$ at the freezing point of copper was determined as 8°, 8°, and 10° (mean value 9°) in three separate experiments, in good agreement with the value 9.5° C., calculated from the value of K determined at the nickel point. Further confirmation was obtained by measuring the apparent temperature of two alumina tubes heated side by side at 1500° C. in a platinum-resistance furnace. One tube was sighted through the prism and sighting tube of the apparatus of Fig. 1, so that the exact conditions of the cooling-curve observations were reproduced. The other tube was sighted directly and the observed difference was 16° C., in exact agreement with that calculated from the data at the nickel point.

The accuracy obtained with the optical pyrometer is difficult to estimate, and was placed by the National Physical Laboratory as $\pm 7^\circ$ at 1300°–1500° C. and $\pm 10^\circ$ C. at 1500°–1900° C. As the above results show, the accuracy for the measurement of steady temperatures at 1500° C. was better than these values suggest. The matching of the disappearing filament is subject to some uncertainty, being dependent on the experience of the observer. At the nickel point steady arrests were obtained which extended over periods of the order of 10 min. During these arrests the filament was repeatedly matched, and in two heating and two cooling curves the total spread of the readings was 2°, 4°, 2°, and 4° C., respectively. At the freezing point of chromium, 1845° C. (see p. 181), well-defined horizontal arrests were obtained, and the total scatter was 7° and 4° C. in two experiments. This scatter is, of course, more serious for alloys which freeze over a range of temperature. In the present work the arrests became more pronounced with increasing temperature, and it seems probable that the errors did not increase very greatly in the range of temperature from 1500° to 1850° C.

* This paper was prepared for publication before full details of the revised International Scale of Temperature, adopted at the Ninth General Conference of Weights and Measures in 1948, were available. All temperatures are therefore expressed in terms of the old (1927) International Scale. On the new scale the freezing point of nickel is 1453° C. and the freezing point of the chromium sample given later as 1845° C. is 1840° C. on the new scale.

D. The Liquidus below 1500° C.

The thermal analyses below 1500° C. were carried out by thermo-couple methods using the apparatus shown in Fig. 3.



In this figure *A*. is a mullite tube 24 in. long, of which the middle 15 in. are heated in a platinum-wound resistance furnace. The lower end of the mullite tube is closed by a water-cooled metal base *B*, and the joint made vacuum tight by Apiezon W sealing compound. A platinum/platinum-13% rhodium thermocouple is introduced at the bottom of the apparatus through the glass tube *C*, and passes upward into the thermocouple pocket of the crucible *D* which stands on an alumina block *E* resting on an inner mullite tube *F*. Immediately below the crucible the wires of the thermocouple are protected by the alumina tube *G*. In order to reduce the loss of manganese by volatilization the crucible is provided with an alumina lid *H* bored with an off-centre hole to accommodate an alumina thermocouple sheath *K* which can be used as a stirrer and in which the immersion thermocouple (see below) is contained.

The upper end of the mullite tube *A* is closed by a water-cooled brass

KEY.

- A* Outer mullite tube.
- B* Water-cooled base-piece.
- C* Glass tube.
- D* Alumina thermocouple crucible.
- E* Alumina disc.
- F* Inner mullite tube supporting crucible.
- G* Alumina thermocouple sheath.
- H* Alumina lid, formed from inverted crucible.
- J* Tantalum or zirconium foil.
- K* Alumina stirrer and sheath for immersion thermocouple.
- L* Argon supply and vacuum system.
- M* Metal bellows.

FIG. 3.—Apparatus for Cooling Curves below 1500° C.

collar containing holes for the insertion of the sheath *K* and a tube *L* through which the apparatus can be evacuated, and filled with purified argon; all the cooling-curve experiments were done in an atmosphere of this gas. The stirrer is moved up and down either by means of a flexible metal bellows or through a piece of rubber tubing. With this apparatus a rate of cooling of the order of $1^{\circ}\text{--}3^{\circ}$ C./min. can be obtained by making small regular adjustments of a Variac transformer, and a 50-g. ingot freezing at a constant temperature gives a most satisfactory arrest lasting for 15 to 20 min.

In the work on manganese-chromium alloys the thermocouple was rapidly contaminated by the action of manganese vapour. This produced a variation in composition along the wires, and accuracy could only be obtained by calibration under the exact conditions of the cooling-curve experiments. The method adopted was to take the cooling curve at a slow rate ($1^{\circ}\text{--}3^{\circ}/\text{min.}$) of cooling and as soon as the arrest was well established, the immersion thermocouple (see Fig. 3) was pushed down into the sheath *K*. Alternate readings were then taken from the two thermocouples, and after steady conditions had been established the immersion couple was withdrawn. In this way a direct calibration of the lower thermocouple was obtained in each experiment, and as the immersion thermocouple was recalibrated frequently, accurate results were obtained in spite of the contamination of the lower thermocouple.* The alloys melting at the lower temperatures were stirred continuously during the taking of a cooling curve. Above 1400° C., the thermocouple wires were very easily broken by the shaking resulting from the stirring of the alloy, and cooling curves were therefore taken with unstirred alloys. In view of the slow rate of cooling and pronounced nature of the thermal arrests, it is unlikely that inaccuracy was introduced by lack of stirring. The exact sequence of events in an experiment is described in the Section dealing with the determination of the solidus (p. 176).

In the earlier experiments with the apparatus of Fig. 3, chemical analysis indicated that some of the ingots contained as much as 0·4% nitrogen, although others under what appeared to be identical conditions contained only 0·04% of this element. The removal of the nitrogen proved to be extremely difficult, and after exhaustive tests it was shown that at high temperatures some of the mullite tubes were slightly permeable to nitrogen. No other material was found which would withstand the action of manganese vapour † at high temperatures,

* Experiment showed that these precautions were essential and that the ordinary method of calibrating against the gold point, used by some investigators, was not reliable with contaminated couples.

† Even with mullite tubes failure occurred after every six to ten experiments.

and the policy adopted finally was to surround the cooling-curve crucible with a cylinder of zirconium foil which absorbed most of the nitrogen before it reached the alloy; we have to thank Mr. A. R. Powell for this suggestion. At the same time the argon was purified scrupulously by passing over heated copper turnings to absorb oxygen, and then through a drying tower filled with calcium chloride. The resulting gas was passed over a heated mixture of magnesium and lime which absorbs nitrogen more rapidly than does magnesium alone, and then through a second drying tower before being admitted to the furnace. By these means the nitrogen content of the alloys was kept below 0·1%.

E. The Determination of the Solidus.

The solidus was determined by the method of heating curves, and for alloys freezing below 1500° C. the general procedure was to use an ingot previously melted in the induction furnace. This was used for a heating curve in which the solidus was approached at a rate of about 4°–6° C./min., and under these conditions a well-defined solidus arrest was obtained, the end-point of which was sufficiently sharp to give a liquidus point to within 5° C. The alloy was then slowly cooled and the liquidus point determined accurately from the thermal arrest, and as soon as the alloy was totally solid it was maintained at a temperature of about 30° C. below the melting point for a period of the order of half an hour. After this homogenization treatment a second heating curve and cooling curve were taken, and in general the arrests on the two cooling curves were in very good agreement; if any difference existed the value from the second cooling curve was preferred because any loss of manganese by volatilization meant that the analysis of the final ingot referred to the second rather than to the first cooling curve. The arrest on the second heating curve was also in surprisingly good agreement with that on the first heating curve with the unannealed ingot from the induction furnace melt, indicating that diffusion in the solid state occurs rapidly just below the melting point.

In the chromium-rich alloys the experimental difficulties became considerable as the melting point of chromium (1845° C.) was approached. Crucible failures were frequent, and some experiments also had to be abandoned because of the formation of a dendritic deposit in the alumina sighting tubes; this last trouble was probably due to slight contamination of the alumina by sodium oxide. In some cases it was necessary to determine the solidus point from the initial heating curve with the furnace-cooled ingot. This was thought justifiable because the experiments described above show clearly that the method

is reasonably accurate for the alloys of intermediate composition, and the form of the diagram is such that with increasing chromium content the liquidus and solidus are closer together so that less coring is to be expected in the furnace-cooled ingot.

In general a solidus curve determined by the method of heating curves tends to be too low because any variation in composition results in the specimen beginning to melt at a temperature lower than that corresponding to the mean composition. It was therefore necessary to check the results obtained from the heating-curve experiments by the microscopic examination of quenched ingots. For this purpose the furnace-cooled ingots were first homogenized by heating for 72 hr. at 1150°-1300° C. in an atmosphere of purified argon. Loss of manganese by volatilization was greatly reduced by placing the alloys in alumina crucibles the open ends of which were closed by flat plates of alumina tied on with tantalum wire. The crucibles were then heated in a mullite tube, one end of which was hemispherically sealed, and the other closed by a water-cooled end-piece through which the tube could be evacuated and then filled with purified argon. The mullite tube was heated in a horizontal platinum-resistance furnace, controlled by a Foster temperature regulator. For the solidus experiments small specimens of the homogenized alloys were heated for periods of 30 min. in a vertical tube furnace, the general arrangements of which are shown in Fig. 4. After trying many methods it has been found best to place the specimen in an alumina collar surrounded by zirconium foil as a safeguard against contamination by nitrogen. The specimen in its container is suspended by tantalum wire which in turn hangs from a short horizontal piece of 5-amp. fuse wire fastened to two heavy copper leads. This arrangement is similar to that of Gayler³ and at the moment of quenching the bottom of the furnace tube is opened so that on blowing the fuse the specimen falls into a bucket of water.

The first series of solidus points determined by the quenching method was made before the danger of contamination by nitrogen had been appreciated, and the points were lower than those obtained from the heating curves; in some cases the difference was as much as 30° C. Conclusive evidence was obtained that the mullite tubes were slightly permeable to nitrogen at high temperatures, and, as in the liquidus work, the nitrogen content of the alloys was reduced very considerably by the special purification of the argon and the use of the zirconium foil. As shown later (p. 184) the results obtained by the quenching and heating-curve methods were brought into agreement. Once this had been done the solidus was established by thermal analysis

alone, because with such very reactive alloys there is no doubt that the relatively small specimens used for the microscopic method are more likely to be contaminated.

F. Equilibrium in the Solid State.

For the determination of the phase boundaries of the alloys in the solid state the furnace-cooled alloys were first given the homogenization

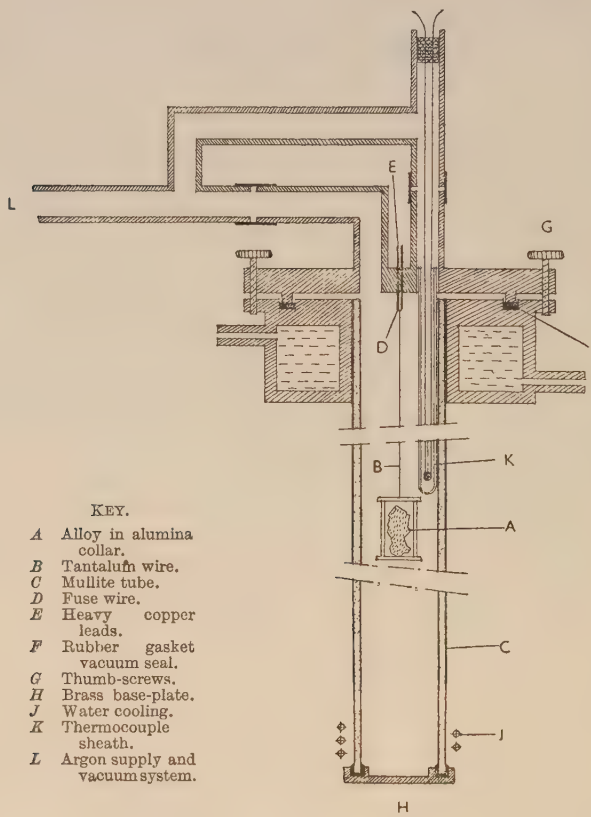


FIG. 4.—Vertical Quenching Furnace.

treatment referred to on p. 177, except that for the manganese-rich alloys a temperature of 1150° C. was used. As manganese undergoes an allotropic transformation at 720° C., it was necessary to anneal some of the alloys at comparatively low temperatures, and for this purpose the specimens were sealed in hard glass or silica tubes, and

annealed in horizontal tubular resistance furnaces controlled by Foster temperature regulators; the accuracy of the control was of the order of $\pm 2^\circ \text{C}$. At higher temperatures it was necessary to protect the alloys from contact with silica, and the specimens were placed in alumina collars contained in sealed, evacuated silica tubes. In this way it was possible to give prolonged annealing treatments at temperatures up to 1100°C ., without any contamination of the alloys, but the method failed at higher temperatures owing to a reaction between the alumina and silica. The reaction could be prevented by wrapping the alumina collar in zirconium foil, but this greatly increased the space required for each specimen and also interfered with rapid quenching. It was not found practicable to anneal in small sealed tubes above 1200°C ., owing to severe contamination by nitrogen.

The vertical tube furnace of Fig. 4 was not suitable for prolonged annealing at high temperatures because the tantalum wire failed after a few hours. The annealing experiments were therefore carried out in a horizontal platinum-wound resistance furnace, a mullite tube sealed at one end being placed in the furnace. The open end of the mullite tube projected about 6 in. from the furnace and was closed by a water-cooled end-piece through which the tube could be evacuated and filled with argon. The specimen itself was placed in an alumina collar, the ends of which were covered by flat pieces of alumina tied on by tantalum wire in order to reduce the loss of manganese by volatilization. As in the work on the liquidus and solidus, the methods for avoiding contamination by nitrogen were improved as the work progressed, and in some experiments the alumina collars were wrapped in zirconium or tantalum foil in order to absorb nitrogen.

G. Preparation for Microscopic Examination.

Alloys containing up to about 70% manganese were tough and could be sawn up, ground, and polished by the usual methods. Alloys lying outside the limits of the chromium solid solution were extremely brittle and broke into fragments on squeezing in a vice. The best results for the brittle alloys were obtained by giving the specimen a preliminary grinding on a slowly revolving emery wheel, followed by very careful hand grinding on oiled, graded emery papers. After grinding on 000 emery paper the brittle specimen was polished with a mixture of magnesia and water on a rotary wheel. The resulting sections of manganese-rich alloys always contained cracks and holes, but these did not prevent the development of the structure by etching. For alloys at the manganese end of the system the most satisfactory etching reagents were alcoholic nitric acid and alcoholic hydrochloric

acid. The chromium-rich alloys became passive in strong acids and were etched with dilute ($N/10$) aqueous hydrochloric acid.

H. X-Ray Methods.

X-ray methods were used both for the identification of phases and for the determination of some phase boundaries by the lattice-spacing technique. The manganese-rich alloys were so brittle that on grinding in an agate mortar a fine powder was obtained which gave sharply resolved $K\alpha$ doublets at the high-angle end of a Debye-Scherrer film. For this reason some of the phase-boundary measurements were made with powders prepared directly from lump specimens annealed to equilibrium at the temperatures concerned. In other cases the powder was re-annealed in an evacuated silica capillary which was quenched by plunging into water so that the capillary broke and the filings were exposed to the water. In a third series of experiments the quenching was carried out without breaking the silica capillary. The X-ray methods were the standard techniques used in this laboratory, and have been described elsewhere.⁴

J. Analysis of Alloys.

All the analytical work in the present investigation was done by Messrs. Johnson, Matthey and Company, Ltd., and the authors must express their thanks to Mr. A. R. Powell for the great skill and interest he showed in this work. In the cooling-curve work nearly all ingots were sectioned and examined microscopically, after which the entire ingot was dissolved for analysis. For the reasons described above the nitrogen contents of all the ingots referred to in Table I were determined. A small portion of insoluble residue was usually obtained, and in many cases this was analysed completely for MnO , Cr_2O_3 , SiO_2 , and Al_2O_3 . The details of the analyses are given in Appendix II (p. 194). The general effect of adding manganese to chromium was to reduce the oxide content considerably and to replace Cr_2O_3 by a much smaller amount of MnO . Thus in the alloy containing 61.33% manganese the total insoluble matter was 0.22%, and this contained MnO 0.06%, SiO_2 0.05%, Al_2O_3 0.09%. It was not possible to say how much of the alumina was a genuine constituent of the alloy, and how much was merely mechanical inclusion from the sighting tube, thermocouple sheath, or crucible. The refractories used contained no silica, and it is thought that the small amounts of silica detected in some analyses were mechanical inclusions from the grinding wheels used to remove surface layers. For the equilibrium diagram the insoluble residue was ignored, and the analytical percentages of the two metals scaled

up to 100. In the detailed tables which accompany this paper the percentages of insoluble matter are given, but the actual purity of the alloys is usually greater than the figures suggest, because accidental inclusions from refractories and grinding wheels could not be avoided.

In the alloys used for the microscopical work the analyses were carried out on the actual specimens used for microscopic examination. In all cases both chromium and manganese were determined, and with many alloys the percentages of nitrogen and insoluble material were also obtained; these details are given in Appendix III. In many cases portions of the furnace-cooled ingots were analysed after different heat-treatments and, as will be seen from the tables, the results were usually in good agreement. In the diagrams the full points always refer to alloys which were analysed after annealing at the temperature concerned, whilst for the open points the composition is that from a specimen from the same ingot annealed at another temperature. As no evidence was obtained of markedly uneven composition of the ingots, there is no reason to suppose that the compositions of the open points in the diagrams are seriously in error.

III.—THE FREEZING POINT OF CHROMIUM.

The freezing point of chromium was determined as 1845° C. for a sample which gave a horizontal arrest lasting for 12 min. Analysis of the ingot showed the presence of 0·011% nitrogen and gave a residue of 0·44% insoluble Cr_2O_3 , corresponding with 0·14% oxygen. In order to examine the effect of oxygen a further experiment was carried out using chromium which had not received hydrogen treatment. The resulting freezing point was 1836° C.; the ingot contained no nitrogen and gave a total insoluble residue of 0·70%, of which 0·64% was Cr_2O_3 , corresponding with 0·19% oxygen. From this we estimate the freezing point of pure chromium to be 1860° C.

The above figures may be compared with the value 1830° C. given by Adcock,² whose value should perhaps be increased by 10°–15° C., because it was obtained by means of an optical pyrometer calibrated against the freezing point of iron which was assumed to be 1527° C., whereas the value now accepted is 1539° C. Like the present authors, Adcock found it impossible to melt chromium free from oxygen, but he gave no analytical details of the ingot used. Some authorities consider the most accurate determination of the melting point to be the value 1890° C. obtained by Grube and Knabe.⁵ These authors used electrolytic chromium melted in hydrogen, but no preliminary deoxidizing treatment appears to have been given, and the final ingot was not analysed. It seems probable to us that the high value was

due to inaccurate pyrometry. Values given by other investigators have varied between 1500° and 1920° C., and of these the low values are undoubtedly the result of contamination by oxygen and nitrogen. From the work of Wahlin⁶ it appears probable that the high values obtained from relatively impure chromium were due to faulty corrections to allow for the fact that optical pyrometers were sighted on the surface of the metal instead of under black-body conditions. We do not discuss these figures here because none of the workers concerned gave analytical data for the ingots used.

IV.—THE LIQUIDUS AND SOLIDUS.

The thermal arrest points obtained in the determination of the liquidus and solidus are given in Table I, and are plotted in Fig. 5.

TABLE I.—*Liquidus and Solidus Experiments.*

Alloy No.	Weight-% Mn	Atomic-% Mn	Liquidus, ° C.	Solidus, ° C.
10M.	9.52	9.06	1811H.	1716H.
18M.	18.96	18.14	...	1634H.
28M.	27.90	26.81	...	1568H.
29M.	28.77	27.66	1718C.	...
43M.	42.86	41.53	1645H.; 1638C.	1479H.
61M.	61.44	60.14	1497C.	1362H.
72L.	70.94	69.80	1400C.	1313H.
73L.	72.64	71.55	1395C.	1310H.
80L.	80.60	79.73	1321C.	1284H.
84L.	82.60	81.80	1306C.	1276H.
82LA.	83.07	82.29	1301C.	1275H.
83L.	83.32	82.54	1303C.	1277H.
85LB.	86.67	86.02	1292C.	1276H.
88L.	87.75	87.15	1282C.	1268H.
92LB.	91.64	91.21	1268C.	1259H.
97L.	97.77	97.64	1252C.	1247H.
99L.	98.78	98.58	1250C.	1246H.
100L.	Pure Mn	Pure Mn	1244C.	...

Note : In this table H. and C. denote arrests on heating and cooling curves, respectively.

Owing to a failure of the refractory sighting tube, the liquidus point for alloy 9.06 * is from a heating and not from a cooling curve, but in view of the tests referred to on p. 176 we do not think it likely that any appreciable error has been introduced, because the arrest was pronounced and its end-point well marked.

There is a wide solid solution of manganese in chromium, and the liquidus and solidus curves fall smoothly with increasing manganese

* For convenience all alloys are referred to in terms of their atomic percentages of manganese.

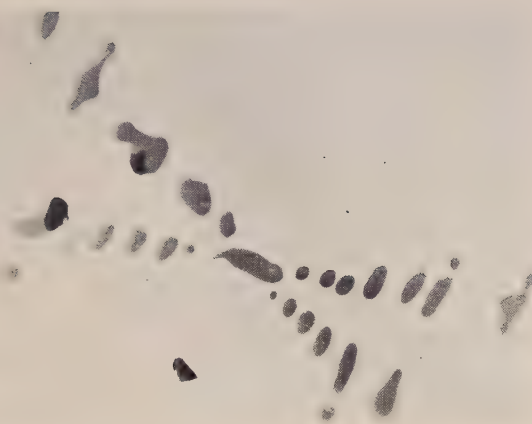


FIG. 8.—Oxide particles in alloy made from untreated chromium.
Unetched. $\times 400$.



FIG. 9.—Oxide particles in alloy made from hydrogen-treated chromium. Unetched. $\times 750$.

[To face p. 182.]

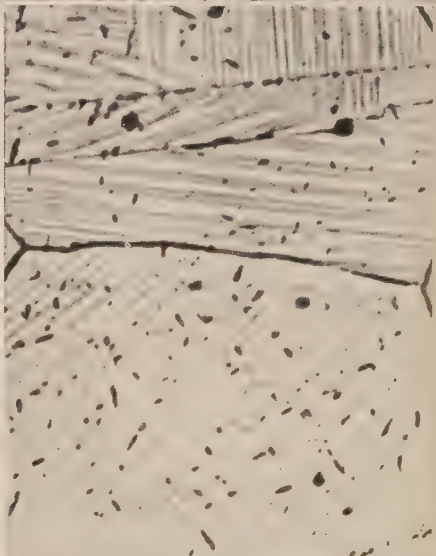
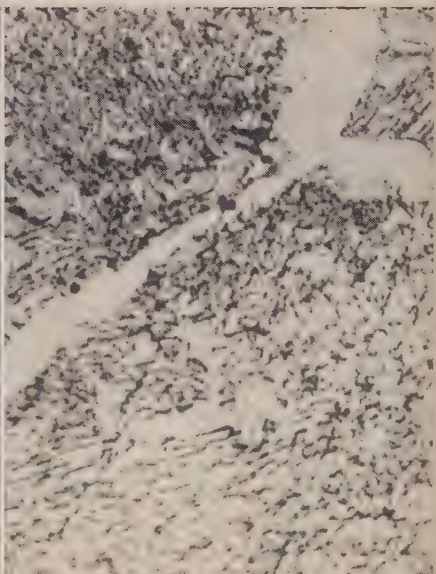


FIG. 10.—Alloy 73M (73.83 at.-% manganese) quenched from 1005° C. Etched with alcoholic hydrochloric acid. Crystals of θ in α -chromium solid solution. $\times 400$.

FIG. 11.—Alloy 88N (89.5 at.-% manganese) quenched from 1030° C. Etched with alcoholic nitric acid. Decomposed γ_{Mn} + θ . $\times 1000$.

FIG. 12.—Alloy 82L (81.8 at.-% manganese) quenched from 702° C. Etched with alcoholic nitric acid. Crystals of α_{Mn} in θ . $\times 1000$.

FIG. 13.—Alloy 92M (91.67 at.-% manganese) quenched from 1210° C. Etched with alcoholic nitric acid. γ_{Mn} phase showing twin structure. $\times 250$.

content down to 1310° C., where the solidus shows a short peritectic horizontal corresponding to the formation of the θ phase. In Fig. 5 the freezing point of chromium has been placed at the actually determined value of 1845° C., rather than at the value 1860° C. deduced as the true freezing point in the complete absence of oxygen (see p. 181).

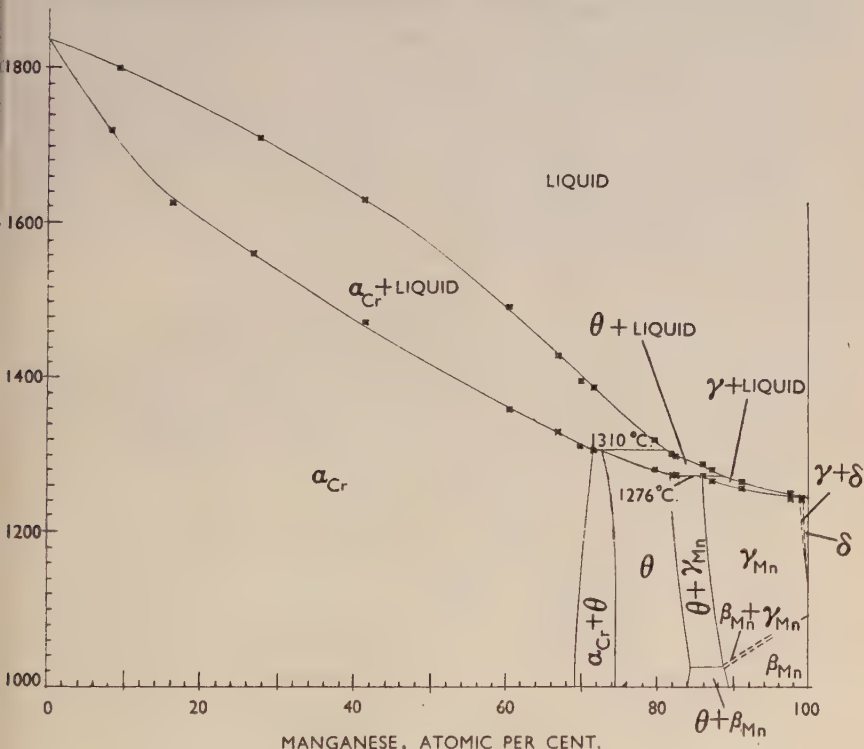
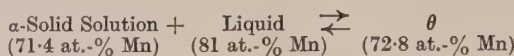


FIG. 5.—The Liquidus and Solidus.

As explained before, the addition of manganese decreased the oxygen content of the alloys, and resulted in the gradual replacement of Cr_2O_3 by MnO . This made it difficult to apply corrections for the effect of the small amounts of oxygen on the liquidus points of alloys of intermediate composition, and for this reason it was thought better to record the actual experimental results. The curve drawn in Fig. 5 may be as much as 15° C. too low at 100% chromium, but at 50% manganese the error is unlikely to exceed 5° C.

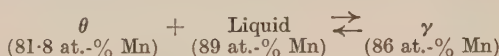
The θ phase is of variable composition and appears to be based on
VOL. LXXVI.

the formula CrMn₃. The peritectic reaction taking place at 1310° C. may be represented :



The peritectic heat of reaction appears to be very small,* and no definite arrests were obtained on cooling curves, although the microstructures of the cooling curve ingots showed the presence of both α and θ phases in the alloys concerned.

The change in direction of the liquidus at the 1310° C. peritectic point is slight, and with further increase in manganese content the curve continues to fall to 1276° C., where a second peritectic reaction occurs in which the θ phase reacts with liquid to form a solid solution of chromium in γ -manganese. The compositions of the phases taking part in this reaction are :



The horizontal portion of the solidus is thus longer than in the 1310° C. peritectic reaction, but the change in the direction of the liquidus is very slight. The latent heat of the peritectic transformation is again small * and no peritectic horizontals were present on the cooling curves, although a slight flattening of the curve after the primary arrest was noted in some of the alloys concerned.

From 1276° C. the liquidus and solidus curves continue to fall to the melting point of pure manganese (1244° C.). Alloy 98.6 gave a primary arrest at 1250° C., followed by a well-defined secondary arrest at 1246° C., indicating the presence of a peritectic reaction in which the γ phase reacts with liquid to form a solid solution of chromium in δ -manganese. There was, however, no secondary arrest on the cooling curve of alloy 97.6, and no γ/δ arrests were detected in the solid state for alloys containing more than 1 at.-% manganese, so that the solid solubility of chromium in δ -manganese is small.

The solidus points referred to above were all obtained from arrests on heating curves. In Fig. 6 the full line shows the solidus curve from Fig. 5, and the different points indicate the microstructures of the alloys after quenching from the temperatures concerned. It will be seen that the microstructures are in agreement with the results of the thermal analysis, and the latter method (p. 177) may therefore be regarded as

* The failure to detect the peritectic arrests on cooling curves may, of course, have been due to lack of diffusion preventing the reactions proceeding to an appreciable extent after the first film of the new solid phase had been formed. The homogenization experiments suggested, however, that diffusion occurs rapidly immediately below the solidus.

justified, because the alloys are those in the region of the peritectic compositions, where coring effects are likely to be greatest.

V.—THE SOLID SOLUTION OF MANGANESE IN CHROMIUM.

Annealing experiments have shown that at low temperatures the chromium-base solid solution breaks up into additional phases, and

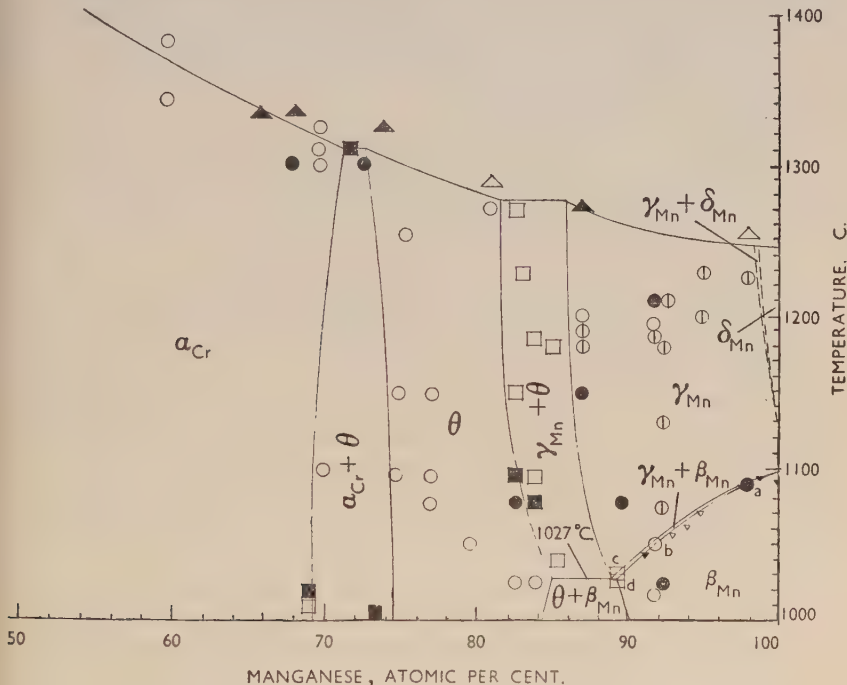


FIG. 6.—Constitution of Manganese-Rich Alloys Above 1000° C.

KEY.

- ○ Homogeneous alloys.
- Decomposed alloys.
- □ Two-phase alloys.
- ▲ △ Alloys containing chilled liquid.
- ▼ ▽ Cooling-curve arrests.

Solid points are analysed compositions.

as equilibrium is reached extremely slowly, the part of the diagram below 1000° C. is being made the subject of a separate investigation. The results obtained at the higher temperatures are shown in Fig. 6, from which it will be seen that with decreasing temperature the solubility of manganese in chromium diminishes from 71.4 at.-% at the

1310° C. peritectic horizontal to 69 at.-% at 1000° C. In these experiments the alloys were given the preliminary homogenization treatment referred to on p. 177, followed by annealing for 24–100 hr. at the lower temperatures; the exact annealing times are given in Appendix III. The chromium-base solid solution is hard and tough, in marked contrast to the θ phase and the solid solutions in α - and β -manganese. In the region of 40 at.-% manganese the chromium-base solid solution has an extraordinary affinity for nitrogen, and on prolonged annealing some alloys were converted entirely into a white nitride phase even though the pressure of nitrogen was very small; this phenomenon is described in a separate paper.¹²

Owing to the formation of new phases at low temperatures the lattice spacings of the solid solution in chromium were not determined in detail. The lattice spacing of pure chromium was determined as 2.8791 kX., whilst that of alloy 37.8 was 2.8832 kX.

VI.—THE θ PHASE.

The limits of composition of the θ phase above 1000° C. are shown in Fig. 6, whilst Fig. 7 shows the diagram from 60–100% manganese at lower temperatures. The θ phase is brittle and is of variable composition, and the furnace-cooled ingots show a cored structure which is removed by annealing at high temperatures. The $(\alpha + \theta)$ phase field is narrow, and the $(\alpha + \theta)/\theta$ boundary curves so as to make the two-phase region more restricted at high and at low temperatures. Fig. 10 (Plate XXI) shows the structure of a typical two-phase $(\alpha + \theta)$ alloy after quenching from 1005° C.

On the manganese side of the θ -phase region, the $(\theta + \gamma\text{-Mn})$ field is narrow, and in alloys quenched from this region it was impossible to retain the γ -manganese phase undecomposed. Fig. 11 (Plate XXI) shows the structure of alloy 89.5 after quenching from 1030° C.; the structure consists mainly of decomposed γ with θ in the grain boundaries. At lower temperatures, where the θ phase exists in equilibrium with β - or α -manganese, the two-phase fields are much wider. Fig. 12 (Plate XXI) shows the structure of alloy 81.8 after quenching from 702° C., and here crystals of α -manganese are clearly apparent in a ground-mass of the θ phase. For the determination of the equilibrium diagram in the region of the θ phase, the furnace-cooled ingots were given a homogenization treatment of 72 hr. at 1150° C., and then re-annealed for periods varying from 24 hr. at the higher temperatures to 4 weeks at 552° C. All alloys were quenched after the final annealing, but it was not desirable to quench after the homogenization treatment because the brittle nature of the alloys resulted in the penetration of

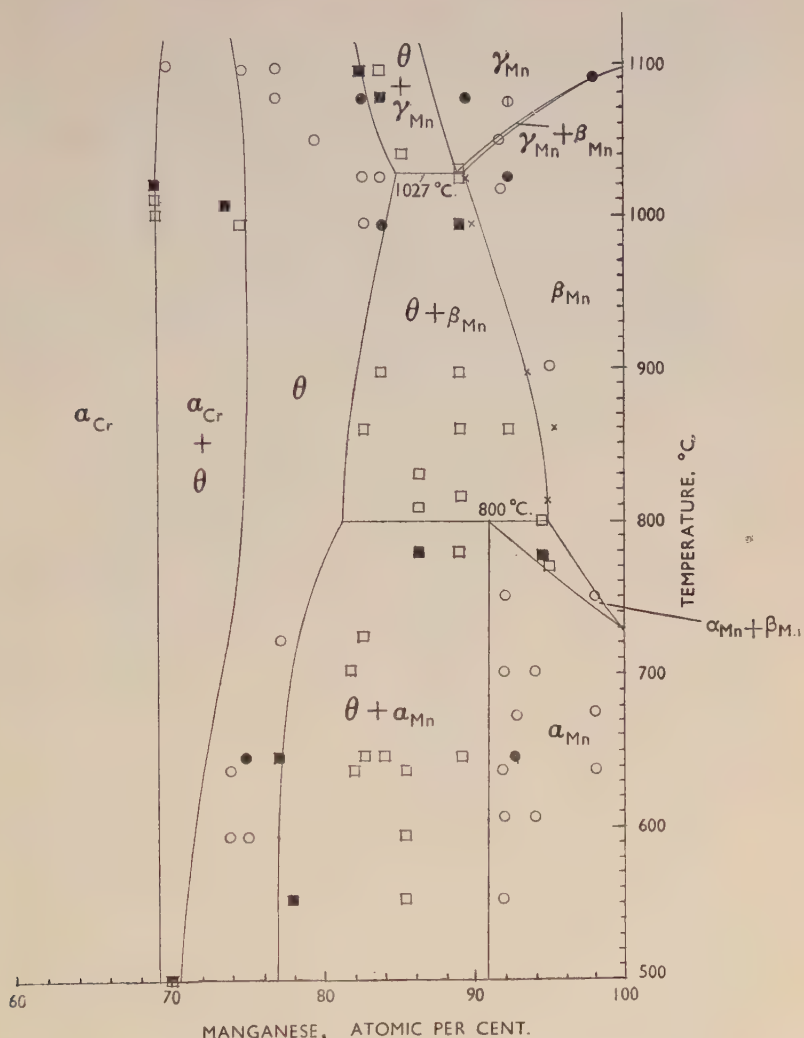


FIG. 7.—Constitution of Manganese-Rich Alloys Below 1100° C.

KEY.

- ○ Homogeneous alloys.
- □ Decomposed alloys.
- □ Two-phase alloys.
- × Phase boundary from lattice parameter.

Solid points are analysed compositions.

cracks by water, so that corrosion occurred and oxygen was introduced on further annealing. The details of the annealing treatments and the full analyses are given in Appendix III.

The θ phase gives rise to a complex diffraction pattern which does not appear to be that of a cubic structure. Table II gives the angles of the lines on a Debye-Scherrer film for chromium radiation.

TABLE II.—*Debye-Scherrer Powder Photograph of Alloy 77N (Homogeneous θ Phase.)*

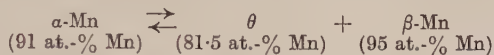
Unfiltered Cr radiation was used for these photographs, but nearly all the lines listed below are believed to be α lines. Resolved α_1 , α_2 doublets are bracketed together. The lines have been roughly classified by visual observation as strong (s.), medium-strong (ms.), medium (m.), and weak (w.). The addition of the letter d indicates that the line was diffuse.

Line	Bragg Angle	Line	Bragg Angle
ms.	77.186° } α_2	Several vvw. unmeasurable lines, probably β lines)	
s.	76.723° } α_1	w. 59.159°	
w.	76.036°	(Several vvw. lines)	
w.	75.424° } α_2	m. 40.458°	
w.	75.137° } α_1	w. 38.520°	
w.	73.329°	s. 37.332°	
m.	71.677° } α_2	s. 36.645°	
ms.	71.368° } α_1	s. 35.532°	
ms.	70.498°	ms. 34.202°	
ms.	70.294°	s. 33.591°	
s.	68.812°	s. 32.475°	
wd.	68.248°	w. 31.978°	
msd.	67.366°	w. 31.042°	
wd.	66.884°	m. 30.254°	
s.	66.190°	w. 29.286°	
w.	64.851°		

VII.—THE SOLID SOLUTIONS IN THE ALLOTROPIC FORMS OF MANGANESE.

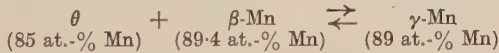
Manganese exists in four allotropic forms, all of which can take limited amounts of chromium into solid solution. The low-temperature modification, α -manganese, has a complex crystal structure and is stable up to 727° C., at which temperature it changes into β -manganese which also has a complicated crystal structure. The $\alpha \rightleftharpoons \beta$ transformation shows marked temperature hysteresis, and the true equilibrium temperature cannot be determined by heating or cooling curves. The temperature 727° C. is given by Potter and Lukens⁷ as the most probable value, and is based on (a) the heat-content curves for manganese at high temperatures, and (b) the solubility of hydrogen in manganese at different temperatures. α -Manganese is able to dissolve almost

10 at.-% chromium, and as will be seen from Fig. 7 the temperature of the $\alpha \rightleftharpoons \beta$ transformation is raised by the addition of chromium. At 800° C. the solid solution in α -manganese undergoes a peritectoid transformation into a solid solution in β -manganese and the θ phase. The compositions of the phases concerned are :



In pure manganese the β modification is stable between 727° C. and about 1095° C., at which temperature it changes into γ -manganese, which has a face-centred tetragonal structure. The $\beta \rightleftharpoons \gamma$ transformation does not show appreciable temperature hysteresis, and in the present work the transformation temperature was determined as 1091° C., in agreement with the results of Dean and his collaborators,⁸ whose values were $1092^\circ \pm 3^\circ$ C. on a heating curve and $1090^\circ \pm 3^\circ$ C. on a cooling curve. The good agreement between the results of heating and cooling curves suggests that true equilibrium is established, because it is difficult to see how a heating curve could give too low a value. On the other hand Naylor⁹ obtained a value of $1101^\circ \pm 5^\circ$ C. by the heat-content method, and Potter and Lukens⁷ one of $1099^\circ \pm 3^\circ$ C. by the method based on the solubility of hydrogen. They considered these values to be more probable because the metal was maintained for a longer period at the temperatures concerned. These methods are, however, indirect, and we consider that the results obtained by thermal analysis should be given at least an equal weight, and have therefore taken the most probable value to be 1095° C.

As will be seen from Fig. 6, the temperature of the $\beta \rightleftharpoons \gamma$ transformation is lowered by the addition of chromium, until at 1027° C. there is a eutectoid horizontal corresponding to the reaction :



The β/γ line was determined by microscopic methods, the critical alloys being marked *a*, *b*, *c*, and *d* in Fig. 6. The two-phase ($\beta + \gamma$) field was too narrow for direct observation and has been inserted from theoretical considerations. As will be seen from Fig. 7, the addition of chromium resulted in the β/γ arrests on cooling curves becoming slightly lower than the values determined by microscopic methods.

The solubility of chromium in β -manganese is at a maximum at the 1027° C. eutectoid, and the $\theta + \beta_{\text{Mn}}/\beta_{\text{Mn}}$ solubility curve was determined by a combination of microscopic and X-ray methods. The lattice-spacing data are given in Table III, and the solubility points which they indicate are shown in Fig. 7. The points lie on a smooth

TABLE III.—*Lattice Spacings of the Solid Solution of Chromium in β-Manganese.*

Alloy	Wt.-% Mn	Wt.-% Cr	Total Mn + Cr	Wt.-% N₂	At.-% Cr	Lattice Spacing, kX.
Pure Mn	99.98	Nil	...	6.3018
98 Mn	97.96	2.02	99.98	...	2.13	6.2958
95M.	94.91	5.17	100.08	...	5.44	6.2921
93N.	92.70	7.30	100.00	0.05	7.68	6.2902

Two-Phase Alloys.

Alloy	Temperature, ° C.	Lattice Spacing, kX.
93N.	816	6.2924
88N.	812	6.2922
88N.	994	6.2883
88N.	897	6.2913
88N.	1025	6.2877
89L.	1020	6.2876
88N.	860	6.2939(?)

curve agreeing with the microstructures except for one point which is clearly incorrect. It is thought that this was the result of faulty quenching, because the tube containing the alloy did not break on entering the quenching water.

The γ -modification of manganese is stable between 1095° C. and 1133° C. in pure manganese. It has a face-centred tetragonal structure with $a = 3.774$ kX. and $c/a = 0.938$, but recent investigations have shown that in many alloy systems the solid solution in γ -manganese gradually becomes cubic with increasing percentage of the alloying element. In the present work it was found extremely difficult to retain the γ phase by quenching, and brittle decomposed structures were usually obtained. Two alloys, however, were quenched so as to consist mainly of the homogeneous γ phase, and Fig. 13 (Plate XXI) shows the microstructure of such an alloy. The beginning of decomposition can be seen in the grain boundaries and mass of the grain, and there is a well-developed twin structure consisting of some large twins and a large number of fine twins. A very similar structure has recently been reported by Worrell¹⁰ in a copper-manganese alloy and has led Zener¹¹ to suggest that γ -manganese may really be cubic. Worrell analysed his photomicrographs using a stereographic net and was able to show they were all consistent with the assumption that the large twins were {111} and the fine twins {110}. A full analysis has not been

carried out in the present work, but although for some grains agreement with the hypothesis was found, in others no fit seemed possible.

Pure manganese is now thought to undergo a transformation at 1133° C., into a further modification δ -manganese. This modification has never been isolated, and the evidence for its existence is that well-defined thermal arrests are found on heating and cooling curves, and are supported by the heat-content and hydrogen-solubility data. In the present work the $\gamma \rightleftharpoons \delta$ transformation was determined as 1133° C. on heating curves and 1132° C. on cooling curves, in good agreement with the values 1133° and 1134° C., given by the U.S. Bureau of Mines⁸ for heating and cooling curves, respectively. The methods of heat content and hydrogen solubility gives values of $1137^\circ \pm 5^\circ$ C., and $1138^\circ \pm 3^\circ$ C., respectively, and are thus again slightly higher. As explained on p. 184, the cooling curve of alloy 98·6 showed a primary arrest followed by a secondary arrest at 1246° C., i.e. higher than the melting point of manganese, whereas the curve for alloy 97·6 showed one arrest only. It follows, therefore, that the temperature of the $\gamma \rightleftharpoons \delta$ transformation is markedly raised by very small amounts of chromium, and the homogeneous δ phase field is extremely narrow.

VIII.—LATTICE-SPACING RESULTS.

Owing to the formation of one or more intermediate phases at low temperatures the lattice spacings of the primary solid solution of manganese in chromium were not determined. The lattice spacing of pure chromium was found to be 2·8791 kX. at 25° C., while an alloy containing 37·81% manganese had a spacing of 2·8832 kX. at the same temperature. The parameters were calculated from Debye-Scherrer powder photographs, using chromium radiation, and standard extrapolation methods were employed. The lattice parameter of pure α -manganese was found to be 8·894 kX., in good agreement with previous workers' results. Addition of chromium decreases this lattice spacing, and an alloy with 7·5% chromium had a spacing of 8·888 kX.

Pure β -manganese was found to have a spacing of 6·3018 kX. at 25° C., and this value is slightly higher than the value 6·300 kX. usually given in the literature. The spacings of the β -manganese solid solution are given in Table III.

IX.—DISCUSSION.

The equilibrium diagram of Figs. 6 and 7 shows that the solubility limit of chromium in the α , β , and γ forms of manganese is approximately the same, and is much less than the solubility of manganese in chromium. In the case of the α - and β -manganese modifications

the solubility (in atomic per cent.) is about one-third that of iron, and this suggests that these complex crystal structures are disturbed less by a slight excess of $3d$ and $4s$ electrons than by a slight deficiency. Except for binary alloys with the neighbouring elements iron and chromium, the range of composition of the α -manganese phase always appears to be small; the solubility range of the β -manganese phase increases still further, however, in alloys of manganese with cobalt. The factors affecting the stability of the different manganese phases will be discussed more fully in another paper.

The existence of the intermediate θ phase, stable up to the solidus, is rather unexpected in view of the similar size-factors and electron characteristics of the two metals. The position and extent of the phase field, and the X-ray diffraction data indicate that the θ phase is not related to the various isomorphous intermediate phases of the σ (iron-chromium) type.

ACKNOWLEDGEMENTS.

The authors must express their gratitude to Sir Cyril Hinshelwood, F.R.S., for laboratory accommodation, and to Dr. F. M. Brewer for many other facilities which have greatly encouraged the present research.

THE INORGANIC CHEMISTRY LABORATORY,
THE UNIVERSITY MUSEUM,
OXFORD.

APPENDIX I.

PREPARATION OF THE ALLOYS.

The first alloys were prepared in a spark-gap induction furnace at the National Physical Laboratory as explained on p. 170, but apart from minor details the method was identical with that used at Oxford, where a valve-operated generator was used. The apparatus used was the same as that shown in Fig. 1, except for the alumina sighting-tube arrangement which was replaced by a glass window so that the surface of the metal charge could be observed. All the alloys were melted in recrystallized alumina crucibles, and for the alloys of high chromium content the crucibles had a lining of thoria. No molybdenum heating sleeve was employed, so that the vigorous stirring action of the eddy currents thoroughly mixed the two metals.

As explained on p. 170, the chromium and manganese were both given a preliminary deoxidizing treatment in the induction furnace, and this also served to remove the large quantities of hydrogen present in the electrolytic metals. For the preparation of the alloys the

refractory materials were first out-gassed by intermittent heating with the generator on minimum power until the charge was bright red and no further gases were evolved. The furnace tube was evacuated by a Metro-Vickers O2 oil-diffusion pump backed by a two-stage DR1 rotary pump; during the first stages of the degassing glow discharges were produced inside the silica furnace tube by the action of the H.F. currents.

It was not possible to melt the alloys *in vacuo* owing to the violent discharges produced by the metal vapour present above about 800° C. Purified hydrogen was admitted through the top inlet tube and the conditions adjusted so that a slight stream of hydrogen was drawn through the tube while the pressure remained constant at about two-thirds of an atmosphere. The power was quickly raised until the alloy could be seen to be molten, after which it was reduced slightly to avoid overheating and loss of manganese. The alloy was maintained liquid for a period varying from 10 min. to $\frac{1}{2}$ hr., and it was solidified and remelted two or three times at intervals. Finally, the hydrogen was pumped away until the pressure reached about 10 cm. of mercury, at which stage the generator was switched off and the remainder of the hydrogen pumped off. This procedure usually produced a sound ingot free from the large blow-holes which were obtained if the alloy was allowed to solidify completely before pumping off the hydrogen.

In most cases the crucible had to be broken before the ingot could be extracted, but occasionally a crucible was used a second time. Loss of manganese by volatilization amounted to up to 10 g. in a 60-g. ingot, and it was therefore difficult to prepare alloys of a given composition, particularly in the chromium-rich region.

The generator used was a valve oscillator of the Colpitts type and had a maximum output power of 5 kW., the frequency of the oscillations being 800 kc./sec. The water-cooled work coil of the generator was made of slightly flattened $\frac{1}{4}$ -in. dia. copper tubing, wound into a coil about $3\frac{1}{2}$ in. in dia. and 12 in. long, and was situated concentric with and outside the centre portion of the silica furnace tube. The power output from the generator could be smoothly adjusted over a wide range, and the frequency was sufficiently high to heat efficiently even finely divided charges. This was not the case with the spark-gap generator used in the early work, and "bridging" difficulties were often encountered in preparing the first alloys.

APPENDIX II.

TABLE IV.—*Detailed Analyses of Alloys in Table I.*

No. of Alloy	Wt.-% Mn	Wt.-% Cr	Nitrogen	Cr ₂ O ₃	MnO	Al ₂ O ₃	SiO ₂	Total Insoluble
Cr H ₂ -treated	0.011	0.44
Cr untreated	Nil	0.64	0.70
10M.	9.48	90.08	0.006	0.14	0.17	...	0.10	0.42
18M.	18.89	80.72	0.012	0.10	0.08	...	0.16	0.33
28M.	27.77	71.76	Nil	0.03	0.23	...	0.10	0.37
29M.	28.74	71.15	Nil	Trace	0.06	...	0.05	0.12
43M.	42.83	57.09	0.018	0.01	0.04	0.05	0.04	0.14
61M.	61.33	38.49	0.024	...	0.06	0.09	0.05	0.22
72L.	70.96	29.07	0.048
73L.	72.47	27.29	0.018	0.21
80L.	80.50	19.37	0.15	0.08
84L.	82.36	17.35	0.06	0.13
82LA.	82.82	16.88	0.09	0.11
83L.	83.15	16.64	0.094	0.11
85LB.	86.54	13.31	0.006	0.11
88L.	87.66	12.24	Nil	0.04
92LB.	91.60	8.36	0.042
97L.	97.69	2.23	0.08	0.10
99L.	...	1.21	0.05	0.04

APPENDIX III.

DETAILS OF ANALYSES AND HEAT-TREATMENT OF ALLOYS.

These details have, with the authors' agreement, been deposited in the Library of the Institute and are available for consultation by those interested.

REFERENCES.

1. L. Pauling, *Phys. Rev.*, 1938, [ii], **54**, 899.
2. F. Adcock, *J. Iron Steel Inst.*, 1926, **114**, 117 P.; 1931, **124**, 99 P.
3. M. L. V. Gayler, *J. Iron Steel Inst.*, 1933, **128**, 293 P.
4. H. J. Axon and W. Hume-Rothery, *Proc. Roy. Soc.*, 1948, [A], **193**, 1.
5. G. Grube and R. Knabe, *Z. Elektrochem.*, 1936, **42**, 793.
6. H. B. Wahlin, *Phys. Rev.*, 1948, [ii], **73**, 1459.
7. E. V. Potter and H. C. Lukens, *Trans. Amer. Inst. Min. Met. Eng.*, 1947, **171**, 401.
8. R. S. Dean, J. R. Long, T. R. Graham, E. V. Potter, and E. T. Hayes, *Trans. Amer. Soc. Metals*, 1945, **34**, 443.
9. B. F. Naylor, *J. Chem. Physics*, 1945, **13**, 329.
10. F. T. Worrell, *J. Appl. Physics*, 1948, **19**, 929.
11. C. Zener, "Elasticity and Anelasticity of Metals", p. 162. Chicago : 1948.
12. S. J. Carlile and W. Hume-Rothery, *J. Inst. Metals*, this vol., p. 195.

A NOTE ON THE EFFECT OF NITROGEN **1215** ON THE STRUCTURES OF CERTAIN ALLOYS OF CHROMIUM AND MANGANESE, AND ON THE EXISTENCE OF AN INTER- MEDIATE NITRIDE PHASE.*

By S. J. CARLILE,† B.A., and W. HUME-ROTHERY,‡ M.A., D.Sc.,
F.R.S., MEMBER.

SYNOPSIS.

Chromium-manganese alloys absorb nitrogen readily at high temperatures, and in the range 20-65 wt.-% manganese a white nitride phase is formed even though the pressure of nitrogen is very low. Experiments are described in which, when alloys were annealed above 1000° C. in mullite tubes filled with argon, the nitride phase was formed as a result of a very slight permeability of the mullite to nitrogen. Photomicrographs of the growth of the nitride phase and the development of acicular structures are shown. A powder X-ray diffraction photograph suggests that the white phase is a new substance, possibly of the formula $(\text{CrMn})_3\text{N}$, and is not one of the previously known chromium nitrides.

I.—INTRODUCTION.

In another paper¹ experimental work on the equilibrium diagram of the system chromium-manganese is described, and reference is made to the extreme readiness with which these alloys absorb nitrogen. In the present note a description is given of the range of alloys in which contamination by nitrogen at low pressure may result in the production of a non-metallic nitride phase.

At temperatures above 1000° C. the equilibrium diagram of the system chromium-manganese shows the existence of (1) a wide solid solution of manganese in chromium extending to about 70% manganese, (2) an intermediate phase denoted θ in the region 75-80% manganese, and (3) considerable solid solutions based on the β and γ modifications of manganese. All the alloys absorb nitrogen readily at high temperatures, but the effects described below were observed only in the region 20-65% manganese.

II.—PREPARATION AND MICROSTRUCTURES OF ALLOYS.

The alloys described in the present work were prepared from the purest electrolytic chromium, which was further purified by treatment

* Manuscript received 3 August 1949.

† Lecturer in Physics, Huddersfield Technical College.

‡ Royal Society Warren Research Fellow, Oxford.

for 6 hr. at 1400° C. in a very slow stream of hydrogen. By this means the oxide content of the chromium was reduced to amounts which varied from 0·08 to 0·4% (these figures refer to total "insoluble material"), and on alloying with manganese the oxide content diminished still further owing to reduction of chromic oxide by manganese. The manganese used was electrolytic metal which had been heated in hydrogen in order to remove superficial oxidation.

Alloys in the range 0–70 wt.-% manganese were prepared by melting the constituent metals in thoria-lined A.R.R. alumina crucibles in an H.-F. induction furnace using an atmosphere of hydrogen at 2/3 atmospheric pressure.* After thorough melting, the power was cut off, and as soon as the alloy was solid the hydrogen was pumped away and the alloy allowed to cool *in vacuo*. The furnace-cooled ingots in the above range of composition showed the normal cored structure of a solid solution, and in a few cases occasional white particles were present in the manganese-rich areas. Fig. 1 (Plate XXII) shows the structures of alloy 47 † in the furnace-cooled state, and fine, small, white crystals are apparent in the darkly etched areas. From what follows it is clear that the white crystals are a nitride phase, although chemical analysis showed that the nitrogen contents of the furnace-cooled alloys were very low, the actual figures varying from an amount too small to be detected analytically to a maximum of 0·08%.

For the determination of the equilibrium diagram, portions of the furnace-cooled ingots were homogenized by heating at 1300° C. in a closed mullite tube, using an atmosphere of argon which had been purified by passing over a mixture of magnesium turnings and lime at red heat. After this treatment samples were annealed for further periods above 1000° C. in a closed mullite tube heated in either a horizontal or vertical platinum-wound resistance furnace; in the latter case the specimen was suspended by a tantalum wire. Microscopic examination showed that as the annealing progressed, particles of a white constituent were gradually formed. Fig. 2 (Plate XXII) shows this effect for alloy 42 after annealing for 48 hr. at 1185° C. It was at first thought that this indicated the gradual formation of a superlattice or of an intermediate phase analogous to that of the σ phase in the iron-chromium alloys, since alloy 35, after annealing under different conditions (see below) for 353 hr. at 1025° C., was

* The furnace system was thoroughly degassed before the hydrogen was admitted.

† For convenience the alloys are referred to in terms of the weight percentages of manganese, and as the compositions are not critical the nearest whole number is used. Alloy 47 is thus an alloy containing 47 wt.-% manganese.

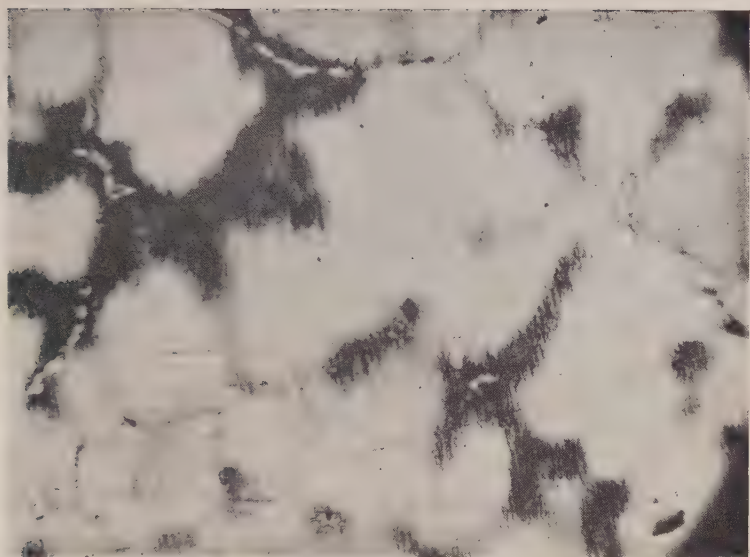


FIG. 1.—Alloy No. 47. Furnace-cooled. Cored solid solution with traces of nitride phase. $\times 500$.

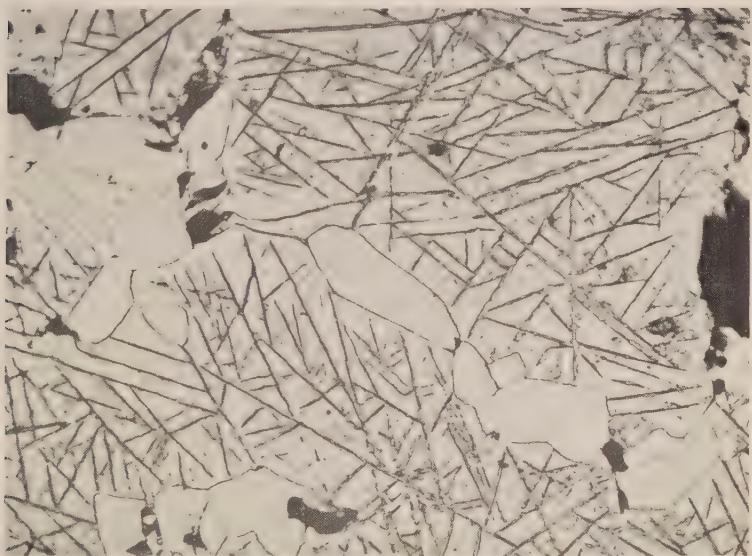


FIG. 2. —Alloy No. 42. Annealed for 48 hr. at 1185° C. and quenched in water. White particles of nitride phase forming in acicular solid solution. $\times 400$.

Both etched in $N/10$ aqueous HCl.

[To face p. 198.]

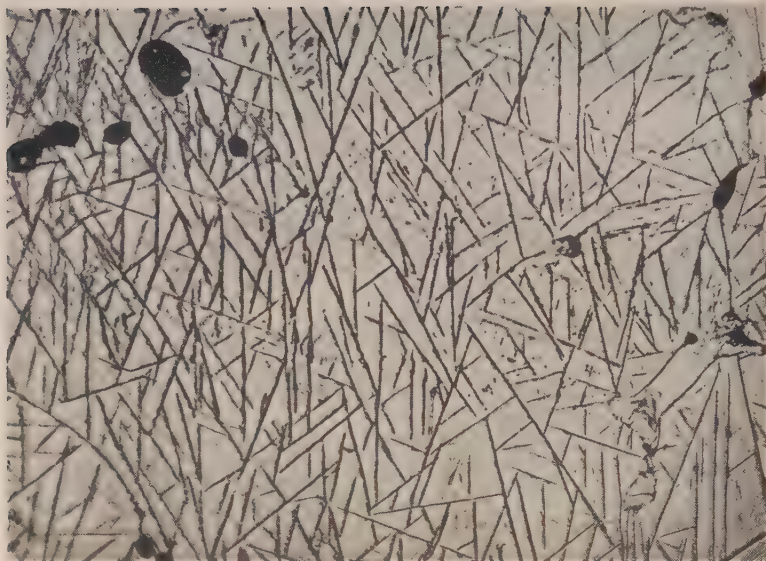


FIG. 3.—Alloy No. 39. Annealed for 30 min. at 1461° C. and quenched in water.
Fine acicular structure. $\times 350$.

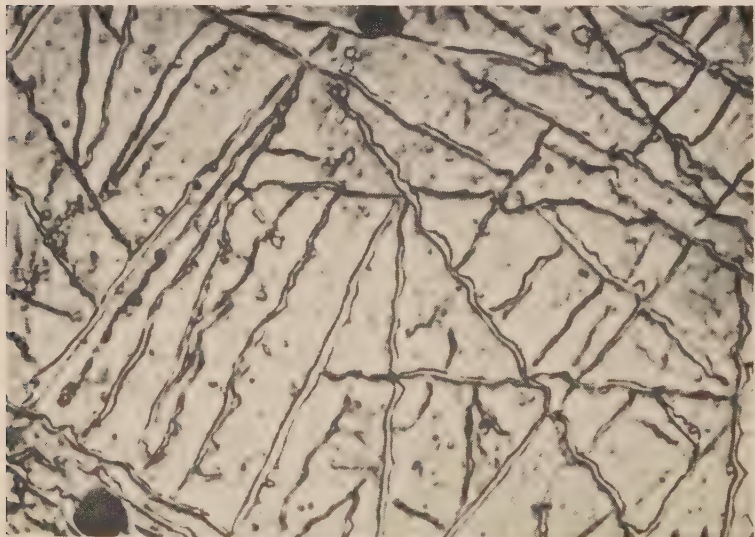


FIG. 4.—Alloy No. 44. Annealed for 24 hr. at 1200° C. and quenched in water.
Acicular structure. $\times 1000$.

Both etched in $N/10$ aqueous HCl.

entirely converted to a hard, brittle, white phase. At the same time acicular structures were frequently observed in the annealed and quenched alloys. Examples of these are shown in Fig. 3 (Plate XXIII) for alloy 39 after annealing at 1461° C. for 30 min. and quenching in water. In some alloys the micro-sections showed merely fine acicular markings, but in others the "needles"^{*} were very much thicker and their constituent material had the same etching characteristics as the white particles in Fig. 2. Fig. 4 (Plate XXIII) shows the structure of alloy 44 after annealing for 24 hr. at 1200° C. These acicular markings suggested that contamination by nitrogen was occurring during the annealing experiments, and this was confirmed by chemical analysis. As explained in the previous paper,¹ a careful investigation showed that the mullite tubes were very slightly permeable to nitrogen at high temperatures, and the affinity of the alloys for nitrogen appears to be so great that in spite of the use of an atmosphere of argon, a gradual absorption of nitrogen by the specimen took place during the annealing treatment. The correctness of this interpretation was shown by the fact that when specimens were annealed in sealed silica capsules at a temperature of 1000° C. the amount of the white constituent did not increase beyond that of the original furnace-cooled ingot. It is to be noted, however, that at higher temperatures silica itself becomes slightly permeable by nitrogen.

III.—THE COMPOSITION AND CHARACTERISTICS OF THE NITRIDE PHASE.

As explained above, the continued annealing of alloy 35 resulted in a gradual absorption of nitrogen until the entire specimen was converted into the white nitride phase.

		<i>A</i>	<i>B</i>
Chromium	.	63.38	65.97
Manganese	.	33.55	22.67
Nitrogen	.	3.15	8.10
Insoluble Cr ₂ O ₃	3.44 = 1.08% oxygen
		100.08	100.18

A specimen annealed for 360 hr. at 1000° C. in a sealed mullite tube containing argon gave the results shown in column *A* above, which clearly indicate a considerable absorption of nitrogen. The micro-structure of the specimen showed the presence of both the white phase and of the chromium-base solid solution, and the experiment was made

* The needles are, of course, really the intersections of thin plates with the plane of the specimen.

at a late period in the research with full precautions of vacuum technique, purification of argon, and sealing of the tube. Slight permeability of the mullite tube to nitrogen appears to be the only way by which the absorption of nitrogen could have occurred, and the figures show that the white phase does not contain oxygen.

In the earlier stages of the work another portion of alloy 35 was annealed for 186 hr. at 1025° C. in a silica tube which was evacuated with a water pump and then sealed. The resulting structure showed both the white phase and the chromium-base solid solution. A portion of the specimen was re-annealed for a further period of 167 hr. at 1025° C., after which the interior of the alloy consisted entirely of the white phase, while the exterior was covered with a thin greenish layer. As much as possible of this layer was removed, and the analysis of the remaining small pieces of the alloy gave the results shown in column *B* above. These anneals were done before the vacuum technique had been improved, and it is possible that a little air may have leaked into the tube during the experiment; alternatively, the oxide content may have been the result of annealing a specimen which had previously been quenched.* The decrease in the manganese content of the main bulk of the alloy suggests that some manganese was lost by volatilization, and that the surface layer contained more manganese oxide than would be expected from the original composition of the alloy.† The figures in column *A* suggest strongly that under the conditions of the experiment the alloy is attacked by nitrogen rather than by oxygen because it is improbable that the mullite tube would have been permeable to nitrogen and not to oxygen. If, therefore we regard the 3·44% of insoluble Cr₂O₃ in column *B* as associated with the surface layer,‡ the remaining percentages of chromium, manganese, and nitrogen are equivalent to a formula Cr_{56·1}Mn_{18·3}N_{25·6}, or approximately (CrMn)₃N.

A Debye-Scherrer photograph was taken of the brittle white substance of column *B*, and Table I gives the angles and visually estimated intensities of the diffraction lines, which do not appear to be those of a cubic lattice, and are not those of the chromium nitrides whose diffraction patterns have been described by Blix.²

The atom of manganese is larger than that of chromium, so that if phases of the form (CrMn)₂N or (CrMn)N were produced we should expect their lattice spacings to be greater, and hence their diffraction

* With brittle manganese-rich alloys it was found that when a specimen had been quenched in water, it could not be re-annealed without introducing oxygen.

† The difference between the figures in columns *A* and *B* cannot be reconciled with a mere volatilization of manganese.

‡ The brittle nature of the alloy would prevent a complete removal of the surface.

lines to be at smaller angles than those for the pure chromium nitride phases. As will be seen from Table I, the white phase gives two strong lines at $33\cdot85^\circ$ and $34\cdot43^\circ$, while Cr_2N and CrN give no strong or medium

TABLE I.—*X-Ray Diffraction Lines Given by Cr_2N , CrN , and the Nitride Phase Present in the Cr-Mn System (Cr Radiation.)*

Nitride Phase in System Cr-Mn		Cr_2N		CrN	
Angle	Intensity	Angle	Intensity	Angle	Intensity
26·67	Very weak	26	Very weak	26·8	Weak
28·66	Weak	28	Very weak	28·7	Strong
29·52	Medium	28·7	Medium	30·3	Medium
30·51	Medium	29·7	Medium	33·6	Strong
30·99	Weak	31·0	Medium	45·3	Weak
31·77	Medium	32·8	Strong	52·4	Very strong
33·85	Strong	40·0	Weak	56·5	Very weak
34·43	Strong	44·8	Medium	60·5	Very weak
41·14	Very weak	49·2	Weak	66·1} α_1	
45·79	Medium	56·5	Weak	66·4} α_2	Strong
50·41	Very weak	56·6	Strong	73·0} α_1	
52·69	Medium	63·1	Weak	73·3} α_2	Strong
57·35	Weak	65·8	Strong		
57·84	Strong	74·0} α_1	Weak		
62·31	Weak	74·2} α_2			
64·83	Weak	78·5} α_1			
67·37	Strong	78·8} α_2	Strong		
76·25	Strong				
83	Medium *				

* Very diffuse.

NOTE: The data for the X-ray diffraction patterns of the phases Cr_2N and CrN are those given by Blix.²

lines between $33\cdot6^\circ$ and $44\cdot8^\circ$. The diffraction pattern for the white phase does not indicate the presence of Cr_2O_3 or of MnO , and it appears that the phase is a new substance.

IV.—CONCLUSION.

The work described above shows conclusively that the chromium-manganese alloys concerned possess an extraordinary affinity for nitrogen, and that even though the pressure of nitrogen is extremely low they may be entirely converted into a nitride phase which is not chromium nitride. It is feared that this characteristic will prevent alloys with a chromium-manganese base from being suitable for use at high temperatures.

ACKNOWLEDGEMENT.

The authors must express their thanks to Professor Sir Cyril Hinshelwood, F.R.S., for laboratory accommodation and many other facilities which have greatly encouraged the present work.

THE INORGANIC CHEMISTRY LABORATORY,
THE UNIVERSITY MUSEUM, OXFORD.

REFERENCES.

1. S. J. Carlile, J. W. Christian, and W. Hume-Rothery, *J. Inst. Metals*, this vol., p. 169.
2. F. Blix, *Z. physikal. Chem.*, 1929, [B], 3, 229.

OVERHEATING PHENOMENA IN ALUMINIUM- 1216 COPPER-MAGNESIUM-SILICON ALLOYS OF THE DURALUMIN TYPE.*

By J. CROWTHER,† M.Sc., F.I.M., MEMBER.

SYNOPSIS.

The incidence of quench-cracking in components made from aluminium alloy sheet to the aircraft specification D.T.D. 610B led to an examination of the dependence on chemical composition of the effective solidus temperature of alloys of this general type. Overheating was assessed by the appearance of quench-cracking and reduced ductility in tensile specimens and of quenched liquid in microsections of a series of experimental alloys covering a wide range of silicon and magnesium contents, and was related to the solidus of the alloys as given by thermal arrests on heating.

The aluminium corner of the quaternary aluminium-copper-magnesium-silicon system was examined at a constant 4% copper content, and the solidus was found to correspond closely with that of the more complex alloys. The solidus was characterized by three invariant planes: the eutectics $\text{Al} + \text{CuAl}_2 + (\text{AlCuMgSi}) + \text{Si}$ at $509^\circ\text{C}.$, and $\text{Al} + \text{CuAl}_2 + \text{Al}_2\text{CuMg} + \text{Mg}_2\text{Si}$ at $506^\circ\text{C}.$, and a plane involving $\text{Al}, \text{CuAl}_2, \text{Mg}_2\text{Si}$, and (AlCuMgSi) at $514^\circ\text{C}.$.

The 514° and $509^\circ\text{C}.$ planes and the variant $\text{Al} + \text{CuAl}_2 + (\text{AlCuMgSi})$ region between them largely determined the solidus of the commercial alloys under consideration.

I.—INTRODUCTION.

THE original Duralumin, which established itself as an aircraft material during the first World War, was essentially an alloy of aluminium, copper, and magnesium. Iron and silicon were always present as impurities, and manganese was added deliberately, but these elements did not play an essential part in the development of the properties of the alloy by heat-treatment.

The heat-treatment given to the alloy was a solution treatment at about $490^\circ\text{C}.$, when most of the copper and magnesium were taken into solid solution and retained on quenching into water; spontaneous precipitation of an intermetallic compound caused a marked increase in strength during the next few days, a phenomenon now well known as "age-hardening". This material is still in wide use as a general-purpose alloy, but in the last decade there has been an increasing use of a modified alloy in which an increased silicon content allows a further heat-treatment at temperatures of $150^\circ\text{--}200^\circ\text{C}.$ to give a considerable improvement in

* Manuscript received 8 April 1949.

† Research Metallurgist, James Booth and Company, Ltd., Birmingham.

proof stress by precipitating one or more compounds containing silicon. Typical load-elongation curves for the two alloys are given in Fig. 1.

To obtain the highest mechanical strength on precipitation the greatest possible concentration of alloying elements is required in the aluminium-rich solid solution before quenching, which is achieved by solution treating the alloy at as high a temperature as is practicable, the limiting condition being usually the commencement of fusion. Aluminium has a strong tendency to form compounds with its alloying elements,

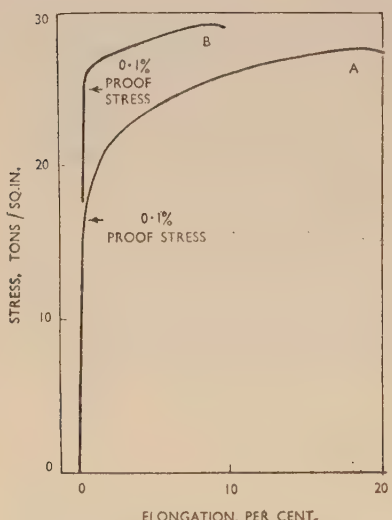


FIG. 1.—Typical Load-Elongation Curve for Naturally Ageing and Artificially Ageing Duralumin-Type Alloys.

- A. Aged at room temperature.
B. Aged at 180° C.

composition is not fully understood, and the present work arose out of an investigation of the sporadic occurrence of quench-cracking in sheet material to the aircraft specification D.T.D. 610B.

The composition limits specified in D.T.D. 610B are :

Cu	Mn	Mg	Fe	Si
3.5-4.8	≥1.2	≥0.6	≥1.0	≥1.5%

The Practical Significance of Overheating.

“Overheating”, as applied to aluminium-base alloys, is a rather diffuse term with somewhat different meanings for the manipulator and the micrographer. The former recognizes overheating by the appear-

and these in general form eutectic systems with the parent metal, so that the solidus of the saturated solid solution is defined by well-marked eutectic planes. Complex alloys, such as the Duralumins now under discussion (containing copper, magnesium, silicon, manganese, and iron), may contain many different intermetallic compounds, and the solidus temperature may be significantly altered by relatively slight changes of chemical composition. In the commercial heat-treatment of these alloys it is common practice to heat to within 5° C. of the solidus temperature, even with large batches of material, and on occasion partial liquefaction may occur. The precise dependence of the solidus temperatures on chemical

ance of significant practical defects in heat-treated parts, such as blisters, quench-cracks, and low ductility after quenching; the latter more specifically by the appearance of quenched liquid in the microstructure of the material. These two methods of assessment are by no means always in agreement, and the limit of temperature to which a metal specimen may be heated without practical detriment is not necessarily the true solidus of the material, for at any given alloy composition it may vary appreciably with the homogeneity of the material, the nature of the component heat-treated, the method of treating, and the intended service application.

Probably the only unmistakable external evidence of overheating in an aluminium alloy is the actual exudation on the metal surface of drops of liquid. In the alloys under consideration this liquid is always of much higher magnesium content than the parent metal and readily oxidizes to give a dirty grey appearance. This exudation occurs only when the solidus temperature is considerably exceeded, so that the liquid phase forms a continuous and extensive grain-boundary network, and is encountered only rarely.

A commonly accepted indication of overheating is the formation of numerous small blisters, but, although this particular type of blistering frequently does accompany overheating, it is really symptomatic of the effect of gas in sub-surface discontinuities, which may be caused by the appearance of liquid but may also be connected with defects in the solid metal. The gas for blister formation (generally hydrogen) is available only if it has been previously dissolved in the metal or has been supplied by reaction with the furnace atmosphere, and in the relative absence of gas liquefaction does not produce blisters. Hence, blistering does not always indicate overheating, and absence of blisters certainly does not mean absence of overheating.

Quench-cracking is a type of fracture, generally intergranular, caused by stresses set up during quenching, and is greatly facilitated by the liquid films produced by overheating. Here again, the effect is not really symptomatic of overheating, but rather of quenching stresses and, although the amount of stress required to cause cracking is much lower when liquid is present, cracking can occur in the absence of liquid. On the other hand, in cases where quenching stresses are kept low by virtue of the small size of the component or the slow rate of cooling, cracking may be absent even when liquefaction is obvious.

Sheet material clad with aluminium to increase its corrosion-resistance is appreciably less susceptible to quench-cracking than unclad material of the same composition, since the aluminium presents a continuous unmelted surface.

Boundary liquefaction produces a film of liquid of eutectic composition, and on cooling this generally solidifies to a more or less continuous band of intermetallic compound, unbroken by the aluminium-rich phase of the eutectic, which attaches itself to the aluminium-rich material already present as the major part of the alloy. This intergranular film is relatively hard and brittle and, if present in quantity, markedly reduces the ductility of the alloy as a whole; once formed, it cannot be re-absorbed into the matrix except by a protracted re-solution treatment, and definite overheating is therefore damaging even in instances in which it does not induce quench-cracking.

This fact should be particularly borne in mind in cases where quenching is slightly delayed, so that the boundary liquid freezes during the transfer of the metal from the furnace to the quenching medium, at a time when the cooling is relatively slow. The subsequent rapid cooling in quenching acts on a completely solid metal and does not normally produce cracking, but the boundary films persist and may affect ductility in the cold; too great a delay before quenching, of course, allows some separation of hardening constituents with consequent reduction in final strength.

The temperature at which liquefaction begins depends on the metallurgical condition of the material. In the cast condition eutectic material is already present as a more or less continuous grain-boundary network, and on reheating the various eutectics which may be present simply melt on reaching the characteristic temperature of each one. In most cast alloys coring effects during freezing lead to the liquid finally solidifying being richer in alloying elements than it would be if in equilibrium, and this may give in the cast structure eutectics of lower melting points than would be expected. Subsequent heating and mechanical working tend to homogenize the material and to eliminate the variations in composition which give an abnormally low solidus, and hence the more the material is homogenized by heating and working the nearer will its solidus approach the equilibrium value. In practice, heavy extrusions and forgings in which a cast structure is still evident may show overheating at temperatures somewhat below those safely withstood by the same material in the form of sheet. Liquefaction in such cases may be confined to small scattered areas of slightly higher alloy content.

This lowering of the solidus as a result of lack of homogeneity obviously occurs only when freezing can proceed through the normal final eutectic of equilibrium to one of lower freezing point; if the normal eutectic is the lowest that can be formed, then heterogeneity simply increases the amount of this eutectic without affecting the actual solidus temperature.

Various degrees of overheating may be recognized in the micro-structure, but the practical implication can often be assessed only when the conditions of treatment and subsequent service are known.

Gross overheating, producing a structure such as is shown in Fig. 21 (Plate XXIV), renders an alloy unfit for use even if it is not quench-cracked or blistered. The milder form shown in Fig. 22 (Plate XXIV) is very likely to cause cracking in any large or complicated component, but if the part escapes cracking by virtue of its small size, of its aluminium cladding, or of delay in quenching, it may be perfectly satisfactory for normal service although possibly it is of lower than normal ductility. In cases where quenching stresses are not low, cracking may be caused by very much less obvious overheating, such as that shown in Fig. 23 (Plate XXIV), which would have no measurable effect on the tensile properties at room temperature. In some alloys, particularly when the grain-size is large, much liquid may be produced within the grains in the form of more or less spherical globules (Fig. 24, Plate XXIV), which, as would be expected, appear to have very little effect on either the quench-cracking or the mechanical properties of the quenched alloy; they are almost always accompanied, however, by some measure of boundary liquefaction.

In special conditions of service, as when the material is subjected to fatigue stressing or corrosion, any tendency to form intercrystalline networks may have special significance, and the effects of moderate overheating become more important.

Numerous articles have appeared in the literature dealing with one or other of the many aspects of overheating in the common Duralumin-type alloys, but they are, in general, confined to the grosser and more obvious phenomena, and were of little use in providing a basis for the present investigation. The cases of technical overheating illustrated are of obvious blistering or exudation, and the micrographs are generally of structures showing complete and thick grain-boundary liquefaction, often deliberately produced at temperatures well above the known solidus of the material examined.

For example, Keller and Bossert,¹ in discussing the micrography of Alcoa 24S (4.4% copper, 1.5% magnesium, with manganese and silicon), show an overheated structure produced at a temperature of 980° F. (527° C.), which is 25° C. above the temperature at which they state overheating begins. Less complete boundaries are illustrated by Hoffmann-Möckel² and by Stelljes.³ A striking series of photographs is given by Panseri and Monticelli,⁴ who illustrate a variety of exudations and blisters, finely liquefied grain boundaries, and isolated globules of eutectic.

The actual temperatures at which overheating begins have not, in

general, been closely defined. As noted above, Keller and Bossert state that overheating in 24S takes place at 936° F. (502° C.). Panseri and Monticelli report that liquid first appears at 520° C. in a Duralumin-type alloy of unspecified composition. Stelljes shows considerable liquefaction at 520° C. in an alloy of the composition :

Cu	Mn	Mg	Fe	Si
4.2	0.34	0.83	0.40	0.51%

His micrograph of the structure at 510° C. is too heavily etched to show the presence of any small amount of liquefaction at that temperature.

The constitution of the alloys examined has not been much discussed. Stelljes speaks of eutectics of "aluminium + copper + magnesium silicide" melting at about 510° C., and "aluminium + copper + silicon" at 525° C., and, as a constituent, "CuAl₂ containing silicon". Heising and Burkart,⁵ in examining the eutectic in cracks near spot welds in 24S, state that published information on the aluminium-copper-magnesium-manganese system gives no guide to the eutectics involved. They illustrate a eutectic reported as "aluminium + CuAl₂ + (AlCuFeMn or Mg₂Si)", but which closely resembles Fig. 32 (Plate XXV) of the present work, showing Al + CuAl₂ + Al₂CuMg.

Several excellent photomicrographs are included in the paper on general aluminium alloy metallography by Mason, Metcalfe, and Mott.⁶ Globules and a grain-corner pool are illustrated, all with clearly resolvable eutectic structures, but the constituent phases are not reported.

II.—PRELIMINARY INVESTIGATION.

In attempting to find the reason for the occasional incidence of quench-cracking in components made from aluminium-coated Duralumin sheet to aircraft specification D.T.D. 610B, it became apparent that the temperature at which overheating took place varied significantly within the range of composition permitted by the specification. Published work was of little help in assessing this variation, but its existence was clearly demonstrated by preliminary tests in which the microstructures of quenched sheet samples were correlated with the thermal arrests obtained on heating small chill-cast bars. The work was extended by a brief examination of the relevant portion of the basic aluminium-copper-magnesium-silicon system, and finally by a more complete check of the quench-cracking, tensile properties, and microstructures of a number of sheet alloys of commercial type, but covering a wide range of composition.

The investigation was begun by determining the thermal arrests in samples of sheet material which had cracked in quenching. Small pieces

of sheet were clamped around the bare junction of a thermocouple, enclosed in a small crucible, and heated slowly in a resistance furnace. Inverse-rate curves taken during heating through the range 490°–530° C. generally showed fairly well-defined arrests between 510° and 515° C., but on subsequent cooling from 530° C. the arrest temperatures were always lower by some 2°–6° C. Careful checking of the experimental technique left no doubt that this difference was real; general experience suggested that the arrest on heating was the more exact and that the lower temperature obtained on cooling was a result of supercooling of the last traces of liquid.

Larger amounts of similar alloys were melted in crucibles to determine the usual inverse-rate curves on freezing and remelting, and the same order of difference was found between the two sets of arrests. The melts were not stirred during freezing, since the significant final arrest resulted from the freezing of a very small amount of liquid in an already rigid matrix.

The temperatures of the lowest arrests on heating did approximate to those producing quench-cracking and slight grain-boundary liquefaction in the sheet alloys, and it was decided to investigate the over-heating phenomena in this type of alloy on a somewhat wider basis, using as criteria the arrest temperatures on heating, the microstructures of quenched specimens, and the incidence of quench-cracking and reduced ductility in quenched tensile test-pieces.

The experimental alloys were melted in a laboratory wire-wound furnace, using 99.85% aluminium, 99.9 + % magnesium, electrolytic copper, commercial silicon, and master alloys made by dissolving electrolytic manganese, or commercial soft iron wire, in aluminium. The melts were of 200 or 400 g., as required, and were cast into $5 \times \frac{3}{4}$ in. dia. round bar and $120 \times 60 \times 8$ mm. slab, both heavily chilled. The slab was hot and cold rolled to 1-mm. strip for heat-treatment as micro-specimens and tensile test-pieces. The round bar provided an analytical sample, an as-cast microsection, and a cylinder for thermal analysis. A small button of each melt was allowed to freeze relatively slowly in an alumina-lined crucible to give a coarse separation of constituents to aid identification, although its structure, of course, did not necessarily agree with that of the chill-cast sample.

For thermal analysis, the chill-cast cylinder $\frac{3}{4}$ in. in dia. $\times 1\frac{1}{4}$ in. long was drilled axially to a depth of about $\frac{7}{8}$ in. to take the bare junction of a 22-S.W.G. Chromel/Alumel thermocouple. It was placed inside a small crucible in a wire-wound tubular furnace and heated slowly, an inverse-rate curve being determined between 490° and 550° C. with a heating rate of 2°–4° C./min. A Cambridge null-point bench thermo-

couple potentiometer, sensitive to 1 microV., was used, with temperature intervals of about $1\frac{1}{4}$ ° C. (50 microV.). The thermocouple was carefully calibrated at the freezing points of 99.99% aluminium and a pure aluminium-copper eutectic, and periodically checked at the latter temperature and at the arrest temperature of one of the test cylinders which had a well-defined arrest at 513° C.

TABLE I.—*Effects of Magnesium and Silicon Contents on Arrests in Alloys Containing 4.2% Copper, 0.6% Manganese, and 0.7% Iron.*

Cast No.	Mg, %	Si, %	Arrests, ° C.
R. 647	0.2	0.4	533 (531-537)
648	"	0.6	531.5 (527-536)
568a	"	0.8	530 (522-534)
649	"	1.0	
569a	"	1.25	513,* 519 (517-522)
650	"	1.5	515.5
651	0.4	0.4	514, 529 * (521-534)
652	"	0.6	513,* 523.5 (517-531)
563a	"	0.8	512.5, 525 * (515-529)
564a	"	1.0	512,* 519 (516-525)
565a	"	1.15	510.5,* 516 (514-519)
566a	"	1.3	508,* 510 ? (508-511)
567a	"	1.6	509
653	0.6	0.4	513.5
654	"	0.6	513
558a	"	0.7	513
677	"	0.8	513.5
559a	"	0.95	513
560a	"	1.05	513.5,* 521 (519-524)
561a	"	1.3	511.5
562a	"	1.45	510,* 525 (520-528)
770	"	1.7	509,* 524.5 (509-531)
771	"	2.0	508.5, 524 (509-532)
772	"	2.5	510, 527.5 * (514-541)
773	"	3.0	509.5, 526 * (514-529), 538 (529-544)
774	"	3.5	509, 526 * (512-532), 544.5 (532-549)
665	0.8	0.4	513.5
656	"	0.6	513.5
657	"	0.8	513
658	"	1.0	513.5,* 529 (527-534)
659	"	1.2	511.5,* 529 (521-535)
660	1.0	0.4	513
661	"	0.6	513.5
662	"	0.8	514,* 533 (527-535)
663	"	1.0	514,* 531 (525-535)
664	1.2	0.4	513
665	"	0.6	513,* 535 (529-541)
666	"	0.8	515
667	1.4	0.4	513
668	"	0.6	513.5

a denotes alloy of analysed composition.

* " larger arrest.

() " range of extended arrest and follows the peak temperature.

TABLE II.—Effect of Copper, Manganese, and Iron on Arrests in Alloys Containing 0·6% Magnesium and 0·8% Silicon.

Cast No.	Cu, %	Mn, %	Fe, %	Mg, %	Si, %	Arrests, °C.
R. 674	5·0	0·6	0·7	0·6	0·8	514,* 541 (530–544)
677	4·2	"	"	"	"	513·5
675	3·5	"	"	"	"	514
676	2·0	"	"	"	"	513·5 ...
678	4·5	Nil	"	"	"	513·5
679	"	0·6	Nil	"	"	515

* denotes larger arrest.

() " range of extended arrest and follows the peak temperature.

TABLE III.—Effect of Homogenization at 500° C. on Arrests in Alloys Containing 4·2% Copper, 0·6% Manganese, and 0·7% Iron.

Cast No.	Mg, %	Si, %	Arrests, °C.	
			Before homogenization	After homogenization
R. 569a	0·2	1·25	513,* 519 (517–522)	513,* 519
563a	0·4	0·8	512·5, 525 * (515–529)	525·5 (519–526)
564a	"	1·0	512,* 519 (516–525)	513
565a	"	1·15	510·5,* 516 (514–519)	511
566a	"	1·3	508,* 510 ? (508–511)	508
567a	"	1·6	509	507·5
558a	0·6	0·7	513	512,* 518 (515–519)
559a	"	0·95	513	511
560a	"	1·05	513·5,* 521 (519–524)	512·5,* 523 (515–524)
561a	"	1·3	511·5 *	512,* 525 ?
562a	"	1·45	510,* 525 (520–528)	509

a denotes alloy of analysed composition.

* " larger arrest.

() " range of extended arrest and follows the peak temperature.

Heat-treatment was carried out on small pieces of strip for micro-examination or on blanked test-pieces with $2\frac{1}{4} \times 0\cdot5$ in. parallel for determining the tensile properties after natural ageing. An electrically heated salt-tank $12 \times 8 \times 10$ in. deep was carefully stabilized at the required temperature with a Sunvic energy regulator, and the specimens were immersed, held for 30 min., and water quenched. The temperature was measured with the same thermocouple and potentiometer as were used for thermal analysis, and temperatures were maintained during the solution treatment to within $\pm 1^\circ$ C.

The compositions of the chill-cast alloys are listed in Tables I, II, and III, together with the temperatures of thermal arrests on heating. Table I deals with the alloys cast to examine the effect of magnesium and silicon contents in alloys containing nominally 4·2 copper, 0·6% manganese,

and 0.7% iron; Table II deals with a short series in which variations in copper, manganese, and iron content were made while the magnesium and silicon contents were maintained constant at 0.6% and 0.8%, respectively; and Table III compares the arrests found in the same specimens as in Table I before and after homogenization for 24 hr. at 500°C.

Fig. 2 is a plot of the alloys of constant copper, manganese, and iron contents showing how the lowest arrest temperature obtained on heating a chill-cast alloy varied with the magnesium and silicon contents. The

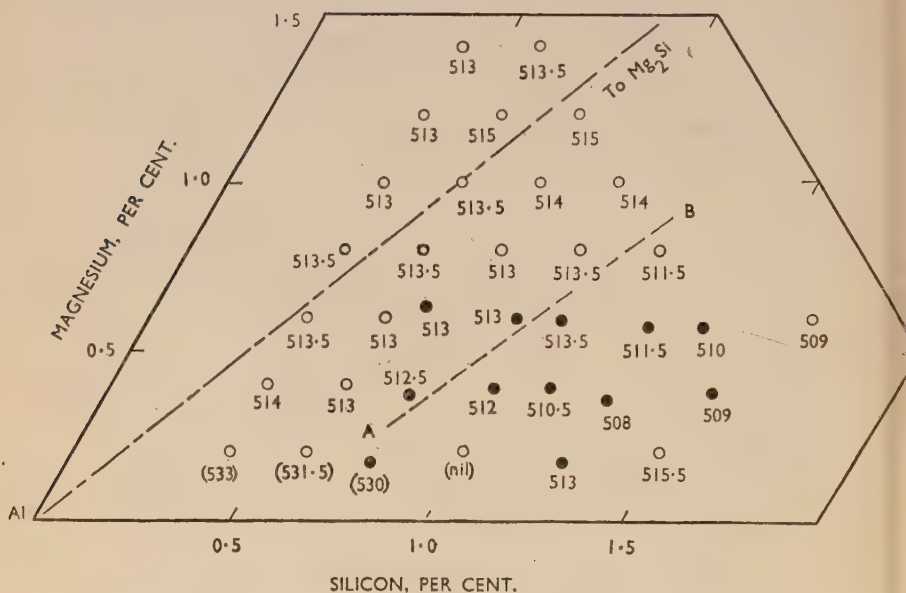


FIG. 2.—Lowest Arrest Temperatures of Al-Cu-Mg-Si-Mn-Fe Alloys.

● Analysed.
○ Nominal.

line joining the aluminium corner to the composition Mg_2Si is included. It is apparent that the arrests fell into two groups; those on the higher-magnesium side of the line AB showed a constant temperature of about $513.5^\circ C.$, while for those on the higher-silicon side the temperature fell steadily to about $509^\circ C.$ This is shown very clearly by the section at constant magnesium (0.6%) given in Fig. 3, where the range is extended to 3.5% silicon.

Table II shows that the arrest at about 513.5° C. was present in all the alloys containing 0.6% magnesium and 0.8% silicon over the range 5.0%-3.5% copper, but was absent when the copper content was reduced

to 2%. Absence of iron or manganese did not alter the arrest temperature.

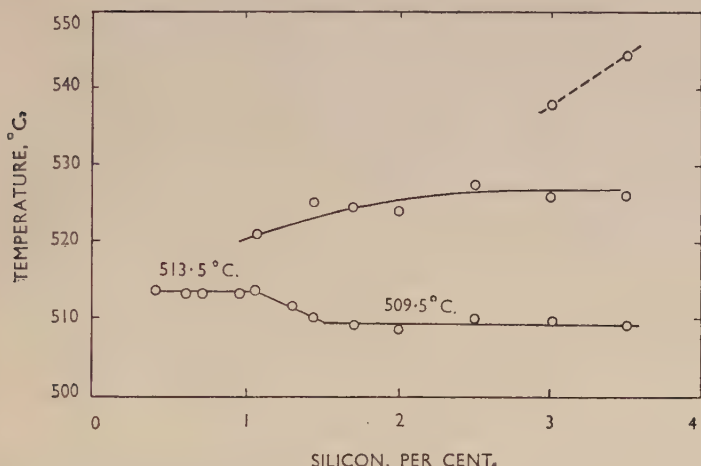


FIG. 3.—Effect of Silicon Content on Arrest Temperature in Alloys Containing Copper 4.2, Magnesium 0.6, Manganese 0.6, Iron 0.7%.

TEMPERATURE

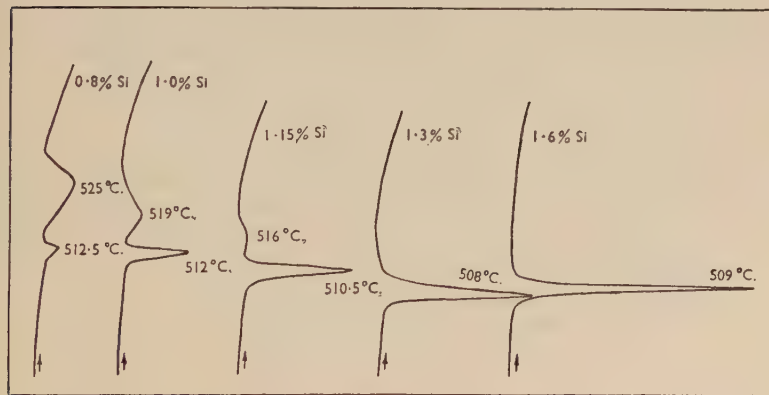


FIG. 4.—Inverse-Rate Heating Curves on Alloys Containing Copper 4.2, Magnesium 0.4, Manganese 0.6, Iron 0.7%.

Homogenization of the alloys given in Table III for 24 hr. at 500° C. did not significantly alter the temperature of any arrest, but caused the disappearance of the lowest arrest in the alloy containing 0.4% magnesium, 0.8% silicon, presumably by taking into solution the constituents of the responsible eutectic.

A significant factor in overheating is, of course, the amount of liquid produced on exceeding the lowest eutectic temperature, and the increase in amount with increasing silicon content for a constant magnesium content is well shown by the magnitudes of the arrests in the series for 0.4% magnesium (Fig. 4).

Table IV gives the results of microscopic examination of sheet specimens quenched from temperatures between 510° and 520° C. It distinguishes between various degrees of grain-boundary liquefaction, from the first thin films of constituent to a continuous boundary with a definite eutectic structure; this appeared first, as usual, at grain corners. Globules with an obvious two- or three-phase structure generally appeared at the same time as the first indications of boundary liquefaction. These globules were randomly distributed throughout the matrix and probably occurred at the site of particles of CuAl₂ or other participating constituent left undissolved on solution treatment. Since such an appearance of eutectic involves a concentration of copper, magnesium, and silicon by diffusion through the solid, it takes time for full accomplishment.

The temperatures at which overheating became visible microscopically agree reasonably well with the arrest temperatures which are included in Table IV. The discrepancies may be ascribed to two causes: in cases where the solidus is determined by a eutectic obviously freezing over a range of temperature (e.g. Cast R.568), the lower temperature limit is not determinable by a thermal curve; while a small arrest in a thermal curve on a chill-cast specimen may be given by a eutectic which is eliminated during the subsequent working into sheet.

It is obvious that complete correlation cannot be expected between thermal curves on chill-cast material and heat-treatment phenomena in wrought material which should be well homogenized, but the results given above show that, except when the amount of eutectic was very small in an alloy near the boundary of the aluminium-rich solid solution, there was a very useful agreement between the two.

Tensile tests were carried out on quenched sheet material to find the effect of overheating on ductility. The small cast slabs used at this stage provided only one tensile specimen of each alloy at each temperature, and the strip tested was not, of course, representative of normal commercial material. Table V does, however, present an interesting correlation between overheating and loss of ductility. It is also interesting that even in these small specimens quench-cracking occurred in alloy R.562 (0.6% magnesium, 1.4% silicon) at 514° C., and that most of the alloys, even when damaged by overheating, showed a negligible amount of blister.

This preliminary work showed that alloys in the range examined

TABLE IV.—Microstructures of Quenched Samples.

Cast No.	Analysis		Heating Arrests, °C.	Quenching Temperature.			
	Mg, %	Si, %		510° C.	512° C.	514° C.	518° C.
R.568	0.2	0.8	530 (622-534)	No fusion.	No fusion.	No fusion.	No fusion.
569	0.2	1.3	513,* 519 (517-522)	No fusion.	No fusion.	No boundaries, Very occasional globules.	Occasional bound- aries, Large globules.
R.563	0.4	0.8	512.5, 525*	No fusion.	No fusion.	No fusion.	No fusion.
564	0.4	1.0	512, 519 (516-525)	No fusion.	No fusion.	No fusion.	Some boundaries. Coarse globules.
565	0.4	1.1	510.5,* 516 (514-519)	Traces of bound- ary.	Traces of bound- ary.	Occasional bound- aries.	Some boundaries. Coarse globules.
566	0.4	1.3	508,* 510? (508-511)	Some globules. No boundaries. Some globules.	Some globules. Occasional bound- aries.	Some globules. Some boundaries.	Some boundaries. Coarse globules.
567	0.4	1.6	509	Occasional bound- ary pools. Globules.	Some globules. Some globules. No boundaries found.	Occasional bound- ary networks. Globules.	Occasional bound- ary networks. Globules.
R.558	0.6	0.7	513	No fusion.	No fusion.	No fusion.	No boundaries. Few globules.
559	0.6	0.9	513	No fusion.	No fusion.	No fusion.	No boundaries. Some large globules.
560	0.6	1.1	513.5, 521, (519-524)	No fusion.	Traces of bound- ary.	Traces of bound- ary.	Traces of bound- ary.
561	0.6	1.3	511.5	Some boundaries, Numerous small globules.	Some globules. Numerous small globules.	Some globules. Numerous small globules.	Some globules. Numerous small globules.
562	0.6	1.4	510,* 525 (520-528)	Patches of con- tinuous bound- ary.	Occasional bound- aries.	Some boundaries. Large globules.	Many continuous boundaries. Large globules.

* Denotes larger arrest.

() Denotes range of extended arrest.

TABLE V.—Mechanical Tests on Quenched Specimens.

Cast No.	Analysis		Quenching Temperature			Proof Stress, U.T.S., Elongation	Proof Stress, U.T.S., Elongation	Proof Stress, U.T.S., Elongation
	Mg, %	Si, %	508° C.	511° C.	514° C.			
R.568	0.2	0.8	13-25-20, no blistering	12-22-14, no blistering	14-26-18, no blistering	11-21-18, v. slight blistering	14-24-20, no blistering	14-25-20, no blistering, U.T.S., elongation
569	0.2	1.3	13-25-19, no blistering	14-25-13, no blistering	13-25-18, no blistering	14-25-17, no blistering	12-20-14, v. slight blistering	13-22-12, slight blistering
R.563	0.4	0.8	12-22-17, slight blistering	14-27-17, no blistering	14-26-18, v. slight blistering	15-27-20, no blistering	14-25-20, no blistering	13-22-12, slight blistering
564	0.4	1.0	11-17-4, v. slight blistering	14-26-17, no blistering	15-27-21, v. slight blistering	15-27-16, no blistering	14-26-16, v. slight blistering	14-26-16, v. slight blistering
565	0.4	1.1	13-25-19, heavy blistering	15-25-12, no blistering	14-22-12, v. slight blistering	15-25-17, v. slight blistering	14-24-9, v. slight blistering	14-24-9, v. slight blistering
566	0.4	1.3	14-24-13, v. slight blistering	13-23-19, v. slight blistering	13-23-19, v. slight blistering	14-26-18, no blistering	14-21-0, no blistering	14-21-0, no blistering
567	0.4	1.6	15-26-16, slight blistering	14-23-8, v. blistering	12-20-10, v. slight blistering	14-27-26, v. slight blistering	15-25-12, v. slight blistering	15-25-12, v. slight blistering
R.558	0.6	0.7	12-24-17, slight blistering	15-26-22, v. slight blistering	15-27-26, slight blistering	15-25-12, v. slight blistering	15-26-22, v. slight blistering	15-26-22, v. slight blistering
559	0.6	0.9	12-23-17, v. slight blistering	15-27-21, v. slight blistering	14-21-9, blistering	15-24-7, v. slight blistering	14-23-8, v. slight blistering	14-23-8, v. slight blistering
560	0.6	1.1	12-25-18, no blistering	14-16-15, v. slight blistering	15-26-17 v. slight blistering	13-23-10, moderate blistering	13-22-10, heavy blistering	13-22-10, heavy blistering
561	0.6	1.3	13-25-20, slight blistering	13-20-7, v. slight blistering	15-24-9, v. slight blistering	15-26-20, moderate blistering	13-21-6, moderate blistering	13-21-6, moderate blistering
562	0.6	1.4	11-21-12, moderate blistering	14-17-3, heavy blistering	4-4-0, heavy blistering, cracks	4-4-0, v. heavy blistering, cracks	4-4-0, heavy blistering, cracks	4-4-0, heavy blistering, cracks

Proof stress and ultimate tensile stress are in tons/in.², and elongation in %.

could be divided into two groups having solidus temperatures around 513.5° and 509° C., respectively, with a transitional zone between the two, and that the temperature seemed to be determined by the magnesium : silicon ratio rather than by the absolute amount of either element. Micrographic work on the alloys established the significant phases present, but the complete correlation of the arrests with the constitution was not possible. The further extension of the work was, therefore, along two main lines. First, the preparation of sheet materials of similar compositions to those already examined but in larger quantity to allow more extensive examination; and secondly, a more detailed investigation of the constitution of the alloys, which soon resolved itself into an examination of part of the quaternary system aluminium-copper-magnesium-silicon. This latter study will be discussed first, since its results are important in explaining the practical overheating phenomena observed in the more complex sheet alloys.

III.—THE AL-CU-MG-SI SYSTEM.

For a proper explanation of the arrests and microstructures observed in the tests reported above, it was obviously desirable to identify the phases present and examine their relationships to each other. To do this adequately for the six-component system (Al-Cu-Mg-Si-Fe-Mn) was out of the question, but since only the very lowest arrests were of interest, it appeared reasonable to examine only the quaternary system (Al-Cu-Mg-Si). It was known⁷ that iron and manganese form compounds separating at temperatures relatively near the liquidus, and although an Al-Cu-Mn compound had been reported⁸ to be involved in the age-hardening of Duralumin-type alloys, the preliminary work described above indicated that neither manganese nor iron affected the temperatures of the lowest eutectics. Iron and manganese would undoubtedly remove some silicon and possibly copper from the melt, and might thus displace the field of existence of the significant eutectics, but they could reasonably be expected not to alter the temperatures at which those eutectics melted. It will be seen later that this simplification was adequately justified.

Review of Literature.

Considering its importance for commercial alloys, the Al-Cu-Mg-Si system has been little treated in the literature. Of its component ternary systems, the phases present in the aluminium corners of the Al-Cu-Si⁹ and Al-Mg-Si¹⁰ diagrams have been sufficiently established, and the constitution at 460° C. of the Al-Cu-Mg system has recently been clarified by the work of Little, Hume-Rothery, and Raynor.¹¹ The

Al-Cu-Si diagram shows a simple ternary eutectic at 525° C., developing from the respective binary eutectics Al + Si at 577° C. and Al + CuAl₂ at 548° C. In the Al-Mg-Si system, two ternary eutectics, Al + Mg₂Si + Si at 559° C. and Al + Mg₂Si + Al₃Mg₂ at 450° C. lie one on each side of the pseudo-binary eutectiferous system Al-Mg₂Si, with a eutectic temperature of 595° C.

The system Al-Cu-Mg contains two ternary compounds co-existing with the aluminium-rich solid solution, called *S* and *T* by Nishimura.¹² The one of lower magnesium content, *S*, has been shown¹¹ to be Al₂CuMg; with Al and CuAl₂ it forms a ternary eutectic whose freezing point was given by Nishimura and by Urazov and Petrov¹³ as 500° C. The second compound, *T* (approximately Al₆CuMg₄), is formed peritectically from *S* and gives a ternary eutectic with Al₃Mg₂.

The aluminium corner of the quaternary system Al-Cu-Mg-Si therefore involves seven known phases: α solid solution, CuAl₂, *S*, *T*, Al₃Mg₂, Mg₂Si, and silicon, of which Al₃Mg₂ and *T* are not to be expected in the Duralumin-type alloys under discussion, in which the copper content substantially exceeds the magnesium. To these, the work of Dix, Sager, and Sager¹⁴ added an eighth, a quaternary compound reported later by Petrov¹⁵ to be Al₄CuMg₅Si₄ or Al₄CuMg₄Si₄. This has a field of existence intruding between those of Mg₂Si and silicon, and it appears to be formed from Mg₂Si by a peritectic reaction.

TABLE VI.—List of Eutectics in Al-Cu-Mg-Si Alloys.

Eutectics	Temp., °C.	Cu, %	Mg, %	Si, %	Source
Al + CuAl ₂ . . .	548	33	
Al + Al ₃ Mg ₂ . . .	450	...	33	...	
Al + Si . . .	577	11.7	
Al + Mg ₂ Si . . .	595	...	8.3	4.7	
Al + Mg ₂ Si + Si . .	557	...	5.5	14	
Al + Mg ₂ Si + Al ₃ Mg ₂ .	450	...	33	0.1	
Al + CuAl ₂ + Si . .	525	26	...	6	
Al + CuAl ₂ + <i>S</i> . .	500	27	6	...	Nishimura ¹²
Al + <i>T</i> + Al ₃ Mg ₂ . .	447	3	32	...	Nishimura ¹²
Al + CuAl ₂ + Mg ₂ Si . .	517	28	6	3.5	Mondolfo ¹⁶
Al + CuAl ₂ + <i>Q</i>	Töllner ¹⁷
Al + CuAl ₂ + <i>Q</i> + Si . .	520	26	2	5	Mondolfo ¹⁶
	509.4	24.7	1.7	8.3	Töllner ¹⁷

S = Al₂CuMg.

T = Al₆CuMg₄, approximately.

Q = Al₄CuMg₅Si₄, "

Mondolfo¹⁶ reports two eutectics in the quaternary system which are not present in the ternaries, namely:

		Cu, %	Mg, %	Si, %
Al + CuAl ₂ + Mg ₂ Si . . .	517° C.	28	6	3.5
Al + CuAl ₂ + Al ₄ CuMg ₅ Si ₄ + Si . .	520° C.	26	2	5

OVERHEATING IN DURALUMIN-TYPE ALLOYS.

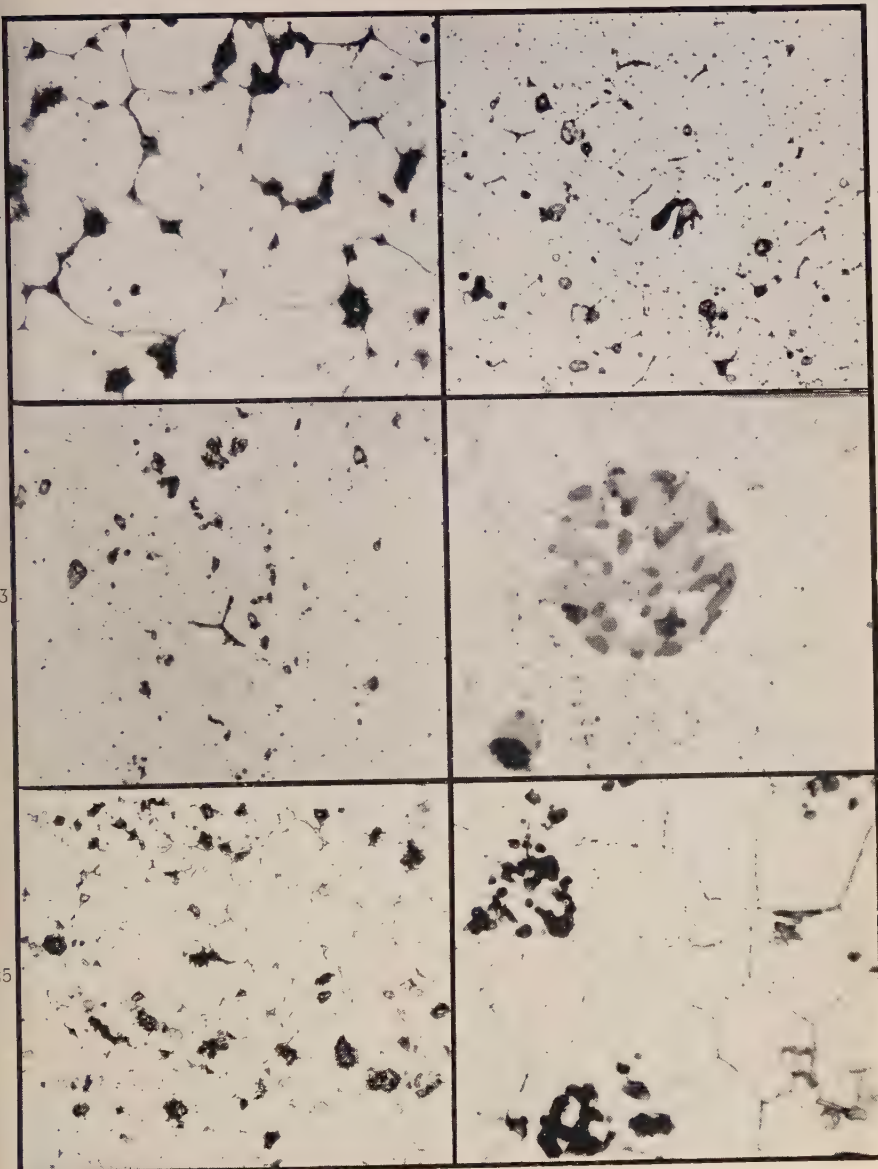


FIG. 21.—Gross overheating in alloy XK 816, water quenched from 520° C. $\times 500$.
 FIG. 22.—Moderate overheating in alloy XK 823, water quenched from 517° C. $\times 500$.
 FIG. 23.—Trace of overheating in commercial Duralumin sheet. $\times 500$.
 FIG. 24.—Globule consisting mainly of Al, CuAl₂, and Q, with some Si. $\times 1500$.
 FIG. 25.—“Messy” structure of alloy XK 828, water quenched from 520° C. $\times 500$.
 FIG. 26.—Dotted boundary in alloy XK 825, water quenched from 517° C. $\times 1500$.

All etched in 0·5% HF.

[To face p. 216.]

EUTECTICS IN AL-CU-MG-SI ALLOYS CONTAINING 4% COPPER.

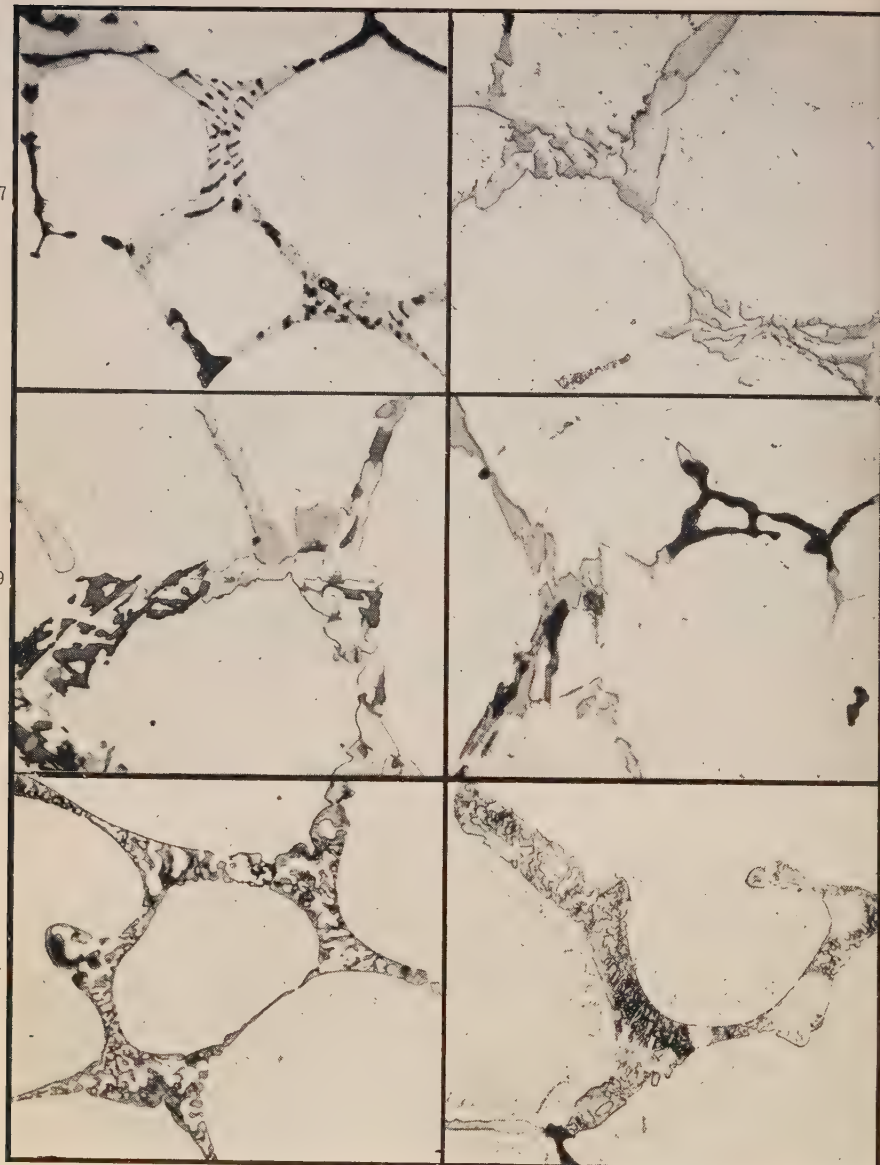
FIG. 27.—Al + Mg₂Si and Al + CuAl₂ + Mg₂Si.FIG. 28.—Al + Q and Al + CuAl₂ + Q.FIG. 29.—Al + Si and Al + CuAl₂ + Q + Si.FIG. 30.—Al + Mg₂Si passing to Al + Q along a grain boundary.

FIG. 31.—Al + S.

FIG. 32.—Al + CuAl₂ and Al + CuAl₂ + S.All etched in 0·5% HF. $\times 500$.

Töllner¹⁷ studied the micrography of Al-Cu-Mg-Si alloys, and mentions a quaternary compound Q_{Si} apparently identical with $Al_4CuMg_5Si_4$ and forming a quaternary eutectic:

	Cu, %	Mg, %	Si, %
$Al + CuAl_2 + Q_{Si} + Si$	24.7	1.7	8.3

which is not in agreement with Mondolfo.

Dix, Sager, and Sager¹⁴ give a temperature of 510.5° C. for a eutectic of unspecified constitution which apparently initiated melting in an alloy containing α , $CuAl_2$, Mg_2Si , and the $AlCuMgSi$ compound.

The various eutectics described in the literature are listed in Table VI.

Experimental Investigation.

The experimental work described below was concerned with the Al-Cu-Mg-Si system at a constant copper content of 4%. The limiting

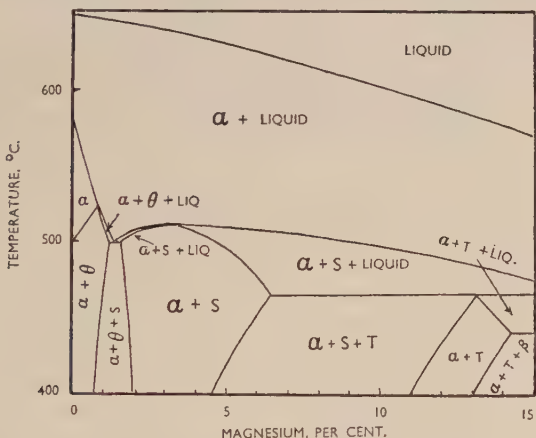


FIG. 5.—4% Copper Section of Aluminium-Copper-Magnesium Diagram.
(After Nishimura,¹² with modifications according to Hume-Rothery.)

vertical sections of the constituent Al-Cu-Mg and Al-Cu-Si ternary systems are shown in Figs. 5 and 6. Only incomplete information on which to base these sections was available in the literature, but the ones deduced are sufficiently accurate for the present purpose and are consistent with the experimental data on the quaternary alloys examined.

Both diagrams start from the aluminium-copper binary system²² at 4% copper, where the liquidus temperature is about 625° C., the solidus 585° C., and the lower limit of the α solid solution is about 505° C. Addition of either magnesium or silicon at this last temperature causes the appearance of $CuAl_2$.

The 4% copper section of the Al-Cu-Mg system given in Fig. 5 is based mainly on the work of Nishimura,¹² and is characterized by rapid lowering of the solidus with increasing magnesium content to about 500° C. at the $\alpha + \text{CuAl}_2 + S$ eutectic, followed by a slight rise in the $\alpha + S$ region. The rest of the diagram was of no significance in the investigations here reported. The $(\alpha + \text{CuAl}_2)/(\alpha + \text{CuAl}_2 + S)$ and $(\alpha + \text{CuAl}_2 + S)/(\alpha + S)$ boundaries have been adjusted to agree at 460° C. with those determined by Little, Hume-Rothery, and Raynor,¹¹ whose data also allow the calculation of the positions of these boundaries at 500° C. as at about 1.5% and 1.7% magnesium, respectively.

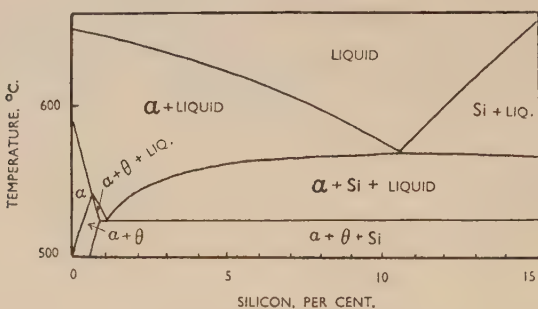


FIG. 6.—4% Copper Section of Aluminium-Copper-Silicon Diagram.
(From data of Matsuyama.¹⁸)

The general form of Fig. 6, for the 4% copper section of the Al-Cu-Si system, is based on Matsuyama.¹⁸ The ternary eutectic temperature is variously given as 525° C.^{9, 19} and 522° C.^{18, 20} The information on the $\alpha/(\alpha + \text{CuAl}_2)$ and $(\alpha + \text{CuAl}_2)/(\alpha + \text{CuAl}_2 + \text{Si})$ boundaries is conflicting^{8, 20, 21} and sometimes not in agreement with the accepted binary solid-solubility limits, but it seems established that the solubility of silicon is reduced only slightly by the presence of copper. In Fig. 6, the $(\alpha + \text{CuAl}_2)/(\alpha + \text{CuAl}_2 + \text{Si})$ boundary has been put at 0.6% silicon at 500° C. and 0.8% at the eutectic temperature.

The third side of the diagram considered would be the vertical section at 4% copper developed from the binary magnesium-silicon system, but no information is available from which to construct this. The binary system itself²³ is well known, and is characterized by the presence of the compound Mg_2Si , which forms eutectics with magnesium and with silicon. The general form of this diagram persists in the aluminium corner of the Al-Mg-Si system, and Fig. 7 gives the 4% magnesium, 4% silicon section for comparison with the similar one at 4% copper deduced in Fig. 14 from the results of the present investigations.

The experimental examination of the quaternary system had one main object, that of finding out whether it showed the two constant-temperature planes found in the solidus of the more complex alloys, and if so, to establish the nature of the eutectics involved. The work was confined, therefore, to Al-Cu-Mg-Si alloys of a constant copper content (4%) and to the region of the actual solidus, except when examination at higher temperatures was desirable to demonstrate the order of separation of the various constituents during freezing. It consisted largely of determining arrests during the heating of chill-cast alloys and checking the phases and eutectics shown in more coarsely separated, slowly frozen material, but was extended by the micro-examination of specimens quenched after isothermal treatments.

The alloys were made from 99.9% aluminium and hence contained about 0.05% iron, except in the case of the ternary Al-Cu-Mg alloys, which were based on 99.99% aluminium so as to be free from silicon. They were melted in alumina-lined crucibles and cast as previously described into chill-cast $\frac{3}{4}$ -in.-dia. rod and 8-mm. thick slab, together with small frozen slugs. The compositions of the alloys examined are plotted in Fig. 8. The temperatures of the lower arrests found on heating chill-

cast material are given in a similar ternary plot in Fig. 9, and various vertical sections are presented in Figs. 10-13. The correspondence between the solidus in this quaternary system at 4% copper and that of the Duralumin-type alloys examined previously is obvious, particularly on comparing Figs. 10 and 3. The portion of the system of greatest interest was, of course, that most nearly corresponding to the composition and constitution of the commercial alloys, but these are close to the limits of the α solid solution, where identification of undissolved constituents is difficult because of their small amount and particle size, thermal arrests are not well defined, and control of chemical composition must be precise if the field is to be covered uniformly. Since this

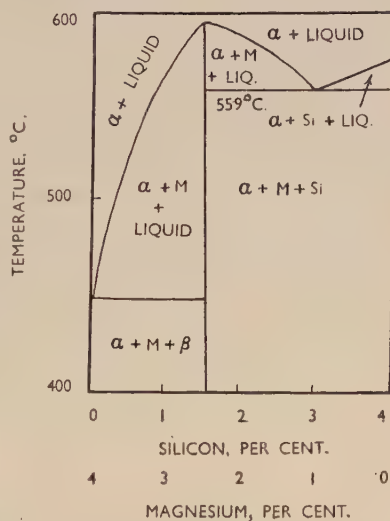


FIG. 7.—Section 4% Magnesium, 4% Silicon of Aluminium-Magnesium-Silicon Diagram ($M = Mg_2Si$).

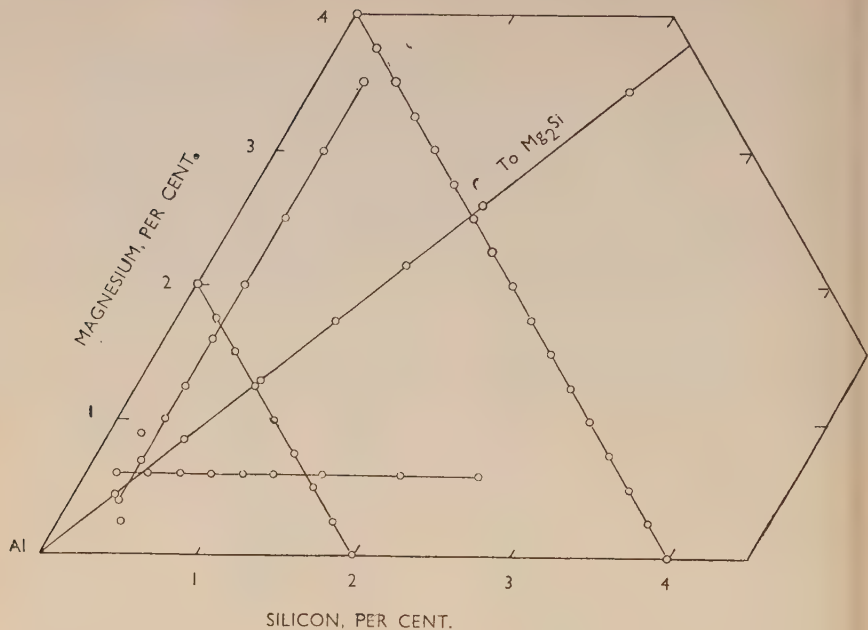


FIG. 8.—Aluminium-Copper-Magnesium-Silicon Alloys Examined in 4% Copper Section.

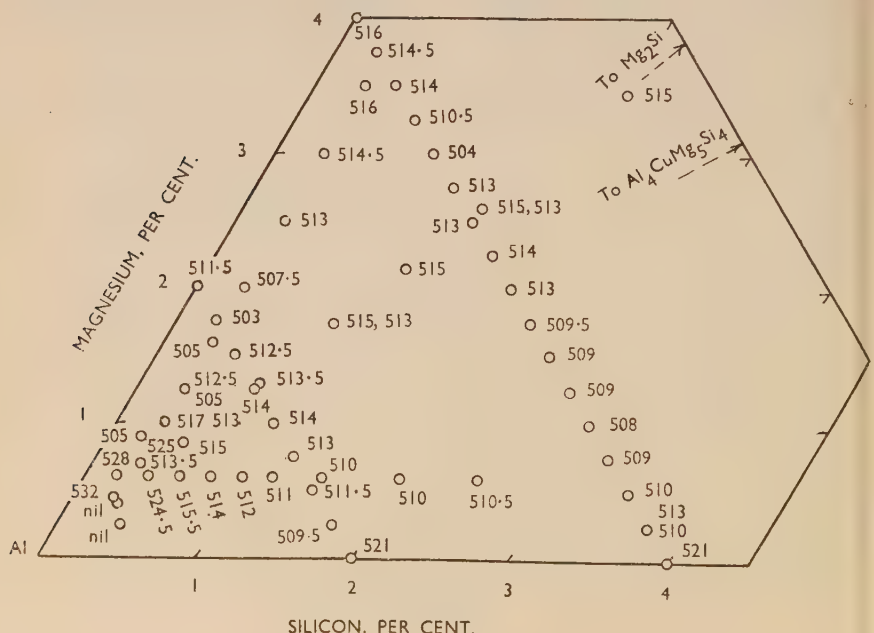


FIG. 9.—Lowest Arrests Occurring on Heating Alloys of Fig. 8.

investigation was aimed at determining non-variant solidus temperatures rather than phase-field limits, most of the work was done at the higher

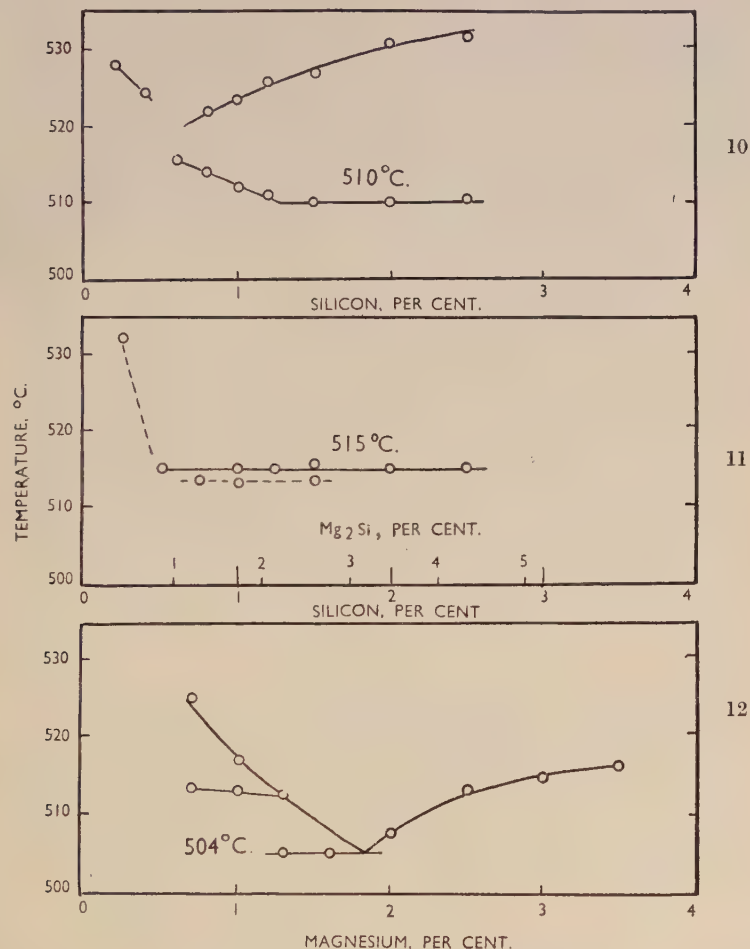


FIG. 10.—Vertical Section at 0·6% Magnesium.

FIG. 11.—Vertical Section along line Al-Mg₂Si.

FIG. 12.—Vertical Section at 0·3% Silicon.

silicon and magnesium contents, in particular along the section 4% magnesium, 4% silicon. This section cut adequately across all the phase fields which radiated from the aluminium corner, and allowed easy identification of phases and eutectic temperatures. Alloys were made

in steps of $\frac{1}{4}\%$ from 4% copper, 4% magnesium to 4% copper, 4% silicon, and the results of their examination are given in Fig. 14.

No attempt was made to attain equilibrium, but all the structures obtained were capable of straightforward explanation, and the four-phase constant-temperature planes of the solidus were well defined, at least in temperature.

The solidus of the 4 : 4 section was first determined by the arrests during the heating of chill-cast cylinders, and the microstructures of slowly frozen melts allowed the identification of all the phases expected, namely α , CuAl_2 , S , Mg_2Si , Q , and Si; no other phases were found. Their modes of separation during freezing were generally determinable, and it

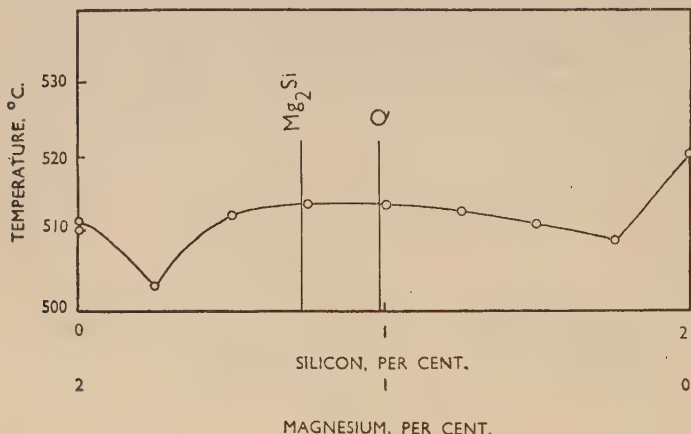


FIG. 13.—Vertical Section 2% Magnesium, 2% Silicon at 4% Copper.

was clear that the diagram comprised two distinct parts corresponding to excess of silicon or of magnesium over the composition Mg_2Si . Near the Mg_2Si ratio the final separation was a distinctive ($\text{Al} + \text{CuAl}_2 + \text{Mg}_2\text{Si}$) eutectic (Fig. 27, Plate XXV). At higher silicon contents this was replaced first by ($\text{Al} + \text{CuAl}_2 + Q$) (Fig. 28, Plate XXV), then by ($\text{Al} + \text{CuAl}_2 + Q + \text{Si}$) (Fig. 29, Plate XXV), and finally by ($\text{Al} + \text{CuAl}_2 + \text{Si}$). It was also apparent that an earlier separation on freezing of a binary ($\text{Al} + \text{Mg}_2\text{Si}$) eutectic was succeeded as the silicon content was increased by ($\text{Al} + Q$), and that over a certain range of composition Q formed peritectically from Mg_2Si . The sequence along a grain boundary from script Mg_2Si to angular Q is shown in Fig. 30 (Plate XXV). Near the silicon end of the section the corresponding separation was ($\text{Al} + \text{Si}$). On the magnesium-rich side of Mg_2Si the final separations were either ($\text{Al} + S$) (Fig. 31, Plate XXV) or ($\text{Al} + \text{CuAl}_2$), with

(Al + CuAl₂ + S) (Fig. 32, Plate XXV) over a narrow range of composition. (Al + Mg₂Si) preceded all these except in the case of the alloy containing no silicon.

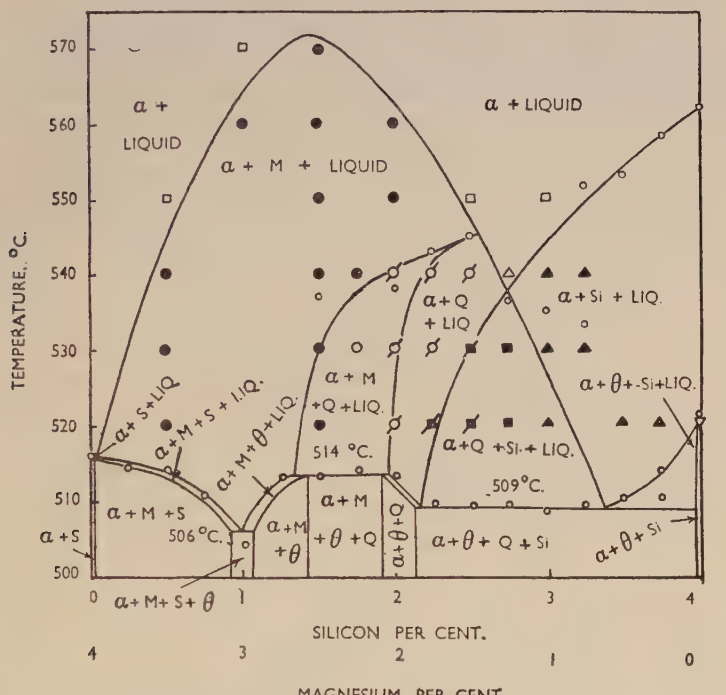


FIG. 14.—Section 4% Magnesium, 4% Silicon at 4% Copper.

Symbols including / indicate specimens with evidence of $M \rightarrow Q$ peritectic reaction.

$M = \text{Mg}_2\text{Si}$.

° indicates thermal arrest on heating.

□	$a + L$	○	$a + M + Q + L$	$a + Q + Si + L$
●	$a + M + L$	○	$a + M + Q + L$	$a + Q + Si + L$
▲	$a + Si + L$	○	$a + Q + L$	$\} Q \text{ sheath}$
△	$a + Q + L$			$a + Q + Si + L$ (with cored Q)

To confirm these deductions on the order of freezing, small portions of the slowly frozen slugs were immersed in a molten nitrate bath at suitable controlled temperatures, held for 5 min., and quenched. Micro-examination then allowed easy distinction to be made between the fine structure of the portions which had been liquid at the quenching temperature and the coarser structure of the original material. This time at temperature was not long enough to cause serious diffusion, and thus the

unmelted portions represented reasonably accurately the structure of the alloy at that temperature during its original freezing. The results of these experiments are contained in Fig. 14, which includes also the heating arrests; approximate phase boundaries are drawn.

The existence of three constant-temperature regions in the solidus is well brought out. The highest, at 514° C., is associated with Al, CuAl₂, Mg₂Si, and Q. At slightly higher silicon contents freezing continues through a range of temperatures as the eutectic (Al + CuAl₂ + Q)

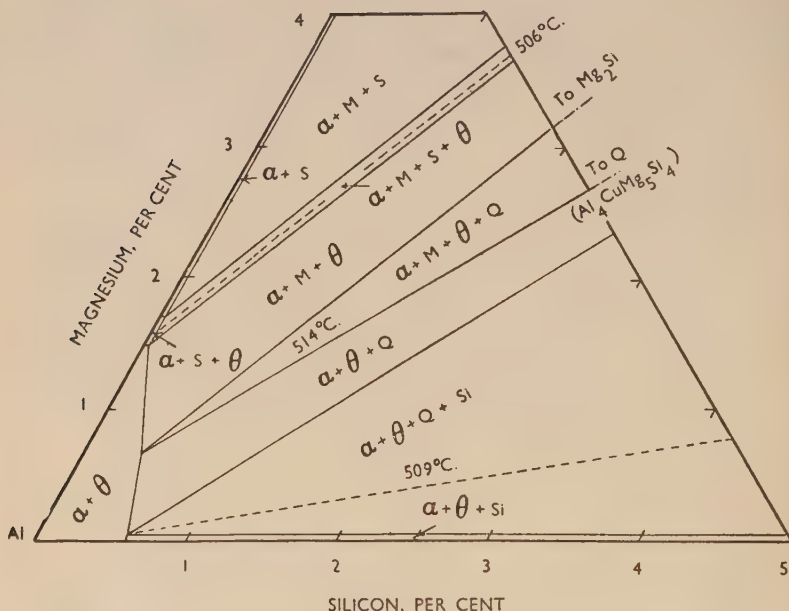


FIG. 15.—Solidus of Al-Cu-Mg-Si System at 4% Copper (approx. 510° C.).

to the second constant-temperature plane at 509° C., corresponding to the quaternary eutectic (Al + CuAl₂ + Q + Si). At lower silicon contents the temperature drops sharply to the (Al + CuAl₂ + S + Mg₂Si) plane at 506° C.; the eutectic (Al + CuAl₂ + S (with Mg₂Si)) was found only very close to the minimum in the solidus, as indicated by thermal analysis (3% magnesium, 1% silicon). The existence and range of the variant fields (Al + CuAl₂ + Q + liquid) and (Al + CuAl₂ + Mg₂Si + liquid) in Fig. 14 could properly be established only by careful isothermal treatments of homogenized material. The general form of the section is a logical development of the 4% magnesium, 4% silicon section of the copper-free system shown in Fig. 7.

On the basis of the above work, Fig. 15 was constructed to show the probable form of the system in the aluminium corner of the Al-Cu-Mg-Si system at a constant copper content of 4%. It shows the sequence and approximate extent of the various phase fields, and although it cannot claim to define their boundaries with the accuracy required of an equilibrium diagram, it throws considerable light on the phenomena really under consideration, namely the overheating temperatures of commercial alloys. The solidus temperatures reported in Fig. 15 for the three main constant-temperature areas were checked against the melting points of alloys corresponding to the compositions reported by Nishimura, Mondolfo, and Töllner, respectively, for the eutectics ($\alpha + \text{CuAl}_2 + S$), ($\alpha + \text{CuAl}_2 + \text{Mg}_2\text{Si}$), and ($\alpha + \text{CuAl}_2 + Q + \text{Si}$). The results are given in Table VII. The microstructures of these alloys were found to be as reported in the literature.

TABLE VII.—*Eutectic Melting Points.*

Eutectic	Composition			Melting Point			
	Cu, %	Mg, %	Si, %	Cast	°C.	Cast	°C.
$\alpha + \text{CuAl}_2 + S$	27	6	Nil	R.680	506.5	R.948	507
$\alpha + \text{CuAl}_2 + \text{Mg}_2\text{Si}$	28	6	3.5	681	515	949	514
$\alpha + \text{CuAl}_2 + Q + \text{Si}$	25	1.7	8.3	682	508.5	950	509.5

The temperature observed for the ($\alpha + \text{CuAl}_2 + Q + \text{Si}$) eutectic agrees very well with Töllner's value of 509.4° C. That for the ($\alpha + \text{CuAl}_2 + \text{Mg}_2\text{Si}$) eutectic is 3° C. lower than Mondolfo's value of 517° C., and that for the ($\alpha + \text{CuAl}_2 + S$) eutectic 6° C. or so higher than the value of 500° C. given by Nishimura. Such differences are unexplained, but are of considerable importance in considering heat-treatment temperatures. Fig. 15 is not strictly an isothermal section, but may be regarded as approximating to one with a mean temperature of 510° C., since practically all the solidus temperatures measured were within the range 506°–514° C.

A very small α phase field intrudes into the aluminium corner at 510° C. and at higher temperatures grows at the expense of the neighbouring ($\alpha + \text{CuAl}_2$) field. The ($\alpha + \text{CuAl}_2$) field extends between the limits 1.5% magnesium at 506° C. and 0.7% silicon at 509° C., the boundary between these limits being drawn approximately linearly in the figure for lack of any precise information. The solidus of this ($\alpha + \text{CuAl}_2$) field and of the succeeding α field rises steeply towards the aluminium corner, where it attains the temperature of 585° C. of the binary aluminium-copper system at 4% copper. The ($\alpha + \text{CuAl}_2$) field at the temper-

ature of the diagram is in contact with seven other phase fields, namely, $(\alpha + \text{CuAl}_2 + \text{Si})$, $(\alpha + \text{CuAl}_2 + Q + \text{Si})$, $(\alpha + \text{CuAl}_2 + Q)$, $(\alpha + \text{CuAl}_2 + Q + \text{Mg}_2\text{Si})$, $(\alpha + \text{CuAl}_2 + \text{Mg}_2\text{Si})$, $(\alpha + \text{CuAl}_2 + \text{Mg}_2\text{Si} + S)$, and $(\alpha + \text{CuAl}_2 + S)$, and is separated by a narrow gap from the remaining two fields of the aluminium corner $(\alpha + \text{Mg}_2\text{Si} + S)$ and $(\alpha + S)$. The $(\alpha + S)$ and $(\alpha + \text{CuAl}_2 + S)$ fields are probably very narrow, any appreciable amount of silicon causing the appearance of Mg_2Si . In the 4% magnesium, 4% silicon section shown in Fig. 14, two of the four-phase constant-temperature regions of the solidus are prominent, $(\alpha + \text{CuAl}_2 + \text{Mg}_2\text{Si} + Q)$ at 514°C . and $(\alpha + \text{CuAl}_2 + Q + \text{Si})$ at 509°C ., but these have only point contact with the $(\alpha + \text{CuAl}_2)$ boundary and consequently near this boundary the variant fields $(\alpha + \text{CuAl}_2 + \text{Mg}_2\text{Si})$ and $(\alpha + \text{CuAl}_2 + Q)$ are predominant. The four-phase area $(\alpha + \text{CuAl}_2 + \text{Mg}_2\text{Si} + S)$ is narrow and of constant width throughout the diagram, and the $(\alpha + \text{Mg}_2\text{Si} + S)$ field becomes of importance only in alloys of higher magnesium content than was considered in this work.

It should be borne in mind that only one of these four-phase fields, $(\alpha + \text{CuAl}_2 + Q + \text{Si})$ at 509°C ., represents a final eutectic actually composed of significant amounts of all four phases. Microsections corresponding to the $(\alpha + \text{CuAl}_2 + \text{Mg}_2\text{Si} + S)$ field are apparently made up of a binary $(\alpha + \text{Mg}_2\text{Si})$ eutectic followed by a ternary $(\alpha + \text{CuAl}_2 + S)$ eutectic, although in fact this latter is most probably a quaternary in which the amount of Mg_2Si is too small to be observed with certainty. The $(\alpha + \text{CuAl}_2 + \text{Mg}_2\text{Si} + Q)$ field has not been examined in sufficient detail to determine its exact derivation; the eutectics $(\alpha + \text{CuAl}_2 + \text{Mg}_2\text{Si})$ and $(\alpha + \text{CuAl}_2 + Q)$ and the peritectic $\text{Mg}_2\text{Si} \rightarrow Q$ reaction have been observed, and the constancy of the solidus temperature in this region has been confirmed, but the precise form of the diagram in Fig. 15 is not rigidly established and needs further investigation. The general form of the solidus is, however, sufficiently clear to be used as a basis for explaining the observations on overheating which form the main subject of this paper.

The result of the earlier thermal analyses on chill-cast cylinders (Fig. 2) may now be reviewed in the light of Fig. 15. More critical examination of the arrests previously regarded as constant around 514°C . shows them to be slightly higher close to the $\text{Al}-\text{Mg}_2\text{Si}$ line and to fall away slowly on each side, thus agreeing in general with the phase fields depicted in Fig. 15. This small but systematic variation in temperature (about 2°C .) could not be regarded as significant until supported by the evidence now available from a wider range of alloys.

The accompanying photomicrographs (Figs. 27-32, Plate XXV)

show characteristic features of the micrography of the alloys examined. All specimens were finished with alumina on Selvyt for preliminary visual examination, since this polished the *Q* phase slightly, and silicon definitely, in relief, making their identification easier when in small particles. For photography a flat surface was obtained with magnesia on felt. All specimens were swabbed with 0·5% hydrofluoric acid, which allowed identification of all phases except when they were present as very small particles.

Under these circumstances CuAl_2 was easily recognizable as slightly pink, outlined particles, and *S* was coloured brown. In the ternary ($\text{Al} + \text{CuAl}_2 + S$) field, which always had a very fine structure, it was sometimes necessary to etch further with nitric acid or caustic soda to distinguish between CuAl_2 and the scattered globules of aluminium within the eutectic.

The quaternary compound *Q* was very similar in colour to CuAl_2 , but was slightly harder. In the ternary or quaternary eutectics it was generally continuous with CuAl_2 , and no etching boundary developed between them; but *Q* then appeared more bluish in tint, particularly on slight defocusing. Hot 10% caustic soda solution darkened CuAl_2 , but not *Q*. Mg_2Si and silicon were readily identified.

Photographs were taken with panchromatic plates, Pointolite illumination, and a yellow filter (Ilford Micro 4).

IV.—OVERHEATING EXPERIMENTS ON DURALUMIN ALLOYS.

Simultaneously with the examination of the constitution of the Al-Cu-Mg-Si system at 4% copper, further work was carried out on the overheating of wrought Duralumin-type alloys, and the results of the two aspects of the work were correlated.

The alloys examined were made in 15-lb. melts and chill cast as $9 \times 4 \times 1$ -in. slabs which were hot and cold rolled to 0·048-in. thick strip for heat-treatment. Specimens $9 \times 1\frac{1}{2}$ -in. were solution treated in a salt bath, as previously described, at temperatures of 508°, 511°, 514°, 517°, and 520° C., and subsequently given a precipitation treatment of 1 hr. at 200° C., also in salt. These specimens each provided a standard tensile test-piece and a section for micro-examination.

The analysed compositions of the alloys are listed in Table VIII. Figs. 16, 17, and 18 show, for each quenching temperature used, the dependence of the 0·1% proof stress, ultimate tensile stress, and percentage elongation, respectively, on the magnesium and silicon contents of alloys containing nominally 4·2% copper, 0·6% manganese, and 0·5% iron. The numerical values of these properties (rounded to the nearest 0·5 ton/in.² or 0·5%) are appended to the open circles marking

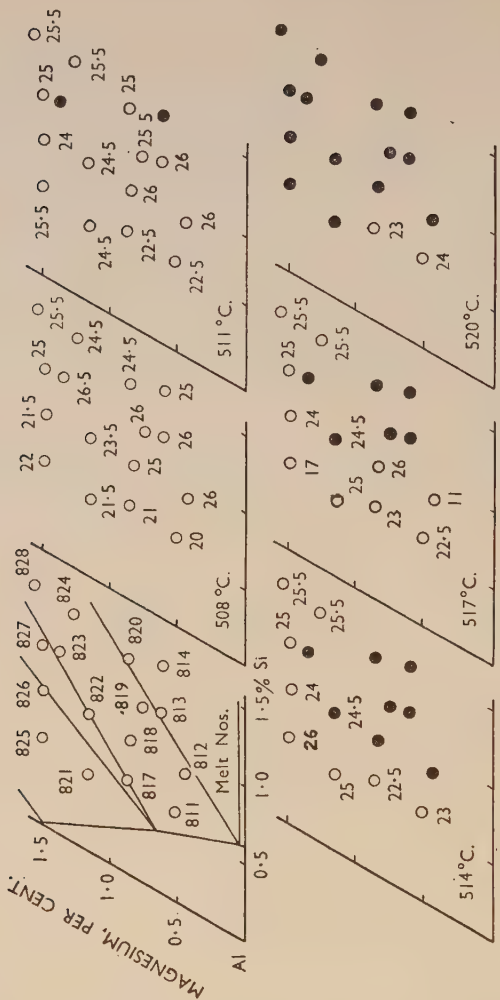


FIG. 16.—0.1% Proof Stress of Quenched Al-Cu-Mg-Si Alloys.

the composition of each alloy tested : the full circles refer to alloys which quench-cracked at the temperature in question and were, therefore, not available for tensile test. These diagrams also show the approximate boundaries at the solidus temperature of the various phase fields in the quaternary Al-Cu-Mg-Si system, as suggested in Fig. 15.

The effect of composition on overheating is most strikingly brought out by the elongation figures given in Fig. 18. No cracking occurred at 508° C. and elongations of 5.5-12.5% were obtained. At 511° C. there was cracking in the alloy XK. 814, which was most probably

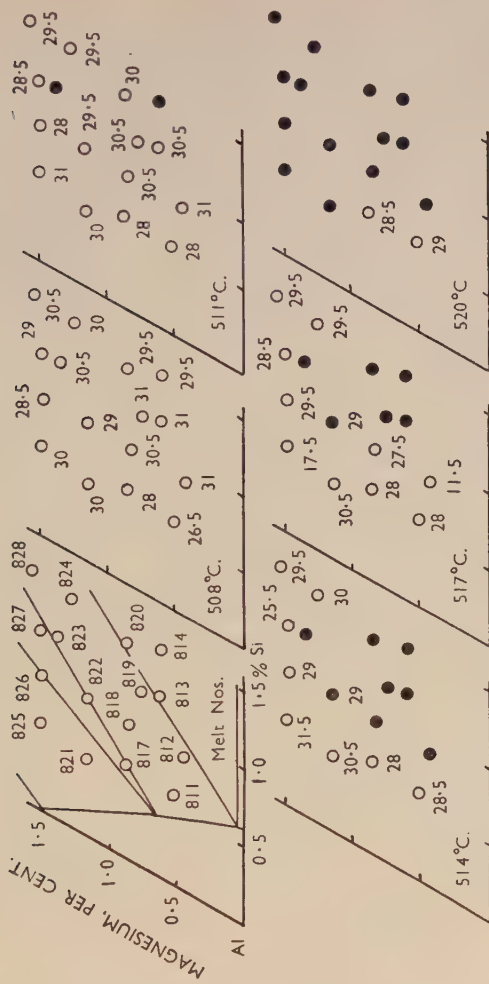


FIG. 17.—Ultimate Tensile Stress of Quenched Al-Cu-Mg-Si Alloys.

in the field of the $(\text{Al} + \text{CuAl}_2 + Q + \text{Si})$ eutectic, melting at 509° C. , and in XK. 823, which, although of lower Si : Mg ratio, had an abnormally high copper content. A significant drop in elongation was shown by almost all the alloys.

At 514° C. six more alloys quench-cracked, all in the composition range corresponding to the $(\text{Al} + \text{CuAl}_2 + Q)$ eutectic in the quaternary system, and hence melting between 509° and 514° C. Alloys 824 and 828 showed an anomalous freedom from cracking which could not be explained by variation in copper, manganese, or iron content.

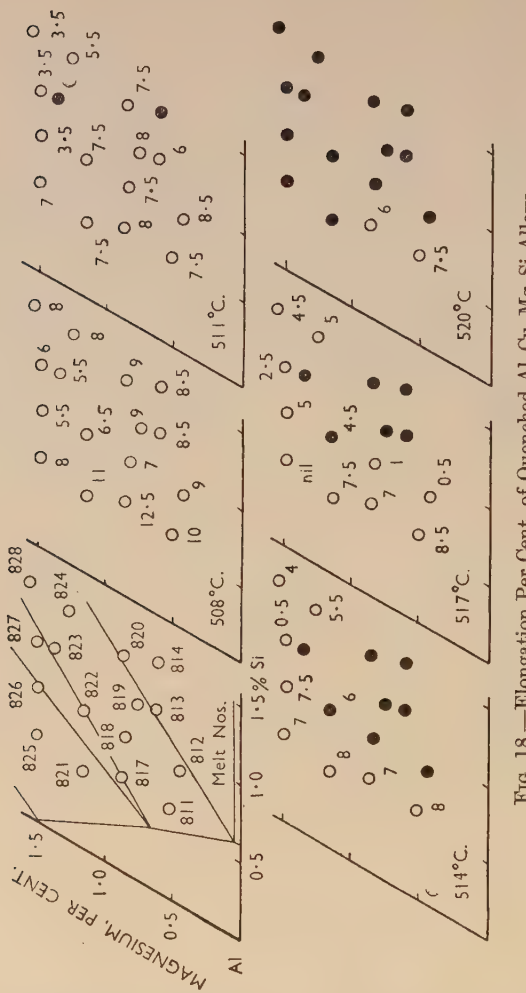


FIG. 18.—Elongation Per Cent. of Quenched Al-Cu-Mg-Si Alloys.

At 517°C . damage was shown by the same alloys, and it is interesting to note that alloys 812 and 818 did not quench-crack, although they showed negligible elongation when subsequently tested. At this temperature alloy 825 was completely embrittled, on the magnesium side of the $\text{Al}-\text{Mg}_2\text{Si}$ line. At 520°C . all alloys cracked with the exception of 811 and 817; of these, 811 was very close to the $(\alpha + \text{CuAl}_2)$ field and 817 contained only a small amount of the eutectic of highest melting point ($\text{Al} + \text{CuAl}_2 + \text{Mg}_2\text{Si}$).

The behaviour on quenching could thus be correlated quite signifi-

TABLE VIII.—*Compositions and Microstructures of Alloys Used in Overheating Experiments.*

Microstructure as Quenched from :

Cast No.	Composition					508° C.	511° C.	514° C.	517° C.	520° C.
	Cu, %	Mg, %	Si, %	Fe, %	Mn, %					
XK.809	4.4	0.83	0.80	0.13	0.10	No liquefaction.	Occasional short <i>B</i> .	Some short <i>B</i> .	Short thick <i>B</i> .	Many thick and short <i>B</i> . Many thick <i>C</i> and short <i>B</i> . "Messy", patches, no "Messy", "messy". Some <i>B</i> "messy".
810	4.3	0.85	0.77	0.21	0.39	No liquefaction.	Very occasional <i>B</i> .	Very occasional short <i>B</i> .	Scattered small rings.	Many areas continuous <i>B</i> "messy". Many clusters <i>B</i> , some <i>G</i> .
811	4.1	0.50	0.57	0.60	0.69	No liquefaction.	Occasional <i>B</i> and thin <i>C</i> , some <i>G</i> .	Very occasional short <i>B</i> .	Many areas continuous <i>B</i> "messy".	Many clusters <i>B</i> , some <i>G</i> .
812	4.1	0.43	0.85	0.55	0.69	Occasional short thick <i>B</i> , some <i>G</i> .	Occasional short thick <i>B</i> , some <i>G</i> .	Much discontinuous <i>B</i> , small <i>G</i> .	"Messy" bands.	Numerous short <i>B</i> .
813	4.4	0.69	1.13	0.58	0.70	Occasional clusters thick <i>B</i> .	Occasional short <i>B</i> .	Numerous short <i>B</i> .	Many <i>B</i> , "messy".	General heavy <i>C</i> .
814	4.4	0.59	1.34	0.54	0.67	Occasional clusters thick <i>B</i> .	Areas of thick <i>C</i> .	Thick at every <i>C</i> .	Thick <i>C</i> and many <i>B</i> .	Clusters of fine <i>B</i> .
815	3.2	0.85	0.89	0.57	0.73	No liquefaction.	Short <i>B</i> and frequent small particles in <i>B</i>	Some short thick <i>B</i> .	Some short thick <i>B</i> , grain etch. Continuous <i>B</i> and thick <i>C</i> .
816	5.4	0.90	0.89	0.60	0.69	No liquefaction.	No liquefaction.	Patches of short <i>B</i> .	Full of etched pits "Messy", "messy".	"Messy", "messy".
817	4.2	0.85	0.89	0.57	0.58	No liquefaction.	Occasional short <i>B</i> .	Occasional short <i>B</i> .	Full of etched pits "messy". Some <i>B</i> clusters.	Some <i>B</i> clusters.
818	4.1	0.81	0.85	0.59	0.58	No liquefaction.	Occasional short <i>B</i> .	Few short <i>B</i> and <i>C</i> .	Scattered thick <i>B</i> .	Large <i>C</i> pools, thick short <i>B</i> .
819	4.2	0.74	1.10	0.54	0.61	Many short thick <i>B</i> .	Few short <i>B</i> .	Many <i>C</i> and discontinuous <i>B</i> .	Some <i>B</i> networks.	Large <i>C</i> pools.
820	4.1	0.83	1.36	0.55	0.59	No liquefaction.	General <i>C</i> .	Areas of short <i>B</i> .	Scattered thin net-works.	General "messy", few real <i>B</i> .
821	4.1	1.12	0.49	0.49	0.60	Many short thick <i>B</i> and <i>C</i> .	All <i>B</i> etched as fine dots.	Very slight <i>B</i> .	Isolated thick net-works.	"Messy", short <i>B</i> .
822	4.1	1.12	0.87	0.53	0.63	No liquefaction.	Occasional thick <i>B</i>	Very many <i>C</i> .	Isolated <i>B</i> and dotted <i>B</i> .
823	4.5	1.33	1.15	0.62	0.67	No liquefaction.	Many thick <i>C</i> , small <i>G</i> .	Very many tiny <i>C</i> .	Very many <i>C</i> .	Pools heavy <i>C</i> and some <i>B</i> .
824	4.0	1.23	1.43	0.48	0.60	Traces <i>B</i> .	Some short thick <i>B</i> .	Very many tiny <i>C</i> .	Complete very thin <i>B</i> , short thick <i>B</i> .	Some short <i>B</i> .
825	4.0	1.47	0.56	0.50	0.62	Some short thick <i>B</i> .	All <i>B</i> etched finely, dotted, short thick <i>B</i> .	Many very small <i>G</i> .	Areas large <i>B</i> parti-cles in relief.	Many streaks of "messy", few <i>B</i> .
826	4.1	1.45	0.85	0.52	0.60	Occasional <i>C</i> .	All <i>B</i> etched dotted, some short thick <i>B</i> .	Some fine <i>B</i> .	Small clusters <i>B</i> .	Full of small <i>C</i> and pools.
827	4.1	1.47	1.13	0.49	0.62	Occasional <i>C</i> .	Some short thick <i>B</i> , some dotted <i>B</i> .	Some short thick <i>B</i> .	"Messy", many small <i>C</i> .	Many small <i>C</i> .
828	4.1	1.52	1.48	0.52	0.61	Occasional <i>B</i> .	Some short thick <i>B</i> .	Occasional <i>B</i> .	Thin <i>B</i> .	Fine <i>B</i> , small <i>C</i> .
829	4.1	0.85	0.85	0.04	0.06	No liquefaction.	<i>B</i> dotted.

C indicates definite liquefaction at grain corners (junctions).

B indicates abnormal structure at grain boundaries.

G indicates rounded globules.

cantly with the metallographic features demonstrated in Section III; the correlation was necessarily not completely quantitative, since the phase boundaries were not established precisely, and also because the alloys were deliberately not homogenized to bring them into equilibrium, and hence they contained the lower-melting eutectics ($\text{Al} + \text{CuAl}_2 + Q + \text{Si}$) and ($\text{Al} + \text{CuAl}_2 + Q$) nearer to the $\text{Al}-\text{Mg}_2\text{Si}$ line than would be the case under equilibrium conditions.

Incidentally, the diagrams show a surprisingly small variation in mechanical properties for the undamaged alloys over the whole range of magnesium and silicon contents. Very notable is the identity of tensile strength of alloy 812 (0.4% magnesium, 0.8% silicon) with alloy 828 (1.5% magnesium, 1.5% silicon). The 0.1% proof stress varied somewhat widely, being apparently highest for the ($\text{Al} + \text{CuAl}_2 + Q$) field. For most of the alloys which could be examined over a range of temperature, there was a slight but consistent increase in strength with increasing temperature of quenching. It should be borne in mind that the standard precipitation treatment given was not necessarily the optimum for all alloys, and that the mechanical properties displayed should not be regarded as typical of material produced on a commercial scale.

Figs. 19 and 20 are concerned with the effect of the other elements—copper, manganese, and iron—on an alloy containing 0.8% magnesium and 0.8% silicon, and show proof stress, ultimate stress, and elongation plotted against temperature of quenching for each uncracked specimen. It is apparent from Fig. 19 that 5.2% copper gave the strongest material, but caused cracking at 511°C . as compared with 514°C . for the normal material containing 4.2% copper; whilst with 3.2% copper the alloy could be heated to 520°C . without cracking, but had then not quite attained the same strength. The metallography of these alloys of varying copper contents was not studied, but it is reasonable to conclude that at the higher copper content the field of the 509°C . eutectic moves to lower magnesium and silicon contents and at lower copper contents moves to higher magnesium and silicon contents.

From Fig. 20, it is clear that with lower manganese and iron contents the alloys containing 4.2% copper, 0.8% magnesium, and 0.8% silicon, could be quenched from higher temperatures without cracking, but the significance of this is not known. If iron and manganese played a part in removing copper and silicon as complexes at high temperatures, the opposite effect would be expected.

The microstructures of all the quenched specimens were carefully examined in an attempt to correlate quench-cracking with the incidence of grain-boundary liquefaction. The microsections were given the best

possible surface finish with magnesia and were examined after an etch with 0·5% hydrofluoric acid just sufficient to show normal unliquefied grain boundaries as faint watery lines. A magnification of 500 dia. was standardized for general examination, although higher magnifications were employed for the resolution of fine structures. Sodium hydroxide and nitric acid etches were used from time to time, but in

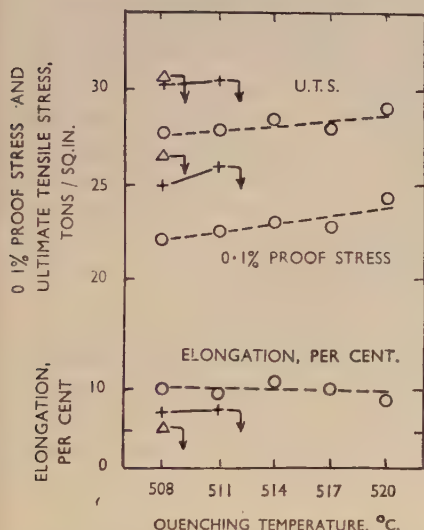


FIG. 19.—Effect of Copper on Properties of Alloy Containing Magnesium 0·8, Silicon 0·8%.

KEY.
 △ 5·2% copper.
 + 4·2% copper.
 ○ 3·2% copper.

↓ signified that the alloy cracked at the next highest temperature.

general the hydrofluoric etch was preferred, because it allowed better differentiation of boundary phases.

The results are summarized in Table VIII. Several distinctive metallographic features could be associated with particular ranges of composition or temperatures of quenching. Of the specimens quenched at 508° C., the majority showed no indication at all of liquefaction, although in a few alloys occasional minute rod-like particles were to be seen in the grain boundaries. As the quenching temperature was raised, signs of liquefaction appeared in more and more specimens and increased

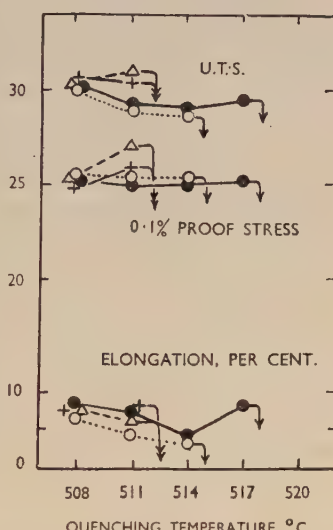


FIG. 20.—Effect of Manganese and Iron on Properties of Alloy Containing Copper 4·2, Magnesium 0·8, Silicon 0·8%.

KEY.
 + 1·1% (manganese + iron).
 △ 0·6% (manganese + iron).
 ○ 0·23% (manganese + iron).
 ● 0·1% (manganese + iron).

in extent until, at 520° C., practically every specimen showed the well-known grain-boundary films and grain-corner pools of obviously overheated material. Significant differences could, however, easily be recognized in the mode of liquefaction of different specimens and could be attributed to the different eutectic liquids responsible. The alloys in which the eutectic ($\text{Al} + \text{CuAl}_2 + Q + \text{Si}$) would be expected generally liquefied in what might be termed the orthodox manner. As the temperature was raised, short, clearly defined rods and "hooks" appeared in the grain boundaries (Fig. 22, Plate XXIV), extending into complete networks and finally into obvious grain-boundary pools (Fig. 21, Plate XXIV). Alloys near the $\text{Al}-\text{Mg}_2\text{Si}$ line, in which the ($\text{Al} + \text{CuAl}_2 + \text{Mg}_2\text{Si} + Q$) field would be the critical plane, gave a much less complete development of grain-boundary films, and at 517° and 520° C. showed a random distribution of ragged pools of rapid-etching eutectic which gave the microstructure an appearance most aptly described as "messy" (Fig. 25, Plate XXIV). In the alloys 821 and 825, which were most definitely on the magnesium-rich side of the $\text{Al}-\text{Mg}_2\text{Si}$ line, the grain boundaries etched completely at all temperatures, as discontinuous fine dots at the lower temperatures and as continuous very fine lines at the higher ones. This was probably to be attributed to a small amount of the ($\text{Al} + \text{CuAl}_2 + S$) eutectic which melts at 506° C. (Fig. 26, Plate XXIV). The alloy 826 combined this behaviour with the development of "messy" areas in the specimens quenched from 517° and 520° C.

This series of sheet alloys showed very few rounded globules of eutectic within the grains, in marked contrast to those of the first series. It can only be assumed that the better homogenization and a greater degree of working of the second series removed most of the local heterogeneities which caused the globule formation in the earlier alloys. That some heterogeneity on a micro-scale still existed in the present series was evident from the local variations in amount of liquefaction; such heterogeneity was, however, not dissimilar from the amount shown by commercially produced sheet of this type.

In general, therefore, the results of the quench-cracking experiments were in agreement with the microstructural indications, and as might be expected from the solidus temperatures determined for the $\text{Al}-\text{Cu}-\text{Mg}-\text{Si}$ quaternary system. Significant amounts of quenched liquid first appeared in the alloys of highest Si : Mg ratio, and hence nearest to the field of the ($\text{Al} + \text{CuAl}_2 + Q + \text{Si}$) eutectic melting at 509° C. This eutectic developed characteristically at grain boundaries. Alloys nearest the $\text{Al}-\text{Mg}_2\text{Si}$ line required the highest temperature for damage by overheating, not only because the solidus was highest but also because

the liquid appeared mainly as disconnected pools and hence did not so drastically weaken the structure. The alloys examined did not include any of Si : Mg ratio low enough to be really in the field of the (Al + CuAl₂ + S) eutectic, melting at 506° C.

V.—GENERAL DISCUSSION.

The work reported above was intended to examine the effective solidus temperature of commercial Duralumin-type alloys containing approximately 4% copper, 0.7% manganese, 0.6% magnesium, 0.6% iron, 0.8% silicon, and to investigate the effect of variation in chemical composition, particularly variation of the magnesium and silicon contents. Thermal arrests obtained on heating chill-cast alloys indicated a solidus characterized by two constant-temperature regions at 509° and 514° C. The onset of liquefaction and the incidence of quench-cracking in sheet alloy confirmed these temperatures, and established an essential difference in the mode of liquefaction in the two regions.

A brief examination of the quaternary system Al-Cu-Mg-Si at constant 4% copper content revealed the existence of identical solidus planes in that system and showed them to belong to (Al + CuAl₂ + (AlCuMgSi) + Si), 509° C., and (Al + CuAl₂ + Mg₂Si with (AlCuMgSi)), 514° C., with a variant region of (Al + CuAl₂ + (AlCuMgSi)) between.

At higher Mg : Si ratios than that corresponding to Mg₂Si, a further constant-temperature plane existed, that of (Al + CuAl₂ + Al₂CuMg (in the presence of Mg₂Si)), at 506° C.

It was demonstrated that the highest solidus temperatures existed at Mg : Si ratios close to that of Mg₂Si; these alloys possessed the greatest resistance to quench-cracking, not only because of their high solidus temperatures but also because the characteristic mode of liquefaction was in disconnected pools. At higher silicon contents, the temperature at which damage by overheating occurred decreased; the solidus temperature fell and the (Al + CuAl₂ + (AlCuMgSi)) and (Al + CuAl₂ + (AlCuMgSi) + Si) eutectics appeared preferentially as grain-boundary films. At higher magnesium contents the solidus fell to 506° C. and the (Al + CuAl₂ + Al₂CuMg) eutectic formed at the grain boundaries, but this region was not critically examined. An interesting result of the qualitative dependence of the structure on the Mg : Si ratio was the fact that an alloy containing only 0.5% magnesium and 0.57% silicon quenched-cracked at 514° C., whereas another with 1.5% of each element did not; whilst the tensile properties of the two alloys as quenched at 511° C. showed the former to be slightly the stronger.

The identity of temperature of the constant-temperature planes in the quaternary system Al-Cu-Mg-Si and the more complex Al-Cu-Mg-

Si-Mn-Fe system of the Duralumin-type alloys suggested that neither iron nor manganese entered into the constitution of the final eutectics, and hence these elements affected only the extent of the solidus phase fields in a secondary manner by removing a certain amount of copper and silicon from the melt at temperatures near the liquidus. This was not in agreement with the results of cracking tests on alloys with varying manganese and iron contents, but this aspect of the problem was not examined further.

In conclusion, it should be pointed out that although quench-cracking was fairly consistently obtained in these experimental alloys, this was probably due to the very rapid quench which was possible, and that in commercial practice cracking, even of distinctly overheated material, is of relatively infrequent occurrence.

ACKNOWLEDGEMENTS.

The author wishes to record his indebtedness to Miss B. H. Thornelow, who made the small-scale melts and carried out the thermal analysis, and to Mr. F. G. Abbott, who bore the brunt of the extensive micro-graphic work; to Mr. C. Smith, F.I.M., Chief Metallurgist of Messrs. James Booth and Company, Ltd., for his counsel at all stages of the work; and to Mr. D. H. H. Clarke, M.A., A.M.I.Mech.E., for his continued interest and for permission to publish the results.

REFERENCES.

1. F. Keller and R. A. Bossert, *Metal Progress*, 1942, **41**, 63.
2. E. Hoffmann-Möckel, *Aluminium*, 1939, **21**, 759.
3. Herm. A. J. Stelljes, *Aluminium*, 1936, **18**, 601.
4. C. Panseri and M. Monticelli, *Alluminio*, 1939, **8**, 183.
5. J. R. Heising and E. H. Burkart, *Metal Progress*, 1942, **42**, 1027.
6. N. H. Mason, G. J. Metcalfe, and B. W. Mott, *J. Inst. Metals*, 1944, **70**, 197.
7. H. W. L. Phillips and P. C. Varley, *J. Inst. Metals*, 1943, **69**, 317.
8. V. Fuss, "Metallography of Aluminium and Its Alloys". London : 1936 (Chapman and Hall).
9. A. G. C. Gwyer, H. W. L. Phillips, and L. Mann, *J. Inst. Metals*, 1928, **40**, 297.
10. H. W. L. Phillips, *J. Inst. Metals*, 1941, **67**, 257.
11. A. T. Little, W. Hume-Rothery, and G. V. Raynor, *J. Inst. Metals*, 1944, **70**, 491.
12. H. Nishimura, *Nippon Kinzoku Gakkai-Si*, 1937, **1**, 8.
13. G. G. Urazov and D. A. Petrov, *Zhur. Fiz. Khim.*, 1946, **20**, 387.
14. E. H. Dix, Jr., G. F. Sager, and B. P. Sager, *Trans. Amer. Inst. Min. Met. Eng.*, 1932, **99**, 119.
15. D. A. Petrov, *Acta Physicochim. U.R.S.S.*, 1937, **4**, 505.
16. L. F. Mondolfo, "Metallography of Aluminium Alloys". New York : 1943 (John Wiley and Sons).
17. H. Töllner, *Aluminium-Arch.*, 1940, (34).
18. K. Matsuyama, *Kinzoku no Kenkyu*, 1934, **11**, 461.
19. G. G. Urazov, S. A. Pogodin, and G. M. Zomoruev, *Mineral. Syrie i Tsvet. Metally*, 1929, **4**, 160; and *Izvest. Inst. Fiziko-Khim. Anal.*, 1931, **5**, 157.
20. C. Hisatsune, *Mem. Coll. Eng. Kyoto Imp. Univ.*, 1935, **9**, 18.
21. W. Hofmann and H. Wiehr, *Aluminium*, 1940, **22**, 592.
22. G. V. Raynor, *Inst. Metals Annotated Equilib. Diagr.* No. **4**, 1944.
23. M. Hansen, "Der Aufbau der Zweistofflegierungen". Berlin : 1936 (Julius Springer).

THE MECHANISM OF DEFORMATION IN 1217 METALS, WITH SPECIAL REFERENCE TO CREEP.*

By W. A. WOOD,† D.Sc., MEMBER, and W. A. RACHINGER,‡ M.Sc.

SYNOPSIS.

A study has been made of the changes in crystalline structure produced at various temperatures when a metal is subjected to the slow rate of strain typical of the creep process and also to the relatively rapid rate associated with ordinary mechanical testing. Measurements were made at the same time of the strength developed in the metal under the various conditions of deformation. The object was to investigate the underlying mechanisms of deformation and in particular the relation of deformation by creep to the more familiar deformation by slip. The results show that the grains develop a sub-structure of a size determined by the temperature and rate of strain. The mechanism of deformation changes from slip to creep as the elements of the sub-structure exceed a certain size. For a given rate of strain the size of the elements in the sub-structure is larger the higher the temperature; for a given temperature the elements are smaller the more rapid the rate of strain. The strength and strain-hardening capacity of a metal decrease as the sub-structure becomes coarser, and on this observation an explanation of creep is based.

I.—INTRODUCTION.

IN recent work a study was made of the mechanism by which a metal deforms at elevated temperatures, with special reference to the slow, continued deformation under constant stress which has become known as creep.¹ The mechanism was shown to be quite different from the familiar mechanism of slip which characterizes deformation at normal temperatures and at the usual rates of straining. The main difference was that as the temperature was raised and the rate of deformation was lowered, the slip process became progressively superseded by one which resulted in the dissociation of the grains into quite coarse elements, and which permitted deformation by the relative movement of these elements in the grains without the formation of slip lines or without reference to specific slip planes.

In recent years attention has been drawn to the presence of sub-structures in metallic grains, especially by Lacombe and Beaujard,² Cahn,³ and Guinier and Tennevin.⁴ Their work deals in the main,

* Manuscript received 30 March 1949.

† Acting-Professor of Metallurgy Research, Baillieu Laboratory, University of Melbourne, Australia.

‡ Aeronautical Research Laboratories, Department of Supply and Development, Melbourne, Australia.

however, with recovered or recrystallized grains. There may be some connection with the sub-structures studied here, but the present work differs fundamentally in tracing a sub-structure arising in *deformed* grains in a manner varying according to the mode of deformation.

The principal factors determining the sub-structure under consideration appear to be : (a) temperature of deformation, (b) rate of strain, (c) grain-size of the metal, (d) degree of previous cold work, and (e) the purity of the metal. In the present paper the factors studied are mainly the temperature and the rate of strain, aluminium being used as the test material. In addition, the variations produced by these factors in the size and perfection of the sub-structure have been correlated with the rate of strain-hardening developed during the course of deformation. In particular, it has been shown that with a sufficiently coarse sub-structure the rate of strain-hardening is negligibly small, and this condition has been put forward, therefore, as that permitting the process of creep.

II.—EXPERIMENTAL.

1. *Method of Straining.*

In creep testing a specimen is normally subjected to a constant load at a given temperature, and the deformation measured over a long period of time. In the present tests it was decided to deform the test specimens at a given temperature but at an approximately constant rate of strain from the beginning of the test. It was realized that, as with creep experiments, this is an arbitrary method of testing. But it has some advantages. It makes the rate of strain the controlling factor, as distinct from an applied load; and, after all, it is the strain in the metal which directly determines the changes in internal structure. Further, the specimens can be in a standard annealed condition before the constant rate of strain is imposed, whereas in the ordinary creep test the constant rate of strain in the secondary stage is preceded by the unknown effects of the deformation in the primary stage. Finally, it lends itself to a continuous-recording method of measuring the strength, for it is a simple matter to insert a weigh-bar in series with the test specimen and read off the tension required to extend the specimen at any moment from an extensometer indicating the elastic strain in the weigh-bar.

The apparatus constructed for the purpose was quite straightforward and need hardly be described in detail. One end of the specimen was held fixed, while the other was linked by a connecting rod to one end of the weigh-bar. The further end of the latter was joined by a wire cable to a pulley which extended the specimen as it rotated. The pulley was fixed to the final spindle of a chain of gears, with a step-down ratio

38,000,000 to 1, driven by a synchronous motor. The rate of strain was obtained from the angular rotation of the gear wheels and checked by final measurements between calibration marks on the specimen. The rate of strain obtained in this way was 0·1% extension per hr., which, it was found, was as fast as could be conveniently imposed without losing the structural changes shown in the previous paper to be characteristic of secondary creep. The term "slow straining" in the present paper will refer to specimens extended at this rate.

Specimens could be extended also at approximately 10% per min., a rate considered comparable with the rates used in ordinary tensile testing. For this purpose the "fixed" end of the specimen was attached by a connecting rod to an adjustable yoke which permitted the specimen to be stretched directly by a screw movement turned by hand. This will be referred to as "rapid straining".

At each temperature of testing, a special feature was made of comparing the changes in structure of specimens strained at the above slow and rapid rates.

The usual precautions were taken to ensure that during a test the tension was exerted axially along the specimen and weigh-bar, by having universal joints between the specimen grips and the various connecting rods and cables. In addition, the specimen itself could be surrounded by a furnace capable of maintaining a uniform temperature along the gauge length.

The standard form of specimen adopted was that of a flat tensile test-piece, 0·036 in. thick and with a parallel gauge length of $2 \times \frac{1}{2}$ in. It was found easier to obtain a uniform structure across flat specimens than across large cylindrical specimens such as would normally be used in creep testing.

For convenience the same form of specimen was used for the weigh-bar, but in this case the material was mild steel. The stresses involved in extending the aluminium were never more than a few tons/in.² and therefore were well within the elastic range of the steel. The elastic strain was determined by two Tuckerman extensometers attached one on each side of the weigh-bar, and the equivalent tension was obtained from preliminary experiments giving the stress-strain relationship for the weigh-bar under direct loading.

It would be difficult to obtain an absolutely uniform rate of extension of a test-piece under the above conditions if the desired rate of strain were very low, because of the stretching of the weigh-bar itself and variations in the gear-wheels. But at the rates of strain employed in the present work, changes due to these factors were not significant.

2. Material and Procedure.

The material studied was aluminium of 99.98% purity, kindly supplied by the British Aluminium Company, Ltd., in the form initially of cold-rolled sheet. From this, specimens were machined to the dimensions already indicated and then annealed to give a grain-size of approximately 0.1 mm. Apart from a few coarse-grained specimens prepared for special tests, this grain-size was adopted as standard.

The specimens were then polished electrolytically in a standard bath of perchloric acid and acetic anhydride so as to avoid any preliminary cold working of the surfaces. They were subjected to a preliminary examination by X-ray diffraction to ensure that the grains were of the appropriate average size and were structurally as perfect as possible. The X-ray method found most useful was that of back-reflection from a stationary specimen. The radiation employed was the cobalt $K\alpha$ which, with a specimen-film distance of 10 cm., gave the (420) reflection ring with the $\alpha_1\alpha_2$ doublet well resolved. An essential feature of the initial condition of the specimens was that the grains should give a ring consisting of sharp spots well separated from each other.

The procedure then was to take at least two specimens and strain them at a selected temperature, one specimen being strained at the slow rate and the other at the rapid rate. At comparable degrees of extension the specimens were cooled, and a note was made of the changes in structure, as shown by the changes produced in the initially polished surfaces and in the state of the X-ray reflection spots. At the same time these changes were studied in relation to the plot of stress against extension, which was given by the extensometer indications on the weigh-bar. The procedure was then repeated with similar specimens at other temperatures which in practice ranged from 500° C. to room temperature, in steps of some 50° C.

III.—RESULTS.**1. Development of the Sub-Structure in an Individual Grain.**

Before proceeding to the main body of the results it will be convenient to consider a special case designed to bring out specifically the changes produced by the deformation in the individual grain. For this purpose it was necessary to use a relatively coarse-grained specimen, so that the X-ray reflections were widely separated on the reflection ring; any spread of the reflections caused by deformation did not then result in overlapping. These special conditions were met in the present experimental arrangements by the use of specimens of 1 mm. grain-size, in contrast to the otherwise standard grain-size of 0.1 mm.

The results in this Section, therefore, refer to specimens of such a

grain-size subjected to slow and rapid straining respectively, at a fixed elevated temperature, namely 350° C. The observations will serve to simplify the interpretation of the changes found in the standard finer-grained material which are discussed later. They bring out, in particular, the quite different effects of the two rates of straining.

(a) *Structural Changes During Slow Straining.*

The effects of slow straining are described by reference to a typical specimen examined after extensions of 3·8, 8·7, 13·5, and 25·4%, carried out at the slow rate of 0·1% per hr. The changes are illustrated by X-ray photographs and a photomicrograph. It is desired to draw attention to the following points.

(i) *Evidence for the Sub-Structure.*—Fig. 1 (Plate XXVI), the X-ray photograph from the specimen before straining, shows a few single reflection spots, each evidently from a single grain of homogeneous orientation. Figs. 2 and 3 (Plate XXVI), obtained after straining to 3·8 and 8·7% extension, show that the initial reflections have split into groups of smaller, sharp spots scattered over a short arc. This comparison constitutes a simple but conclusive proof that the original grains have broken down into discrete smaller elements distinguished by differences in orientation. (In these Figures, the same point on the specimen was photographed as nearly as possible, but perfect repetition was impossible owing to extension of the specimen; the photographs show, however, to a close approximation, changes in the same initial reflection spots.)

(ii) *Scatter of Orientation in Sub-Structure.*—It is useful to note first the high sensitivity of the X-ray back-reflection method in detecting changes of orientation. Under the present conditions, a change in orientation of an element of the sub-structure by 1° would move the corresponding reflection spot approximately 5 mm. along the circumference of the reflection ring. It will be noted from Figs. 2 and 3 that the secondary reflection spots are separated by about 0·5 to 1 mm. and are scattered over arcs of length from 1·5 to 2 cm. Therefore it can be concluded that the neighbouring elements of the sub-structure differ in orientation by about 0·1°-0·2° and that the range of scatter over a whole grain is of the order of 4° or 5°. This order of change was typical of other specimens examined.

It was found further that the divergence in orientation of the elements from the parent grain grew rapidly in the early stages of deformation, but then tended to a steady value, which was of the order of the 5° just mentioned.

(iii) *Perfection of the Elements of the Sub-Structure.*—The X-ray back-

reflection method is also highly sensitive to volume distortion of the atomic lattice, which results in diffusion of the X-ray reflections. It was found, however, that very soon after the beginning of deformation, the reflection spots were always quite sharp, and moreover remained sharp throughout subsequent deformation. The sharpness may be noted by reference to Figs. 2 and 3 (Plate XXVI). It was concluded, therefore, that each element of the structure was internally virtually free from distortion and became at least as perfect as the structure of the original annealed grains. Any distortion present was small and was presumably entirely confined to the sub-boundaries between the elements, where it would be too localized for detection.

(iv) *Size of Sub-Structure.*—The size of the elements was estimated from the number of spots formed on the reflection arcs, and for the case under consideration was about 10^{-3} cm. It will be shown later that this size is a function of the temperature and rate of strain. The point to which it is desired to draw attention here is the general observation that for a given temperature and rate of strain the size of the elements tended to a definite value with increasing extension of the specimen. This conclusion followed from the fact that the number of reflection spots on the arcs was virtually the same after 25·4% extension as after 3·8 and 8·7%; it was the same even after the specimen had been extended by some 50% to fracture.

(v) *Microstructure.*—The photomicrograph in Fig. 4 (Plate XXVI), obtained after 25·4% extension, illustrates the further observation that when the deformation is such as to produce the coarse sub-structure described above, it takes place by a mechanism other than the familiar one of slip; for the photograph shows no signs of slip lines. Instead, the polished surface of the grains exhibits irregular markings which confer a cellular appearance. This, together with the X-ray evidence of the breaking down of the grains to form a sub-structure, is taken to indicate a process whereby the grains deform by relative movement of the coarse elements of the sub-structure.

The magnification of Fig. 4 is 100 dia., so that one grain occupies most of the field. A short length of the original grain boundary is included at the bottom left-hand corner. This illustrates the apparent thickening which is characteristic of creep deformation and which is due presumably to relative movement at the boundaries of neighbouring grains. The photograph illustrates also, however, the network of markings produced by deformation within the grain and, in the centre of the field, shows a thickening of these markings which was often to be observed. This was considered to confirm the relative movement at the sub-boundaries between the elements of the sub-structure.

(vi) *Cell Mechanism*.—Slow deformation at an elevated temperature thus takes place by a distinct mechanism characterized by dissociation of the grains into the coarse elements and the absence of slip formations. In the previous paper¹ this was described as the “cell mechanism” to distinguish it from the normal mechanism of deformation by slip. For convenience the same expression will be retained in the present paper.

(b) *Structural Changes During Rapid Straining.*

The next observations refer to a specimen comparable with the above but strained at the rapid rate. They demonstrate the fundamental differences in behaviour of the structure at the slow and rapid rates of strain.

(i) *X-Ray Structure*.—The X-ray examination showed very marked differences, as is evident from Figs. 5 and 6 (Plate XXVII), which were obtained after a specimen had been extended by 3·3 and 7·5% respectively. These photographs show that the original single reflection spots, which were comparable with those in Fig. 1, become transformed into arcs which now consist of irregular diffuse reflection spots superposed on a strong background of continuous line. Therefore the difference from the effects of slow straining is that while the grains still break up into elements of different orientation these elements are irregular in size, probably distorted in structure, and accompanied by very fine fragments which produce so many reflections that the larger spots appear to coalesce. There is no longer a division of the grains into a clearly marked sub-structure of perfect elements.

(ii) *Microstructure*.—This aspect of the structure is illustrated by Fig. 7 (Plate XXVII), obtained after 7·5% extension, which shows the further fundamental difference that the rapid extension has taken place wholly by the slip mechanism, in contrast with the slow straining at the same temperature which took place predominantly by the cell mechanism. The slip lines on rapid straining are sharp and well marked and, as is also shown by the photograph, the apparent thickening of the grain boundaries noted in the slow deformation is also absent.

The preceding results on coarse-grained material thus characterize the features of the sub-structure formed in the separate grains by deformation at an elevated temperature, and serve also to distinguish between the cell mechanism characteristic of slow deformation and the slip mechanism characteristic of rapid deformation. In the following Sections are described the modifications produced in these sub-structures when the temperature of deformation is altered. These modifications are shown best by reverting to the standard fine-grained specimens, and the further results refer only to such material.

2. Sub-Structure Formed by Slow Straining at Different Temperatures.

The next observations are most conveniently presented by reproducing side by side the X-ray photographs and photomicrographs obtained from specimens subjected to similar elongations at different temperatures. The illustrations then form the following series, in which even numbers refer to X-ray photographs and odd numbers to the photomicrographs, the latter being at 100 dia. magnification.

	Condition before straining.		
Fig. 8 (Plate XXVII).			
Figs. 9, 10 (Plate XXVIII).	After 7%	slow extension at 350° C.	
Figs. 11, 12 (Plate XXVIII).	" 8%	"	300° C.
Figs. 13, 14 (Plate XXIX).	" 9%	"	250° C.
Figs. 15, 16 (Plate XXIX).	" 9%	"	200° C.
Figs. 17, 18 (Plate XXX).	" 8%	"	150° C.
Figs. 19, 20 (Plate XXX).	" 8%	"	110° C.
Figs. 21, 22 (Plate XXXI).	" 9%	"	20° C. (room temperature).

(a) *Variation in Size of Sub-Structure with Temperature.*

The observations in this Section will show that the slow deformation at each temperature proceeds by essentially the same mechanism, namely the dissociation of the grains into relatively perfect elements; but that the size of the elements becomes systematically smaller as the temperature of deformation is reduced.

To illustrate the above points it is convenient to begin with the structure formed at 350° C. and to consider the X-ray photographs. First, it will be noted that the sharp reflection spots typical of the original material are replaced after deformation at 350° C. by a set of equally sharp but more numerous spots. It will be clear at once from the previous discussion of the coarse-grained specimens, that this multiplication of the reflection spots provides a straightforward proof that the grains have dissociated into discrete elements. Further, the sharpness of the secondary reflections shows also, as before, that the elements are as perfect in structure as the annealed parent grains. Finally, the size of the elements, as estimated from the number of reflections, is approximately 7×10^{-4} cm.; this size may be regarded as typical of the slow deformation at 350° C., since it was found that the number of spots on the ring did not change appreciably after still further deformation.

Next, the effect of reducing the temperature of deformation may be seen by referring to the succession of X-ray photographs covering the range from 350° to 20° C. This series, viewed as a whole, shows at once a systematic progression in the number of reflection spots on the rings as the temperature is reduced. Thus at 350° C. the spots are well separated, while at 20° C. they are packed so closely that the diffraction

ring appears continuous. The number of spots on the rings is known to be proportional to the number of reflecting elements in the volume covered by the incident X-ray beam and therefore inversely proportional to their size. Consequently the multiplication of the spots as the temperature of deformation decreases indicates in a direct manner a systematic and progressive reduction in size of the sub-structure. Approximate estimates of the size of the elements are: 7×10^{-4} cm. at 350° C., 5×10^{-4} cm. at 300° C., decreasing regularly through 2×10^{-4} cm. at 150° C. to roughly 10^{-4} cm. at room temperature.

At each temperature the individual reflection spots are relatively sharp and discrete. Even at room temperature the individual spots can just be discerned on the original negative and print, even though the ring might at first sight appear continuous. Therefore, at each temperature, deformation has proceeded by a similar relative movement of the discrete elements into which the grain has dissociated, and these elements, whatever their size, have remained relatively perfect in internal structure. This latter point is especially interesting in connection with the slow deformation at room temperature; it means that extensive lattice distortions are not an inevitable or essential accompaniment of plastic deformation, as is so often assumed.

(b) *Transition from the Cell to the Slip Mechanism of Deformation.*

It will next be shown that there is a transition from the cell mechanism to the mechanism of deformation by slip as the elements composing the sub-structures become less than a critical size.

This point is brought out by a comparison of the corresponding X-ray photographs and photomicrographs obtained at the various temperatures of deformation and set out according to the above list of illustrations. As already indicated, the cell mechanism is marked by an absence of slip lines. Now this absence is to be noted in the photomicrographs corresponding to deformation at the higher temperatures of 350° , 300° , and 250° C. But as the temperature of deformation decreases to 200° C. slip lines make their appearance in occasional grains, although the lines are rather thick, irregular, and widely spaced. When the temperature is further reduced to 150° C. it will be seen that most of the grains have deformed by slip and that the slip lines are sharper and more regular; while at the still lower temperatures of 110° and 20° C. the deformation is wholly by slip, with the lines relatively sharp and closely spaced. Therefore there is a transition from the cell mechanism to the slip mechanism at about 200° - 150° C.

This change from the cell to the slip mechanism is of special interest when it is recalled that the corresponding X-ray photographs show only

a progressive refinement of the sub-structure as the temperature of deformation is reduced from 350° C.; there is no abnormality in the range 200°–150° C. Therefore it is reasonable to conclude that the appearance of the slip mechanism is associated with a reduction in the elements of the sub-structure to a size less than a critical value, which in the present conditions of experiment is approximately 4×10^{-4} cm., the size reached about 200° C. Thus it would appear that at each temperature the mechanism of deformation requires the formation of a sub-structure, but that the boundaries of the elements tend to become defined by specific crystallographic slip planes as the size of the sub-structure becomes small.

The photographs show further that there is a general relation between the size of the elements and the spacing of the slip lines. As the sub-structure increases in size with increasing temperature of deformation, the slip lines become more widely spaced, as well as more irregular and apparently thicker. It is hoped to follow this relation further in other work. It suggests that the elements of the sub-structure may correspond at first with the regions between the slip lines; and it might then explain why the coarse sub-structures show so little distortion as a result of deformation; for it could be assumed that any distortion essential to the deformation was confined to a few atomic planes about the slip planes or sub-boundaries which, in the coarse sub-structures, become reduced in number.

Although a value has been given for the size of the elements at the transition from the cell to the slip mechanism, it will be evident that this critical size might vary under different conditions of experiment, involving, for example, different rates of strain and specimens of different purity or grain-size. The important point, however, is that such a transitional size exists, whatever its absolute value.

3. Variation of Sub-Structure with Rate of Strain.

In this Section it will be shown that, at a given temperature of deformation, the average size of the elements in the sub-structure decreases as the rate of strain is increased, and that the resulting sub-structure is roughly equivalent to that which would be produced by less rapid deformation at a lower temperature.

Then conclusions follow drawn from a comparison of the structures of the slowly strained specimens just discussed with those of specimens extended by comparable amounts at the same temperatures at the rapid rate of strain, which was approximately 10% per min. The evidence is again best presented by reproducing side by side the X-ray photographs

and the corresponding photomicrographs, and this is done for the selection of temperatures indicated in the following list :

Figs. 23, 24 (Plate XXXI).	After 9% rapid extension at 200° C.
Figs. 25, 26 (Plate XXXII).	" 12% "
Figs. 27, 28 (Plate XXXII).	" 8% "
Figs. 29, 30 (Plate XXXIII).	" 9% "
Figs. 31, 32 (Plate XXXIII).	" 8% "

It is convenient to begin with the changes produced by deformation at 200° C. and then to proceed to higher temperatures. For below 200° C. the changes in the specimens were similar to each other and characteristic of ordinary deformation by slip at room temperature; thus the X-ray reflection rings were always almost continuous, indicating breakdown to a crystallite formation of very small size, while the micro-structure showed only the familiar systems of sharp slip lines.

At 200° C., however, the structure begins to change. As shown by Figs. 23 and 24 (Plate XXXI) the grains are still traversed by slip lines, but the diffraction ring exhibits a few discrete spots superposed on the continuous ring. Some growth of the sub-structure has therefore taken place.

At 250° C., the presence of discrete reflection spots has become emphasized. The deformation, however, has taken place mainly by the slip mechanism.

At 350° C., definite signs appear of transition from the slip to the cell mechanism of deformation. In some grains slip lines are virtually absent, while in the remaining grains the slip lines have become more irregular and widely spaced. Also, in the X-ray photograph, the discrete nature of the reflection spots may be easily distinguished.

If, now, the photographs of the specimens strained at 200°, 250°, and 350° C. are compared with the earlier photographs of specimens strained at the same temperatures but at the slower rate, it will be quite clear that the main effect of the more rapid deformation is to reduce the size, and possibly the regularity, of the sub-structure associated with each temperature.

It is of interest to consider the effects of still higher temperatures of deformation. It might be added first, perhaps, that even at 400° and 500° C. deformation occurred without recrystallization, presumably because the specimens were initially well annealed, and the internal deformation resulting from the extensions employed was always below the threshold value required for recrystallization at the working temperatures. None of the effects described in the present paper involves recrystallization.

The interesting feature of the experiments at the higher temperatures

is that they show a transition to the cell mechanism of deformation even at the rapid rate of strain. Thus at 400° C., as indicated by Figs. 29 and 30 (Plate XXXIII), the transitional stage is quite evident. At 500° C., illustrated by Figs. 31 and 32 (Plate XXXIII), this transition is practically complete. For it will be seen that the X-ray ring consists entirely of sharp spots corresponding to the formation of the coarse sub-structure, while the photomicrograph shows a virtual absence of slip lines and the apparent thickening of the grain boundaries typical of the cell mechanism. These photographs in fact bear a distinct resemblance to those obtained after slow straining at 250° C., as will be evident on referring to Figs. 13 and 14 (Plate XXIX).

The observations in this Section may thus be summarized by the statement that the sub-structure depends as much on the rate of strain as on the temperature of straining. Under the present conditions of experiment the rapid straining at an elevated temperature had the same effect on the crystalline structure as the slow straining at a temperature approximately 200° C. lower.

4. Relation of Sub-Structure to Mechanical Strength.

The following concluding observations show that the mechanical strength of the metal, as defined by the resistance to applied deformation, depends primarily on the size of the sub-structure produced by the deformation. The greater the size of the elements the less the resistance to deformation, and when the size becomes sufficiently coarse the resistance is negligible. This latter condition is then identified with that responsible for "creep".

The strength developed by a specimen during elongation could be obtained continuously from the extensometers attached to the weigh-bar, as indicated earlier in describing the apparatus. This stress was plotted against extension for the various specimens. The mechanical behaviour thus shown was correlated with the changes in structure exhibited by the same specimens with the following results.

(a) Specimens Subjected to Slow Straining.

It is convenient to discuss first the specimens subjected to slow straining. The strain-hardening characteristics obtained in the above manner for specimens deformed at temperatures from 20° to 350° C. are given by the curves in Fig. 33, which show the following features.

(i) At each temperature, the strength of a specimen increases initially at a relatively rapid rate and then at a much slower but steady rate; this second stage is reached more rapidly the higher the temperature of deformation. It is considered that the initial stage corresponds with the



FIG. 1.—Coarse-Grained Specimen, Initial Condition.

FIG. 2.—Above After 3·8% Slow Extension at 350° C.

FIG. 3.—Above After Further Extension to 8·7%.

FIG. 4.—Microstructure After Extension to 25·4%. $\times 100$.



[To face p. 248.]

5

6

7

8



FIG. 5.—Coarse-Grained Specimen, 3.3% Rapid Extension at 350° C.
FIG. 6.—Above After Further Strain to 5.7%.

FIG. 7.—Microstructure of Above Specimen After 7.5% Extension. $\times 100$.
FIG. 8.—Initial State of Fine-Grained Material.

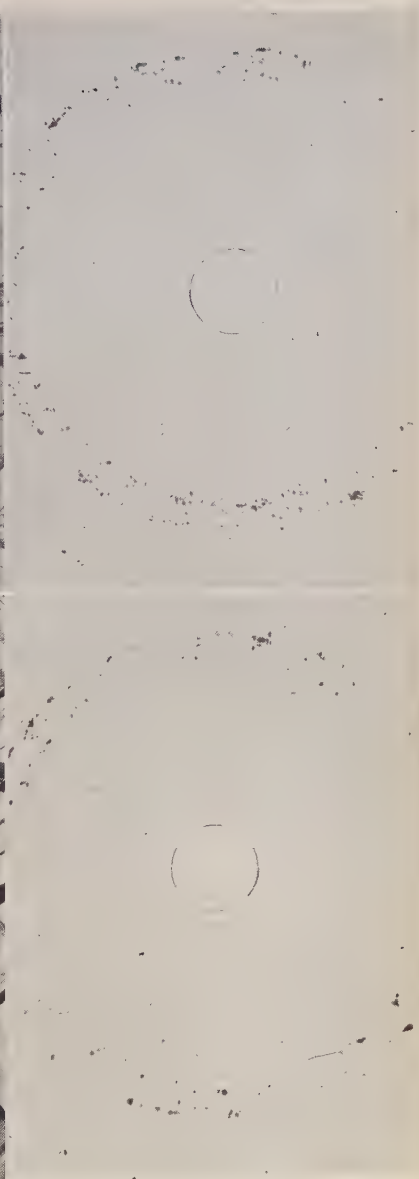
PLATE XXVIII.



9



11



10

Figs. 9 and 10.—After 7% Slow Strain at 350° C.

Figs. 11 and 12.—After 8% Slow Strain at 300° C.

Photomicrographs. $\times 100$.

13



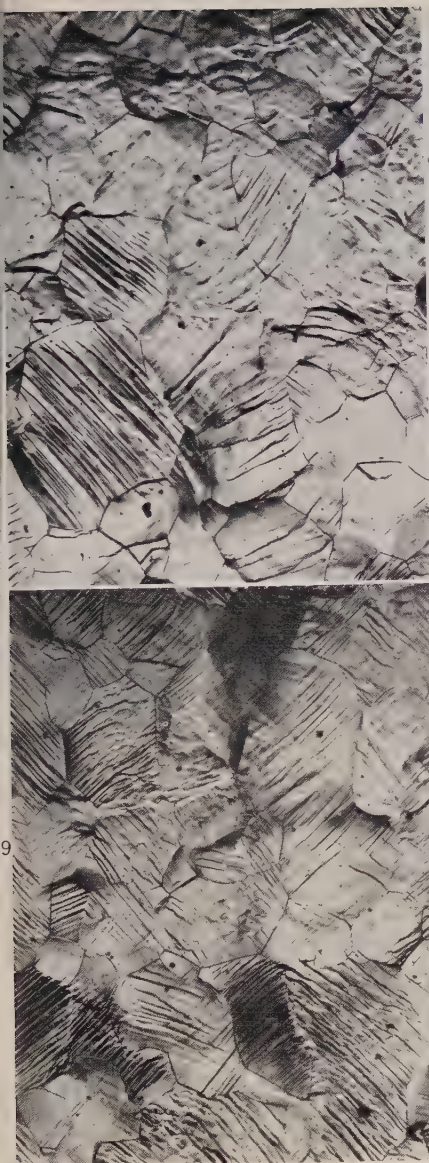
15



1



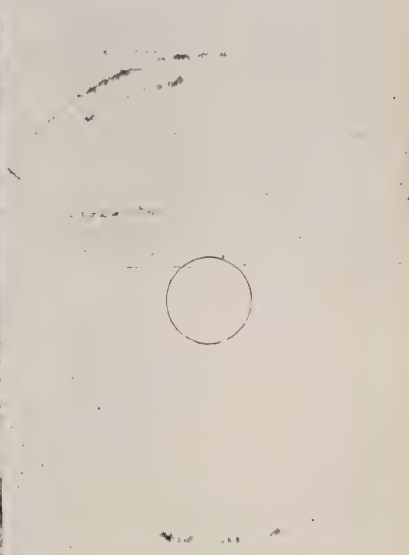
Figs. 13 and 14.—After 9% Slow Strain at 250° C.
Figs. 15 and 16.—After 9% Slow Strain at 200° C.
Photomicrographs. $\times 100$.



FIGS. 17 and 18.—After 8% Slow Strain at 150° C.
FIGS. 19 and 20.—After 8% Slow Strain at 110° C.
Photomicrographs. $\times 100$.



18



20

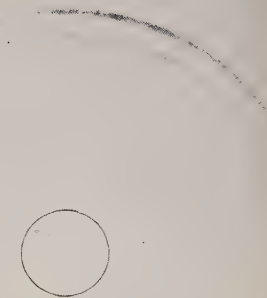
21



23



2



24



FIGS. 21 and 22.—After 9% Slow Strain at 20° C.
FIGS. 23 and 24.—After 9% Rapid Strain at 200° C.
Photomicrographs. $\times 100$.



26



28

Figs. 25 and 26.—After 12% Rapid Strain at 250° C.
Figs. 27 and 28.—After 8% Rapid Strain at 350° C.
Photomicrographs. $\times 100$.

Lawrence Bragg⁵ in discussing the yield of metals by slip. Bragg has shown that an element will yield at a shear strain of approximately $d/2L$, where d is the atomic spacing and L the size of the element. It has been shown here that slow deformation at elevated temperatures, however, does not occur by slip. But the same general criterion may also be expected to govern the movement of one element past another in the cell mechanism of deformation. For it is reasonable to suppose that, as in slip, the relative movement must occur in discrete steps of one atomic spacing along the common sub-boundary. However, the whole of the element cannot jump at one instant. At some moment, therefore, the front part of the element in the direction of the applied stress must undergo a relative displacement of one atomic distance, leaving the rear part to follow at a later moment. Without any knowledge of the detailed mechanism, it can be said that in the interval the element will be under an average tensile strain of d/L , and that therefore a critical average stress of Ed/L will be involved in the relative movement of the neighbouring elements, E being Young's modulus. Such a stress would, of course, not be uniform along the element, but in view of the very small value of the elastic displacements of atoms under mechanical stress relative to the displacements due to thermal vibration, it is doubtful whether any stress could be uniform in elements as small as those under consideration.

In any event it is interesting to apply the above criterion to the observed strengths of the elements in the sub-structure. The cases are taken from Fig. 33 of a specimen extended 6% at room temperature and one extended the same amount at 300° C. The curves show that the first specimen at this extension has a strength of 3000 lb./in.², and the second 800 lb./in.². In Section 2 (a), the corresponding sizes of the elements in the sub-structures were estimated to be respectively $L = 10^{-4}$ cm. and $L = 5 \times 10^{-4}$ cm. The calculated strengths associated with these values according to the above criterion, taking E as 10⁷ lb./in.² and d as 2.86 Å., are respectively 2860 and 600 lb./in.². Considering the rough nature of the assumptions, these compare very favourably with the observed values of 3000 and 800 lb./in.².

Further, the above considerations taken in conjunction with the experimental observations provide a direct explanation of the main feature of creep, namely the secondary stage in which extension proceeds continuously under constant stress. For the observations show that at a sufficiently elevated temperature and slow rate of strain the size of the sub-structure tends to a constant value with increasing strain. Therefore the strength, or resistance to deformation, similarly will tend to a constant value. The metal will then creep under a fixed load.

(b) *Specimens Subjected to Rapid Straining.*

It has already been shown that if, at a given temperature, the rate of strain is increased, the average size of the elements in the sub-structure is decreased. It follows from the above considerations, therefore, that the increased rate of strain should automatically invoke an increased resistance to the applied deformation.

The observations recorded in Table I clearly confirm the point. In this Table the strength developed in the specimens subjected to the rapid rate of strain is given. Since a much shorter time was available for making the observations, compared with the slowly strained specimens, measurements were confined to fewer stages during the deformation. In the same table, for comparison, the values of the strength developed by the slowly strained specimens are given for the same stages of extension. The comparison demonstrates at once the point under consideration.

TABLE I.—*Resistance to Deformation Developed in Specimens Extended at Different Rates of Strain.*

Temperature, °C.	Elongation, %	Resistance, lb./in. ²	
		Rapid Strain	Slow Strain
20	4·0	3220	2620
	8·0	5430	3360
200	6·4	3040	1370
	8·7	4260	1500
250	2·6	1800	820
	5·8	2220	1100
300	12·0	2950	1530
	6·6	2500	800

IV.—DISCUSSION.

The implications of the present results are : (i) that the process of deformation involves the formation of a sub-structure in the grains, (ii) that the size of the sub-structure is a systematic function of temperature and rate of deformation, and (iii) that this size then largely determines the mechanical strength exhibited by the metal during deformation.

The production of definite sub-structures by deformation was pointed out many years ago by Wood ⁷ and also by Goss ⁸ in America. But this work in the main was confined to metals deformed at room temperature and at the rates of strain normally used in cold working and mechanical testing. Since, as already indicated, the question of a sub-structure has attracted more and more attention in recent years, it may

be of interest to note how the results of the present authors stand in relation to those of other workers.

The position will be simplified by distinguishing between sub-structures in annealed grains and sub-structures developed in deformed grains.

Annealed Grains.—The structure of annealed grains or large single crystals is always imperfect. The early X-ray work of Darwin and Bragg showed that the imperfection consisted of a relative tilt of elements of the structure, which they described as a mosaic. The size of the mosaic elements was considered to about 10^{-4} cm., and the angular inclinations to vary between a few seconds and some minutes of arc, according to the degree of imperfection. However, this sub-structure was believed to arise essentially through accidents of growth of the crystal. Lacombe and Beaujard² have recently revealed sub-structures in large annealed grains by using chemical methods. These methods are less sensitive than the X-ray method, and possibly for that reason the structures thus revealed appear to be very coarse, being of the order of the entire grain-size of the specimens used by the present authors. It is difficult to see any relation between either of these types of sub-structure and those studied in this paper, a fundamental difference being that the latter are a systematic function of the conditions of deformation.

Deformed Grains.—Sub-structures have been observed in deformed metal which has been heated to a stage preceding recrystallization, that is, after recovery; and these sub-structures, as shown by Crussard,³ produce spotted X-ray reflection arcs at first sight not dissimilar to those shown in the present paper to arise during creep. The question arises whether in fact they are the same.

Before discussing this point, it will save confusion to recall that in practice the term "recovery" refers to metal which has been heat-treated after relatively rapid deformation applied at a low temperature, usually room temperature.

The question then becomes: Is the sub-structure formed after heating a cold-worked specimen to a given temperature the same as that formed by deforming the metal actually at that temperature? The answer is, no. Experiments on this point have been specially made, and they show that the effect of heating the cold-worked specimen is merely to remove internal strains and distortions and so to reveal more clearly in the X-ray photograph the sub-structure already formed by the low-temperature deformation. A little growth of the sub-structure before recrystallization is to be observed on prolonged heating at the recovery temperature or at higher temperatures, but the increase is found to be insignifi-

cant. The important point is that the size of the sub-structure is related to the initial temperature and rate of deformation rather than to the temperature of subsequent heating. Therefore, the authors regard the sub-structures noted in recovery from rapid cold deformation as, at most, only a special case of the sub-structures investigated in their work. This work shows that the sub-structure increases systematically in size as the temperature of deformation is increased and the rate of deformation is decreased. The sub-structure formed by rapid cold deformation and associated with "recovery" is therefore relatively fine. It is impossible to produce in that way the coarser, clean-cut sub-structure associated with the cell mechanism, because the latter involves a slow deformation at an elevated temperature.

Sub-structures are formed also in hot-worked metals, and the further question might be raised whether these are the same as those studied in the present paper. The answer again is that they might be regarded as a very special case, belonging to the type described in the paper in considering the effects of the rapid deformation at various elevated temperatures. Experiments show that prolonged heating of such hot-worked specimens at the same or even higher temperatures produces no really significant change in the sub-structure before recrystallization. The structure again is related to the initial conditions of deformation rather than to subsequent heat-treatments. Therefore it is impossible in this way to produce the sub-structures associated with creep because of the initial difference in the rate of strain.

It will be advisable in future to define the term recovery more closely. In the broadest sense, the sub-structures associated with the cell mechanism are products of "recovery" in that they must be preceded by some process of breakdown in the grains. But neither this process nor the resulting sub-structure is the same as that associated with "recovery" as usually defined. For the initial process takes place without slip-line formations, and the final sub-structure is considerably coarser. It will be necessary, therefore, to distinguish between recovery from cold deformation, recovery from hot deformation, and recovery from slow or rapid deformation.

REFERENCES.

1. G. R. Wilms and W. A. Wood, *J. Inst. Metals*, 1949, **75**, 693.
2. P. Lacombe and L. Beaujard, *J. Inst. Metals*, 1947-48, **74**, 1.
3. R. Cahn, *Proc. Phys. Soc.*, 1948, **61**, 136.
4. A. Guinier and P. Tennevin, *Compt. rend.*, 1948, **226**, 1530.
5. W. L. Bragg, *Nature*, 1942, **149**, 511.
6. W. A. Wood and W. A. Rachinger, *J. Inst. Metals*, 1949, **75**, 571.
7. W. A. Wood, *Trans. Faraday Soc.*, 1935, **31**, 1248; *Proc. Roy. Soc.*, 1939, [A], **172**, 231.
8. N. P. Goss, *Trans. Amer. Soc. Metals*, 1945, **34**, 630.
9. C. Crussard, *Rev. Mét.*, 1944, **41**, 111.

ON THE MECHANISM OF OXIDATION OF 1218 NICKEL-PLATINUM ALLOYS.*

By O. KUBASCHEWSKI,† Dr.phil.nat.habil., MEMBER, and
(Frl.) ORTRUD VON GOLDBECK,‡ Dr.rer.nat.

SYNOPSIS.

The mechanism of oxidation of binary alloys at high temperatures is discussed on the basis of measurements of the oxidation rate, between 600° and 1100° C., of nickel-platinum alloys containing 0–90 at.-% platinum, and the theoretical considerations put forward by C. Wagner.

The experimental results are expressed in terms of a "corrosion constant", K_0 , which is the ratio of the square of the decrease in thickness of the metal layer caused by oxidation to the time. At 850° and 1100° C. K_0 is almost constant for periods up to 100 hr., suggesting that a simple kinetic process determines the rate at these temperatures. At 600° C. neither the parabolic nor the exponential law of oxidation applies. For a given temperature K_0 is also independent of concentration up to 85 at.-% platinum, and it is smaller than the diffusion rate of nickel in nickel-platinum alloys. These observations suggest that a diffusion process within the oxide layer determines the rate of oxidation. The heat of activation is determined from the $\log K_0 - 1/T$ diagram and is a constant (35,500 cal.) up to 85 at.-% platinum. The corresponding value for the diffusion of nickel in platinum is 43,100 cal. From the five kinetic reactions which can be conceived as determining the rate of oxidation of nickel-platinum alloys, the diffusion rate of Ni^{++} ions (over vacant lattice sites) is finally selected as the most probable. This agrees with the conclusion reached by Wagner for the oxidation of nickel.

The conclusions drawn in the present paper may be generally applicable to other similar alloys, and may even be extended, with certain limitations, to binary systems in which both constituents are oxidizable.

I.—INTRODUCTION.

INVESTIGATIONS of the oxidation of alloys have hitherto been carried out for the most part empirically and for commercial reasons.¹ Such research is indeed very important, in view of the great losses of metal due to oxidation and the need to develop high-temperature materials for industrial use. Very little, however, has been done on the fundamental side of the problem. A knowledge of the mechanism of oxidation, of the rate-determining factors, and of the interaction of various oxides or ions would provide a sounder basis for an understanding of the whole problem, and would probably simplify the search for alloys of good oxidation-resistance.

* Manuscript received 6 May 1949.

† Formerly Reader in Physical Chemistry at the Technische Hochschule, and Senior Assistant at the Kaiser-Wilhelm Institut für Metallforschung, Stuttgart, Germany.

‡ Formerly Research Student at the Technische Hochschule, Stuttgart, Germany.

The little fundamental knowledge available at present has been critically surveyed by C. Wagner.² A correlation between the time-laws of oxidation of pure metals and the volume ratio :

$$\frac{\text{Molecular volume of oxide}}{\text{Atomic volume of metal}} \left(\frac{1}{\phi} \right)$$

was postulated and discussed in the almost classic paper of Pilling and Bedworth,³ which, with the publications of Tammann and his co-workers^{4, 5, 6} on the validity of the various time-laws, forms the nucleus of the fundamental work done hitherto. Attempts have been made more recently by Gulbransen and Hickman⁷ to gain a fundamental, knowledge of the oxidation of alloys from electron-diffraction patterns of the oxide layers.

In the work described below it was considered that an investigation of the mechanism of oxidation could most profitably be carried out on a simple binary system. The nickel-platinum system was chosen for the following reasons :

(1) Of the two constituent elements only nickel is oxidized, platinum being too electropositive to form oxides under normal conditions.

(2) Nickel forms only one oxide, NiO.

(3) The oxidation of nickel has frequently been investigated, using metal of various degrees of purity. (This work has been reviewed elsewhere by the present authors.⁸)

(4) The mechanism of oxidation of pure nickel has been discussed in several papers by Wagner,^{2, 9} who concluded that the diffusion of Ni^{++} ions over vacant lattice sites and of electrons is the rate-determining factor.

(5) Platinum and nickel form a continuous series of solid solutions having a disordered structure above 600° C.¹⁰

(6) Conjectures about the dependence of the oxidation of alloys of nickel with electropositive metals on concentration have been put forward, also by Wagner,² and a private discussion of these ideas between Wagner and one of the authors at least partly initiated this work.

The present paper describes experiments on the oxidation of a range of nickel-platinum alloys for various lengths of time and at various temperatures and oxygen pressures, and gives the conclusions drawn from the experimental results. The results of some earlier oxidation tests on gold-nickel and platinum-nickel alloys containing low percentages of nickel¹¹ are included in the discussion.

II.—EXPERIMENTAL METHOD.

The oxidation of metals may be observed by visual methods, by changes in weight, or by measurement of changes in pressure in the surrounding gas. Of these, the method of weighing after successive periods of treatment was selected.

The alloys were produced from carbonyl nickel powder and pure platinum. The compressed powder mixtures were melted in a Tammann furnace *in vacuo*, and the alloys were cooled slowly, rolled, and cut into small plates ($12 \times 6 \times 0.5$ mm.), which were finally polished.

In each experiment two of these plates were placed, always in the same position, in an alumina boat, contained in a Pythagoras tube, open at both ends, which was put into an automatically regulated electric resistance furnace (with nickel-chromium wire windings or, for experiments at the higher temperatures, silicon carbide rods). The furnace was tilted to provide a continuous stream of air through the Pythagoras tube. Under these conditions, formation of nickel nitride would not be expected.

The boats were removed from the furnace after various periods of treatment and placed in a desiccator until they had cooled to room temperature.

The temperature was measured with a calibrated platinum/platinum-rhodium thermocouple placed adjacent to the boat. Temperature fluctuation was regulated to within $\pm 3^\circ$ C.

A micro-balance was used for weighing, to an accuracy of ± 0.002 mg. After weighing, the alumina boats with the test plates were returned to the furnace and the weight increase was thus determined in several stages up to a total of 100 hr.

Plates which were only slightly oxidized in the first experiment were used for a further experiment after being polished to a depth sufficient to ensure that the layer impoverished in nickel in the first experiment had been removed. Heavily oxidized test-pieces were not used again.

The experimental errors introduced in temperature measurement, weighing, &c., have not been considered in detail, as they are small compared with those which arise from contamination of the surface, formation of active points, and other surface effects, which cannot be estimated. The rate constant of oxidation of any particular alloy was found to be reproducible well within $\pm 50\%$, which is quite a satisfactory figure for kinetic measurements on reactions involving solids.

The alloys used contained nominally 10.0, 14.7, 20.0, 25.0, 27.0, 40.0, 50.0, 60.0, 75.0, 80.0, and 100.0 at.-% nickel. The temperature range investigated was 600° - 1100° C. and in two cases 600° - 1350° C.

III.—RESULTS AND CONCLUSIONS.

From considerations of space it is not proposed to tabulate all the separate weight determinations. To illustrate the scope of the experimental work, however, the complete measurements carried out on the alloy containing 20 at.-% platinum are given in Table I.

TABLE I.—*Oxidation Rate of a Nickel–Platinum Alloy Containing 20 at.-% Platinum.*

1100° C.		850° C.		600° C.		
Time, hr.	k' , g. ³ cm. ⁻⁴ sec. ⁻¹	Time, hr.	k' , g. ³ cm. ⁻⁴ sec. ⁻¹	Time, hr.	k' , g. ³ cm. ⁻⁴ sec. ⁻¹	k''
	$\times 10^{-9}$		$\times 10^{-10}$		$\times 10^{-12}$	$\times 10^{-4}$
4.5	4.12	4.0	4.01	4.0	3.34	0.61
19.75	9.70	8.0	4.19	8.0	3.75	0.74
43.25	7.65	12.0	4.06	11.75	3.58	0.84
67.25	8.25	25.75	4.23	19.0	2.99	0.93
105.5	7.20	38.75	4.60	28.25	2.90	1.08
...	...	75.0	4.71	52.3	2.90	1.39
4.5	4.25	100.0	4.36	81.0	2.84	1.67
19.75	5.83	100.75	2.59	1.74
43.25	10.10	4.0	3.81
67.25	7.23	8.0	5.81	4.0	3.42	0.45
105.5	8.24	12.0	5.58	8.0	3.21	0.68
...	...	25.75	5.75	11.75	3.27	0.81
...	...	38.75	5.89	19.0	2.55	0.86
...	...	75.0	4.80	28.25	2.79	1.06
...	...	100.0	4.80	52.3	2.18	1.21
...	81.0	2.03	1.44
...	...	4.0	2.29	100.75	1.94	1.51
...	...	13.75	1.70
...	...	17.35	1.51

Provided that the surface area of the test sample and the concentration of the reacting gas remain constant during oxidation, that the rate-determining factor remains the same, and that dense oxidation layers are formed, the so-called parabolic law of oxidation :

$$\Delta\xi^2 = 2kt \dots \dots \dots \dots \quad (1)$$

holds good for pure metals at high temperatures.^{3, 12, 13, 14} In this equation, $\Delta\xi$ is the thickness of the oxide layer after time t . If $\Delta\xi$ is expressed in cm. and t in sec., k has the dimension cm.² sec.⁻¹. It is sometimes convenient to use the increase in weight (in g. of oxide) per cm.² of surface area (Δm) in place of thickness, and since $\Delta\xi$ and Δm are proportional :

$$\Delta\xi = \Delta m / \rho \dots \dots \dots \dots \quad (2)$$

(ρ = density of the oxide) and equation (1) can be expressed in the form

$$\Delta m^2 = k't \dots \dots \dots \dots \quad (3)$$

k' having the dimension g.² cm.⁻⁴ sec.⁻¹.

If the oxide layer is porous, i.e. non-protecting, a linear time-law applies:

$$\Delta m = k^*t \dots \dots \dots \dots \quad (4)$$

Equation (4) is generally valid for metals having a volume ratio ($\frac{1}{\phi}$) less than unity. Alloys of magnesium, a metal of this type, have recently been studied by Leontis and Rhines.¹⁵ The volume ratio of nickel is greater than unity, namely $\frac{1}{\phi} = 1.67$. This type of metal generally obeys equation (3) at least approximately.

At low temperatures, an exponential law⁵

$$\Delta m = k'' \log t \dots \dots \dots \dots \quad (5)$$

has also been observed in a number of instances, e.g. for iron below 200° C.,¹⁶ and for zinc up to 400° C.¹⁷ There are several explanations for this behaviour,^{2, 14, 17, 18} none of which is, however, fully satisfactory in its present state.

In Table I the information on the oxidation of nickel-platinum alloys is presented as k' values, calculated from the increase in weight in g. NiO/cm.² and the time in sec. It is seen that k' is almost constant over oxidation periods up to 100 hr. at 1100° and 850° C. There is, however, a remarkable decrease in the values of k' with time at 600° C. Furthermore, k'' values calculated for this temperature increase with time, so neither equation (3) nor equation (5) holds at 600° C.

This is found to be the tendency of all the other alloys and also of very pure nickel (carbonyl nickel, twice remelted *in vacuo*): at 1100° C. k' is almost constant; at 850° C. and with the lower nickel concentrations the slight decrease in the values of k' with time becomes a little more pronounced; and at 600° C. k' decreases with time, though k'' always increases.

From this it may be concluded that a simple and uniform kinetic process determines the rate at high temperatures. It is known from diffusion measurements (e.g. by Matano¹⁹) that any effect arising from the state of aggregation (grain-size, &c.) becomes more serious at low temperatures and may modify or mask the true values. Something similar may be envisaged as applying to diffusion in the oxide layer. On the one hand the effect may be explained by the primary formation of a thermochemically unstable oxide layer with high permeability for

diffusing ions, which is gradually transformed during oxidation into a stable layer of lower permeability.² On the other hand, since the highest values of oxidation fit best in the $\log k' - 1/T$ diagram (see below), it is more likely that local transitory resistances caused by variations in orientation of the oxide aggregates reduce the actual rate of ionic interchange in the crystal, and that this effect is more pronounced at low temperatures. It may be found useful to carry out further work on oxidation in conjunction with electron-microscope investigations of the layers.

It is at first surprising to find no tendency towards the linear law (equation 4) at low concentrations of nickel. Since nickel is the only component oxidized, the volume of the metallic phase related to 1 g.-atom of nickel increases, while the molecular volume of the oxide phase remains constant, i.e. the volume ratio, $\frac{1}{\phi}$, decreases. The critical value of unity is attained at 32 at.-% platinum. At greater concentrations of platinum the volume ratio is less than unity. Nevertheless the square-root law (equation 3) still applies. It must be concluded, therefore, that, in growing, the oxide layer covers the surface of the alloy completely without forming any pores. This result is quite different from the behaviour of a pure metal with a volume ratio < 1 , such as magnesium.¹⁵

A critical concentration is, however, to be expected when the additions of the electropositive metal become too large to permit complete covering of the surface by oxide, thus causing pore formation. This critical concentration will be indicated by the approach of the weight increase to the linear law (equation 4). This was not observed with the alloys under investigation, even at a concentration of 85 at.-% platinum.

Comparative measurements with gold-nickel alloys containing 15.0 and 25.2 at.-% gold¹¹ showed a pronounced increase of k' with time, if calculated by means of equation 3, i.e. the linear law is approached. The oxidation is also more rapid with the gold-nickel alloys than with the platinum-nickel alloys of the same concentration. Actually no chemical difference is found between additions of gold or platinum, as neither takes part in oxide formation. The reason for the observed difference in behaviour must lie in the larger atomic volume of gold (10.2 cm.^3) compared with that of platinum (9.1 cm.^3), and the critical concentration, mentioned above, is therefore lower in the case of the gold-containing alloys.

In Table II are summarized the mean values of k' derived from the increases in weight at all the temperatures and concentrations investigated. For 1100° and 850° C. the average values of all the determinations on alloys of each concentration are taken. For 600° C., however,

where k' is not constant, the maximum value is taken, as this generally compares best with the high-temperature values in the $\log k\text{-}1/T$ diagram. There is generally a drop to about $\frac{1}{2} - \frac{2}{3}$ of this maximum value after 100 hr.

TABLE II.—*Oxidation Rate (k'), Corrosion Constant (K_0), and Heat of Activation (Q) for the Oxidation of Nickel-Platinum Alloys (Average Values).*

Plati- num, at.-%	Volume Fraction of Nickel	k' , g. ² cm. ⁻⁴ sec. ⁻¹			K_0 , cm. ² sec. ⁻¹			Q, cal.
		1100° C.	850° C.	600° C.	1100° C.	850° C.	600° C.	
0	1.00	$\times 10^{-9}$	$\times 10^{-10}$	$\times 10^{-12}$	$\times 10^{-11}$	$\times 10^{-12}$	$\times 10^{-14}$	33,500
20.0	0.745	13.9	10.6	13.9	5.45	4.15	5.45	35,200
25.0	0.684	7.3	4.25	3.6	5.25	3.05	2.5	(41,500)
40.0	0.522	(12.7)	(3.6)	(2.0)	10.7	3.05	1.68	35,000
50.0	0.422	4.15	3.33	3.4	5.9	4.9	4.9	(36,000)
60.0	0.327	{ 3.81	(2.07)	(1.9)*	8.4	4.6	4.15	33,000
73.0	0.212	{ 0.5	1.46	6.76 *	8.94	5.9	24.0 *	(32,800)
75.0	0.195	0.85	4.58	1.83 *	2.85	16.6	6.75 *	35,400
80.0	0.155	0.21	0.24	0.079	3.5	3.8	1.2	35,000
85.3	0.111	0.12	0.066	0.098	3.7	2.1	3.05	33,000
90.0	0.075	(0.002)	(0.002)	(0.004)	0.14	0.13	0.26	(31,000)

* According to the detailed study of the platinum-nickel system by Esch and Schneider,¹⁰ a very slow order-disorder transformation occurs with the alloys containing 45–60 at.-% platinum at 590°–625° C. On the basis of the Hedvall principle that substances considerably activate a kinetic process while in a state of transformation,²⁴ the values of k' in this concentration range are probably not true constants, but are affected by the transformation and may therefore be too high.

The values for alloys containing 25 and 14.7 at.-% nickel were interpolated from the earlier measurements,¹¹ which were carried out after oxidation times up to 10 hr. only, but mainly over 4 hr.† The values in brackets are derived from a few short-time investigations only and are therefore more unreliable.

These results make possible the verification of the theoretical speculations by Wagner² concerning the dependence of the rate constant of oxidation on the concentration of an alloy consisting of an oxidizable and an electropositive metal. Wagner recommended the introduction of a new constant, which he calls the "corrosion constant", K_0 . This is related not to the increase in thickness of the oxide layer, $\Delta\xi$, as in equation (1), but to the decrease of thickness of metal, $\Delta\xi^*$, due to oxidation. If a positive sign is given to both quantities and if the ratio of the volumes of the metallic and the oxide phases containing the same

† The break in the $\log k\text{-}1/T$ curve at 25% nickel cited in the earlier publication¹¹ was disproved in the present work. The alloys used in the earlier work were not produced by the author, and the effect recorded may have been due to contamination and not have represented the true values for the binary alloys.

amount of metal is designated ϕ (see p. 256), the following equation holds :

$$\Delta\xi^* = \phi \cdot \Delta\xi \quad \dots \dots \dots \quad (6)$$

From this, the relationship

$$\Delta\xi^* = \phi \sqrt{2kt} = \sqrt{2K_0t} \quad \dots \dots \dots \quad (7)$$

is derived from equation (1), and K_0 is calculated from k by the equation :

$$K_0 = k \cdot \phi^2 \quad \dots \dots \dots \quad (8)$$

K_0 has the dimension $\text{cm.}^2 \text{ sec.}^{-1}$, and according to Wagner it can be directly correlated with diffusion constants in alloys.

The value of ϕ for pure nickel and nickel oxide is $6.6 : 10.0 = 0.66$. Values of ϕ for the alloys are obtained by dividing this figure by the volume fraction of the nickel. (This allows for the dilution or "expansion" of the nickel.)

The values of K_0 calculated from those of k' are given in Table II. As the corrosion constant will probably find more general application in future, an example of one of these calculations may be given. If k' is $4.15 \times 10^{-9} \text{ g.}^2 \text{ cm.}^{-4} \text{ sec.}^{-1}$;

$$k = \frac{\Delta\xi^2}{2t} = \frac{k'}{2\phi^2} = \frac{4.15 \times 10^{-10}}{2 \times 7.45^2} = 3.74 \times 10^{-11} \text{ cm.}^2 \text{ sec.}^{-1};$$

$$\phi = \frac{\text{molecular volume of Pt-Ni}}{\text{molecular volume of NiO}} \quad (\text{both containing 1 g.-atom of nickel}) \\ = \frac{6.6}{0.522} \times \frac{1}{10.0} = 1.26. \quad \text{Hence} \quad K_0 = k\phi^2 = 3.74 \times 10^{-11} \times 1.26^2 = 5.93 \times 10^{-11} \text{ cm.}^2 \text{ sec.}^{-1}.$$

By making a number of simplifying assumptions, Wagner has concluded that in a binary metallic system, such as nickel-platinum, K_0 should be constant over a wide range of concentration, provided that the diffusion rate D of the oxidizable metal in the alloy is higher than the corrosion constant, K_0 . The diffusion rate of nickel in platinum is known at one concentration. It was measured by Kubaschewski and Ebert²⁰ for an alloy having an initial composition of 14.7 at.-% nickel, and amounts to $1.05 \times 10^{-10} \text{ cm.}^2 \text{ sec.}^{-1}$ at 1100° C. and $3.1 \times 10^{-12} \text{ cm.}^2 \text{ sec.}^{-1}$ at 850° C. The respective values of K_0 are 3.7×10^{-11} and $2.1 \times 10^{-12} \text{ cm.}^2 \text{ sec.}^{-1}$. The ratio K_0/D is therefore less than unity, so that the condition stipulated by Wagner is fulfilled.

It will be seen from Table II and Fig. 1 that the values of K_0 can well be considered constant at all three temperatures for concentrations up to 80 at.-% platinum, thus conforming to Wagner's prediction and suggesting that the oxidation rate is determined by a diffusion process

in the oxide layer. The decrease in value of K_0 on reducing the concentration beyond a certain critical value was also predicted by Wagner, indicating that another diffusion process (possibly one in the alloy phase) becomes the rate-determining factor. It is, however, not intended to pursue his considerations further, since in this range the simplifying assumption no longer necessarily applies. This assumption is largely that of a constant dissociation pressure of NiO. This is certainly very much increased owing to the effect of the free energy of alloy formation

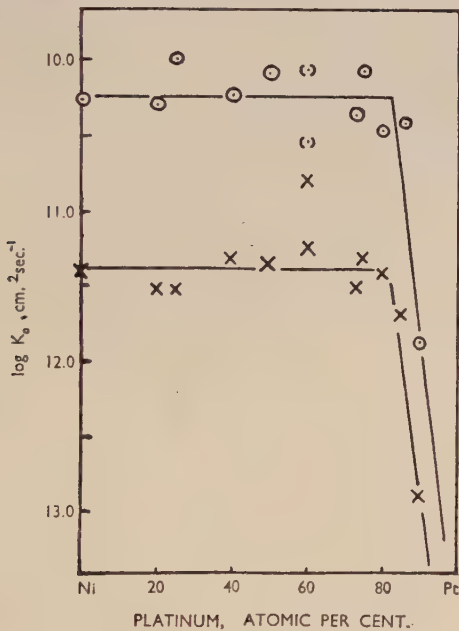


FIG. 1.—Relation Between $\log K_0$ and Alloy Composition.
○ 1100° C. × 850° C.

(platinum-nickel) which is not known, but may very well be more than 10,000 cal./g.-atom nickel at low concentrations of nickel.

In Fig. 2 the values of $\log K_0$ are plotted against the reciprocal of the absolute temperature. If a uniform kinetic process is responsible for oxidation, straight lines are to be expected for each concentration in the $\log K_0 - 1/T$ diagram. The number of temperatures investigated is too small to make this result quite conclusive. The drawing of straight lines can, however, be justified from general experience. The equation

$$K_0 = Ae^{-Q/RT} \quad \dots \quad \dots \quad \dots \quad \dots \quad \dots \quad (9)$$

corresponding to Arrhenius's equation for diffusion processes, where A and Q are constants, has frequently been proved. The values of the activation energy, Q , have been calculated from the straight lines in Fig. 2, and are also tabulated in Table II. It will be seen that all values of Q are approximately equal to that for pure nickel, suggesting that the same rate-determining process governs the oxidation of alloys of all the compositions investigated.

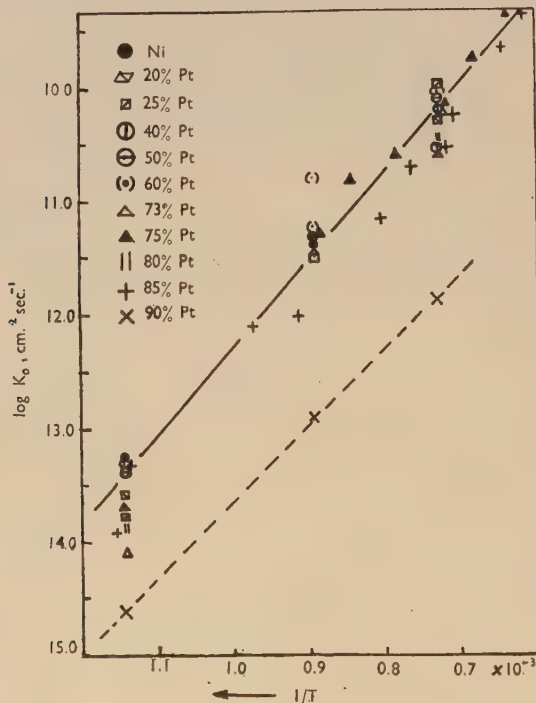


FIG. 2.—Relation Between $\log K_0$ and $1/T$. (T = Absolute Temperature.)

A few other experiments on oxidation at various oxygen pressures, though not systematic, may also be mentioned. These were carried out with various mixtures of oxygen and nitrogen containing 100, 20, 7, and 3% oxygen, in the same apparatus with the addition of a gas-circulating pump, on nickel and the alloys containing 20 and 40 at.-% platinum. While no regularity in the influence of the oxygen concentration was found, a slight decrease (not more than 25%) in oxidation rate was found on reducing the oxygen concentration from 100 to 3%.

From all this experimental evidence, final conclusions concerning the mechanism of oxidation may be drawn. Fig. 3 presents a scheme of the oxidation process, the arrows indicating the various factors that may determine the oxidation rate as follows : (1) the diffusion of nickel in nickel-platinum alloys, (2) the transition of nickel atoms in the oxide layer, forming Ni^{++} ions and electrons, (3) the diffusion of these ions and electrons in the oxide layer to the phase boundary NiO/O_2 , (4) the diffusion of O^{--} ions in the opposite direction, or (5) the reaction of Ni^{++} ions with the molecular oxygen of the gas phase.

If the first factor were rate-determining, the activation energy of oxidation and that of diffusion of nickel would be expected to be equal. The activation energy of the diffusion of nickel in platinum for an alloy containing 14·7 at.-% nickel was calculated from previous measurements²⁰ to be 43,100 cal.; the average value of the activation energies

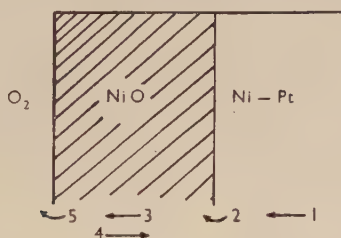


FIG. 3.—Possible Mechanisms of Oxidation.

found in the present work is 35,500 cal., a difference too great to be explained by experimental inaccuracies. Factor 1 is also excluded by Wagner's considerations, mentioned above, and by the experimental observation that the ratio K_0/D is much less than unity, whereas it should be equal to or greater than unity if metallic diffusion were the rate-determining factor. Factor 2 is also excluded, for if this were responsible for the reaction rate, the absolute values of K_0 and Q should show much greater variation with concentration than they do. No. 2 may, however, be the rate-determining factor at high concentrations of platinum, where the sudden drop in K_0 occurs (Fig. 1), the value of Q for the diffusion of nickel being higher than that for oxidation even at the high concentrations. (The value of Q for 90 at.-% platinum is, however, not quite definite, as the actual values of the oxidation rate are so low that any small experimental error may alter the slope considerably.) If factor 5 were the rate-determining factor, the influence of oxygen pressure should be much greater than was actually observed, and should be proportional to the square root of the pressure.

We are left, therefore, with Nos. 3 and 4, between which the present work is unable to distinguish. It is, however, generally assumed that the diffusion of metallic ions occurs in preference to that of the oxygen ions,^{2, 18, 21} since the latter have so much larger an ionic diameter. It is therefore more likely that the diffusion of Ni^{++} ions plus electrons in the oxide determines the oxidation rate. This conclusion is arrived at independently of any assumption regarding the mechanism of oxidation of pure nickel. The similar values of Q in Table II and the constancy of K_0 suggest in addition that the same mechanism applies both to pure nickel and to the alloys, which may be considered as confirmation both of the conclusions reached by Wagner for pure nickel^{2, 9} and of those reached in the present work.

The question remains whether the energy of activation of the electrons or of that of the ions is the greater, i.e. the rate-determining factor. This problem was solved by Cabrera, Terrien, and Hamon,²² who showed that the oxidation rate of thin aluminium films is the same with or without the application of ultra-violet rays. That means that the oxidation rate is determined by the diffusion rate of the metal ions. One is probably justified in extending this conclusion as a generalization to other metals, including nickel.

The results reported in the present paper may be considered of general significance in that they substantiate previous theoretical predictions. It would be useful to correlate such measurements with determinations of the velocity of ionic migration in the oxide layers and of the free energy of alloy formation. Neither value is known for the materials used, however. The transference numbers of nickel ions in molten nickel oxide (relative to the velocity of the electrons) was recently determined by Schrag,²³ but could not be related to a definite temperature and cannot be used to evaluate the absolute velocity of ionic migration.

Finally, it should be possible to extend the knowledge gained with alloys containing one inert constituent, to binary alloys in which both constituents are oxidizable. This will, of course, involve careful analysis of the oxide layer formed. It may reasonably be expected that the same laws apply in such cases as in that of nickel-platinum alloys. It will possibly be found that the oxidation rate of the less electropositive metal governs the total oxidation rate over the greater range of concentration according to the rules formulated above, the more electropositive metal acting in this range as an "inert component" only. At higher concentrations of this metal, however, two reactions originating from the two constituent metals probably overlap.

Very small additions of alloying elements to a given metal may give

rise to quite different mechanisms owing mainly to changes in the atomic structure of the oxide layer.⁹ These phenomena must be the subject of separate investigation.

REFERENCES.

1. W. Hessenbruch, "Metalle und Legierungen für hohe Temperaturen". Berlin : 1940 (J. Springer).
2. C. Wagner, "Chemische Reaktionen der Metalle". Leipzig : 1940 (Akademische Verlagsgesellschaft Becker u. Erler).
3. N. B. Pilling and R. E. Bedworth, *J. Inst. Metals*, 1923, **29**, 529.
4. G. Tammann, *Z. anorg. Chem.*, 1920, **111**, 78.
5. G. Tammann and W. Köster, *ibid.*, 1922, **123**, 196.
6. G. Tammann and H. Bredemeier, *ibid.*, 1924, **136**, 337.
7. E. A. Gulbransen and J. W. Hickman, *Trans. Amer. Inst. Min. Met. Eng.*, 1947, **171**, 306.
J. W. Hickman and E. A. Gulbransen, *ibid.*, p. 344.
J. W. Hickman and E. A. Gulbransen, *ibid.*, p. 371.
- E. A. Gulbransen and W. S. Wysong, *Metals Technol.*, 1947, **14**, (6); and *A.I.M.M.E. Tech. Publ. No. 2224*.
- E. A. Gulbransen and W. S. Wysong, *Metals Technol.*, 1947, **14**, (6); and *A.I.M.M.E. Tech. Publ. No. 2226*.
8. O. Kubaschewski and O. von Goldbeck, *Z. Metallkunde*, 1948, **39**, 158.
9. C. Wagner and K. E. Zimens, *Acta Chem. Scand.*, 1947, **1**, 547.
10. U. Esch and A. Schneider, *Z. Elektrochem.*, 1944, **50**, 268.
11. O. Kubaschewski, *Z. Elektrochem.*, 1943, **49**, 446.
12. J. S. Dunn, *Proc. Roy. Soc.*, 1926, [A], **111**, 203, 210.
13. W. Feitknecht, *Z. Elektrochem.*, 1929, **35**, 142.
14. U. R. Evans, *Trans. Electrochem. Soc.*, 1943, **83**, 335.
15. T. E. Leontis and F. N. Rhines, *Trans. Amer. Inst. Min. Met. Eng.*, 1946, **166**, 265.
16. W. H. J. Vernon, *Trans. Faraday Soc.*, 1935, **31**, 1670.
17. W. H. J. Vernon, E. I. Akeroyd, and E. G. Stroud, *J. Inst. Metals*, 1939, **65**, 301. (See also remarks in discussion by U. R. Evans, T. P. Hoar, N. F. Mott, G. Shearer, and A. B. Winterbottom.)
18. N. F. Mott, *Trans. Faraday Soc.*, 1940, **36**, 472; 1947, **43**, 429.
19. C. Matano, *Jap. J. Physics*, 1934, **9**, 41.
20. O. Kubaschewski and H. Ebert, *Z. Elektrochem.*, 1944, **50**, 138.
21. E. Scheil and K. Kiwit, *Arch. Eisenhüttenwesen*, 1935-36, **9**, 405.
22. N. Cabrera, J. Terrien, and J. Hamon, *Compt. rend.*, 1947, **224**, 1558.
N. Cabrera and J. Hamon, *ibid.*, 1713.
23. G. Schrag, *Metallforschung*, 1947, **2**, 25.
24. J. A. Hedvall, "Reaktionsfähigkeit fester Stoffe". Leipzig : 1937 (J. A. Barth).

THE ALUMINIUM-TIN PHASE DIAGRAM AND 1219 THE CHARACTERISTICS OF ALUMINIUM ALLOYS CONTAINING TIN AS AN ALLOY- ING ELEMENT.*

By A. H. SULLY,[†] M.Sc., Ph.D., F.Inst.P., MEMBER, H. K. HARDY,[‡] M.Sc.,
Ph.D., A.R.S.M., A.I.M., MEMBER, and T. J. HEAL,[§] B.Sc., A.Inst.P.

SYNOPSIS.

A redetermination has been made of the liquidus curve of the aluminium-tin system and the solid solubility of tin in aluminium. The liquidus curve confirms the results of Gwyer and of Crepaz. There is a simple eutectic at about 0·5% aluminium and 3·6° C. below the melting point of tin.

The results of metallographic examination, ageing tests, and precise lattice-parameter measurements place the solubility of tin in aluminium as just below 0·05 wt.-% at 530° C., and well below 0·02 wt.-% at 165° C.

The metallurgy of tin as an alloying element in aluminium alloys is described with reference to the structures of such alloys. Aluminium alloys containing tin may, for convenience, be divided into three classes : (a) those in which tin is a major constituent, (b) those in which tin is a soluble constituent, and (c) those in which the tin is affected by the presence of another element, such as magnesium.

Alloys in the first group contain a more or less continuous network of tin-rich eutectic, the effect of which is illustrated by the poor high-temperature tensile properties of a number of aluminium-tin alloys.

Although the solid solubility of tin in aluminium is only very slight, it is sufficient to exert a considerable influence on the response to heat-treatment of certain commercial alloys, such as the alloy containing 4·5% copper (D.T.D. 304).

Finally, it is shown that other elements may combine with tin to form a compound and so suppress its normal effects. This is the case in Duralumin-type alloys, containing magnesium in addition to copper, in which small quantities of tin have no appreciable effect on forgeability or ageing characteristics.

INTRODUCTION.

THE chief use of tin in aluminium-base alloys is for anti-friction bearings, some of which contain 5–10% tin. Tin has sometimes been added to aluminium alloys in small quantities to improve their castability, although there is some doubt about the validity of this claim. Other minor uses of tin in aluminium alloys are mentioned in the literature, including improvement of corrosion-resistance to chloride ions and free-machining properties.

* Manuscript received 21 April 1949.

[†] Principal Physicist, Fulmer Research Institute, Ltd., Stoke Poges, Bucks.

[‡] Physical Metallurgist, Fulmer Research Institute, Ltd., Stoke Poges, Bucks.

[§] Physicist, Fulmer Research Institute, Ltd., Stoke Poges, Bucks.

The first object of this investigation was to check the equilibrium diagram. In particular, it was considered desirable to determine the order of the solid solubility of tin in aluminium, since values quoted in the literature varied from 0 to 20%. This work is described in Part A of the paper.

The properties of aluminium-tin binary alloys and of some more complex aluminium alloys containing tin were then examined in the light of the aluminium-tin phase diagram, and the second purpose of this paper is to give an account of the behaviour of aluminium alloys containing tin, as a function of the manner in which the tin is distributed (Part B).

A.—THE ALUMINIUM-TIN PHASE DIAGRAM.

I.—PREVIOUS WORK.

Liquidus and Solidus.

The most reliable of the early work is that of Gwyer,¹ which showed a smooth curve for the liquidus with no irregularities (Fig. 1). The eutectic arrest on the cooling curve was found with as little as 1.2 at.-% tin (5.1 wt.-%). Earlier workers^{2, 3, 4} had observed irregularities such as a minimum and a maximum in the region 75–85% tin, whereas others^{5, 6} confirmed Gwyer's results.

Later work by Crepaz⁷ confirmed Gwyer's liquidus curve. Losana and Carozzi⁸ placed the eutectic at 0.58% aluminium and 229° C. compared with the 232° C. of Gwyer. Kaneko and Kamiya⁹ determined the eutectic as 1.3% aluminium. It may be noted here that the liquidus curve given by Mondolfo¹⁰ when reviewing the literature on the aluminium-tin system differs considerably from the experimental curves of Gwyer and of Crepaz.

Solid Solubility of Tin in Aluminium.

The results given for the solid solubility show very great discrepancies, estimates varying from nil (Gwyer,¹ Crepaz⁷) to 2% (Gotō and Mishima¹¹), 2% at room temperature (Zamotorin^{12, 13}), 10%,³ and even 20%.⁵ Gwyer based his conclusions on the eutectic arrest which he observed on the cooling curve of the 5% tin alloy. The higher values, which were obtained on specimens in the cast condition, are undoubtedly the result of using metallographic techniques which would now be regarded as unsuitable.

Zamotorin's results¹² were based on measurements of the hardness, electrical resistance, and temperature coefficient of electrical resistance,

carried out on bars and wires of aluminium-tin alloys which had been annealed for 60 days at 200° C. and slowly cooled to room temperature (Fig. 2). The deflection at about 2% tin was interpreted as indicating the solubility at room temperature.

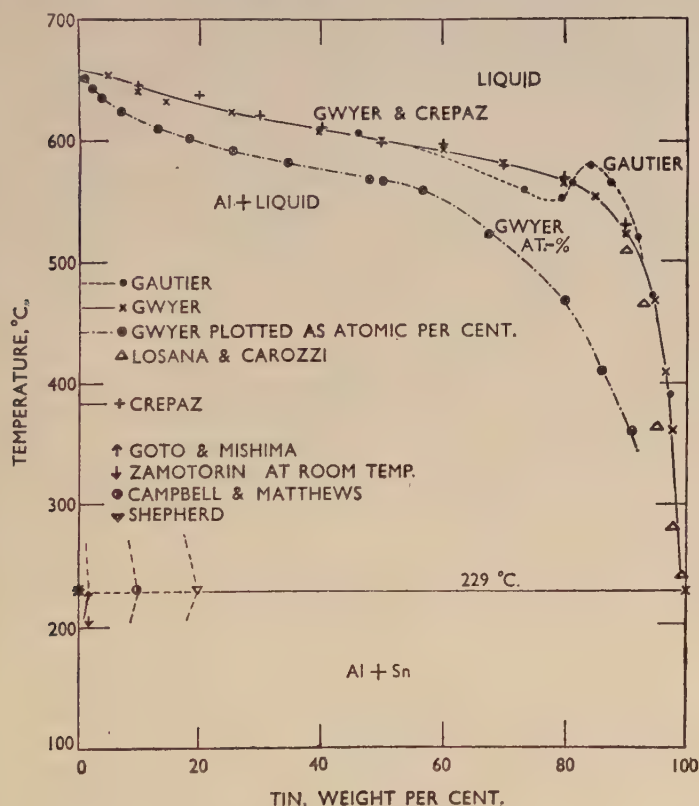


FIG. 1.—The Aluminium-Tin Equilibrium Diagram According to Previous Work.
Eutectic composition $\sim 99.5\%$ tin.

While the present work was in progress, Nielsen and Nekervis¹⁴ quoted unpublished work of Fink, indicating that the solubility is approximately 0.05% tin at 500° C. and not more than a few thousandths of one per cent. at the eutectic temperature.

II.—METHODS OF INVESTIGATION.

A redetermination of the liquidus curve and eutectic temperature was made by thermal analysis, using inverse-rate cooling curves.

Micrographic and X-ray examinations were carried out on chill-cast specimens across the whole diagram to confirm the absence of phases other than those of the primary metals.

Three experimental techniques have been used to obtain the solid solubility of tin in aluminium at 530° and 165° C.: (1) Metallographic examination of wrought alloys, (2) lattice-parameter measurements on

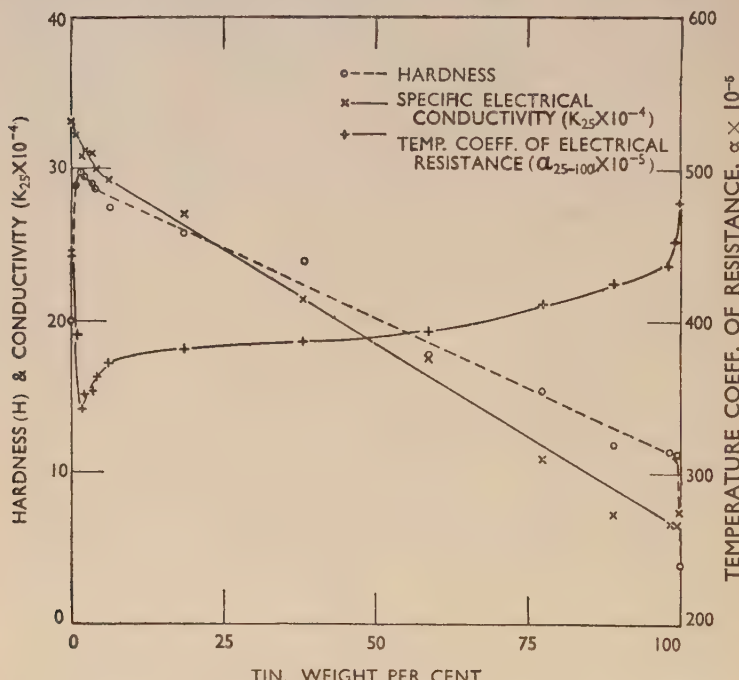


FIG. 2.—Variation of Certain Properties with Composition in Aluminium-Tin Wires Annealed for 60 days at 220° C. (Zamotorin¹²). The hardness tests are on cast bars.

filings, and (3) tests on chill-cast alloys to determine the extent of precipitation-hardening.

The alloys were all prepared from super-purity aluminium (99.99%+) obtained from the British Aluminium Company, Ltd., and from Chempur tin (approaching 99.99%).

Preparation of Alloys for the Liquidus Determination.

Melting was carried out in high-purity graphite crucibles in a resistance furnace, the high-tin alloys being protected from oxidation

by broken graphite rods on the surface and by a cover of carbon dioxide. The melts were thoroughly stirred before pouring.

Alloys were prepared having the following nominal tin contents : 0, 0.5, 1, 2, 4, 8, 12, 16, 20, 30, 40, 50, 60, 65, 70, 75, 80, 85, 90, 92, 95, 97, 99, 99.5, 99.75, 100%. They were cast, at a temperature about 100° C. above the liquidus, into $\frac{1}{2}$ -in.-dia. chill moulds of very substantial section made from an aluminium alloy. The billets were used for the examination of the structure of chill-cast alloys and were remelted for thermal analysis.

Preparation of Alloys for Solid-Solubility Determinations.

The aluminium was melted in a graphite crucible and degassed with chlorine through an alumina tube; the tin was then added and the melt well stirred. High-frequency melting was used for all except the 0.02% tin alloys of Fig. 19, which were melted in a resistance furnace.

The range of composition covered was from 0.01% to 1.0% tin. All the alloys were analysed and were found to be very close to the nominal compositions. Analysis of the super-purity aluminium showed < 0.001% silicon and 0.002% iron.

All the alloys were water-chill cast into $1\frac{1}{4}$ -in.-dia. billets. Those for forging were scalped to 1.1 in. dia. and cold forged to $\frac{1}{2}$ in. square. Samples for metallographic examination were taken at this stage.

Solution heat-treatment was carried out for not less than 16 hr., and usually 24 or 48 hr., at 530° C., followed by water quenching. Ageing was carried out for 16 hr. at 165° C.

Thermal Analysis.

The liquidus and eutectic temperatures were obtained from inverse-rate cooling curves. The thermal-analysis equipment is illustrated diagrammatically in Fig. 3; it could be adjusted to give the same rate of cooling at both the liquidus and eutectic temperatures.

Samples for thermal analysis consisted of 25–27 ml. of molten metal. In all cases the temperature was initially raised to about 700° C. to ensure complete solution of the aluminium dendrites. Carbon dioxide was used as a protective atmosphere for the higher-tin alloys.

The metal was stirred continuously with a graphite rod during the test. The temperatures were measured potentiometrically using a Chromel/Alumel thermocouple in an alumina sheath. In the course of the investigation the thermocouples were calibrated on 18 occasions against the melting points of aluminium, zinc, and tin. The maximum alteration between successive calibrations was $\frac{1}{4}$ ° C. The rate of

cooling used was normally between 2 and 4° C./min. The overall accuracy of the determinations is probably better than $\pm \frac{1}{4}$ ° C. After the cooling curves had been obtained, the alloys were remelted and chill cast for chemical analysis.

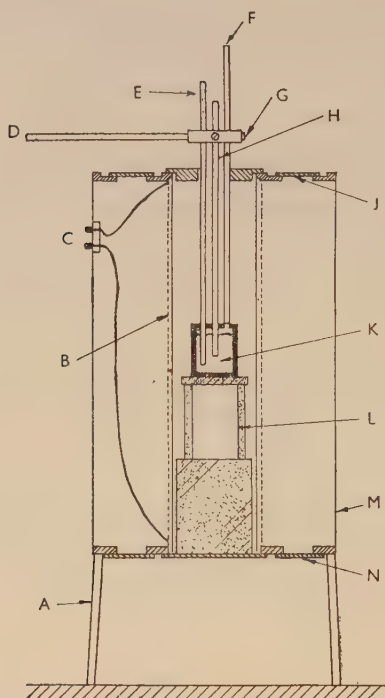


FIG. 3.—Diagrammatic Representation of Thermal Analysis Furnace Suitable for Variable Rates of Cooling.

KEY.

A	Supporting stand.	G	Grub screw.
B	Silica furnace tube with windings covered by Alundum cement.	H	Thermocouple sheath.
C	Terminals connected to variable transformer.	J	Removable split ring.
D	Supporting arm for sheath, &c.	K	Metal in graphite crucible.
E	Stirrer.	L	Refractory tube on refractory block.
F	CO ₂ inlet tube.	M	Terminal shield.
		N	Removable ring.

Metallographic Technique.

After some initial difficulties, a polishing procedure was adopted, which varied only in details from a method developed for strong aluminium alloys.¹⁵ The specimens were rubbed down on 0, 00, and 000 emery papers flooded with a mixture of paraffin oil and liquid

paraffin. They were then polished by hand on Selvyt pads with Brasso, heavy magnesia, and finally light magnesia. It was found essential to wash the magnesia off the specimens as rapidly as possible, since if this was not done shallow corrosion pits were formed. Electrolytic polishing was not suitable for alloys containing more than 4% tin and was used only for the solid-solubility determinations.

Etching the polished specimens was attended by only limited success. A solution of ammonium persulphate was least unsatisfactory. In general, the specimens were examined unetched, except for any attack which occurred during polishing.

For the metallographic examination carried out to determine the solubility of tin in aluminium, mechanical polishing was unsuitable and electrolytic polishing was employed. The micro-specimens were rubbed down to 000 emery, using a light machine oil as a lubricant. A modification of De Sy and Haemers' solution was employed for electrolytic polishing,¹⁶ consisting of four parts of absolute alcohol to one part of perchloric acid. The voltage was controlled at 10–15 V. and the current density was about 0·2 amp./cm.² The specimens were polished in stages of 2½ min.

The polished specimen, still in the anode holder, was then washed either in water or alcohol and immediately etched for 1 min. by swilling with 1% Analar hydrofluoric acid in distilled water. The specimen was dried and examined and then etched for a further 30 sec. It is essential to use high-purity reagents and to standardize the etching conditions. The specimens must be swilled rather than immersed in the etchant, as the slightest trace of tin in the solution will lead to bad pitting of subsequent specimens.

III.—THE LIQUIDUS.

The thermal-analysis results have been plotted in Fig. 4. The liquidus takes the form of a perfectly smooth curve. It confirms the average curve of Gwyer and Crepaz, although it is a few degrees higher between 50–80% tin. No evidence was found of any liquid immiscibility.

The eutectic concentration was confirmed as being about 0·5% tin, although no attempt was made to fix this accurately. In the alloy containing 30% tin the eutectic arrest was determined as 227·9° C. In alloys with 50, 70, 90, 95, 99, 99·5, and 99·75% tin, the arrest occurred at either 228·5° or 228·3° C., the last three alloys giving the latter value. This variation of 0·2° C. in the arrest point represents a variation in thermo-e.m.f. of only 0·01 mV. On the basis of these measure-

ments the eutectic temperature has been taken as 228.3° C., a value somewhat lower than that of earlier investigations.

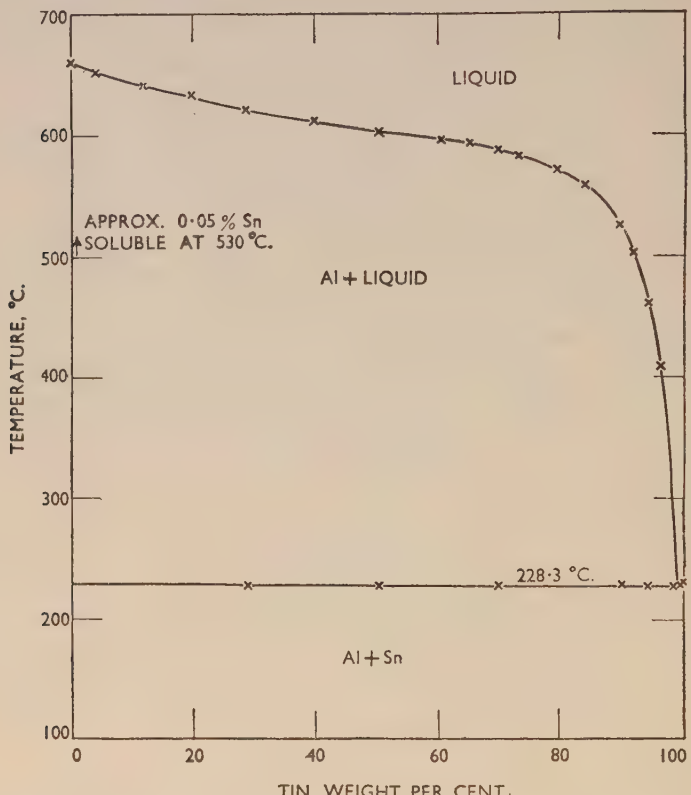


FIG. 4.—The Aluminium-Tin Equilibrium Diagram from Thermal Analysis. Solid solubility of tin in aluminium approx. 0.05% at 530° C. Eutectic composition ~99.5% tin.

IV.—STRUCTURE OF CHILL-CAST ALLOYS.

Up to 99% tin the structure consisted of primary aluminium with interdendritic pools of tin-rich material (Figs. 5-7, Plate XXXIV). Up to 20% tin the structure was typical of aluminium alloys containing a degenerate eutectic.

The aluminium dendrites in a background of the tin-rich phase in the 95% tin alloy were frequently darkened by corrosion (Fig. 7). The 99% tin alloy showed a few very small corroded areas, probably due to primary particles of aluminium.

X-Ray Examination.

A Debye-Scherrer examination was made of two samples of 200-mesh filings from the annealed chill-cast billets. The filings were heat-treated in a vacuum for 64 and 79 days at 200° and 100° C., respectively; the X-ray photographs showed no lines due to phases other than aluminium and tin. Lines due to tin were detected at all compositions from 0·6% tin upwards.

Hardness Tests.

Hardness test results are given in Table I. The scatter of results on the chill-cast alloys is too great to show whether small tin additions raise the hardness of pure aluminium, as reported by Zamotorin for material of commercial purity (Fig. 2). This was also true in the other conditions of heat-treatment in Table I.

TABLE I.—*Hardness Test Results on Chill-Cast Aluminium-Tin Alloys Made from Super-Purity Aluminium and Chempur Tin.*

Tin Content, wt.-%	As chill cast (B.H.N. 2/20/15)	Heated 7 days at 300° C. and water quenched (V.P.N. HD1).	Heated 7 days at 300° C., compressed 50%, heated 14 days at 300° C. and water quenched (V.P.N. HD1)	Compressed 50%, heated 62 days at 200° C. and water quenched		Compressed 50%, heated 9 days at 500° C. and water quenched* (V.P.N. HD1)	Compressed 30%, heated 10 days at 400° C. and water quenched (V.P.N. HD1)
				V.P.N. HD1	B.H.N. 2/20/15		
0	16·3	18·4	20·2	29·5 *	26·3 *	19·9	17·1
0·5	20·7	17·5	18·0	29·5 *	23·5 *	20·1	18·4
1·0	19·0	17·5	17·5	29·9 *	24·3 *	21·3	19·9
2·0	21·0	19·9	16·7	28·8 *	26·3 *	18·6	18·9
4·0	19·4	21·0	17·5	28·8 *	24·5 *	20·8	19·6
8·1	26·9	20·0	17·0	29·8 *	25·9 *
11·8	20·5	18·8	18·1
16·4	20·9	21·7	20·3
18·6	19·3	19·3	16·9
29·9	19·3	...	20·0
53·2	20·5	20·5	17·3
70·4	18·6	...	20·6
90·0	16·2
94·8	16·7
99·0	19·1
100·0	7·2

* These specimens were incompletely recrystallized after heat-treatment. All other worked and heat-treated specimens were completely recrystallized.

B.H.N. = Brinell hardness number. V.P.N. = Vickers diamond pyramid hardness number.

The strengthening effect of small aluminium additions to tin is well confirmed. The aluminium-tin eutectic is considerably harder than pure tin.

V.—SOLID SOLUBILITY OF TIN IN ALUMINIUM.

Metallographic Examination.

The microstructure of alloys containing 0, 0·025, and 0·05% tin is illustrated in Figs. 9–14 (Plate XXXV). Super-purity aluminium (Figs. 9 and 10) showed no ageing effects and the grain boundaries were only weakly delineated. The reason for the pits in the background is not clear, but they may be due to gas porosity. The number of such pits increased with increasing tin content, and in alloys with tin contents of several per cent. the pits were obviously due to porosity.

In the solution-heat-treated condition the 0·025% tin alloy was very similar to super-purity aluminium (Fig. 11). Precipitation occurred on ageing at 165° C. (Fig. 12).

Precipitation also occurred when alloys containing 0·05% tin and more were aged (Fig. 14). In the solution-heat-treated condition the 0·05% tin alloy showed discontinuous dots in the grain boundaries. These became more continuous with increasing tin content.

The quantity of "precipitate" in the aged specimens is greatly in excess of the amount to be expected in such weakly alloyed materials. Hence, the structures shown in Figs. 12 and 14 must be taken as being due to an etching effect associated with the tin-rich regions, the etching characteristics of the naturally and artificially aged materials being markedly different.

The metallographic evidence indicates that the solubility at 165° C. is probably considerably below 0·02% tin. At 530° C. it is just below 0·05%, the pits at the grain boundaries of Fig. 13 probably corresponding to tin which was liquid during solution heat-treatment. A rather similar technique has been used by Fink, Willey, and Stumpf¹⁷ for determining the solid solubility of sodium in aluminium. The presence of small pits in specimens electrolytically polished in a solution of fluoboric acid was taken by them as evidence for the existence of an undissolved sodium-rich phase.

Age-Hardening of Aluminium-Tin Alloys.

Determinations were made of the 0·1% and 0·2% proof stresses, ultimate tensile stress, and elongation of a series of alloys containing 0–0·1% tin. These alloys were water-chill cast and were tested after being solution heat-treated for 16 hr. at 530° C., quenched in cold water, and aged either for 15 days at room temperature or for 16 hr. at 165° C. Two specimens were tested in each condition of heat-treatment.

The 0·1% and 0·2% proof stresses showed similar variations with

tin content; the values of the 0·2% proof stress are plotted in Fig. 21. The ultimate tensile stress was largely independent of tin content in the naturally aged condition, varying between 2·78 and 3·99 tons/in.² After artificial ageing there was a more systematic change from about 3 to about 3·7 tons/in.² for the super-purity aluminium and 0·1% tin alloy, respectively. The elongation showed erratic variations between 35 and 55%, depending on the crystal size and orientation.

As shown in Fig. 21, the proof-stress values increased with increasing tin content. The further rise on artificial ageing of tin-containing alloys is well marked. The difference between the averaged curves reaches a maximum at about 0·05% tin, suggesting that the solubility at 530° C. is of this order, although in view of the scatter of results too much significance should not be attached to this. Similarly, the averaged curves suggest that the solubility at 165° C. is below 0·01% tin, but, here again, the scatter of results precludes an accurate assessment. However, the solubility at this temperature is certainly well below 0·02% tin, in agreement with the metallographic examination.

Lattice-Parameter Measurements.

Lattice-parameter measurements were made on three of the materials used for the survey of the entire system, namely pure aluminium and the 1% and 8% tin alloys. In addition, in view of the metallographic evidence of solubility at 530° C., it was decided to see whether parameter measurements on the alloys prepared for the solubility determination would give any additional evidence of solubility at temperatures of that order. Small billets were taken after cold forging

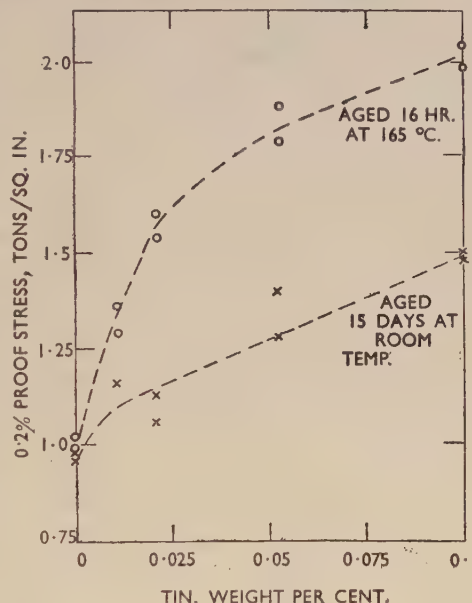


FIG. 21.—Proof Stress of Aluminium-Tin Alloys. Water chill cast, solution heat-treated 16 hr. at 530° C., quenched in cold water, and aged as indicated.

to $\frac{1}{2}$ in. square and heat-treated for 48 hr. at 520° C. in a salt bath; the surface layers were then skimmed off and a considerable quantity of filings taken with a dead smooth file. These filings were cleaned with benzene and particles of iron from the file were removed with a magnet. To prevent silicon pick-up, the filings were packed in alumina tubes and then sealed off in Pyrex tubes after evacuation and degassing.¹⁸ After heat-treatment for 18 hr. at 520° C. , the tubes were quenched into an ice/water mixture from a specially constructed quenching furnace. The tubes shattered on quenching, and the powders gave diffraction patterns with sharp, well-resolved lines.

The films were taken with 200-mesh powder in a 19-cm. Debye-Scherrer camera, using unfiltered cobalt radiation which gave the (420) and (331) α doublets at 81° - 82° and 74° , respectively, and the (422) β line at 78° . The Nelson-Riley extrapolation¹⁹ was used to evaluate the parameters. The wave-lengths and the conversion factor used were those given by Bragg.²⁰ The refractive-index correction was applied. The results obtained are given in Table II.

TABLE II.—*Lattice-Parameter Measurements on Aluminium-Tin Alloys.*

Alloy No.	Composition	Heat-Treatment Applied to Filings	Lattice Parameter at 25° C. , kX. units
F. 76	Super-purity Al	18 hr. at 520° C. , I.Q.	4·0413 ₈
F. 77	0·025% Sn alloy	" " "	4·0414 ₇
F. 78	0·055% "	" " "	4·0416 ₃
F. 79	0·098%	" " "	4·0416 ₇
F. 80	0·19%	" " "	4·0415 ₃
F. 81	0·50%	" " "	4·0415 ₂
F. 82	1·00%	" " "	4·0415 ₃
F. 79	0·098% "	18 hr. at 520° C. , I.Q. plus 16 hr. at 165° C. , I.Q.	4·0414 ₅
	Super-purity Al	64 days at 200° C. , I.Q.	4·0414 ₀
	1% Sn alloy	" " 200° C. , I.Q.	4·0413 ₅
	8%	" " 200° C. , I.Q.	4·0414 ₅

Average of the values for Alloys F. 78-82 given above = 4·0415₈ kX.

Average of the values for Super-purity Al given above = 4·0413₉ kX.

I.Q. = Quenched into iced water.

The measurements were very carefully carried out, and the temperature of the specimens was controlled within closer limits than $\pm \frac{1}{2}^\circ\text{ C.}$ during the exposures. It is considered that the relative accuracy of the parameter values quoted is $\pm 0·00005$ kX. unit.

The mean of the two values for pure aluminium is 4·0413₉ kX. units, which is in good agreement with the values of Hume-Rothery*

* Published value with correction for refractive index of +0·00003 kX. unit not made in original.

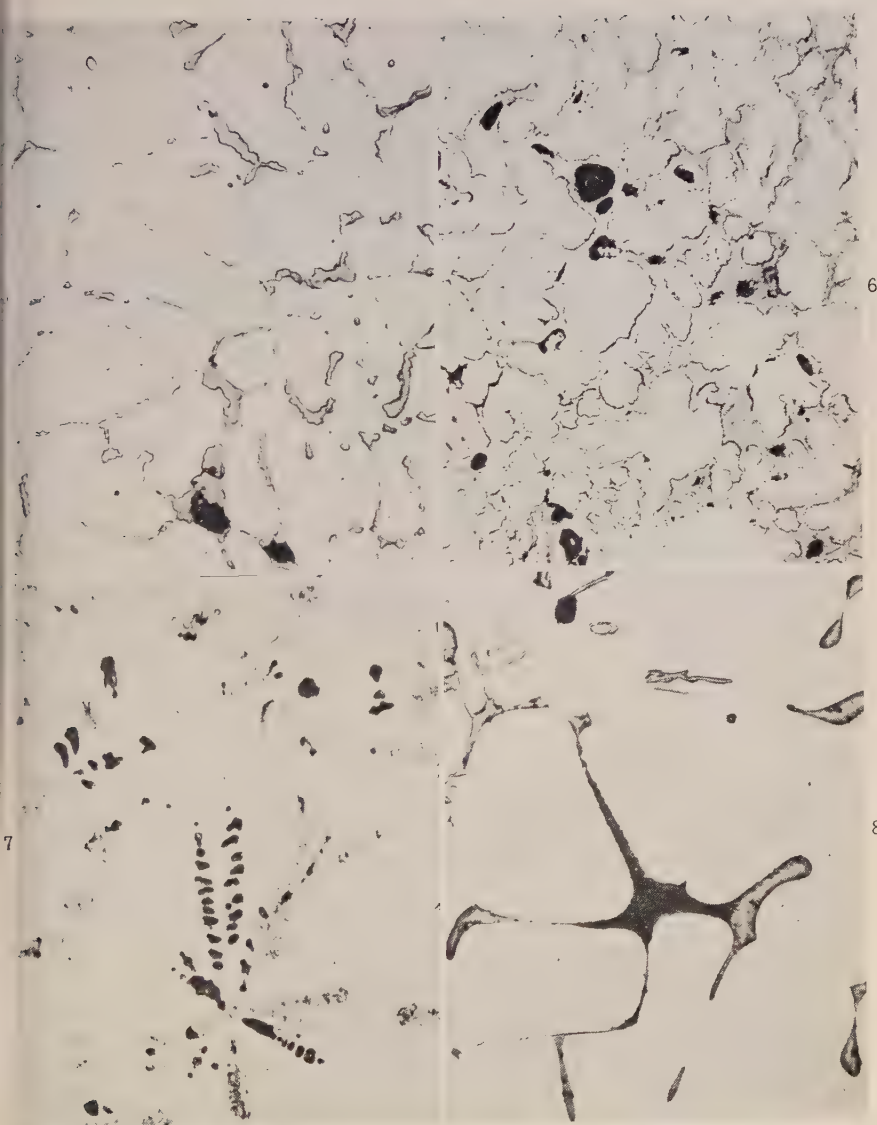


FIG. 5.—Aluminium-12% Tin Alloy, chill cast. Al light, Sn-rich half-tone. $\times 500$.
FIG. 6.—Aluminium-50% Tin Alloy, chill cast. Al light, Sn-rich half-tone. $\times 500$.
FIG. 7.—Aluminium-95% Tin Alloy, chill cast. Al dark or mottled, Sn-rich light. $\times 500$.
FIG. 8.—Aluminium-10% Tin Alloy, sand cast. Al light, Sn half-tone, Mg_2Sn dark. $\times 250$.

[To face p. 280.]



FIGS. 9 and 10.—Super-Purity Aluminium.

FIGS. 11 and 12.—Aluminium-0.025% Tin Alloy.

FIGS. 13 and 14.—Aluminium-0.05% Tin Alloy.

All electrolytically polished and etched in $\frac{1}{2}\%$ HF. All $\times 250$.
Left-hand side: solution heat-treated at 530° C .

Right-hand side: solution heat-treated and then aged at 165° C .

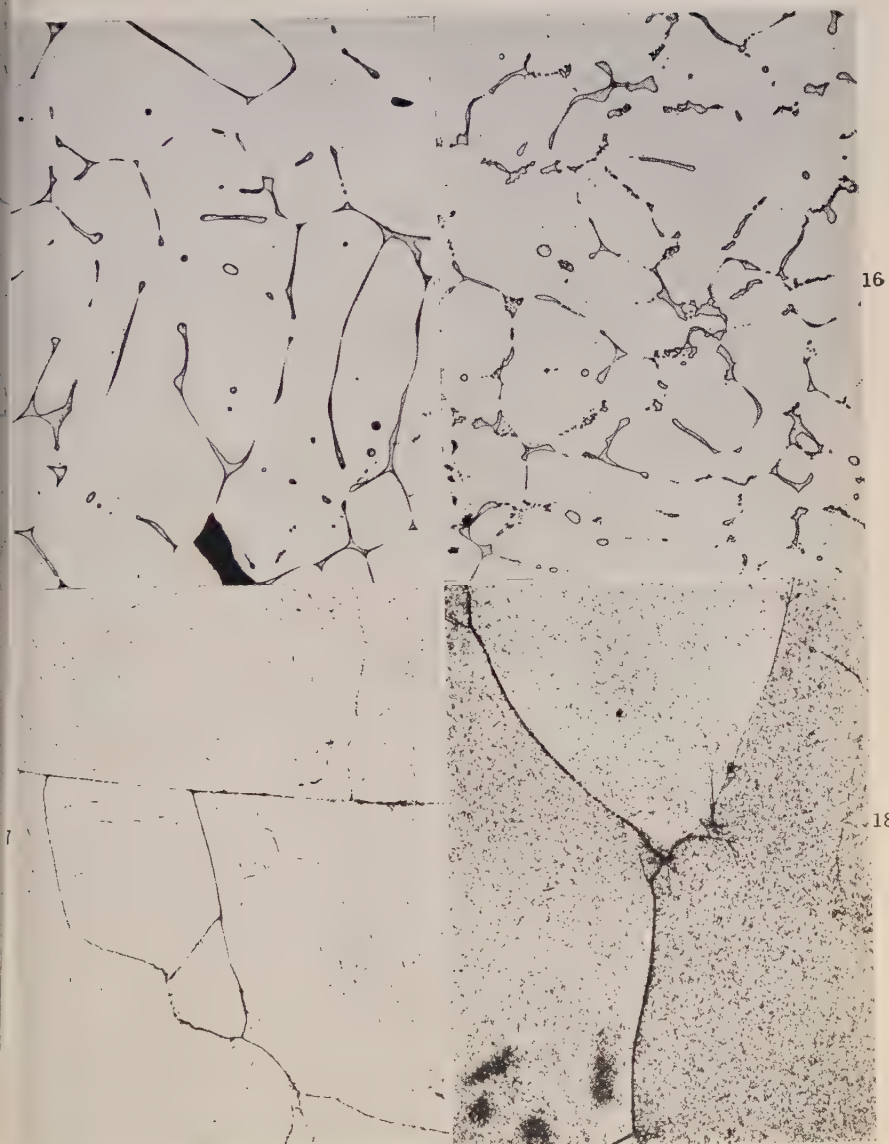
FIG. 15.—Aluminium-10% Tin Alloy, sand cast. Al light, Sn half-tone. $\times 100$.FIG. 16.—Aluminium-10% Tin-1% Nickel Alloy, sand cast. Al light, Sn half-tone. $\times 100$.FIG. 17.—Aluminium-4% Copper Alloy. Solution heat-treated and aged 24 hr. at 190°C .Etched in 25% HNO_3 at 70°C . for 2 min. $\times 250$.

FIG. 18.—Aluminium-4% Copper-0.05% Tin Alloy. Same treatment as Fig. 17.

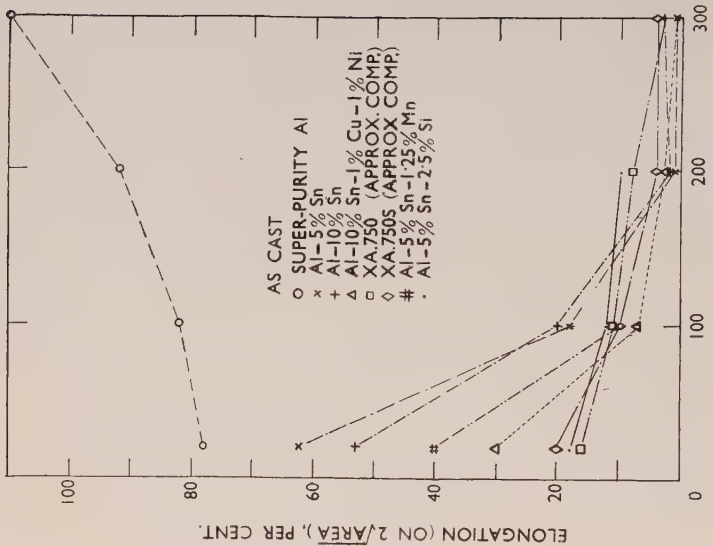


FIG. 19.—Variation of Maximum Stress with Temperature.

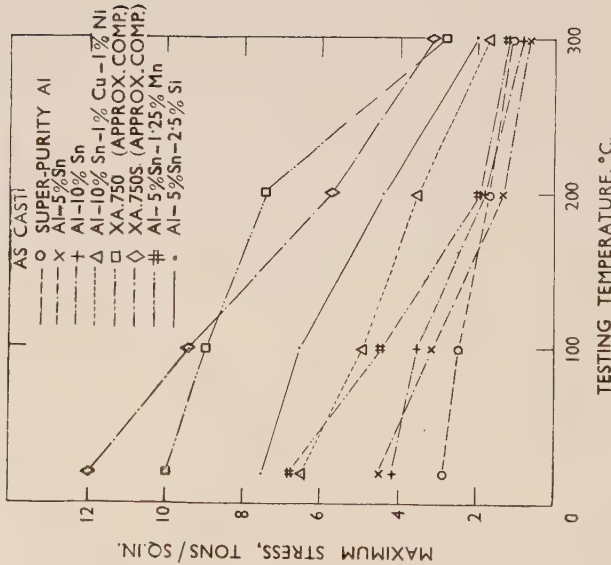


FIG. 20.—Variation of Elongation with Temperature.

4·0413₇,²¹ Jette and Foote, 4·0413₉,²² and Wilson 4·0413₄,²³ For the specimens heat-treated at 520° C., the mean of the parameters of the alloys containing 0·05–1·0% tin, which on the metallographic evidence should be saturated, is 4·0415₈ kX. units. The difference between the mean parameters, i.e. 0·0001₉ kX. units, is considered to be definite evidence of the solubility of tin, and the figures suggest that the solubility limit is less than, but close to, 0·05%.

In view of the evidence from mechanical tests and metallographic examination of ageing after 16 hr. at 165° C., the alloy containing 0·1% tin was aged under these conditions in vacuum and the parameter again measured. The value obtained—4·0414₅ kX. units, which is a reduction of 0·0002₂ kX. units from the previous value for this alloy—supports the argument that significance may be attached to the parameter evidence of the solubility of tin.

VI.—DISCUSSION OF RESULTS.

In confirmation of earlier work, the aluminium-tin equilibrium diagram has been found to be of the simple eutectiferous type, the eutectic being very close to the tin side of the diagram and 3·6° C. lower than the melting point of tin.

The solid solubility of tin in aluminium may be taken as just below 0·05 wt.-% at 530° C. and considerably below 0·02% at 165° C. The value at 530° C. is close to that given by Fink,¹⁴ viz. approximately 0·05% at 500° C. The small difference in the two results may be due either to the slightly different temperatures or to lack of attainment of complete equilibrium at 530° C.

It is clear that the inflections found by Zamotorin at 2% tin on plotting different physical properties against composition (Fig. 2) are not the results of solubility effects.

This type of solubility curve, in which the solubility reaches a maximum at a temperature higher than that of the eutectic, has been termed a “reverse saturation curve” by Scheil.²⁴ It has been found in silver-lead alloys²⁵ and in several other systems²⁶ where there is a considerable difference between the melting points of the metals and also between the sizes of the atoms.

B. TIN AS AN ALLOYING ELEMENT IN ALUMINIUM ALLOYS.

I.—CLASSIFICATION OF ALLOYS BASED ON THEIR TIN DISTRIBUTION.

Aluminium alloys containing tin may, for convenience, be discussed in three groups :

- (a) Those in which tin is a major constituent.
- (b) Those in which tin is a soluble constituent.
- (c) Those in which the tin is combined with another element, such as magnesium.

Alloys of the first group possess in the cast condition a more or less continuous network of the tin-rich eutectic, which, although exerting comparatively little effect at room temperature, has a predominant influence on their properties at somewhat higher temperatures.

Alloys in the second group contain only a small quantity of tin. Although the solubility of tin is very low, it is shown to be capable of exerting a pronounced influence on the ageing characteristics of aluminium-copper alloys, such as D.T.D. 304.

The typical effects of tin are lost in the third group of alloys, in which it is combined with other alloying elements. This is illustrated by the behaviour of Duralumin-type alloys containing magnesium, in which small tin additions are without influence on the forgeability and ageing characteristics.

It may be noted that although aluminium-copper-tin alloys were used at one time and tin has been claimed to improve the castability of aluminium alloys, this has not been confirmed by hot-tear tests of the type used by Lees,²⁷ which have been carried out on D.T.D. 304 and D.T.D. 424 alloys containing tin additions up to 2%.

The small effect of limited tin additions is not unexpected, since the addition of 2 wt.-% tin to aluminium alloys results in an addition of only approximately 0·7% by volume of tin eutectic. The increase in eutectic index²⁷ resulting from the tin addition is therefore small, and in addition aluminium-tin eutectic persists in liquid form down to a temperature of 228° C., thereby enormously extending the solidification range.

II.—ALUMINIUM ALLOYS CONTAINING TIN AS A MAJOR CONSTITUENT.

Aluminium-base bearing alloys form the chief class of materials in this group. These generally contain about 5–7% tin, together with small quantities of other elements, such as copper, nickel, and silicon.^{28, 29}

Typical of such alloys are Alcoa XA 750 and XA 750S. The bearings are normally used in the cast and stabilized condition, the additional alloying elements being present to improve their strength.

The tin-rich eutectic occurs interdendritically in the form of films and pools. The bearing behaviour will undoubtedly be influenced by the tin distribution, the effect of various factors on which has been investigated.* The basic alloy chosen contained 10% tin and the structure as sand-cast is shown in Fig. 15 (Plate XXXVI). The chill-cast alloy possesses a similar structure, but on a much smaller scale. Variations in the rate of pouring and in the pouring temperature in the range covered were found to be without influence on the tin distribution in both cold and heated metal moulds.

Additions of silicon, zinc, magnesium, and manganese were found to have no substantial effect on the dendrite size or on the distribution of tin in either chill- or sand-cast 10% tin alloy. Only nickel, or possibly nickel plus copper, had the effect of reducing the film-forming tendency of the tin. The structure of an aluminium-10% tin-1% nickel alloy is shown in Fig. 16 (Plate XXXVI), from which it will be seen that the tin has solidified in the form of more isolated pools. A similar effect due to the simultaneous addition of nickel and copper was not reproducible in duplicate tests.

The presence of magnesium caused the appearance of a new phase, brown in colour and liable to be somewhat corroded during polishing (Fig. 8, Plate XXXIV). This is believed to be Mg_2Sn .

The mechanical properties of aluminium-tin alloys were investigated by preparing alloys made from super-purity aluminium, with additions of 5 and 10% tin. Super-purity alloys were also made containing 10% tin with 1% of both nickel and copper, and 5% tin with either 1½% manganese or 2½% silicon. Alloys made from commercial-purity aluminium and approximating in composition to the commercial alloys Alcoa XA 750 and XA 750S, were also prepared. The results of tensile tests, which were carried out at both room and elevated temperatures, are set out in Figs. 19 and 20,* Plate XXXVII.

Dealing first with the properties at room temperature, it is clear that tin additions have caused a substantial increase in the tensile strength of super-purity aluminium. There is a slight reduction in ductility at room temperature in the binary alloys made from super-purity aluminium, but these alloys are very much more ductile than the alloys made from commercial-purity aluminium, or alloys in which additions of copper and nickel, or manganese, or silicon are also made.

A most striking effect, however, occurs in tensile tests carried out

* In all cases the experimental details are given in the Appendix.

at elevated temperatures below the melting point of the aluminium-tin eutectic. Even at the comparatively low temperature of 100° C. there is a very marked drop in ductility in all the aluminium-tin alloys in this series. The ductility of super-purity aluminium, on the other hand, increases with increase in temperature, which is the normal effect of elevated temperatures on the ductility of most alloys tested below the solidus temperature.

At elevated temperatures the fractures of the alloys were interdendritic. The fall in ductility is greatest for the binary aluminium-tin alloy, whereas the commercial alloys and the aluminium-5% tin- $2\frac{1}{2}$ % silicon alloy, although possessing lower ductility at room temperature, retained their ductility with increasing temperature to a greater extent, and above 150° C. possessed a higher elongation than the other alloys.

It has been shown by Hanson and Sandford³⁰ that the tin-aluminium eutectic in the form of sheet is liable to a reduction in strength due to atmospheric corrosion. There is experimental evidence, however, that the results shown in Figs. 19 and 20 are not due to such extraneous influences. The room-temperature properties were redetermined after previous exposure of the alloys in air at 100° or 200° C. and were found to be unaffected, while high-temperature tests in an oil bath out of contact with air gave similar values to those obtained in air.

The tensile strength of the cast tin-aluminium eutectic has been given as 5.2 tons/in.², with 27% elongation, compared with 1.4 tons/in.² and 69% for pure tin.³⁰ The variation of tensile properties of the tin-aluminium eutectic with temperature is not known, but Homer and Plummer³¹ have shown that the tensile properties of pure tin fall steeply and almost linearly with increasing temperature to a very low value near the melting point.

Thus, at room temperature, the tin-aluminium eutectic is comparable in strength with, if not stronger than, the aluminium matrix, and, under stress, homogeneous deformation may occur, associated with appreciable ductility. Since the melting points of tin and the tin-aluminium eutectic are within 4° C. of each other, it may be assumed that the eutectic shows the same sharp fall in strength with increasing temperature as is shown by pure tin, whereas the fall in strength of the aluminium matrix is much less rapid. At elevated temperatures, therefore, the strength and ductility of the aluminium-tin alloys are determined primarily by the pulling apart of the eutectic films. These are so thin that even though they may have a high ductility the overall deformation of the specimen at fracture is low.

The behaviour of the binary aluminium-tin alloys and the complex

commercial alloys containing nickel and copper is in agreement with the microstructural observations that the tin films are most continuous in the pure aluminium-tin alloys. The commercial alloys do not show the same marked drop of elongation with increasing temperature as do the binary aluminium-tin alloys.

The further conclusion can be drawn from Figs. 19 and 20 (Plate XXXVII) that the hot working of alloys containing fairly large tin additions directly from the cast state is likely to be difficult, if not impossible.

III.—ALUMINIUM ALLOYS CONTAINING TIN AS A SOLUBLE CONSTITUENT.

It was observed in the work on the phase diagram that the slight solubility of tin in aluminium was sufficient to cause considerable age-hardening, after solution treatment and quenching. After ageing for 16 hr. at 165° C., the 0·2% proof stress of the alloy containing 0·05% tin is increased from 1·3 to 1·8 tons/in.² (Fig. 21, p. 279). Very little is known about the influence of this solubility on aluminium alloys in general, but it has been found that small quantities of tin can exert a relatively large effect on the ageing of aluminium-copper alloys containing 4·0–5·0% copper. A search made simultaneously with the experimental work showed that the effect has been described in the patent literature,³² but apparently not elsewhere.

The properties and heat-treatments of the cast aluminium-4 $\frac{1}{2}$ %

TABLE III.—*Specification Figures for Commercial-Purity Aluminium-4 $\frac{1}{2}$ % Copper Alloy.*

Specification No.	Heat-Treatment	Properties as Sand-Cast		
		0·1% Proof Stress, tons/in. ²	Max. Stress, tons/in. ²	Elongation % on 2 in.
D.T.D. 298	More than 12 hr. at 525°–545° C., water quenched. May be reheated to 130° C. for 1–2 hr., otherwise naturally aged.	11 *	14	7
D.T.D. 304	12–16 hr. at 525°–545° C., water quenched. Aged 6–18 hr. at 120°–170° C.	14 *	18	4
D.T.D. 361	Not less than 16 hr. at 535°±10° C., quenched in water or oil. Aged 8–16 hr. at 165°±5° C.	20 *	21	1

* D.T.D. expected minimum for proof stress.

TABLE IV.—*Tensile Test Results on D.T.D. Bars of Al-4½% Cu-0·12% Si-0·3% Fe-0·2% Ti Alloys Containing Various Quantities of Tin.*

Solution heat-treated 16 hr. at 535° C., quenched in cold water, and aged 15 days at room temperature.

Reference No.	0·1% Proof Stress, tons/in. ²	Maximum Stress, tons/in. ²	Elongation, %	Vickers Diamond Pyramid Hard- ness No.
<i>Tin-free alloy.</i>				
M 73/1	6·8	16·1	11	80·5
M 73/3	6·6	16·6	11	...
<i>Alloy containing 0·05% Sn.</i>				
F 334/1	5·0	12·0	7	78·8
F 334/3	5·0	12·0	...*	...
<i>Alloy containing 0·1% Sn.</i>				
F 333/1	4·8	11·6	8	78·5
F 333/3	4·8	14·3	10	...
<i>Alloy containing 0·25% Sn.</i>				
M 74/1	4·4	13·6	...*	68·6
M 74/3	4·6	10·4	5	...
<i>Alloy containing 0·5% Sn.</i>				
M 77/1	4·0	9·6	6	64·8
M 77/3	4·6	11·4	...*	...

* Broke in shoulder.

copper alloy are listed, together with the relevant specifications, in Table III. Tables IV, V, and VI give the tensile properties obtained after natural and after artificial ageing on such an alloy made from aluminium of commercial purity, with and without tin additions. It will be seen that the tin-containing alloys show a much lower response to natural ageing, but a marked increase in properties after artificial ageing. This is particularly noticeable in the hardness and proof-stress values. Similar results are shown by high-purity alloys (Table VII). It may be noted that 0·05 wt.-% tin is equivalent to just over 0·01 at.-% tin.

The alloys with the higher tin contents in Tables IV and V show an undue brittleness. Comparison of Tables III, V, and VI shows that it is difficult to meet the properties called for in D.T.D. 361 in the aluminium-copper alloys free from tin. By a judicious balance of alloy purity, tin content, and casting temperature, however, the properties are readily obtainable with the specified heat-treatment.

Subsequent experience has shown that the scatter of elongation values in Tables IV and V was associated with a high pouring temperature. A pouring temperature of 620° C. gave the results shown in Table VI.

TABLE V.—Tensile Test Results on D.T.D. Bars of Al-4½% Cu-0·12% Si-0·3% Fe-0·2% Ti Alloys Containing Various Quantities of Tin.

Solution heat-treated 16 hr. at 535° C., quenched in cold water, and aged 16 hr. at 165° C.

Reference No.	0·1% Proof Stress, tons/in. ²	Maximum Stress, tons/in. ²	Elongation, %	Vickers Diamond Pyramid Hard- ness No.
<i>Tin-free alloy.</i>				
M 73/1	13·7	19·6	4	99·4
M 73/4	13·2	20·4	4	109
<i>Alloy containing 0·05% Sn.</i>				
F 334/2	20·0 *	20·0	1	136
<i>Alloy containing 0·1% Sn.</i>				
F 333/2	20·7 *	22·3	1	140
F 333/4	21·9 *	22·9	1	...
<i>Alloy containing 0·25% Sn.</i>				
M 74/2	18·4	18·6	... †	138
M 74/4	16·8	17·4	... ‡	139
<i>Alloy containing 0·5% Sn.</i>				
M 77/2	20·2	21·4	... †	...
M 77/4	20·0	21·2	2	128

* 0·05% proof stress, tons/in.²

† Broke in shoulder.

‡ Broke at gauge mark.

Micro-examination confirmed the increased rate of ageing of the alloys containing tin. This is illustrated in Figs. 17 and 18 (Plate XXXVI), where an ageing treatment at 190° C. has been carried out

TABLE VI.—Tensile Test Results on D.T.D. Bars of Al-4½% Cu-0·12% Si-0·15% Fe-0·15% Ti Alloys Containing Various Quantities of Tin, Cast at 670° C.

Solution heat-treated 16 hr. at 530° C., quenched in cold water, and aged 16 hr. at 165° C.

0·1% Proof Stress, tons/in. ²	Maximum Stress, tons/in. ²	Elongation, %
<i>Tin-free alloy.</i>		
15·6	22·1	6
15·0	19·2	4
<i>Alloy containing 0·05% Sn.</i>		
23·5	25·2	2
23·3	24·9	2
23·5	25·5	2
22·6	24·8	2

TABLE VII.—*Hardness Values on Super-Purity Aluminium-4% Copper Alloys with Tin Additions, Sand Cast, Solution Heat-Treated for 16 hr. at 530° C., and Aged as Indicated.*

Alloy	Vickers Diamond Pyramid Hardness No.	
	Aged 15 days at room temp.	Aged 16 hr. at 165° C.
Al-4% Cu . . : :	79	113
Al-4% Cu-0.025% Sn : .	71	121
Al-4% Cu-0.05% Sn . .	65	142

to show the effect more clearly. The tin-containing alloy shows a much more marked development of precipitation than the tin-free alloy. The increased rate of artificial ageing would be accounted for if it is assumed that the particles of tin precipitate first and act as nuclei on which the precipitation of copper can occur. It is, however, difficult to account for the slower natural ageing of the alloys containing tin on this basis.

A very tentative explanation of this effect may be advanced by considering the relative sizes of tin and copper atoms in relation to aluminium. Taking the closest distance of approach of the atoms in the pure substance as a measure of their size,³³ it is clear that copper atoms are smaller than aluminium atoms, whereas tin atoms are larger. This is confirmed by their behaviour when dissolved in aluminium. Copper atoms cause the aluminium lattice to contract,²¹ whilst there are indications that it is expanded by tin atoms (Table II). It is visualized that these conditions may give rise to a preferred atomic arrangement during solution heat-treatment, when the lattice strain due to a large tin atom can be relieved by a collection of smaller copper atoms around it. The strain energy associated with such a collection of atoms would then be smaller than that due to the atoms individually. This is analogous to the collection of solute atoms around a dislocation which has been postulated by Cottrell.³⁴ If this aggregation of copper-tin atoms is sufficiently stable, it will resist rearrangement during natural ageing, with the result that natural ageing will be retarded and lower properties may be expected. On artificial ageing, the tin atoms may be expected to precipitate, and as a consequence the collection of copper atoms will be favourably placed for rapid precipitation at the stage when its rearrangement becomes possible. This explanation is very tentative and is unlikely to give a complete picture. It does not preclude the formation of an aluminium-copper-tin precipitate on

artificial ageing. Its chief merit lies in providing a basis for future experimental work.

IV.—ALUMINIUM ALLOYS CONTAINING TIN COMBINED WITH OTHER ELEMENTS.

The normal effect of tin will be suppressed if it combines with other elements present in the alloys. Cook and Chadwick have found that

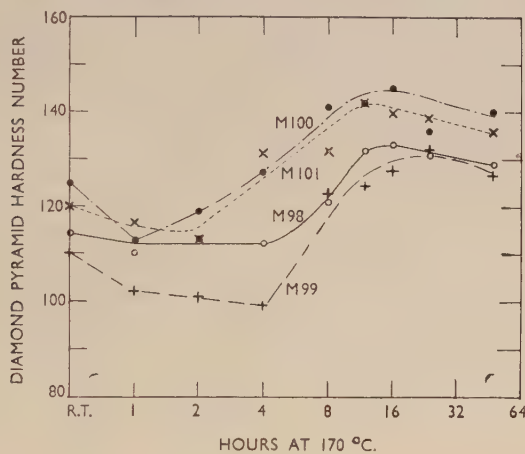


FIG. 22.—Artificial Ageing Curves at 170° C.

KEY.
—○— M98. 4½% Cu, 0·5% Mg.
-+— M99. 4½% Cu, 0·5% Mg + 0·3% Sn.
—●— M100. D.T.D. 364A.
---x--- M101. D.T.D. 364A + 0·3% Sn.

up to 0·3% tin has no effect on the natural ageing of a sheet alloy containing 4% copper and 0·6% magnesium (B.S.S. L3).³⁵ Information on artificially aged alloys was provided by studying the effect of a similar quantity of tin on forged aluminium-4½% copper and aluminium-4½% copper-0·5% magnesium alloys and an aluminium alloy containing 4½% copper, 0·7% silicon, 0·8% iron, 0·7% manganese, 0·5% magnesium, 0·15% titanium, conforming to D.T.D. 364A. This quantity of tin made the straight aluminium-copper alloy so hot-short that it was unforgeable directly from the cast state, and further work on this alloy was abandoned. The alloys containing magnesium forged satisfactorily, even in the presence of tin.

Natural and artificial ageing was followed by hardness tests. The natural-ageing curves of the tin-free and tin-containing alloys with magnesium were fairly similar, in agreement with the results of Cook and Chadwick.³⁵ On ageing at 170° C., the tin-containing alloys were slightly softer than those free from tin, but the differences were not very great (Fig. 22).

Tensile test results after ageing at room temperature and for 16 hr. at 170° C. are given in Tables VIII and IX, from which it will be seen that 0·3% tin has had little effect in either condition.

The conclusions to be drawn are that 0·3% tin is without influence on the forgeability or ageing characteristics of Duralumin-type alloys containing 0·5% magnesium. If all the tin were associated with

TABLE VIII.—*Tensile Test Results on $\frac{3}{4}$ -in.-Square Forged Bars Solution Heat-Treated at 510° C., Quenched in Cold Water, and Naturally Aged for 8 Days.*

Alloy	0·1% Proof Stress, tons/in. ²	Maximum Stress, tons/in. ²	Elongation, %
Al-4½% Cu-0·5% Mg . . . {	16·4	25·8	29
	15·3	25·7	33
Al-4½% Cu-0·5% Mg-0·3% Sn {	14·8	25·5	29
	14·7	25·6	32
D.T.D. 364A *	15·7	28·6	23
	15·7	27·8	27
D.T.D. 364A + 0·3% Sn . . {	15·0	28·0	25
	14·9	28·0	24

* Composition as given in Table IX.

TABLE IX.—*Tensile Test Results on $\frac{3}{4}$ -in.-Square Forged Bars, Solution Heat-Treated at 510° C., Quenched in Cold Water, and Aged for 16 hr. at 170° C.*

Alloy	0·1% Proof Stress, tons/in. ²	Maximum Stress, tons/in. ²	Elongation, %
Al-4½% Cu-0·5% Mg . . . {	21·2	26·6	17
	22·4	28·1	13
Al-4½% Cu-0·5% Mg-0·3% Sn {	19·9	26·0	17
	20·0	25·9	13
D.T.D. 364A *	24·0	29·2	11
	24·6	28·8	13
D.T.D. 364A + 0·3% Sn . . {	24·0	28·7	13
	24·0	27·8	13

* 4½% copper, 0·7% silicon, 0·8% iron, 0·7% manganese, 0·5% magnesium, 0·15% titanium, remainder aluminium.

magnesium in the ratio Mg_2Sn , which seems very likely in view of the freedom from hot-shortness, the effective magnesium content would be reduced by about 0·1%. This would not have a very marked influence on the ageing characteristics and thus the results are readily understood.

V.—DISCUSSION.

The properties due to tin in aluminium alloys have been described for the three types into which aluminium-tin alloys may conveniently be divided.

In the case in which tin combines with other elements present in the alloy, the presence of tin is not beneficial, but neither is it necessarily detrimental. Where tin is a major constituent, the properties are determined chiefly by the properties of the tin-aluminium eutectic, and in the as-cast condition such alloys have low ductility at elevated temperatures and cannot be hot forged.

It has been shown that as a soluble element tin may have a pronounced influence on the ageing characteristics of aluminium-copper alloys. A small quantity of tin may be beneficial for the purpose of producing the maximum ductility in the solution-heat-treated condition and the maximum hardness, proof stress, and ultimate tensile strength in the artificially aged condition.

ACKNOWLEDGEMENTS.

The authors and the Fulmer Research Institute are indebted to the Tin Research Institute, by whom the research was sponsored, for permission to publish this paper. The authors also wish to express their thanks to Mr. E. A. G. Liddiard, M.A., F.I.M., Director of Research, Fulmer Research Institute, for advice during the course of the investigation, and to their colleagues Mr. E. A. Brandes, B.Sc., A.R.C.S., F.I.M., and Mr. A. G. Provan, B.Sc., A.R.T.C., who prepared the alloys on which the work was conducted, Mr. G. N. Cale, B.Sc., and Mr. G. Willoughby, L.I.M., for mechanical-test data, and Mr. H. H. Smith, A.R.I.C., and Mr. J. A. McBain for chemical analyses.

APPENDIX.—DETAILS OF EXPERIMENTAL WORK ON ALUMINIUM ALLOYS CONTAINING TIN.

Tin Distribution as Affected by Pouring Conditions and Alloying Elements.

The effect on the microstructure of the aluminium-10% tin alloy was examined for pouring temperatures of 675°, 700°, 725°, 750°, and 800° C. with slow, medium, and rapid rates of pouring; casting was carried out into a 1½-in.-dia. sand mould and into ½-in.-dia. hot and cold dies.

In addition aluminium-10% tin alloys were examined containing (a) 1% copper, 1% nickel, (b) 1% zinc, (c) 1% magnesium, (d) 2½% silicon, (e) 2½% manganese, together with minor variations in iron and silicon content. These alloys were cast into the same types of mould, at 725° C., with the medium speed of pouring.

Tensile Tests at Elevated Temperatures.

The following materials were prepared by high-frequency melting :

- (a) Super-purity aluminium.
- (b) Super-purity aluminium + 5% tin.
- (c) Super-purity aluminium + 10% tin.
- (d) Super-purity aluminium + 10% tin + 1% nickel + 1% copper.
- (e) Super-purity aluminium + 5% tin + 1¼% manganese.
- (f) Super-purity aluminium + 5% tin + 2½% silicon.
- (g) An alloy approximating in composition to commercial alloy Alcoa XA 750 (6·5% tin, 1% copper, 1% nickel, 0·5% magnesium, 0·8% silicon, 0·12% iron, remainder commercial-purity aluminium).
- (h) An alloy approximating in composition to the commercial alloy Alcoa XA 750S (6·5% tin, 1% copper, 1% nickel, 2·5% silicon, 0·16% iron, remainder commercial-purity aluminium).

They were water-chill cast as billets 1 in. dia. × 9 in. long, from which sub-standard test-pieces of 0·423 in. dia. were machined. Tensile testing was carried out at room temperature, 100°, 200°, and 300° C. in accordance with the requirements of British Standard Specification No. 1094.

Cast and Heat-Treated Aluminium-4½% Copper Alloy.

D.T.D. test-bars were prepared in aluminium alloys containing 4½% copper, 0·12% silicon, 0·3% iron, 0·22% titanium, with and without

small additions of tin. Melting was carried out in Salamander crucibles in an oil-fired furnace. The melts were degassed with chlorine and poured into baked sand moulds.

The test-bars were solution heat-treated in a circulating air furnace for 16 hr. at 535° C., followed by quenching in cold water. They were aged for 15 days at room temperature or 16 hr. at 165° C.

Forged Duralumin-Type Alloys.

Water-chill-cast ingots were prepared in the following alloys of commercial purity :

(a) Aluminium-4½% copper-0·15% titanium.

(b) Aluminium-4½% copper-0·5% magnesium-0·15% titanium.

(c) D.T.D. 364A (4½% copper, 0·7% silicon, 0·8% iron, 0·7% manganese, 0·5% magnesium, 0·15% titanium).

and in the same alloys containing approximately 0·3% tin.

The billets were pre-heated at 450° C. and hot forged from this initial temperature. Billets of 1·1 in. dia. were forged to 0·5 in. square, reheated, and flattened to 0·2 in. thick for hardness test-pieces. Billets of 2½ in. dia. were hot forged to ¾ in. square. All the alloys forged satisfactorily, except the aluminium-4½% copper alloy containing tin. This was very hot-short and broke up at the first blow.

Specimens for hardness and tensile testing were solution heat-treated at 510° C. and quenched in cold water. These were allowed to age at room temperature or were artificially aged at 170° C.

Analysis.

By adjusting the concentration of the reagents, the normal method for the analysis of tin in aluminium alloys by oxidizing from stannous to stannic chloride with potassium iodate solution can be used for low tin contents. The method is quite suitable for tin concentrations down to 0·05%, and with care it is satisfactory for 0·025% tin, but below this value the accuracy falls off.

REFERENCES.

1. A. G. C. Gwyer, *Z. anorg. Chem.*, 1906, **49**, 311.
2. H. Gautier (and — Rolland-Gosselin), *Compt. rend.*, 1896, **123**, 109; and *Bull. Soc. d'Encour.*, 1896, [v], 1, 1293; also "Contribution à l'Etude des Alliages", p. 93. Paris: 1901.
3. W. Campbell and J. A. Mathews, *J. Amer. Chem. Soc.*, 1902, **24**, 253.
4. W. C. Anderson and G. Lean, *Proc. Roy. Soc.*, 1903, **72**, 277.
5. E. S. Shepherd, *J. Physical Chem.*, 1904, **8**, 233.
6. R. Lorenz and D. Plumbridge, *Z. anorg. Chem.*, 1913, **83**, 243.
7. E. Crepaz, *Giorn. Chim. Ind. Appl.*, 1923, **5**, 115.
8. L. Losana and E. Carozzi, *Gazz. Chim. Ital.*, 1923, **53**, 546.

9. K. Kaneko and M. Kamiya, *Nippon Kōgyō Kwai Shi*, 1924, **40**, 509; seen in abstract only, *Met. Abs. (J. Inst. Metals)*, 1926, **36**, 436.
10. L. F. Mondolfo, "Metallography of Aluminium Alloys", p. 41. New York : 1943 (John Wiley & Sons).
11. M. Gotō and T. Mishima, *Nippon Kōgyō Kwai Shi*, 1923, **39**, 714; seen in abstract only, *Met. Abs. (J. Inst. Metals)*, 1926, **36**, 433.
12. M. I. Zamotorin, *Trudy Leningrad. Indust. Inst.*, 1936, (4), 23.
13. M. I. Zamotorin, *Metallurg*, 1936, (11), 103.
14. W. L. Fink, quoted by H. P. Nielsen and R. J. Nekervis, *Metals Handbook (Amer. Soc. Metals)*, 1948, p. 1166.
15. H. K. Hardy, *Metal Treatment*, 1944, **11**, (37), 37.
16. A. De Sy and H. Haemers, *Aluminium*, 1942, **24**, (3), 96.
17. W. L. Fink, L. A. Willey, and H. C. Stumpf, *Metals Technol.*, 1948, **15**, (2); *A.I.M.M.E. Tech. Publ.* No. 2339.
18. W. Hume-Rothery. Private communication.
19. J. B. Nelson and D. P. Riley, *Proc. Phys. Soc.*, 1945, **57**, 160.
20. W. L. Bragg, *J. Sci. Instruments*, 1947, **24**, 27.
21. H. J. Axon and W. Hume-Rothery, *Proc. Roy. Soc.*, 1948, [A], **193**, 1.
22. E. R. Jette and F. Foote, *J. Chem. Physics*, 1935, **3**, 605.
23. A. J. C. Wilson, *Proc. Phys. Soc.*, 1941, **53**, 235.
24. E. Scheil, *Z. Metallkunde*, 1942, **34**, (4), 96.
25. E. Raub and A. von Polaczek-Wittke, *Z. Metallkunde*, 1942, **34**, (4), 93.
26. E. Raub and A. Engel, *Metallforschung*, 1946, **1**, (3), 78.
27. D. C. G. Lees, *J. Inst. Metals*, 1946, **72**, 343.
28. British Patent Nos. 470,248; 472,248.
29. H. Y. Hunsicker, *Machine Design*, 1947, **19**, (1), 121.
30. D. Hanson and E. J. Sandford, *J. Inst. Metals*, 1935, **56**, 191.
31. C. E. Homer and H. Plummer, *Tech. Publ. Internat. Tin. Research Develop. Council, Series A*, No. 57, 1937.
32. U.S. Patent No. 2,062,329, 1936.
33. W. Hume-Rothery, "The Structure of Metals and Alloys", *Inst. Metals Monograph and Rep. Series*, No. 1, 1945, p. 40.
34. A. H. Cottrell, *Phys. Soc. : Rep. of Conf. on Strength of Solids*, 1948, p. 30.
35. M. Cook and R. Chadwick, *J. Inst. Metals*, 1942, **68**, 169.

GRAIN REFINEMENT OF ALUMINIUM AND 1220 ITS ALLOYS BY SMALL ADDITIONS OF OTHER ELEMENTS.*

By MYRIAM D. EBORALL,† B.A.

(Communication from the British Non-Ferrous Metals Research Association.)

SYNOPSIS.

The effect of eight elements on the grain-size of sand-cast pure aluminium, and also that of titanium and boron on the grain-size of some aluminium alloys, has been studied. Several methods of adding titanium to the melts were used, and the efficiency of transfer of titanium was determined in each case. It was found that titanium, zirconium, and vanadium were the most effective grain refiners of pure aluminium, but that boron, although having little influence on the grain-size of pure aluminium, refined the grain of the copper-bearing alloys, its efficiency increasing with the copper content.

The grain-refining action of the added elements is not satisfactorily explained, but it is shown that (i) the presence of primary particles of intermetallic compounds is not necessary to initiate refinement, (ii) a peritectic reaction does not necessarily produce fine grains, and (iii) all the facts cannot be explained on the theory that grain-size is controlled by concentration gradients in the semi-solid casting.

The grain-size of aluminium containing small amounts of the grain-refining elements was markedly affected by the pouring temperature; this was not accounted for by the corresponding variations in rate of freezing in the mould.

The efficiency of transfer of titanium to the melts varied with the method of addition, and the efficiency of potassium titanofluoride was considerably reduced by the presence of magnesium in the melt. There was only a small variation in optimum titanium content with the method of addition.

I.—INTRODUCTION.

THE possibility of producing fine-grained aluminium alloy castings by adding small quantities of certain elements to the melt has long been well known, but, although several attempts had been made to explain the observed facts before the present work was started, the mechanism remained incompletely understood.

The experiments described below were undertaken in order to obtain a wider range of data than was already available, and it was hoped that, in the light of the results, the grain-refining mechanism might be elucidated. It is shown that none of the theories current when the work was carried out was capable of accounting for all the experimental data, but

* Manuscript received 28 July 1949. The work described in this paper was made available to members of the B.N.F.M.R.A. in confidential research reports issued over the period 1945–47.

† Investigator, British Non-Ferrous Metals Research Association, London.

later work in the Association's laboratories has proved more conclusive and Cibula¹ has now accounted for the grain refinement of aluminium alloys by added elements.

The available information on the grain refinement of metals and alloys by small additions of other elements showed that the elements known to be most effective form peritectics with the basis metal, e.g. titanium and zirconium with aluminium, zirconium with magnesium, iron with copper, &c., and an examination was therefore made of the grain-refining effect of some elements thought to form such systems with aluminium, those selected being titanium, zirconium, niobium, molybdenum, chromium, vanadium, tungsten, and boron. These were added in various small quantities to aluminium of high purity.

The effects of titanium and boron on various aluminium-base alloys were also studied. In this later work, several methods of adding the titanium were used, in order to determine whether the amount of titanium necessary to give complete grain refinement varied according to the way it was introduced into the melt. The same results showed the efficiency of transfer of titanium from three different sources to the melts.

Particular attention was given to determining whether the presence of primary particles of the compounds between aluminium and the added elements is necessary for grain refinement.

II.—PREVIOUS WORK.

The grain-refining influence of titanium and niobium on aluminium and its alloys has been referred to by many authors, and occasional mention has been made of the effect of other elements.

Röhrig² stated that the addition of 0·01% titanium to aluminium prohibits the growth of columnar crystals and leads to a fine-grained structure, and Dumas³ asserts that, in 99·5% aluminium, 0·02% titanium reduces the grain diameter from 3 to 1 mm. by precipitation of $TiAl_3$ in a very finely dispersed form. Panseri and Guastalla⁴ state that the addition of 0·35% titanium to the eutectic aluminium-silicon alloy gives a fine-grained structure, while Böhm⁵ overcame coarse-grained structures, caused by heating two complex aluminium-base alloys to 830° C., by the addition of 0·2% titanium. This amount was also said to refine the aluminium-silicon alloy containing 10% of silicon. Slater and Parker⁶ and Wells⁷ found that 0·15% titanium was necessary to ensure a consistently small grain-size in aluminium alloys, although smaller quantities produced an effect whose magnitude varied with the composition of the alloy.

The alloys of aluminium containing magnesium as a main alloying element appear to be a special case, and, although they are refined by titanium additions, it is necessary to add a little more titanium each time the alloys are remelted (Dumas³). These alloys were shown by Rosenhain and his colleagues⁸ to absorb proportionately more titanium from titanium tetrachloride, with selective elimination of magnesium, than does pure aluminium.

Wells⁷ also investigated the effect of niobium additions, and found that 0·02% had some effect, while 0·1% gave the maximum refinement, reducing the grain diameter of several alloys and also that of pure aluminium to one-tenth.

The use of vanadium for the grain refinement of aluminium is mentioned by Dumas³ and by Mondolfo.⁹

Reimann¹⁰ observed that 0·45% molybdenum gave a fine-grained structure to aluminium.

The only systematic study of the effect of boron appears to be that of Slater and Parker,⁶ who made additions of up to 0·5% to various alloys and found them to be ineffective in aluminium of commercial purity and of varying efficacy in a selection of commercial alloys.

III.—MATERIALS.

(a) *Metals and Alloys.*

Super-pure aluminium was used as the basis material throughout, to avoid possible complications due to the presence of minor alloying elements. Super-pure magnesium (99·99%, <0·0001% iron), cathode copper, and 99·99% zinc were used as the main alloying constituents. Salamander pots and iron stirrers and skimmers, well coated with alundum, were used in preparing the melts. There was a certain amount of silicon pick-up, but, in general, iron and silicon contamination of the magnesium-free alloys was only 0·02% or less of each element. The silicon contents of the aluminium-magnesium alloys containing 0·5% and 10% magnesium were 0·01% and 0·04%, respectively.

(b) *Hardeners.*

The compositions of the hardeners are given in Table I. Commercial hardeners were used except for those containing titanium, tungsten, and vanadium, which were prepared as follows :

Titanium : potassium titanofluoride was stirred into aluminium at 1000° C.

Tungsten and Vanadium : equal weights of 99·8% tungstic oxide and 120-mesh aluminium powder, or 99·8% vanadium oxide

and cryolite, were pelleted and plunged into molten aluminium at 1000° C.

TABLE I.—*Composition of Hardeners.*

Main Alloying Element, %		Iron Content, %	Silicon Content, %
Ti	0·45	0·026	0·058
	1·11	0·02	0·06
	1·42	0·08	n.d.
	0·99	0·008	n.d.
Zr	4·5	0·12 (nom.)	...
Mo	13·7	0·31	0·30
Cr	11·0	0·45	0·21
Nb	5·5	1·13	...
V	4·9	0·06	0·45
W	5·3	0·03	0·05

(c) *Chemicals.*

The potassium titanofluoride and borofluoride and the titanium tetrachloride used were of ordinary commercial purity.

IV.—EXPERIMENTAL PROCEDURE.

(a) *Effect of Added Elements and of Casting Temperature on Pure Aluminium.*

The main series of tests in the first part of the work was made on aluminium with the following additions: titanium, zirconium, vanadium, molybdenum, tungsten, niobium, chromium, and boron; amounts varied from 0·03% to 1·5%, the details being given in Table II. Each melt weighed 1 kg., and was sufficient to provide four bars $\frac{3}{4}$ in. in dia. and 4 in. long with heads $1\frac{1}{2}$ in. deep and $1\frac{3}{8}$ in. in dia. These bars were poured in succession into green Mansfield sand moulds from 1000°, 900°, 800°, and 700° C., respectively. Before each bar was poured the melt was heated to 1000° C., allowed to cool to the pouring temperature, and fluxed with a mixture consisting of two parts of sodium chloride and one part of sodium fluoride. Above 900° C. the degassing of the melts by the flux was not very efficient. The vanadium and tungsten alloys were not superheated, but were simply cast at 75° C. above the liquidus.

The grain-size at a point $1\frac{1}{2}$ in. below the base of the neck was exam-

TABLE II.—Effect of Added Elements on Grain-Size of Aluminium.
Casting Temperature 700° C.

Element	Content, %	Grain-Size (see p. 301)
Ti	0.034	C + E _M
	0.046	E _C
	0.078	E _M
	0.125	E _{VF}
	0.17	E _{VF} ‡
	0.19	E _{VF}
	0.25	E _{VF}
	0.44	E _{VF}
Zr	<0.05	NC
	0.21	E _C
	0.28	E _{VF}
	0.29	E _F
	0.32	E _{VF} , NC †
	0.36	E _F
	0.45	E _F ‡
V	0.18	C + E _C ‡
	0.49	NC + E _C
	0.62	E _M + E _F
	0.85	E _F
	1.5 *	E _{VF}
Mo	0.21	NC ‡
	0.25	NC
	0.36	E _M
	0.48	E _F
	0.68	E _F
	1.09	E _F
	1.41	NC
W	0.16	C + NC ‡
	0.25	C + NC
	0.56	E _F + E _{VF}
Nb	0.04	NC ‡
	0.055	E _M
	0.10	NC + E _M
	0.16	E _M
	0.18	E _M
Cr	0.045	NC
	0.07	NC
	0.15	NC + E _F
	0.30	NC
	0.75	C
	1.27	C ‡
B	0.07 *	NC ‡
	0.11 *	NC
	0.13 *	NC
	0.25 *	NC + E _M
	0.32 *	NC + E _M

* Nominal.

† Duplicate specimens.

‡ Lowest concentration of added element at which primary particles of intermetallic compound were detected (by micro-examination).

ined by preparing a section cut at right angles to the axis of the bar, the surfaces being machined and polished in the usual way. The reagent used for macro-etching was that due to Arrowsmith, Wolfe, and Murray,¹¹ consisting of 37 parts of water, 12 parts of concentrated nitric acid, and 1 part of hydrofluoric acid. The same solution diluted ten times was used when micro-etching to detect the presence or absence of primary particles of intermetallic compounds. The heads of a few of the bars were sectioned vertically and macro-etched to detect segregation effects.

Analyses were made on small chill bars cast immediately after pouring the sand-cast bars at 900° C.

(b) *Effect of Rate of Cooling on Pure Aluminium.*

To distinguish between the effect of pouring temperature and the resultant variation in rate of cooling, the same alloys were cast from 700° C., after preheating to 1000° C., into dry Mansfield sand at various temperatures. This procedure gave a similar variation in the rate of cooling to that caused by the use of the different casting temperatures.

(c) *Effect of Added Elements on Aluminium Alloys.*

Titanium was added, by three different methods, to aluminium-magnesium alloy melts containing 0·5, 1, 5, or 10% magnesium. Boron was added to aluminium-copper alloys (2, 4, 6, 8, and 10% copper), to aluminium-magnesium alloys (0·5, 2, 5, and 10% magnesium), to aluminium-zinc alloys (7·7, 12, and 25% zinc), and to a single aluminium-silver alloy (8% silver).

The melts (750 g.) were made at 750° C., and if potassium titano- or boro-fluoride or titanium tetrachloride were used, they were added at this stage, the titano- and boro-fluorides as dry powders sprinkled on the surface of the melts, and the tetrachloride via a dry silica tube, the upper end of which was connected to the top and bottom of a drip-feeding reservoir so that the liquid dripped regularly into the tube under its own pressure head. Any dross was then removed, and the melts were treated with 2% (of the weight of the melt) of the degassing flux, which was allowed to remain on the surface for 5 min. The melt was then vigorously stirred and cooled to 700° C. for casting.

With the aluminium-magnesium alloy melts, this procedure was varied by omitting the degassing flux and cleaning up the surface of the melt with Hydrasal (a carnallite-base flux) immediately before casting. Most of these alloys were cast into silica sand inhibited with 2% of boric acid, but in a few cases, noted in the Tables, they were cast into Mansfield sand moulds, the surfaces of which had been well dusted with boric acid.

The lower parts of the bars, on which the grain-size determinations were made, were analysed for titanium (chemically) or for boron (spectrographic qualitative analysis only with some alloys), and in most cases a specimen for centrifuging (see below) was machined from the $1\frac{1}{2}$ in. of the bar immediately below the feeder head.

(d) *Grain-Size Measurement.*

The grain-sizes of the bars were classified by reference to typical macrostructures, which are reproduced in Figs. 1–6 (Plate XXXVIII) as follows :

- (i) C Columnar (9.5 mm. long, 7.5 mm. dia.).
- (ii) NC Narrow columnar (9.5 mm. long, 1.2 mm. dia.).
- (iii) E_C Coarse equi-axial (1.9 mm. dia.).
- (iv) E_M Medium equi-axial (1.2 mm. dia.).
- (v) E_F Fine equi-axial (0.6–0.9 mm. dia.).
- (vi) E_{VF} Very fine equi-axial (0.45 mm. dia. and less).

The figures in brackets are the dimensions of typical crystals, and grain refinement is considered complete when the grain-size designated E_{VF} is attained.

(e) *Detection of Primary Particles.*

In the experiments with small additions of other elements to aluminium, the presence or absence of the respective intermetallic compounds was determined by metallographic examination of a large number of fields in the cross-section of the bar. A more sensitive technique was used in the experiments on the effect of boron and titanium additions to aluminium-base alloys : a specimen was machined from the bar (see above) and centrifuged for 1 min. at 600 r.p.m. and $6\frac{1}{2}$ in. radius, at a temperature just above the liquidus temperature of the basis alloy. Microsections taken perpendicular to the axis of rotation revealed a segregate of primary particles when these had been present in the original cast bar.

V.—RESULTS.

1. *Pure Aluminium Melts.*

(i) *Effect of Added Elements, of Pouring Temperature, and of Rate of Cooling on the Grain-Size of Aluminium.*

Some of the results obtained in the series of tests described in Section IV (a) are given in Table II, which shows the grain-size of the bars cast at 700°C . and also gives the lowest concentration of added element at which primary particles of intermetallic compounds were detected by

micro-examination of the alloys as cast. Titanium, vanadium, and zirconium were by far the most effective grain-refining agents, niobium, molybdenum, and tungsten having a moderate effect, and boron and chromium hardly any.

Considerable difficulty was experienced in obtaining reproducible results with zirconium, presumably owing to segregation; the alloys seldom had the composition to be expected from the amount of hardener added. Sections from the extreme bottom of several bars had the same grain-size as those in the normal position, but when the heads of some of these bars were sectioned the grain-size was found to be very variable, and segregation had evidently occurred during cooling after casting.

It was found impossible to obtain a niobium content of more than 0·2%, using the normal technique, although nominal quantities well in excess of this were added.

Micro-examination revealed primary particles of intermetallic compounds in all these systems, and the relation between such particles and grain-size is discussed below. The constitution of the alloys is considered in the Appendix (see p. 313).

TABLE III.—*Effect of Mould Temperature on Grain-Size of Aluminium-Titanium Alloys.*

Titanium, %	Pouring Temperature 700° C.					Green Sand Mould at Room Temperature.			
	Dry Sand Mould Temperature, ° C.					Pouring Temperature, ° C.			
	500 *	400	300	200	100	1000 *	900	800	700 †
0·12	E _F	E _F	E _{VF}	E _M	E _{VF}	C + E _C E _M	E _M	E _M	E _{VF} E _{VF}
0·17	E _F	E _F	E _{VF}	E _{VF}	E _{VF}				

* Freezing time about 5 min.

† Freezing time about 2 min.

The alloys containing titanium, zirconium, niobium, and molybdenum generally showed a considerable decrease in grain-size with casting temperature, although very little effect was noticed with pure aluminium or with alloys containing boron or chromium. The decrease was most marked in the system aluminium-titanium (see Table III). Tests on this and other systems in which the freezing time was increased from 2 to 5 min. (a) by casting at 1000° C. or (b) by casting at 700° C. into preheated moulds, showed that the rate of cooling in the mould did not cause this variation in grain-size, but that the history of the melt before casting was more important.

(ii) Effect of Titanium from Various Sources on the Grain-Size of Aluminium.

The effect of titanium additions from three different sources on the grain-size of unalloyed aluminium is shown in Table IV, where the presence or absence of primary particles of $TiAl_3$ is also noted. With all methods of addition, some decrease in grain-size is noticeable at

TABLE IV.—Effect of Titanium Additions (from Various Sources) on Grain-Size of Unalloyed Aluminium.

750-g. melts. Casting temperature 700° C.

Specimen No. MSU	Source of Titanium	Titanium, % (analysis)	Grain-Size (see p. 301)	Primaries †
*	...	n.d. (spect.)	C	
*	Al/Ti	0·05	E _C	
*	Al/Ti	0·08	E _M	
2	Al/Ti	0·12	E _F	—
11	Al/Ti	0·15	E _{VF}	+
*	C	
116	K ₂ TiF ₆	<0·02	NC	—
113	K ₂ TiF ₆	0·04	E _M + E _F	—
110	K ₂ TiF ₆	0·07	E _M + E _F	—
107	K ₂ TiF ₆	0·08	E _F + E _{VF}	—
5	K ₂ TiF ₆	0·11	E _{VF}	—
26	K ₂ TiF ₆	0·13	E _{VF}	+
20, 23	K ₂ TiF ₆	0·14, 0·14	E _F , E _{VF}	—, —
*	C	
8	TiCl ₄	0·05	NC + E _F	—
32	TiCl ₄	0·08	E _C + E _F	—
38	TiCl ₄	0·10	E _M	
14	TiCl ₄	0·14	E _F	+
35	TiCl ₄	0·15	E _F	—
17	TiCl ₄	0·20	E _{VF}	+

* From Table II.

† + present, — absent, as indicated by micro-examination of centrifuged samples. A blank in this column indicates that no sample was centrifuged.

titanium contents of 0·05% or less, and grain refinement increases with titanium content. The amount of titanium required for complete grain refinement varies slightly with the method of addition, being 0·08–0·11% titanium (potassium titanofluoride), 0·12–0·15% titanium (aluminium–titanium hardener), or 0·15–0·2% titanium (titanium tetrachloride). Potassium titanofluoride gives a mixed grain-size at low titanium contents. In each case, primary particles of $TiAl_3$ first appear at titanium contents of about 0·13%.

(iii) Efficiency of Transfer of Titanium from Various Compounds to Aluminium.

As might be expected, the use of the hardener gave the theoretical titanium content. It may be important to note that the hardener alloy was dilute and that solution of $TiAl_3$ in the melt may have been facilitated for this reason. Potassium titanofluoride was also very efficient, giving about 90% transfer, but titanium tetrachloride was less successful, the efficiency of transfer being only about 30%.

2. Aluminium-Base Alloy Melts.

(i) Titanium Additions to Aluminium-Magnesium Alloys.

Titanium additions were made, by all three methods, to aluminium-magnesium alloys containing 0·5, 1, 5, and 10% magnesium, and the results are given in Tables V, VI, and VII.

TABLE V.—Effect of Titanium Additions (from Aluminium-Titanium Hardener) on Grain-Size of Aluminium-Magnesium Alloys, and Efficiency of Transfer of Titanium.

750-g. melts. Casting temperature 700° C.

Specimen No. MSU	Magnesium, % (nominal)	Titanium, % (nominal)	Titanium, % (analysis)	Efficiency of Transfer, %	Grain-Size (see p. 301)	Primaries †
153 *	0·5	NC + EC	
228	0·5	0·075	0·06	80	EF	
222	0·5	0·10	0·09	90	EF	
177	0·5	0·15	0·16	100	EVF	—
150 *	1	NC + EC	
231	1	0·075	0·07	93	EF	
225	1	0·10	0·09	90	EF	
180	1	0·15	0·16	100	EVF	+
50	5	EC	
240	5	0·01	0·007 ‡	70	EM	
210	5	0·025	0·02(3)	92	EM	
207	5	0·05	0·05(5)	100	EM	
165	5	0·075	0·07	95	EM	
159	5	0·10	0·09	90	EM	
41	5	0·15	0·14	94	EF	—
156	5	0·18	0·18	100	EVF	+
62	10	EM	
168	10	0·05	0·05	100	EM	+
162	10	0·075	0·07	95	EF	+
137 *	10	0·10	0·11	100	EVF	+
53	10	0·15	0·12	80	EVF	

* Moulds made of Mansfield green sand dusted with boric acid.

† + present, — absent, as indicated by micro-examination of centrifuged samples. A blank in this column indicates that no sample was centrifuged.

‡ Analysed by a more sensitive method than the other samples.

TABLE VI.—Effect of Titanium Additions (from Potassium Titanofluoride) on Grain-Size of Aluminium-Magnesium Alloys, and Efficiency of Transfer of Titanium.

750-g. melts. Casting temperature 700° C.

Specimen No. MSU	Magnesium, % (nominal)	Titanium, % (nominal)	Titanium, % (analysis)	Efficiency of Transfer, %	Grain-Size (see p. 301)	Primaries †
153 *	0.5	NC + E _C	
171	0.5	0.15	0.07	47	E _F	—
248	0.5	0.20	0.13	65	E _M + E _F	—
251	0.5	0.25	0.16	64	E _M + E _F	—
216	0.5	0.30	0.18	60	E _{VF}	+
150 *	1	NC + E _C	
174	1	0.15	0.04	27	E _F	—
219	1	0.30	0.17	56	E _F	—
50	5	E _C	
44	5	0.15	0.01	7	E _C	—
62	10	E _M	
213	10	0.10	0.01	10	E _M	
56	10	0.15	0.01	7	E _F	—

* Moulds made of Mansfield green sand, dusted with boric acid.

† + present, — absent, as indicated by micro-examination of centrifuged samples. A blank in this column indicates that no sample was centrifuged.

Inspection of these tables shows that the amount of titanium required to give the minimum grain-size (E_{VF}) in the alloys of highest magnesium content was only about half that required for the alloys of low magnesium content.

The efficiency of transfer of titanium to the melts was 100% for the hardener alloy, 20–40% for the titanium tetrachloride, and very variable (5–65%) for the titanofluoride. The latter material quickly formed a hard crust when it was sprinkled on the surface of a melt, and no further reaction was apparent. The results with the tetrachloride do not confirm Rosenhain's⁸ observation that the efficiency of transfer is greater in the case of aluminium-magnesium alloys than in that of aluminium.

In all these experiments, as with those on pure aluminium, considerable grain refinement was obtained in the single-phase alloys, although full refinement occurred at the lowest compositions containing primary particles of TiAl₃ type. The alloys refined by titanium tetrachloride additions showed some very tiny primary particles of a different type at all titanium contents; these particles did not appear to affect the grain-size. The constitution of these alloys is discussed in the Appendix (see p. 313).

TABLE VII.—*Effect of Titanium Additions (from Titanium Tetrachloride) on Grain-Size of Aluminium-Magnesium Alloys, and Efficiency of Transfer of Titanium.*

750-g. melts. Casting temperature 700° C.

Specimen No. MSU	Magnesium, % (nominal)	Titanium, % (nominal)	Titanium, % (analysis)	Efficiency of Transfer, %	Grain-Size (see p. 301)	Primaries †
153 *	0.5	$E_C + E_M$	+ , very tiny
134 *	0.5	0.54	0.08	15	E_M	-
260	0.5	0.36	0.16	44	E_F	-
234	0.5	0.54	0.16	30	E_F	+ , $TiAl_3$ type
150 *	1	$E_C + E_M$	-
131 *	1	0.54	0.06	11	$E_M -$	+ , few, very tiny
263	1	0.36	0.14	39	E_M	-
237	1	0.54	0.27	50	E_{VF}	+ , $TiAl_3$ type
50	5	E_C	
128 *	5	0.18	0.09	50	E_M	+
125 *	5	0.36	0.17	47	E_{VF}	+
47	5	0.54	0.18	33	E_{VF}	
62	10	E_M	
122 *	10	0.18	0.06	33	E_F	+
59	10	0.54	0.075	14	E_{VF}	+
119 *	10	0.36	0.15	41	E_{VF}	

* Moulds made of Mansfield green sand, dusted with boric acid.

† + present, — absent, as indicated by micro-examination of centrifuged samples. A blank in this column indicates that no sample was centrifuged.

(ii) *Boron Additions to Aluminium Alloys.*

Boron was added to the alloys by means of potassium borofluoride. Alloys containing 2–10% copper, 7–25% zinc, or 0.5–10% magnesium were studied, and the results are given in Tables VIII–XI.

(a) *Aluminium-Copper Alloys* (Tables VIII and IX).—The effect of boron on the grain-size of these alloys was largely determined by the copper content, and some of the results from Table VIII are re-arranged in Table IX to bring out this point. Boron contents of the order of 0.04% sufficed to give the maximum grain-refining effect at any copper content, the occasional higher contents given in Table VIII having no effect on the trend of the grain-size change with increasing copper content.

Spectrographic comparison of the bars MSV17, 32, and 29 (Table VIII) showed that the efficiency of the transfer of boron (about 10% in

most cases) to the melts decreased with decreasing temperature of addition.

TABLE VIII.—*Effect of Boron Additions on Grain-Size of Aluminium-Copper Alloys.*

750-g. melts. Casting temperature 700° C.

Temperature of additions 750° C. unless otherwise stated.

Specimen No. MSV	Copper, % (nominal)	Boron, %		Grain-Size (see p. 301)	Primaries †
		Nominal	Actual		
20	NC	
5	...	0.50	0.055	NC + E _M	+
83, 116, 140 }	2	{E _M , E _M , N _C	
152, 149 }	2	0.50	0.065	{E _M , E _M E _M }	+
107					
23, 170	4	E _C , E _C	
227	4	0.30	0.045	E _F	+
36	4	0.75	0.050	E _F	+
11	4	0.50	0.17	E _F	+
86, 173	6	E _C , E _C	
233	6	0.30	0.040	E _F	+
110	6	0.50	0.040	E _F	+
200	6	0.75	0.070	E _F	
230	6	0.40	...	E _F	
26, 141	8	E _C , E _C	
38	8	0.25	...	E _M	-
29 (700° C.)	8	0.50	...	E _M	+
32 (720° C.)	8	0.50	...	E _F	+
194	8	0.40	...	E _F	+
197	8	0.30	0.045	E _F	+
17	8	0.50	0.055	E _{VF}	+
89, 144	10	E _C , E _C	
203	10	0.40	...	E _F	+
224, 236	10	0.30	0.065 *	E _{VF}	+
113	10	0.50	0.035	E _{VF}	+

* MSV 236.

† + present, - absent, as indicated by micro-examination of centrifuged samples. A blank in this column indicates that no sample was centrifuged.

Primary particles, shown by X-ray examination to have the AlB₂ structure, were present in aluminium and in all the copper-bearing alloys at 0.3% boron (nominal) or more, and in some cases the same constituent was also present in the eutectic of the as-cast or centrifuged alloys. The grain-size did not appear to be governed by the presence of these primary particles.

TABLE IX.—Effect of a Fixed Amount of Boron (Nominal 0.5%) on Aluminium-Copper Alloys of Varying Copper Contents.

750-g. melts. Casting temperature 700° C. Primary particles of AlB_2 present in all cases.

Specimen No. MSV	Copper, % (nominal)	Grain-Size in Absence of Boron	Grain-Size with Boron Addition	Actual Boron Content, %
5	...	NC	NC + E_M	0.055
107	2	E_M	E_M	0.065
11	4	E_C	E_F	0.17
110	6	E_C	E_F	0.040
17	8	E_C	E_{VF}	0.055
113	10	E_C	E_{VF}	0.035

(b) Aluminium-Zinc Alloys (Table X).—A few experiments were made in which boron was added to aluminium containing 7.7, 12, or 25% zinc. The results were somewhat obscured by the fact that the melts free from boron did not give a very reproducible grain-size, particularly at 12% zinc, but it appeared that there was some grain refinement by boron. Comparative spectrographic analyses showed that all these alloys contained about the same amount of boron.

TABLE X.—Effect of Boron Additions on Grain-Size of Aluminium-Zinc Alloys.

750-g. melts. Casting temperature 700° C.

Specimen No. MSV	Zinc, % (nominal)	Boron, % (nominal)	Grain-Size (see p. 301)	Primaries *
92, 119	7.7	...	E_F, E_F	
122	7.7	0.50	E_F, E_{VF}	+
77, 131, 143, } 155, 158 }	12	...	{ $E_C, E_{VF}, C,$ E_C, E_C	
218	12	0.30	E_F	+
125	12	0.50	E_F	+
95, 134, 146, } 161, 163 }	25	...	{ $E_F, E_C, E_C,$ E_C, E_C	
221	25	0.30	E_{VF}	+
128	25	0.50	E_{VF}	+

* + present, — absent, as indicated by micro-examination of centrifuged samples. A blank in this column indicates that no sample was centrifuged.

In all cases where boron was added, primary particles of AlB_2 were found, and this compound sometimes also appeared in the eutectic. There were too few experiments with this alloy system for any conclusion to be drawn as to the relation between primary particles and grain refinement.

(c) *Aluminium-Magnesium Alloys* (Table XI).—Attempts were made to add boron to alloys containing 0·5, 2, 5, and 10% magnesium, with the results shown in Table XI. The borofluoride rapidly formed a hard dross, and spectrographic analysis showed that transfer of boron to melts containing magnesium was very low, as was the transfer of titanium from potassium titanofluoride to similar alloys. Slight refinement was obtained in some melts to which boron was added (as potassium borofluoride) in amounts of 0·05% or over. Spectrographic analyses showed that, at 0·5% magnesium, boron entered the alloy progressively with increasing nominal boron content, but at 2% magnesium the maximum actual boron content was reached at a nominal 0·05% boron. Even lower boron contents were obtained at higher magnesium contents, and at 10% magnesium only a trace of boron was found.

TABLE XI.—*Effect of Boron Additions on the Grain-Size of Aluminium-Magnesium Alloys.*

750-g. melts. Casting temperature 700° C.
Additions as potassium borofluoride, except where marked (Al/B).

Specimen No. MSV	Magnesium, % (nominal)	Boron, % (nominal)	Grain-Size (see p. 301)	Primaries †
257	0·5†	...	NC + EC	
212	0·5	0·05	NC + EC	+
191	0·5	0·10	EF	+
215	0·5	0·15	NC + EC	+
254	2	...	EC	
209	2	0·05	EM	—
188	2	0·10	EC	+
179	2	0·40	EM	+
248	5	...	EC	
206	5	0·05	EM	+
185	5	0·10	EM	+
176	5	0·40	EM	+
65	5	0·50 *	EF	+
62 (Al/B)	5	0·50 ‡	EF	—
251	10	...	EM	
182	10	0·10	EC	+

* 0·020% boron actual.

† + present, — absent, as indicated by micro-examination of centrifuged samples. A blank in this column indicates that no sample was centrifuged.

‡ 0·025% boron actual.

In the only case where an aluminium-boron hardener was used, a finer grain was obtained than in any other bar, and this specimen had a higher boron content than the other alloys containing 5% magnesium.

The refinement appeared to be unrelated to the appearance of primary particles. These, where seen, were mostly very tiny and rod-like and were only revealed by an oil-immersion lens, but in two of the specimens, MSV 215 and 65, they were definitely of the AlB_2 type in form and colour.

(d) *Aluminium-Silver Alloy.*—One pair of experiments was made in which a nominal 0·5% boron was added from potassium borofluoride to aluminium containing 8% silver. The "blank" alloy had medium equi-axial grains and the boron-containing alloy fine equi-axial grains. Primary particles of AlB_2 type were present in the latter.

VI.—DISCUSSION OF RESULTS.

1. *Grain Refinement.*

Three possibilities were considered in endeavouring to account for the results obtained : firstly, that primary particles of intermetallic compounds caused grain refinement by acting as nuclei for crystallization; secondly, that only those elements forming peritectic systems with aluminium gave very fine-grained alloys; thirdly, that concentration gradients in the solidifying casting were the governing factor. These possibilities are discussed separately below.

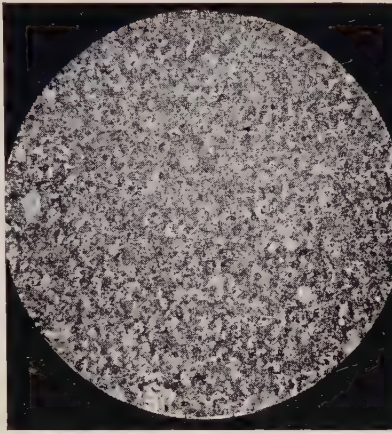
(i) *The Relation of Primary Particles of Intermetallic Compounds to Grain-Size.*

In Tables II, IV-VIII, X, and XI are given the lowest concentrations of added elements which produced primary particles of intermetallic compounds under the conditions obtaining. Although such particles are always present in the specimens having the grain-size designated E_{VF} , many coarse-grained specimens also contained such particles. It is also apparent that those elements causing grain refinement have some effect, although not the full effect, at concentrations lower than those giving compound formation. From these observations, it was deduced that, although primary particles of the intermetallic compounds may play some part in promoting full grain refinement, they were not essential for its initiation. The possibility that "foreign nuclei", as defined by Mitsche,¹² are responsible for grain refinement is, however, not precluded by these results.

(ii) *Grain Refinement and Peritectic Systems.*

Iwasé, Asato, and Nasu,¹³ having studied several different systems, put forward the theory that systems in which peritectic reactions occurred were particularly liable to give fine-grained castings. They

TYPICAL MACROSTRUCTURES OF CAST ALUMINIUM ALLOYS.

FIG. 1.—C. Columnar structure with central coarse equiaxed patch. $\times 4$.FIG. 2. NC. Narrow columnar crystals. $\times 4$.FIG. 4.—Em. Medium equiaxed crystals. $\times 4$.FIG. 3.—Eo. Coarse equiaxed crystals. $\times 4$.FIG. 5.—Ef. Fine equiaxed crystals. $\times 4$.FIG. 6.—EvF. Very fine equiaxed crystals. $\times 4$.

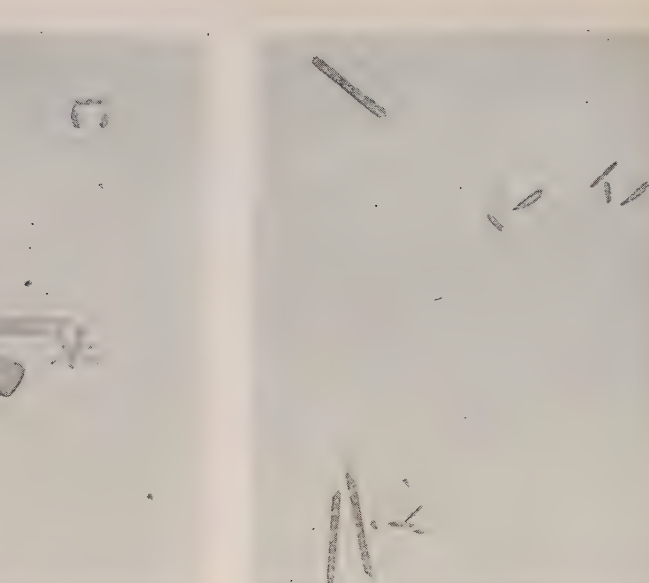


FIG. 7.—Al-Ti System : 0·5% Ti. $TiAl_3$ in aluminium solid solution. Unetched. $\times 250$.

FIG. 8.—Al-Zr System : 0·45% Zr. $ZrAl_3$ in aluminium solid solution. Unetched. $\times 250$.



FIG. 9.—Al-Mo System : 0·68% Mo. $MoAl_3$ dark, sheathed by $MoAl_5$, half-tone, in aluminium solid solution. Unetched. $\times 250$.

FIG. 10.—Al-Nb System : 0·18% Nb. Al-Nb compound, composition unknown. Unetched. $\times 250$.

FIG. 11.—Al-Cr System : 1·27% Cr. CrAl_7 in aluminium solid solution. Unetched.
 $\times 250$.

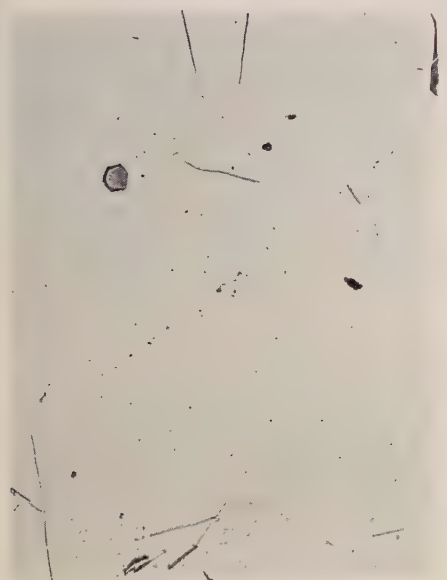


FIG. 12.—Al-B System : 0·25% B. AlB_2 in aluminium solid solution. Unetched.
 $\times 250$.

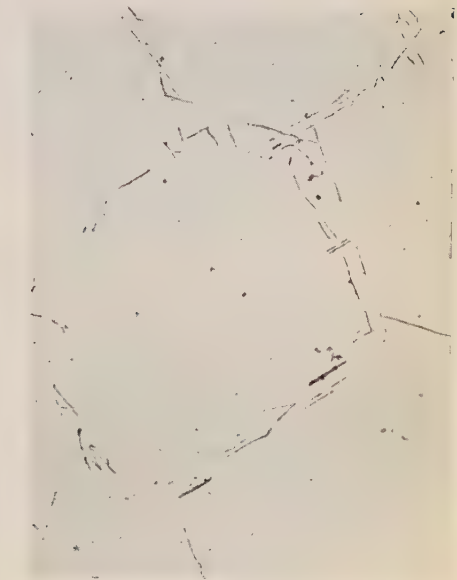


FIG. 13.—Al-B System : 0·07% B. Aluminium solid solution and eutectic. Etched.
 $\times 150$.

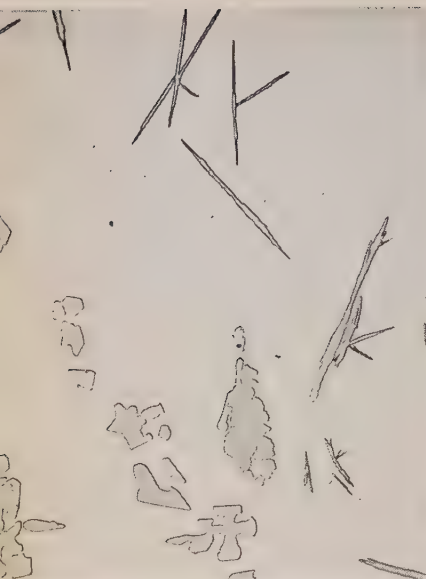


FIG. 14.—Al-W System : 1·5% W. Sand cast at 825° C. Unetched. $\times 150$.

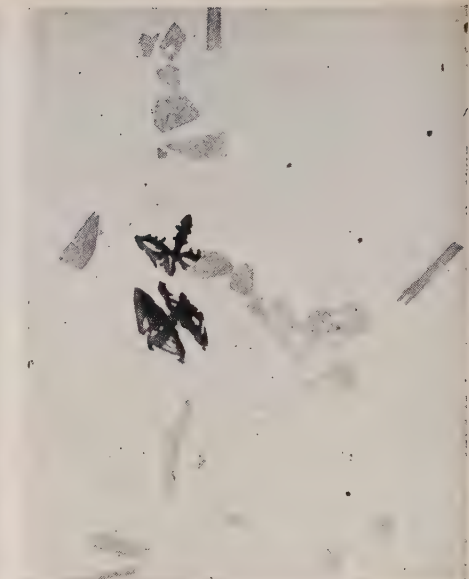


FIG. 15.—Al-V System : 1·5% V. Sand cast at 815° C. Unetched. $\times 150$.



FIG. 16.—Al-Mg Alloy : 5% Mg, 0·17% Ti. Segregate on centrifuged sample. Unetched. $\times 400$.

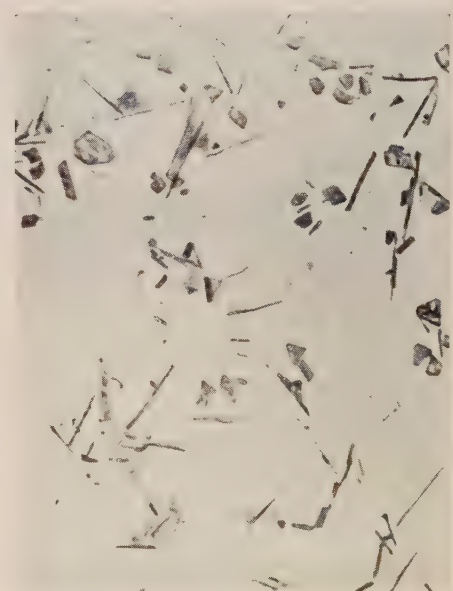


FIG.—17. Al-Mg Alloy : 10% Mg, 0·07% Ti. Eutectic in immediate neighbourhood of segregate. Unetched. $\times 400$.

PLATE XLII.



FIG. 18.—Al-Zn Alloy : 12% Zn, 0·5% B. Eutectic in "as-cast" alloy.
Unetched. $\times 200$.



FIG. 19.—Al-Zn Alloy : 12% Zn. Microradiograph. $\times 100$, Cu
radiation, Ni filter.

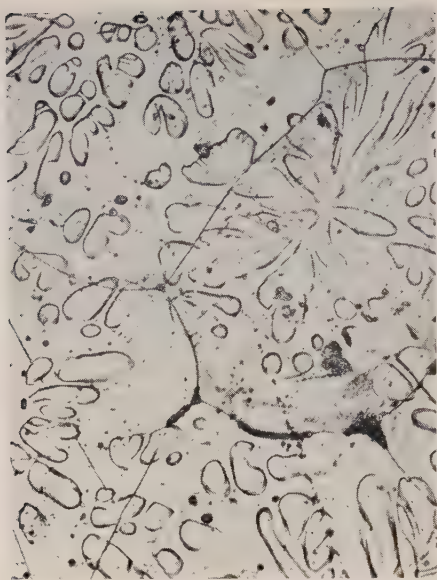


FIG. 20.—Grain Growth in Cast Aluminium-Titanium Alloys. Grain boundaries crossing dendrites. 0·12% Ti, sand cast from 800° C. Etched. $\times 100$.



FIG. 21.—High-Purity Aluminium Quenched in Water from 1000° C. Sub-boundary structures. Etched. $\times 100$.



FIG. 22.—High-Purity Aluminium Quenched in Water from 800° C. Sub-boundary structures. Etched. $\times 100$.

thought that the peritectic reaction caused fragmentation of the primary particles, with the consequent production of a large number of small nuclei. All the addition elements used in the present work, except boron and niobium, form peritectic systems with pure aluminium (see Appendix, p. 313). No reliable information was available when the work was started about the binary systems aluminium–boron and aluminium–niobium, or about any of the ternary systems studied. The most efficient grain refiners were titanium, zirconium, and vanadium, and in the alloys of these metals with aluminium, although considerable refinement occurred at hypo-peritectic compositions, the peritectic composition was reached before grain refinement was complete. Chromium, however, although forming a peritectic system with aluminium, is practically without effect on the grain-size, even when present in hyper-peritectic quantities. It is clear that, although the most powerful grain refiners do, in fact, form peritectics with aluminium, the peritectic reaction is not in itself the governing feature.

(iii) *The Effect of Concentration Gradients in the Solidifying Alloy on the Final Grain-Size.*

Northcott¹⁴ has elaborated the theory that equi-axial crystals are formed in alloys by the production of a concentration gradient within the melt as soon as solidification begins at the mould face. The liquid in the immediate region of the solid particle becomes impoverished or enriched in the added element, according to the type of system, and, as a result of this, has a lower melting point than the liquid nearer the centre of the casting, which is of average composition. The advancing liquidus isothermal thus produces a shower of crystals deposited from the liquid of average composition, separated from the previously solidified metal by a layer of molten metal. This process occurs repeatedly, and an equi-axial grain structure is the result.

This theory may be extended somewhat, as follows : all other things being equal, the greater the difference in composition between the first-formed solid and the residual liquid, the greater effect will separation of primary crystals have upon the composition of the liquid in their neighbourhood, and the greater will be the distance over which the influence of such effects will be exerted. Consequently, the second row of primary particles will be formed at a greater distance from the first row. The effect of diffusion, however, will be to reduce the concentration gradient in the liquid, and thus the distance between the rows of primaries, and these two factors will operate in opposite senses. It is likely, therefore, that systems showing small differences in composition between the initial solid and the residual liquid will have fine grains, provided that

the composition interval is great enough to avoid complete annulment of the concentration gradient by diffusion.

The theory should be applicable to both peritectic and eutectic systems, the grain-refining effect of the concentration gradient varying in a complex way with the relative and absolute slopes of the liquidus and solidus curves. A number of peritectic and eutectic systems have been examined in the present work, and while the grain refinement observed in some of the binary alloys could be attributed to concentration-gradient effects, the different behaviour of aluminium–boron and aluminium–copper–boron alloys is not readily explicable on this basis, nor will the theory account for the (admittedly small) variation in titanium content giving full grain refinement of aluminium.

2. *Effect of Casting Temperature and Rate of Cooling on Grain-Size.*

In the main series of tests it was seen that bars cast in green sand from high temperatures were generally coarser grained than bars cast from low temperatures. This might have been due to differences in rate of cooling either in the mould or in the temperature range 1000°–700° C. The tests reported in Table III suggest that some change occurs in the melt during cooling in the pot to the low pouring temperatures, the change promoting grain refinement, and that the rate of cooling after pouring is less important.

VII.—CONCLUSIONS.

The effects of small additions of elements forming peritectic systems with aluminium on the grain-size of this metal and its alloys have been studied. Many of the elements have a marked grain-refining effect, but, since chromium has little effect, the occurrence of a peritectic is not thought to be an essential feature in the formation of fine grains.

In some of the systems examined the grain-refining effects of the added elements are considerable when the amounts added are too small to produce primary particles of their respective compounds with aluminium, and it is concluded that such particles are not essential to the grain-refining mechanism. The grain-refining effect was usually a maximum when the peritectic composition was reached, but the minimum titanium content giving maximum refinement varied slightly with the method of addition, and this also indicates that the peritectic reaction is not of itself important.

While some of the results could be explained by a theory relating grain-size to concentration gradients in the semi-solid casting, this theory is not adequate in all cases, and, in particular, the grain refinement of

the aluminium-copper alloys by boron, which has only a small effect on pure aluminium, is not easily explained by the concentration-gradient theory.

The grain-refining effects of some of these elements depend partly on the thermal history of the melt. There are indications that some change promoting coarse grain occurs on superheating and that this is reversed by slow cooling from the superheating temperature to the lower casting temperature.

ACKNOWLEDGEMENTS.

The author's thanks are due to the Director and Council of the British Non-Ferrous Metals Research Association for permission to publish this work, and to Mr. W. A. Baker, B.Sc., F.I.M., for much helpful discussion.

APPENDIX.

CONSTITUTION AND METALLOGRAPHY OF THE ALLOYS.

1. Available Information.

(i) *Aluminium-Titanium System.*

Fink, Van Horn, and Budge¹⁵ gave a diagram showing a eutectic between aluminium and the compound $TiAl_3$ at 0·03–0·04% titanium and 659·8° C., and a peritectic at 0·18% titanium and 665·1° C. This, however, postulated the existence of an aluminium-titanium compound other than $TiAl_3$ between 665·1° and 659·8° C., for which there was no X-ray or other evidence. These authors later modified their diagram, as a result of some work on the conductivities of alloys of the two metals carried out by Willey, to a simple peritectic system, in which the reaction :



occurs at 665·1° C., and the solid solubility of titanium is given as 0·28%. Bohner¹⁶ found a break in the conductivity curve at 0·23% titanium.

Nishimura and Matsumoto¹⁷ state that the peritectic occurs at 0·05% titanium and 665° C.

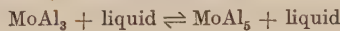
(ii) *Aluminium-Zirconium System.*

Fink and Willey¹⁸ are the only authors who have published any detailed work on the system aluminium-zirconium. Their diagram shows a peritectic at 0·11% zirconium and 660·5° C., the solid solubility being 0·28% zirconium at this temperature and 0·05% zirconium at

500° C. The compound has the formula $ZrAl_3$ and appears light grey in polished sections.

(iii) *Aluminium-Molybdenum System.*

Yamaguchi and Simizu,¹⁹ in attempting to establish the diagram of this system, found two compounds having the formulæ $MoAl_3$ and $MoAl_5$, the second being formed by the peritectic reaction :



at 703° C., and appearing in the microsections as a sheath round the $MoAl_3$ particles. At this temperature the liquid contains 0·24% molybdenum. They state that no solid solubility of molybdenum in aluminium could be detected by X-ray methods or by hardness tests.

(iv) *Aluminium-Chromium System.*

There seems to be some difference of opinion between the workers on this system as to the solid solubility of chromium in aluminium. Estimates vary from 3·1% (Knappwost and Nowotny²⁰) to 0·7% (Hofmann and Wiehr²¹) just below the melting point. Fink and Freche²² give the solid solubility as 0·77% at the peritectic temperature 661° C., and state that up to 0·4% chromium may be added without altering the melting point of pure aluminium. All authors are agreed that the compound formed at concentrations above the peritectic composition is $CrAl_7$.

(v) *Aluminium-Boron System.*

The most recent work on this system was carried out by Hofmann and Jäniche.²³ They found that boron was quite insoluble in solid aluminium and that there was no eutectic between aluminium and AlB_2 , contrary to the opinion of Haenni,²⁴ who found a eutectic between 15 and 18% boron. The compound AlB_2 is hexagonal and forms hexagonal leaflets in which the aluminium atoms occupy a simple hexagonal lattice and the boron a network analogous to that of graphite. Alloys having up to 1% boron contain AlB_2 ; above this content AlB_{12} also occurs.

(vi) *Aluminium-Niobium System.*

The compound $NbAl_3$ has been described and its structure studied by Brauer.²⁵

(vii) *Aluminium-Vanadium System.*

The solid solubility of vanadium in aluminium was reported by Roth²⁶ to be 0·37%. Only an approximate equilibrium diagram, based

on unpublished work by Mondolfo,⁹ is available; it indicates a peritectic reaction at approximately 0·1% vanadium and 660° C.

(viii) *Aluminium-Tungsten System.*

The only extensive data published on the aluminium-tungsten system are by Clark,²⁷ according to whose work a peritectic reaction occurs in alloys of very low tungsten content at 660° C., at which temperature the solid solubility is 1·5-1·8%.

(ix) *Ternary Alloys.*

There appears to be no published information regarding the systems aluminium-magnesium-titanium, aluminium-copper-boron, aluminium-zinc-boron, aluminium-magnesium-boron, and aluminium-silver-boron.

2. *Compounds and Solubilities Observed.*

No attempt was made to obtain equilibrium conditions in any of this work, but the concentration at which primary particles of a second constituent first appeared in the cast or centrifuged specimens was noted for each system.

(i) *Binary Alloys.*

Figs. 7-15 (Plates XXXIX-XLI) show the phases observed in the various systems. A very few particles of $TiAl_3$ were observed in the alloys containing 0·17% titanium, cast at 1000° C., and 0·19% titanium, cast at 900° C. Bearing in mind that the alloys are out of equilibrium, this is in good agreement with the work of Fink, Van Horn, and Budge,¹⁵ who found that the peritectic reaction occurred at 0·18% titanium, i.e. at higher titanium contents the primary crystals would be $TiAl_3$.

The systems aluminium-niobium and aluminium-molybdenum are particularly interesting. The constituent $NbAl_3$ appeared in very small quantities in alloys containing as little as 0·04% niobium, but was not formed in any considerable quantity until the niobium content was between 0·10% and 0·18%. The compound assumes small perfect geometrical shapes and shows a great tendency to polish in relief and therefore is probably very hard.

The peritectic reaction found by Yamaguchi and Simizu¹⁹ in the aluminium-molybdenum system is clearly illustrated in Fig. 9 (Plate XXXIX). No particles of compound were revealed by ordinary microscopic methods in alloys containing less than 0·21% molybdenum even after annealing for 36 hr. All the specimens showed marked coring on etching. This seems to indicate that there is some solid solubility of

molybdenum in aluminium, contrary to the opinion of the Japanese workers. Hardness measurements were therefore made on a series of aluminium-molybdenum alloys, the specimens being taken from the bars cast at 700° C. The results are given in Table XII, which shows that the hardness is very slightly increased by additions of molybdenum even when no primary particles of MoAl_5 are present. Although more refined methods were not used, it seems fairly certain that there is some solid solubility of molybdenum in aluminium.

TABLE XII.—*Hardness of the Aluminium-Molybdenum Alloys.*

Bars cast at 700° C.

Molybdenum, %	Hardness No. (Vickers)
0·00	17·5
0·21	18·1
0·25	20·0

The alloys containing zirconium did not show any recognizable particles of ZrAl_3 below 0·45%, cast at 800° C. (Fig. 8, Plate XXXIX), while those containing chromium showed particles of CrAl_7 at 1·27% (Fig. 11, Plate XL) and no such particles at 0·75% chromium.

The structure shown in Fig. 13 (Plate XL) was obtained in some aluminium–boron alloys, but whether the eutectic consists only of aluminium and AlB_2 or whether some impurities, such as iron or silicon, form a part of it, was not determined.

In the tungsten alloys, small geometrically shaped particles were present at 0·25% tungsten, and possibly also at 0·16%, which was apparently close to the peritectic composition. At higher alloy contents the particles sometimes assumed pronounced dendritic forms, and in alloys with 0·75% tungsten or more a second constituent appeared as sections of plates. The structure of the 1·5% tungsten alloy is shown in Fig. 14 (Plate XLI). These constituents are similar in appearance to the γ and δ phases shown by Clark,²⁷ in whose diagram γ is formed from δ by a peritectic reaction at 0·5% tungsten, and 687° C. The γ phase was often seen associated with the plates (δ phase) or in broken elongated shapes as though formed from them.

Two constituents were present in the vanadium alloys: a dark dendritic constituent appeared in alloys containing 1·5% vanadium (Mondolfo⁹ suggests 1·7% as the lower limit for the formation of this phase); and a lighter constituent, seen in Fig. 15 (Plate XLI) which was, in places, to be seen growing from the dendrites of the dark com-

pound, and was also present as very small dispersed particles in alloys containing only 0·2% vanadium.

(ii) *Ternary Alloys.*

(a) *The System Aluminium-Magnesium-Titanium.*—When titanium was added from the pure aluminium-titanium hardener, or from titanium tetrachloride, the aluminium-magnesium-titanium alloys containing 0·5 and 1% magnesium showed primary particles at titanium contents of 0·09-0·16%, and microscopic examination revealed that these had a similar appearance to $TiAl_3$. At 5% magnesium and 0·17-0·18% titanium, two compounds were present, one appearing very pale under the microscope and the other somewhat darker. The pale compound was sometimes seen surrounding the darker and may be formed from it and the liquid by a peritectic reaction. A similar effect was observed at 0·17% titanium added as titanium tetrachloride. The typical appearance is shown in Fig. 16 (Plate XLI). In the 10% magnesium alloy, at 0·05% titanium and more there appears to be one primary compound only, the very pale constituent observed in the 5% magnesium alloy. Fig. 17 (Plate XLI) shows the aluminium-magnesium eutectic in the immediate neighbourhood of the segregated particles in this alloy. The rod-shaped constituent in the eutectic is evidently due to titanium, and since it did not occur in the parts of the specimen remote from the centrifuged segregate, it might be inferred that the rods are all primary particles and their apparent association with the eutectic in some areas is fortuitous. X-ray analysis of centrifuged segregates revealed one compound only at 5% magnesium and 0·17% titanium and another only at 10% magnesium and 0·05-0·07% titanium. Neither constituent was $TiAl_3$ or elementary titanium.

(b) *The Ternary Systems Containing Boron.*—Primary particles, shown by X-ray analysis to have the AlB_2 structure, were present in the aluminium-copper-boron alloys containing 0·03% boron or more.

The metallography of those alloys containing zinc is very interesting. In all cases where boron was added primary particles of AlB_2 were identified by X-ray analysis, and these sometimes also appeared in the eutectic. The "blank" alloys showed no eutectic at 7·7 and 12% zinc, but a considerable quantity of unresolved eutectic at 25% zinc. The addition of 0·30-0·50% boron to 7·7 and 12% zinc alloys produced a large quantity of eutectic, the new constituent having the acicular or sometimes script-like appearance shown in Fig. 18 (Plate XLII). Attempts to detect this constituent by X-ray analysis have failed, but the presence, in the 12% zinc alloy, of a constituent of greater density than the basis alloy is clearly revealed in the radiograph reproduced in

Fig. 19 (Plate XLII). At 25% zinc no sign of this constituent was seen, although spectrographic analysis showed that these bars contained about the same amount of boron as did the alloys of lower zinc content, and a phase boundary has evidently been crossed between 12% and 25% zinc.

The actual boron contents of the aluminium-magnesium-boron alloys were probably very low. Primaries, where seen, were mostly very tiny and rod-like and were revealed only by an oil-immersion lens, but in two of the specimens, MSV 215 and 65, they were definitely of AlB_2 type in form and colour.

Particles of AlB_2 were present in the aluminium-silver-boron alloy.

3. *Grain Growth in Cast Aluminium-Titanium Alloys.*

The alloys of aluminium with titanium show marked coring on etching with the solution previously described (p. 300). The shape and outlines of the dendrites are clearly revealed and the grain boundaries are also shown by this etch. It was noticed that in many of the specimens of these alloys the grain boundaries were very straight, frequently forming roughly hexagonal grains and meeting in angles of 120° . Also, the grain boundaries crossed the dendrites in many places, as illustrated in Fig. 20 (Plate XLIII). These two observations can only be explained by assuming that the grain boundary has moved since the end of solidification, as it would otherwise pass entirely between the dendrites. Specimens were next cut from bars which had been allowed to cool to room temperature in the mould and were kept cool throughout preparation for micro-examination, but these nevertheless also showed grain growth. Finally, a rectangular bar was cast having a very good cast surface. It was allowed to cool in the mould and was etched electrolytically without delay and without further surface treatment. The grain boundaries were still observed to cross the dendrites. It was concluded that grain growth can occur after solidification in cast aluminium-titanium alloys without the application of external work and without further heat-treatment.

It is very probable that such grain growth occurs in pure aluminium also, as the grain boundaries are again straight and meet in regular angles. Since no dendrites are shown up by etching, however, it is not possible to be certain of this. Similar observations have been made by other workers in aluminium and high-purity aluminium-zinc and aluminium-copper alloys. These observations are explained by C. S. Smith's recent paper²⁸ on the effects of interfacial energies on micro-structure.

4. Sub-Boundary Structures in High-Purity Aluminium.

Figs. 21 and 22 (Plate XLIII) show the structure of high-purity aluminium, water-quenched from 1000° and from 800° C., respectively. It can be seen that the etching reagent has revealed a structure within the individual grains. This sometimes takes the form of a more or less perfect hexagonal network (Fig. 21, top right-hand corner, and Fig. 22, centre), and sometimes of a series of parallel lines and pits. In all cases micro-examination at higher magnifications reveals that the sub-boundaries are actually rows of etch pits and not particles of oxide or other constituent, although it is possible that they originated in minute particles of impurity segregated on particular planes in the crystals, as postulated by Northcott.²⁹ Spectrographic analysis of one of these specimens gave the following results :

Cu	Fe	Mn	Si	Ti	Ni	Mg
0·006%	<0·05%	0·001%	<0·005%	<0·003%	Trace	<0·01%

From previous chemical analyses it is probable that the iron content is in fact less than 0·02%. It is evident that, if these structures are caused by impurities other than oxygen, extremely small quantities are capable of producing them. No attempt has been made to investigate this further, and the observation is merely recorded as a matter of interest.

REFERENCES.

1. A. Cibula, *J. Inst. Metals*, 1949-50, **76**, 321.
2. H. Röhrig, *Metallwirtschaft*, 1931, **10**, 105.
3. A. Dumas, *Rev. Mét.*, 1944, **41**, 273.
4. C. Panseri and B. Guastalla, *Alluminio*, 1941, **10**, 202.
5. E. Böhm, *Aluminium*, 1938, **20**, 168.
6. I. G. Slater and R. T. Parker. Unpublished work, B.N.F.M.R.A.
7. S. A. E. Wells, *Proc. Inst. Brit. Found.*, 1942-43, **36**, 215; also *Metal Ind.*, 1943, **63**, 114, 139.
8. W. Rosenhain, J. D. Grogan, and T. H. Schofield, *J. Inst. Metals*, 1930, **44**, 305.
9. L. F. Mondolfo, "Metallography of Aluminium Alloys". New York : **1943** (John Wiley and Sons).
10. H. Reimann, *Z. Metallkunde*, 1922, **14**, 119.
11. J. C. Arrowsmith, K. J. B. Wolfe, and G. Murray, *J. Inst. Metals*, 1942, **68**, 109.
12. R. Mitsche, *Carnegie Schol. Mem.*, *Iron Steel Inst.*, 1934, **23**, 65; 1936, **25**, 41.
13. K. Iwasé, J. Asato, and N. Nasu, *Sci. Rep. Tōhoku Imp. Univ.*, 1936, [i], **Honda Anniv. Vol.**, 652.
14. L. Northcott, *J. Inst. Metals*, 1938, **62**, 101.
15. W. L. Fink, K. R. Van Horn, and P. M. Budge, *Trans. Amer. Inst. Min. Met. Eng., Inst. Metals Div.*, 1931, 421.
16. H. Bohner, *Z. Metallkunde*, 1927, **19**, 288.
17. H. Nishimura and E. Matsumoto, *Nippon Kinzoku Gakkai-Si*, 1940, **4**, 339.
18. W. L. Fink and L. A. Willey, *Trans. Amer. Inst. Min. Met. Eng.*, 1939, **133**, 69.
19. K. Yamaguchi and K. Simizu, *Nippon Kinzoku Gakkai-Si*, 1940, **4**, 390.

20. A. Knappwost and H. Nowotny, *Z. Metallkunde*, 1941, **33**, 153.
21. W. Hofmann and H. Wiehr, *Z. Metallkunde*, 1941, **33**, 369.
22. W. L. Fink and H. R. Freche, *Trans. Amer. Inst. Min. Met. Eng.*, 1933, **104**, 325.
23. W. Hofmann and W. Jäniche, *Z. Metallkunde*, 1936, **28**, 1.
24. P. Haenni, *Rev. Mét.*, 1926, **23**, 342.
25. G. Brauer, *Z. anorg. Chem.*, 1939, **242**, 1.
26. A. Roth, *Z. Metallkunde*, 1940, **32**, 356.
27. W. D. Clark, *J. Inst. Metals*, 1940, **66**, 271.
28. C. S. Smith, *Trans. Amer. Inst. Min. Met. Eng.*, 1948, **175**, 15.
29. L. Northcott, *J. Inst. Metals*, 1936, **59**, 225.

THE MECHANISM OF GRAIN REFINEMENT 1221 OF SAND CASTINGS IN ALUMINIUM ALLOYS.*

By A. CIBULA,† M.A., A.I.M., STUDENT MEMBER.

(Communication from the British Non-Ferrous Metals Research Association.)

SYNOPSIS.

The work described in this paper was carried out to determine the mechanism of, and secure greater control of, the grain refinement of aluminium casting alloys of the solid-solution type and, in particular, to find ways of preventing grain coarsening and increasing the efficiency of refinement.

Measurements of the undercooling before solidification in castings of various aluminium alloys were correlated with the grain-sizes. Large additions of certain metals (e.g. copper and nickel) to pure aluminium partly refined the columnar structure to a coarse equi-axial one; this is ascribed to concentration gradients in the liquid round solidifying dendrites, which retarded crystal growth and the release of heat of fusion and thus allowed the interior of the casting to undercool and new crystallites to form there.

When very small additions of the powerful grain-refining elements (e.g. titanium, boron, niobium, and zirconium) were made to pure aluminium, no undercooling was detected, indicating the presence of nuclei which facilitated the formation of crystallites of solid solution; but very fine equi-axial grain structures were obtained only when elements were present which produced concentration gradients during solidification and thus restricted growth of the first-formed crystals and allowed other nuclei to become centres of crystallization. Grain coarsening, due to the removal of nuclei from the melt by superheating, sedimentation, or the passage of gases, was also studied.

The experiments showed that, except in melts containing boron, the nuclei were not crystals of the intermetallic compounds of the refining metals with aluminium; theoretical considerations suggested that they were particles of the simple interstitial carbides of these transition metals. These conclusions were confirmed by further experiments with aluminium-titanium alloys, in which titanium carbide particles were detected by X-ray examination after being concentrated by centrifuging the molten metal.

I.—INTRODUCTION.

It is well known that grain refinement ‡ results in a considerable improvement in the properties of many casting alloys; the effect on

* Manuscript received 28 July 1949. The work described in this paper was made available to members of the B.N.F.M.R.A. in confidential research reports issued during 1948 and 1949.

† Research Investigator, British Non-Ferrous Metals Research Association, London.

‡ The term grain refinement in this paper refers to changes in macrostructure; refinement of microstructure, such as that obtained by modification of the aluminium-silicon eutectic alloys, is not considered.

the tensile properties of high-strength cast aluminium alloys, for example, is described in another paper.¹ Because of these advantages, methods of grain refinement have been developed empirically for several casting alloys, in particular the magnesium- and aluminium-base alloys, and to explain these and other changes in grain-size many different mechanisms have been proposed. They are mainly, however, of two kinds; the first includes those which suggest a restriction of crystal growth during solidification, for example by concentration gradients in the liquid metal surrounding crystallites of solid,^{2, 3, 4} or by adsorption of an alloying element on to the surface of the crystallites⁵; explanations of the second kind assume the presence of nuclei which facilitate crystallite formation, such as particles of intermetallic compounds,⁶ constituents due to impurity elements,^{7, 8} or even fragments of the original solid-solution lattice.^{7, 9}

Grain refinement of castings in aluminium alloys of the solid-solution type is obtained by the addition of small amounts of elements such as titanium, niobium, and boron. Several workers have asserted that refinement by titanium, which forms a peritectic system with aluminium,¹⁰ is due to nucleation of solid-solution grains by crystals of the intermetallic compound $TiAl_3$, round which the peritectic reaction occurs. Eborall¹¹ therefore studied the reduction of grain-size produced by the addition of titanium and several similar elements (zirconium, molybdenum, chromium, niobium, vanadium, and tungsten), to determine firstly, whether the formation of a peritectic system with aluminium results in grain refinement, and secondly, whether the minimum addition of each metal was that necessary for the formation of intermetallic compounds, that is, the peritectic point concentration.

The results indicated that although most of the elements which cause grain refinement also form peritectic systems with aluminium, nevertheless the presence of primary crystals of the intermetallic compounds was not an essential part of the mechanism; for in some alloys—those with titanium or zirconium—marked reduction of grain-size occurred at concentrations of these elements too small to produce their respective compounds, whereas the presence of crystals of intermetallic compound in other alloys produced only slight refinement. Furthermore, no reduction in grain-size occurred in alloys containing chromium, which forms a peritectic system with aluminium.

These results led to the alternative suggestion that grain refinement was due to restriction of crystal growth by concentration gradients, which were effective because of the particular solidus and liquidus slopes and/or diffusion rates encountered in these alloys of the peritectic systems. However, measurements of grain-sizes showed¹² that similar grain

refinement did not occur in alloys with several elements (iron, cobalt, nickel, manganese, lead, antimony, bismuth, and beryllium) which form eutectics close to 100% aluminium, although in these systems the liquidus and solidus slopes and the ranges of solid-solution formation were not very different from those in the peritectic systems, and several of the elements were transition elements similar to the grain-refining metals.

The measurement of undercooling was considered to be a likely method of distinguishing between the mechanism of grain refinement in various aluminium alloys, since any mechanism of crystal-growth restriction should retard the liberation of latent heat and thus increase undercooling effects, whereas a nucleation mechanism should reduce undercooling. These effects were investigated in experiments described in the next Section, and the conclusions were partly confirmed by some grain-size effects observed in further experiments described in Section III. The results suggested that nuclei were present in certain alloys, and the identities of these particles are considered in Sections IV and V.

II.—UNDERCOOLING IN ALUMINIUM ALLOY CASTINGS.

(a) *Previous Work.*

The results obtained by Eborall¹¹ showed that grain refinement in aluminium-titanium alloy castings occurred at concentrations much lower than those at which the intermetallic compound $TiAl_3$ could be detected metallographically. Ruddle¹³ observed that considerable undercooling occurred in castings of super-pure aluminium and aluminium-copper alloys, but not in alloys containing about 0·1% titanium, suggesting the nuclei were present in melts to which this amount of titanium had been added. It was therefore considered possible that increasing the titanium content would have an effect on the undercooling at solidification of aluminium alloys corresponding to the reduction in grain-size, and that eventually, when $TiAl_3$ crystals were present, undercooling would vanish if such particles served as centres of crystallization.

(b) *Experimental Procedure.*

(1) *Materials.*

In the work described in this and subsequent Sections, super-pure aluminium (99·99%) was used for making up all melts, including the hardener alloys. The batches of this metal were not large enough for only one to be used throughout the whole series of experiments, but no differences in undercooling were noticed in castings from the different batches used.

Lead (99.99%) and copper (O.F.H.C. foil) were added as such to the melts and other metals were added as hardener alloys prepared as described in Table I and of the tabulated compositions, the impurities being estimated spectrographically.

TABLE I.—Composition and Preparation of Hardeners.

Mark	Alloy	Composition	Impurities *	Method of Preparation
NKY 2	Al-Ti	1.75% Ti	0.13% Si; traces of Fe, Mg, Cu.	Potassium titanofluoride stirred into molten aluminium at 1000°–1100° C. 90% recovery of titanium.
NKY 4	Al-Ti	2.33% Ti		
NLA 5	Al-Nb	0.70% Nb	0.03% Fe; 0.06% Si; traces of Cu, Mg, Ti.	Niobium powder of high (spectrographic) purity pressed into pellets with aluminium powder and dissolved in molten aluminium at 1100° C. under KF flux.
NSO 1	Al-Ta	0.41% Ta	<0.02% Fe; <0.03% Si; traces of Cu, Mg, Ti.	Tantalum powder of high (spectrographic) purity pressed into pellets with aluminium powder and dissolved in molten aluminium at 1050° C.
NSM 1	Al-Mo	2.64% Mo	<0.02% Fe; <0.03% Si; traces of Cu, Mg, Mn, Ti.	99.9% sheet molybdenum dissolved in aluminium at 1000° C.
NSK 1	Al-Zr	1.69% Zr	0.02% Fe; <0.03% Si; traces of Cu, Mg, Mn, Ti.	Zirconium metal dissolved in aluminium at 1000° C.
NSH 1	Al-Cr	7.4% Cr	0.02% Fe; <0.03% Si; traces of Cu, Mg, Mn, Ti.	Electrolytic chromium dissolved in aluminium at 1000° C.
NLC 4	Al-B	0.27% B	0.08% Si; 0.03% Fe.	Potassium borofluoride stirred into molten aluminium at 1000°–1100° C. Recovery of boron, 15%.
NJU 2	Al-Ni	22.3% Ni	<0.01% each of Fe and Si; traces of Mg, Cu, Ti.	99.9% nickel pellets dissolved in molten aluminium.
NJY 1	Al-Mn	11.8% Mn	<0.05% Si; 0.02% Fe; traces of Mg, Cu, Ti.	99.99% electrolytic manganese dissolved in molten aluminium.
NKA 5	Al-W	5.3% W	0.05% Si; 0.03% Fe; traces of Cu, Mg, Ti.	Tungstic oxide (99.9%) reduced with aluminium powder by plunging mixture under molten aluminium at 1000° C.; the reaction was vigorous; 60% of tungsten recovered.
NJZ 3	Al-V	4.9% V	0.45% Si; 0.06% Fe; traces of Cu, Mg, Mn, Ti.	Vanadium pentoxide (99.8%) reduced by addition to molten aluminium at 1000° C. via cover of molten cryolite.

* The trace of titanium detected in these hardeners was not considered sufficient to vitiate the results of grain-size determinations and undercooling measurements, for the reasons discussed below.

(2) Melting and Casting.

All melts, including the hardeners, were made in Salamander crucibles which had been coated with a wash of 99% alumina cement. The iron and silicon contents of castings in super-pure aluminium which

had been melted using this technique were 0·006% and 0·004%, respectively : the most important source of impurities in other melts was therefore the hardeners, and the magnitude of the impurities can be judged from the compositions in Table I. The crucibles were placed in an Inconel vessel which was heated in an electric furnace and in which an atmosphere of dry nitrogen was maintained, so that degassing treatments and possible resultant complications could be avoided.

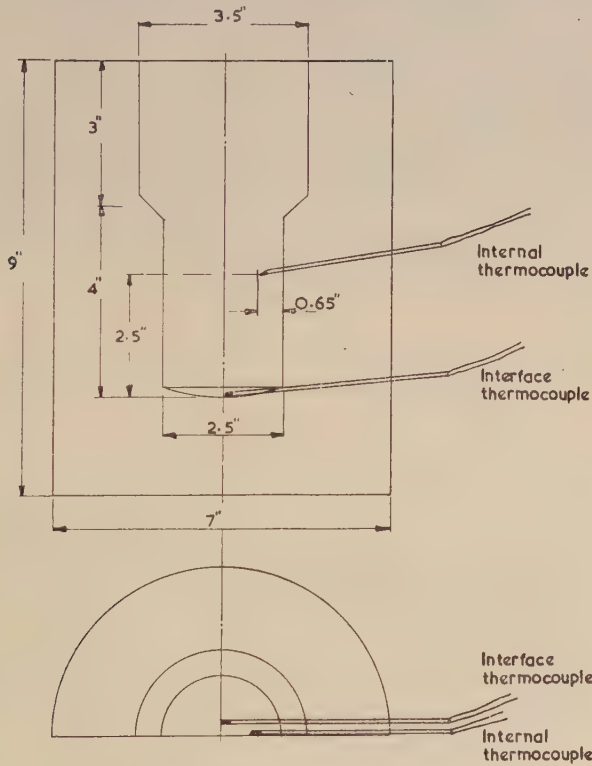


FIG. 1.—Position of Thermocouple in Half-Mould.

The alloys for undercooling measurements were made in approximately $2\frac{1}{2}$ -kg. melts; the temperatures before casting were measured with a 16-S.W.G. Chromel/Alumel thermocouple, the hot junction of which was coated with alumina cement.

The castings, the dimensions of which are shown in Fig. 1, were made by pouring the melts directly into the mould cavities, which were in dry synthetic sand bonded with 5% bentonite.

(3) Measurement of Undercooling.

A technique for the measurement of temperature changes within solidifying castings had been developed by Ruddle,¹³ and this was used in the present work.

Undercooling was measured by thermocouples introduced into the mould cavity before pouring the melt; for this purpose a vertically split moulding flask was used, the two halves being rammed and baked separately. Thermocouples were fixed with alundum cement into grooves in the dry sand at the parting line, and the two halves of the mould were then clamped together with the thermocouples protruding into the cavity.

The thermocouples were of 28 B. & S. gauge (0.3 mm. dia.) Chromel P and Alumel wires, protected up to 2 mm. from the weld by twin-bore fused-silica sheathing which held the couples in position. The tip of each thermocouple was covered with a thin wash of a proprietary sodium silicate–fireclay cement which protected the weld from attack without making the response of the thermocouple to temperature changes unduly slow.

Usually, two thermocouples were introduced into each casting. One was at a point on the metal–mould interface where the undercooling required for initial solidification could be measured. The position selected was close to the centre of the base, 7 mm. away from the parting line, and 0.5 mm. off the sand face; the thermocouple entered the side of the casting and approached the metal–mould interface from the metal side at an angle of 10°, so that errors in temperature measurement due to conduction along the couple wires were at a minimum. Precautions were taken to prevent the formation of a flash at the parting line, since solidification would then have commenced at the edge of the fin rather than at the thermocouple junction. The second thermocouple was placed with the weld at a point where it might record the undercooling in front of growing dendrites. Several positions were tried, two of which are shown in macrosections of some of the castings in Figs. 4–11 (Plates XLIV–XLVI); the position finally adopted was midway between the central axis and the sand face, as shown in Fig. 1.

Examination of sections of the castings through the thermocouple tips did not reveal evidence of interference with the growth of columnar grains by the thermocouple and silica sheathing.

The major part of the thermocouple e.m.f. was balanced by a back e.m.f. generated by a calibrated potentiometer; the residual potential, which was less than 1 mV., was measured after amplification by a Tinsley straight-line D.C. amplifier, on an ink-recording milliammeter.

PLATE XLIV.

FIG. 5.—Section of Casting in High-Purity Aluminium, Cast at 760° C. $\times \frac{1}{2}$.



FIG. 4.—Surface of Casting in High-Purity Aluminium, Cast at 760° C. $\times \frac{1}{2}$.



[To face p. 326.]

FIG. 6.—Surface of Casting in Aluminium-
0·01% Titanium Alloy, Cast at 760° C. $\times \frac{1}{2}$.

FIG. 7.—Section of Casting in Aluminium-
0·01% Titanium Alloy, Cast at 760° C. $\times \frac{1}{2}$.

FIG. 8.—Section of Casting in Aluminium-
0·5% Copper Alloy, Cast at 760° C. $\times \frac{1}{2}$.

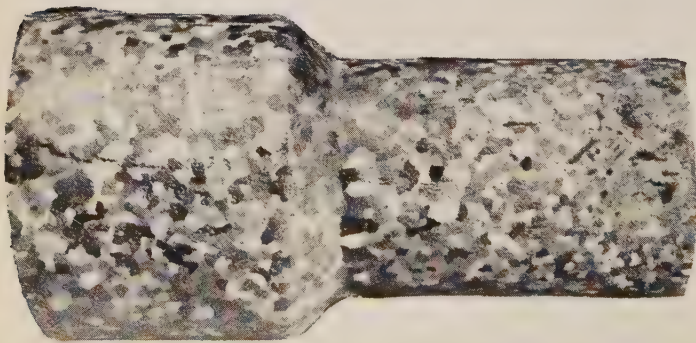


PLATE XLVI.

FIG. 11.—Section of Casting in Aluminium-
4% Copper Alloy, Cast at 750° C. $\times \frac{1}{2}$.



FIG. 10.—Section of Casting in Aluminium-
2% Copper Alloy, Cast at 755° C. $\times \frac{1}{2}$.



FIG. 9.—Section of Casting in Aluminium-
0·5% Copper-0·01% Titanium Alloy,
Cast at 760° C. $\times \frac{1}{2}$.





FIG. 14.—Section of Casting in Aluminium-0·04% Boron Alloy, Superheated to 960° C. before Casting at 760° C. $\times \frac{1}{2}$.



FIG. 13.—Section of Casting in Aluminium-0·04% Boron Alloy, Cast at 760° C. $\times \frac{1}{2}$.



FIG. 12.—Surface of Casting in Aluminium-0·04% Boron Alloy, Cast at 760° C. $\times \frac{1}{2}$.

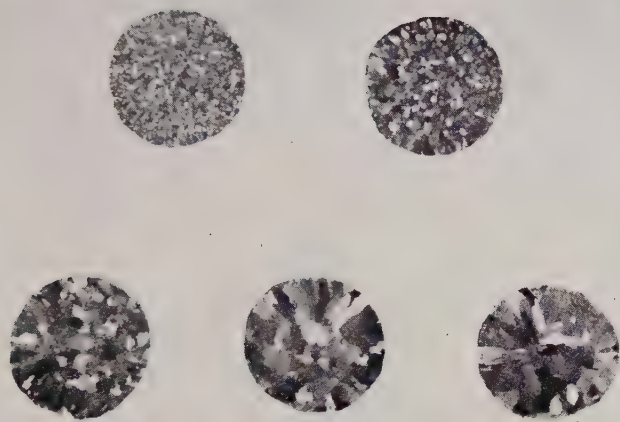


FIG. 15.—Grain Coarsening Produced by Passing Argon Through an Aluminium-0·15% Titanium Melt at 760° C. First bar cast from initial melt, others at 15-min. intervals. $\times 1$.

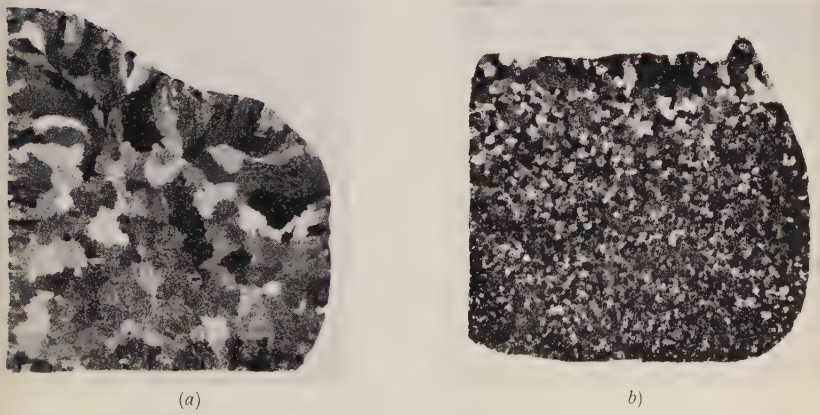


FIG. 16 (a).—Coarse Grain-Size in Aluminium-Titanium Alloy Centrifuged for 15 min. at 690° C.
(b).—Similar Specimen after Heating for 15 min. at 690° C. in Stationary Centrifuge. $\times 3$.



FIG. 17.—Section of Centrifuged Aluminium-0.1% Titanium Alloy, Initially Fine Grained. $\times 2000$.



FIG. 18.—Section of Aluminium-0.12% Titanium Alloy Centrifuged After Grain Coarsening with Nitrogen. $\times 2000$.



FIG. 19.—Section of Centrifuged Aluminium-0.2% Niobium Alloy, Initially Fine Grained. $\times 2000$.



FIG. 20.—Section of Aluminium-0.14% Titanium Alloy, Centrifuged After Grain Coarsening with Nitrogen and Refining by Graphit Addition. $\times 2000$.

Full-scale (4 in.) deflection of the recorder was given by an input of 1 mV., equivalent to 23.6° C. at 660° C. Temperature changes of 0.25° C. could be detected, and in some cases the sensitivity was even better than this.

The thermocouples were calibrated where necessary, either during solidification of the casting, at the melting point of aluminium or the aluminium-copper eutectic, or before assembling the mould, at the melting point of aluminium. The cooling rate was determined over a 10° C. range above the liquidus temperature. Undercooling was determined by measurement of recalescence when the latter was complete; in some alloys only partial recalescence occurred near the surface of the casting, and in these cases the difference between the liquidus temperature recorded by the internal thermocouple and the temperature minimum preceding recalescence recorded by the surface couple was measured. Examples of the use of each method are described in presenting the results.

During the initial part of the cooling curves, considerable temperature fluctuations accompanying turbulence in the melt were observed, but in alloys cast with a superheat of 100° C. or more, the record became smooth and the cooling rate steady before solidification started.

(c) *Results and Discussion.*

The undercooling characteristics of aluminium and its alloys were of three types, exemplified respectively by high-purity aluminium, high-purity aluminium-copper alloys, and alloys containing titanium; corresponding differences occurred in the macrostructures of castings of these alloys. The behaviour of these three groups of alloys will be described in turn, followed by a comparison with the results obtained from a few alloys of aluminium with other metals.

(1) *High-Purity Aluminium Castings.*

No undercooling was detected at points in the interior of the castings, normal cooling curves being recorded. At the metal-mould interface, however, considerable undercooling occurred, as shown in Fig. 2, followed by sharp and complete recalescence which evidently prevented undercooling from extending into the casting to the internal thermocouple and, moreover, indicated that crystal growth in the undercooled layer was rapid and unrestricted once solidification had begun.

In some records a reduction in the rate of cooling occurred just before the point of maximum undercooling was reached, suggesting that solidification had started at a point on the base remote from the thermo-

couple tip; the recorded temperature minima during undercooling were in such cases, therefore, not necessarily those at which the first crystallites formed.

The results of these measurements of undercooling close to the metal-mould interface are shown in Table II. Considerable undercooling occurred with all pouring temperatures, though with the lowest superheat of 50° C., turbulence, shown by fluctuations in the cooling curve, had not stopped when undercooling occurred.

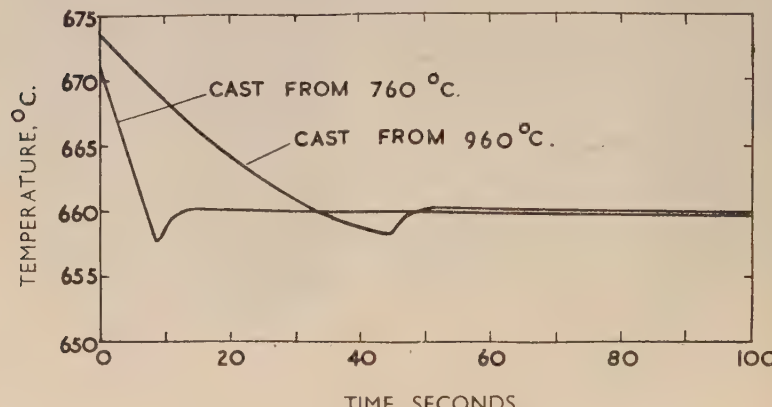


FIG. 2.—Undercooling at Metal-Mould Interface of Castings in High-Purity Aluminium Cast from 760° and 960° C.

All castings were columnar in structure, some of the coarsest grains having an area of about 50 cm.² on the surface of the casting. The grain-sizes at the surfaces are noted in Table II, column 6, and Figs. 4 and 5 (Plate XLIV) are photographs of the etched surface and a vertical section, respectively, of a casting poured at 760° C. The smaller grain-sizes and undercooling in the casting poured at 710° C. are discussed later.

TABLE II.—Undercooling at the Base of Sand Castings of High-Purity Aluminium.

Mark	Casting Temp., °C.	Superheat, °C.	Rate of Cooling, °C./sec.	Undercooling, °C.	Approx. Average Grain Dia. at Surface of Casting, cm.
NOP 6 .	710	50	3.6	0.7	0.7
NOP 3, 4, 5 .	760	100	1.8	1.9, 2.9, 2.2	3-4
NOP 7, 9 .	860	200	0.75	0.9, 2.6	5
NOP 8 .	960	300	0.45	1.7	5

To summarize, marked undercooling was necessary for solidification to begin in high-purity aluminium. Recalescence was rapid, indicating that crystal growth was unrestricted, and solidification continued on an advancing front without further undercooling and without the formation of new grains.

(2) *High-Purity Aluminium-Copper Alloys.*

In alloys containing 4% copper or more, the eutectic arrest was marked and was used to calibrate the thermocouples; in alloys of lower copper content it was necessary to calibrate the thermocouples in pure aluminium before assembling the mould. The results of undercooling measurements in hypo-eutectic alloys containing 0·5–16% copper are shown in Table III.

TABLE III.—*Undercooling in Sand Castings of High-Purity Aluminium-Copper Alloys, Cast from 100° C. Above Liquidus Temperature.*

Mark	Copper Content, %	Thermocouple at Interface			Internal Thermocouple		Structure of Casting
		Rate of Cooling, °C./sec.	Under-cooling, °C.	Recal-escence, °C.	Rate of Cooling, °C./sec.	Under-cooling and Recal-escence, °C.	
NOP series	0	1·8	1·9–2·9	1·9–2·9	1·2	0	Columnar
NOU 31	0·5	1·6	2·4	2·4	
NOU 19	1	1·3	0·2	
NOU 20	1	1·1	0·5	
NOU 29	1	1·8	3·9	3·9	1·1	0·8	
NOU 18	2	1·9	3·3	3·3	...	0·9	Predominantly columnar; shrinkage pipe
NOU 22	2	1·0	0·8	
NOU 21	2	1·9	3·5	3·5	
NOU 24	2	1·0	0·7	
NOU 28	2	2·0	2·1	2·1	...	0·5	
NOU 11	4	1·8	5·6	2·2	1·2	2·4	Predominantly equi-axial; scattered shrinkage cavities
NOU 25	8	1·8	5·0	2·9	1·1	2·3	
NOU 26	16	1·5	4·5	1·2	1·2	2·6	

In all castings, marked undercooling occurred at the metal-mould interface, increasing irregularly with the copper content up to 4%; however, recalescence was complete only in alloys containing up to 2% copper, and then (unlike super-pure aluminium) only when the thermo-

couple was removed from the mould wall by more than about 0·3 mm., so that the chilling effect was reduced.

The persistence of undercooling at the casting surface in alloys of increasing copper content was accompanied by a spread of undercooling into the casting, as measured by the internal thermocouple (column 7 of Table III). Internal undercooling was slight in low-copper alloys, but increased with copper content up to 4%, after which it was approximately constant. Cooling curves for the interface and internal thermocouples in the 8% copper alloy are shown in Fig. 3.

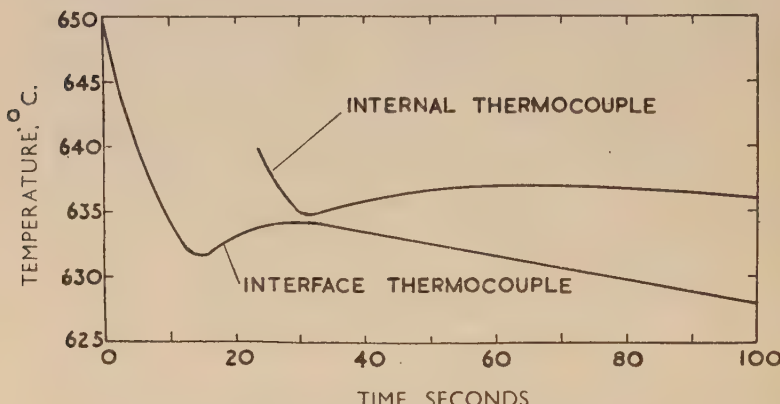


FIG. 3.—Undercooling in Casting of Aluminium-8% Copper Alloy at Metal-Mould Interface and Internally. Casting temperature = 740° C.

In determining the extent of undercooling at both thermocouple positions in these alloys, it was assumed that recalescence at the internal couple was virtually complete and that the maximum temperatures recorded there after undercooling were the liquidus temperatures for the alloys. This assumption neglects the changes in liquid composition due to the formation of solid during recalescence, and the resultant error was estimated to be 0·5° C. in the aluminium-16% copper alloy, decreasing to less than 0·2° C. in the aluminium-4% copper alloy. The values for the liquidus temperatures obtained in this way did in fact agree well with those given in the equilibrium diagram published by Raynor,¹⁴ the differences being less than 1° C.

Corresponding to these undercooling effects, changes in macro-structure occurred, examples of which are shown in Figs. 8, 10, and 11 (Plates XLV and XLVI). In alloys containing up to 2% copper, the structures were predominantly columnar, though progressively broken

up by scattered equi-axial grains. At 4% copper the castings were largely equi-axial in structure, as shown in Fig. 11, and little further refinement of the structure occurred with rise in copper content from 4 to 16%. A further noticeable feature was the replacement of the shrinkage pipe by a shallow surface depression and dispersed porosity when equi-axial grains took the place of columnar growth.

The grain boundaries in these alloys were uneven and interpenetrating, a feature characteristic of alloys freezing over a long temperature range, which is undoubtedly due in part to the restriction of the growth of solid-solution dendrites by concentration gradients in the surrounding liquid. It is known that crystal growth is most rapid in certain lattice directions and this initiates the formation of dendritic crystals; when the solid differs in composition from the liquid, and in consequence a concentration gradient appears in the surrounding liquid, growth is controlled by the extent to which the concentration gradients are dissipated by diffusion. This occurs most readily near the tips of the dendrite arms, and consequently their inherent tendency to become long and slender is enhanced by the presence of the concentration gradients. The arms of neighbouring dendrites therefore tend to interpenetrate, with the result that the grain boundaries appear irregular.

The observed variations in undercooling, recalescence, and grain-size can also be explained in terms of the restriction of crystal growth by concentration gradients. The point of maximum undercooling on the cooling curve occurs at the moment when the rate of release of latent heat balances the net rate of heat abstraction by the mould and the surrounding metal. If crystal growth and the corresponding release of latent heat are restricted, the melt may cool below the temperature at which crystallites first appear at the surface; for the same reason recalescence may be incomplete and the undercooling can spread into the interior of the casting. These effects will be more marked the greater the restriction on crystal growth, and this clearly increases with copper content because the difference between the composition of the crystallites and that of the neighbouring liquid increases with the copper content of the alloys examined. Thus the observed undercooling is explained by the growth-restricting effect of the concentration gradients.

The undercooling in turn accounts for the observed variations in grain-size, in the following manner. In pure aluminium, undercooling at the mould wall is followed by rapid recalescence as soon as the first crystallites are formed, and further solid is deposited preferentially on to these crystals. With increasing contents of copper, undercooling spreads further into the casting and this causes new crystallites to form

in the interior, in numbers which increase with the degree of undercooling, so that the columnar growth is eventually replaced by a coarse equi-axial structure. It is unlikely that the increasing degree of undercooling with increasing copper content is due to greater difficulty of formation of new crystallites; the degree of undercooling is more likely to be a measure of the restriction of crystal growth in alloys of higher copper content. This restriction by concentration gradients has been postulated in many papers,^{2, 3, 4} and the theory is supported by the results described in another published recently.¹⁵

The interpretation given above is consistent with Tammann's classical theory of crystallization from melts, and it conforms with the pasty solidification of aluminium-4% copper alloys and the skin formation in pure aluminium described by Ruddle.¹³

The concentration gradients and hence their growth-restricting effects should depend upon the absolute composition interval between the liquid and co-existing solid, and upon the slopes of the liquidus and, to a lesser extent, the solidus curves. This view is confirmed by the fact that in aluminium—4% copper and aluminium—4% nickel alloys the above factors are of the same order, and castings in both alloys have similar equi-axial structures under similar casting conditions.

The freezing ranges in castings in these two alloys are widely different, however, owing to the dissimilar eutectic temperatures. Furthermore, in the series of aluminium-copper alloys, the observed freezing range under the non-equilibrium conditions was greatest in the casting containing 2% copper, which was still largely columnar. The freezing range does not, therefore, appear to be a factor directly controlling grain-size.

(3) *Alloys Containing Titanium.*

Several castings were made in aluminium-titanium alloys containing 0.002%–0.1% titanium, using a constant pouring temperature of 760° C. (100° C. superheat). In no case was undercooling detected in the casting, either at the surface or internally; the change in direction of the cooling curve recorded by the interface thermocouple at the solidification temperature was very sharp.

The grain-sizes of the castings are given in Table IV. Even at the lowest titanium contents investigated, there was a marked reduction in the size of the grains on the surfaces of the castings. However, with titanium contents up to 0.04% the grains within the casting were still columnar, though reduced in cross-section; this is illustrated in Figs. 6 and 7 (Plate XLV) which are photographs of an etched surface and section respectively of a casting containing 0.01% titanium (cf. Figs. 4 and 5, Plate XLIV).

TABLE IV.—*Grain-Sizes of Sand Castings in Aluminium-Titanium and Aluminium-Copper-Titanium Alloys.*

Mark	Copper Content, %	Titanium Addition, %	Grain Dia. on Surface of Casting, cm.	Internal Grain Structure and Dia., cm.
NOP 3, 4, & 5 .	0	0	3-4	Columnar
NKZ 20 .	0	0.002	0.6-0.7	Columnar
NKZ 5 & 6 .	0	0.01	0.2-0.3	Columnar
NKZ 9 .	0	0.04	0.07	Equi-axial; 0.07
NKZ 1 .	0	0.10	0.04	Equi-axial; 0.04
NOU 31 .	0.5	0	Coarse and variable 0.1	Columnar
NLD 3 .	0.5	0.01	Coarse and variable 0.1	Equi-axial; 0.1-0.3
NOU 11 .	4	0	Coarse and variable 0.1	Coarse equi-axial
NLD 1 .	4	0.01		Equi-axial; 0.1

The virtual suppression of undercooling indicates that crystallite formation is greatly facilitated by the addition of as little as 0.002% titanium. The production of equi-axial structures may be explained as follows. In alloys of greater titanium contents the titanium dissolved in the melt produces concentration-gradient effects like those described for the aluminium-copper alloys, and the deposition of solid on to the crystallites formed at the mould wall is hindered; at titanium contents of 0.04% or more, this restriction is sufficient to cause further deposition of solid to occur preferentially on to new crystallites formed inside the casting, rather than on to those already existing at the mould wall. Repetitions of this growth-hindering process, followed by the formation of successive series of new crystallites, result in an equi-axial structure.

This mechanism is essentially similar to that already described to explain the formation of equi-axial structures in aluminium-copper alloys, and differs only in the fact that new crystallites are formed much more readily when titanium is present, so that the necessary growth restriction is much smaller. It is possible that even in the presence of titanium, some slight undercooling is necessary for the formation of a crystallite; but if this is so, it is not detectable with the present apparatus.

Concentration-gradient effects should be at their maximum, in aluminium-titanium alloys, at or above the peritectic point composition, so that increasing titanium additions up to this composition should favour the formation of more and more new crystals and consequently a progressively finer grain-size, as was found by Eborall.¹¹

If these views are correct, concentration gradients due to the presence of elements other than titanium should also increase the grain refinement caused by small titanium additions. In conformity with this, the presence of 0.5% copper changed the structure of the alloy containing

0·01% titanium from columnar to equi-axial, as shown in Table IV and Fig. 9 (Plate XLVI), and the alloy containing 4% copper and 0·01% titanium had a much more uniformly fine equi-axial grain structure. No undercooling was detected at primary solidification in any of these castings in aluminium-copper-titanium alloys.

The eutectic arrests in the alloys of higher copper content were preceded by about 0·5° C. undercooling, both in the presence and in the absence of titanium; this means that titanium additions did not facilitate the separation of CuAl₂.

To summarize the results described in this Section, crystallites form much more readily in melts to which titanium has been added, so that solidification occurs without detectable undercooling and the resultant grain-size is considerably reduced. New crystallites cannot form in the interior of the casting, however, unless the crystal growth is slightly restricted by concentration gradients caused by the presence of the titanium itself or of other alloying elements.

(4) Undercooling in Other Aluminium Alloys.

Undercooling measurements were made in a few aluminium alloys of several other systems, in order to determine whether the added element increased or decreased undercooling. It was important, in view of the effect of small titanium additions, that this and similar elements should be absent from the hardener alloys. A trace of titanium was detected spectrographically in these alloys but, as it was present to the same extent (about 0·001%) in the pure aluminium in which the hardener was diluted, and as it did not in fact prevent undercooling in many of the alloys, it was not considered sufficient to obscure the effect of the main alloying element. The results of these experiments are given in Table V. The alloys were cast with 100° C. superheat.

Of the binary alloys investigated, those which contained elements which are strong grain refiners of aluminium or its alloys solidified without detectable undercooling, when sufficient alloying element had been added to reduce the surface grain-size to approximately 0·7 cm. or less. The molybdenum-containing alloy, for example, did not undercool before the solid solution was formed; on the other hand, the chromium-containing alloy, which was hyperperitectic in composition and showed a pronounced primary-solidification inflection in the cooling curve, undercooled considerably before the formation of the solid solution, even in the presence of intermetallic compound crystals.

Niobium and boron, which are strong grain refiners in alloys of aluminium but not in the pure metal, nevertheless prevented undercooling when added to pure aluminium, and the surfaces of the castings

TABLE V.—Undercooling in Aluminium Alloy Sand Castings.

Mark	Alloy System	Alloy Content		Interface Under-cooling, °C.	Internal Under-cooling and Recalescence, °C.	Grain Structure of Casting
		Wt.-%	At.-%			
NOU 11, 25, 26	Al-Cu	4-16	1.75- 7.5	4.5-5.5	2.3-2.6	Coarse equi-axial.
NKB 16	Al-Ni	4.0	1.9	4.3	2.1	Coarse equi-axial.
NKG 16	Al-Mn	1.0	0.49	1.9	0	Columnar; 7 cm. dia. on surface of casting.
NKH 29	Al-Pb	0.8	0.10	1.9	0	Columnar.
NSH 2	Al-Cr	1.3	0.67	1.8	<0.1	Columnar; 2.5 cm. dia. on surface of casting.
NSM 2	Al-Mo	0.5	0.14	0	0	Fine equi-axial, 0.05-0.2 cm., plus narrow columnar in upper parts.
NLF 1	Al-B	0.04	0.10	0	0	Predominantly narrow columnar, 0.1-0.15 cm. on surface of casting.
NLB 1	Al-Nb	0.20	0.058	0	0	Predominantly narrow columnar, 0.1-0.15 cm. on surface of casting.
NSO 2	Al-Ta	0.01	0.0015	0	0	Columnar; 0.5 cm. on surface.
NKZ 20	Al-Ti	0.003	0.0015	0	0	0.6-0.7 cm. on surface; columnar.
NSK 2	Al-Zr	0.01	0.003	2.8	0	2-3 cm. on surface.
NSK 3	Al-Zr	0.1	0.030	0.5	0	2 cm. on surface.
NSK 4	Al-Zr	0.25	0.074	0	0	0.12 cm. on surface.
NKK 16	Al-V	0.1	0.053	0.8	0	1-2 cm. on surface.
NKK 7	Al-V	0.25	0.13	0.25	0	0.8-1 cm. on surface.
NKL 17	Al-W	0.4	0.059	0.4	0	1-2 cm. on surface.
NKL 18	Al-W	0.7	0.10	0	0	0.05-0.1 cm. on surface and internally.

became fine grained even though the columnar structure persisted internally, as illustrated in Figs. 12 and 13 (Plate XLVII). This structure is similar to that observed in aluminium containing only small amounts of titanium and is presumably due to the same cause, namely the absence of concentration gradients in the binary alloys.

The nickel-containing alloy, in which grain refinement by concentration gradients was believed to occur, solidified with an equi-axial structure, after undercooling both at the surface and internally to an extent similar to that observed in the aluminium-copper alloys.

(5) Further Discussion of Results.

The results of the undercooling and grain-size measurements described in this Section suggest that there are two mechanisms of grain

refinement in aluminium alloys, one exemplified by aluminium-copper alloys and the other by aluminium-titanium alloys.

In the aluminium alloys with elements such as copper, nickel, and silicon, grain refinement is relatively slight and can be explained by assuming that concentration gradients in the liquid metal restrict crystal growth, causing increased undercooling at the surface of the casting and the appearance of undercooling in the interior of the casting, the latter being associated with the production of equi-axial grains. In binary alloys with iron, cobalt, manganese, lead, bismuth, and antimony, these concentration gradients are not sufficient to change the columnar to an equi-axial structure.

Elements which produce marked grain refinement of aluminium or its alloys belong to the second group. In alloys with these elements crystallites can form without detectable undercooling, which suggests that the primary cause of grain refinement in such alloys is not restriction of crystal growth (though this plays an important part in allowing new grains to form in the interior of the casting), but the presence of nuclei on which the solid solution can crystallize without detectable undercooling.

In aluminium-titanium alloys, undercooling is prevented and the grain-size is decreased by very small additions which, according to the published equilibrium diagrams,¹⁰ are much below those necessary for the formation of $TiAl_3$ crystals. Furthermore, the experiments described in subsequent Sections show that the grain-size and undercooling may be strongly affected by temperature cycles well above the published liquidus temperatures, where the intermetallic compound should be in solution. For these reasons, the nuclei in aluminium-titanium alloys cannot be $TiAl_3$, but are probably compounds of titanium with an element other than aluminium.

In the next Section are described some further experiments which can be explained by the presence of nuclei in the melt, and throw some light on their identity.

III.—SOME GRAIN-SIZE EFFECTS DUE TO THE PRESENCE OF NUCLEI IN ALUMINIUM ALLOY MELTS.

(a) *Alloys Containing Titanium.*

(1) *Effects of Superheating.*

There are many references in the literature to grain coarsening of aluminium and other alloys produced by superheating the melts before casting from the normal temperatures; a similar effect was observed by Eborall¹¹ in alloys of aluminium with titanium, zirconium, and

molybdenum. Dumas¹⁶ describes experiments in which the effect of superheating an aluminium-magnesium melt was destroyed by the addition of 25-50% of new metal after superheating.

TABLE VI.—*Effect of Superheating on Undercooling in Sand Castings of Aluminium-0·01% Titanium Alloys.*

Mark	Superheating and Casting Temp.	Undercooling at Surface, °C.	Grain Structure and Dia. of Grains on Surface of Casting, cm.
NKZ 5 & 6	Heated to 760° C. and cast after stirring.	0	Columnar; 0·2-0·3
NKZ 7	Heated to 860° C. stirred and cast.	0·5	Columnar; 2·5
NKZ 8	Heated to 860° C., cooled to 760° C. in 20 min. with stirring, and cast.	1·4	Columnar; 1·3
NKZ 22 & 23	NKZ 7 & 8 castings remelted to 760° C. and cast.	0	Columnar; 0·2-0·3

To obtain further information, undercooling measurements were made in aluminium-0·01% and 0·04% titanium alloys superheated and cast from various temperatures; some of the results are given in Table VI. Analyses showed that no losses of titanium occurred during melting and superheating.

Superheating the 0·01% titanium alloy to 860° C. caused grain coarsening accompanied by undercooling at solidification; the effect did not disappear when the melt was cooled to 760° C. before casting, though the grains were less coarse, but the finer grain-size returned after remelting and casting, and no undercooling was then detected. Only grain coarsening, without undercooling, occurred after superheating the 0·04% titanium alloy to temperatures up to 960° C.

These results may be simply explained by assuming solution of the nuclei in the molten metal as the temperature is raised, and reprecipitation on solidification and remelting. In other work,¹ observations indicated that reprecipitation may occur merely on cooling from the coarsening temperature to a low pouring temperature (680°-700° C.), castings made below this temperature being very fine grained without pre-solidification.

The super-pure aluminium ingot used in this work contained a trace of titanium, less than 0·001%. The fact that the grain-size and undercooling observed in pure aluminium cast with only 50° C. superheat were both smaller than when superheats of 100° C. or more were used (Table II), is probably due to the presence of this trace of titanium. The casting temperature (760° C.) employed in most of the work described

in this paper was, evidently, sufficiently high to prevent this small inherent titanium content from masking the undercooling effects produced by other elements such as copper and nickel.

(2) Effects of Prolonged Holding Above Liquidus Temperature.

Castings of $\frac{3}{4}$ in. dia. in aluminium-0.19% titanium and aluminium-4% copper-0.15% titanium alloys, showed progressive grain coarsening when poured at intervals from melts held at 760° C. (approximately 100° C. above the liquidus temperatures for these alloys), for periods up to 20 hr. The grain-sizes of the two alloys increased from 0.25 to 2.0 and from 0.35 to 1.0 mm., respectively, and they were not affected by stirring the melt before casting. No change in titanium content occurred.

This grain coarsening was presumably due to growth or agglomeration of the nucleating particles (and consequently a reduction in their number) on holding at a constant temperature, and not to removal by gravity segregation, as this would have been affected by stirring. The original fine grain-size could be largely restored by subsequent super-heating to 975° C., followed by solidifying and remelting; this treatment apparently dissolved and reprecipitated the nuclei in their original form.

(3) Gravity Segregation.

During the course of a study of thermal gradients in castings,¹³ it was observed after sectioning a 5-in.-dia. cylinder sand cast in an aluminium-0.15% titanium alloy, that a 1-in. zone of coarse columnar grains had grown from the upper surface of the cylinder. This zone was sharply separated from the very fine equi-axial-grained region constituting the remainder of the casting. The coarse-grained zone contained 0.06% titanium, which normally is sufficient to produce marked refinement. The outer surface of the coarse columnar zone was fine grained.

An obvious explanation of this structure is that the primary solid-solution crystals, which were denser than the melt, had sunk as they were formed, and that they had removed all effective nuclei from the upper part of the casting by depositing solid on to them, with subsequent gravity segregation. If this was the case, and if the titanium provided the nuclei, only a small proportion of the original titanium content was present in the form which could act as nuclei, because the coarse-grained region had a substantial titanium content.

Similar grain-size variations have been observed in castings in alloys of aluminium with zirconium, molybdenum, and tungsten.

(4) *Effect of Passing Gases Through the Melt.*

Various gases were passed at 1 l./min., through a silica tube coated with alumina, into melts of aluminium containing 0·12–0·17% titanium, held at 760° C. Bars of $\frac{3}{4}$ in. dia were cast at 15-min. intervals.

When nitrogen, argon (each dried over P_2O_5), air, or hydrogen was used, the test-bars became progressively coarser grained and after 45 min. consisted largely of columnar grains; examples of test-bars cast from metal in which argon was used are shown in Fig. 15 (Plate XLVIII). It was found that treatment at 700° C. required longer times to produce columnar grains, but the use of a covering of 50:50 potassium chloride/magnesium chloride flux made the process much more rapid.

Although analyses showed that no reduction of titanium content occurred during the passage of the gases, the metal resulting from these treatments was inherently coarse grained; it could be melted and superheated to 950° C. (in alumina-coated crucibles), solidified, remelted, and cast, or taken through a variety of other melting cycles, with no reduction in grain-size, providing the pouring temperature of the final casting was near to or above the temperature at which the alloy had been coarsened initially. These facts indicated that nuclei had been removed from the melts, presumably by physical adherence to the gas bubbles or flux particles. If this were the case, the analyses showed that, of the titanium content of 0·15%, less than 0·01% was in the form of nuclei.

In other experiments on an aluminium–0·29% titanium alloy, treatment with nitrogen at 760° C. resulted in an increase in grain-size from 0·15 to 1·5 mm. without loss of titanium; this titanium content is above the peritectic point composition (0·15%),^{10, 11} and if $TiAl_3$ particles formed on cooling from 760° C. were responsible for grain refinement, all the test-bars should have been fine grained.

When chlorine was used in these experiments, instead of the gases mentioned above, the alloy containing 0·15% titanium increased in grain-size only to 0·5 mm., which was no greater than was observed after the alloy was merely held at 760° C. without passing any gas through the melt. The reaction between the chlorine and the melt was highly exothermic, and care was therefore taken to avoid a rise in the temperature of the melt, which would itself have caused grain coarsening; this often occurs when chlorine is used for degassing aluminium alloys.

(b) *Alloys Containing Boron.*(1) *Effect of Superheating.*

The solubility of boron in molten aluminium increases¹⁷ from 0·04% at 675° C. to 0·08% at 750° C., larger amounts of boron resulting in the

formation of the constituent AlB_2 in the form of hexagonal plates. Experiments were made with binary alloys containing 0·01, 0·02, and 0·04% boron to examine the effect on grain-size and undercooling of superheating in the range 760°–960° C. This is well above the highest temperatures at which the AlB_2 crystals could be out of solution in these alloys and, therefore, if grain refinement is due to nucleation by AlB_2 , superheating in this range should have little effect upon the ultimate grain-size.

The grain structures of these castings were similar to those of aluminium containing very small amounts of titanium; that is, the surface grain-size was much reduced, but the internal structure was still columnar, with the exceptions noted below.

The results, some of which are given in Table VII, showed that superheating had only a small effect on alloys containing boron, unlike those with titanium, but there was a tendency for grain-sizes to decrease slightly. AlB_2 particles were observed at 0·04%, very few at 0·02%, and none at 0·01% boron.

TABLE VII.—*Effect of Superheating on Grain-Size and Undercooling of Aluminium-Boron Alloys Cast at 760° C.*

Mark	Boron Content, %	Superheating Temp., ° C.	Grain Dia. on Surface, mm.	Undercooling at Surface, ° C.
NLF 1, 2 .	0·04	760	1·0–1·5; 1·5–2·0	0
NLF 3 .		860	0·8	0
NLF 12, 13 .		960	0·3–1; 1	0
NLF 7 .	0·01	760	10–15	0·7
NLF 10 .		860	8	0·2

An exceptional feature was observed in the 0·04 boron alloys which had been superheated to 960° C.; the castings, illustrated in Fig. 14 (Plate XLVII), exhibited a variable central zone of very fine equi-axial grains and the remainder of the structure was also largely equi-axial instead of columnar. These effects were associated with increased amounts of a semi-continuous grain-boundary constituent, present to some extent in all the alloys containing boron and particularly prominent in the fine-grained central zone. It is possible that the grain-boundary constituent was partly due to an increased pick-up of an impurity element, and indicated a slight restriction of crystal growth necessary for crystallites to form round new nuclei in the liquid metal, thus producing a fine grain-size.

IV.—THE IDENTITY OF NUCLEI IN MELTS CONTAINING TITANIUM AND OTHER TRANSITION-ELEMENT GRAIN REFINERS.

Of those elements which have been found to be grain refiners of aluminium or its alloys, namely, titanium, zirconium, molybdenum, niobium, tantalum, vanadium, tungsten, and boron, all but the last are transition elements and, for reasons which will become apparent, they are considered here separately; boron is discussed in the next Section. The first compounds to be considered as nuclei were the intermetallic compounds with aluminium.

(a) *Intermetallic-Compound Crystals as Nuclei.*

The results described above confirm the conclusion of Eborall¹¹ that it is unlikely that grain refinement in aluminium-titanium alloys is due to the presence of $TiAl_3$ crystals, for the following reasons:

(i) As little as 0·003% titanium is sufficient to cause some grain refinement and to prevent undercooling, whereas Eborall¹¹ found 0·13–0·15% titanium was required to form the $TiAl_3$ constituent, and Fink, Van Horn, and Budge fixed the peritectic point composition, by a different method, at 0·15% titanium.¹⁰

(ii) Temperature cycles in the range 760°–960° C. have a marked effect on the grain-size and undercooling of alloys containing 0·01 and 0·04% titanium, though these temperatures are well above the liquidus for the binary aluminium-titanium system and should therefore have no influence on the distribution of $TiAl_3$ crystals.

(iii) Passing gases through an aluminium-titanium melt above the liquidus temperature resulted in grain coarsening, without removal of titanium in amounts greater than 0·01% from alloys of 0·12–0·29% titanium; the coarse-grained material of 0·29% titanium contained $TiAl_3$ particles.

(iv) The results of other melt treatments described below are incompatible with grain refinement being due to the presence of $TiAl_3$ crystals.

There seems to be no evidence to identify the nuclei as intermetallic compounds in melts containing other transition elements which are grain refiners. Furthermore, in aluminium-chromium alloys the crystals of intermetallic compound neither cause grain refinement nor prevent considerable undercooling before the separation of the solid solution at the peritectic temperature.

For these reasons other compounds of the refining elements were considered as possible nuclei, particularly those with elements likely to be

present in molten aluminium or its environment, such as oxygen, nitrogen, carbon, and hydrogen. The factors considered were stability in the presence of molten aluminium and dissolved alloying elements, and similarity of lattice structure with that of aluminium, though the latter may not be an essential condition; some property, possibly additional to these, was sought, which was specific to the powerful grain-refining elements. It was found that these conditions were satisfied by the carbides of the refining elements; other compounds either were unlikely to be stable in molten aluminium (for example, oxides and certain hydrides and nitrides) or possessed no property by which the grain-refining transition elements could be differentiated from the others (for example, the nitrides, which are discussed in more detail below).

(b) *Carbide Particles as Nuclei.*

(1) *Carbides Formed by the Transition Metals.*

The transition metals have the notable property of forming interstitial compounds with the elements carbon, nitrogen, hydrogen, and boron. These compounds were investigated by Hägg, reviews of whose work have been published by Westgren¹⁸ and by Hofer.¹⁹

Unlike the typically ionic compounds formed by carbon with elements such as aluminium, beryllium, and calcium, the carbides of the transition elements show marked metallic properties. They are of two types : (i) The first has simple cubic or hexagonal structures, simple formulæ, and high stability; these carbides are noted for their high melting points and hardness and have prominent metallic properties such as supraconductivity, opacity, and the capacity to form solid solutions. (ii) Carbides of the second type, formed by other transition elements, have more complex structures and formulæ, lower stability, and are less metallic in character.

The formation of the simple interstitial structures was shown by Hägg to depend solely on an atomic-size relationship. When the ratio of the radius of the carbon atom (0.77 Å.) to that of the metal atom is less than 0.59 (varying slightly with the atomic period), the carbon atoms can occupy interstitial positions in a simple metal lattice and the highly stable interstitial carbides are formed. When the ratio is greater than 0.59 and the carbon atoms are too large to occupy these interstices, complex lattices of the metal atoms are necessary and the less stable complex carbides are formed (e.g. Fe₃C). Table VIII shows the way in which carbide formation varies with atomic size in each period; the free energies of formation at 727° C.^{21, 22} and the closest distances of approach of the metal atoms in the carbides^{20, 23} are also given. The

grain refiners and probable grain refiners have been enclosed by heavy lines in Table VIII.

TABLE VIII.—*Carbides of the Transition Elements.*

Element	Sc	Ti	V	Cr	Mn	Fe	Co	Ni	
R_c/R_m	0.48	0.53	0.59	0.62	0.60	0.61	0.62	0.62	
Formula	SeC	TiC	VC; V ₂ C	Cr ₃ C ₂ Cr ₄ O	Mn ₃ C; Mn ₄ O	Fe ₃ O	?Co ₃ O	Ni ₃ O	
Structure	Cubic	Cubic	Cubic; Hex. c.p.	Complex formulæ and structures.					
Closest distance of approach of metal atoms, Å.	...	3.06	2.93	
Free energy of formation (+ΔG) cal./g.-atom of carbon	...	-55,000	High	-18,000	-23,000	+1,000	+ve	+8,000	
Element	Y	Zr	Nb	Mo		Ma	Ru	Rh	Pd
R_c/R_m	0.43	0.49	0.54	0.57		...	0.58	0.57	0.56
Formula	YC ₂	ZrC	NbC	MoC	Mo ₂ C
Structure	Tetra-gonal	Cubic	Cubic	Hex.	Hex. c.p.	No stable carbides known.			
Closest distance of approach of metal atoms, Å.	...	3.31	3.14	2.90	2.99				
Free energy of formation (+ΔG) cal./g.-atom of carbon	...	-56,000	Highly negative	-600					
Element	La, Ce	Hf	Ta	W		Re	Os	Ir	Pt
R_c/R_m	0.41- 0.48	0.49	0.54	0.57		0.56	0.58	0.57	0.55
Formula	MC ₂	HfO	TaC; Ta ₂ C	WO	W ₂ O
Structure	Tetra-gonal	...	Cubic & Hex. c.p.	Hex. simple	Hex. c.p.
Closest distance of approach of metal atoms, Å.	3.14; 3.09	2.90	2.99
Free energy of formation (+ΔG) cal./g.-atom of carbon	Highly negative	Highly negative	

There is a coincidence of simple interstitial carbide formation and grain refinement, and it is notable that this correlation distinguishes between molybdenum and chromium which respectively refine and do not refine the grain-size of aluminium. It can also be seen that there is

a close similarity of the metal-atom lattices in the simple cubic carbides to the face-centred cubic lattice of solid aluminium in which the closest distance of approach of the aluminium atoms is 2.86 Å. The difference between corresponding interatomic distances is greatest in the case of aluminium and zirconium carbide, being 16% (so far as figures are available). In the simple hexagonal carbides the similarity of structures still exists if one compares the closest distance of approach of the metal atoms in the close-packed planes of the carbide lattices and the aluminium lattice, in which corresponding interatomic distances are again very similar.

To indicate the stability of the carbides in the presence of aluminium, the free energies of formation of these compounds should be compared with that of aluminium carbide, which at 727° C. is -4000 cal./g.-atom of carbon.²¹ Only in the case of molybdenum is the stability of the wrong order; however, it is possible that the published work from which Kelley²¹ selected the best value was inaccurate, as it proved to be in the case of chromium.²² The free-energy figures refer to the phases in the free state, and although account should therefore be taken of the reduction of the activity of the alloying element when dissolved in aluminium, no data have been published to allow for this correction. Although no figures are available for some of the carbides, an indication of their stability is given by their extremely high melting points (e.g. TaC, 4150° C.; MoC, 2840° C.) and hardness.

These observations strongly suggest that the grain-refining nuclei are simple interstitial carbides. If this is correct, Table VIII indicates that three other elements—scandium, hafnium, and tantalum—should also cause marked refinement of aluminium, since these three elements also form cubic interstitial carbides. Aluminium-tantalum alloys were therefore examined (see Table V) and were found to be very fine grained at 0.4% tantalum (chill cast) and to solidify without undercooling in the case of 0.01% tantalum alloy sand castings. The other elements, which are not easily available, have not yet been examined.

When the radius ratio (carbon atom : metal atom) is less than 0.48, dicarbides are formed in which two carbon atoms occupy each interstice; this distorts the lattice in the direction of the diatomic carbon groups into a tetragonal structure. Cerium, for example, forms the dicarbide CeC₂, with dimensions $a = 3.87$, $c = 6.48$ Å. No figures for the stabilities of these carbides have been published, but they are probably high. Undercooling and grain-size measurements in alloys containing up to 5% cerium have shown that nucleation by primary particles does not occur in these alloys, undercooling effects and changes in grain-size being similar to those observed in aluminium-copper alloys. It can

therefore be concluded that if the stability of the dicarbides is sufficient to ensure their presence in molten aluminium containing up to 5% cerium, they do not facilitate crystallization.

(2) *Other Interstitial Compounds.*

The transition elements form interstitial compounds with nitrogen and hydrogen which have lattice dimensions similar to those of the carbides. However, it is unlikely that these compounds form the nuclei in aluminium-alloy melts, as several of the hydrides become unstable below the melting point of aluminium, and some of the nitrides, for example vanadium nitride, are less stable than aluminium nitride. It is probable therefore that aluminium nitride would be formed rather than the nitrides of the transition elements, when the latter are in solution in aluminium. Moreover, owing to the smaller size of the nitrogen atom, simple interstitial nitrides can be formed by several elements, for example chromium, which cannot form the corresponding carbides and do not cause grain refinement of aluminium alloys.

(3) *Significance of the Formation of Peritectic Systems.*

If the identification of nuclei as carbide particles is correct, a satisfactory explanation is thus provided for the somewhat puzzling association of peritectic systems with grain refinement observed in earlier work on aluminium alloys.

The peritectic point occurs at the intersection of two liquidus curves which slope in the same direction. Nearly all the transition elements form stable compounds with aluminium, and in these alloy systems there are therefore steeply rising liquidus curves, at which intermetallic compounds separate, fairly close to 100% aluminium. The liquidus curve for the formation of the solid solution, however, rises with increase in alloy content only, apparently, when the atomic radii of aluminium and the solute element are very similar, and only in such cases is a peritectic system formed; this is shown in Table IX. In other cases the melting point of the solid solution is depressed by alloying additions and a eutectic system is formed.

The formation of a peritectic system with aluminium and the existence of a simple interstitial compound with carbon are therefore both functions of the atomic radius of the transition element, and these two properties very nearly coincide because the aluminium and carbon atoms have radii suitable for this to occur.

(4) *Lattice Registration and Nucleation.*

Although the evidence presented in this Section suggests that similarity of lattices is necessary if solid particles are to act as nuclei

TABLE IX.—Equilibrium Systems Formed by Transition Elements with Aluminium.

Element	Sc	Ti	V	Cr	Mn	Fe	Co	Ni
Approx. difference ²⁷ in atomic radii, %	+11; +12	+2	-8	-5; -13	-10	-12 to -13		
Type of system	?	Peri-tectic	Peri-tectic	Peri-tectic	Eutec-tic	Eutectic		
Grain refinement	?	Yes	Yes	No	No	No		
Element	Y	Zr	Nb	Mo	Ma	Ru	Rh	Pd
Approx. difference ²⁷ in atomic radii, %	+26	+10	0	-5	?	-8	-6	-4
Type of system	?	Peri-tectic	Peri-tectic	Peri-tectic	?	?	?	?
Grain refinement	?	Yes	Yes	Yes	?	...	?	...
Element	La, Ce...	Hf	Ta	W	Re	Os	Ir	Pt
Approx. difference ²⁷ in atomic radii, %	+20 to +35	+10	0	-4	?	-7	-5	-3
Type of system	Ce forms eutectic	?	?	Peri-tectic	?	?	?	Eutec-tic
Grain refinement	No	?	Yes	Yes	?	?	?	?

for crystallization, it is often stated in the literature that any small particle may do this by providing a surface on to which solid can be deposited. The conditions which must be satisfied for nucleation by foreign particles to occur are discussed in the Appendix (p. 354); the discussion lends support to the view that nucleation by foreign particles is easier the closer the registration between the lattices of the nuclei and of the aluminium solid solution. It is clear from the foregoing that the carbides of the powerful grain refiners (excepting boron) have favourable structures, but, so far as information is available, the compounds of these elements with aluminium have more complex structures which are less likely to satisfy the requirements of a nucleus. This is in accordance with the experimental observations.

There is evidence from different sources that crystals of one substance may nucleate the deposition of another if the lattice dimensions are similar, and when this occurs the lattice orientations of the two solids are simply related.* Royer²⁵ found that differences in lattice dimensions

* The influence of the nature of the interatomic binding is apparently not clearly understood; however, in the case of the carbide nuclei discussed in the present work, the interatomic bonds are predominantly metallic in nature and it seems reasonable to assume that this would facilitate the nucleation of aluminium crystals.

of up to 16% can be tolerated in the case of halides deposited from solution on to crystals of lead sulphide, potassium or sodium chloride, and mica. Thomson²⁶ has reviewed several other instances, including the deposition of metals from the vapour phase.

C. S. Smith²⁷ has suggested that any impurity which is precipitated from solution when a liquid metal solidifies, may assume a structure identical with that of the solid metal, and some of these minute "rafts" may be stable on remelting to a low temperature, and therefore able to act as nuclei during subsequent solidification. As shown by Eborall,¹¹ however, aluminium alloys can be made fine grained by the introduction of certain elements from molten or volatile salts, and since previous solidification is not involved Smith's explanation cannot apply in these cases.

(c) *Experiments on the Identification of Nuclei in Melts Containing Titanium.*

(1) *Grain Coarsening by Manganese and Chromium.*

Manganese forms a carbide which is of the complex type but is also fairly stable. It seemed possible, therefore, that the presence of a high concentration of manganese, relative to that of titanium, might cause the reaction :



to proceed from left to right and hence prevent grain refinement by titanium and possibly cause undercooling to occur, assuming TiC to be responsible for the grain refinement. Experiments were made with an aluminium-1% manganese-0.002% titanium alloy, and the results are compared in Table X with similar results from aluminium-1% manganese and aluminium-0.002% titanium alloys.

The results show that: (i) The presence of 1% manganese in the 0.002% titanium alloy has resulted in a marked grain coarsening, the grain-size of this casting being closely similar to that of super-purity aluminium with no added titanium; (ii) the coarsening is accompanied by undercooling at solidification; and (iii) the grain-size of super-purity aluminium is also increased by the addition of 1% manganese; this is presumably due to the effect of the manganese on the slight inherent titanium content of super-purity aluminium (0.001%).

A similar effect was considered probable with chromium additions because its complex carbide is also fairly stable; the results reported in Table X confirmed that chromium behaves similarly to manganese, though its coarsening effect is less marked. A better indication of the coarsening action of chromium and manganese can be seen by comparison

with the effect of an addition of 1% copper, which, on the other hand, increases the grain refinement due to the added titanium, for the reasons discussed above.

TABLE X.—*Grain Coarsening by Manganese and Chromium Additions to Aluminium-Titanium Alloy.*

Mark	Alloy Composition *	Undercooling at Casting Surface, °C.	Grain-Size on Surface of Casting, cm.
NOP 3, 4, 5 .	Al (super-purity)	1·9-2·9	3·5
NKZ 20 .	Al-0·002% Ti	0	0·6-0·7
NKG 16 .	Al-1% Mn	1·9	7
NKG 17 .	Al-1% Mn-0·002% Ti	1·5	3
NSH 2 .	Al-1·3% Cr	1·8	2·5
NSH 3 .	Al-1·4% Cr-0·002% Ti	0·7	1·5
NOU 29 .	Al-1% Cu	3·9	Up to 1·5
NOU 6 & 7 .	Al-1% Cu-0·002% Ti	0	0·3-0·4

* Titanium quoted is the amount added and excludes the inherent titanium content (0·001%) of the aluminium.

(2) Concentration of Nuclei and X-Ray Examination.

Melts of 12 g. of aluminium-0·1% titanium alloys were centrifuged in an apparatus developed by Baker.²⁸ The specimens were machined to fit into a closed graphite crucible and placed in a furnace on the horizontal arm of a centrifuge; the acceleration developed was 140 g. To obtain a smooth surface suitable for subsequent examination of the bases of the specimens, the metal was electrolytically polished before centrifuging and a polished graphite disc was fitted into the bottom of the crucible.

The use of graphite for this purpose, though not desirable, since carbides were to be looked for, could not be avoided, as no other material could be prepared as a polished disc which was not attacked by molten aluminium. However, there was no sign of any reaction between the aluminium alloy and the graphite, and control experiments with aluminium-titanium alloys from which nuclei had been removed, revealed no sign of carbide formation due to combination with the graphite base.

A normally fine-grained aluminium-titanium alloy was centrifuged for 15 min. at 690° C., i.e. above the aluminium-titanium liquidus temperature, and then solidified while the machine was stationary. The resulting metal was coarse grained, except in the layer adjacent to

the base; but a specimen melted in the same crucible in the stationary centrifuge remained fine grained. These results are shown in Fig. 16 (a) and (b) (Plate XLVIII), and indicate that the nuclei had been segregated to the base of the crucible (the left of the specimen in Fig. 16(a)).

It was possible to estimate the size of the nuclei from the time required to coarsen the grain-size by centrifuging, assuming them to be spherical particles of titanium carbide and using Stokes's law. The smallest particles were estimated to be 0.4μ in dia.

A coarse-grained centrifuged specimen was then sectioned and polished, and the edge in contact with the base of the crucible was examined at a high magnification; a typical field is shown in Fig. 17 (Plate XLIX). Small particles were observed whose size agreed well with the estimated figure, which, at the magnification used, corresponds to 0.8 mm. and greater. They tended to polish into relief very easily, as indicated in the Figure, and eventually were torn from the surface; this may be the reason for the ragged edge of the specimen. The particles were often square in cross-section, and rotation of the specimen between crossed Nicols indicated that they had a cubic lattice.

The base of the other half of the specimen was examined by X-rays at glancing-angle incidence, in an oscillating camera. The pattern obtained agreed with the structure of TiC, within the degree of accuracy of the camera. A more accurate analysis was obtained by extracting the carbide in 1 : 1 hydrochloric acid from scrapings from the base, and examining the residue in a powder camera; the value $a_0 = 4.321 \pm 0.003$ kX. units was obtained for the face-centred cubic lattice, in excellent agreement with recently published values for titanium carbide ($a_0 = 4.319^{29}$ and $a_0 = 4.329$ kX. units.³⁰) Another sample centrifuged at 760° C. yielded similar results.

Two specimens from aluminium-titanium alloys which had been coarsened by bubbling nitrogen through them when molten, as described above, were centrifuged at 690° and 760° C.; no X-ray pattern corresponding to TiC was obtained from these specimens and, as far as could be ascertained metallographically, no TiC particles were present (see Fig. 18, Plate XLIX).

An approximate estimation of the number of particles in a fine-grained alloy indicated that at 680° C. they were several hundred times as numerous as the number of grain centres, which means that very few become effective nuclei. The number of carbide particles estimated corresponds to a carbon content of only 0.0002%–0.002%, that is 0.001–0.01% of titanium carbide.

These centrifuging experiments were repeated on aluminium alloys containing 0.2% niobium, 0.1% tantalum, and 0.3% zirconium; the

alloys were all coarse grained after centrifuging. In the zirconium alloys, $ZrAl_3$ crystals were too numerous for any other small particles to be detected. In the other alloys, small cubic particles were observed, but they were too few to produce an X-ray diffraction pattern; the particles in the niobium alloy are shown in Fig. 19 (Plate XLIX).

(3) *Removal of Nuclei and Addition of Carbon and Other Substances.*

A stock of coarse-grained aluminium-0·15% titanium alloy was made by passing nitrogen through the liquid metal at 700°-720° C. Additions were then made to 500-g. batches of this alloy which were melted in alumina-lined crucibles or, if fluxes were used, in recrystallized pure alumina crucibles. The substances were added at 950° C., so that any compounds formed which might serve as nuclei should be dissolved; the metal was then chill-cast to precipitate the nuclei as fine particles. Their presence was sought by remelting the alloy to a low temperature (720°-740° C.) and measuring the grain-size of a bar sand-cast from the melt. Control experiments were made, with no additions, with each batch of coarse-grained alloy and each crucible material used; bars from these melts were columnar in structure.

Almost complete grain refinement could be obtained by the addition of an equal weight of super-pure aluminium, allowing for the decrease in titanium content. The nuclei formed by titanium, therefore, contain an element present in 99·99% aluminium. The results of other additions, and spectrographic analyses of various fine- and coarse-grained alloys, indicated that the element combined with titanium in the nuclei was not detectable spectrographically, nor was it hydrogen or oxygen.

Carbon was added in various forms, and it was found that its effect depended very much on whether the additions were made through a flux, and if so on the nature of the flux.

(i) *Additions without a Flux.*—Direct additions of carbon as pure powdered graphite or graphite rods produced only partial and inconsistent refinement, the minimum grain-size average being 0·75 mm., whereas a normal aluminium-0·15% titanium alloy melted and cast in the same way had a grain-size of 0·25 mm. These results were apparently due to the poor contact between the metal and the carbon, since no indication of a reaction was observed, even in one melt which was heated to 1300° C. in contact with a graphite rod. No greater reduction in grain-size occurred when carbon was added as carbon tetrachloride vapour, carbon monoxide, acetylene, or high-carbon steel, though in each case carbon was produced.

(ii) *Additions through a Potassium Chloride Flux.*—No refinement of the columnar structure occurred when graphite was added, the flux

merely coating a graphite rod which was otherwise unaffected. As mentioned in Section III, a chloride flux facilitated the removal of nuclei from a fine-grained alloy by a gas passed through the melt. It has also been observed that a similar flux can prevent grain refinement of magnesium-aluminium alloys by superheating²⁸ or by carbon additions.³¹

(iii) *Additions through a Potassium Fluoride Flux.*—A graphite rod was completely disintegrated when this flux was used, and the finest grain-sizes were obtained in castings from the melt. However, the flux alone produced a partial refinement of the grain-size to 0·9 mm., possibly owing to small carbonate impurities in the flux, to attack of the alumina crucible, or carbon pick-up from the atmosphere. Melting in crucibles of silicon carbide or fused magnesia (which contains carbonate) without graphite additions, also resulted in the finest grain-sizes.

Two specimens from castings refined in this manner were centrifuged and examined as described above. In both alloys small cubic particles were observed which were too few in number to produce an X-ray diffraction pattern, but were similar to those identified previously as titanium carbide. In addition to these cubic particles, many small needles or plates were present; both kinds of particles are shown in Fig. 20 (Plate XLIX).

The small plates were present at the inside as well as the outside faces of the centrifuged specimens. The X-ray patterns from these specimens agreed well with that of aluminium carbide; as the density of this compound is very close to that of liquid aluminium, the effect of centrifugal force on the plates would be strongly influenced by association with other particles, such as the denser cubes of titanium carbide (as suggested in Fig. 20, Plate XLIX), and this would explain the existence of the plates at both faces of the specimens. Particles similar to these aluminium carbide plates have been observed in several alloys which had at some stage been melted under a fluoride flux in graphite crucibles.

V.—THE IDENTITY OF NUCLEI IN MELTS CONTAINING BORON.

No experiments were made which have given direct evidence of the identity of the nuclei in melts containing boron, but the following facts suggest that the nuclei are crystals of AlB_2 which are formed during solidification.

In the experiments made with aluminium-boron alloys, crystals of the intermetallic compound AlB_2 were visible at 0·02% boron, which is just sufficient to cause grain refinement on the surface of the casting;

furthermore, grain-sizes were only slightly affected, possibly not significantly, by superheating the melt before casting at 760° C., which is above the liquidus temperature for the compound AlB₂.

The aluminium atoms in this compound are arranged on a simple hexagonal lattice³² in which the interatomic distance is 3.00 Å., which is close to the figure for the normal aluminium lattice, 2.86 Å. Structurally, therefore, AlB₂ appears capable of nucleating the crystallization of aluminium.

Although boron also forms a very stable compound with carbon, B₄C, this compound has a rhombohedral structure which is quite different from that of aluminium.

VI.—SUMMARY AND CONCLUSIONS.

(a) General Mechanism of Grain Refinement.

As indicated in Section II, the observations on grain-sizes and undercooling in a variety of aluminium-base alloys are interpreted as showing that grain refinement in any given case is due to one of the following :

(1) Restriction of crystal growth by concentration gradients, associated with increased undercooling at the surface of the casting and, more particularly, with the spread of undercooling into the interior of the casting, the latter condition producing an equi-axial structure. The grain refinement produced by this mechanism in aluminium alloys with copper, nickel, lead, &c., is relatively slight until a large proportion of the alloying element is present, and is never very marked.

(2) The presence of nuclei upon which the aluminium solid solution crystallizes easily, this being associated with the virtual suppression of undercooling. This mechanism alone, e.g. in aluminium alloyed with very small proportions of titanium, will only refine a coarse columnar structure to a much finer but still columnar one, and will not produce the equi-axial structures characteristic of marked grain refinement.

(3) The combined effects of concentration gradients and of nuclei, grain refinement then being very marked and again associated with the virtual suppression of undercooling, although it is possible that very slight undercooling occurs and that it is the function of the concentration gradients to produce this. This marked grain refinement occurs in aluminium alloyed with substantial proportions of titanium, zirconium, vanadium, molybdenum, or tungsten, where the alloying element provides both the concentration gradient and the nuclei.

In some other alloys of aluminium with powerful grain-refining elements, notably niobium and boron, the range of composition over

which the solid solution is formed is very restricted, primary particles of the respective compounds with aluminium appearing in alloys containing only 0·02% boron or 0·04% niobium.¹¹ In these systems, therefore, the alloying element fails to produce the concentration-gradient effect, and maximum refinement is obtained only if another element, e.g. copper, is added to provide the restriction of crystal growth. Thus, the theory accounts satisfactorily for an earlier observation¹² that boron and niobium have a relatively slight grain-refining action when added to super-pure aluminium, although they refine aluminium-base alloys markedly.

The above outline of the grain-refinement mechanism accounts satisfactorily for all the observations made to date in this research on the grain refinement of aluminium and its alloys. For example, the effects of superheating aluminium-titanium and aluminium-copper-titanium alloys are attributed to a decrease in the number of nuclei by particle growth or agglomeration or to solution of the nuclei in the melt at high temperatures, which would explain the observed grain coarsening and recurrence of undercooling.

(b) *The Identity of Nuclei in Fine-Grained Alloys.*

In alloys of aluminium with the grain refiners which are transition metals, the effects of these elements are first observed at contents which are sometimes too small to cause the appearance of their compounds with aluminium. From considerations of the stability and crystal structures of the compounds formed by the transition elements with several non-metals, and from experimental evidence, it is concluded that the nuclei are carbides of the grain-refining metals; these carbides contain carbon atoms in interstitial positions in simple metal-lattice structures of which the dimensions are similar to those of the aluminium lattice. Certain transition metals, notably chromium and manganese, form complex carbides, the structures of which differ markedly from that of aluminium, and these transition elements do not cause grain refinement.

It is considered that the identity of the grain-refining nuclei in aluminium alloys refined with titanium is established. In the case of the other grain-refining transitional elements, the identification of the nuclei as the respective carbides of the elements is based on indirect evidence, but this is considered to leave little room for doubt.

Boron forms with aluminium a compound, the lattice dimensions of which also conform with those of aluminium, and it is possible that like the above carbides this compound provides nuclei on which crystallites of solid metal can readily form.

ACKNOWLEDGEMENTS.

The author is indebted to the Director and Council of the British Non-Ferrous Metals Research Association for permission to publish this paper, and to members of the Association's Sub-Committee on the Grain Refinement of Light Alloys for advice on the conduct of the research. The author gratefully acknowledges the advice and assistance received from his colleagues, particularly Mr. W. A. Baker, B.Sc., F.I.M., Mr. R. W. Ruddle, M.A., A.I.M., Mr. E. C. W. Perryman, B.A. (who made the difficult metallographic preparations), and Miss J. M. Silcock and Mr. J. Fox (who made the X-ray examinations).

APPENDIX.

The Formation of Crystallites in a Melt.

The respective effects of undercooling and of nucleation by foreign particles upon the rate of crystallite formation may be illustrated

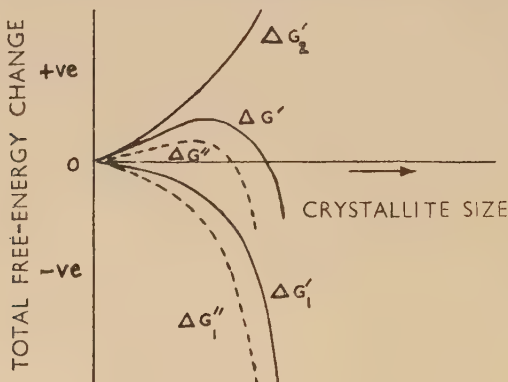


FIG. 21.—Effect of Undercooling on Free Energy of Formation of Crystallite.

diagrammatically using the method of Becker, described by Mehl and Jetter.³³ The total free-energy change in the formation of a crystallite, $\Delta G'$ in Fig. 21, is the sum of two terms :

$$\Delta G' = \Delta G'_1 + \Delta G'_2 \quad \dots \dots \dots \quad (1)$$

where $\Delta G'_2$ is the work of formation of the crystallite-liquid interface, which is positive and is proportional to the square of the linear dimensions of the crystallite; and $\Delta G'_1$ is the negative free-energy change resulting from the phase change at a given degree of undercooling, which is

proportional to the cube of the crystallite diameter. The resultant $\Delta G'$ reaches a maximum at a certain particle size; crystallites of this size may grow with decreasing free energy and are therefore stable, whereas smaller crystallites tend to redissolve. The frequency with which stable crystallites may form decreases with the height of the free-energy maximum as the initial work necessary to overcome the energy barrier must arise from random energy fluctuations in the melt. This energy barrier may be reduced in two ways:

(i) *By Greater Undercooling.*—With a greater degree of undercooling the term $\Delta G'_1$ increases (numerically), e.g. to $\Delta G''_1$ (Fig. 21), whereas the free energy of surface formation, $\Delta G'_2$, may be regarded as approximately constant over these small temperature intervals. The resultant

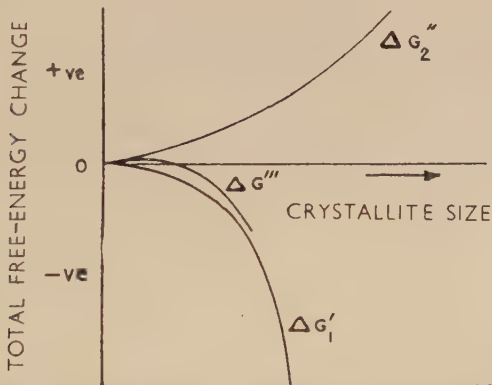


FIG. 22.—Effect of Foreign Nuclei on Free Energy of Formation of Crystallite.

$\Delta G''$ thus reaches a lower maximum, at a smaller crystallite size, and the rate of crystallite formation is therefore increased by the greater undercooling.

(ii) *By the Presence of Foreign Particles.*—The effect of nucleation by foreign particles at, say, the undercooling corresponding to $\Delta G'_1$ in Fig. 21, is a reduction of the free energy of formation of the crystallite surface, shown by a reduction of G'_2 to G''_2 in Fig. 22, and a lower maximum in the final curve for $\Delta G'''$. Crystallite formation is again, therefore, more frequent. Since the rate of crystal growth also increases with the degree of undercooling, an increase in the rate of crystallite formation near the true melting point, caused by foreign nuclei, is more effective in reducing the resultant grain-size than is an equal increase in the rate of crystallite formation caused by undercooling.

Only certain types of foreign particles will reduce the free energy

required to create the new interfaces when a crystallite is formed, and it is only to these nuclei that Fig. 22 refers; other particles may be ineffective. The properties which enable a foreign particle to act as a nucleus may be derived as follows :

In equation (1) above,

$$\Delta G_1 = \text{free energy change due to phase change} \\ = K_1 \times \text{volume of solid crystallite} \quad \dots \dots \dots \quad (2)$$

where K_1 corresponds to a degree of undercooling, ΔT_1 , and is zero when $\Delta T = 0$.

$$\Delta G_2 = \text{free-energy change due to the formation of new interfaces.} \\ = \Sigma(K_{AB} \times \text{area of interface } A/B) \quad \dots \dots \dots \quad (3)$$

where K_{AB} is the free-energy content per unit area of the interface A/B . In the following, where equation (3) is used,

$K_{SL} \equiv$ Solid metal-liquid metal interface.

$K_{SP} \equiv$ Solid metal-foreign particle interface.

$K_{LP} \equiv$ Liquid metal-foreign particle interface.

The interfacial free-energy contents may be treated³⁴ as forces acting in the respective interfaces (i.e. "surface tensions"). Ideally

the relation between K_{SL} , K_{LP} , and K_{SP} governs the angles of contact of the interfaces, as in Fig. 23, such that :

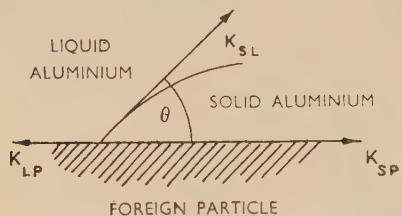


FIG. 23.—Relation Between Interfacial Free-Energy Contents and Angles of Contact.

$$K_{LP} = K_{SP} + K_{SL} \cos \theta \quad (4)$$

This idealized relationship is used below to investigate the effects of the properties of the interfaces upon crystallite formation; in practice this assumption must be

qualified because the shape of the crystallite and the angles of contact will also be controlled by crystal forces and by the variation of rates of growth with lattice direction.

Three types of crystallite formation may occur, theoretically, as in (a), (b), and (c) below.

Type (a).

$$K_{SP} > K_{SL} + K_{LP} \quad \dots \dots \dots \quad (5)$$

The angle of contact θ is 180° , and new crystallites are therefore formed as spheres (minimum surface area : volume ratio), either touching the foreign particle or away from it, and the free energy of the surface of the crystallites is not affected by the presence of the particles;

nucleation therefore occurs as in a melt free from such inclusions. Re-arranging equation (5),

$$K_{SL} + K_{LP} - K_{SP} \ll 0.$$

$K_{SL} + K_{LP} - K_{SP}$ is the work per unit area required to part a crystallite of solid aluminium from the surface of a foreign particle, when immersed in liquid aluminium,* and is known as the "work of adhesion". Hence, when the work of adhesion is less than zero (i.e. adhesion is unstable), crystallite formation occurs as in a melt free from foreign particles.

Type (b).

$$K_{LP} > K_{SL} + K_{SP} \dots \dots \dots \quad (6)$$

$$\begin{aligned} \Delta G &= \Delta G_2 + \Delta G_1 \\ &= (K_{SL} + K_{SP} - K_{LP}) \times \text{area of film} \\ &\quad - K_1 \times \text{volume of film} \dots \dots \dots \quad (7) \end{aligned}$$

<0 at all stages in the growth of the crystallite, since both terms are negative.

The smallest of these crystallites is therefore stable (even slightly above the true melting point, when K_1 is negative).

Since $K_{LP} \gg K_{SL} + K_{SP} \dots \dots \dots \quad (6)$

$$K_{SL} + K_{LP} - K_{SP} \gg 2K_{SL} \dots \dots \dots \quad (8)$$

The quantity of $2K_{SL}$ is the work of cohesion of two surfaces of solid metal in liquid; thus, when the work of adhesion of solid metal to a foreign particle is greater than the work of cohesion of solid metal crystallite formation occurs very readily, the work of formation being negative at all stages, at a temperature at or below the melting point.

Type (c).

Between Types (a) and (b), a continuous range of crystallite formation is possible, such that:

$$\left. \begin{aligned} K_{LP} &< K_{SL} + K_{SP} \\ K_{SP} &< K_{SL} + K_{LP} \end{aligned} \right\} \dots \dots \dots \quad (9) \quad (10)$$

and θ lies between 0° and 180° , as, for example, in Fig. 23. It may be assumed that, at least initially, the crystallite is approximately in the shape of a spherical cap, the base angles being fixed by the relation above in equation (4). Then

$$\Delta G = \Delta G_2 + \Delta G_1 \dots \dots \dots \quad (1)$$

$$\begin{aligned} &= [K_{SL} \cdot 2\pi r^2 (1 - \cos \theta)^2 + (K_{SP} - K_{LP})\pi r^2 \sin^2 \theta] \\ &\quad - \left[K_1 \frac{\pi r^3}{3} (1 - \cos \theta)^2 (2 + \cos \theta) \right] \end{aligned}$$

* This follows, since in destroying the solid metal-particle interface ($\equiv K_{SP}$), two new interfaces, solid-liquid ($\equiv K_{SL}$) and particle-liquid ($\equiv K_{LP}$), are created.

where r is the radius of the spherical cap.

$$\Delta G \text{ is a maximum when } \frac{\partial \Delta G}{\partial r} = 0,$$

$$\text{i.e. when } r = \frac{2[2K_{SL} + (K_{SP} - K_{LP})(1 + \cos \theta)]}{K_1(1 - \cos \theta)(2 + \cos \theta)}$$

$$\text{and } \Delta G_{\max.} = \frac{4\pi}{3} \frac{[2K_{SL} + (K_{SP} - K_{LP})(1 + \cos \theta)]^3}{K_1^2(1 - \cos \theta)(2 + \cos \theta)^2}$$

$$\text{But from equation (4), } \cos \theta = \frac{K_{LP} - K_{SP}}{K_{SL}}$$

Substituting for θ ,

$$\Delta G_{\max.} = (K_{SL} + K_{SP} - K_{LP})^2 (2K_{SL} + K_{LP} - K_{SP}) \frac{4\pi}{3K_1^2} \quad (11)$$

This expression decreases continuously from $\frac{16\pi}{3K_1^2} K_{SL}$, when $K_{LP} + K_{SL} - K_{SP} = 0$, (i.e. Type (a)), to zero when $K_{LP} + K_{SL} - K_{SP} = 2K_{SL}$ (i.e. Type (b)). (Outside these limits, the values of θ given by equation (11) are unreal, crystallites forming as in Types (a) and (b) above.)

The values of ΔG are plotted in Fig. 24 against W_A , the work of adhesion of solid metal to foreign particle, over the three ranges of crystallite formation.

To summarize, crystallite formation occurs more readily with a corresponding reduction in undercooling, in the presence of foreign nuclei to which the work of adhesion (of solid metal) is greater than zero; when the work of adhesion is equal to or greater than the work of cohesion of solid metal (as in Type (b) above), crystallites are more stable than the liquid phase at all particle sizes and undercooling should be impossible.

Metallurgical Implications.

The factors which increase the work of adhesion of solid metal to a foreign surface are presumably :

- (i) Attractive forces between the atoms of the solid metal and of the foreign particle;
- (ii) Absence of strain in the metal lattice at the nucleus–metal interface.

The first factor is also that which leads to the formation of stable solutions or intermetallic compounds, that is, it would lead to solution of the foreign particle. If solution is not to occur, the stability of the compound forming the foreign nuclei must be very high.

The second factor requires a fairly close structural relation between the lattices of solid metal and the foreign particle.*

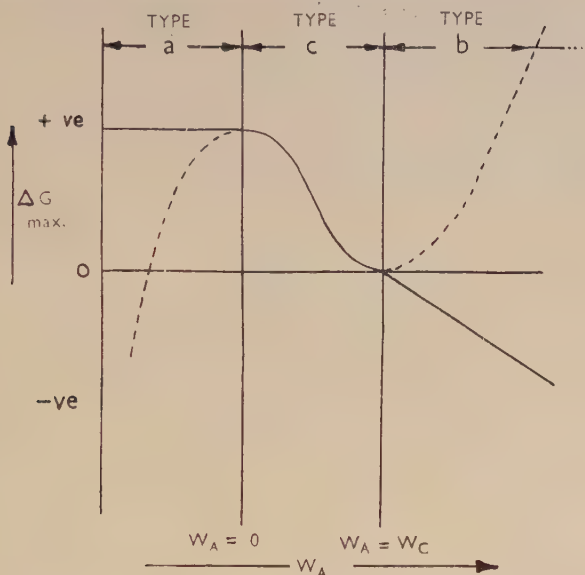


FIG. 24.—Variation of Maximum Free Energy Required for Formation of Crystallites with Work of Adhesion.

KEY.

Type *a*: crystallite formation and undercooling not affected by presence of particles.

Type *b*: crystallites form as films on foreign particles with no undercooling.

Type *c*: crystallites form more readily on foreign particles with diminished undercooling.

W_A = work of adhesion of solid metal to surface of foreign particle.

W_G = work of cohesion of solid metal.

These conditions of high stability, structural similarity, and attractive atomic forces are apparently all satisfied in the case of aluminium by the simple interstitial carbides of the transition elements, if the observations and conclusions in the body of the paper are correct; these observations suggest that crystallite formation of Type (*c*) occurs.

* Van der Merwe,³⁵ from consideration of a model in which interatomic forces were represented by springs, similarly concluded that a limiting lattice misfit exists which allows the formation of an oriented nucleus on a substrate; he found the limiting difference to be 9%, or somewhat greater if there are strong attractive forces between the deposited atoms and the substrate.

REFERENCES.

1. A. Cibula and R. W. Ruddle, *J. Inst. Metals*, 1949-50, **76**, 361.
2. R. Genders and G. L. Bailey, "The Casting of Brass Ingots" (B.N.F.M.R.A. Research Monograph No. 3), p. 59. London : 1934.
3. H. Hanemann and W. Hofmann, *Z. Metallkunde*, 1937, **29**, 149.
4. L. Northcott, *J. Inst. Metals*, 1939, **65**, 173.
5. L. Northcott, *J. Inst. Metals*, 1938, **62**, 101.
6. K. Iwasé, J. Asato, and N. Nasu, *Sci. Rep. Tōhoku Imp. Univ.*, 1936, [i], **Honda Anniv. Vol.**, 652.
7. R. Mitsche, *Carnegie Schol. Mem. Iron Steel Inst.*, 1934, **23**, 65 ; 1936, **25**, 41.
8. L. Horn and G. Masing, *Z. Electrochem.*, 1940, **46**, 109.
9. A. Latin, *J. Inst. Metals*, 1940, **66**, 177.
10. W. L. Fink, K. R. Van Horn, and P. M. Budge, *Trans. Amer. Inst. Min. Met. Eng., Inst. Metals Div.*, 1931, 421 ; and discussion (p. 436).
11. M. D. Eborall, *J. Inst. Metals*, 1949-50, **76**, 295.
12. A. Cibula. Unpublished work, B.N.F.M.R.A.
13. R. W. Ruddle, *J. Inst. Metals*, 1950, **76** (in the press).
14. G. V. Raynor, *Inst. Metals Annotated Equilib. Diagr. No. 4*, 1946.
15. P. Lacombe and L. Beaujard, *Rev. Mét.*, 1947, **44**, 65.
16. A. Dumas, *Rev. Mét.*, 1944, **41**, 273.
17. W. L. Fink and L. A. Willey, "Metals Handbook" (Amer. Soc. Metals), **1948**, p. 1155.
18. A. Westgren, *J. Franklin Inst.*, 1931, **212**, 577.
19. L. J. E. Hofer, *U.S. Bur. Mines Rep. Invest. No. 3770*, 1944.
20. R. W. G. Wyckoff, "The Structure of Crystals". 2nd Edition. New York : 1931. Supplement, 1935. (Reinhold Publishing Corp.)
21. K. K. Kelley, *U.S. Bur. Mines Bull. No. 407*, 1937.
22. K. K. Kelley, F. S. Boericke, G. E. Moore, E. H. Huffmann, W. M. Bangert, *U.S. Bur. Mines Tech. Paper No. 662*, 1944.
23. H. J. Goldschmidt, *J. Iron Steel Inst.*, 1948, **160**, 345.
24. W. Hume-Rothery, "The Structure of Metals and Alloys", *Inst. Metals Monograph and Rep. Series No. 1*, 1947.
25. L. Royer, *Compt. rend.*, 1925, **180**, 2050.
26. G. P. Thomson, *Proc. Phys. Soc.*, 1948, **61**, 403.
27. C. S. Smith, *J. Metals*, 1949, **1**, (III), 204.
28. W. A. Baker. Unpublished work, B.N.F.M.R.A.
29. A. G. Metcalfe, *J. Inst. Metals*, 1947, **73**, 591.
30. J. T. Norton and A. L. Mowry, *J. Metals*, 1949, **1**, (III), 133.
31. Brit. Patent, No. **608,942**.
32. W. Hofmann and W. Jäniche, *Z. Metallkunde*, 1936, **28**, 1.
33. R. F. Mehl and L. K. Jetter, "Symposium on Age-Hardening of Metals" (Amer. Soc. Metals), **1940**, p. 342.
34. N. K. Adam, "The Physics and Chemistry of Surfaces". London : 1941 (Oxford University Press).
35. J. H. van der Merwe, "Crystal Growth", *Discussions Faraday Soc. No. 5*, 1949, 201.

THE EFFECT OF GRAIN-SIZE ON THE TENSILE PROPERTIES OF HIGH-STRENGTH CAST ALUMINIUM ALLOYS.* 1222

By A. CIBULA,† M.A., A.I.M., STUDENT MEMBER, and R. W. RUDDLE,‡
M.A., A.I.M., MEMBER.

(Communication from the British Non-Ferrous Metals Research Association.)

SYNOPSIS.

The work described was carried out to determine the cause of the deterioration in mechanical properties of castings in certain high-strength aluminium alloys, when high melting and pouring temperatures are used, and to explain the very adverse effects of a large grain-size in these alloys.

By varying the superheating temperature before casting, test-bars having different grain-sizes were produced from metal cast at the same temperature, thus making it possible to distinguish between the effects of grain-size and other factors depending upon the casting temperature. In this way, coarse- and fine-grained test-bars in aluminium-4·5% copper alloy (D.T.D. 304) were poured at each of several selected casting temperatures in the range 680°-900° C. Some results obtained with aluminium-10% magnesium alloy (D.T.D. 300A) are also presented.

The tensile properties of these alloys were found to increase markedly with decrease in grain-size, owing primarily to changes in the form of the intergranular shrinkage cavities; the effect is greatest in the heat-treated alloys which contain only small amounts of brittle intergranular constituents. The adverse effects of high melting temperatures were due to the resultant increase in grain-size; methods of minimizing this grain coarsening are suggested.

I.—INTRODUCTION.

IT is well known that the casting characteristics of light alloys are substantially improved by grain refinement and, in particular, that fine-grained materials are less prone to hot-tearing than coarse-grained materials of the same composition.^{1, 2} It is also recognized that the grain-size of cast alloys may have important effects upon their tensile properties, and the present paper provides new information on this point.

Certain of the heat-treated aluminium casting alloys are notorious in that their tensile properties are extremely sensitive to superheating and to pouring temperature, high temperatures having a markedly

* Manuscript received 24 August 1949. The work described in this paper was made available to members of the B.N.F.M.R.A. in a confidential research report issued in 1949.

† Investigator, British Non-Ferrous Metals Research Association, London.

‡ Head of Melting and Casting Section, British Non-Ferrous Metals Research Association, London.

adverse effect. This is true, for example, of the high-strength aluminium-4.5% copper (D.T.D. 304) and aluminium-10% magnesium (D.T.D. 300A) alloys.

High casting temperatures are undesirable as they may lead to excessive oxidation of the melt and to increased pick-up of gas and other impurities. However, even when these adverse effects are eliminated by careful melting and degassing, high superheating and pouring temperatures result in a deterioration in the tensile properties of the casting. Since the deterioration is associated with marked grain coarsening, it seemed probable that this factor is one of the major causes. To investigate this was the main purpose of the present work. There are a number of ways in which increased grain-size may affect the tensile properties of a cast alloy. First, it may increase the solution heat-treatment time required to ensure substantially complete homogeneity, and thus render the times given in the specifications inadequate; secondly, the large grain-size may influence the distribution and form, and possibly the amount, of the micro-shrinkage voids. In anisotropic metals grain-size has a direct influence on the tensile properties, but in the (cubic) alloys under discussion the direct effect of variations in grain-size of the cast alloys can be expected to be small.⁴

Where the deterioration in properties is caused by pouring from a high temperature, it is also possible that resultant changes in the temperature gradients in the casting will have adverse effects on the soundness, and hence the strength, of the casting.^{1, 3} Other work on the grain refinement of light alloys^{3, 5} has indicated methods of producing castings of different grain-sizes from the same pouring temperature, and thus in the present work it has been possible to distinguish between the effects of grain-size and of temperature gradients.

The most convenient material for the present study was the 4.5% copper alloy (D.T.D. 304), and this was accordingly used for most of the work. A few results obtained with the aluminium-10% magnesium alloy (D.T.D. 300A) by other workers^{8, 12} are also included.

II.—EXPERIMENTAL TECHNIQUE.

(a) *Materials.*

The material used in most of the work was commercial D.T.D. 304 alloy ingot of the composition shown in Table I.

Some castings were also made from melts of similar copper content prepared from commercial-purity aluminium (99.7%) and a copper hardener alloy; grain-refining additions of boron or titanium hardener alloys were made to these melts. The compositions of the hardener

TABLE I.—Composition of Materials Used.

Alloying Element	D.T.D. 304 Commercial Ingot	Aluminium-Boron Hardener, NLC 6	Aluminium-Titanium Hardeners		Aluminium-Copper Hardener	O.P. Aluminium
			NKY 10	NKY 20		
Copper, %	4.82	0.002	0.02	...	50	...
Titanium, %	0.12	<0.002	1.71	2.20	...	0.002
Boron, %	0.28
Iron, % ...	0.18	0.01	<0.03	0.13
Silicon, % ...	0.10	0.07	0.13	0.10

alloys are also shown in Table I; the copper hardeners were made by adding cathode copper (99.99%) to molten super-purity aluminium (99.99%) and the boron and titanium hardeners by adding potassium borofluoride or potassium titanofluoride to super-purity aluminium at approximately 1050° C.

(b) Melting and Casting.

All the melts were made in Salamander crucibles heated in a gas-fired injector furnace, and were degassed when required by bubbling chlorine through the metal for 15 min.; freedom from dissolved gas was checked by the reduced-pressure solidification test¹ and/or by subsequent density determinations on sand-cast D.T.D. test-bars.

Temperatures were measured to within 5° C., using a Chromel/Alumel thermocouple.

All melts were poured into D.T.D. test-bar moulds inclined at about 45° to the vertical at the beginning of casting; the moulds were made from synthetic sand and were used green. Except where otherwise stated, the pouring time for each bar was 8–12 sec. To obtain a large range of grain-sizes and, in particular, a variation of grain-size in castings poured at the same temperature, certain series of castings were made from melts which had been considerably superheated before pouring in order to obtain the coarsest grain-sizes, and other series were made from melts which were quickly heated to the casting temperature. The effect of dissolved gas in castings of different grain-sizes was examined by omitting the chlorine treatment in certain cases. Except where variations are described below the details of the two alternative melting procedures were as follows:

(1) Melts of 10–12 kg. were superheated to approximately 950° C. and degassed with chlorine. The crucibles were then removed from the furnace, and, while the metal was cooling, two test-bars were poured at each selected casting temperature down to 680° C.

All castings made from melts which were not degassed contained some gas picked up during superheating to 950° C.

(2) Melts of 5 kg. were heated rapidly to each selected casting temperature and two test-bars were immediately cast; the gas content of these bars increased with the casting temperature. The remainder of each melt was then returned to the hot furnace and degassed; frequent readings were taken to ensure that the strongly exothermic reaction did not cause the temperature to rise above the selected casting temperature, and the flow of chlorine was varied to maintain an approximately constant temperature. Two further test-bars were then cast, the reduced-pressure gas test being generally omitted in order to minimize the temperature drop before pouring.

(c) *Examination of Castings.* —

(1) *Grain-Size Determinations.*

Sections of the test-bars immediately adjacent to the lengths removed for heat-treatment and tensile testing were polished and etched in Keller's reagent. The grain diameters were measured with a scale, at a low magnification appropriate to the grain-size of the specimen.

(2) *Determination of Porosity.*

The percentage of voids in each bar was determined before heat-treatment by comparing the density with that of void-free material of the same composition (2.80 g./c.c.).

(3) *Heat-Treatment and Tensile Properties.*

The test-bars were given the following heat-treatment in a forced-air circulation furnace :

Solution treatment : 18 hr. at 535° C. and quenched in water.

Ageing treatment : 16 hr. at 140° C. and air cooled.

In one series of experiments the solution times were extended to 100 hr. Standard tensile test-pieces of 0.564 in. dia. were machined from the bars, and the ultimate tensile strength (U.T.S.) and elongation were determined.

III.—RESULTS AND DISCUSSION.

(a) *The Relation Between Casting Temperature, Grain-Size, and Tensile Properties.*

The tensile properties and grain-sizes of bars cast with and without previous superheating from respectively gas-free and from gassy melts

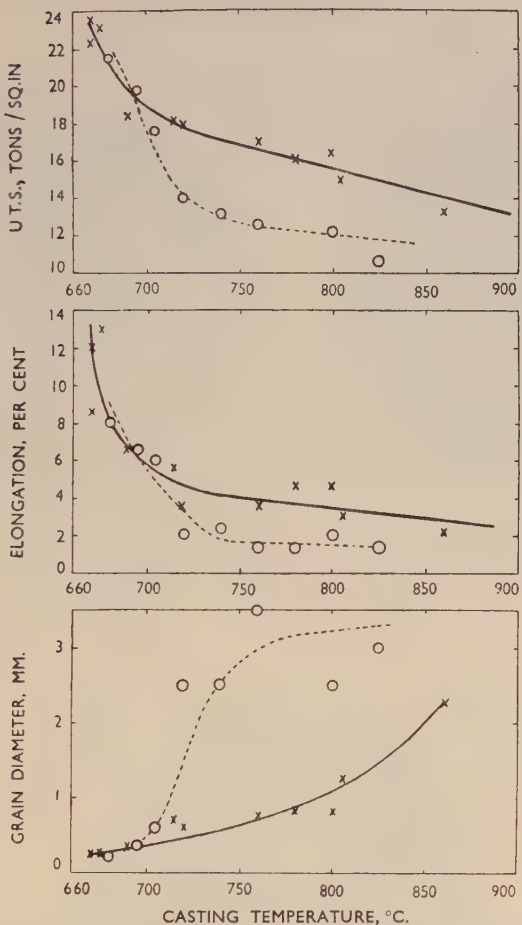


FIG. 1.—Variation of U.T.S., Elongation, and Grain-Size of Test-Bars Cast in Gas-Free D.T.D. 304 Alloy from Various Temperatures.

$\text{O} - \text{---} \text{O}$ denotes melts superheated before casting.

$\times - \text{---} \times$ denotes melts not heated above the casting temperature.

are shown plotted against casting temperatures in Figs. 1 and 2. These results show that :

- (1) The U.T.S. and elongation of castings from degassed melts heated to the casting temperature and poured, fall sharply as the casting temperature is raised, particularly in the range 680°–720° C.; above this temperature they fall below the minimum values specified in D.T.D. 304.

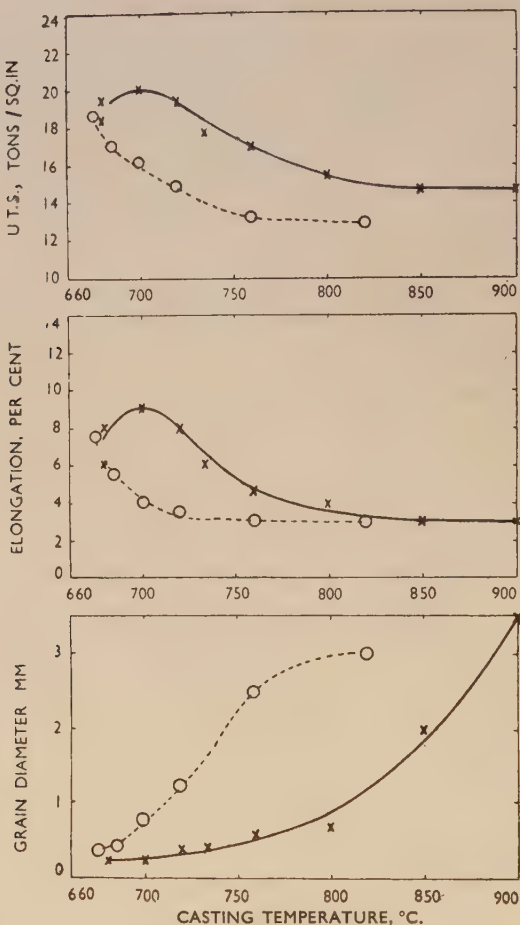


FIG. 2.—Variation of U.T.S., Elongation, and Grain-Size of Test-Bars Cast in Gassy D.T.D. 304 Alloy from Various Temperatures.

○ --- ○ denotes melt superheated before casting.
 × --- × denotes melt not heated above the casting temperature.

(2) Castings from melts superheated to 950° C. and subsequently poured at 825°–720° C. have tensile properties considerably lower than the corresponding bars poured without superheating. However, when the pouring temperature of superheated melts falls below 720° C., a rapid improvement occurs in the tensile properties of the castings, and at about 700° C. they differ little from those obtained from bars from non-superheated melts.

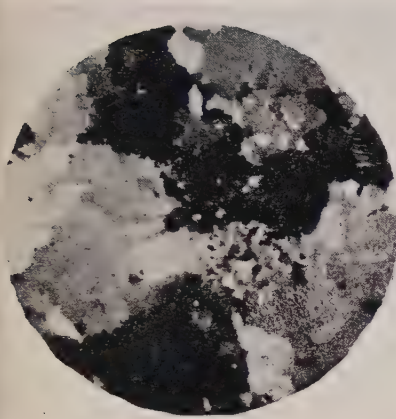


FIG. 3.—Grain-size of test-bar in D.T.D. 304 alloy cast at 760° C. after superheating.
 $\times 4$.

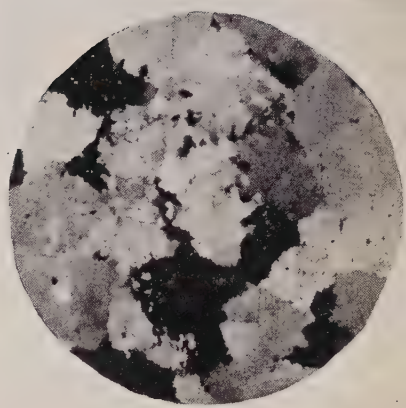


FIG. 4.—Grain-size of test-bar in D.T.D. 304 alloy cast at 720° C. after superheating.
 $\times 4$.

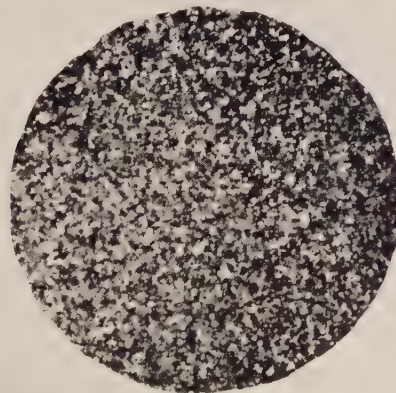


FIG. 5.—Grain-size of test-bar in D.T.D. 304 alloy cast at 680° C. after superheating.
 $\times 4$.

[To face p. 366.]



FIG. 6.—Microstructure of as-cast test-bar of fine grain-size (0.25 mm.) in D.T.D. 304 alloy. $\times 65$.

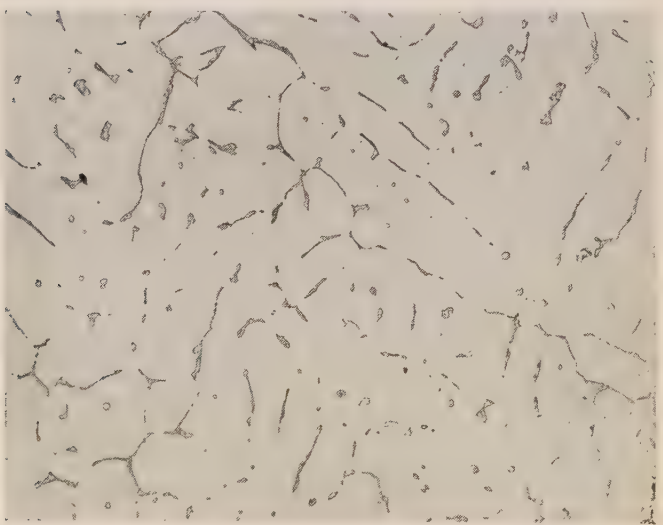


FIG. 7.—Microstructure of as-cast test-bar of coarse grain-size (2.5 mm.) in D.T.D. 304 alloy. $\times 65$.



FIG. 8.—Distribution of voids in fine-grained test-bar in D.T.D. 304 alloy. Grain-size 0.25 mm.; voids 0.8%. $\times 20$.

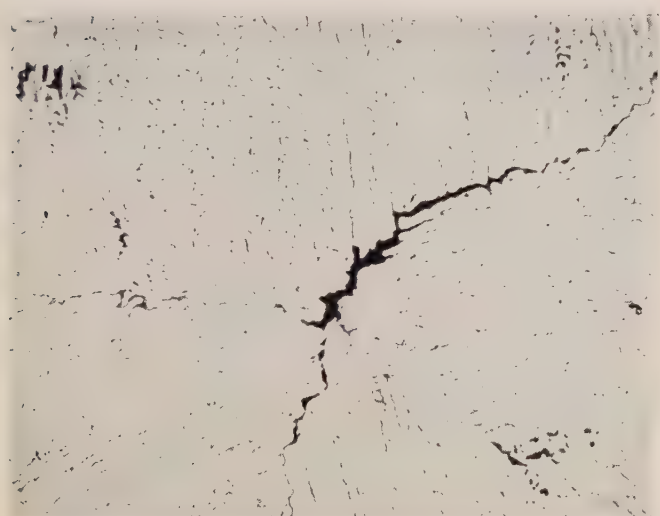


FIG. 9.—Distribution of voids in coarse-grained test-bar in D.T.D. 304 alloy. Grain-size 4 mm.; voids 0.8%. $\times 20$.

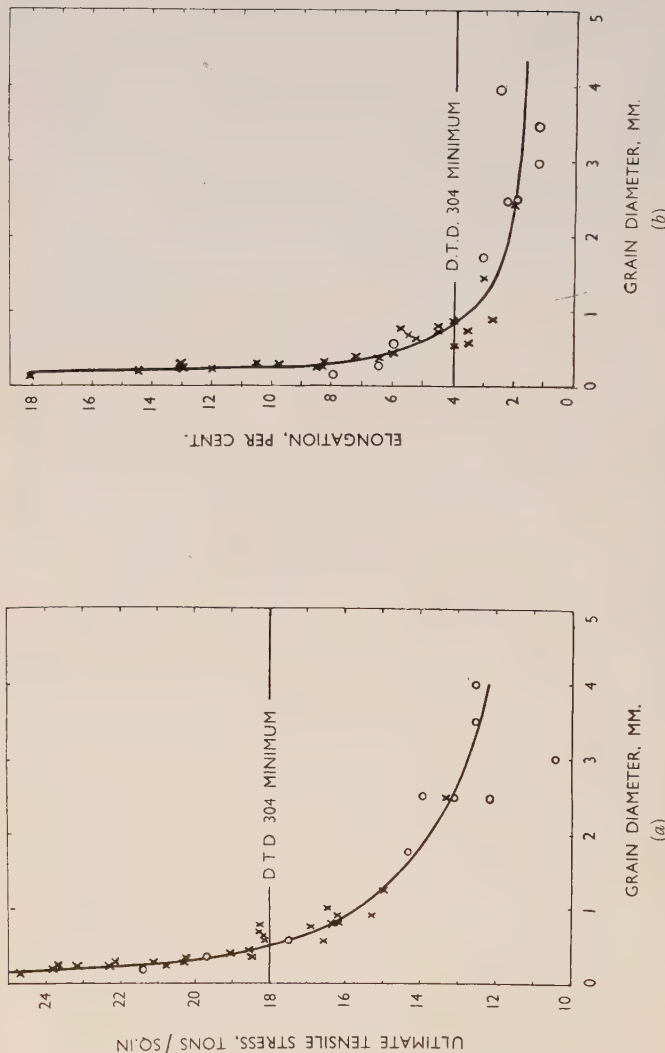


FIG. 10.—Variation of (a) U.T.S. and (b) Elongation with Grain-Size of Test-Bars in D.T.D. 304 Alloy.
 ○ denotes melt not heated above casting temperature.
 × denotes melt superheated before casting.

(3) Corresponding to these changes in tensile properties as the casting temperature is raised, the grain-size increases from 0·2–0·3 mm., when cast at 680° C., to 2·3 mm., when cast at 860° C., and, by extrapolation of the curves in Fig. 1, to 3·5 mm. at 950° C.; this coarse grain-size persists in the castings poured at lower temperatures after superheating, until, at approximately 720° C., a sudden decrease in grain-size occurs, coinciding with the sharp increase in U.T.S. and elongation. This change in grain-size is illustrated in Figs. 3–5 (Plate L) which show the grain structures of castings poured at 760°, 720°, and 680° C. after superheating.

Other work by one of the authors⁵ has shown that such changes of grain-size are due to the presence, in melts containing titanium, of grain-refining nuclei which dissolve as the temperature is raised, but remain in supersaturated solution on cooling again, so that a large grain-size results (as in Figs. 3 and 4). At low temperatures the nuclei may reprecipitate and lead to fine-grained castings, as in Fig. 5, but under some conditions reprecipitation and the return of the fine grain-size occur only after solidification and remelting.⁵

The relation between U.T.S. and grain-size is shown clearly in Fig. 10 (Plate LIII), in which the values for all test-bars cast from degassed melts are plotted, including results taken from other work described below. The points fall closely about a single curve and show a close dependence of U.T.S. and elongation upon grain-size. The casting temperature appears to influence the results only to the extent that it affects the grain-size; this is confirmed by other results presented below. Another interesting point that emerges from Fig. 10 is the steepness of the curve at small grain diameters and, consequently, the possibility of obtaining very high U.T.S. and elongation values as a result of increased grain refinement; it must be noted, moreover, that the highest values obtained in the present work approach those of wrought alloys of similar composition.

Similar changes in grain-size occur in castings from gassy melts. The U.T.S. and elongation values show much the same variations as those obtained from gas-free castings, but they are lower in test-bars of the finest grain-sizes and, since they fall off less rapidly with increase in casting temperature, are slightly higher for coarse-grained metal.

(b) *The Cause of the Deleterious Effects of Grain Coarsening.*

(1) *The Effect of Grain-Size on Solution Heat-Treatment Times.*

To discover whether coarse-grained test-bars required longer solution times to achieve sufficient homogeneity, the effect of varying this

heat-treatment upon the properties of bars of different grain-size was examined. Three sets of ten test-bars were cast with grain-sizes of 0.2, 0.8, and 3.5 mm., respectively, by selecting appropriate super-heating and casting temperatures; to minimize the drop in temperature while each series of bars was cast, the pouring time was reduced to 3-5 sec. per bar. These bars were then solution heat-treated at 535° C. and two bars of each grain-size were quenched after selected intervals of time up to 100 hr. The bars were then precipitation-treated, machined, and tested.

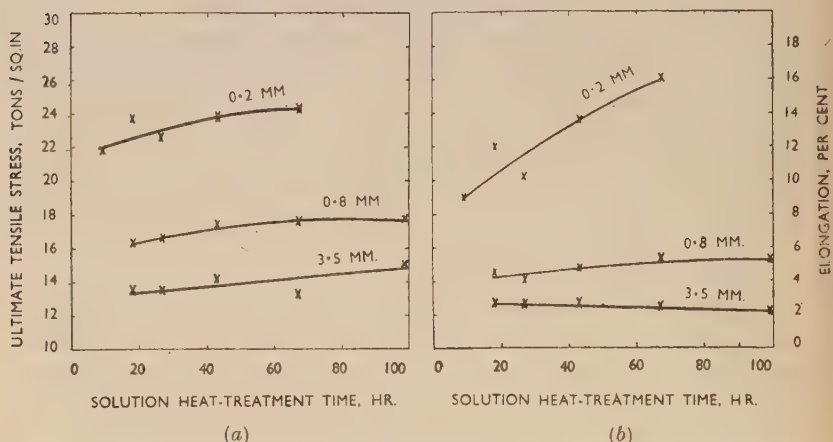


FIG. 11.—Effect of Solution Heat-Treatment Time on (a) U.T.S. and (b) Elongation of D.T.D. 304 Alloy Test-Bars of Various Grain-Sizes.

The results of U.T.S. and elongation determinations are shown in Fig. 11. They show that the poor tensile properties of coarse-grained bars are not much improved by prolonging the solution-treatment time. The effect of grain-size upon the tensile properties is not explained, therefore, by its influence on the homogenization time.

These results are consistent with the as-cast microstructures of bars of different grain-sizes: examples of the structures of fine- and coarse-grained bars given in Figs. 6 and 7 (Plate LI) show that the distribution of the CuAl₂ constituent is similar in the two cases. Since this distribution controls the distances through which diffusion must take place, it also indicates the order of the times required for homogenization.

In bars of the finest grain-sizes the dendritic structure is only just apparent, and the CuAl₂ occurs almost entirely at the grain boundaries. In the coarse-grained bars, on the other hand, the dendritic structure is very pronounced and most of the CuAl₂ is situated in the interstices

between the dendrite arms. The result is that the CuAl₂ distribution is very little affected by change in grain-size, and only a small effect on the minimum solution heat-treatment times is therefore to be expected in sand castings.

The reason for the apparent improvement in properties produced by increasing the solution-treatment times of the fine-grained bars is not clear. It may be due to the solution of traces of CuAl₂ undissolved after 18 hr.; in coarse-grained bars this effect is likely to be masked by the effect of porosity (see below).

(2) *The Effect of Grain-Size Upon the Amount and Distribution of Porosity.*

The mean percentage voids of the test-bars tended to increase with grain-size, probably owing to the diminution of mass feeding in coarse-grained bars, but the scatter was very large. The correlation of tensile properties with total porosity was small, and it was therefore concluded that the close dependence of tensile properties upon grain-size was not primarily due to variations in mean porosity. The effect of this factor may be judged by comparison of Figs. 1 and 2, relating to gas-free and gassy metal; the latter contained 0·7–2·5% voids compared with 0·1–1·0% for the gas-free castings poured from the same temperatures.

Micro-examination showed that grain-size had a very marked effect upon the form and distribution of the voids. In both fine- and coarse-grained bars the porosity occurred largely at the boundaries of the macro-grains and only to a minor extent between the dendrite arms. The voids were therefore much larger in coarse-grained metal and were elongated along the grain boundaries, as comparison of Figs. 8 and 9 (Plate LII) shows.*

It is to be expected that voids of the kind shown in Fig. 9 will be much more detrimental to tensile properties than those shown in Fig. 8. The effect of grain coarsening upon tensile properties may therefore be attributed mainly to this variation in the size and particularly in the shape of the voids, the increase in the total volume of voids being a minor factor.

(c) *The Prevention of Grain Coarsening on Superheating.*

(1) *The Use of Boron as a Grain Refiner.*

Information from a member firm⁶ and the results of work by the Association⁵ on grain refinement by boron showed that the grain-sizes of

* For purposes of comparison, bars containing the same percentage voids were chosen for Figs. 8 and 9; since the coarse-grained bars tended to be high in voids, a fine-grained bar containing a small amount of gas was used for Fig. 8.

castings refined in this manner were less affected by variation of the casting temperature. Test-bars conforming in composition to D.T.D. 304 were therefore cast, in which 0·03, 0·04, or 0·08% boron was substituted for titanium; some of the results obtained are shown in Fig. 12.

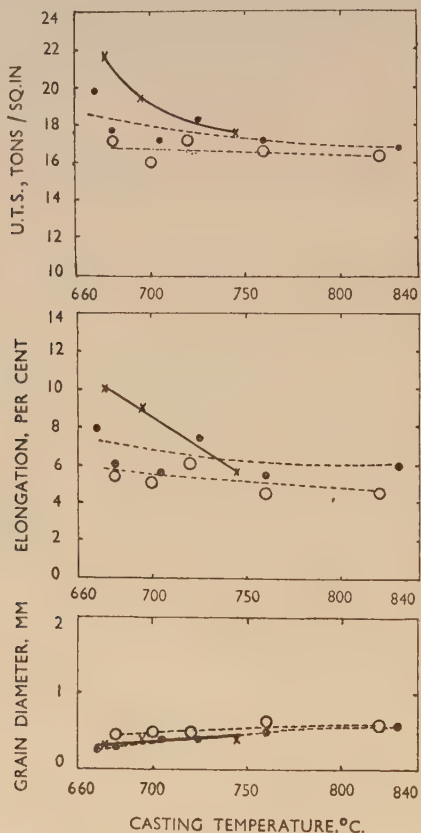


FIG. 12.—Variation of U.T.S., Elongation, and Grain-Size of Test-Bars of D.T.D. 304 Alloy Containing Boron Cast from Various Temperatures.

● --- ● 0.045% B
 ○ --- ○ 0.03% B } superheated to 950° C. before casting.
 × --- × 0.03% B, not heated above casting temperature.

The grain-size in castings containing 0·03% boron increased with casting temperature only to 0·4 mm. at 750° C., and superheating to 950° C. before casting had little greater effect. The deterioration in tensile properties was also reduced, and the elongation did not fall below 4% nor the U.T.S. below 16 tons/in.², even with the highest casting

temperatures. The addition of 0·045% boron resulted in somewhat finer grain-sizes and slightly higher mechanical properties.

The addition of boron appeared greatly to increase the gas pick-up on melting, since longer periods of degassing were necessary. Moreover, even after degassing was complete according to the reduced-pressure solidification test, the percentage of voids in the test-bars was high (0·8-2%), and this suggested that mould reaction had occurred, as the voids appeared partly as pinholes just beneath the surface. The addition of 2% boric acid to the moulding sand did not reduce the porosity.

There is no mention in the literature of mould reaction due to boron, and it was thought possible that the reaction was caused by potassium inadvertently introduced into the hardener during preparation. However, this element could not be detected spectrographically, and prolonged degassing should have removed it from the melt had it been present; furthermore, the titanium hardeners which were prepared in a similar manner caused no mould reaction in metal cast under the same conditions. It was therefore concluded that the mould reaction described above was due to the presence of boron.

Further castings were made containing 0·08% boron, and 0·04% beryllium was added to the melt to prevent mould reaction. Although the increase in grain-size with casting temperature was even further reduced in test-bars poured below 760° C., the voids were still above 0·5%, and this prevented an improvement in mechanical properties corresponding to the finer grain-sizes, an effect similar to that caused by dissolved gas shown in Fig. 2.

Grain coarsening due to superheating can thus be much reduced by the use of boron instead of titanium, but owing to slight mould reaction the advantage of higher tensile properties is obtained only when melting temperatures above 760° C. are necessary.

(2) *Increasing the Effectiveness of Titanium.*

Sicha and Boehm⁷ have shown in a recent paper that the extent to which grain coarsening occurs on raising the casting temperature depends upon the titanium content of the alloy, only small increases in grain-size occurring with 0·4% titanium. If the use of a high casting temperature is essential, the fall in tensile properties may therefore be minimized by the addition of further titanium in the form of a hardener alloy. However, in alloys containing large amounts of titanium, the improvements in tensile properties are less than might be expected from the fine grain-sizes so obtained,⁷ presumably because the presence of $TiAl_3$ particles has a harmful effect. Moreover, increasing the titanium

content has the disadvantage of greater expense. A better solution would be to increase the efficiency of grain refinement at normal titanium contents, and it might then be possible even to reduce the amounts required. Other work⁵ on the grain refinement of aluminium alloys has led to the conclusion that the action of titanium is due to the formation of particles of titanium carbide in the melt which nucleate the formation of crystallites of solid solution, though only a very small proportion of the refining metal is in this effective form. Grain coarsening caused by a rise in temperature of the melt is believed to be due to solution of these particles, and an obvious way to reduce this undesirable effect is to increase the proportion of the added titanium which is combined with carbon in the form of small particles of carbide.

Some of the carbon needed to form titanium carbide particles is supplied by the aluminium of the alloy, but it is believed that a large proportion is derived from the titanium hardener; this is supported by evidence obtained earlier which showed that the refinement produced by titanium varies with the source and method of introduction of the titanium.¹¹ It therefore seemed likely that the efficiency of titanium hardeners would vary—in particular commercial hardeners might contain insufficient carbon to yield maximum refinement.

To prepare a highly effective hardener it is therefore necessary to ensure that carbon is readily accessible to the melt during its preparation; this should be the case when the hardener is prepared from potassium titanofluoride which, when molten, strongly attacks the Salamander crucible and graphite stirring rods. A series of 3-kg. melts to D.T.D. 304 composition was therefore prepared, using two titanium hardener alloys made in this way of the compositions quoted in Table I. Each melt was heated to a different maximum temperature, at which two test-bars were cast after degassing, as described previously.

The tensile strengths, elongations, and grain-sizes of these bars are plotted against casting temperature in Fig. 13, and the curve obtained in Fig. 1 for castings from commercial D.T.D. 304 ingot has been added for comparison.

These results show that the grain coarsening in castings poured at high temperatures is less when titanium is added as an alloy prepared in the manner described, the two hardeners differing somewhat in this respect. The tensile properties show a corresponding improvement, and with casting temperatures above 700° C. the U.T.S. values are 3 tons/in.² higher than the values obtained with commercial ingot, the specification minimum not being reached until a casting temperature of 800° C. is used.

Methods of still further increasing the effectiveness of titanium additions are being investigated.

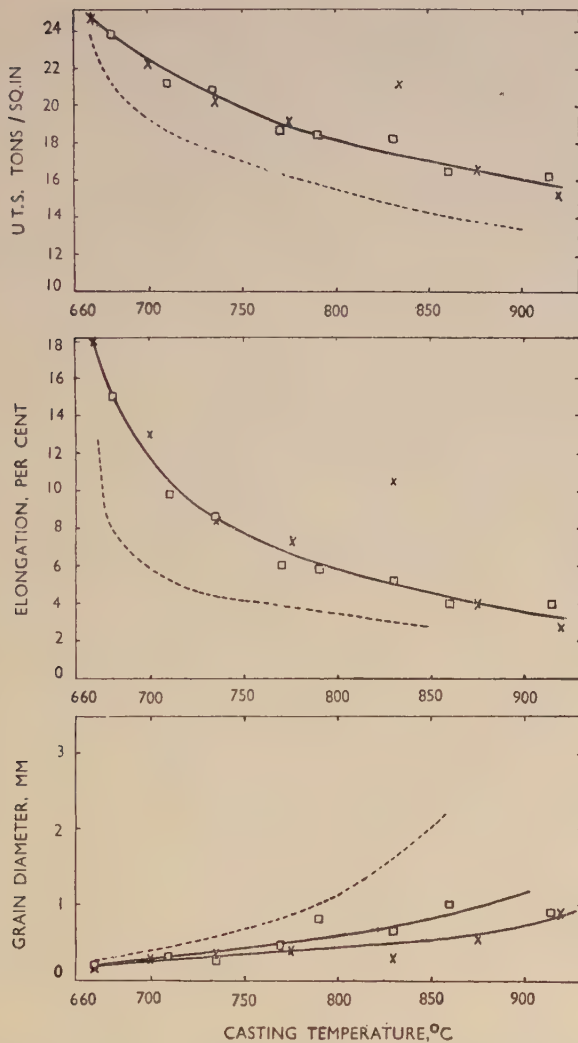


FIG. 13.—Effect of Source of Titanium on U.T.S., Elongation, and Grain-Size of Test-Bars of D.T.D. 304 Alloy Cast from Various Temperatures.

\times — \times denotes titanium added as hardener NKY 10.

\square — \square " " " NKY 20.

— denotes commercial D.T.D. 304 alloy ingot.

(d) Further Discussion and Practical Recommendations.

Although only one alloy, D.T.D. 304, was studied in the present work, the conclusions to be drawn from the results obtained are not confined to

this alloy. For example, Rutherford⁸ and Mincher¹² have both studied the effect of grain-size on the tensile properties of an aluminium-10% magnesium alloy * (D.T.D. 300A) and have obtained curves closely similar to Fig. 10 (Plate LIII); Rutherford's and Mincher's results are summarized in Fig. 14.

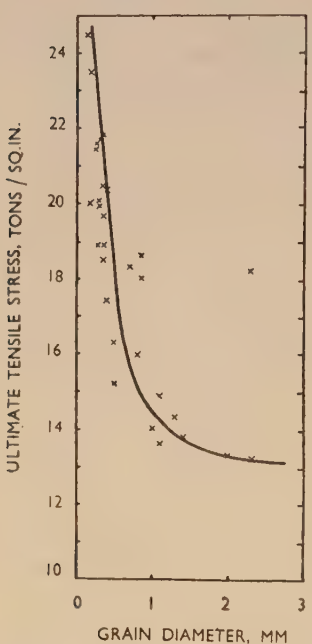


FIG. 14.—Variation of U.T.S. with Grain-Size of Test-Bars Cast in D.T.D. 300A Alloy.

ence on the tensile properties of alloys of the kind investigated in the present work, and accounts for the fact that grain-size effects are very much less marked in alloys containing large amounts of brittle intergranular constituents. Alloys of this second kind were investigated by Baker,¹⁰ who showed that grain refinement of the non-heat-treated alloys 4L11 (7% copper) and 3L5 (14% zinc, 2.5% copper) produced no improvement in test-bars low in voids, and only moderate improvement in unsound castings. The strength of heat-treated test-bars in Y alloy (4% copper, 2% nickel, 1.5% magnesium) was, however, substantially improved by grain refinement.

Only one section thickness—a 1-in.-dia. bar—was investigated in the

* Silicon content approx. 0.15%; iron content approx. 0.2%.

† On the other hand, a hard (e.g. aged) solid solution would be more sensitive to micro-porosity than the homogeneous and ductile solid solution.

In the discussion of two papers on the effects of micro-porosity in magnesium-base casting alloys,⁹ reference was made to the fact that the harmful effect of micro-porosity varies in severity with the ductility of the materials, and that, in particular, in solution-treated magnesium-8% aluminium alloys, consisting essentially of a homogeneous and ductile solid solution, a given amount of micro-porosity would be more harmful than in an alloy of the same composition but in the as-cast state. The reason suggested was that the latter contains substantial amounts of a brittle constituent at the grain boundaries and the substitution of cavities for part of this constituent would have relatively little ill effect.†

This explains why the effect of grain-size on the distribution and form of porosity has such a noticeable influ-

present work, but here again the results obtained are probably of general applicability with the reservation that increasing the section thickness, by retarding the rate of solidification, may possibly encourage the reprecipitation of dissolved nuclei in castings poured from high temperatures.

It is possible that pouring the bars very slowly would result in increased soundness in the bars of coarser grain-size, and this would have the effect of raising the lower part of the tensile properties/grain-size curves (Fig. 10, Plate LIII).* However, the curves obtained with the pouring rates used in this work are likely to be representative of the effect of grain-size on the tensile properties of the less sound parts of industrial castings.

The practical recommendations emerging from this work and listed below are therefore not necessarily confined to 1-in. bars in alloys of the D.T.D. 304 type, but are likely to be generally applicable to sand-cast aluminium alloys which (i) freeze over a range of temperature and are therefore likely to contain dispersed intergranular shrinkage voids, and (ii) are substantially free from brittle grain-boundary constituents and are therefore liable to be seriously harmed by intergranular porosity.

Recommendations.

(1) Melting temperatures should be kept as low as possible. It is particularly important to control the temperature of the metal during degassing with chlorine, as the strongly exothermic reaction of chlorine with aluminium can produce a rapid and considerable rise in the temperature of the metal.

(2) If a high melting temperature is unavoidable or if the metal is accidentally overheated, the resultant grain coarsening and consequent reduction in tensile properties may be minimized by adding a suitable quantity of titanium hardener after degassing and just before pouring. The titanium hardener should be substantially gas-free and should preferably be prepared in such a manner that it contains an adequate carbon content.

(3) In other work⁵ grain coarsening in castings from melts containing titanium was obtained not only after superheating, but also (i) after standing for prolonged periods at relatively low temperatures, and (ii) when gases other than chlorine, e.g. nitrogen, were passed through the melt, particularly under a flux cover. From those observations and from the present work it is clearly important to avoid prolonged standing periods and to restrict to a minimum the amount of nitrogen or other

* Similarly, increasing the rate of solidification of well-fed castings, e.g. by chill casting, is likely to reduce the adverse effect of coarse grain-size, by increasing the soundness of the casting.

inert gas used for degassing if the optimum tensile properties are to be obtained. Again, additions of suitable titanium hardeners before pouring will be helpful in this respect.

IV.—SUMMARY AND CONCLUSIONS.

The evidence discussed in this paper warrants the following conclusions :

(1) Grain refinement modifies the form of intergranular shrinkage cavities in cast aluminium alloys and thereby improves the tensile properties of the materials, the effect being small when the material contains brittle intergranular constituents, but very marked when such constituents are absent or present only in small amounts.

(2) In test-bars of a high-strength heat-treated aluminium-4·5% copper alloy, a change in grain-size from 2 to 0·2 mm. is associated with an increase in strength from 14 to 19–23 tons/in.², and in elongation from about 2·5 to over 10%, the improvement being due primarily to associated changes in the form of the porosity in the cast material.

(3) Grain coarsening of the aluminium-4·5% copper alloy becomes marked when the metal is heated to temperatures exceeding 720° C.; it can be minimized (i) by adding to the melt a suitably prepared aluminium-titanium-carbon alloy and (ii) by adding boron to the melt. Of these remedies the first is preferable because the presence of boron promotes gas absorption in the mould and the resulting decrease in the soundness of the casting partly offsets the beneficial effect of grain refinement.

ACKNOWLEDGEMENTS.

The authors are indebted to the Director and Council of the British Non-Ferrous Metals Research Association for permission to publish this paper, and to Mr. W. A. Baker, B.Sc., F.I.M., for helpful advice and criticism.

REFERENCES.

1. W. A. Baker, *J. Inst. Metals*, 1945, **71**, 165.
2. D. C. G. Lees, *J. Inst. Metals*, 1946, **72**, 343.
3. R. W. Ruddle, *J. Inst. Metals*, 1950, **78**, (in the press).
4. J. T. Hobbs, Jr., "Grain Control in Industrial Metallurgy". (*Amer. Soc. Metals*), **1949**, p. 209.
5. A. Cibula, *J. Inst. Metals*, 1949–50, **76**, 321.
6. P. C. Varley, Private communication from The British Aluminium Company, Ltd.
7. W. E. Sicha and R. C. Boehm, *Trans. Amer. Found. Soc.*, 1948, **56**, 398.
8. N. B. Rutherford, Unpublished work, B.N.F.M.R.A.
9. G. B. Partridge, *J. Inst. Metals*, 1945, **71**, 635 (discussion).
W. A. Baker, *ibid.*, 640 (discussion).
10. W. A. Baker, Unpublished work, B.N.F.M.R.A.
11. M. D. Eborall, *J. Inst. Metals*, 1949–50, **76**, 295.
12. A. L. Mincher, Unpublished work, B.N.F.M.R.A.

A METHOD OF IMPROVING THE PRESSURE-TIGHTNESS OF LEAD-FREE GUN-METAL SAND CASTINGS.* 1223

By W. H. GLAISHER,† B.Sc., MEMBER.

(Communication from the British Non-Ferrous Metals Research Association.)

SYNOPSIS.

Castings of lead-free gun-metal (e.g. 88 : 10 : 2 and 88 : 8 : 4 copper-tin-zinc alloys) should contain a small amount of gas, as this leads to a more uniform distribution of the unsoundness and tends to prevent the development of interconnected cavities, such as may cause failure in the hydraulic test, particularly in the case of poorly fed castings. Control of the gas content of lead-free gun-metal is difficult, though complete removal of the gas can readily be effected.

The paper describes an investigation into the effect of adding phosphorus, as phosphor-copper, to degassed metal before pouring, so as to cause a controlled amount of gas absorption, resulting from the reaction of the residual phosphorus with the moisture of the sand mould. The D.T.D. test-bar and two inadequately fed discs were used for the experiments. By the use of phosphorus, the pressure-tightness of the disc castings could be markedly improved, the best castings being equal to those in leaded gun-metal, while their mechanical properties were better. The soundness and quality of the D.T.D. test-bar were, however, inferior to those in leaded gun-metal. The control of residual phosphorus content (0·04–0·08% being the optimum for the disc casting) and the effects of pouring temperature and section thickness, are discussed.

I.—INTRODUCTION.

IN previous work¹ by Baker, Child, and the present author, it was shown that for castings containing poorly fed sections but required to be pressure-tight, gun-metals containing lead (e.g. 85 : 5 : 5 : 5 copper-tin-zinc-lead alloy) were more suitable than phosphor-bronzes and lead-free gun-metals. For the test casting employed in that work, the leaded gun-metals were best used in the gas-free condition, whereas with the lead-free gun-metal, pressure-tightness was most likely to be obtained when the metal contained a small amount of gas. It was not found easy to control the gas content of melts closely, and even with the optimum gas content there was less certainty of obtaining

* Manuscript received 28 July 1949. The work described in this paper was made available to members of the B.N.F.M.R.A. in a confidential research report issued in 1945.

† Research Investigator, British Iron and Steel Research Association, Sheffield; formerly Research Investigator, British Non-Ferrous Metals Research Association, London.

pressure-tightness than with the gas-free leaded gun-metals. Complete removal of gas from the melt is, however, quite simple.

Further work showed that with phosphorus contents above about 0·02%, the lead-free gun-metal reacted with the steam formed in sand moulds in the same way as has been reported¹ for phosphor-bronzes containing more than 0·3% phosphorus. It was shown that in the case of the phosphor-bronzes, the reaction with steam might be put to good account by influencing the distribution of unsoundness with beneficial effects on pressure-tightness; in the present work the possibilities of taking advantage of these effects with lead-free gun-metals have been studied. The results of these and earlier tests are analysed graphically.

II.—EXPERIMENTAL DETAILS.

(a) Materials.

The alloys were prepared from cathode copper, commercial-purity tin (99·7%+), electrolytic zinc, and commercial phosphor-copper.

Melts were made either from the virgin metals or from ingots and headers from previous melts. Two compositions were used, namely 88 : 10 : 2 and 88 : 8 : 4 copper-tin-zinc alloys, with phosphorus additions up to 0·2%.

(b) Melting.

All melts were made in gas-fired furnaces, and were of 20–120 lb. each. Several methods of degassing, which have been described in detail by Baker and Child,² were used. They were :

(i) *Scavenging with Air or Nitrogen*.—A vigorous stream of the gas was bubbled through the melt by means of a silica tube for 5 min., with a lid on the crucible. In some cases a charcoal cover was used with air-blowing treatments.

(ii) *Degassing with Manganese Ore*.—The manganese ore powder (crude manganese dioxide) was placed in the bottom of the crucible when charging, about 2% of the charge weight being used.

(iii) *Plunging Marble Chips or Lump Manganese Ore*.—For this purpose a Salamander tube of 1½ in. inside dia., $\frac{5}{8}$ in. wall thickness, and 3 ft. long, closed at one end, was used. About 0·25% marble chips or 1% lump manganese ore (i.e. percentage of weight of charge) was placed in the open end of the tube and held in position by a piece of copper foil. When the melt was ready for degassing the tube was pushed into the melt, open end

first, and held down by means of an inverted crucible placed on the other end. The degassing tube was left in the crucible for 3–5 min., during which time a steady evolution of gas occurred. All melts for which this method of degassing was used were made under charcoal, which prevented splashing during degassing.

(iv) *Oxidation of the Melt.*—The molten copper and tin were oxidized by means of a flux before the zinc was added. The flux used contained equal parts of dry sand, borax, and copper oxide.

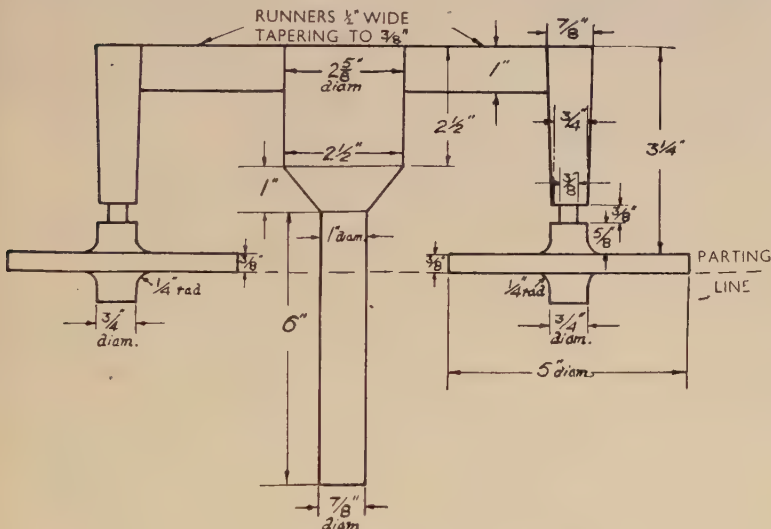


FIG. 1.—D.T.D. Test-Bar and Pressure-Tightness Test Discs.

All these treatments were fully effective, and where no reaction with the sand occurred, high densities in the range 8.75–8.83 g./c.c. were always obtained.

Phosphorus additions (in the form of phosphor-copper), as stated in the tables and text, were made and stirred in 1–2 min. before pouring. The actual phosphorus content of the melt was estimated in all cases.

Melts were poured at 1180° C., unless otherwise stated.

(c) *Test Castings.*

The castings used were the D.T.D. test-bar and the casting combining a D.T.D. test-bar with two inadequately fed discs, used in the previous work¹ and illustrated in Fig. 1. All the results in the present

paper were obtained on tests in which both of the discs cast were $\frac{3}{8}$ in. thick.

(d) *Examination of Castings.*

Densities were determined on a 5·12-in. length cut from the bottom of the D.T.D. test-bar. British Standard test-bars were subsequently machined from these bars for tensile tests.

Pressure-tightness tests were made at 200 lb./in.² air pressure on the disc castings, both before machining and, when the castings did not leak, after machining $\frac{1}{16}$ in. from both faces, the fillet at the boss being completely removed.

Tensile test-pieces 1 in. wide and $\frac{1}{4}$ in. thick were made from strips cut from the discs in such a way as to include the area directly under the boss.

III.—RESULTS AND DISCUSSION.

(a) *Effects of Residual Phosphorus.*

For ease of presentation and discussion the results from the two alloys 88 : 10 : 2 and 88 : 8 : 4 are here considered together. When examined separately the results are very similar.

Including some figures taken from the earlier work,¹ results from about 70 melts made under comparable conditions are available, i.e. degassed melts poured at a standard temperature of 1180° C. Not all the tests were made on all the melts, e.g. tensile tests were not carried out on many of the discs cast in the earlier work, but there is nevertheless a considerable body of results for each test. For reasons of space individual results are not given here; instead the results are plotted in the form of two graphs. In Fig. 2 the properties of the castings are plotted against phosphorus content, while in Fig. 3 they are plotted against the density of the D.T.D. test-bars from each melt, in the same way as in the earlier paper.¹ As before, the points on these graphs were obtained by taking the average properties of all castings falling within either small ranges of phosphorus content or small ranges of density (of the D.T.D. test-bar). Overlapping ranges were used, so that each test result is taken into account twice in the figures. Fig. 3 is included because it was thought desirable to show the results plotted in the same way (i.e. on a density basis) as in the earlier paper,¹ but the results are most easily interpreted from Fig. 2.

From this Figure the effects of small residual phosphorus contents are immediately clear. Both the density and tensile strength of the D.T.D. test-bars fall progressively as the phosphorus content is increased. Pressure-tightness, however, improves rapidly, the proportion of discs which were pressure-tight when machined rising from

below 20% with phosphorus contents less than 0·01% to over 90% with 0·05% residual phosphorus. When the phosphorus content exceeds 0·08%, pressure-tightness slowly falls again, only 70% of discs being pressure-tight with 0·12% phosphorus. The strength of

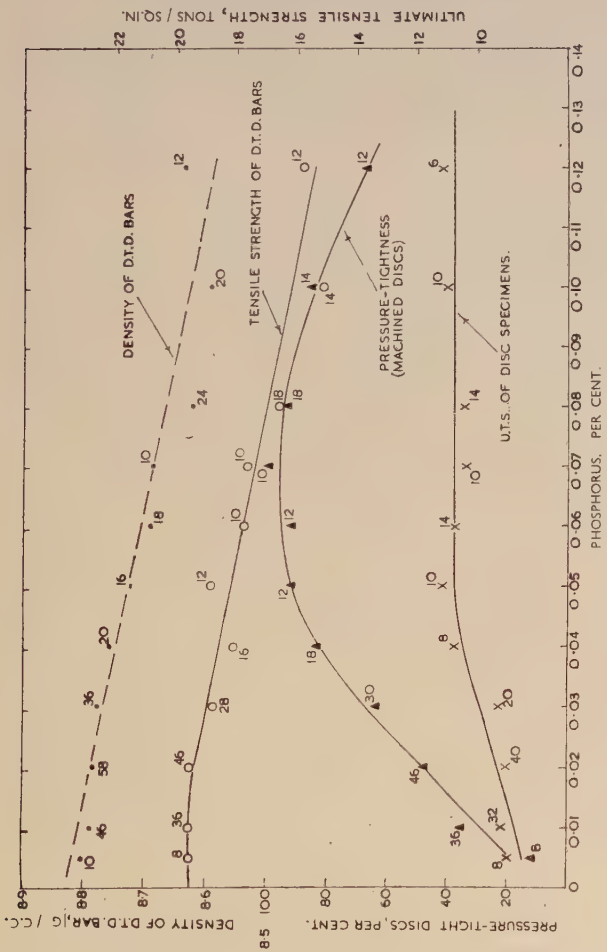


FIG. 2.—Properties of Castings Plotted Against Phosphorus Content.

Note: Each point represents the average results within a range of phosphorus content of 0·02%, except the points at 0·005%, which refer to the range 0·0–0·01% phosphorus, and the points at 0·08, 0·10, and 0·12%, each of which refers to a range of 0·04% phosphorus.

specimens cut from the discs also rises with phosphorus content up to about 0·05%, after which it remains steady up to 0·12% phosphorus.

In previous work¹ the pressure-tightness of lead-free gun-metals was found to vary with the initial gas content of the melt, and a graph was plotted of pressure-tightness against density of the D.T.D. test-

bar, as in Fig. 3. The best pressure-tightness was found to occur within a narrow range of gas content, and in this range 75% of the discs were pressure-tight. In the present work, however, when pressure-tightness is plotted against phosphorus content there is a considerable

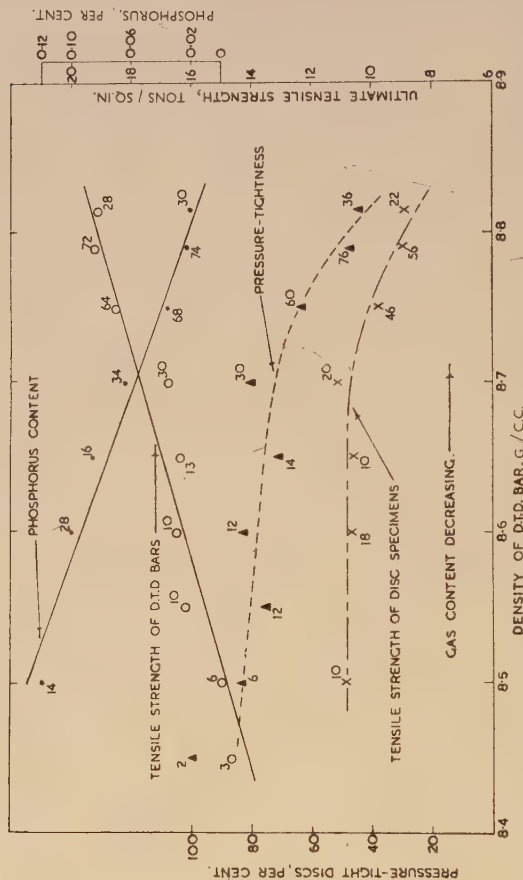


FIG. 3.—Phosphorus content, tensile strength of D.T.D. test-bars, and pressure-tightness and strength of disc castings plotted against gas content of metal as indicated by density of D.T.D. test-bars. Pouring temperature 1180° C.

Note: Each point represents the average results over a density range of 0.10 g./c.c., except points \blacktriangle and \times , which refer to the range 8.40–8.50 g./c.c.; and all points at 8.79 and 8.815 g./c.c., which refer to the ranges 8.75–8.83 and 8.80–8.83 g./c.c., respectively. Each result is therefore taken into account twice.

range, viz. from 0.04 to 0.1% phosphorus, in which over 80% of discs are pressure-tight.

Where the properties of the castings are plotted against the density of the D.T.D. test-bar (Fig. 3), the variation of pressure-tightness is rather less marked, the maximum being about 80%. There is, however, no falling off with the lowest densities. The strength of specimens cut from the discs shows a similar variation, increasing with the first fall

of density and then remaining stationary. The tensile strength of the D.T.D. test-bars decreases steadily with density.

Thus, with residual phosphorus contents of 0·04–0·08%, good pressure-tightness combined with fairly high D.T.D. test-bar strengths (16–19 tons/in.²) and strengths of 10–11 tons/in.² in specimens cut from the discs, may be expected. Both the latter are slightly better than the best obtainable with the leaded gun-metals previously tested (86 : 7 : 5 : 2 and 85 : 5 : 5 : 5 copper-tin-zinc-lead alloys), while the pressure-tightness is equal to that obtained in the best density ranges with these alloys.

(b) *Phosphorus Additions Required.*

The amount of phosphorus which must be added to ensure a given residual phosphorus content depends on the time when it is added and on the degassing method used. There is least loss, and the desired content can most easily be attained, if the phosphorus is added very shortly before pouring and after degassing. One or two minutes should be allowed for deoxidation to take place. Under these conditions the losses to be expected are as follows :

Where degassing is by scavenging either with nitrogen or with air under a charcoal cover or by plunging into the melt marble chips or manganese ore, the loss of phosphorus is about 0·02%, and this amount in excess of the content required should be added. Where manganese ore is charged with the metal, the phosphorus loss is 20–40% of the addition, for additions of 0·05–0·2% phosphorus made 2–5 min. before pouring. Thus, for final phosphorus contents of 0·04–0·08%, the additions required are 0·06–0·12%. With flux degassing the loss is of the same order.

TABLE I.—*Reduction in Phosphorus Content Effected by Additions of Manganese Ore.*

Amount of Mn Ore Charged	Melting Time	Max. Temp. Reached, °C.	Phosphorus, %	
			At Start	At Finish
1·5%	1 hr. 25 min. (starting with furnace cold)	1140	0·10	0·033
2%	1 hr. 25 min. (starting with hot furnace)	1270	0·12	0·013

The above recommendations presuppose that there is no phosphorus present before the additions are made. Where scrap charges are used,

this may not always be the case, but the uncertainty this would introduce is avoided if manganese ore is charged with the metal. Results given in Table I show that amounts of phosphorus well above the amounts likely to be present in charges of gun-metal scrap are substantially removed. The Table refers to melts of 100 lb. of 88:8:4 gun-metal.

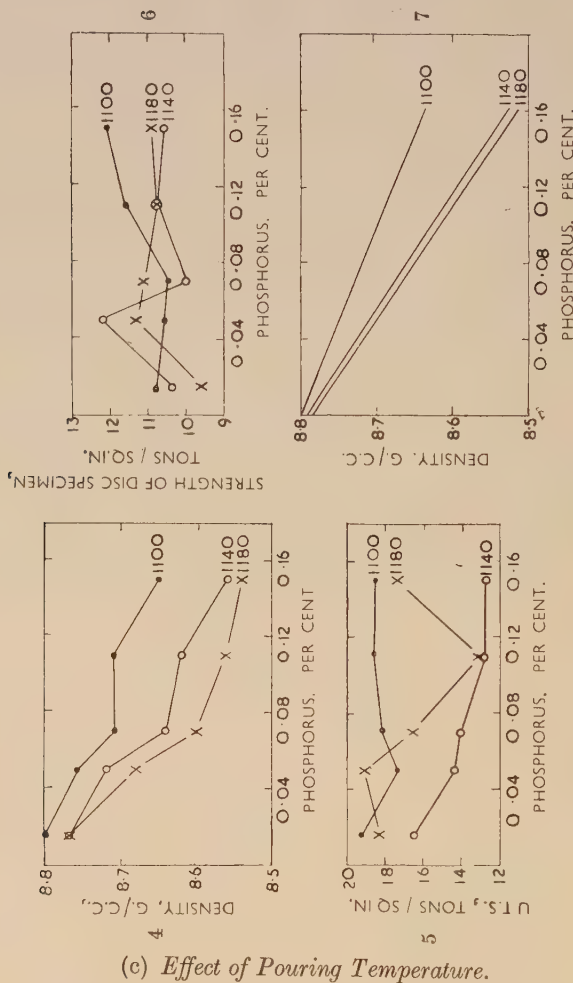


FIG. 4.—Effect of pouring temperature on density of D.T.D. test-bars.
 FIG. 5.—Effect of pouring temperature on strength of D.T.D. test-bars.
 FIG. 6.—Effect of pouring temperature on strength of disc specimens.
 FIG. 7.—As Fig. 4, but with some additional results.

(c) Effect of Pouring Temperature.

The amount of mould reaction caused by small amounts of phosphorus has been found to vary with the pouring temperature. Figs. 4-6 show graphically the results obtained in a series of five melts of

different phosphorus contents from which two bars and two discs were cast at each of three pouring temperatures, 1180°, 1140°, and 1100° C. The amount of mould reaction decreased with fall in pouring temperature, but there was no regular change in physical properties. The bars cast at 1100° C. gave the most consistent tensile strength, while those cast at 1140° C. gave the lowest strength in every case. There was no regular change in the strength of specimens cut from the disc castings.

Some further bars were cast at each temperature in an effort to determine why the bars cast at 1140° C. had the lowest strengths. These bars were examined for distribution of unsoundness by radiography and by density determinations on short lengths of the bars, and micro-examinations were also made. The radiographs were made on strips $\frac{1}{4}$ in. thick and the full length and width of the bar, machined from its centre. There was very little sign of unsoundness at any pouring temperature on those made on bars containing 0·015% phosphorus, but in bars containing 0·09% phosphorus much patchy unsoundness could be seen in bars cast at 1140° C., particularly near the top of the bars, considerably less in those cast at 1180° C., and none in the bars cast at 1100° C.

The distribution of unsoundness along the length of the bars, as determined by density measurements on 1-in. lengths cut from the as-cast bars, bore no relation to that observed by radiography, and appeared to depend more on the phosphorus content than on the pouring temperature. With 0·015% phosphorus, irrespective of pouring temperature, the soundest part of the bar was the centre, with the density falling slightly towards each end. With 0·09% phosphorus the soundest part was at the top, with rather greater unsoundness near the bottom.

Micro-examination revealed that although the amount of unsoundness present varied greatly, its form and distribution were similar in all cases, i.e. convex-sided cavities tending to concentrate towards the centre of the section. With the larger amounts of unsoundness there was a tendency for these to be connected by fissures. Neither the form nor the distribution of the unsoundness appeared to be related to the grain-size of the bars.

The above examination revealed no reason for the lower strength of bars cast at 1140° C., except that there is a tendency in bars cast at this temperature for unsoundness to concentrate in patches, the tendency being more marked with a phosphorus content of 0·09% than with a much lower phosphorus content. Examination made earlier¹ of the distribution of unsoundness in D.T.D. test-bars of phosphor-

bronze (*a*) unsound through sand reaction, and (*b*) unsound through the presence of dissolved gas in the melt, showed that the distribution was the same in either case. This probably applies also in the case of the gun-metals, that is, had bars containing unsoundness due to dissolved gas been examined, similar results would have been obtained to those observed on bars containing unsoundness due to sand reaction.

In Fig. 7 the relation between the density of the D.T.D. test-bar and the phosphorus content is shown for the three casting temperatures. Some results additional to those shown in Fig. 4 are taken into account, and it appears that on an average as much unsoundness due to the reaction occurs in bars poured at 1140° C. as in those poured at 1180° C. There is about half as much in bars poured at 1100° C. Hence, in using the sand reaction as a means of securing pressure-tightness, somewhat higher phosphorus contents are necessary in castings poured at temperatures below 1140° C.

Table II shows pressure-test results on the discs cast from the five melts mentioned above.

Of the discs cast in the alloy containing 0·015% phosphorus, those that leaked at all leaked in the unmachined condition. At the higher phosphorus contents all the discs were pressure-tight before machining. The highest pouring temperature is the most suitable for this casting, but even with the less suitable temperatures the effect of phosphorus is still beneficial.

TABLE II.—*Pressure Tests on Machined Discs Poured at Various Temperatures.*

Pouring Temp., °C.	Phosphorus, %				
	0·015	0·05	0·07	0·11	0·15
1180	L	VSL	NL	NL	NL
	NL	NL	NL	NL	VSL
1140	VSL	NL	VSL	NL	SL
	NL	NL	*	VSL	VSL
1100	VRL	NL	NL	NL	NL
	L	*	VSL	VSL	NL

NL = No leak. L = leak. VSL = very slight leak. VRL = very rapid leak.

* Not tested.

IV.—CONCLUSIONS.

The tests reported above show that a considerable improvement in the pressure-tightness of poorly fed castings in lead-free gun-metals of the 88 : 10 : 2 and 88 : 8 : 4 copper-tin-zinc type can be obtained

by ensuring the presence of certain amounts of residual phosphorus in the metal after deoxidation. The effect is due to a reaction between the phosphorus-containing alloys and the moisture present in sand moulds, which results in a more favourable distribution of unsoundness than that occurring in degassed alloys in which the reaction does not take place.

For the particular test casting and pouring temperature used in the present work, suitable phosphorus contents are from 0·04 to 0·08%. With pouring temperatures below 1140° C., rather more phosphorus is required to produce the same amount of reaction.

In selecting the most suitable phosphorus content, both the pouring temperature and the section of the casting should be considered. For a given pouring temperature castings of heavy section are likely to require less phosphorus than castings of light section.

To ensure the desired residual phosphorus content a slightly greater addition must be made, the excess depending on the method of degassing used and the time at which the addition to the melt is carried out.

With the test casting used, made under the described conditions, pressure-tightness test results as good as those for the leaded gun-metals can be obtained, with rather better tensile test results both on D.T.D. test-bars and on the badly fed section cut from the disc.

It must be stressed that to secure satisfactory results the metal must be free from gas before pouring. The most satisfactory method of ensuring this is to charge manganese ore with the metal at the start of melting. This has the added advantage of removing small amounts of phosphorus which may be present when the charge contains scrap, so that the desired final phosphorus content can be easily obtained.

ACKNOWLEDGEMENTS.

The author's thanks are due to the Director and Council of the British Non-Ferrous Metals Research Association for permission to publish this paper.

REFERENCES.

1. W. A. Baker, F. C. Child, and W. H. Glaisher, *J. Inst. Metals*, 1944, **70**, 373.
2. W. A. Baker and F. C. Child, *J. Inst. Metals*, 1944, **70**, 349.

THE CONSTITUTION OF THE SILVER-RICH 1224 SILVER-MAGNESIUM-ZINC ALLOYS.*

By PROFESSOR G. V. RAYNOR,† M.A., D.Sc., MEMBER OF COUNCIL,
and R. A. SMITH,‡ B.Sc., STUDENT MEMBER.

SYNOPSIS.

In continuation of previous work on the factors affecting ternary equilibrium in copper- and silver-rich alloys, the system silver-magnesium-zinc has been examined by micrographic methods, with confirmatory X-ray experiments. Isotherms have been established at 650°, 450°, and 250° C. Except at 250° C., continuous solid solutions are formed between the two body-centred cubic 3/2 electron compounds which exist in the binary silver-magnesium and silver-zinc systems. At 250° C., the complex hexagonal ζ phase of the silver-zinc system is stable; this phase, however, persists over only a very small range of magnesium content (1 at.-%), and the cubic phase stretches from the silver-magnesium axis almost to the silver-zinc axis. A very narrow two-phase region separates the ternary ζ and β phases. At 250° C. the primary solubility isothermal is almost a straight line joining the binary limits, but as the temperature rises the boundary becomes slightly concave towards the silver-rich corner of the diagram. The homogeneity range of the silver-zinc β phase is slightly increased on the addition of magnesium. The β phase enters into equilibrium with the γ and Mg_3Ag phases, and not with any of the intermetallic compounds of the magnesium-zinc system.

The form of the equilibria is discussed in relation to atomic size effects and electron : atom ratios. The shape of the primary solubility isothermal at 650° C. is consistent with the relief by one solute of the distortion caused by the other solute, but this does not appear to be true at low temperatures. The persistence of the body-centred cubic β phase across the ternary diagram from the silver-magnesium axis almost to the silver-zinc axis indicates that, although in systems where the sizes of the solute atoms do not differ as widely as in this system the ranges of homogeneity of 3/2 electron compounds may be interpreted in terms of the effective size-factor in the ternary alloys, when the solute size-factors with respect to the solvent differ widely, other factors have to be considered. The most important factor in such cases involves the sizes of the respective solute atoms in comparison with the lattice spacings of the binary 3/2 electron compounds into which they are introduced.

I.—INTRODUCTION.

IN previous papers^{1, 2, 3} contributions have been made to the general theory of ternary equilibrium in alloys based on copper and silver as solvents. It has been shown that the existence of electrochemical interaction between the two solutes has an important influence on the forms of the isothermal diagrams. Thus, in the system silver-magnesium-tin, the maximum electron : atom ratio attained by the primary

* Manuscript received 11 April 1949.

† Professor of Metal Physics, University of Birmingham.

‡ Research Student, University of Birmingham.

solid-solubility isothermal occurs at such a composition that magnesium and tin are present in the proportions required to form Mg_2Sn .³ The compositions at which the close-packed hexagonal ζ phase of the silver-tin system becomes unstable with respect to the body-centred cubic β' phase of the silver-magnesium system also correspond with the atomic ratio 2 Mg : 1 Sn.

From a study of the systems silver-antimony-zinc,² silver-magnesium-tin,³ and copper-aluminium-silicon,⁴ it appears that the ranges of homogeneity of 3/2 electron compounds in ternary alloys may be interpreted in terms of the effective size-factors in the ternary systems. If, in the system *ABC*, the size-factors of the solutes *B* and *C* with respect to the solvent *A* are respectively F_B and F_C , then to a first approximation the effective size-factor for a ternary alloy containing *X* at.-% of *B* and *Y* at.-% of *C* may be written as $\frac{XF_B + YF_C}{X + Y}$.¹

It is known, from the data summarized by Hume-Rothery, Reynolds, and Raynor,⁵ that in binary alloys of copper and silver with metals of the *B* Sub-groups, the crystal structures assumed by the 3/2 electron compounds depend upon the value of the size-factor. In general, close-packed hexagonal structures appear at low size-factors (approximately - 6 to + 5), while outside these limits body-centred cubic phases are favoured. The cubic structure is unlikely to occur within the size-factor range - 4·5 to + 3. Increasing solute valency favours the hexagonal structures, while increasing temperature favours the cubic structures. Similar considerations appear to apply to the ternary alloys mentioned. Thus, in the system silver-antimony-zinc, the hexagonal silver-antimony 3/2 electron compound persists from the size-factor of + 0·52 characteristic of the binary alloys to an effective size-factor in the ternary system of - 5·7. At this stage it enters into equilibrium with the cubic phase of the silver-zinc system, which persists from a binary size-factor of - 7·7 to an effective value of - 7·0. The 3/2 electron compounds in the ternary alloys therefore occupy ranges of effective size-factor which are closely similar to the ranges of size-factor over which the same structures exist in binary alloys. Similar indications are given by the systems silver-magnesium-tin and copper-aluminium-silicon.

In extension of this work, the ternary system silver-magnesium-zinc has been investigated. This was selected for the following reasons:

(1) The crystal structures of the 3/2 electron compounds in the component binary silver-magnesium and silver-zinc systems are both body-centred cubic at high temperatures. At low temperatures, however, the crystal structures of the two phases are different; the silver-

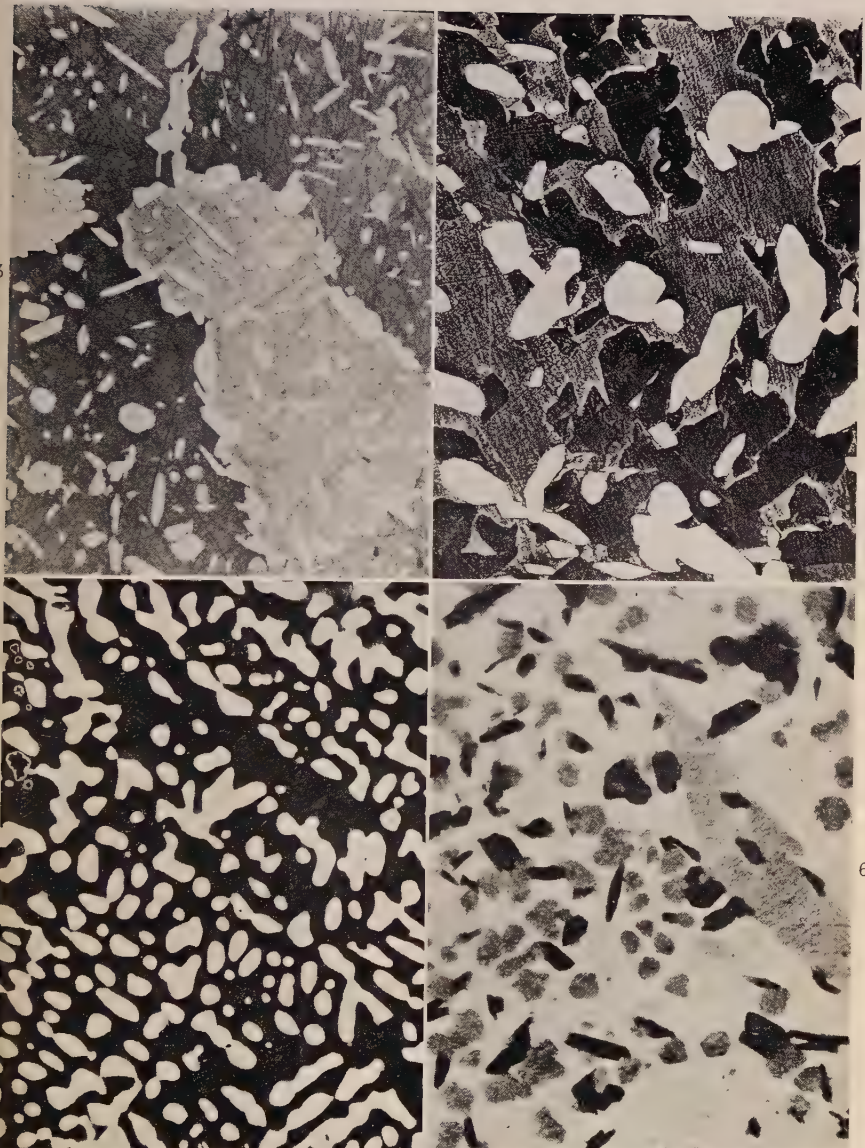


FIG. 3.—Alloy 3·0/42, Annealed at 250° C. Etched in dilute potassium chromate solution. α (white) in and around β grains. $\times 50$.

FIG. 4.—Alloy 1·0/44·0, Annealed at 250° C. Etched in dilute chromic acid solution, followed by ammonia and hydrogen peroxide. α (white) + ζ (black) + β (half-tone). $\times 150$.

FIG. 5.—Alloy 35/30, Annealed at 450° C. Etched in dilute picric acid solution. γ (white) + Mg_3Ag (black). $\times 400$.

FIG. 6.—Alloy 20/40, Annealed at 250° C. Etched in dilute chromic acid solution. γ (white) + Mg_3Ag (black) + β (half-tone). $\times 400$.

zinc phase transforms on cooling below 260° C. to a complex hexagonal structure.

(2) Both solutes are divalent, so that additional complications due to variations in the charges on the solute ions, and to variations in the total solute percentage required to maintain a given electron : atom ratio, should be absent.

(3) The silver-magnesium 3/2 electron compound is ordered, owing to the relatively high electrochemical factor, whereas the corresponding silver-zinc phase shows no ordering.

(4) The effective size-factor in the ternary system varies from -7.77 for the silver-zinc alloys to $+10.65$ for the silver-magnesium alloys. This is a much larger variation than in the systems previously examined, and is approximately symmetrically distributed on either side of zero size-factor. It was therefore of interest to examine whether the stability of the hexagonal modification of the silver-zinc 3/2 electron compound would be increased as the effective size-factor was varied towards zero by the substitution of magnesium for zinc. If this occurred, it would be expected that the temperature of the transformation from the cubic to the hexagonal structure would rise to a maximum at the compositions corresponding with an effective size-factor of zero.

Isothermal diagrams at 650°, 450°, and 250° C. have been established by micrographic and X-ray examination of a large number of ternary alloys, in order to examine the behaviour of the hexagonal silver-zinc phase.

II.—THE BINARY SYSTEMS.

1. *The Silver-Magnesium System.*

This binary system is adequately established for the purposes of the present work, and the equilibrium diagram is shown in Fig. 1. The silver-rich portion (up to 40 at.-% magnesium) has been determined by Andrews and Hume-Rothery,⁶ while the region from 80 to 100 at.-% magnesium is due to Payne and Haughton.⁷ The solid solubility of silver in magnesium according to Hume-Rothery and Butchers⁸ is restricted. The composition region between 40 and 80 at.-% is taken from Hansen.⁹ The solid solubility of magnesium in silver has a maximum value of 29.3 at.-% at the eutectic temperature (759.3° C.), and decreases to a value of 26.5 at.-% at 300° C. The β' phase, which has a crystal structure of the caesium chloride type, extends between approximately 35 and 65 at.-% magnesium at high temperatures; the homogeneity range decreases from approximately

30 at.-% at 600° C. to 23 at.-% at 200° C. The manner in which the liquidus and solidus curves rise to a maximum at the composition AgMg is indicative of the high electrochemical factor in this system.⁵

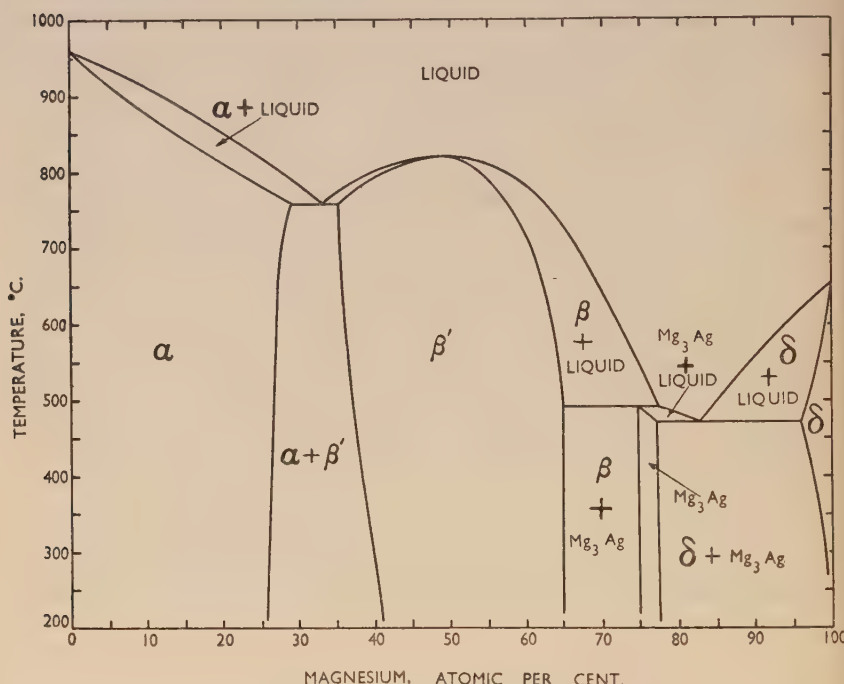


FIG. 1.—Equilibrium Diagram for the Silver-Magnesium Alloys.

2. The Silver-Zinc System.

The equilibrium diagram of the silver-zinc system, according to Andrews, Davies, Hume-Rothery, and Oswin,¹⁰ has been accepted for the present work, and is shown in Fig. 2. The solid solubility of zinc in silver is 32.1 at.-% at the peritectic temperature of 709.8° C., and increases with decreasing temperature to a maximum of 40.2 at.-% at 258°. Below this temperature, the primary solid solution is in equilibrium with the complex hexagonal ζ phase, and the solid solubility decreases, as the temperature falls, to 36.7 at.-% of zinc at 200° C.

The range of homogeneity of the body-centred cubic β phase decreases from approximately 20 at.-% at 650° C. to 5 at.-% at 260° C.

The boundaries of the ζ phase diverge as the temperature decreases, and the range of homogeneity increases to 9 at.-% at 200° C. According to Owen and Edmunds,¹¹ the crystal structure of ζ is a complex

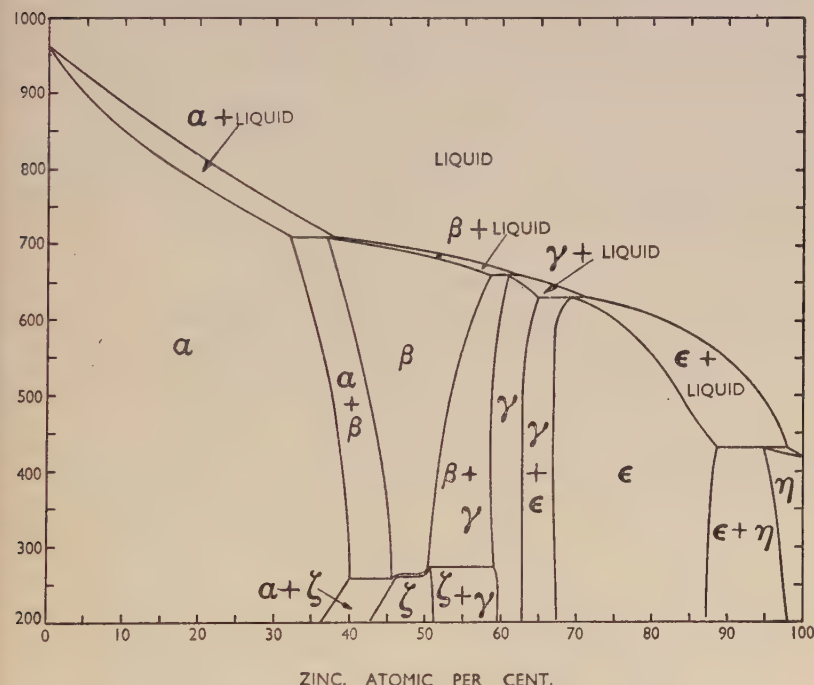


FIG. 2.—Equilibrium Diagram for the Silver-Zinc Alloys.

modification of the close-packed hexagonal structure, with 54 atoms in the unit cell.

The γ phase has a restricted range of homogeneity based upon the composition Ag_5Zn_8 , and has the complex cubic γ -brass structure typical of electron compounds with an electron : atom ratio of 21/13.

3. The Magnesium-Zinc System.

This system is not of great importance for the present work, and the equilibrium diagram need not therefore be reproduced. The intermetallic compounds MgZn , MgZn_2 , and $\text{Mg}_2\text{Zn}_{11}$ occur, with a limited range of homogeneity in each case.

III.—MATERIALS USED.

For the preparation of the binary and ternary alloys used throughout the work, the following materials were used:

(1) Assay silver, 99.99% pure, supplied by Messrs. Johnson, Matthey and Company, Ltd.

(2) Magnesium, 99.95% pure, supplied by Messrs. F. A. Hughes and Company, Ltd.

(3) Pure zinc, which was kindly presented by the Imperial Smelting Corporation, Ltd., of Avonmouth, and in which the only elements detected spectrographically were: lead 0.0001%, cadmium 0.00005%, calcium 0.0001%.

IV.—EXPERIMENTAL METHODS.

The alloys were prepared by adding small pieces of zinc and magnesium to molten silver in an electrically heated Salamander crucible, using potassium chloride as a flux. After thorough stirring, the molten alloys were cast into cold copper moulds.

For all heat-treatments, specimens were enclosed in evacuated hard-glass tubes and annealed in tubular resistance furnaces, which were automatically controlled by Foster regulators. Temperatures were measured with a platinum/platinum-rhodium thermocouple used in conjunction with a deflection potentiometer. In general, the chill-cast alloys were heated slowly to 650° C., or to 550° C. in the case of alloys rich in solute, in order to absorb low-melting solute-rich material without partial melting. After an homogenizing treatment at 650° or 550° C., the specimens were cooled to the required annealing temperature, at which they were annealed for periods of the order of 7–9 days before quenching in cold water.

For micrographic examination, new surfaces of the quenched alloys were exposed, and prepared in the usual manner. Etching techniques are referred to below (Section V). The structures of several alloys were confirmed by X-ray analysis; for this purpose filings were prepared from the quenched alloys, and were reheated to the quenching temperature for the relief of mechanical strain. After this treatment the filings were rapidly cooled, and, without sieving, mounted with Canada Balsam on a hair or a fine glass fibre. Diffraction patterns were obtained in a 9-cm. Debye-Scherrer X-ray camera, using copper K_{α} radiation.

Owing to the volatility and ease of oxidation of the solute metals magnesium and zinc, all critical alloys were chemically analysed. The actual specimens used in the micrographical work were submitted for

analysis, after removal of the extreme outer surfaces to avoid errors due to volatilization losses during annealing. Several alloys were analysed for all three components; the totals of the three percentages were satisfactory, so that in general only the zinc and silver percentages were determined.

In the following sections, it will be necessary to refer to individual alloys, which are described in terms of their alloy content. Thus, an alloy containing 10 at.-% magnesium and 15 at.-% zinc is denoted by the term "alloy 10/15".

V.—METALLOGRAPHY.

During the course of the work, only phases based upon those present in the silver-magnesium and silver-zinc alloys were observed. Since the most important section of the work was concerned with the range of homogeneity of the ζ phase in the ternary isothermals, several etching reagents were used in attempts to distinguish between the β and ζ phases.* Two reagents were found to be of general utility. These were :

(1) A solution of 20 g. of chromium trioxide and 1.5 g. of sodium sulphate in 100 c.c. of water, diluted before use with its own volume of distilled water. Specimens were etched by swabbing or by immersion; the time of etching was rarely critical, and varied considerably for different types of microstructure.

(2) A saturated solution of picric acid in alcohol, frequently diluted before use with an equal volume of water. Etching times were again not critical.

Solution (1) was used extensively for silver-rich alloys, and solution (2) for alloys lying to the solute-rich side of the β -phase area in the ternary diagrams. In certain cases, as, for instance, in the examination of three-phase ($\beta + \gamma + \text{Mg}_3\text{Ag}$) structures, both reagents were used on the same alloy. A summary of the etching results obtained with these reagents is given in Table I.

The use of a saturated solution of potassium dichromate in 2% aqueous sulphuric acid was abandoned at an early stage in the work, owing to its tendency to develop abnormally pronounced contrasts between differently orientated grains of the β phase. Several other reagents of general usefulness for the primary solid solution were found to be incapable of distinguishing between β and ζ .

* In the description of the ternary system at elevated temperatures, the symbol β is used throughout to denote the body-centred cubic phase, since, although it is known that at room temperature the structure is ordered at least up to 30 at.-% zinc, it was not found possible to define the superlattice limits at higher temperatures.

TABLE I.—Results of Etching Tests.

Etching Reagent	Phase	Colour	Remarks
Chromic acid solution.	α	white	Shows a pink tinge when present with the ζ phase.
	β	brown	Shade varies with grain orientation.
	ζ	white	Appears bluish in presence of β phase.
	γ	white	Appears brown in presence of ζ phase.
Picric acid solution .	β	white	Shows a pink tinge in presence of γ phase.
	Mg_3Ag	white	
		brown	Shade varies somewhat with composition.

A series of representative microstructures is shown in Figs. 3, 4, 5, and 6 (Plate LIV).

VI.—EXPERIMENTAL RESULTS.

The results obtained may be conveniently summarized in the form of isothermal diagrams at 650°, 450°, and 250° C.

1. The 650° C. Isothermal.

For the experiments at 650° C., chill-cast specimens were slowly heated over several days to the annealing temperature, and held there for 9 days. The results are given in Fig. 7, in which analysed alloys have been distinguished by shading the appropriate symbols. The microstructures of the duplex alloys were relatively large-grained, and the typical twinned structure of the α phase could be developed by several etching reagents. As expected, at this temperature there is a complete range of ternary solid solutions between the body-centred cubic 3/2 electron compounds in the silver-magnesium and silver-zinc systems.

As shown by the close composition bracket between alloys 7·64/25·63 and 7·59/26·16, which consist respectively of the α phase and the ($\alpha + \beta$) phases, the solid-solubility boundary is not a straight line joining the two binary limits. The deviation is in the direction of increasing solute percentages. The boundary below 20 at.-% zinc has been drawn in conformity with the relative proportions of the phases in the duplex alloys and cannot differ significantly from that shown in Fig. 7.

The ($\alpha + \beta$)/ β boundary is less adequately established by the ex-

perimental points plotted, but must deviate from linearity in the same sense as the $\alpha/(\alpha + \beta)$ phase boundary.

The temperature of 650° C. is only slightly below the $\beta +$ liquid $\rightleftharpoons \gamma$ peritectic in the silver-zinc system, and is considerably above the

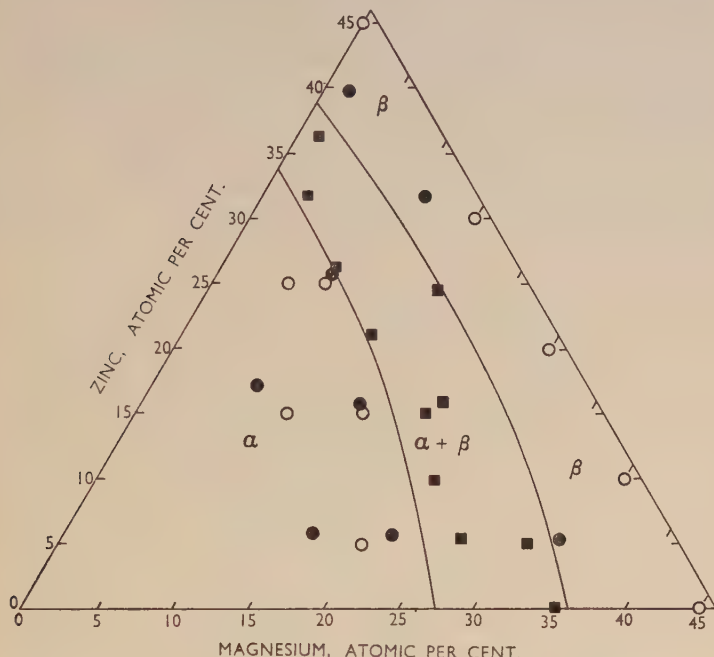


FIG. 7.—The System Silver-Magnesium-Zinc; 650° C. Isothermal.

$\beta +$ liquid $\rightleftharpoons \text{Mg}_3\text{Ag}$ peritectic in the silver-magnesium system. Except near the silver-zinc axis, therefore, the solute-rich boundary of the ternary β phase involves equilibrium with the liquid, and has not been investigated in the present work.

2. The 450° C. Isothermal.

The alloys already annealed at 650° C. were resealed *in vacuo*, and heated for 16 hr. at this temperature. They were then very slowly cooled to 450° C. and annealed at this temperature for 7 days. The microstructures observed were very similar to those observed at 650° C. Alloy 1·91/39·75, however, changed from homogeneous β to $(\beta + \alpha)$, as would be expected from the rate of change with temperature of the solubility of zinc in silver. Alloy 32·95/5·3 also changed from β to

($\alpha + \beta$). The results of these experiments are shown in Fig. 8; no evidence of any three-phase region was obtained. Of the alloys near the α solubility limit, 12.58/21.01, 7.59/26.16, and 2.95/31.67 changed from ($\alpha + \beta$) at 650° C. to α at 450° C.

Further alloys were prepared for the investigation of the solute-rich boundaries of the β -phase area. These were also annealed for 7 days at 450° C.; the results of the micrographic examination are included in Fig. 8. The $\beta/(\beta + \text{Mg}_3\text{Ag})$ boundary is adequately located

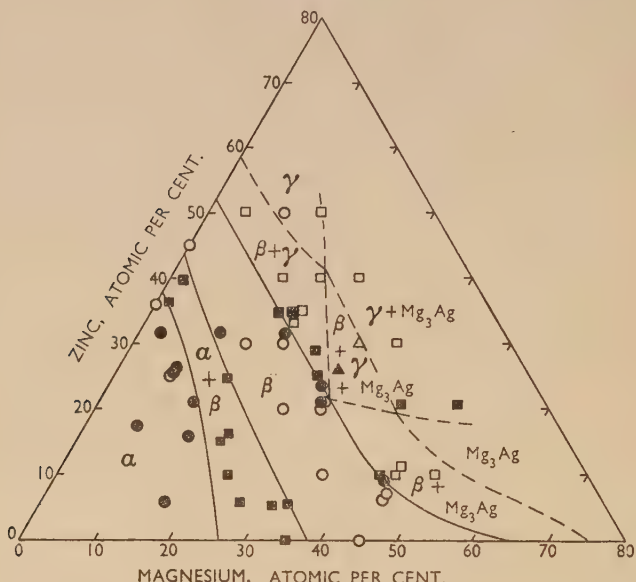


FIG. 8.—The System Silver—Magnesium—Zinc; 450° C. Isothermal.

by the close composition bracket between alloys 43.78/9.14 (β) and 43.13/9.29 ($\beta + \text{Mg}_3\text{Ag}$). The boundary between the β and ($\beta + \gamma$) phase fields is also located by composition brackets between the alloys 17.29/34.81 ($\beta + \gamma$) and 19.47/31.42 (β), and between the alloys 27.09/25.04 ($\beta + \gamma$) and 28.29/23.44 (β). Two alloys, 29.27/25.93 and 30/30, contained the β , γ , and Mg_3Ag phases. These results, taken in conjunction with the other results plotted, enabled the approximate positions of the remaining phase boundaries to be drawn in Fig. 8 as broken lines.

At 450° C., therefore, continuous solid-solution formation still occurs between the two body-centred cubic 3/2 electron compounds.

At higher solute percentages, equilibrium occurs between the γ and Mg_3Ag phases (see Fig. 5, Plate LIV), which must both project some distance into the ternary diagram. There is a three-phase ($\beta + \gamma + Mg_3Ag$) triangle, the boundaries of which have been approximately located.

3. The 250° C. Isothermal.

The silver-rich portion of the 250° C. isothermal was determined by re-annealing, for 7 days at 250° C., portions of alloys cooled very slowly from their previous annealing temperature. As shown in Fig. 9, only the structure of alloy 12·58/21·01 showed any marked change from those observed at 450° C. Examination of the binary silver-zinc

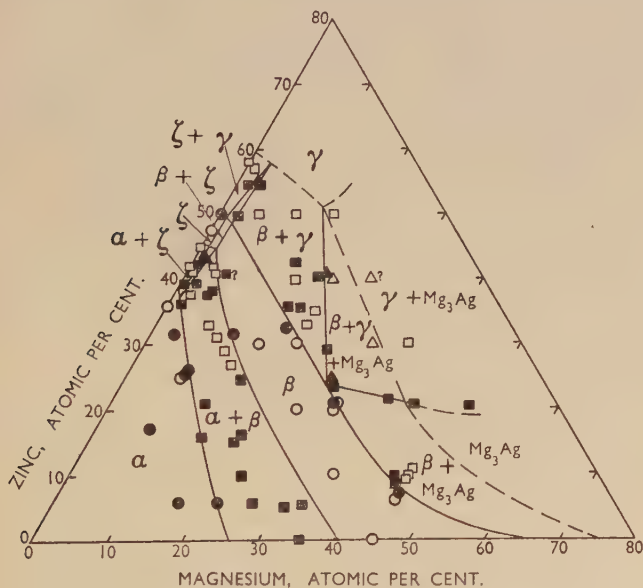


FIG. 9.—The System Silver-Magnesium-Zinc; 250° C. Isothermal.

alloy 0/44, however, showed that the phase present in addition to the α phase was different from that present in the ternary alloys. This was confirmed by X-ray examination, and the new phase was identified with the ζ phase of the silver-zinc system. These results indicated that a three-phase ($\alpha + \beta + \zeta$) triangle should exist close to the silver-zinc axis. Further alloys were prepared to define this field. Some of the results of the examination of these alloys are given in Fig. 9;

Fig. 10 shows the complete results in the region of the ζ phase on a larger scale. Although no alloy was actually placed in the two-phase ($\beta + \zeta$) field, the recognition of two ($\alpha + \beta + \zeta$) alloys, one ($\gamma + \beta + \zeta$) alloy, three ternary ($\alpha + \zeta$) alloys, and two ternary ($\zeta + \gamma$) alloys adequately defines the form of the equilibria in this region.

The positions of the $\beta/(\beta + \text{Mg}_3\text{Ag})$ and $\beta/(\beta + \gamma)$ boundaries were determined by the annealing of alloys cooled very slowly from 550° or

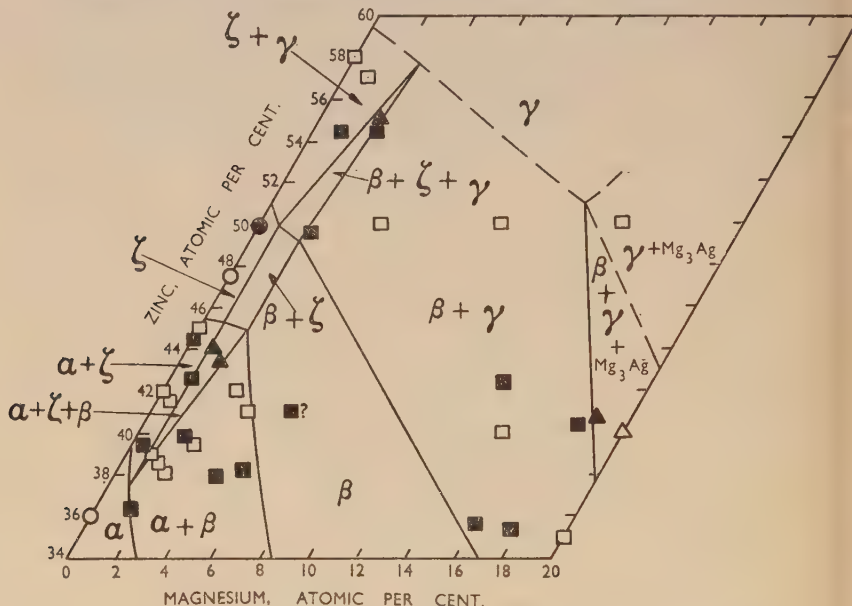


FIG. 10.—The System Silver—Magnesium—Zinc; Enlarged Portion of 250° C. Isothermal.

450° C. and then held for 7 days at 250° C. These boundaries are accurately fixed by the composition brackets plotted in Fig. 9. At this temperature, the sides of the three-phase ($\beta + \gamma + \text{Mg}_3\text{Ag}$) triangle are relatively accurately defined by the plotted points.

The isothermal diagram at 250° C. is therefore of considerable interest; the most striking feature is the persistence, almost to the silver-zinc axis, of the body-centred cubic structure based on AgMg . This structure is maintained until practically the whole of the magnesium has been replaced by zinc. The ternary primary solid-solubility isothermal at this temperature approaches more closely to the ideal case than at higher temperatures. The presence of a restricted homo-

geneous ζ field in the ternary diagram involves the presence of three-phase ($\alpha + \beta + \zeta$) alloys (see Fig. 4, Plate LIV) and of ($\gamma + \beta + \zeta$) alloys. As at 450° C., equilibrium between γ and Mg₃Ag occurs, and three-phase ($\beta + \gamma + \text{Mg}_3\text{Ag}$) alloys (see Fig. 6, Plate LIV) are observed. The positions of the boundaries of this three-phase triangle imply that the γ phase of the silver-zinc system can take up approximately 14 at.-% magnesium, while the Mg₃Ag phase can dissolve approximately 20 at.-% zinc.

The X-ray Debye-Scherrer technique was employed to confirm the indications of the micrographic work, and to ensure that the phases present had been correctly identified. Diffraction patterns were obtained as previously described, and compared with standard diffraction patterns obtained from the binary phases. The results were particularly helpful in the region of the diagram shown in Fig. 10. In the course of this work, it was observed from the diffraction patterns of alloys 45/0, 35/10, 25/20, and 15/30, obtained at room temperature from alloys annealed at 250° C., that superlattice lines were present in all four cases. The caesium chloride arrangement characteristic of AgMg thus persists, at low temperatures, at least up to 30 at.-% zinc. Attempts to investigate the temperature range of stability of the ternary superlattice by high-temperature X-ray photography were unsuccessful, owing to the reactive nature of the alloys at high temperatures, and the volatility of magnesium and zinc, which tended to produce very diffuse X-ray reflections.

VII.—DISCUSSION OF THE RESULTS.

Certain features of the isothermal diagrams for the silver-magnesium-zinc system are of interest, and may be considered separately.

1. *The Primary Solid-Solubility Isotherms.*

The forms of the primary solid-solubility isotherms in ternary systems have been discussed by Hume-Rothery,¹² who distinguishes four cases. Where both solutes are of favourable size-factor with respect to the solvent, the ternary isotherms approximate to straight lines joining the corresponding binary solubility limits. If, however, one solute markedly increases the distortion of the solvent lattice produced by the other solute, the ternary solid solubility tends to be more restricted than in the ideal case. On the other hand, the ternary solid solubility tends to exceed the ideal solubility if one solute relieves the distortion produced by the other. Thus, if the atomic diameter of one solute is large enough for the solubility to be relatively restricted

the alloy may be regarded as a solvent framework containing regions of marked expansion, which can be more easily accommodated if there are regions of contraction produced by the presence of another solute of smaller atomic diameter than the solvent. This conception is, however, inappropriate if the solid solution in the solvent of the metal of larger atomic diameter is not dilute. In this case, the alloy is to be regarded as a framework of both solvent and solute atoms, with an increased lattice spacing; the small atoms of the second solute may then be of unfavourable size-factor with respect to the alloy framework, leading to a more restricted ternary solid solution than in the ideal case.

In the system under consideration, the zinc atom is smaller than that of silver, and, although the valency of zinc is one unit higher than that of silver, the solution of zinc contracts the solvent lattice. Magnesium has a larger atom than silver and expands the lattice of silver, though to a somewhat smaller extent than would be expected on general principles. The distortion produced by the large magnesium atoms may therefore be relieved by the small zinc atoms, so that, provided the ternary solution may be regarded as dilute, the solubility would be expected to be somewhat larger than that corresponding to a straight line joining the binary limits.

The 650° C. isothermal (Fig. 7) shows that the solubility isothermal is concave towards the silver-rich corner, corresponding to a slightly larger solubility than in the ideal case. It would appear, therefore, that the boundary is consistent with mutual relief of distortion by the solutes, in spite of the fact that the solution is not dilute, but extends to more than 30 at.-% of solute. At 250° C., however (Fig. 9), this tendency has disappeared, and the boundary corresponds very closely to the ideal case; the relative amounts of the phases present in the ($\alpha + \beta$) alloys suggest that the boundary may be slightly convex towards the silver-rich corner. The experiments at 450° C. show that the α boundary is of the same form as at 650° C. At this temperature, the form of the boundary may be regarded as roughly intermediate between those at 650° and 250° C. In considering the form of solubility isothermals, therefore, the effect of temperature must be taken into account. At low temperatures, the introduction of large magnesium atoms into the contracted silver-zinc alloy lattice is difficult, so that no increase in solubility occurs, there being probably a slight tendency towards a decrease. As the temperature rises, the effect of thermal agitation leads to an effective expansion of the silver-zinc lattice, and the large magnesium atoms may become more easily accommodated, so that some mutual relief of lattice distortion may occur. At low

temperatures, the alloy behaves as a concentrated solution, but at high temperatures, as a dilute solution. This type of change with temperature may be expected in all cases where the ternary solid solubility is relatively high.

2. *The 3/2 Electron Compounds.*

At 650° C., as would be expected, the two body-centred cubic 3/2 electron compounds are mutually soluble in each other. At 450° C. the same remains true, while the fact that, at 250° C. (which is below the temperature of the $\beta \rightleftharpoons \zeta$ transformation in the silver-zinc alloys), the homogeneous ζ area is very restricted, indicates that no stabilization of the ζ occurs on the addition of magnesium in spite of the trend of the effective size-factor towards zero. It is probable that this is due to the large difference between the sizes of the zinc and magnesium atoms. In the first place, the crystal structure of the ζ phase is not a simple close-packed hexagonal structure, but a complex structure with 54 atoms per unit cell. Its range of homogeneity in the binary system is narrow, indicating that the correct geometry of the structure can be maintained only if the deviation from the equi-atomic ratio is comparatively small. It is probable that, just as in the case of concentrated primary solid solutions, the introduction of the large magnesium atom into the complex hexagonal structure of small lattice spacing causes too large a local strain for stability. The β phase has a body-centred cubic structure, which is by comparison open and more easily able to accommodate large atoms. The effect of replacing small zinc atoms in the ζ structure by magnesium atoms is thus to cause a breakdown of the structure in favour of the cubic structure. Conditions at the silver-magnesium axis are somewhat different; here the structure is simple and open, and the effect of introducing zinc atoms may well be to relieve the distortion due to magnesium and to stabilize the body-centred cubic phase.

The general principle, that the ranges of homogeneity of 3/2 electron compounds in ternary systems tend to correspond with similar ranges of effective size-factor to those in which the same structures are found in the corresponding binary alloys, thus needs modification in cases where the solute atoms are respectively bigger and smaller than that of the solvent, and the difference between the atomic sizes of the solutes is large. In such cases, especially where one of the 3/2 electron compounds has a complex structure, allowance must be made for the difficulty of forcing large atoms into relatively close-packed structures in which the interatomic distances are on the average smaller than in the pure solvent. This implies that, by analogy with primary solid

solutions, there is a size-factor range within which the general principle may be expected to apply, and outside which the ranges of homogeneity of 3/2 electron compounds depend more intimately on distortion effects. Thus, in the systems silver-antimony-zinc, silver-magnesium-tin, and copper-aluminium-silicon the ranges of homogeneity of the 3/2 electron compounds correspond approximately with the same size-factor range as in the corresponding binary alloys; in the present system this does not occur. The size-factors of the various solutes with respect to the solvent are collected in Table II.

TABLE II.—*Size-Factors of Solvent and Solutes.*

Solute	Solvent	Size-Factor	Difference
Sb	Ag	+ 0.5}	—
Zn	Ag	— 7.8}	8.5
Mg	Ag	+10.7}	18.5
Sn	Ag	— 3.0}	13.7
Al	Cu	+ 6.6}	—
Si	Cu	— 8.4}	15.0

From the present work it may be suggested that the interpretation of the ranges of ternary 3/2 electron compounds in terms of effective size-factors is valid only if the difference in the size-factors of the two solutes with respect to the solvent does not exceed 15, the size-factor being expressed as $\frac{(d_{\text{solute}} - d_{\text{solvent}})100}{d_{\text{solvent}}}$, where d denotes the appropriate atomic diameter.

Along the $\beta/(\beta + \gamma)$ boundaries of Figs. 8 and 9, the β phase is in equilibrium with another electron compound (the γ phase of the silver-zinc system). These boundaries occur at constant atomic percentages of silver, so that, at a given temperature, the electron : atom ratio along the boundary remains constant. This behaviour is typical of equilibrium between electron compounds and is shown in several other systems. Along the $\beta/(\beta + \text{Mg}_3\text{Ag})$ boundary, however, the electron : atom ratio rises at first slowly and then more rapidly as the magnesium content increases. Thus, at 450° C., the electron : atom ratio increases from 1.52 at the corner of the $(\beta + \gamma + \text{Mg}_3\text{Ag})$ triangle to 1.65 at the silver-magnesium axis. The tendency is, therefore, for the whole solute-rich boundary of the ternary body-centred cubic phase to occur at a constant electron : atom ratio close to 1.5; this tendency is opposed, at zinc contents of less than 10 at.-%, by the tendency towards perfect ordering of the silver and magnesium atoms, which is responsible for the abnormally wide range of homogeneity of the silver-magnesium phase.

3. The General Form of the Equilibria.

It has been shown³ that in the system silver-magnesium-tin, the compound Mg_2Sn enters into equilibrium with the body-centred cubic 3/2 electron compound. In the present system, none of the binary compounds $MgZn$, $MgZn_2$, or Mg_2Zn_{11} enters into equilibrium with the 3/2 electron compounds. In this connection it is significant that the highest heat of formation in the magnesium-zinc system is 4.2 kg. cal./g.-atom ($MgZn_2$), which is appreciably lower than that of Mg_2Sn (5.6 kg. cal./g.-atom). Compounds occurring on the magnesium-zinc axis are therefore less likely to enter into equilibrium with the β phase than the compound Mg_2Sn .² A quantitative analysis of the equilibria to be expected in terms of the heats of formation is not possible, since, for silver-magnesium alloys, only heats of mixing, which cannot be corrected to heats of formation without latent- and specific-heat data, are known.

The experiments indicate that the γ and Mg_3Ag phases enter into equilibrium, and that both phases have appreciable ranges of homogeneity in the ternary system. At 250° C., the γ phase extends to 14 at.-% magnesium, while the Mg_3Ag phase can take up approximately 20 at.-% zinc. At 450° C., the position of the $(\beta + \gamma)/(\beta + \gamma + Mg_3Ag)$ boundary indicates that the solubility of magnesium in the γ phase has increased with rising temperature to 20 at.-%. The experiments on the $(\beta + Mg_3Ag)/(\beta + \gamma + Mg_3Ag)$ boundary are insufficient to assess the solubility of zinc in Mg_3Ag at 450° C.

The main conclusion to be drawn from this work is that, where the size-factors of the two solutes differ in sign and also appreciably in magnitude, the factors affecting the equilibrium between the two 3/2 electron compounds are not necessarily the same as in cases where the size-factor difference is less serious. The evidence obtained suggests that, if the size-factors of the two solutes with respect to the common solvent do not differ by more than 15 units, the ranges of effective size-factor over which the cubic and hexagonal phases are stable in the ternary alloys correspond approximately with the ranges of size-factor over which they are stable in the corresponding binary alloys. If, however, the size-factor difference is greater than this, it is necessary to consider specifically the effect of introducing large atoms into a lattice which is contracted relatively to the solvent, and of introducing small atoms into a relatively expanded lattice.

ACKNOWLEDGEMENTS.

This research was carried out in the Metallurgy Department of the University of Birmingham, under the general supervision of Professor D. Hanson, D.Sc., to whom the authors' thanks are due for his interest and support. The authors must also acknowledge the valuable assistance of Mr. G. Welsh in the experimental work, and the analytical work of Mr. P. Wingrove.

The authors express their gratitude to the Department of Scientific and Industrial Research, the Royal Society, the Chemical Society, and Imperial Chemical Industries, Ltd., for generous financial assistance.

REFERENCES.

1. G. V. Raynor, *Phil. Mag.*, 1948, [vii], **39**, 212.
2. G. V. Raynor, *Phil. Mag.*, 1948, [vii], **39**, 218.
3. G. V. Raynor and B. R. T. Frost, *J. Inst. Metals*, 1949, **75**, 777.
4. F. H. Wilson, *Trans. Amer. Inst. Min. Met. Eng.*, 1948, **175**, 262.
5. W. Hume-Rothery, P. W. Reynolds, and G. V. Raynor, *J. Inst. Metals*, 1940, **66**, 191.
6. K. W. Andrews and W. Hume-Rothery, *J. Inst. Metals*, 1943, **69**, 485.
7. R. J. M. Payne and J. L. Haughton, *J. Inst. Metals*, 1937, **60**, 351.
8. W. Hume-Rothery and E. Butchers, *J. Inst. Metals*, 1937, **60**, 345.
9. M. Hansen, "Der Aufbau der Zweistofflegierungen". Berlin : 1936 (Julius Springer).
10. K. W. Andrews, H. E. Davies, W. Hume-Rothery, and C. R. Oswin, *Proc. Roy. Soc.*, 1941, [A], **177**, 149.
11. E. A. Owen and I. G. Edmunds, *J. Inst. Metals*, 1938, **63**, 291.
12. W. Hume-Rothery, *Phil. Mag.*, 1936, [vii], **22**, 1013.

